

8-2016

Development of a Pilot-Scale Polymerization Facility and Monomer Preparation for the Determination of Reactivity Ratios for Tetrafluoroethylene (TFE)-Based Copolymers

Daniel A. Hercules
Clemson University

Follow this and additional works at: https://tigerprints.clemson.edu/all_dissertations

Recommended Citation

Hercules, Daniel A., "Development of a Pilot-Scale Polymerization Facility and Monomer Preparation for the Determination of Reactivity Ratios for Tetrafluoroethylene (TFE)-Based Copolymers" (2016). *All Dissertations*. 2169.
https://tigerprints.clemson.edu/all_dissertations/2169

This Dissertation is brought to you for free and open access by the Dissertations at TigerPrints. It has been accepted for inclusion in All Dissertations by an authorized administrator of TigerPrints. For more information, please contact kokeefe@clemson.edu.

DEVELOPMENT OF A PILOT-SCALE POLYMERIZATION FACILITY AND
MONOMER PREPARATION FOR THE DETERMINATION OF REACTIVITY
RATIOS FOR TETRAFLUOROETHYLENE (TFE)-BASED COPOLYMERS.

A Dissertation
Presented to
the Graduate School of
Clemson University

In Partial Fulfilment
of the Requirements for the Degree
Doctor of Philosophy
Chemistry

by
Daniel A. Hercules
August 2016

Accepted by:
Dr. Joseph S. Thrasher, Committee Chair
Dr. Darryl D. DesMarteau
Dr. Stephen E. Creager
Dr. William T. Pennington

Abstract

The addition of a pilot-scale tetrafluoroethylene (TFE) polymerization facility at Clemson University has enabled this academic institution to not only prepare TFE in kilogram quantities but also to store it and copolymerize it in safe conditions. The facility is used to prepare equimolar mixtures of TFE/CO₂ from the pyrolysis of potassium perfluoropropionate in approximately quantitative yields. The TFE is separated from the mixture and stabilized by D-limonene by scrubbing CO₂ from the aforementioned mixture. With the development of high technology software and hardware, the facility has been used to study the relative reactivity ratios of various polymerizations systems like the copolymerization of TFE with sulfonyl fluoride-substituted vinyl ethers [(perfluoro-3-oxa-4-pentene sulfonyl fluoride [DOW monomer] and perfluoro-2-(2-fluorosulfonylethoxy) propyl vinyl ether [PSEPVE]), methyl perfluoro(4-oxa-5-hexanoate) (DEVE), and perfluoro 8-cyano-5-methyl-3,6-dioxa-1-octene (8CNVE)], and vinylidene difluoride (VDF), in the presence and absence of CO₂. Some results from these studies as well as further details on the facility will be presented.

Dedication

I dedicate this work first to God, creator of the universe that all we scientists explore but will never comprehend. I dedicate this dissertation secondly to my wife, Shelby L. Hercules for her unconditional support, patience, and love, which have been my motivation to endure during these years of hard work. Quiero dedicar también éste trabajo de graduación a mi mamá Dora Hércules Ramírez; su apoyo incondicional y los sacrificios durante toda su vida que han sido para ayudarme a salir adelante: esto y mucho más ha sido y será invaluable por el resto de mi vida.

And in every way my family but for blood, I dedicate this work to the Emmons family, for their incredible fraternal and emotional support. To Robert M. Emmons, Marilyn Sue Emmons, and Aidil Emmons for becoming to me what anyone would hope for a father, mother, and grandmother. Your support, prayers, encouragements, and love will never be forgotten and I thank God for blessing me with the opportunity to be close to y'all during these years here at Clemson University.

Acknowledgments

This dissertation is first and foremost a product of the incredible patience and guidance from my advisor Dr. Joseph S. Thrasher. I have been blessed with an endless amount of his kindness and support, and his teachings will accompany me for the rest of my life. Secondly, I want to thank my colleague and friend, Cameron A. Parrish, for his grace, patience, and great support while we were shoulder to shoulder in the lab figuring out solutions to the multiple scientific barriers that we needed to surpass. I specially thank my committee members (Dr. Darryl D. DesMarteau, Dr. Stephen E. Creager, and Dr. William T. Pennington) for their patience and recommendations. Special thanks to the Clemson University machine shop team as a whole for their incredible help, friendliness, and willingness to assist me and the research team with an endless amount of projects that helped develop the project herein detailed. To the administrative body of the Chemistry Department (Heather Shelton, Sharon Smith, Diane Harris, Will Wanamaker, Barbara Lewis) for their great help and great attitude to serve. I thank Dr. Christopher P. Junk for his solidarity and open door policy to ask him as many questions as I wanted. To Dr. Bruno Ameduri for his endless encouragement and support. Special thanks to Dr. Alexander Marchione and Dr. Rebecca Dooley at The Chemours Company for their invaluable help determining the compositions of some of my copolymers. To the Bacher family (Vernon,

Mariah and Dinah) for blessing us with their friendship and company. To the Deavers family, for their encouragement and friendship. To the Thatcher family (Jonathan and Shanon) for supporting us through a deep friendship, prayer, and words of encouragement. To my closest friends in Costa Rica (Mauricio Orozso, Alicia Ortega, Ileana Brenes, Marietta Monestel, and Yamileth Mesen) for their help, support, words of encouragement, and emotional support at the time of my departure to come here to the United States of America to start my Doctoral work. To my great friend Ronald Castro for introducing me to the world of chemistry and always pushing me to be better. Special acknowledgements to Rina Moncada for her incredible support during my younger years. Special acknowledgement to Bob Benjamin from Texas Instruments, and Ravi Patel from Marwadi Education Foundation in India for their incredible support and help during the development of the data acquisition system herein described. To my various undergrad students for their willingness to work late and unusual hours towards to help in my projects. Special thanks to Dr. Olt E. Geiculescu, Dr. Iqbal Sharif, and Dr. Andrej V. Matsnev for their help, lessons, and encouragement during my years at Clemson University.

Lastly, special acknowledgement to B. M. Hercules who has been my inseparable companion in the endless long nights of work and writing.

Table of Contents

	Page
Title Page	i
Abstract	ii
Dedication	iii
Acknowledgments	iv
List of Tables	xii
List of Figures	xx
Disclaimer	lvii
Chapter 1 Minor Research and Noncommercial Co- and Terpolymers of Tetrafluoroethylene	1
1.1. Introduction	1
1.2. Co- and Terpolymers of Tetrafluoroethylene and Non Fluorine-Containing Alkenes	4
1.3. Co- and Terpolymers of Tetrafluoroethylene and Polyfluoroalkenes	10
1.4. Co- and Terpolymers of Tetrafluoroethylene and Perfluoroalkenes	23
1.5. Co- and Terpolymers of Tetrafluoroethylene with Cyclic Monomers and Tetrafluoroethylene-based Photoresist Materials	27
1.6. Future Work and Conclusions	36
1.7. Dissertation Summary	39
1.8. References	40

Table of Contents (Continued)

	Page
Chapter 2 Development of Academic Tetrafluoroethylene (TFE) Polymerization Facilities	62
2.1. Introduction.....	62
2.2 First Generation	74
2.3 Second Generation	78
2.4 Third Generation at Clemson University	83
2.4.1. Equipment Installed In The Tetrafluoroethylene Facility.....	99
2.4.2. Safety and Control Section	103
2.4.3. Data Acquisition (DAQ) System	114
2.4.4. Gas Handling System.....	114
2.4.5. Reactor Setup	123
2.5. Summary	126
2.6. References.....	128
Chapter 3 Preparation of Tetrafluoroethylene from the Pyrolysis of Pentafluoropropionate Salts.....	134
3.1. Abstract	134
3.2. Introduction.....	135
3.3. Results and discussion	140
3.4. Conclusions.....	154

Table of Contents (Continued)

	Page
3.5. Experimental	155
3.6. Acknowledgements.....	165
3.7. References.....	166
Chapter 4 Preparation, Characterization, and Relative Reactivity Ratios of Monomers in Poly(VDF- <i>co</i> -TFE)	175
4.1. Introduction.....	175
4.2. Synthesis of VDF.....	176
4.3. Synthesis and Properties of PVDF.....	177
4.4. Synthesis, Uses, and Properties of Poly(VDF- <i>co</i> -TFE).....	178
4.5. Experimental Determination of Relative Reactivity Ratios.....	180
4.6. Results and Discussion	187
4.7. Conclusions.....	222
4.8. Experimental section.....	223
4.9. Sample Calculations.....	232
4.10. References.....	236
Chapter 5 Experimental Determination of Relative Reactivity Ratios of TFE, PSEPVE, PSVE, DEVE, and 8-CNVE in poly(TFE- <i>co</i> -PSEPVE), poly(TFE- <i>co</i> -PSVE), poly(TFE- <i>co</i> -DEVE), and poly(TFE- <i>co</i> -8CNVE)	249
5.1. Introduction.....	249
5.2. Synthesis of PSEPVE and PSVE.....	252

Table of Contents (Continued)

	Page
5.2. Synthesis of PSEPVE and PSVE.....	257
5.3. Synthesis of EVE and DEVE.....	260
5.4. Preparation of 8-CNVE.....	263
5.5. Results and Discussion	264
5.6. Experimental section.....	283
5.7. References.....	292
Appendix A Standard Operational Procedures.....	296
A.1. SOP Related to a Polymerization Reaction.....	297
A.2. SOP for Scrubbing Carbon Dioxide (CO ₂) from TFE/CO ₂ Mixture.	316
A.3. SOP for Leak Check in Vacuum Line in the Reaction Room for Transferring TFE from a Large Cylinder to High Pressure Cylinder Through Transfer Cylinder.....	325
A.4. SOP for Transferring TFE from a Large Cylinder to a Small Transfer Cylinder (500 cm ³ volume).....	326
A.5. SOP for Transferring TFE From a Transfer Cylinder to a High Pressure Cylinder (500 cm ³ volume).....	327
A.6. SOP for Transferring TFE at Hunter Barricade.	329
Appendix B List of Necessary Components Used in the Construction of the TFE Barricade.	335
B.1. Parts Used in the Control and Reaction Room.....	335
B.2. Parts Used in the Gas Handling System.....	336

Table of Contents (Continued)

	Page
B.3. Parts Used in the Valve Control Panel.	337
B.4. Parts Used in the Radical Initiator and Cooling Lines.	338
B.5. Parts Used in the BPR Array.....	339
B.6. Parr Instruments Inc. Reactor System.	344
Appendix C Data Acquisition Software Code Reference.....	347
C.1. Form1.vb Code and Form Details.	349
C.2. Intro.vb Code and Form Details.....	371
C.3. Complete Programming Code Reference.....	372
Appendix D Supplementary Information for Chapter 3.	415
Appendix E Supplementary Information for Chapter 4.....	505
E.1. Differential scanning calorimetry (DSC) Information.	505
E.2. Thermo Gravimetric Analysis (TGA) Information.	519
E.3. Powder X-ray Diffraction (XRD) analysis of samples of poly(VDF- <i>co</i> -TFE).	532
E.4. Characterization of poly(VDF- <i>co</i> -TFE) using fluorine-19 nuclear magnetic Resonance (¹⁹ F NMR) spectroscopy	539
Appendix F Supporting Information for Chapter 5.	549
F.1. ATR-FTIR results of commercial samples of poly(TFE- <i>co</i> -PSEPVE).....	549
F.2. Equivalent Weight Results Obtained from FTIR Sample Analysis.	556
F.3. Experimental Results from Polymerization Reactions of poly(TFE- <i>co</i> -PSEPVE)..	565

Table of Contents (Continued)

	Page
F.4. Experimental Results from Polymerization Reactions of poly(TFE- <i>co</i> -PSVE).....	567
F.5. Experimental Results from Polymerization Reactions of poly(TFE- <i>co</i> -DEVE).....	574
F.5. Fluorine-19 NMR Characterization of PSEPVE, PSVE, DEVE and 8-CNVE Monomers.	587

List of Tables

	Page
Table 1.1. Major commercial co- and terpolymers of tetrafluoroethylene. ^{4,5}	3
Table 1.2. Different compositions of the system poly(TFE-co-VAc) reported in the literature. ⁴¹	5
Table 1.3. Terpolymers prepared using TFE, VAc, and PDMSMA. ⁴²	6
Table 1.4. Ranges of compositions and their relation to the properties of poly(TFE-ter-VDF-ter-HFP). ⁸²	12
Table 1.5. Reported polymer compositions. ^{96,97}	17
Table 1.6. Composition of terpolymers poly(TFE-ter-E-ter-NFH) used in the study of crystal phase transition temperatures. ¹⁰⁷	19
Table 1.7. List of polymers made and their composition. Each row in the table denotes a different example in the patent. ¹⁴⁷	35
Table 1.8. Final compositions of co- and terpolymers reported. ^{148,149}	36
Table 1.9. Reactivity ratios for copolymers of TFE. ¹²	38
Table 2.1. Chronological order of development of TFE polymerization facilities.....	71
Table 1. Thermogravimetric data analysis (TGA) for CF ₃ CF ₂ C(O)O-M ⁺ (where M = Li ⁺ , Na ⁺ , K ⁺ , Cs ⁺ , Mg ²⁺ , Ca ²⁺ , or Ba ²⁺).	149

List of Tables (Continued)

	Page
Table 2. Mass percent of metal fluoride remaining at the end of each TGA – theoretical versus experimental.	150
Table 4.1. Other monomers that have been copolymerized with VDF.	175
Table 4.2. Reactivity ratios of VDF and TFE in poly(VDF- <i>co</i> -TFE).	180
Table 4.3. Summary of differential scanning calorimetry (DSC) data on samples of PVDF, poly(VDF- <i>co</i> -TFE), and PTFE.	189
Table 4.4. TGA results for the samples of poly(VDF- <i>co</i> -TFE) studied.	194
Table 4.5. TGA results for the samples of poly(VDF- <i>co</i> -TFE) by range of composition.	195
Table 4.6. Permutations of triads, pentads, and heptads present in poly(VDF- <i>co</i> -TFE).	203
Table 4.7. ¹⁹ F NMR spectroscopy assignments for the different VDF sequence distributions. ⁶³	206
Table 4.8. Reaction data: target compositions and final compositions of poly(VDF- <i>co</i> -TFE) in presence (light red) and absence (light blue) of CO ₂	211
Table 4.9. Parameters evaluated for obtaining reactivity ratios using the Fineman and Ross as well as the Kelen and Tüdös method in presence (light red) and absence (light blue) of CO ₂	211

List of Tables (Continued)

	Page
Table 4.10. Reactivity ratios of VDF and TFE in poly(VDF- <i>co</i> -TFE) in the presence and absence of CO ₂ at 83 °C.	215
Table 4.11. Reaction data: target compositions and final compositions of poly(VDF- <i>co</i> -TFE) in presence of CO ₂	233
Table 5.1. FTIR band assignments of poly(TFE- <i>co</i> -PSEPVE). ²⁰	267
Table 5.2. Results of analysis of commercial samples of Nafion [®] resin using the ATR-FTIR method.	269
Table 5.3. Experimental Reactivity Ratios for samples of poly(TFE- <i>co</i> -PSEPVE). Samples S1-S5 were prepared in absence of CO ₂ while samples S6-S10 were prepared in presence of CO ₂	273
Table 5.4. Experimental reactivity ratios of TFE and PSVE in poly(TFE- <i>co</i> -PSVE).....	278
Table 5.5. Experimental reactivity ratios of TFE and DEVE in poly(TFE- <i>co</i> -DEVE)...280	
Table 5.7. Monomer composition in the preparation of poly(TFE- <i>co</i> -PSEPVE).....	286
Table A.1. List of all the components located in the diagrams for the gas handling system and reaction room.	309
Table A.1 Continued. List of all the components located in the diagrams for the gas handling system and reaction room.	310

List of Tables (Continued)

	Page
Table B.1. List of components, manufacturers and prices used in the Control and Reaction Room.....	335
Table B.2. List of components, manufacturers and prices used in the gas handling system located in the reaction room.....	336
Table B.3. List of components, manufacturers and prices used in the air actuated valve panel located in the reaction room.	337
Table B.4. List of components, manufacturers and prices used in the radical initiator solution feed line system.....	338
Table B.5. List of components, manufacturers and prices used in the BPR Array.	339
Table C.1. Component names and function for Form 1 as shown in Figure C.3.	350
Table C.2. Component names and function for the “Port Configuration” tab as shown in Figure C.4.	354
Table C.3. Component names and function for the “Channel Names” tab as shown in Figure C.5.	356
Table C.4. Component names and function for the “Channel ON / OFF” tab as shown in Figure C.6.	357

List of Tables (Continued)

	Page
Table C.5. Component names and function for the “Calibration Parameters” tab, shown in Figure C.8.	360
Table C.6. Component names and function for the “Data Logging” tab as shown in Figure C.9.	362
Table C.7. Component names and function for the “Other Options” tab as shown in Figure C.10.	368
Table C.8. Component names and function for the “Processed Data” tab as shown in Figure C.11.	369
Table C.9. Properties for the component called “Timer1.”	371
Table D.1. Sample and crystal data for sodium pentafluoropropionate.	453
Table D.2. Data collection and structure refinement for sodium pentafluoropropionate.	454
Table D.3. Atomic coordinates and equivalent isotropic atomic displacement parameters (\AA^2) for sodium pentafluoropropionate. $U(\text{eq})$ is defined as one third of the trace of the orthogonalized U_{ij} tensor.	455
Table D.4. Bond lengths (\AA) for sodium pentafluoropropionate.	456

List of Tables (Continued)

	Page
Table D.5. Bond angles ($^{\circ}$) for sodium pentafluoropropionate.	457
Table D.6. Anisotropic atomic displacement parameters (\AA^2) for sodium pentafluoropropionate. The anisotropic atomic displacement factor exponent takes the form: $-2\pi^2[h^2a^{*2}U_{11} + \dots + 2hka^*b^*U_{12}]$	459
Table D.7. Sample and crystal data for potassium pentafluoropropionate.	461
Table D.8. Data collection and structure refinement for potassium pentafluoropropionate.	462
Table D.9. Atomic coordinates and equivalent isotropic atomic displacement parameters (\AA^2) for potassium pentafluoropropionate. $U(\text{eq})$ is defined as one third of the trace of the orthogonalized U_{ij} tensor.	463
Table D.10. Bond lengths (\AA) for potassium pentafluoropropionate.	469
Table D.11. Bond angles ($^{\circ}$) for potassium pentafluoropropionate.	474
Table D.12. Anisotropic atomic displacement parameters (\AA^2) for potassium pentafluoropropionate. The anisotropic atomic displacement factor exponent takes the form: $-2\pi^2[h^2a^{*2}U_{11} + \dots + 2hka^*b^*U_{12}]$	496
Table E.1. Summary of differential scanning calorimetry (DSC) data on samples of PVDF, poly(VDF- <i>co</i> -TFE), and PTFE.	506

List of Tables (Continued)

	Page
Table E.2. TGA results for the samples of poly(VDF- <i>co</i> -TFE) studied.....	519
Table E.3. Reaction data: target compositions and final compositions of poly(VDF- <i>co</i> -TFE) in presence (light red) and absence (light blue) of CO ₂	539
Table F.1. Ratios of absorbances used for the experimental determination of equivalent weight linear regressions (Method I, II, and III).....	555
Table F.2. Experimental determination of constants used for the equivalent weight calculation of samples of poly(TFE- <i>co</i> -PSEPVE) as detailed by the method published in the Chinese patent literature. Samples were prepared in absence of CO ₂	557
Table F.3. Experimental determination of constants used for the equivalent weight calculation of samples of poly(TFE- <i>co</i> -PSEPVE) as detailed by the method published in the Chinese patent literature. Samples were prepared in precense of CO ₂	558
Table F.4. Experimental results for acid base titration of commercial samples of poly(TFE- <i>co</i> -PSEPVE) originally obtained in the sulfonyl fluoride form from DuPont.....	560

List of Tables (Continued)

	Page
Table F.5. Composition analysis for the feed and final monomer composition on experimental samples of poly(TFE- <i>co</i> -PSEPVE). Samples S1-S5 were prepared in absence of CO ₂ , while samples S6-S10 were prepared in presence of CO ₂	565
Table F.6. Fineman and Ross, and Kelen and Tüdös parameters for the determination of reactivity ratios of the monomers in poly(TFE- <i>co</i> -PSEPVE). Samples S1-S5 were prepared in absence of CO ₂ , while samples S6-S10 were prepared in presence of CO ₂	566
Table F.7. Calculation of initial composition molar fractions of monomer feed for the preparation of samples of poly(TFE- <i>co</i> -DEVE).....	579
Table F.9. Fineman and Ross parameters used to calculate the relative reactivity ratios of DEVE and TFE in the samples of poly(TFE- <i>co</i> -DEVE) obtained experimentally.....	581

List of Figures

	Page
Figure 1.1. Polymerization scheme in supercritical CO ₂ for the system poly(TFE-ter-VAc-ter-PDMSMA). ⁴²	6
Figure 1.2. Polymerization and hydrolysis scheme of poly(TFE-co-VAc) to form poly(TFE-ter-VAc-ter-VA). ^{44,46}	7
Figure 1.3. Chemical structure of the monomer MDO used to prepare poly(TFE-co-MDO). ⁴⁷	8
Figure 1.4. Reaction scheme for the system poly(TFE-ter-P-ter-FA3). ⁹³	15
Figure 1.5. Reaction schemes for general polymerization products (top) versus preferred polymerization composition (bottom) manufactured for fuel barrier materials. ⁹⁴	16
Figure 1.6. Reaction scheme for poly(TFE- <i>ter</i> -E- <i>ter</i> -NFH) (top) and poly(TFE- <i>ter</i> -E- <i>ter</i> -HFP) (bottom). ¹⁰⁷	18
Figure 1.7. Reaction scheme for the preparation of poly(TFE- <i>co</i> -VPFCP). ^{120,121}	22
Figure 1.8. Reaction scheme for the preparation of poly(TFE- <i>quad</i> -NM- <i>quad</i> -PMVE- <i>quad</i> -DMAH). ¹³¹	26
Figure 1.9. Reaction scheme for the preparation of the general fluoropolymer poly(TFE- <i>co</i> -NOB), where NOB is a norbornene derivative. ¹⁴⁰	29

List of Figures (Continued)

	Page
Figure 1.10. Comonomers used in the etching rate study of TFE polymers for photolithography. ¹⁴²	30
Figure 1.11. Synthetic scheme to endo and exo-isomers of functionalized norbornene (top) and two methods for preparing TFE-based terpolymers (bottom). ¹⁴³	32
Figure 1.12. Reaction scheme for the synthesis of poly(TFE- <i>ter</i> -NB-F-OH- <i>ter</i> -TBA). ¹⁴⁴	32
Figure 1.13. Polymerization scheme for the TFE-norbornene-based materials. ^{145,146}	33
Figure 1.14. Monomers used in the preparation of co-, ter-, quad-, and pentapolymers of TFE. ¹⁴⁷	34
Figure 1.15. Monomers co- and terpolymerized with TFE. ^{148,149}	35
Figure 2.1. Schematic of a barricade setup with its rooms side by side. ²	64
Figure 2.2. Schematic of a reaction cell unit equipped with an earthen berm at the back of the unit. ³	65
Figure 2.3. Schematic for multi-cell barricade setup. Individual cells are numbered 1 through 6. ³	66
Figure 2.4. Containment vessel equipped with a vertical reactor and a polycarbonate viewing port. Reproduced from the literature. ²	69

List of Figures (Continued)

	Page
Figure 2.5. Containment Vessel for the use and handling of TNT. ⁶	70
Figure 2.6. Architectural drawing of TFE barricade at Hunter Laboratories.	76
Figure 2.7. Top: Schematic of TFE barricade and gas handling system located in Hunter Laboratories, Bottom: Diagram of the reactor setup. ²¹⁻²³	77
Figure 2.8. Architectural drawing of the TFE barricade at Shelby Hall in University of Alabama.	79
Figure 2.9. TFE gas handling system of the TFE barricade at Shelby Hall at The University of Alabama.	80
Figure 2.10. Distribution floor plan for the AMRL building section highlighted on the overall outline shown in the bottom right corner of the figure [Drawing provided by Clemson Facilities].	86
Figure 2.11. Architectural drawing of the back view of the reaction room (reproduced with permission from the manufacturer).....	87
Figure 2.12. Architectural drawing of the front view of the reaction room (reproduced with permission from the manufacturer).....	88
Figure 2.13. Architectural drawing of the top view of the reaction room (reproduced with permission from the manufacturer).....	89

List of Figures (Continued)

	Page
Figure 2.14. Architectural drawing of the control room. Left: Front of the control room, Right: diagram of the door and wall construction (reproduced with permission from the manufacturer).	90
Figure 2.15. Architectural drawing of the back view of the control room (reproduced with permission from the manufacturer).	91
Figure 2.16. TFE barricade located at CETL. Left: control room, Right: reaction room. .	93
Figure 2.17. Google Earth picture of AMRL and CETL.	94
Figure 2.18. Zoom of CETL and fenced area.	95
Figure 2.19. Schematic close up of the fenced area in which the barricade is located. The dimensions and overall shape of the parking lot were determined manually at the site. Dimensions are given in feet.	96
Figure 2.20. Architectural drawing of the first floor of CETL (supplied by Clemson facilities). The room marked with the star is the high bay area while the one marked with the square is the support room for installation of analytical equipment.	97
Figure 2.21. Electrical connection diagram. Panel LCM is located on the side of the control room while the Panel LCS is located in the side of the reaction room. The Panel MEL is located inside the support room (aforementioned) inside the CETL facility.	100

List of Figures (Continued)

	Page
Figure 2.22. Original diagram for tracing the power distribution lines from the CETL building to the barricade facility.	102
Figure 2.23. Picture of the cable tray between the reaction room (right) and the control room (left).....	103
Figure 2.24. Picture of the Model 1000-232 Alpha Omega oxygen sensor installed in the control room.....	104
Figure 2.25. Air Actuated valve (Reproduced with permission from Swagelok digital catalog ³⁴).	105
Figure 2.26. Sectional cut of a tube fitting used in the design of an orifice (Reproduced with permission from Swagelok digital catalog ³⁴).	107
Figure 2.27. Picture of a Teledyne Hastings Mass Flow Controller (Obtained Teledyne Hastings Online Catalog ³⁴).	108
Figure 2.28. Picture of a Teledyne ISCO pump Model 1000D (obtained with permission from Teledyne ISCO online catalog ³⁵).	109
Figure 2.29. Cooling coil diagram for the ISCO Pump used in the feed of radical initiator solution.....	109
Figure 2.30. Air-actuated valve control panel located in the control room.	112

List of Figures (Continued)

	Page
Figure 2.31. Schematic of the valve control panel. The three-way valves labeled A through K are located at the panel in the control room. The air actuators labeled AA 1 through AA 12 are located at the reaction room.	113
Figure 2.32. Schematic of the gas handling system at TFE barricade in Clemson University.	116
Figure 2.33. Schematic of the gas handling system at TFE barricade in Clemson University. View of the right side of the system (see Figure 2.34 for the counterpart of the figure).	117
Figure 2.34. Schematic of the gas handling system at TFE barricade in Clemson University. View of the left side of the system (see Figure 2.33 for the counterpart of the figure).	118
Figure 2.35. TFE scrubbing system.	119
Figure 2.36. BPR valve system connection diagram.	120
Figure 2.37. Deionized, deoxygenated water and glove bag system installed in lab 3 at the AMRL building. ³⁷	122
Figure 2.38. Dissolved oxygen sensor YSI ProODO meter (Picture taken from YSI online catalog ²⁵).	122

List of Figures (Continued)

	Page
Figure 2.39. Parr Reactor left side view. Reproduced with permission from Parr Industries (April 2016).	124
Figure 3.1. Reaction scheme for the preparation of TFE/CO ₂ from the pyrolysis of potassium perfluoropropionate.	135
Figure 3.2. Left: X-ray elemental analysis of left over solids after pyrolysis showing the presence of elemental carbon. Right: Electron microscopy image of left over solids after pyrolysis.....	145
Figure 3.3. OPRTEP representation of sodium pentafluoropropionate (50% probability ellipsoids).....	153
Figure 3.4. Ball-and-stick representations of sodium pentafluoropropionate around the sodium atom (left side) and potassium pentafluoropropionate around the potassium atom (right side), respectively. Gray = carbon atom, green = fluorine atom, red = oxygen atom, and blue = alkali metal cation.	154
Figure 3.5. Schematic of 2-Gal autoclave converted into a caustic scrubber. ¹³	162
Figure 4.1. Commercial and non-commercial routes for the manufacture of VDF. ^{21,22,24}	176
Figure 4.2. Three major polymorphs of PVDF. Top Left: alpha form, Top Right: beta form, Bottom: gamma form. ²³	178

List of Figures (Continued)

	Page
Figure 4.3. Possible radical propagation pathways for chain growth for the radical polymerization of VDF with TFE. ⁵⁵	181
Figure 4.4. Diagram of correlation in between a monomer in the feed mixture to the monomer in the final copolymer formed. A: $r_1 > 1$, $r_2 < 1$, B: $r_1 = r_2 = 1$, C: $r_1 = r_2 < 1$, D: $r_1 < 1$, $r_2 > 1$, E: r_1 and $r_2 < 1$, and $r_1 < r_2$, F: azeotropic point. ⁵⁵	186
Figure 4.5. Representative DSC thermogram for a sample of PVDF.....	191
Figure 4.6. Representative DSC thermogram for a sample of poly(VDF- <i>co</i> -TFE) of 80 and 20 mol% of VDF and TFE, respectively. Sample prepared using large block technique.	192
Figure 4.7. Representative DSC thermograph for a sample of poly(VDF- <i>co</i> -TFE) of 80 and 20 mol% of VDF and TFE, respectively. Sample prepared using short block technique.	193
Figure 4.8. Assembly of XRD data for samples of polymers. From top to bottom respectively: PTFE, poly(VDF- <i>co</i> -TFE) with 40 mol% TFE, 30 mol% TFE, 20 mol% TFE, 10 mol% TFE, and PVDF (in its α form).	197
Figure 4.9. Most probable triad diagrams (note that the two reverse representations of 002 and 022 are not displayed). ⁶³⁻⁶⁵	201

List of Figures (Continued)

	Page
Figure 4.10. Schematic of the different steps of a radical copolymerization of TFE with VDF. Termination steps are not shown.	204
Figure 4.11. Typical distribution of signals in the ^{19}F NMR spectrum of poly(VDF- <i>co</i> -TFE). From left to right: sections for signals from 020 (-90 to -96 ppm), 022 (-108 to -116 ppm) and 222 (-117 to -126 ppm) triads. ⁶³	205
Figure 4.12. ^{19}F NMR spectrum of poly(VDF- <i>co</i> -TFE) of 90-10 mol% composition of VDF and TFE, respectively, with integration (provided by our industrial sponsor).....	207
Figure 4.13. Monomer/polymer composition curve for poly(VDF- <i>co</i> -TFE) in presence (red line) and absence (blue line) of CO_2 . Dotted line is a diagonal for ease of visualization of the data.	213
Figure 4.14. Fineman and Ross plot of H and G for poly(VDF- <i>co</i> -TFE) in absence of CO_2	213
Figure 4.15. Fineman and Ross plot of the H and G parameters for poly(VDF- <i>co</i> -TFE) in presence of CO_2	214
Figure 4.16. Kelen and Tüdös plot of ξ and η for poly(VDF- <i>co</i> -TFE) in absence of CO_2	214

List of Figures (Continued)

	Page
Figure 4.17. Kelen and Tüdös plot of ξ and η for poly(VDF- <i>co</i> -TFE) in presence of CO ₂	215
Figure 4.19. Distilled/deoxygenated water setup for preparing polymerization solutions.	225
Figure 5.1. Structures and IUPAC names for TFE, PSEPVE, PSVE, DEVE and 8-CNVE.	250
Figure 5.2. General diagram of a hydrogen fuel cell.	253
Figure 5.3. Diagram of the Chlor-Alkali process.	255
Figure 5.4. Reaction diagrams for the major types of perfluorosulfonyl-terminated ionomer materials that are commercially available.....	256
Figure 5.5. Reaction scheme for the production of PSEPVE. ⁷	257
Figure 5.6. Original synthetic method for making PSVE monomer. ⁹	259
Figure 5.7. Secondary method of preparation of PSVE monomer. ¹⁰	259
Figure 5.8. Improved reaction scheme for the production of PSVE monomer. ⁸	259
Figure 5.9. Synthetic preparation of EVE monomer. ^{13,14}	261
Figure 5.10. Synthetic preparation of DEVE monomer. ¹⁵	262

List of Figures (Continued)

	Page
Figure 5.11. Synthetic preparation of 8-CNVE monomer. ¹⁷	264
Figure 5.12. Linear relationships between the ratios of absorbances and the equivalent weight of poly(TFE- <i>co</i> -PSEPVE). From left to right: Method I, Method III, and Method II.	271
Figure 5.13. Linear Regression of Fineman and Ross method for samples of poly(TFE- <i>co</i> -PSEPVE) prepared in absence of CO ₂	273
Figure 5.14. Linear Regression of Kelen and Tüdös method for samples of poly(TFE- <i>co</i> -PSEPVE) prepared in absence of CO ₂	274
Figure 5.15. Linear Regression of Fineman and Ross method for samples of poly(TFE- <i>co</i> -PSEPVE) prepared in presence of CO ₂	274
Figure 5.16. Linear Regression of Kelen and Tüdös method for samples of poly(TFE- <i>co</i> -PSEPVE) prepared in precense of CO ₂	275
Figure 5.17. Graphical representation of the comparison of the molar fraction of PSEPVE supplied in the monomer feed versus the molar fraction obtained in the copolymer.	275
Figure 5.18. Linear Regression of Finemand and Ross method for samples of poly(TFE- <i>co</i> -PSVE).	279

List of Figures (Continued)

	Page
Figure 5.19. Linear Regression of Finemad and Ross method for samples of poly(TFE- <i>co</i> -DEVE).....	281
Figure 5.20. Graphical representation of the comparison of the molar fraction of DEVE supplied in the monomer feed versus the molar fraction obtained in the copolymer.	282
Figure 5.21. Glassware used to prepare a 3P solution in HFC-4310.....	284
Figure A.1. Gas handling system schematic diagram. A larger format image is included in Appendix B.	311
Figure A.2. Schematic of valves at autoclave heads.....	312
Figure A.3. Schematic for ISCO pump system.....	313
Figure A.4. Connection layout for air actuated valves. The Valve colored in black is located in the reaction room while the ones colored in red are the ones located in the control room.	314
Figure A.5. Schematic of connections for the TFE transferring system at Hunter.....	334
Figure B.1. Diagram of the left side of the gas handling line.	340
Figure B.2. Diagram of the right side of the gas handling line.....	341
Figure B.3. Diagram of the valve panel.....	342

List of Figures (Continued)

	Page
Figure B.4. Diagram of the BPR array.	343
Figure B.5. Reactor side view (reproduced with permission from Parr Instruments Inc.).	344
Figure B.6. Reactor side view (reproduced with permission from Parr Instruments Inc.).	345
Figure B.7. Reactor vessel side view (reproduced with permission from Parr Instruments Inc.).	346
Figure C.1. Visual Studio solution explorer showing the components of the project.	348
Figure C.2. Form 1 active components. Arranged from left to right: StatusStrip containing a label called Status_Label, a timer, a open file dialog box and a folder browse dialog box.....	349
Figure C.3. Form1 main component layout.	351
Figure C.4. Layout of components inside the “Port Configuration” tab labeled as “A” .	354
Figure C.5. Layout of components inside the “Channel Names” tab labeled as “B”	356
Figure C.6. Layout of components inside the “Channel ON / OFF” tab labeled as “C” .	357
Figure C.7. Schematic of LM4040 reference circuit	359

List of Figures (Continued)

	Page
Figure C.8. Layout of components inside the “Calibration Parameters” tab labeled as “D”	361
Figure C.9. Layout of components inside the “Data Logging” tab labeled as “E”	362
Figure C.10. Layout of components inside the “Other Options” tab labeled as “F”	368
Figure C.11. Layout of components inside the “Processed Data” tab labeled as “E”	369
Figure C.12. Introduction form layout	371
Figure D.1. ^1H NMR spectrum of $\text{CF}_3\text{CF}_2\text{C}(\text{O})\text{OH}$ (CD_3CN): δ 10.94 (s) ppm	416
Figure D.2. ^{19}F NMR spectrum of $\text{CF}_3\text{CF}_2\text{C}(\text{O})\text{OH}$ (CD_3CN): δ CF_3 -84.42 (s), CF_2 -123.35 (s) ppm.	417
Figure D.3. ^{13}C NMR spectrum of $\text{CF}_3\text{CF}_2\text{C}(\text{O})\text{OH}$ (CD_3CN): δ $\text{C}(\text{O})$ 158.25 (t, $J_2 = 28.8$ Hz), CF_3 118.01 (qt, $J_1 = 285.2$ Hz, $J_2 = 33.9$ Hz), CF_2 105.90 (tq, $J_1 = 262.7$ Hz, $J_2 = 39.7$ Hz) ppm.	418
Figure D.4. ^1H NMR spectrum of $\text{CF}_3\text{CF}_2\text{C}(\text{O})\text{OCH}_2\text{CH}_3$ (CD_3CN): δ CH_2 4.44 (q, $J_2 = 7.2$ Hz), CH_3 1.34 (t, $J_2 = 7.2$ Hz) ppm	419
Figure D.5. ^{19}F NMR spectrum of $\text{CF}_3\text{CF}_2\text{C}(\text{O})\text{OCH}_2\text{CH}_3$ (CD_3CN): δ CF_3 -84.39 (s), CF_2 123.00 (s) ppm.	420

List of Figures (Continued)

	Page
Figure D.6. ^{13}C NMR spectrum of $\text{CF}_3\text{CF}_2\text{C}(\text{O})\text{OCH}_2\text{CH}_3$ (CD_3CN): δ -157.98 C(O) (t, $J_2 = 28.8$ Hz), 117.80 CF_3 (qt, $J_1 = 285.2$ Hz, $J_2 = 33.9$ Hz), 105.94 CF_2 (tq, $J_1 = 262.7$ Hz, $J_2 = 39.7$ Hz), 64.99 OCH_2 (s), CH_3 12.70 (s) ppm.....	421
Figure D.7. ^{19}F NMR spectrum of $\text{CF}_3\text{CF}_2\text{C}(\text{O})\text{OK}$ (D_2O): δ -83.23 CF_3 (s), CF_2 -120.96 (s) ppm.	422
Figure D.8. ^{13}C NMR spectrum of $\text{CF}_3\text{CF}_2\text{C}(\text{O})\text{OK}$ (D_2O): δ 163.45 C(O) (t, $J_2 = 24.5$ Hz), CF_3 118.66 (qt, $J_1 = 286.3$ Hz, $J_2 = 35.3$ Hz), CF_2 107.15 (tq, $J_1 = 262.7$ Hz, $J_2 = 38.3$ Hz) ppm.	423
Figure D.9. ^{19}F NMR spectrum of $\text{CF}_2=\text{CF}_2/\text{CO}_2$ (CD_3CN): δ -131.77 (s) ppm.	424
Figure D.10. ^{13}C NMR spectrum of $\text{CF}_2=\text{CF}_2/\text{CO}_2$ (gas): δ 143.67 $\text{CF}_2=\text{CF}_2$ (m), 126.69 CO_2 (s) ppm.	425
Figure D.11. FTIR spectra of TFE taken from a stream of gas from the pyrolysis of sodium pentafluoropropionate at 50 Torr (blue line) and 5 Torr (purple line), superimposed with a spectra of TFE (red line) that has been evacuated from all the non-condensable gases, and a spectra of a standard sample of CF_4 collected at 5 Torr (green line).	426
Figure D.12. LC-mass spectrum (ESI, negative ion mode) of potassium pentafluoropropionate.	427

List of Figures (Continued)

Page

Figure D.13. GC-MS spectrum (selective ion mode, SIM) of a sample of the most volatile gases from a pyrolysis of sodium pentafluoropropionate collected under static vacuum. The ions featured are $C_2F_4^+$ (100 m/z), $C_2F_3^+$ (81 m/z), CF_3^+ (69 m/z), $C_2F_2^+$ (62 m/z) and CF_2^+ (50 m/z). The sum of all the areas is labeled as “TIC”. The large bump on the leading edge of the signal is attributed to the CF_3^+ ion characteristic of CF_4 . Notice that the normalization factor for the peak at 69 m/z at 13.60 is about one-half of what it is in Figure S14, indicating that the presents of another species, other than TFE, is giving rise to a more intense peak for CF_3^+ . As shown in Figure S15, 69 m/z or CF_3^+ is the base peak in the mass spectrum of CF_4 .

.....428

Figure D.14. GC-MS spectrum (selective ion mode, SIM) of a sample of gas from a totally degassed collection cylinder of TFE/ CO_2 as the products of a pyrolysis of sodium pentafluoropropionate. The ions featured are $C_2F_4^+$ (100 m/z), $C_2F_3^+$ (81 m/z), CF_3^+ (69 m/z), $C_2F_2^+$ (62 m/z) and CF_2^+ (50 m/z). The sum of all the areas is labeled as “TIC”. Notice that the normalization factor for the peak at 69 m/z for CF_3^+ at 22.66 is now almost double what it is in Figure D.13.429

List of Figures (Continued)

	Page
Figure D.15. GC-MS spectrum of a standard sample of CF ₄ . The CF ₃ ⁺ signal at m/z 69 is the clearly the base peak. The GC-MS spectra shown in Figures S13-S15 were taken on a 30 m, Rxi-5HT column, which is not made for separating permanent gases; small variations in retention times are probably due to differences between manual injections.	430
Figure D.16. Accelerating rate calorimetry (ARC) thermogram of sodium pentafluoropropionate.	431
Figure D.17. Accelerating rate calorimetry (ARC) thermogram of potassium pentafluoropropionate.	432
Figure D.18. Accelerating rate calorimetry (ARC) thermogram of calcium pentafluoropropionate.	433
Figure D.19. TGA thermograms of monovalent pentafluoropropionates. Red line: lithium pentafluoropropionate; black line: sodium pentafluoropropionate; blue line: potassium pentafluoropropionate; and green line: cesium pentafluoropropionate. A metal fluoride is left at the end in each case (from top to bottom): cesium fluoride, potassium fluoride, sodium fluoride, and lithium fluoride.	434

List of Figures (Continued)

	Page
Figure D.20. TGA thermograms of the divalent pentafluoropropionates. Red line: magnesium pentafluoropropionate; blue line: barium pentafluoropropionate; and green line: calcium pentafluoropropionate. A metal fluoride is left at the end in each case (from top to bottom): barium fluoride, calcium fluoride, and magnesium fluoride.....	435
Figure D.21. Thermogravimetric analysis of lithium pentafluoropropionate.....	436
Figure D.22. Thermogravimetric analysis for lithium pentafluoropropionate with detailed information.....	437
Figure D.23. Thermogravimetric analysis of sodium pentafluoropropionate.....	438
Figure D.24. Thermogravimetric analysis for sodium pentafluoropropionate with detailed information.....	439
Figure D.25. Thermogravimetric analysis of potassium pentafluoropropionate.	440
Figure D.26. Thermogravimetric analysis for potassium pentafluoropropionate with detailed information.	441
Figure D.27. Thermogravimetric analysis of cesium pentafluoropropionate.	442
Figure D.28. Thermogravimetric analysis for cesium pentafluoropropionate with detailed information.....	443

List of Figures (Continued)

	Page
Figure D.29. Thermogravimetric analysis of magnesium pentafluoropropionate.	444
Figure D.30. Thermogravimetric analysis for magnesium pentafluoropropionate with detailed information.	445
Figure D.31. Thermogravimetric analysis of calcium pentafluoropropionate.	446
Figure D.32. Thermogravimetric analysis for calcium pentafluoropropionate with detailed information.	447
Figure D.33. Thermogravimetric analysis of barium pentafluoropropionate.	448
Figure D.34. Thermogravimetric analysis for barium pentafluoropropionate with with detailed information.	449
Figure D.35. Powder X-ray diffraction data for pentafluoropropionate salts. From top to bottom: magnesium, lithium, sodium, potassium, cesium, and calcium pentafluoropropionate.	450
Figure D.36. Calculated powder X-ray diffraction pattern for sodium pentafluoropropionate from the single crystal X-ray diffraction data using Mercury and the .cif file.	451

List of Figures (Continued)

	Page
Figure D.37. A comparison of the experimental powder X-ray diffraction pattern (blue) and calculated powder X-ray diffraction pattern (from single crystal data) for potassium pentafluoropropionate.....	452
Figure D.38. Unit cell representation of sodium pentafluoropropionate.	460
Figure D.39. Unit cell representation of potassium pentafluoropropionate.....	503
Figure D.40. Plot of pressure versus time from a procedure for scrubbing CO ₂ from TFE. The blue line represents the pressure of a manifold to which two TFE/CO ₂ source cylinders are connected, but where only one is used as a feed cylinder at a time. The gray line represents the pressure downstream of a regulator (kept constant at 50 psig) connected to the manifold with the TFE source cylinders, and the orange line represents the pressure of the TFE collection cylinder after the CO ₂ has been scrubbed and the TFE has passed through a D-limonene bubbler.....	504
Figure E.1. Representative DSC thermogram for a sample of poly(VDF). Sample was prepared in absence of CO ₂	507
Figure E.2. Representative DSC thermogram for a sample A of poly(VDF- <i>co</i> -TFE) containing 90 mol% VDF and 10 mol% TFE. Sample was prepared in absence of CO ₂	508

List of Figures (Continued)

	Page
Figure E.3. Representative DSC thermogram for a sample B of poly(VDF- <i>co</i> -TFE) containing 80 mol% VDF and 20 mol% TFE. Sample was prepared using short block copolymerization techniques. Sample was prepared in absence of CO ₂	509
Figure E.4. Representative DSC thermogram for a sample B of poly(VDF- <i>co</i> -TFE) containing 80 mol% VDF and 20 mol% TFE. Sample was prepared using large block copolymerization techniques. Sample was prepared in absence of CO ₂	510
Figure E.5. Representative DSC thermogram for a sample of poly(VDF- <i>co</i> -TFE) containing 80 mol% VDF and 20 mol% TFE. Sample was dried from a high conversion polymerization.....	511
Figure E.6. Representative DSC thermogram for a sample C of poly(VDF- <i>co</i> -TFE) containing 70 mol% VDF and 30 mol% TFE. Sample was prepared in absence of CO ₂	512
Figure E.7. Representative DSC thermogram for a sample D of poly(VDF- <i>co</i> -TFE) containing 60 mol% VDF and 40 mol% TFE. Sample was prepared in absence of CO ₂	513
Figure E.8. Representative DSC thermogram for a sample of PTFE.	514

List of Figures (Continued)

	Page
Figure E.9. Representative DSC thermogram for a sample E of poly(VDF- <i>co</i> -TFE) containing 90 mol% VDF and 10 mol% TFE. Sample was prepared in presence of CO ₂	515
Figure E.10. Representative DSC thermogram for a sample F of poly(VDF- <i>co</i> -TFE) containing 80 mol% VDF and 20 mol% TFE. Sample was prepared in presence of CO ₂	516
Figure E.11. Representative DSC thermogram for a sample G of poly(VDF- <i>co</i> -TFE) containing 70 mol% VDF and 30 mol% TFE. Sample was prepared in presence of CO ₂	517
Figure E.12. Representative DSC thermogram for a sample H of poly(VDF- <i>co</i> -TFE) containing 60 mol% VDF and 40 mol% TFE. Sample was prepared in presence of CO ₂	518
Figure E.13. Representative TGA thermogram for a sample of PVDF.....	520
Figure E.14. Representative TGA thermogram for a sample A of poly(VDF- <i>co</i> -TFE) of 90 and 10 mol% of TFE and VDF respectively. Sample was prepared in absence of CO ₂	521

List of Figures (Continued)

	Page
Figure E.15. Representative TGA thermogram for a sample of poly(VDF- <i>co</i> -TFE) of 80 and 20 mol% of TFE and VDF respectively. Sample was prepared in absence of CO ₂ and short block techniques.....	522
Figure E.16. Representative TGA thermogram for a sample of poly(VDF- <i>co</i> -TFE) of 80 and 20 mol% of TFE and VDF respectively. Sample was prepared in absence of CO ₂ and large block techniques.....	523
Figure E.17. Representative TGA thermogram for a sample of poly(VDF- <i>co</i> -TFE) of 70 and 30 mol% of TFE and VDF respectively. Sample was prepared in absence of CO ₂	524
Figure E.18. Representative TGA thermogram for a sample of poly(VDF- <i>co</i> -TFE) of 60 and 40 mol% of TFE and VDF respectively. Sample was prepared in absence of CO ₂	525
Figure E.19. Representative TGA thermogram for a sample of PTFE.....	526
Figure E.20. Representative TGA thermogram for a sample of poly(VDF- <i>co</i> -TFE) of 90 and 10 mol% of TFE and VDF respectively. Sample was prepared in presence of CO ₂	527

List of Figures (Continued)

	Page
Figure E.21. Representative TGA thermogram for a sample of poly(VDF- <i>co</i> -TFE) of 80 and 20 mol% of TFE and VDF respectively. Sample was prepared in presence of CO ₂	528
Figure E.22. Representative TGA thermogram for a sample of poly(VDF- <i>co</i> -TFE) of 70 and 30 mol% of TFE and VDF respectively. Sample was prepared in presence of CO ₂	529
Figure E.23. Representative TGA thermogram for a sample of poly(VDF- <i>co</i> -TFE) of 60 and 40 mol% of TFE and VDF respectively. Sample was prepared in presence of CO ₂	530
Figure E.24. Relation of 10% mass loss temperature determined by TGA and TFE content in poly(VDF- <i>co</i> -TFE) in absence (blue line) and presence (orange line) of CO ₂	531
Figure E.25. Powder X-ray diffraction patterns of a sample of PTFE. The analysis was performed on a sample of PTFE deposited on a silicon wafer. This data is only used for comparison and reference.....	532
Figure E.26. Powder X-ray diffraction patterns of a sample of PVDF.....	533
Figure E.27. Powder X-ray diffraction patterns of a sample of poly(VDF- <i>co</i> -TFE) of composition 90-10 mol% of VDF and TFE, respectively.	534

List of Figures (Continued)

	Page
Figure E.28. Powder X-ray diffraction patterns of a sample of poly(VDF- <i>co</i> -TFE) of composition 80-20 mol% of VDF and TFE, respectively. Note: the sharp peaks at 38.5 and 44.7 deg are characteristic of the aluminum pan.....	535
Figure E.29. Powder X-ray diffraction patterns of a sample of poly(VDF- <i>co</i> -TFE) of composition 70-30 mol% of VDF and TFE, respectively.	536
Figure E.30. Powder X-ray diffraction patterns of a sample of poly(VDF- <i>co</i> -TFE) of composition 60-40 mol% of VDF and TFE, respectively.	537
Figure E.31. Assembly of powder X-ray diffraction patterns of polymer samples. From top to bottom respectively: PTFE, poly(VDF- <i>co</i> -TFE) with 40 mol% TFE, 30 mol% TFE, 20 mol% TFE, 10 mol% TFE, and PVDF.	538
Figure E.32. ¹⁹ F NMR spectra for a sample of PVDF. The sample was prepared in absence of CO ₂	540
Figure E.33. ¹⁹ F NMR spectra for a sample of poly(VDF- <i>co</i> -TFE) containing 91 mol% VDF and 9 mol% TFE. Sample prepared in absence of CO ₂	541
Figure E.34. ¹⁹ F NMR spectra for a sample of poly(VDF- <i>co</i> -TFE) containing 85 mol% VDF and 15 mol% TFE. Sample prepared in absence of CO ₂	542
Figure E.35. ¹⁹ F NMR spectra for a sample of poly(VDF- <i>co</i> -TFE) containing 82 mol% VDF and 18 mol% TFE. Sample prepared in absence of CO ₂	543

List of Figures (Continued)

	Page
Figure E.36. ^{19}F NMR spectra for a sample of poly(VDF- <i>co</i> -TFE) containing 74 mol% VDF and 26 mol% TFE. Sample prepared in absence of CO_2	544
Figure E.37. ^{19}F NMR spectra for a sample of poly(VDF- <i>co</i> -TFE) containing 92 mol% VDF and 8 mol% TFE. Sample prepared in presence of CO_2	545
Figure E.38. ^{19}F NMR spectra for a sample of poly(VDF- <i>co</i> -TFE) containing 81 mol% VDF and 19 mol% TFE. Sample prepared in presence of CO_2	546
Figure E.39. ^{19}F NMR spectra for a sample of poly(VDF- <i>co</i> -TFE) containing 67 mol% VDF and 33 mol% TFE. Sample prepared in presence of CO_2	547
Figure E.40. ^{19}F NMR spectra for a sample of poly(VDF- <i>co</i> -TFE) containing 64 mol% VDF and 36 mol% TFE. Sample prepared in presence of CO_2	548
Figure F.1. Example spectra for a commercial sample of Nafion [®] 920-SR also denominated as poly(TFE- <i>co</i> -PSEPVE) in the sulfonyl fluoride form.	549
Figure F.2. Example spectra for a commercial sample of Nafion [®] 1000-SR also denominated as poly(TFE- <i>co</i> -PSEPVE) in the sulfonyl fluoride form.	550
Figure F.3. Example spectra for a commercial sample of Nafion [®] 1200-SR also denominated as poly(TFE- <i>co</i> -PSEPVE) in the sulfonyl fluoride form.	551

List of Figures (Continued)

	Page
Figure F.4. Normalized infrared spectra for samples of poly(TFE- <i>co</i> -PSEPVE) featuring the ratios of absorbances used for Method I. A is the spectra for Nafion [®] 1200-SR, B is 1000-SR, and C is 920-SR.....	552
Figure F.5. Normalized infrared spectra for samples of poly(TFE- <i>co</i> -PSEPVE) featuring the ratios of absorbances used for Method II. A is the spectra for Nafion [®] 1200-SR, B is 1000-SR, and C is 920-SR.....	553
Figure F.6. Normalized infrared spectra for samples of poly(TFE- <i>co</i> -PSEPVE) featuring the ratios of absorbances used for Method III. A is the spectra for Nafion [®] 1200-SR, B is 1000-SR, and C is 920-SR.....	554
Figure F.7. Example ATR-FTIR spectra of poly(TFE- <i>co</i> -PSEPVE) of Equivalent Weight of 1116 g/mol.....	559
Figure F.8. Overlay of infrared spectra of poly(TFE- <i>co</i> -PSEPVE) samples used to create the calibration curves. Purple: 927 g/mol, Green: 1019 g/mol, and Red: 1181 g/mol.	561
Figure F.9. Linear correlation in between absorbance ratios and Equivalent weights for samples of poly(TFE- <i>co</i> -PSEPVE). This curve is also denominated Method I.	562
Figure F.10. Linear correlation in between absorbance ratios and Equivalent weights for samples of poly(TFE- <i>co</i> -PSEPVE). This curve is also denominated Method II.	563

List of Figures (Continued)

	Page
Figure F.11. Linear correlation in between absorbance ratios and Equivalent weights for samples of poly(TFE- <i>co</i> -PSEPVE). This curve is also denominated Method III.....	564
Figure F.12. Infrared spectra of experimental samples of poly(TFE- <i>co</i> -PSVE) normalized to the S-F stretch frequency for comparison. In increasing order of EW the samples are 1340, 1420, 1438, and 1509 g/mol.....	567
Figure F.13. TGA analysis comparison of the experimental samples of poly(TFE- <i>co</i> -PSVE) compared to a standard sample of the same polymer of EW of 700 g/mol. EW of samples is as follows: sample 1 is 1340, sample 2 is 1420, sample 3 is 1438, sample 4 is 1509, and sample 5 is 700 g/mol.	568
Figure F.14. TGA results for a sample of poly(TFE- <i>co</i> -PSVE) of EW of 1340 g/mol...	569
Figure F.15. TGA results for a sample of poly(TFE- <i>co</i> -PSVE) of EW of 1420 g/mol...	570
Figure F.16. TGA results for a sample of poly(TFE- <i>co</i> -PSVE) of EW of 1428 g/mol...	571
Figure F.17. TGA results for a sample of poly(TFE- <i>co</i> -PSVE) of EW of 1509 g/mol...	572
Figure F.18. TGA results for a standard sample of poly(TFE- <i>co</i> -PSVE) of EW of 700 g/mol.	573

List of Figures (Continued)

	Page
Figure F.19. Fluorine-19 melt NMR spectra of a poly(TFE- <i>co</i> -DEVE) sample of a composition of 4.3 mol% of DEVE and 95.7 mol% of TFE.	574
Figure F.20. Fluorine-19 melt NMR spectra of a poly(TFE- <i>co</i> -DEVE) sample of a composition of 6.7 mol% of DEVE and 93.3 mol% of TFE.	575
Figure F.21. Fluorine-19 melt NMR spectra of a poly(TFE- <i>co</i> -DEVE) sample of a composition of 8.9 mol% of DEVE and 91.1 mol% of TFE.	576
Figure F.22. Fluorine-19 melt NMR spectra of a poly(TFE- <i>co</i> -DEVE) sample of a composition of 14.2 mol% of DEVE and 85.8 mol% of TFE.	577
Figure F.23. Fluorine-19 melt NMR spectra of a poly(TFE- <i>co</i> -DEVE) sample of a composition of 14.7 mol% of DEVE and 85.3 mol% of TFE.	578
Figure F.24. DSC thermogram of a sample name “A” of poly(TFE- <i>co</i> -DEVE).	582
Figure F.25. DSC thermogram of a sample name “B” of poly(TFE- <i>co</i> -DEVE).	583
Figure F.26. DSC thermogram of a sample name “C” of poly(TFE- <i>co</i> -DEVE).	584
Figure F.27. DSC thermogram of a sample name “D” of poly(TFE- <i>co</i> -DEVE).	585
Figure F.28. DSC thermogram of a sample name “E” of poly(TFE- <i>co</i> -DEVE).	586
Figure F.29. Fluorine-19 NMR spectra (1 of 3 views) of PSEPVE recorded neat.	588

List of Figures (Continued)

	Page
Figure F.30. Fluorine-19 NMR spectra (2 of 3 views) of PSEPVE recorded neat.	589
Figure F.31. Fluorine-19 NMR spectra (3 of 3 views) of PSEPVE recorded neat.	590
Figure F.32. Fluorine-19 NMR spectra (1 of 4 views) of PSVE recorded neat.	592
Figure F.33. Fluorine-19 NMR spectra (2 of 4 views) of PSVE recorded neat.	593
Figure F.34. Fluorine-19 NMR spectra (3 of 4 views) of PSVE recorded neat.	594
Figure F.35. Fluorine-19 NMR spectra (3 of 4 views) of PSVE recorded neat.	595
Figure F.36. Fluorine-19 NMR spectra (1 of 3 views) of DEVE recorded in CD ₃ CN....	597
Figure F.37. Fluorine-19 NMR spectra (2 of 3 views) of DEVE recorded in CD ₃ CN....	598
Figure F.38. Fluorine-19 NMR spectra (3 of 3 views) of DEVE recorded in CD ₃ CN....	599
Figure F.39. Fluorine-19 NMR spectra (1 of 4 views) of 8-CNVE recorded neat.	601
Figure F.40. Fluorine-19 NMR spectra (2 of 4 views) of 8-CNVE recorded neat.	602
Figure F.41. Fluorine-19 NMR spectra (3 of 4 views) of 8-CNVE recorded neat.	603
Figure F.42. Fluorine-19 NMR spectra (4 of 4 views) of 8-CNVE recorded neat.	604

List of Abbreviations and Symbols

μA	micro amperes
2DDO	2-difluoromethylene-1,3-dioxolane
3M	monomer perfluoro-4-(fluorosulfonyl) butyl vinyl ether, ($\text{CF}_2=\text{CFOCF}_2\text{CF}_2\text{CF}_2\text{CF}_2\text{SO}_2\text{F}$)
3P	bis(pentafluoropropionyl) peroxide, ($\text{CF}_3\text{CF}_2\text{C}(\text{O})\text{OOC}(\text{O})\text{CF}_2\text{CF}_3$)
8-CNVE	perfluoro 8-cyano-5-methyl-3,6-dioxo-1-octene, ($\text{CF}_2=\text{CFOCF}(\text{CF}_3)\text{CF}_2\text{OCF}_2\text{CF}_2\text{CN}$)
AA	acrylic acid or air actuator.
AIBN	2,2'-azobis(isobutyronitrile)
AMRL	advanced materials research laboratory
ARC [®]	accelerating rate calorimeter
AREF	analog reference voltage value
Ascarite [®]	sodium hydroxide adsorbed in silica
ASTM	american society for testing and materials
ATR	attenuated total reflectance
ATR-FTIR	attenuated total reflectance Fourier transform infrared spectroscopy
b.p.	boiling point
B2CEVP	bis(2-chloroethyl) vinylphosphonate
BPR	back pressure regulator
BTFE	bromotrifluoroethylene
BTU	british thermal unit
CETL	Clemson engineering technologies laboratory
CF_4	tetrafluoromethane

COC	cyclooctene
COF ₂	carbonyldifluoride
CP	cyclopentene
CPBA	2-cyclopentene-1- <i>tert</i> -butyl acetate
CTFE	chlorotrifluoroethylene
d ₆ -DMSO	deuterated dimethyl sulfoxide
DAQ	data Acquisition System
DCP	dicyclopentene
DCPD	dicyclohexyl peroxydicarbonate
DDO	2,2-bis(trifluoromethyl)-4,5-difluoro-1,3-dioxole
DEVE	methyl perfluoro-(3-oxa-4-hexenoate)
DHF	2,3-dihydrofuran
DMAH	difluoromaleic anhydride
DMCP	3,3-dimethylcyclopropene
DMSO	dimethyl sulfoxide
DOE	design of experiments
DOT	department of transportation
DPG	digital pressure gauge
DSC	differential scanning calorimetry
DTBP	di- <i>t</i> -butyl peroxide
DuPont	E.I. du Pont de Nemours and Company
E	ethylene
E-beam	electron beam
E-K-T	extended Kelen and Tüdös

EVE	methyl perfluoro-(5-methyl-4,7-dioxa-8-nonenoate)
EW	equivalent weight, grams of polymer needed to have 1 mole of acid sites. Equivalent weights are expressed herein g/mol.
FA1	2,3,3-trifluoroallyl alcohol, $\text{CF}_2=\text{CFCH}_2\text{OH}$
FA3	4,5,5-trifluoro-4-penten-1-ol, $\text{CF}_2=\text{CF}(\text{CH}_2)_3\text{OH}$
FA _c	4,5,5-trifluoro-4-penten-1-acetate
FCP	$\text{HOC}(\text{CF}_3)_2$ -functionalized cyclopentene
F-R	Fineman and Ross
FSDFAF	1-fluorosulfony-difluoroacetyl fluoride
FTIR	Fourier transform infrared spectroscopy
g	grams
HCFC-141b	1,1-dichloro-1-fluoroethane
HCFC-142B	1-chloro-1,1-difluoroethane
HD	high definition
HFC	hydrofluorocarbon
HFC-152a	1,1-difluoroethane
HFC-4310	2,3-dihydrodecafluoropentane, $\text{CF}_3\text{CFHCFHCF}_2\text{CF}_3$
HFO-1234-yf	2,3,3,3-tetrafluoropropane
HFP	hexafluoropropylene, $\text{CF}_2=\text{CF}(\text{CF}_3)$
IB	isobutylene
IPP	diisopropyl peroxydicarbonate
IR	infrared
ITA	itaconic acid
K	Kelvin
<i>k</i>	reaction rate constant

K-T	Kelen and Tüdös
L	liters
lbs	pounds
LED	light emitting diode
LWR	line width roughness
M	molarity
M ₁	monomer 1
M ₂	monomer 2
mA	mili amperes
MCU	microcontroller unit
MDO	2-methylene-1,3-dioxepene
MEK	methyl ethyl ketone
MFC	mass flow controller
mil	miliinch
MMA	methyl methacrylate, $\text{CH}_2=\text{C}(\text{CH}_3)\text{CO}_2\text{CH}_3$
MON	monomer
MS	mass spectrometry
MTFP	methyl 2,3,3-trifluoropropenoate, $\text{CF}_2=\text{CFC}(\text{O})\text{OCH}_3$
MTFP	methyl 2,3,3-trifluoropropenoate, $\text{CF}_2=\text{FCO}_2\text{CH}_3$
N117	Nafion [®] membrane with equivalent weight of 1100 and thickness of 7 miliinches
NBVE	<i>n</i> -butyl vinyl ether, $\text{CH}_2=\text{CHOCH}_2\text{CH}_2\text{CH}_2\text{CH}_2$
NFH	nonafluoro-1-hexene
NIST	national institute of standards and technology
NM	trifluoronitrosomethane, CF_3NO

NMR	nuclear magnetic resonance
°C	degree Celsius
P	propylene
PA	pentenoic acid
PDMSMA	poly(dimethylsiloxane)methylacrylate-terminated
PET	poly(ethylene terephthalate)
PFCB	octafluorocyclobutane
PFCP	perfluorocyclopropene
PFIB	perfluoro- <i>iso</i> -butylene, [(CF ₃) ₂ C=CF ₂]
PFSVE	perfluoro(3,6-dioxa-4-methyl-7-octene)sulfonyl fluoride
PID	proportional integral and derivative control algorithm
PMD	perfluoro-4-methyl-1,3-dioxole
PMVE	perfluoromethyl vinyl ether
ppm	parts per million
PPOTESF	2-(1-pentafluoro-2-propenyloxy)-tetrafluoroethanesulfonyl fluoride, CF ₂ =CFCF ₂ OCF ₂ CF ₂ SO ₂ F
PPS	Potassium persulfate
PPVE	perfluoropropyl vinyl ether
PSEPVE	perfluoro-2-(2-fluorosulfonylethoxy) propyl vinyl ether
Psf	pounds per square foot
psia	pounds per square inch absolute
psig	pounds per square inch gauge
PSVE	perfluoro(3-oxa-4-pentene)sulfonyl fluoride
PT	pressure transducer
PTFE	poly(tetrafluoroethylene), (-CF ₂ -CF ₂) _n

PVDF	polyvinylidene difluoride, $(-\text{CF}_2-\text{CH}_2-)_n$
R113	1,1,2-trichloro-1,2,2-trifluoroethane, $\text{CCl}_2\text{FCF}_2\text{C}$
R-140a	1,1,1-tri-chloroethane
rpm	rotations per minute, revolutions per minute
SFVE	perfluoro(3-oxa-4-pentene)sulfonyl fluoride
SL	standard liters
SLM	standard liters per minute
SOP	standard operational procedures
TCP	bis(4- <i>tert</i> -butylcyclohexyl)peroxydicarbonate
T_d	decomposition temperature (5 percent weight loss)
TFBA	<i>tert</i> -butyl- α -fluoroacrylate
TFE	tetrafluoroethylene, $(\text{CF}_2=\text{CF}_2)$
T_g	glass transition temperature
TGA	thermal gravimetric analysis
THV TM	terpolymers of VDF, HFP, and TFE
T_m	melting temperature
TNT	2,4,6-trinitrotoluene
TrFE	trifluoroethylene, $\text{CF}_2=\text{CHF}$
UA	undecylenic acid
UFC	uniform fire code
V2CB	vinyl-2-chloro benzoate
VA	vinyl alcohol
VAc	vinyl acetate
VB	vinyl benzoate

VDF	vinylidene difluoride, $\text{CH}_2=\text{CF}_2$,
VF	vinyl fluoride
VPFCP	vinyl pentafluorocyclopropane
WAXD	wide-angle X-ray diffraction spectroscopy
δ	chemical shift in parts per million

Disclaimer

The author make no warranties, expressed or implied, and assume no liability in connection with any use of the information presented in this dissertation. No one but persons having technical skill in this area of fluorine chemistry should attempt or repeat anything presented herein, and then at their own discretion and risk.

Chapter 1

Minor Research and Noncommercial Co- and Terpolymers of Tetrafluoroethylene

1.1. Introduction

Fluoropolymers have become more and more popular during the last 50 years due to their chemical and thermal resistance and other valued-added properties. Since the discovery of poly(tetrafluoroethylene) (PTFE) by Roy J. Plunkett at DuPont in 1938,^{1,2} not only DuPont, but also other companies have synthesized a number of different compositions in which tetrafluoroethylene (TFE) is a major monomer.

Co- and terpolymers of tetrafluoroethylene (TFE) are ubiquitous in terms of commercial fluoropolymers, and the preparations, properties, and applications of these outstanding materials have been well documented in monographs, book chapters, review articles, as well as in the patent and scientific journal literature. The purpose of this chapter is not to cover these major commercial materials, but rather to overview what is known in the patent and scientific journal literature about research-level TFE-based fluoropolymers and perhaps those TFE-based fluoropolymers that are available only at a minor commercial level.

This chapter will cover co- and terpolymers of TFE with ethylenic and cyclic monomers (non-fluorinated, partially fluorinated, and perfluorinated), with the co- and

terpolymer of TFE and cyclic monomers being an area that became especially important in the 2000s as fluoropolymer chemistry attempted to aid the continuance of Moore's Law with improved materials for photoresists, etc.

Overall, the goal of the chapter is to review the different properties of TFE-based polymers that though have not been highly commercialized, have helped route research in the right direction to obtain samples of commercial value. Since our research group represents one of the few academic laboratories that can safely work with TFE on a kilogram scale,³ it behooves us to be aware of the scientific literature in this field, and it was an instructive exercise for the coauthors to undertake this literature review. A list of the co- and terpolymers of TFE that are excluded from this Chapter is included in Table 1.1. The rationale for these exclusions is based on the fact that a vast number of monographs,⁴⁻¹⁷ book chapters or reviews,¹⁸⁻³³ and journal articles already exist that sufficiently describe the details of such products, and thus they are beyond the scope of this review. Co- and terpolymers of TFE with alkyl vinyl ethers are also excluded from this Chapter since it is the area of research of another member of the research group. Grafted co- and terpolymers of PTFE will also not be covered as well as co- or terpolymers resulting from telomerization or telechelic reactions of TFE with iodoperfluoroalkanes or α,ω -diiodoperfluoroalkanes or polymers resulting from the further elaboration of α,ω diiodoperfluoroalkanes that yield $-(CF_2)_n-$ segments within backbone of the respective polymer. The topic telomerization or telechelic reactions was reviewed by Ameduri and Boutevin in 1997,²⁷ and they and their co-workers have continued to be productive in this

and the latter area.³⁴⁻³⁹ Furthermore, a detailed discussion of recent advances in the area of TFE-based sulfonimide ionomers will also not be included here, as that topic was recently cover in part in another recent review chapter,⁴⁰ and we are planning another review chapter on additional aspects of this subject.

Table 1.1. Major commercial co- and terpolymers of tetrafluoroethylene.^{4,5}

Trademark Name	Family Name	Composition	Manufacturer
Tecnoflon®-BR	Fluoroelastomer	poly(TFE- <i>ter</i> -VDF- <i>ter</i> -P) or poly(TFE- <i>penta</i> -HPF- <i>penta</i> -VDF- <i>penta</i> -E- <i>penta</i> -PMVE)	Solvay Specialty Polymers
Nafion®, Aquivion® PFSA	Perfluorosulfonic acid resin	poly(TFE- <i>co</i> - PFSVE)	Chemours
		poly(TFE- <i>co</i> -SFVE)	Solvay Specialty Polymers
Aflas® 100	Fluoroelastomer	poly(TFE- <i>co</i> -P)	Asahi Glass Co.
Dyneon™ ETFE	Fluorothermoplastic	poly(TFE- <i>co</i> -E)	3M-Dyneon
Tefzel™	Fluoroplastic resin		Chemours
Teflon™ FEP* Neoflon FEP** Dyneon FEP***	Fluorothermoplastic	poly(TFE- <i>co</i> -HFP)	Chemours* Daikin** 3M-Dyneon***
Teflon™ FFR	Fluoroplastic foam resin	Poly(TFE- <i>co</i> -HFP)	Chemours
Aflas® 200	Fluoroelastomer	poly(TFE- <i>ter</i> -VDF- <i>ter</i> -P)	Asahi Glass Co.
Dyneon™ THV™ Dyneon™ HTE Hostaflon TFB	Fluorothermoplastic	poly(TFE- <i>ter</i> -VDF- <i>ter</i> -HFP)	3M-Dyneon
		poly(TFE- <i>ter</i> -HFP- <i>ter</i> -E)	3M-Dyneon
		Poly(TFE- <i>ter</i> -HFP- <i>ter</i> -VDF)	Hoechst
Tecnoflon®-P Tecnoflon®-V Viton B®, Dai-el®***	Fluoroelastomer	poly(TFE- <i>ter</i> -VDF- <i>ter</i> -HFP)	Solvay Specialty Polymers
		poly(TFE- <i>ter</i> -VDF- <i>ter</i> -HFP)	*Chemours, **Daikin
Hyflon® AD Teflon™ AF	Amorphous fluoropolymer	poly(TFE- <i>co</i> -PMD)	Solvay Specialty Polymers
		poly(TFE- <i>co</i> -DDO)	Chemours

Where PFSVE is perfluoro(3,6-dioxa-4-methyl-7-octene)sulfonyl fluoride, SFVE is perfluoro(3-oxa-4-pentene)sulfonyl fluoride, PMD is perfluoro-4-methyl-1,3-dioxole, and DDO is 2,2-bis(trifluoromethyl)-4,5-difluoro-1,3-dioxole.

This Chapter is subdivided into two main sections based on the structure of the primary comonomer being used with TFE and further divided based on either the degree of fluorination or the functionality that the respective comonomers being discussed contain. The two major families of TFE-based co- and terpolymers (as mentioned above) include alkenes and cyclic monomers and photoresist. Sections 1.2, 1.3, and 1.4 include co- and terpolymers of tetrafluoroethylene with alkenes, polyfluoroalkenes, and perfluoroalkenes, respectively. Finally, Section 1.5 contains co- and terpolymers of tetrafluoroethylene with cyclic monomers and tetrafluoroethylene-based photoresist materials.

1.2. Co- and Terpolymers of Tetrafluoroethylene and Non Fluorine-Containing Alkenes

Copolymers of TFE and vinyl acetate (VAc) were prepared by M. Schoichet et al. in supercritical CO₂ in the early 2000s.⁴¹ As shown in Table 1.2, the quantity of TFE in these copolymers ranged from 15 to 66 mol %. A study of water contact angles for the system poly(TFE-*co*-VAc) versus increasing incorporation of TFE revealed that the advancing contact angle remained between 86 and 90° as the receding contact angle increased from 45 to 66°. These data can be compared to the advancing and receding contact angles of PTFE and PVAc of 116°/92° and 69°/33°, respectively.⁴¹

Table 1.2. Different compositions of the system poly(TFE-*co*-VAc) reported in the literature.⁴¹

Sample	TFE (mol %)	VAc (mol %)
poly(TFE- <i>co</i> -VAc)	15	85
poly(TFE- <i>co</i> -VAc)	26	74
poly(TFE- <i>co</i> -VAc)	66	34

Another system that has been studied more as research samples is the terpolymer poly(TFE-*ter*-VAc-*ter*-PDMSMA), where PDMSMA is poly(dimethylsiloxane)-methylacrylate-terminated, as shown in Figure 1.1.⁴² These samples were prepared by solution polymerization using supercritical carbon dioxide as solvent, and the authors highlighted the thermoplastic properties and thermal stabilities of the materials. Each of the samples studied contained TFE in concentrations greater than 55 mol %. More specific concentrations and their percent yields and glass transition temperatures can be seen in Table 1.3. The samples were originally created to combine the best of both worlds, that is, the thermal stability and hydrophobicity of fluoropolymers and the elastomeric properties of polysiloxanes.^{12,42,43} Analysis of the thermal properties revealed that the terpolymers were stable up to 200 °C for prolonged periods of time and that thermal stability increased with both TFE concentration and the degree of crosslinking (as the polymer can be modified to crosslink across the siloxane groups). Crosslinked films of these fluorosilicon polymers were homogenized with dispersions of MgO (2.7%) and Ca(OH)₂ (4%) in methyl ethyl ketone (MEK) with a MEK solution of the polymer (15% w/v) containing bisphenol AF and phosphonium chloride (2% each), followed by solvent evaporation, precuring at 145 °C (30-60 min), and postcuring at 204 °C (16 h). The authors concluded that these

presence of concentrated sulfuric acid, ethanol, and a catalytic amount of water, as shown in Figure 1.2.⁴⁴ These authors did not report the complete hydrolysis of all acetate groups, and the content of TFE in the final product remained greater than 63 mol %. Although a search of the literature reveals that poly(TFE-*co*-VA) has not been or cannot be made by the direct means of copolymerizing vinyl alcohol with TFE or grafting vinyl alcohol with PTFE, several publications include mention of poly(TFE-*co*-VA) being obtained from the hydrolysis of poly(TFE-*co*-VAc) with NaOH at 60 °C for 5 hours.⁴⁵

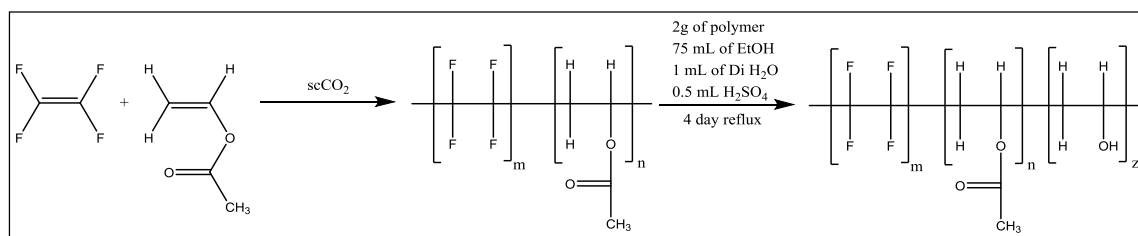


Figure 1.2. Polymerization and hydrolysis scheme of poly(TFE-*co*-VAc) to form poly(TFE-*ter*-VAc-*ter*-VA).^{44,46}

Other polyesters have been prepared by means of radical copolymerization of TFE and 2-methylene-1,3-dioxepene (MDO, Figure 1.3) using 2,2'-azobis(isobutyronitrile) (AIBN) as the radical initiator (known as Vazo™ 64 from DuPont) and *tert*-butyl alcohol as the solvent that have increased biodegradability and water repellency.⁴⁷ Characterization methods such as IR and ¹⁹F and ¹H NMR spectroscopy reveal an alternating copolymer of 52-53 mol % MDO including 5-7 mol % of MDO in dyads. Additionally, terpolymers of TFE, MDO, and isobutylene (IB) were described where IB was basically incorporated as a termonomer in place of some of the MDO (at levels between 16 and 43 mol %). Proton NMR spectroscopy showed that the terpolymers had 5-10 mol % of dyads of both MDO

and IB monomer. Finally, reduction of poly(TFE-*alt*-MDO) with LiAlH₄ proved to be a useful way to synthesize 3,3,4,4,-tetrafluoro-octan-1,8-diol.⁴⁷

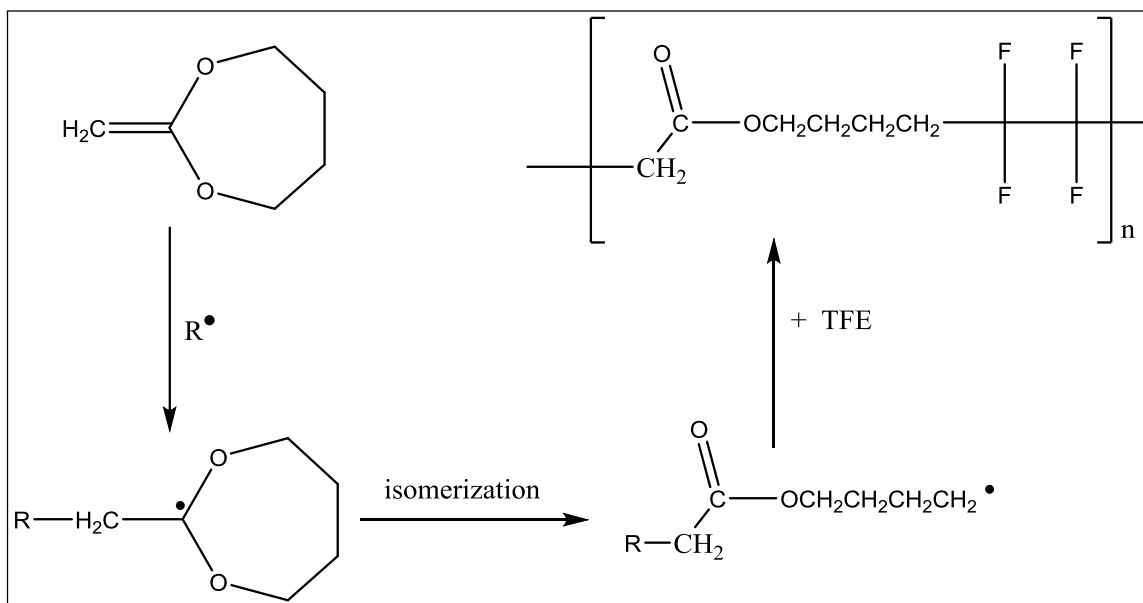


Figure 1.3. Chemical structure of the monomer MDO used to prepare poly(TFE-*co*-MDO).⁴⁷

Kostov et al. in Bulgaria have published a number of studies over the years on the co- and terpolymerization of TFE with a variety of monomers. In one such study, they studied^{48-49,50} the thermal and relaxation properties of poly(TFE-*co*-E) and poly(TFE-*co*-P), since these copolymers are commercial materials their results will not be discussed in further detail here, but other TFE-based fluoropolymers will be.^{43,51,52} For example, Kostov et al. prepared the terpolymer poly(TFE-*ter*-P-*ter*-NBVE), where NBVE is $CH_2=CH-O-CH_2CH_2CH_2CH_2$, by radiation induction in collaboration with Tabata's laboratory in Japan.⁴³ Each of the nonfluorinated monomers gave rise to an alternating polymer structure with TFE, and with increasing concentration of NBVE both the rate of

polymerization and molecular weight of the resulting terpolymers were found to increase. As can be expected, the T_g of the transparent, rubbery terpolymer decreased sharply with increasing NBVE content, but both the thermal and chemical stabilities of the resulting polymer decreased slightly at the same time.⁴³ Brown et al. at the former U.S. National Bureau of Standards [now National Institute of Standards and Technology (NIST)] also prepared copolymers of TFE and isobutylene (IB) under high pressure (5000 atm) via induction by gamma radiation. Copolymers with compositions 30 to 56 mol % TFE were prepared with corresponding T_g 's ranging from 257 to 313 K, and polymers with greater than 45 mol % TFE were found to be crystalline.⁵³

In two separate publications, Kostov and Atanasov describe the preparation and study of co- and terpolymers for ion-exchange applications.^{51,52} In the first study, the preparation and properties of the terpolymers of TFE, HFP, and acrylic acid (AA) were described, and these researchers obtained polymers with ion exchange capacities up to 0.8 meq/g.⁵¹ In the second study, both the aforementioned terpolymers of TFE, HFP, and AA as well as copolymers of TFE and ethylene (E) were sulfonated with an excess of freshly distilled SO_3 in dichloroethane at 273 and 298 K, respectively. In the case of the terpolymers, now with both carboxylate and sulfonate groups, ion exchange capacities were increased to 1.75 meq/g, while the sulfonated copolymers of TFE and E had ion exchange capacities up to 0.70 meq/g. Both types of polymers were also found to have good thermal and film-forming properties.⁵³

1.3. Co- and Terpolymers of Tetrafluoroethylene and Polyfluoroalkenes

Although not technically a polyfluoroalkene, vinyl fluoride (VF) has been used in the preparation of both co- and terpolymers of TFE. As pointed out in more recent findings by Uschold et al.,^{54,55} most early reports on VF/TFE co- and terpolymers required forceful polymerization conditions such as high pressure (122-143 atm),⁵⁶ the use of irradiation for initiation,⁵⁷ or the use of flammable solvents and toxic organometallic reagents, which resulted in polymers with nonionic end groups.⁵⁸⁻⁶⁰ Uschold et al.⁵⁴ were able to find conditions (use of water soluble, free radical initiators; 10 to 120 atm pressure; and 60 to 100 °C polymerization temperatures) by which they could prepare VF/TFE co- and terpolymers with ionic end groups, much more uniform particle size, and improved weather, chemical, and stain resistance. Most recently, Uschold et al.⁵⁵ have produced VF/TFE co- and terpolymers with lower crystallinity, and some of the terpolymers of VF and at least two highly fluorinated monomers, where one of these comonomers has a side chain of at least one carbon atom, are even melt processible. The plasma copolymerization of VF and TFE has also been reported by Golub and Wydeven.⁶¹

It is well known that polyvinylidene fluoride (PVDF) is only 50-70% crystalline,⁶² while PTFE is well known for its remarkably high degree of crystallinity.⁴ Great efforts have been made to produce poly(TFE-*co*-VDF) with different percentages of TFE in order to study its crystallinity and other properties. The particular case of poly(TFE-*co*-VDF) has gained great attention since Lovinger first pointed out its Curie transition between ferroelectric and paraelectric states in 1983.⁶³ The analyzed composition of 81:19 mol %

of VDF to TFE, respectively, was an experimental grade sample of Kynar 7200 manufactured by Pennwalt Corporation (currently Arkema). As the content of TFE increases in poly(TFE-*co*-VDF), the degree of crystallinity increases in the copolymer. This can be interpreted as a random distribution of the two monomers throughout the material. Furthermore, the product of their reactivity ratios is 0.86, as determined by Moggi et al., which further indicates that the copolymer has a random distribution of the two monomers.⁶⁴ Recently, copolymers of TFE and VDF have been prepared in the AMRL laboratory located at Clemson University, both in the absence and presence of carbon dioxide, and the resulting reactivity ratios are comparable to those of Moggi et al., likewise indicative of a random distribution of the monomers in the polymer, which is also confirmed by NMR spectroscopy (*vide infra*).⁶⁴

A potential application of poly(TFE-*co*-VDF) includes the manufacture of high electric energy storage capacitors by means of stacking layers of poly(TFE-*co*-VDF) with layers of poly(ethylene terephthalate) (PET), which has been shown to give energy densities up to 16 J/cm³.⁶⁵ Over the years, many co- and terpolymers of VDF have been prepared in order to take advantage of the special dielectric, piezoelectric, and discharge properties of PVDF. Reasonably large energy storage capacities have been found in these materials with energy densities between 10 to 25 J/cm³.⁶⁶⁻⁷⁶

Copolymers of TFE and VDF have a high degree of crystallinity, and the introduction of HFP as a termonomer strongly reduces the degree of crystallinity in the terpolymer. Such terpolymers of VDF, HFP, and TFE have been commercialized by the 3M Company under the acronym THV™. The materials can exhibit either elastomeric

properties or a combination of elastomeric and thermoplastic properties, depending on the concentration of the monomers.^{77,78} THV™ polymers are used as thermal shrink materials to protect electrical connections, coatings for medical devices due to bio-compatibility, hose and gasoline tank liners, etc.⁷⁹ The low temperature flexibility of the THV™ improves as the content of VDF in the terpolymer increases as seen in Table 1.4. On the other hand, if an excess of VDF exists in the THV™, the material loses its resistance to bases and amines, which are often present in engine oils and coolants as additives.^{80,81}

Table 1.4. Ranges of compositions and their relation to the properties of poly(TFE-*ter*-VDF-*ter*-HFP)⁸².

Property	TFE (mol %)	VDF (mol %)	HFP (mol %)
Elastomer	0-40	20-70	20-60
Thermoplastic / Elastomer	15-30	15-20	13-25
Thermoplastic / Elastomer	80-85	70-80	80-85

Both the compositions and sequence distributions of poly(TFE-*co*-VDF) and poly(TFE-*ter*-VDF-*ter*-HFP) can be determined by ¹⁹F NMR spectroscopy since these polymers have reasonable solubility in polar organic solvents like acetone.⁸³⁻⁸⁸ Traditional characterization of these polymers by one-dimensional NMR spectroscopy generally allowed for an estimate of their compositions as well as characterization of three- and five-carbon sequences,⁸³⁻⁸⁵ but recent multidimensional studies by Rinaldi et al.⁸⁶⁻⁸⁸ have allowed for a complete characterization of the microstructures of these polymers, including several approaches to estimating their compositions, characterization of seven- and nine-carbon sequences in addition to three- and five-carbon sequences, as well as the percentages of VDF monomer inversions.

A pentapolymer of TFE, VDF, vinyl benzoate (VB), bis(2-chloroethyl) vinylphosphonate (B2CEVP), and itaconic acid (ITA) has been prepared in trimethyl phosphate by the reaction of VB, B2CEVP, ITA, and a mixture of TFE and VDF in a 400-mL pressure vessel at 60 °C. A 75% solution of *tert*-butyl peroxyphosphate in mineral spirits was used as the free radical initiator solution.⁸⁹ The resulting pentapolymer had a total of 59.2% fluorine and 0.2% phosphorus by elemental analysis, which corresponded to 0.005 mole of B2CEVP groups per mol of VDF. Infrared spectroscopy and acid-base titrations were used to determine the quantity of the other monomer units in the polymer. Other terpolymers and quadpolymers were reported using the same general method of polymerization, such as poly(VDF-*quad*-TFE-*quad*-VB-*quad*-VAc), poly(VDF-*penta*-TFE-*penta*-VB-*penta*-CTFE-*penta*-ITA), poly(VDF-*ter*-TFE-*ter*-VB), poly(VDF-*quad*-TFE-*quad*-VB-*quad*-CTFE), poly(VDF-*quad*-TFE-*quad*-VB-*quad*-V2CB), of various compositions where VB is vinyl benzoate, VAc is vinyl acetate, V2CB is vinyl-2-chloro benzoate, and ITA is itaconic acid.⁸⁹

Tetrafluoroethylene has been copolymerized with a variety of functionalized trifluorovinyl monomers. For example, Ameduri, Kostov, and coworkers prepared copolymers of TFE with both 2,3,3-trifluoroallyl alcohol ($\text{CF}_2=\text{CFCH}_2\text{OH}$, FA1) and 4,5,5-trifluoro-4-penten-1-ol [$\text{CF}_2=\text{CF}(\text{CH}_2)_3\text{OH}$, FA3] by both free-radical (AIBN initiator) solution and bulk polymerization techniques.⁹⁰ These same copolymers, as well as similar ones with a wider array of functional groups in place of the hydroxyl group, were the subject of a WO patent where the copolymers could be crosslinked and made into

rubbers.⁹¹ These researchers found that the molecular weights of their copolymers were adversely impacted by an allyl chain transfer reaction to the hydroxyl monomers. Monomer FA3 was found to be more reactive than FA1, and polymers resulting from the former were also more thermally stable.⁹⁰ More recently, this same group of researchers prepared the related copolymer of TFE and 4,5,5-trifluoro-4-penten-1-acetate (FAc) by free-radical (*tert*-butyl peroxyvalate initiator) bulk polymerization techniques, and allyl chain transfer to the acetate monomer was again observed.⁹²

Similarly, though under aqueous emulsion polymerization conditions, Ameduri, Kostov, and coworkers prepared a series of terpolymers from tetrafluoroethylene, propylene (P), and FA3.⁹² The primary purposes of this research were to study the role of FA3 as a cure-site monomer in poly(TFE-*co*-P) as well as to study of the properties of the final materials. The polymers were prepared by using a gas mixture of TFE and P with a composition 80:20 mol %, respectively, and the FA3 termonomer was introduced in amounts ranging from 0 to 14.1 mol% (see Figure 1.4). The rate of polymerization was perceived to decrease as the amount of FA3 increased, and the thermal stability of the resulting polymer also decreased in this direction, as determined by TGA with 50% weight loss occurring at a lower temperature. The T_g of the terpolymer was observed to decrease from 0 °C to -4 °C with respect of that of poly(TFE-*co*-P).⁹³

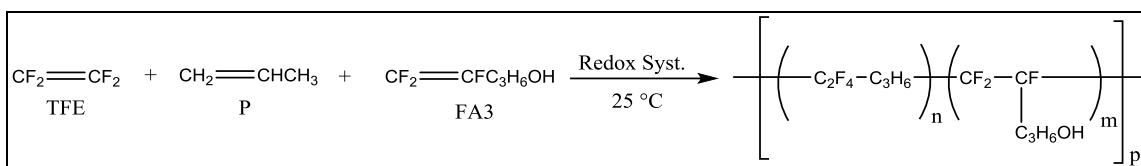


Figure 1.4. Reaction scheme for the system poly(TFE-*ter*-P-*ter*-FA3).⁹³

Researchers at Daikin have prepared another family of TFE-based fluoropolymers that may serve as a barrier or coating material in fuel lines given that they display both good adhesion to other materials and low fuel permeation.⁹⁴ The general combination of monomers (see Figure 1.5) proposed in the patent gives poly(TFE-*co*-CXY=CZR), where X, Y, Z are H, F, or Cl (all the same or different) and R is F, Cl, CF₃ or O(CF₂)₁₋₅F where at least one X, Y, or Z is H. The inventors mention that the preferred TFE comonomer is 2,3,3,3-tetrafluoropropene (HFO-1234-yf) ranging in composition in the final copolymer from 0 to 20 mol %. Additionally, the patent indicates the inclusion of an optional functional group that consists of either a carbonyl group, an amino group, an oxazolyl group, a glycidyl group, an epoxy group, and/or a hydroxyl group to improve adhesion and thereby expands the range of possible applications to either hoses that deliver drug solutions, a container for urea, a tank for fuel, a tube for fuel, a hose for fuel, an underground embedding tube, or an underground embedding hose.⁹⁴ The copolymer of TFE and HFO-1234-yf had been previously reported via radiation polymerization at high pressure by the aforementioned research group at NIST,⁹⁵ where a reactivity ratio study showed that the incorporation of TFE versus HFO-1234-yf was generally disfavored.

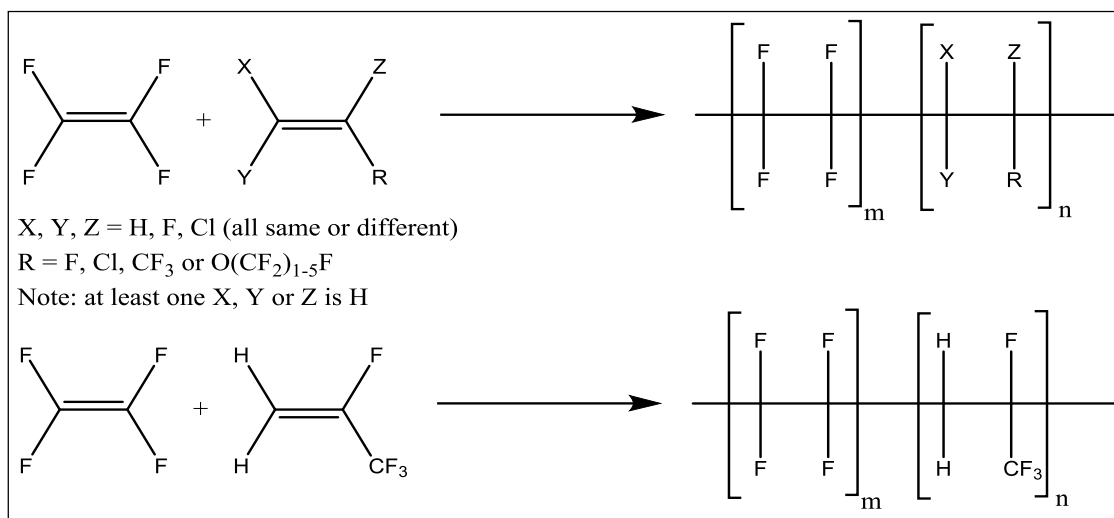


Figure 1.5. Reaction schemes for general polymerization products (top) versus preferred polymerization composition (bottom) manufactured for fuel barrier materials.⁹⁴

In a similar way, other TFE-based materials that exhibit excellent fuel barrier properties, excellent adhesion to other materials, and are capable of maintaining good adhesion to other materials even after contact with a fuel have been reported by Daikin.^{96,97} The polymerizations were carried out in solution using di-*n*-propylperoxydicarbonate as the radical initiator. The polymer samples, compositions, and melting points are included in Table 1.5.^{96,97}

Much of what is in the patent art with respect to copolymers of TFE and chlorotrifluoroethylene (CTFE) appears to be where small amounts of CTFE have been incorporated to either modify or improve the properties of PTFE. On the other hand, few scientific publications have appeared describing poly(TFE-*co*-CTFE) where CTFE (or bromotrifluoroethylene, BTFE) can be a major component.^{57,98-100} For example, Bruk et al. reported the liquid-phase, radiation copolymerization of TFE and CTFE at low temperature (-114 °C to 0 °C),⁹⁸ while Moggi et al. reported the solution copolymerization

of TFE with both CTFE and BTFE at 40 °C over the entire range of monomer compositions.⁹⁹ More recently, a WO patent has appeared describing a TFE-based polymer sheet with excellent water vapor barrier properties for special use as either a solar battery back sheet or in a solar battery module.¹⁰¹ The polymers described in this patent are poly(TFE-*ter*-CTFE-*ter*-AA), where AA is acrylic acid. The materials were prepared by aqueous emulsion polymerization using $F(CF_2)_3C(CF_3)_2CH_2CH_2COONH_4$ as the surfactant and ammonium persulfate as the radical initiator, while slowly adding the acrylic acid drop-by-drop over a 24 hour period. The targeted composition of the polymers ranged from 0.01 to 30 wt % of acrylic acid and 70 wt % or more of CTFE with TFE being the rest of the composition. A preferred composition was not given.¹⁰¹

Table 1.5. Reported polymer compositions.^{96,97}

Polymer Sample	Composition (mol % for each monomer, respectively)	Melting Point (°C)
poly(TFE- <i>ter</i> -E- <i>ter</i> -UA)	61.9-31.9-6.2	209
poly(TFE- <i>quad</i> -E- <i>quad</i> -HFP- <i>quad</i> -UA)	47.6-42.5-9.6-0.3	195
poly(TFE- <i>quad</i> -E- <i>quad</i> -HFP- <i>quad</i> -UA)	46.0-41.3-8.9-3.7	186
poly(TFE- <i>quad</i> -E- <i>quad</i> -HFP- <i>quad</i> -PA)	47.9-42.1-9.6-0.3	196

E = ethylene, HFP = hexafluoropropylene, UA = undecylenic acid, and PA = pentenoic acid.

In addition to the aforementioned copolymer of TFE and HFO-1234-yf, a broader series of copolymers of TFE with other polyfluoroolefins, including $CH_2=CHCF_3$, $CH_2=CHC_3F_7$, $CH_2=C(CF_3)_2$, and *cis*- and *trans*- $CHF=CHCF_3$,¹⁰²⁻¹⁰⁶ was prepared and

studied in the late 1960s and earlier 1970s by the group at NIST. They generally carried out these polymerizations via radiation induction and under high pressure; the copolymers were well characterized, including polymerization rates and reactivity ratios.^{95,102-106} Reactivity ratios have also been reported by the Russian group of Fokin for the radiation-induced copolymerization of TFE with trifluoroethylene.⁵⁷

Research samples of poly(TFE-*ter*-E-*ter*-NFH) have been developed (where NFH is nonafluoro-1-hexene), to study the effect of a bulky group on the crystal lattice as compared to that in poly(TFE-*ter*-E-*ter*-HFP), as shown in Figure 1.6.¹⁰⁷ Both polymers were prepared by means of solution polymerization using a hydrofluorocarbon (HFC) solvent and were characterized by molten-state ¹⁹F NMR spectroscopy, wide-angle X-ray diffraction (WAXD), and differential scanning calorimetry (DSC). The researchers were able to conclude that the short side chains (CF₃ groups) are included in the crystal lattice of the TFE/E chains, whereas the long side chains (C₄F₉ groups) are excluded from the crystal lattice.¹⁰⁷ The compositions made for this study are shown in Table 1.6.

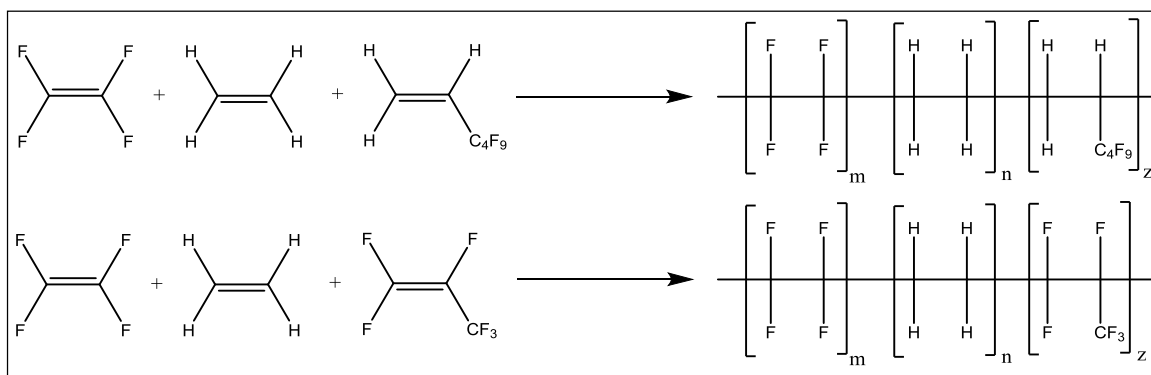


Figure 1.6. Reaction scheme for poly(TFE-*ter*-E-*ter*-NFH) (top) and poly(TFE-*ter*-E-*ter*-HFP) (bottom)¹⁰⁷

Table 1.6. Composition of terpolymers poly(TFE-*ter*-E-*ter*-NFH) used in the study of crystal phase transition temperatures.¹⁰⁷

Sample	Composition in mol %			
	E	TFE	NFH	HFP
poly(TFE- <i>ter</i> -E- <i>ter</i> -NFH)	45.7	53.6	0.8	-
poly(TFE- <i>ter</i> -E- <i>ter</i> -NFH)	45.4	53.2	1.5	-
poly(TFE- <i>ter</i> -E- <i>ter</i> -NFH)	38.6	58.1	3.3	-
poly(TFE- <i>ter</i> -E- <i>ter</i> -HFP)	43.8	53.5	-	2.7
poly(TFE- <i>ter</i> -E- <i>ter</i> -HFP)	42.0	53.4	-	4.6

E = ethylene, TFE = tetrafluoroethylene, NFH = nonafluoro-1-hexene, HFP = hexafluoropropylene.

Poly(TFE-*ter*-E-*ter*-NFH) has been the subject of at least two patents, one from DuPont¹⁰⁸ and the other from Asahi Glass.¹⁰⁹ A composition of poly(TFE-*ter*-E-*ter*-NFH) containing 59.0, 39.5, and 1.5 mol % of TFE, E, and NFH, respectively, was mixed with boron nitride (0.01 to 0.5 wt%) in order to increase the scrape abrasion of this material when used in wire coating applications. The scrape abrasion resistance was more than double that of a copper wire not coated with such a material.¹⁰⁸ The preparation of poly(TFE-*ter*-E-*ter*-NFH) with a composition of 57.2:40.3:2.5 mol % of TFE to E to NFH, respectively, having a melting temperature of 223 °C and a melt viscosity of 240 °C at 110 Pa·s has also been reported in a U.S. patent along with other compositions including 57:40:3 and 58:39:3 mol % of TFE to E to NFH, respectively. These materials have been reported to show good chemical and thermal resistance for the manufacture of nonwoven fibers.¹⁰⁹

T. Watanabe et al. have reported the radiation induced copolymerization of TFE and methyl 2,3,3-trifluoropropenoate [CF₂=CFC(O)OCH₃, MTFP],¹¹⁰ while Weise

reported the MTFP-initiated terpolymerization of TFE, MTFP, and methyl methacrylate [$\text{CH}_2=\text{C}(\text{CH}_3)\text{CO}_2\text{CH}_3$, MMA] at 60 °C and 3000 atm.¹¹¹ In the previous section, ion exchange resins prepared by G. K. Kostov via radiation syntheses were described.^{112,113} This group has also prepared terpolymers of TFE/E and TFE/P with MTFP.¹¹⁴ Alternating polymer structures were found between the electron poor olefins (TFE and MTFP) and the electron rich olefins (E and/or P). Both the polyesters and polycarboxylic acid resins, resulting from hydrolysis under basic conditions, were characterized by IR spectroscopy and physical methods, including molecular weights (4 to 8×10^4 Da), glass transition (263-291 K) and decomposition temperatures for the esters – 646-680 K and the acids – 528-561 K, chemical resistance, degree of hydrolysis (90+%), concentration of ion exchange groups (up to 5.24 equiv/kg), percent swelling, etc. Finally, 50-100 μm films of these ion exchange resins were crosslinked by electron beam (e-beam) irradiation to make membranes suitable for use in chloralkali cells.¹¹⁴

Additional copolymers of TFE and vinyl monomers with a long perfluorinated alkyl chain have been reported in the recent patent literature.¹¹⁵⁻¹¹⁷ In each of these patents, TFE has been copolymerized with $\text{CH}_2=\text{CH}(\text{CF}_2)_n\text{CF}_3$ (where $6 < n < 10$) and other monomers with different length perfluorinated side chains to give fine particles of PTFE and a copolymer ranging from 0.01 to 0.3 mol % of comonomer units. The materials were prepared by aqueous emulsion polymerization using either ammonium perfluorooctanoate^{115,116} or ammonium perfluoro-3,6-dioxaoctanoate ($\text{C}_2\text{F}_5\text{OC}_2\text{F}_4\text{OCF}_2\text{C}(\text{O})\text{O}^-\text{NH}_4^+$) as the surfactant.¹¹⁷ The products are described as core-shell, expanded beading,⁷⁵ porous, expanded articles,⁷⁶ or stretched porous material.¹¹⁷

Okamoto et al. developed a new fluoropolymer composed of TFE and 2-difluoromethylene-1,3-dioxolane (2DDO) for use either as an electro-optical material or as a coating material.^{118,119} The fluoropolymer was prepared via solution polymerization using R-113 as the solvent and perfluoro-*tert*-butyl peroxide as the radical initiator. The composition of TFE to 2DDO in samples of poly(TFE-*co*-2DDO) varied from 4:1 to 20:1 in two examples provided in the referenced U.S. patents, and the copolymer was found to be well soluble in fluorinated solvents such as hexafluorobenzene.^{118,119}

A search of the literature has revealed only a few references describing small vinyl perfluorinated cycloalkanes. However, the successful preparation of vinylpentafluorocyclopropane (VPFCP) gave an opportunity to prepare unsaturated fluoropolymers.^{120,121} VPFCP was found to readily homopolymerize at 40 °C in the presence of a free radical initiator such as bis(perfluoropropionyl)peroxide (3P) to give a white solid (see Figure 2.18) that is insoluble in both common organic solvents and fluorinated solvents. VPFCP was found to copolymerize with TFE, CTFE, and PPVE. However, characterization results (TGA and DSC) indicated a low degree of incorporation of these comonomers. In the corresponding U.S. patent,⁸¹ an example of the copolymerization of VPFCP with TFE was not even given, and in the copolymerizations described in this patent, no copolymers were obtained in greater mass than the initial mass of VPFCP monomer used in the copolymerization.⁸¹

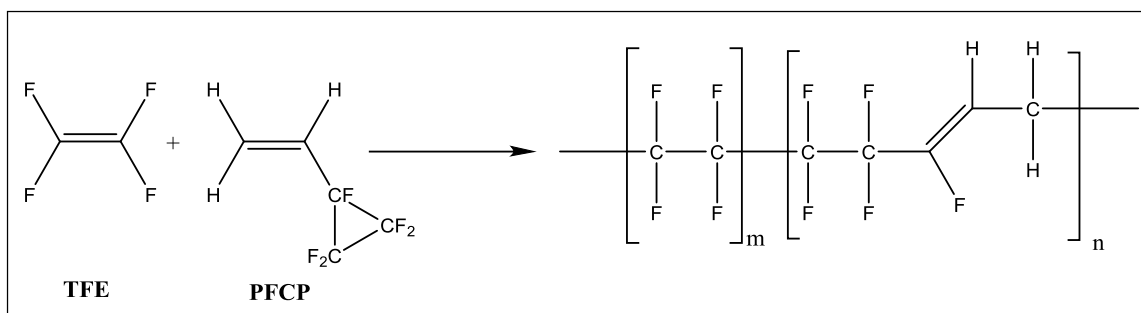


Figure 1.7. Reaction scheme for the preparation of poly(TFE-co-VPFCP).^{120,121}

As a bridge to the next section, a series of poly- and perfluoroethylenic monomers having either a hydroxyl group or fluoroalkyl carbonyl group were prepared and polymerized with comonomers like TFE.¹²² The structures of some of the aforementioned new monomers included $\text{CH}_2=\text{CFC}(\text{CF}_3)_2\text{OH}$, $\text{CH}_2=\text{CFCF}_2\text{OCF}(\text{CF}_3)\text{CF}_2\text{OCF}(\text{CF}_3)\text{C}(\text{CF}_3)_2\text{OH}$, $\text{CF}_2=\text{CFC}(\text{CF}_3)_2\text{OH}$, $\text{CH}_2=\text{CFCF}_2\text{OCF}(\text{CF}_3)\text{CF}_2\text{OCF}(\text{CF}_3)\text{C}(\text{C}_2\text{F}_5)=\text{O}$, $\text{CH}_2=\text{CHCH}_2\text{C}(\text{CF}_3)_2\text{OH}$, among others. Examples of solution polymerization of the first two of these monomers with TFE were also given in the patent, and further chemistry on end group protection was also presented. The new fluoropolymers possessed excellent optical properties and were proposed to be useful as either the base polymer in an antireflective film or as a composition for a photoresist.¹²²

1.4. Co- and Terpolymers of Tetrafluoroethylene and Perfluoroalkenes

Although perfluorocyclopropene (PFCP) and TFE were found not to copolymerize in sealed glass tubes at 80-85 °C under autogenous pressure, they did copolymerize when the polymerizations were carried out in sealed platinum tubes under 3000 atm of pressure. A variety of free radical initiators (AIBN, Bz₂O₂, N₂F₂, 3P, persulfate) were found to be successful. The highest yield of 75% was achieved when using AIBN as the initiator, no solvent, and a mole ratio of 1:3 for PFCP to TFE. Other less successful polymerizations were run with either R-113, the hexafluoropropylene cyclic dimer, or water as a solvent.¹²³⁻

¹²⁵ Like PTFE, poly(TFE-*co*-PFCP) was found to be insoluble in many traditional solvents. Both IR spectroscopy and thermal analyses proved that the material was different than PTFE itself, as additional weak bands were seen in the IR spectrum of the copolymer (1020, 960, and 803 cm⁻¹) and both the T_g (-30 °C) and T_m (290 to 309 °C) were significantly lowered in the copolymer.¹²³⁻¹²⁵

TFE has also been found to copolymerize with hexafluorocyclobutene (perfluorocyclobutene, C₄F₆) to yield polymers that are much more melt extrudable than samples of PTFE prepared in the same way.¹²⁶ This copolymer was prepared in water in one of two ways: (1) benzoyl peroxide as a free radical initiator, a reaction temperature of 79-81 °C, and a pressure of 2000-2500 psi that was maintained by intermittent injections of water or (2) ammonium persulfate as a free radical initiator, an ambient reaction temperature, and a continuously maintained TFE pressure of 50 psi. Copolymers prepared

by both methods could be hot pressed into films, and the composition of the copolymer prepared by the second method was approximately 30% hexafluorocyclobutene.¹²⁶

Co- and terpolymers of TFE and hexafluorocyclopentadiene or perfluorodicyclopentadiene with other fluoromonomers have been prepared by either solution or aqueous emulsion polymerization.¹²⁷ For example, a copolymer that was 71 mol % TFE and 29 mol % hexafluorocyclopentadiene resulted from a solution [perfluoro(dimethylcyclobutane)] polymerization carried out in a sealed platinum tube held at 60 °C and 3000 psi using N₂F₂ as an initiator. A white, film-forming (with a hot press) solid was obtained that had an IR band at 1760 cm⁻¹, which is indicative of fluorocarbon unsaturation remaining in the material. Additionally, a terpolymer of TFE, perfluorodicyclopentadiene, and PMVE was prepared by aqueous emulsion techniques using ammonium perfluorooctanoate as surfactant, potassium persulfate as initiator, a reaction temperature of 55-65 °C, and a pressure of 180 psi. This polymer also displayed the characteristic stretching frequency of 1760 cm⁻¹ in the IR spectrum.¹²⁷

FEP or poly(TFE-*co*-HFP) is a well-known, commercial fluoropolymer; however, the copolymers of TFE with other terminal or branched perfluoroolefins are not so well defined. Nevertheless, such copolymers have been prepared by both aqueous emulsion techniques (ammonium persulfate and sodium perfluorooctanoate were used as initiator and surfactant, respectively) and γ -irradiation techniques (⁶⁰Co source).¹²⁸ The perfluoroolefins studied included hexafluoropropene (C₃F₆), octafluoro-1-butene (1-C₄F₈), octafluoro-*iso*-butene (*iso*-C₄F₈), decafluoro-1-pentene (1-C₅F₁₀), tetradecafluoro-1-heptene (1-C₇F₁₄), and octadecafluoro-1-nonene (1-C₉F₁₈). These

researchers also studied the copolymerization of TFE with hexafluorocyclobutene as described above. A primary reason why these TFE-based copolymers cannot be found in the market place is the fact that their thermal stabilities are markedly reduced (by ca. 100 °C) due to pendant side groups longer than CF₃.¹²⁸

A number of fluoropolymers have been prepared from the reaction of TFE with trifluoronitrosomethane (CF₃NO, NM) with and without other monomers. First, the reaction of TFE with just CF₃NO generally yields a mixture of the cycloadduct perfluoro-2-methyl-1,2-oxazetidine and the linear polymer, and depending upon the conditions of the reaction, one can produce either more of the cycloadduct or of the linear polymer.¹²⁹ When additional monomers, such as CH₃O₂C(CF₂)₃NO (3NN), ONCF₂CF₂COOCH₃ (NCF), and/or ON(CF₂)₃CO₂CH₃ (NCM) are used as comonomers with TFE and CF₃NO, a series of special nitrogen-containing fluoropolymers can be obtained. In this manner poly(TFE-*ter*-NM-*ter*-3NN), poly(TFE-*ter*-NM-*ter*-NCF), and poly(TFE-*ter*-NM-*ter*-NCM) have been reported in the literature.¹³⁰ Although the authors did not elaborate upon the compositions, these polymers do display elastomeric/rubbery properties.

Another interesting family of polymers has been made by TRW Inc. in which TFE was reacted with trifluoronitrosomethane (NM), difluoromaleic anhydride (DMAH), and perfluoromethyl vinyl ether (PMVE).¹³¹ The reactions were carried by simply adding all of the monomers into an enclosed vessel and allowing them to warm in the presence of an organic peroxide catalyst. Some substructures from the literature reference could be modified by adding other vinyl ethers or crosslinking agents. One of the prepared polymers

is shown in Figure 1.8, while poly(TFE-*ter*-NM-*ter*-DMAH) was also reported. One potential application of these materials is to crosslink across the anhydride groups by using a perfluoroalkyl diisocyanate (OCN-R-NCO), where R can be a (CF₂)_n fragment of various lengths or a different spacer, to form cured elastomers for a variety of applications.¹³¹

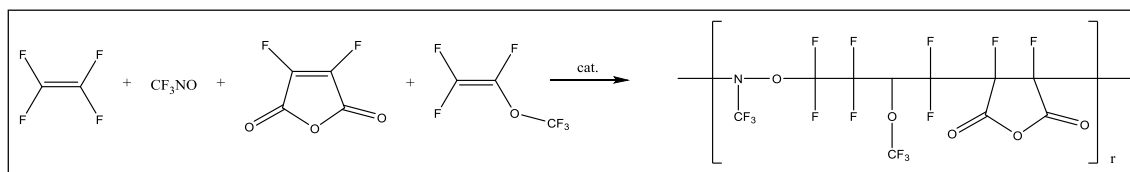


Figure 1.8. Reaction scheme for the preparation of poly(TFE-*quad*-NM-*quad*-PMVE-*quad*-DMAH).¹³¹

A few additional sulfonyl fluoride-terminated perfluorinated monomers and their copolymers with TFE exist beyond those that are found in commercial products for ion-exchange membranes. Both researchers at the DuPont Company and at the Bourgas Technological University in Bulgaria have independently studied the polymerization (solution, aqueous emulsion, and bulk) of 2-(1-pentafluoro-2-propenyloxy)-tetrafluoroethanesulfonyl fluoride (CF₂=CF CF₂OCF₂CF₂SO₂F, PPOTESF) with TFE.^{132,133} In the latter of these studies, Kostov et al. determined the reactivity ratio of the two monomers using the Fineman-Ross method, and their results indicate a random distribution of PPOTESF in the copolymer.⁹³ In a similar way, Kostov et al. studied both the bulk and solution polymerization of TFE with 1-fluorosulfonyl-difluoroacetyl fluoride (FSDFAF), which led them to believe that FSDFAF monomer units were randomly distributed along the polymer backbone. The T_m of this copolymer was also found to be 10-15 °C lower than that of PTFE, and the thermal stability was 360-380 °C.¹³⁴ Finally, in

2009, scientists from Asahi Glass reported on the preparation of a new family of perfluorinated monomers with two sulfonyl fluoride groups per monomer and their copolymers with TFE as well as membranes in the sulfonic acid form. The formula for this new family of monomers is $\text{CF}_2=\text{CF}(\text{CF}_2)_n\text{OCF}_2\text{CF}(\text{R}_{f1}\text{SO}_2\text{F})\text{OCF}_2\text{R}_{f2}\text{SO}_2\text{F}$, where n is 0 or 1, R_{f1} is a single bond or C_{1-6} bivalent perfluoroorganic group, and R_{f2} is a C_{1-6} bivalent perfluoroorganic group.¹³⁵ An obvious rationale of the interest in these new monomers is the potential for increasing the density of ion-exchange groups in the final polymeric membranes.

1.5. Co- and Terpolymers of Tetrafluoroethylene with Cyclic Monomers and Tetrafluoroethylene-based Photoresist Materials

Tetrafluoroethylene-based photoresist materials emerged in the late 1990s, when suddenly the interest in them began to wane around 2005 due to a number of technological challenges for 157-nm photoresist set against alternate approaches in photolithography such as 193-nm immersion photoresist. The use of TFE-based fluoropolymers as photoresist materials originally arose from the need of high transparency at 157 nm coupled with high thermal and chemical stabilities, low surface energies, low dielectric constants, low refractive indices, and low flammabilities.¹³⁶⁻¹³⁸ At the time, most fluoropolymers were not a good choice due to the lack of good solubility in common solvents as opposed to their well-known solubility in highly fluorinated solvents, which can become cost prohibitive. The high crystallinity of PTFE limits its optical applications, hence the need

existed to include at least one comonomer to reduce the crystallinity of the fluoropolymer. Historically, the incorporation of cyclic monomers has demonstrated the ability to greatly reduce the crystallinity of fluoropolymers as well as lower their glass transition temperatures; however, for the optical needs mentioned the other advantageous properties must be maintained.^{139,140} Other desirable properties often required in these polymers include etch resistance, high image contrast, lack of flow of the polymer layer during processing (polymer having a T_g above the desired process temperature, generally 120 to 180 °C), high solubility in common organic solvents to favor use of spin coating techniques, a high molecular weight that enhances mechanical properties without compromising the polymer solubility in the developer, the ability to coat a wide variety of substrates (including silicon), and impurities levels in the range of parts-per-billion.¹⁴¹

Although lots of polymeric structures have been reported in this field, one particular family of polymers (see Figure 1.9) attracted attention since this family is soluble in common organic solvents such as THF, acetone, and 2-heptanone and insoluble in hydrocarbons.¹⁴⁰ The polymers contain a norbornene group (NOB) that has four positions where various substituents can be replaced, e.g., $-\text{OC}_3\text{F}_7$, $-\text{F}$, $-\text{OC}_2\text{H}_5$, $-\text{H}$, $-\text{CF}_3$, $-\text{C}(\text{CF}_3)_2\text{OH}$, or OH . (Other substituents were mentioned in the publication, but an exhaustive coverage of all of the compositions will not be given here.) Some of these materials have absorption coefficients at 157 nm ranging from 1.13 to 1.63 μm^{-1} ,¹⁴⁰ and for the most part, these values are in the lower range of absorption coefficients known for non-fluorinated materials for photolithography; for example, compare to poly(hydrosilsequioxane) 0.06 μm^{-1} , poly(dimethylsiloxane)

1.61 μm^{-1} , poly(vinyl alcohol) (99.7%) 4.16 μm^{-1} , and poly(methylmethacrylate) 5.69 μm^{-1} .¹⁴¹ Thus, finding a fluoropolymer that also enhanced the thermal properties of the required material along with having a lower absorption coefficient became a real task.

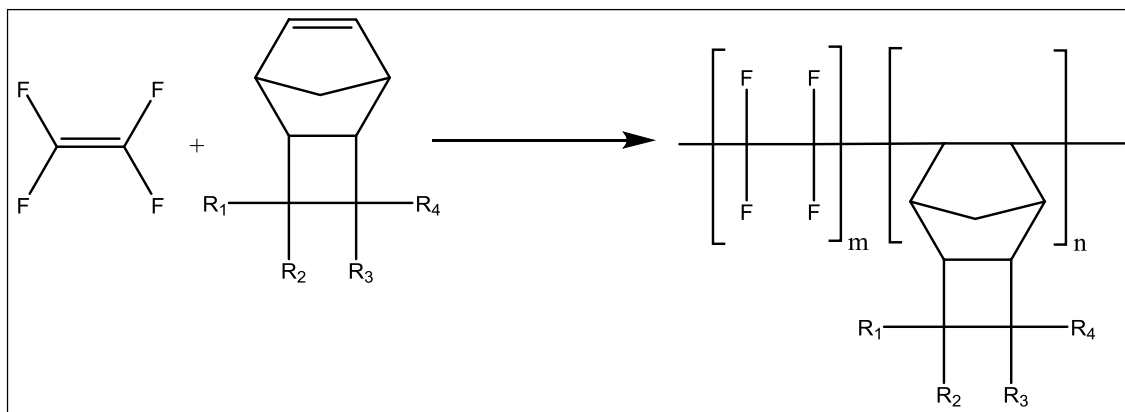


Figure 1.9. Reaction scheme for the preparation of the general fluoropolymer poly(TFE-*co*-NOB), where NOB is a norbornene derivative.¹⁴⁰

Because of their resistance to energetic wavelengths, it has clearly been suggested that fluorinated materials are more appropriate for application in photolithography. A study of the inverse relationship between the level of fluorine incorporation and etch resistance supports this statement.¹⁴² In the same way, etch resistance was found to increase when using a cyclic monomer as compared to an analogous non-cyclic monomer. The structures of monomers that were copolymerized with TFE in this study are shown in Figure 1.10. The polymerizations were carried out under normal solution polymerization conditions (40 °C and maintained for 18–24 h), and the feed ratios of the monomers were varied to give compositions of TFE to ethylenic comonomers in the final polymers as close to 1:1 as possible. Additionally, the polymers were strategically prepared to contain end

groups that would allow the study of both the effects of chain length as well as a $-\text{CF}_3$ versus a $-\text{CF}_2\text{H}$ end group with respect to etch resistance.¹⁴²

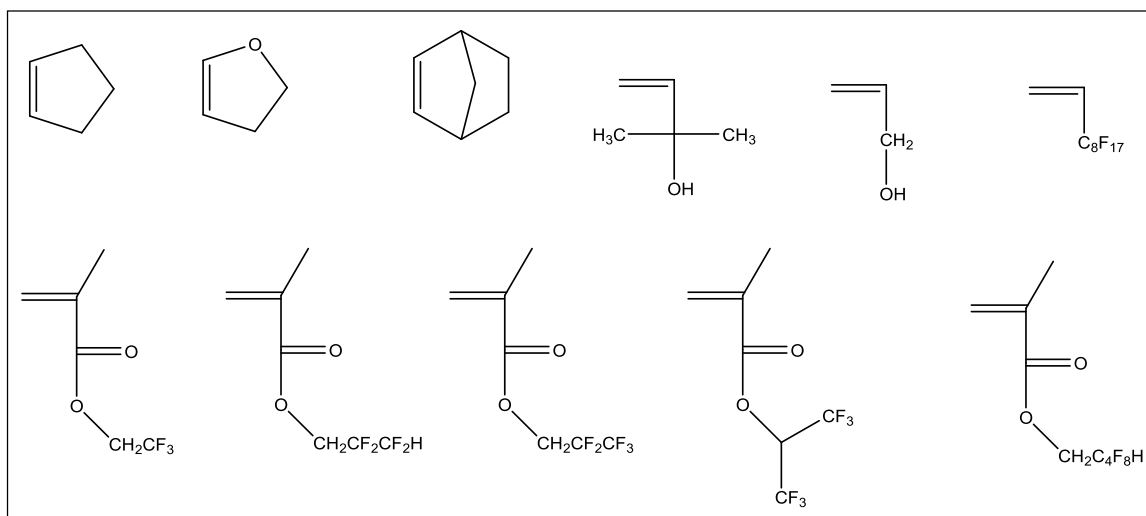


Figure 1.10. Comonomers used in the etching rate study of TFE polymers for photolithography.¹⁴²

The type of fluoropolymers being applied to photolithography not only includes copolymers of TFE but terpolymers as well. A number of reports have appeared in the literature describing the synthesis of very transparent materials made via radical terpolymerization of TFE, and some of these reports will be overviewed below. As shown at the bottom of Figure 1.11, two terpolymers of TFE/norbornene were prepared by radical polymerization at 40 °C for 18–24 h, followed by precipitation of the polymer in hexane and drying under vacuum.¹⁴³ The *exo* polymer was found to give more contrast than the *endo* one. The tests were made by making a 1:1 line and space patterns at 55 nm on a 150 nm thick film. The authors used two methods of polymerization (bottom of Figure 1.11), namely a true terpolymerization (Method A) versus a copolymerization plus partial

derivatization (Method B). It was found that the latter method gave a more stereoselective polymer than the former method, as only the *exo* groups would undergo derivatization. Likewise, deprotection studies showed that only protective groups in the *exo* position changed back to hydroxyl groups, but those in the *endo* position remained unchanged.¹⁴³

Another terpolymer made using a norbornene fluoroalcohol has been reported in the literature.¹⁴⁴ The polymer was prepared using solution polymerization conditions (fluorocarbon solvent and peroxydicarbonate as radical initiator; see Figure 1.12). The terpolymer poly(TFE-*ter*-NB-F-OH-*ter*-TBA), having a composition of 31:45:24 mol% for TFE, NB-F-OH, and TBA, respectively, had an absorption coefficient of $1.98\ \mu\text{m}^{-1}$. Although the material was suitable for making 90 nm 1:1 line and space patterns, the spaces were not clean all the way down to the silicon surface.¹⁴⁴

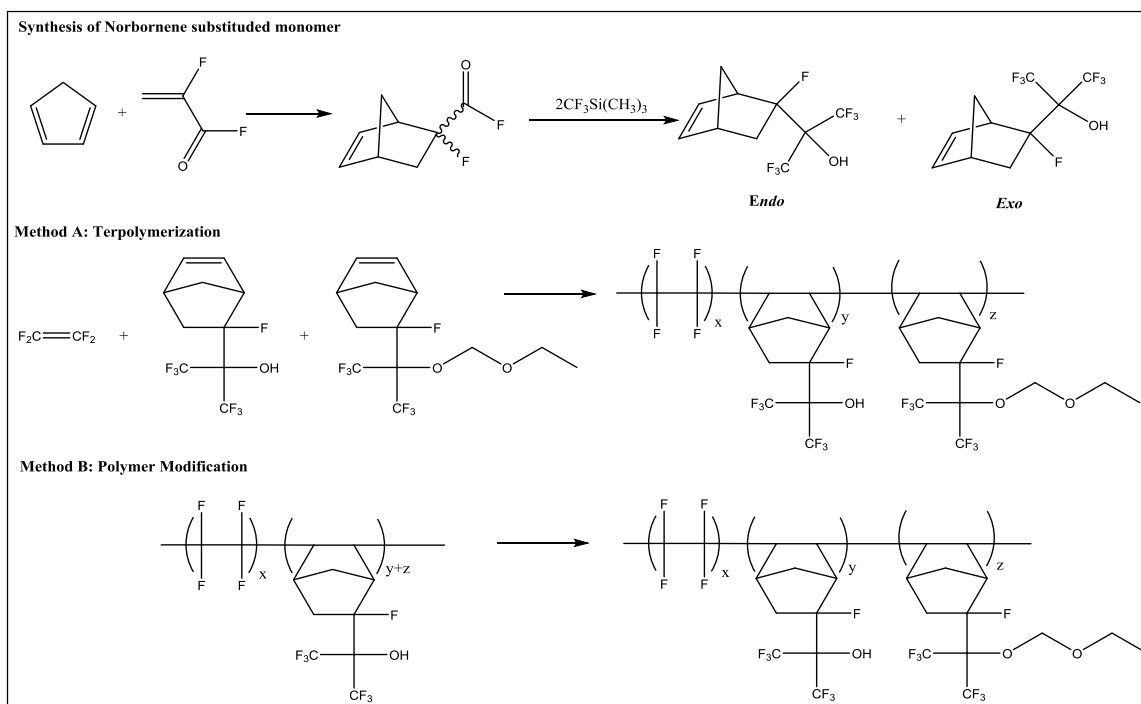


Figure 1.11. Synthetic scheme to endo and exo-isomers of functionalized norbornene (top) and two methods for preparing TFE-based terpolymers (bottom).¹⁴³

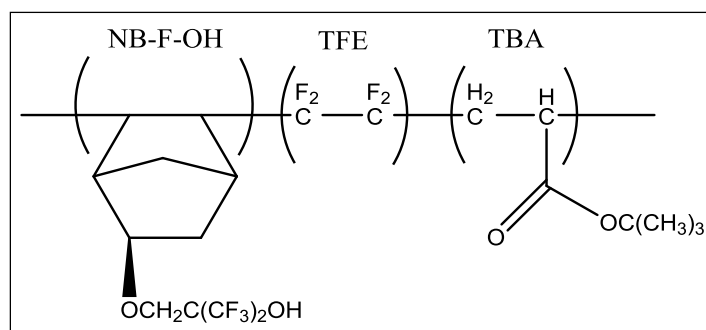


Figure 1.12. Reaction scheme for the synthesis of poly(TFE-*ter*-NB-F-OH-*ter*-TBA).¹⁴⁴

It is known that most of the fluoropolymers made in the early 2000s for the 157 nm photolithography were not appropriate for their intended uses given that they can undergo photolysis at such wavelengths. In more recent years other materials have been able to improve such characteristics as high sensitivity, high resolution, and low line width

roughness (LWR). A copolymer of TFE and a norbornene comonomer (first published in 2003)¹⁴⁵ has been re-studied¹⁴⁵ to reveal some improvements on the aforementioned properties. The reaction scheme is detailed in Figure 1.13, although the solvents or radical initiators used in the process of copolymerizing these monomers were not mentioned in detail in any of the publications.^{143,145}

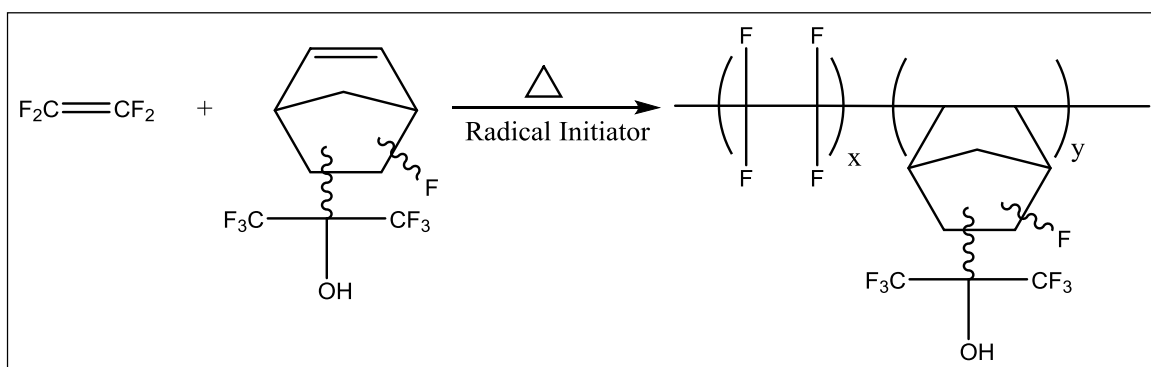


Figure 1.13. Polymerization scheme for the TFE-norbornene-based materials.^{145,146}

By the first publication¹⁴⁵ the authors were only able to measure the performance of 1:1 line and space patterns at 120-130 nm, but in the most recent publication (due to improvements in measuring technology) the same authors have been able to measure the performance of the copolymer at smaller patterns (30-50 nm). Although it could be used safely at 40 nm to obtain a good resolution, the material presents some bridging at such line and space pattern widths at 110 °C.

A more recent publication includes polycyclic alcohol derivatives that have been co- and terpolymerized with TFE to obtain materials for photoimaging compositions and positive- and negative-working photoresist compositions using 157 nm wavelength light.¹⁴⁷ The structures of all the monomers used are shown in Figure 1.14, and the

polymers prepared and their compositions are listed in Table 1.7. Some of these materials have also been used to make photoresist materials. One example is the use of a 2-heptanone solution of the methoxymethyl ether protected poly(TFE-*co*-TCN-di-F-OH) and triphenylsulfonium nonaflate. Other photoresist materials have been prepared correspondingly by using the methoxymethyl ether protected poly(TFE-*co*-NB-di-F-OH) and methoxymethyl ether protected poly(TFE-*ter*-NB-F-OH-*ter*-NB-di-F-OH).¹⁴⁷

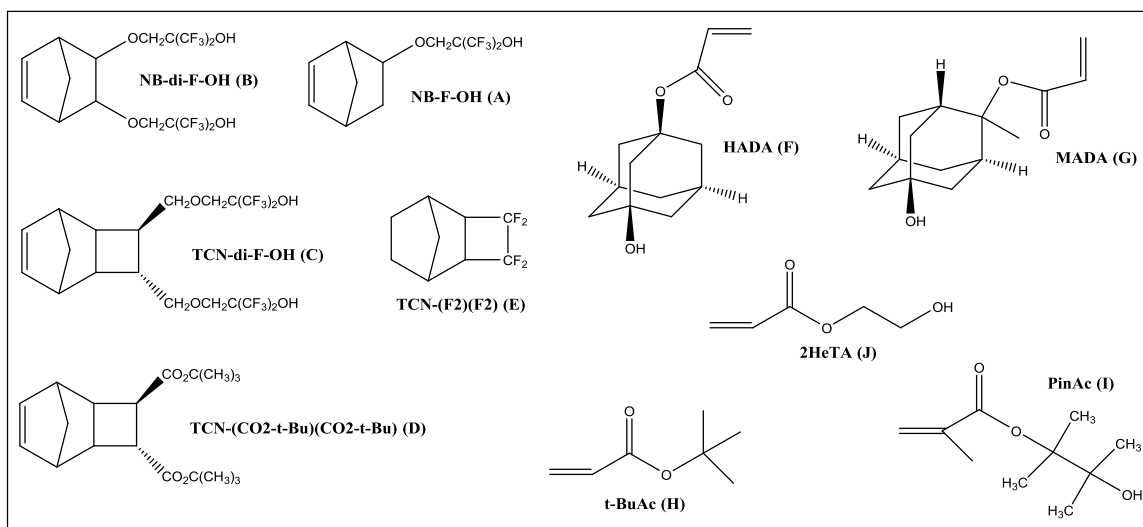


Figure 1.14. Monomers used in the preparation of co-, ter-, quad-, and pentapolymers of TFE.¹⁴⁷

Two important references in the literature^{148,149} show a series of co- and terpolymers of TFE with different monomers such as cyclopentene (CP), cyclooctene (COC), 2,3-dihydrofuran (DHF), 3,3-dimethylcyclopropene (DMCP), dicyclopentene (DCP), *tert*-butyl- α -fluoroacrylate (TFBA), 2-cyclopentene-1-*tert*-butyl acetate (CPBA),

and $\text{HOC}(\text{CF}_3)_2$ -functionalized cyclopentene (FCP). The monomers are shown in Figure 1.15.

Table 1.7. List of polymers made and their composition. Each row in the table denotes a different example in the patent.¹⁴⁷

Polymer Sample	Composition [EA: Elemental Analysis, MP: molar percentage (mol %)]
poly(TFE- <i>co</i> -C)	EA: C = 39.57; H = 3.07; F = 44.74
poly(TFE- <i>co</i> -B)	MP: 54-46
poly(TFE- <i>ter</i> -A- <i>ter</i> -B)	MP: 55-34-11
poly(TFE- <i>ter</i> -A- <i>ter</i> -B)	MP: 55-26-18
poly(TFE- <i>ter</i> -B- <i>ter</i> -G)	MP: 23-33-45
poly(TFE- <i>quad</i> -B- <i>quad</i> -I- <i>quad</i> -F)	EA: C = 46.72; H = 4.66; F = 30.69
poly(TFE- <i>quad</i> -E- <i>quad</i> -B- <i>quad</i> -H)	MP: 32- 26-10-32
poly(TFE- <i>quad</i> -E- <i>quad</i> -B- <i>quad</i> -D)	MP: 48-24-10-18
poly(TFE- <i>penta</i> -E- <i>penta</i> -B- <i>penta</i> -H- <i>penta</i> -J)	EA: C = 45.61; H = 4.02; F = 37.09
poly(TFE- <i>quad</i> -B- <i>quad</i> -J- <i>quad</i> -F)	EA: C = 46.42; H = 4.78; F = 31.61

A = NB-F-OH, B = NB-di-F-OH, C = TCN-di-F-OH, D = TCN-(CO₂-*t*-Bu)(CO₂-*t*-Bu), E = TCN-(F₂)(F₂), F = HADA, G = MADA, H = *t*-BuAc, I = PinAc, and J = 2HEtA.

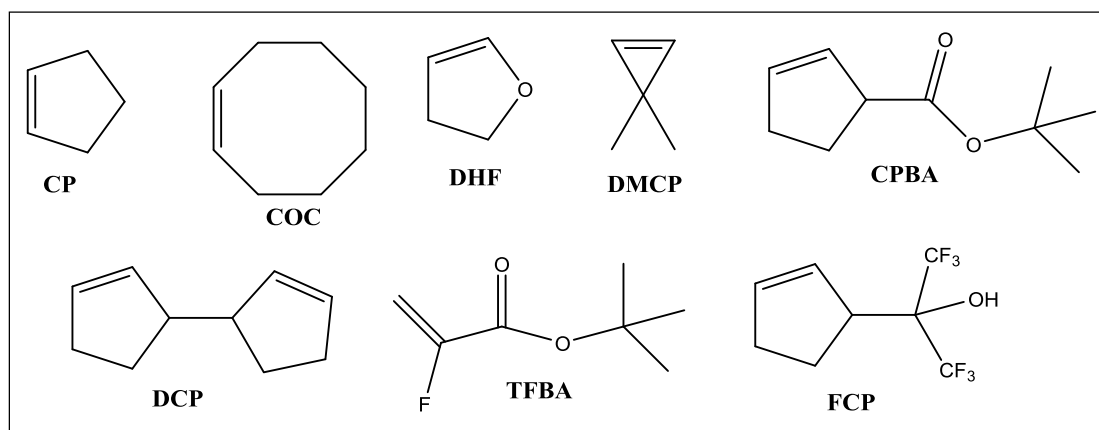


Figure 1.15. Monomers co- and terpolymerized with TFE.^{148,149}

All of the polymerizations were reported to be carried out in HCFC-141B as solvent with TCP [bis(4-*tert*-butylcyclohexyl)peroxydicarbonate] as the initiator. A full list of the final compositions of the polymers as well as their experimentally determined absorption coefficients are shown in Table 1.8. Although the poly(TFE-*co*-DMCP) and poly(TFE-*co*-DCP) copolymers were not tested for their absorption coefficients, they are included in the table in order to account for the materials being prepared.¹⁴⁸

Table 1.8. Final compositions of co- and terpolymers reported.^{148,149}

Polymer Sample	Composition (mol % for each monomer, respectively)	Absorption Coefficient at 157 nm (μm^{-1})
poly(TFE- <i>co</i> -CP)	50-50	0.9
poly(TFE- <i>co</i> -DHF)	50-50	1.0
poly(TFE- <i>co</i> -COC)	52-48	1.1
poly(TFE- <i>co</i> -DMCP)	61-39	-
poly(TFE- <i>co</i> -DCP)	51-49	-
poly(TFE- <i>ter</i> -DHF- <i>ter</i> -TFBA)	23-33-44	3.5
poly(TFE- <i>ter</i> -CP- <i>ter</i> -TFBA)	15-40-45	3.6
poly(TFE- <i>ter</i> -CP- <i>ter</i> -TFBA)	26-34-40	3.7
poly(TFE- <i>ter</i> -CP- <i>ter</i> -TFBA)	7-52-41	4.1
poly(TFE- <i>co</i> -CPBA)	50-50	3.2
poly(TFE- <i>ter</i> -CP- <i>ter</i> -FCP)	50-50	0.7

CP = cyclopentene, COC = cyclooctene, DHF = 2,3-dihydrofuran, DMCP = 3,3-dimethylcyclopropene, DCP = dicyclopentene, TFBA = *tert*-butyl- α -fluoroacrylate, CPBA = 2-cyclopentene-1-*tert*-butyl acetate, and FCP = HOC(CF₃)₂-functionalized cyclopentene.

1.6. Future Work and Conclusions

The present Chapter contains important information regarding non-commercial co- and terpolymers of TFE that have been studied mostly in the past 20 years. It is clear that

the variety of these materials is of equal (or greater) magnitude to the ones that have been commercialized on a large scale, but further work is still to be done exploring different monomers, adding other functional groups to the polymers, and using other post-polymerization processes to enhance the physical and/or chemical properties of the materials. From co- and terpolymers of TFE including alkenes (as discussed in Section 1.2) to those of cyclic monomers and tetrafluoroethylene-based photoresist materials (as shown in Section 1.5), it is clear that the applications of these polymers are vast regardless of the comonomer used.

Furthermore, one of the most important properties (especially for industrial or production purposes) is the reactivity ratio of TFE with that of any of the monomers discussed or excluded in this Chapter. Since reports of reactivity ratios do not appear in the literature very often (perhaps because of confidentiality), an open opportunity is left for researchers to investigate them. The available data for reactivity ratios of the polymers reported in this overview are summarized below in Table 1.9; a few additional data for reactivity ratios of commercial TFE-based copolymers can be found in the cited literature.¹²

Table 1.9. Reactivity ratios for copolymers of TFE.¹²

Polymer	r ₁ (TFE)	r ₂
poly(TFE- <i>co</i> -NBVE) ¹⁵⁰	0.005	0.0015
poly(TFE- <i>co</i> -VAc) ^{42,44}	-0.009	0.95
Poly(TFE- <i>co</i> -IB) ⁵³	0.005	0.021
poly(TFE- <i>co</i> -VF) ⁵⁷	0.06	0.30
poly(TFE- <i>co</i> -VF) ⁵⁸	0.05	0.27
poly(TFE- <i>co</i> -VDF) ⁶⁴	3.73	0.23
poly(TFE- <i>co</i> -VDF) ⁵⁷	0.28	0.32
poly(TFE- <i>co</i> -VDF) ¹⁵¹	0.39 ^a	3.37 ^a
poly(TFE- <i>co</i> -VDF) ¹⁵¹	1.03 ^b	0.87 ^b
poly(TFE- <i>co</i> -FA1) ⁹⁰	2.47	0.41
poly(TFE- <i>co</i> -FA3) ⁹⁰	1.57	0.45
poly(TFE- <i>co</i> -FAc) ⁹²	0.18	0.20
poly(TFE- <i>co</i> -CTFE) ⁵⁷	0.80	1.10
poly(TFE- <i>co</i> -CTFE) ⁹⁹	0.75	1.04
poly(TFE- <i>co</i> -CTFE) ¹⁰⁰	1.0	1.0
poly(TFE- <i>co</i> -BTFE) ⁹⁹	0.82	0.24
poly(TFE- <i>co</i> -CH ₂ =CHCF ₃) ¹⁰⁴	0.12	5.0
poly(TFE- <i>co</i> -CH ₂ =CHC ₃ F ₇) ¹⁰³	0.21	2.3
poly(TFE- <i>co</i> -CH ₂ =CFCF ₃) ⁹⁵	0.37	5.4
Poly(TFE- <i>co</i> -CH ₂ =C(CF ₃) ₂) ⁹⁵	0.58	0.09
poly(TFE- <i>co-trans</i> -CHF=CHCF ₃) ¹⁰²	15.9	0.059
poly(TFE- <i>co-cis</i> -CHF=CHCF ₃) ¹⁰²	11.5	0.17
poly(TFE- <i>co</i> -CF ₂ =CHF) ⁵⁷	1.14	0.46
poly(TFE- <i>co</i> -MTFP) ¹¹⁰	5.0	0.10
poly(TFE- <i>co</i> -MTFP) ¹⁵²	3.0	0.15
poly(TFE- <i>co</i> -PPOTESF) ¹³³	10.02	0.31
poly(TFE- <i>co</i> -PPOTESF) ¹³³	10.81	0.23

NBVE = *n*-butyl vinyl ether, VAc = CH₂=CHCO₂CH₃, IB = CH₂=C(CH₃)₂, VF = CH₂=CHF, VDF = CH₂CF₂, FA1 = CF₂=CFCH₂OH, FA3 = CF₂=CFC₃H₆OH, FAc = 4,5,5-trifluoro-4-ene pentyl acetate, CTFE = chlorotrifluoroethylene, BTFE = bromotrifluoroethylene, TrFE = CF₂=CHF, MTFP = CF₂=CFCO₂CH₃, PPOTESF = CF₂=CFCF₂OCF₂CF₂SO₂F.

^a in the absence of CO₂, ^b in the presence of CO₂.

1.7. Dissertation Summary

As explained in Section 1.6, reactivity ratios are important not only to industry but to academic research centers. My goal has been to lead the construction of a pilot-scale tetrafluoroethylene polymerization facility in order to carry reactions that other academic institutions are not able to perform. By doing this, I have been able to obtain reactivity ratios for several polymer systems that have not been disclosed in detail in the literature. In Chapter 2, I will cover the history of the development of tetrafluoroethylene barricades and the evolution of our facility at Clemson University. In Chapter 3, the improvements of TFE monomer preparation as well as other supporting information will be explained. In Chapter 4, the study of the synthesis of poly(TFE-*co*-VDF) using aqueous emulsion polymerization methods will be explained, as well as, the determination of the reactivity ratios of TFE and VDF in both presence and absence of carbon dioxide via ^{19}F NMR Spectroscopy. The study of the synthesis and determination of reactivity ratios of poly(TFE-*co*-PSEPVE) and poly(TFE-*co*-PSVE), and poly(TFE-*co*-DEVE) using solution polymerization methods, will be explained in Chapter 5. These last three polymer systems have been studied using solution polymerization methods in HFC-4310 and their reactivity ratios have been studied by means of molten state ^{19}F NMR Spectroscopy.

1.8. References

1. Plunkett, R. J. "The History of Polytetrafluoroethylene: Discovery and Development". In *High Perform. Polym., Proc. Symp.*; Seymour, R. B., Kirschenbaum, G. S., Eds.; 1986, pp 261-266.
2. Kauffman, G. B. Teflon – 50 Slippery Years. *Educ. Chem.* **1988**, 25, 173.
3. Hercules, D. A.; Desmarteau, D. D.; Fernandez, R. E.; Clark, J. L.; Thrasher, J. S. "Evolution of Academic Barricades for the Use of Tetrafluoroethylene (TFE) in the Preparation of Fluoropolymers". In *Handbook of Fluoropolymer Science and Technology*; 1st ed.; Iacono, S. T., Iyer, S. S., Smith, D. W., Eds.; John Wiley & Sons: Hoboken, NJ, USA, 2014, pp 415-433.
4. Ebnesajjad, S. *Fluoroplastics. Volume 1: Non-Melt Processible Fluoroplastics: The Definitive User's Guide and Databook*; 2nd ed. Plastics Design Library: Norwich, NY, 2000.
5. Ebnesajjad, S. *Fluoroplastics. Volume 2: Melt Processible Fluoropolymers: The Definitive User's Guide and Databook*; 2nd ed. Plastics Design Library: Norwich, NY, 2003.
6. Ebnesajjad, S. *Introduction to Fluoropolymers: Materials, Technology, and Applications* Elsevier: Waltham, MA, 2013.
7. Ebnesajjad, S. *Fluoropolymer Additives* Elsevier: New York, 2012.

8. Ebnesajjad, S.; Khaladkar, P. R. *Fluoropolymers Applications in Chemical Processing Industries. The Definitive User's Guide and Databook*Plastics Design Library: Norwich, NY, 2005.
9. Drobny, J. G. *Technology of Fluoropolymers*; 2nd ed. CRC Press: Boca Raton, FL, 2009.
10. Okada, D.; Saito, M.; Hayamizu, K. *Perfluorinated Polymer Electrolyte Membranes for Fuel Cells*Nova Science Publishers: New York, 2008.
11. Moore, A. L. *Fluoroelastomers Handbook. The Definitive User's Guide and Databook*William Andrew: Norwich, New York, 2006.
12. Ameduri, B.; Boutevin, B. *Well-Architected Fluoropolymers: Synthesis, Properties and Applications*Elsevier: New York, 2004.
13. *Fluorinated Surfaces, Coatings, and Films*ACS Symposium Series 787: Washington, DC, 2001.
14. *Fluoropolymers 1: Synthesis*Kluwer Academic/Plenum Publishers: New York, 1999.
15. *Fluoropolymers 2: Properties*Kluwer Academic/Plenum Publishers: New York, 1999.
16. *Modern Fluoropolymers: High Performance Polymers for Diverse Applications*John Wiley & Sons: New York, 1997.

17. *Fluorine Chemistry: A Comprehensive Treatment (Encyclopedia Reprint Series)* John Wiley & Sons: New York, 1995.
18. Gangal, S. V.; Brothers, P. D. "Perfluorinated Polymers". In *Kirk-Othmer Encyclopedia of Chemical Technology*; 2015, pp 1-68.
19. Gardiner, J. Fluoropolymers: Origin, Production, and Industrial and Commercial Applications. *Aust. J. Chem.* **2015**, 68, 13.
20. Okamoto, Y.; Mikes, F.; Koike, K.; Koike, Y. "Amorphous Fluoropolymers". In *Handbook of Fluoropolymer Science and Technology*; Smith, D. W., Iacono, S. T., Iyer, S. S., Eds.; John Wiley & Sons: New York, 2014, pp 377-391.
21. Arcella, V.; Merlo, L.; Pieri, R.; Toniolo, P.; Triulzi, F.; Apostolo, M. "Fluoropolymers for Sustainable Energy". In *Handbook of Fluoropolymer Science and Technology*; Smith, D. W., Iacono, S. T., Iyer, S. S., Eds.; John Wiley & Sons: New York, 2014, pp 393-412.
22. Arcella, V.; Troglia, C.; Ghielmi, A. Hyflon Ion Membranes for Fuel Cells. *Ind. Eng. Chem. Res.* **2005**, 44, 7646-7651.
23. Gangal, S. V. "Fluorine-Containing Polymers. Perfluorinated Ethylene-Propylene Copolymers". In *Kirk-Othmer Encyclopedia of Chemical Technology*; 2000, pp.

24. Gangal, S. V.; Brothers, P. D. In *Encyclopedia of Polymer Science and Technology*; 4th ed.; Mark, H. F., Ed.; John Wiley & Sons: Hoboken, 2014; Vol. 9, pp 487-501.
25. Ameduri, B.; Boutevin, B.; Kostov, G. Fluoroelastomers: Synthesis, Properties, and Applications. *Prog. Polym. Sci.* **2001**, 26, 105.
26. "Fluorocarbon Elastomers". In *Kirk-Othmer Encyclopedia of Chemical Technology*; 2000, pp.
27. Ameduri, B.; Boutevin, B. "Telomerization Reactions of Fluorinated Alkenes". In *Topics in Current Chemistry: Organofluorine Chemistry: Fluorinated Alkenes and Reactive Intermediates*; 1997, 192, pp 165-233.
28. Anderson, R. F.; Punderson, J. O. "Poly(tetrafluoroethylene) and Related Fluoroplastics". In *Organofluorine Chemicals and their Industrial Applications*; Banks, R. E., Ed.; Ellis Horwood: Chichester, 1979, pp 235-247.
29. Feiring, A. E. "Fluoroplastics". In *Organofluorine Chemistry: Principles and Commercial Applications*; Banks, R. E., Smart, B. E., Tatlow, J. C., Eds.; Plenum Press: New York, 1994, pp 339-372.
30. Logothetis, A. L. "Fluoroelastomers". In *Organofluorine Chemistry: Principles and Commercial Applications*; Banks, R. E., Smart, B. E., Tatlow, J. C., Eds.; Plenum Press: New York, 1994, pp 373-396.

31. Smith, S. "Fluoroelastomers". In *Preparation, Properties, and Industrial Applications of Organofluorine Compounds*; Banks, R. E., Ed.; John Wiley & Sons: New York, 1982, pp 235-295.
32. Yamabe, M. "Fluoropolymer Coating". In *Organofluorine Chemistry: Principles and Commercial Applications*; Banks, R. E., Smart, B. E., Tatlow, J. C., Eds.; Plenum Press: New York, 1994, pp 397-401.
33. Yamabe, M.; Miyake, H. "Fluorinated Membranes". In *Organofluorine Chemistry: Principles and Commercial Applications*; Banks, R. E., Smart, B. E., Tatlow, J. C., Eds.; Plenum Press: New York, 1994, pp 403-412.
34. Ameduri, B.; Kostov, G.; Brandstadter, S.; Edwards, E. B. Telomer Compositions and Production Processes. WO Patent 2008/019111 A2, Feb 14, 2008.
35. Balague, J.; Ameduri, B.; Boutevin, B. Controlled Step-Wise Telomerization of Vinylidene Fluoride, HexaFluoropropene and Trifluoroethylene with Iodofluorinated Transfer Agents. *J. Fluorine Chem.* **2000**, *102*, 253-268.
36. Hung, M. H.; Ameduri, B. Brazing Compounds. U.S. Patent 8,138,274 B2, Dec 11, 2012.
37. Hung, M. H.; Ameduri, B.; Soules, A.; Boutevin, B. Copolycondensation Polymerization of Fluoropolymers. U.S. Patent 8,247,614 B2, Aug 21, 2012.

38. Hung, M. H.; Ameduri, B.; Tillet, G. Curable Fluoroelastomer Compositions. U.S. Patent 8,288,482 B2, Oct 16, 2012.
39. Soules, A.; Ameduri, B.; Boutevin, B. Original Fluorinated Copolymers Achieved by Both Azide/Alkyne “Click” Reaction and Hay Coupling from Tetrafluoroethylene Telomers. *Macromolecules* **2010**, *43*, 4489.
40. Sharif, I.; Creager, S.; Desmarteau, D. D. "Fluorinated Ionomers and Ionomer Membranes Containing the Bis[(Perfluoroalkyl)sulfonyl]imide Protogenic Group". In *Handbook of Fluoropolymer Science and Technology*; 1st ed.; Iacono, S. T., Iyer, S. S., Smith, D. W., Eds.; John Wiley & Sons: Hoboken, NJ, USA, 2014, pp 521-544.
41. Baradie, B.; Shoichet, M. S. Insight into the Surface Properties of Fluorocarbon–Vinyl Acetate Copolymer Films and Blends. *Macromolecules* **2003**, *36*, 2343-2348.
42. Baradie, B.; Shoichet, M. S. Novel Fluoro-Terpolymers for Coatings Applications. *Macromolecules* **2005**, *38*, 5560-5568.
43. Boutevin, B.; Pietrasanta, Y. The Synthesis and Applications of Fluorinated Silicones, Notably in High-Performance Coatings. *Progress in Organic Coatings* **1985**, *13*, 297-331.

44. Baradie, B.; Shoichet, M. S. Synthesis of Fluorocarbon–Vinyl Acetate Copolymers in Supercritical Carbon Dioxide: Insight into Bulk Properties. *Macromolecules* **2002**, *35*, 3569-3575.
45. Cleek, R. L.; Cully, E. H.; Drumheller, P. D.; Holland, T. A. Polytetrafluoroethylene Co-Polymer Emulsions. U.S. Patent 2014/0072514 A1, Mar 13, 2014.
46. Cripps, H. N. Partially Fluorinated Polyesters from Ketene Acetals and Fluorinated Vinyl Monomers. U.S. Patent 4,906,714, Mar 6, 1990.
47. Bailey, W. J.; Ni, Z.; Wu, S. Free Radical Ring-Opening Polymerization of 4,7-Dimethyl-2-methylene-1,3-dioxepane and 5,6-Benzo-2-methylene-1,3-dioxepane. *Macromolecules* **1982**, *15*, 711-714.
48. Kostov, G.; Nikolov, A.; Atanasov, A. N. *J. Appl. Polym. Sci.* **2001**, *81*, 2626.
49. Kostov, G.; Bessiere, J. M.; Guida-Pietrasanta, F.; Bauduin, G.; Petrov, P. Study of the Microstructure and Thermal Properties of Tetrafluoroethylene–Propylene Elastomers. *European Polymer Journal* **1999**, *35*, 743-749.
50. Kostov, G. K.; Petrov, P. C. Stress-Relaxation Study of Tetrafluoroethylene-Propylene Rubbers. *Polymer* **1995**, *36*, 3683-3686.

51. Kostov, G. K.; Atanassov, A. N. Ion-Exchange Copolymers Based on Tetrafluoroethylene, Hexafluoropropylene, and Acrylic Acid. *J. Appl. Polym. Sci.* **1991**, *42*, 1607-1613.
52. Kostov, G. K.; Atanassov, A. N. SYNTHESIS OF HYDROPHILIC ION-EXCHANGE FLUOROPOLYMERS CONTAINING S U L P H O - A N D B O T H S U L P H O - A N D CARBOXYL GROUPS Sulphonation of TFE-HFP-AAc copolymers. *Eur. Polym. J.* **1991**, *27*, 1331-1333.
53. Brown, D. W.; Lowry, R. E.; Wall, L. A. Glass and Melting Transitions of Copolymers of Tetrafluoroethylene with Propylene and Isobutylene. *J. Polym. Sci., Polym. Phys. Ed.* **1974**, *12*, 1303-1318.
54. Uschold, R. E. Patent. **1998**.
55. Brown, M. J.; Felix, V. M.; Periyasamy, M.; Uschold, R. E. Melt-Processible Vinyl Fluoride Interpolymers of Low Crystallinity. WO Patent 2015/002824 A1, Jan 8, 2015.
56. Coffman, D. D.; Ford, T. A. Vinyl Fluoride Copolymers. U.S. Patent 2,419,009, Apr 15, 1947.
57. Naberezhnykh, R. A.; Sorokin, A. D.; Volkova, E. V.; Fokin, A. V. No Title. *Izv. Akad. Nauk SSSR, Ser. Khim.* **1974**, *23*, 232-235.

58. Sianesi, D.; Caporiccio, G. Polymerization and Copolymerization Studies on Vinyl Fluoride. *Journal of Polymer Science Part A-1: Polymer Chemistry* **1968**, *6*, 335-352.
59. Sianesi, D.; Caporiccio, G. Patent. **1970**.
60. Stilmar, F. B. Patent. **1970**.
61. Golub, M. A.; Wydeven, T. Relative Rates for Plasma Homo- and Copolymerizations of a Homologous Series of Fluorinated Ethylenes. *Plasma Polym.* **1998**, *3*, 35-42.
62. Dillon, D. R.; Tenneti, K. K.; Li, C. Y.; Ko, F. K.; Sics, I.; Hsiao, B. S. On the Structure and Morphology of Polyvinylidene Fluoride–Nanoclay Nanocomposites. *Polymer* **2006**, *47*, 1678-1688.
63. Lovinger, A. J. Ferroelectric Transition in a Copolymer of Vinylidene Fluoride and Tetrafluoroethylene. *Macromolecules* **1983**, *16*, 1529-1534.
64. Moggi, G.; Bonardelli, P.; Bart, J. C. Copolymers of 1,1-Difluoroethene with Tetrafluoroethene, Chlorotrifluoroethene, and Bromotrifluoroethene. *J. Polym. Sci., Polym. Phys. Edit.* **1984**, *22*, 357-365.
65. Carr, J. M.; Mackey, M.; Flandin, L.; Schuele, D.; Zhu, L.; Baer, E. Effect of Biaxial Orientation on Dielectric and Breakdown Properties of Poly(ethylene

- terephthalate)/Poly(vinylidene fluoride-co-tetrafluoroethylene) Multilayer Films. *J. Polym. Sci. Part B: Polym. Phys.* **2013**, *51*, 882-896.
66. Chu, B.; Zhou, X.; Ren, K.; Neese, B.; Lin, M.; Wang, Q.; Bauer, F.; Zhang, Q. M. A Dielectric Polymer with High Electric Energy Density and Fast Discharge Speed. *Science* **2006**, *313*, 334-336.
 67. Zhou, X.; Chu, B.; Neese, B.; Lin, M.; Zhang, Q. M. No Title. *IEEE Trans. Dielect. Electr. Insul.* **2007**, *14*, 1333.
 68. Zhang, Z.; Chung, T. C. M. The Structure-Property Relationship of Poly(vinylidene difluoride)-Based Polymers with Energy Storage and Loss under Applied Electric Fields. *Macromolecules* **2007**, *40*, 9391-9397.
 69. Li, J.; Hu, X.; Gao, G.; Ding, S.; Li, H.; Yang, L.; Zhang, Z. Tuning Phase Transition and Ferroelectric Properties of Poly(vinylidene fluoride-co-trifluoroethylene) via Grafting with Desired Poly(methacrylic ester)s as Side Chains. *J. Mater. Chem. C* **2013**, *1*, 1111-1121.
 70. Vogelsang, R.; Farr, T.; Frohlich, K. No Title. *IEEE Trans. Dielect. Electr. Insul.* **2006**, *13*, 373.
 71. Murata, Y.; Koizumi, N. No Title. *Ferroelectrics* **1989**, *92*, 47.
 72. Liu, Q.; Khatri, I.; Ishikawa, R.; Fujimori, A.; Manabe, K.; Nishiro, H.; Shirai, H. No Title. *Appl. Phys. Lett.* **2013**, *103*, 163503.

73. Ohigashi, H. Piezoelectric Polymers – Materials and Manufacture. *Jap. J. Appl. Phys.* **1985**, 24, 23-27.
74. Kim, J. H.; Park, T. K.; Lee, H.; Lee, D. J. No Title. *Korea Polym. J.* **1995**, 3, 101.
75. Kochervinskii, V. V.; Kiselev, D. A.; Malinkovich, M. D.; Pavlov, A. S.; Malyshkina, I. A. Local Piezoelectric Response, Structural and Dynamic Properties of Ferroelectric Copolymers of Vinylidene Fluoride–tetrafluoroethylene. *Colloid Polym. Sci.* **2015**, 293, 533-543.
76. Guo, Y.; Hoshino, K.; Hanna, J.-i.; Kokado, H. No Title. *Jpn. J. Appl. Phys.* **1992**, 31, 1830.
77. Hull, E.; Johnson, B. V.; Rodricks, I. P.; Staley, J. B. In *Modern Fluoropolymers: High Performance Polymers for Diverse Applications*; Scheirs, J., Ed.; John Wiley & Sons: New York, 1997, p 257-270.
78. Pellerite, M. No Title. *Polym. Prepr. (Am. Chem. Soc., Div. Polym. Chem.)* **2005**, 46, 741.
79. Pacetti, S. No Title. **2008**.
80. Kojima, G.; Kodama, S. In *In Handbook for Fluoropolymer*; Satokawa, T., Shinnbunnsya, N. K., Eds. Tokyo, 1990, p 611-624.

81. Tate, N.; Saito, M.; Sugitani, K., In *Proceedings of JSAE/SAE 2003 Spring Fuels and Lubricants Meeting*, SAE Technical Paper 2003-01-2000, Yokohama, Japan, May 19–22, 2003.
82. Hull, E. J., B. V.; Rodricks, I. P.; Staley, J. B. "THV Fluoroplastic". In *Modern Fluoropolymers*; Scheirs, J., Ed.; Wiley: New York, 1997, pp 257-270.
83. Murasheva, Y. M.; Shashkov, A. S.; Dontsov, A. A. Analysis of the ^{19}F NMR Spectra of Copolymers of Vinylidene Fluoride with Tetrafluoroethylene, and of Vinylidene Fluoride with Tetrafluoroethylene and Hexafluoropropylene. The Use of an Empirical Additive Scheme and of the Principle of Alternation. *Polym. Sci. U.S.S.R.* **1981**, 23, 711-720.
84. Pianca, M.; Bonardelli, P.; Tatò, M.; Cirillo, G.; Moggi, G. Composition and Sequence Distribution of Vinylidene Fluoride Copolymer and Terpolymer Fluoroelastomers. Determination by ^{19}F Nuclear Magnetic Resonance Spectroscopy and Correlation with some Properties. *Polymer* **1987**, 28, 224-230.
85. Luttringer, G.; Meurer, B.; Weill, G. Microstructure of Vinylidene Fluoride and Tetrafluoroethylene Copolymers by High-Resolution ^{19}F Nuclear Magnetic Resonance. *Polymer* **1992**, 33, 4920-4928.
86. Li, L.; Twum, E. B.; Li, X.; McCord, E. F.; Fox, P. A.; Lyons, D. F.; Rinaldi, P. L. 2D-NMR Characterization of Sequence Distributions in the Backbone of

- Poly(vinylidene fluoride- co -tetrafluoroethylene). *Macromolecules* **2012**, *45*, 9682-9696.
87. Li, X.; Baughman, J.; Gao, C.; Li, L.; Rinaldi, P. L.; Twum, E. B.; McCord, E. F.; Wyzgoski, F. J. "Multidimensional NMR of Fluoropolymers". In *Handbook of Fluoropolymer Science and Technology*; 1 ed.; Iyer., S. T. I. a. S. S., Ed.; John Wiley & Sons, Inc.: Hoboken, NJ, USA, 2014, pp 565-598.
 88. Twum, E. B.; McCord, E. F.; Lyons, D. F.; Rinaldi, P. L. Multidimensional ^{19}F NMR Analyses of Terpolymers from Vinylidene Fluoride (VDF)–Hexafluoropropylene (HFP)–Tetrafluoroethylene (TFE). *Macromolecules* **2015**, *48*, 3563-3576.
 89. Chalmers, J. R. Patent. **1969**.
 90. Ameduri, B.; Bauduin, G.; Kostov, G. K.; Petrova, P.; Rousseau, A. Synthesis and Polymerization of Fluorinated Monomers Bearing a Reactive Lateral Group - Part 7. Copolymerization of Tetrafluoroethylene with Omega-Hydroxy Trifluorovinyl Monomers. *J. Appl. Polym. Sci.* **1999**, *73*, 189-202.
 91. Petrova, P.; Ameduri, B.; Kostov, G.; Boutevin, B. Patent. **2000**.
 92. Kostov, G.; Améduri, B.; Boutevin, B.; Bauduin, G.; Stankova, M. Synthesis and Characterization of Original Functional Polymers of Tetrafluoroethylene and 4,5,5-Trifluoro-4-ene Pentyl Acetate. *Journal of Polymer Science Part A: Polymer Chemistry* **2004**, *42*, 1693-1706.

93. Ameduri, B.; Boutevin, B.; Kostov, G.; Petrov, P.; Petrova, P. *J. Polym. Sci., Part A: Polym. Chem.* **1999**, 37, 3991.
94. Takahiro, K.; Tsuyoshi, I.; Seiji, K. Patent. **2010**.
95. Brown, D. W.; Lowry, R. E.; Wall, L. A. Radiation-Induced Polymerization at High Pressure of 2, 3, 3, 3-Tetrafluoropropene in Bulk and with Tetrafluoroethylene. *J. Polym. Sci., Part A: Polym. Chem.* **1971**, 9, 1993-2007.
96. Nakano, Y.; Kouketsu, Y.; Sagisaka, S.; Fukagawa, R.; Murakami, S.; Hirao, T. Patent. **2013**.
97. Nakano, Y.; Kouketsu, Y.; Sagisaka, S.; Murakami, S.; Komori, M.; Inaba, T.; Hirao, T. Patent. **2012**.
98. Bruk, M. B.; Abkin, A. D.; Khomikovskii, P. M.; Kotin, Y. B. Liquid-Phase, Radiation Polymerization of Tetrafluoroethylene and its Copolymerization with Trifluorochloroethylene at Low Temperatures. *Polym. Sci. U.S.S.R.* **1973**, 15, 549-560.
99. Moggi, G.; Bonardelli, P.; Monti, C. Copolymers of Tetrafluoroethene with Chlorotrifluoroethene and with Bromotrifluoroethene. *J. Polym. Sci., Polym. Phys. Ed.* **1985**, 23, 1099-1108.
100. Young, L. J. Copolymerization Parameters. *Journal of Polymer Science* **1961**, 54, 411-455.

101. Hatakeyama, A. Patent. **2012**.
102. Brown, D. W.; Lowry, R. E.; Wall, L. A. Radiation-Induced Polymerization at High Pressure. *J. Polym. Sci., Part A: Polym. Chem.* **1973**, *11*, 1973-1984.
103. Brown, D. W.; Lowry, R. E.; Wall, L. A. Radiation-Induced Copolymerization of Tetrafluoroethylene and 3,3,4,4,5,5,5-Heptafluoropentene-1 Under Pressure. *J. Polym. Sci., Part A: Polym. Chem.* **1970**, *8*, 2441-2452.
104. Brown, D. W.; Wall, L. A. The Radiation-Induced Copolymerization of Tetrafluoroethylene and 3,3,3-Trifluoropropene under Pressure. *J. Polym. Sci., Part A: Polym. Chem.* **1968**, *6*, 1367-1379.
105. Brown, D. W.; Wall, L. A. High -Temperature Aging of Fluoropolymers. *J. Polym. Sci., Part A: Polym. Chem.* **1972**, *10*, 2967-2982.
106. Wall, L. A.; Brown, D. W. Patent. **1974**.
107. Funaki, A.; Arai, K.; Aida, S.; Phongtamrug, S.; Tashiro, K. Influence of Third Monomer on the Crystal Phase Transition Behavior of Ethylene–Tetrafluoroethylene Copolymer. *Polymer* **2008**, *49*, 5497-5503.
108. Favereau, D. A.; Farnsworth, D.; Pasquale, A. J. Patent. **2005**.
109. Taguchi, D.; Iruya, K.; Kotera, S. Patent. **2011**.

110. Watanabe, T.; Momose, T.; Ishigaki, I.; Tabata, Y.; Okamoto, J. Radiation-Induced Copolymerization of Methyl Trifluoroacrylate with Fluoroolefin. *J. Polym. Sci., Polym. Lett. Ed.* **1981**, *19*, 599-602.
111. Weise, J. K. No Title. *Polym. Preprints (American Chemical Society, Division of Polymer Chemistry)* **1971**, *12*, 512.
112. Kostov, G. K.; Atanasov, A. N. Synthesis of Hydrophilic Ion-Exchange Fluoropolymers Containing Sulpho- and both Sulpho- and Carboxyl Groups. *Eur. Polym. J.* **1991**, *27*, 1331-1333.
113. Kostov, G. K.; Kotov, S. V.; Ivanov, G. D. Synthesis of a Copolymer of Tetrafluoroethylene and 1-Fluorosulfonyl-Difluoroacetylfluoride. *J. Appl. Polym. Sci.* **1991**, *42*, 2761-2766.
114. Kostov, G. K.; Matsuda, O.; Machi, S.; Tabata, Y. Radiation Synthesis of Ion-Exchange Carboxylic Fluorine Containing Membranes. *J. Membrane Sci.* **1992**, *68*, 133-140.
115. Sabol, E. A.; Baillie, R. L. Copolymers of Tetrafluoroethylene. U.S. Patent 7,531,611 B2, May 12, 2009.
116. Ford, L. A. Patent. **2015**.
117. Higuchi, S.; Matsuoka, Y.; Kobayashi, S. Polytetrafluoroethylene Aqueous Emulsion and Process for its Production, Polytetrafluoroethylene Aqueous

- Dispersion Obtainable by Using Such an Aqueous Emulsion, Polytetrafluoroethylene Fine Powder, and Stretched Porous Material. U.S. Patent 2012/0202906 A1, Aug 9, 2012.
118. Okamoto, Y.; Koike, Y.; Liu, W.-H.; Guo, Y. Fluorinated Polymers, Method for Producing the Fluorinated Compounds and Polymers. U.S. Patent 7,582,714 B2, Sep 1, 2009.
 119. Okamoto, Y.; Y, K.; Liu, W.-H.; Guo, Y. Patent. **2010**.
 120. Yang, Z.-y. An Extraordinarily Rapid Polymerization of Vinylpentafluorocyclopropane : Highly Stereo- and Regioselective Synthesis of Unsaturated Fluoropolymers. *J. Am. Chem. Soc.* **2003**, *125*, 870-871.
 121. Yang, Z.-Y. Patent. **1995**.
 122. Araki, T.; Komatsu, Y.; Koh, M. Fluorine-Containing Ethylenic Monomer Having Hydroxyl Group or Fluoroalkyl Carbonyl Group and Fluorine-Containing Polymer Prepared by Polymerization of Same. U.S. Patent 7,214,470 B2, May 8, 2007.
 123. Sargeant, P. B.; Krespax, C. G. Fluorocyclopropanes . IV . Copolymers of Perfluorocyclopropene. *J. Polym. Sci., Part A: Polym. Chem.* **1969**, *1*, 1467-1478.
 124. Barkdoll, A. E.; Sargeant, P. B. Halotrifluorocyclopropenes. U.S. Patent 3,634,525, Jan 11, 1972.

125. Barkdoll, A. E.; Sargeant, P. B. Halotrifluorocyclopropenes. U.S. Patent 3,413,275, Nov 26, 1968.
126. Harmon, J. Copolymers of Cyclic Fluorine-Containing Compounds. U.S. Patent 2,511,258, Jun 13, 1950.
127. Harris, J. F. Polymers of Hexafluorocyclopentadiene and Perfluorodicyclopentadiene. U.S. Patent 3,449,304, Jun 10, 1969.
128. Dixon, G. D.; Feast, W. J.; Knight, G. J.; Mobbs, R. H.; Musgrave, W. K. R.; Wright, W. W. Preparation and Thermal Degradation of Copolymers of Tetrafluoroethylene and Perfluoroalkenes. *Eur. Polym. J.* **1969**, 5, 295-306.
129. Barr, D. A.; Haszeldine, R. N. Perfluoroalkyl Derivatives of Nitrogen. Part I . Perfluoro-2-methyl-1 : 2-oxazetidine and Perfluoro(alkylenealkylamines). *J. Chem. Soc.* **1955**, 1881-1889.
130. Oliver, W. H.; Stump, E. C. Patent. **1969**.
131. Jones, R. J. Nitroso Perfluoro Addition Polymers. U.S. Patent 3,761,453, Sep 25, 1973.
132. Krespan, C. G. Patent. **1981**.
133. Kostov, G. K.; Kotov, S. V.; Ivanov, G. D.; Todorova, D. Study on the Synthesis of Perfluorovinyl-Sulfonic Functional Monomer and Its Copolymerization with Tetrafluoroethylene. *J. Appl. Polym. Sci.* **1993**, 47, 735-741.

134. Kostov, G. K.; Kotov, S. V.; Ivanov, G. D. Synthesis of a Copolymer of Tetrafluoroethylene and. *J. Appl. Polym. Sci.* **1991**, *42*, 2761-2766.
135. Kaneko, I.; Watakabe, A.; Tayanagi, J.; Saito, S. Fluorosulfonyl Group-Containing Compound, Method for its Production and Polymer Thereof. U.S. Patent 7,531,610 B2, May 12, 2009.
136. Silva, A. D.; Ober, C. K. "Patterning by Photolithography". In *Functional Polymer Films*; 1st ed.; Knoll, W., Advincula, R. C., Eds.; Wiley-VCH: 2011, pp 475-499.
137. Cefalas, A. C. Current Trends in 157nm Dry Lithography. *Applied Surface Science* **2005**, *247*, 577-583.
138. Rothschild, M.; Bloomstein, T. M.; Fedynyshyn, T. H.; Liberman, V.; Mowers, W.; Sinta, R.; Switkes, M.; Grenville, A.; Orvek, K. Fluorine—an Enabler in Advanced Photolithography. *Journal of Fluorine Chemistry* **2003**, *122*, 3-10.
139. Crawford, M. K.; Farnham, W. B.; Feiring, A. E.; Feldman, J.; French, R. H.; Leffew, K. W.; Petrov, V. A.; Schadt, F. L.; Zumsteg, F. C. Fluoropolymers for 157 nm Lithography: Performance of Single Layer Resists. *J. Photopolym. Sci. Tech.* **2002**, *15*, 677-687.
140. Feiring, A. E.; Crawford, M. K.; Farnham, W. B.; Feldman, J.; French, R. H.; Junk, C. P.; Leffew, K. W.; Petrov, V. A.; Qiu, W.; Schadt, F. L.; Tran, H. V.; Zumsteg, F. C. New Amorphous Fluoropolymers of Tetrafluoroethylene with Fluorinated

- and Non-Fluorinated Tricyclonones. Semiconductor Photoresists for Imaging at 157 and 193 nm. *Macromolecules* **2006**, *39*, 3252-3261.
141. Feiring, A. E.; Crawford, M. K.; Farnham, W. B.; Feldman, J.; French, R. H.; Junk, C. P.; Leffew, K. W.; Petrov, V. A.; Qiu, W.; Schadt, F. L.; Tran, H. V.; Zumsteg, F. C. Design of Very Transparent Fluoropolymer Resists for Semiconductor Manufacture at 157 nm. *J. Fluorine Chem.* **2003**, *122*, 11-16.
 142. Koh, M.; Ishikawa, T.; Araki, T.; Aoyama, H.; Yamashita, T.; Yamazaki, T.; Watanabe, H.; Toriumi, M.; Itani, T. The Study on Dry Etch Resistance of Fluorine Functionalized Polymers. *Proc. SPIE – Int. Soc. Opt. Eng.* **2002**, *4690*, 486-496.
 143. Ishikawa, T.; Kodani, T.; Yoshida, T.; Moriya, T.; Yamashita, T.; Toriumi, M.; Araki, T.; Aoyama, H.; Hagiwara, T.; Furukawa, T.; Itani, T.; Fujii, K. Dissolution Behavior of Tetrafluoroethylene-based Fluoropolymers for 157-nm Resist Materials. *Journal of Fluorine Chemistry* **2004**, *125*, 1791-1799.
 144. Crawford, M. K.; Farnham, W. B.; Feiring, A. E.; Feldman, J.; French, R. H.; Leffew, K. W.; Petrov, V. A.; Schadt, F. L.; Zumsteg, F. C. Single Layer Fluoropolymer Resists for 157 nm Lithography. *J. Photopolym. Sci. Technol.* **2003**, *5039*, 80-92.
 145. Toriumi, M.; Ishikawa, T.; Kodami, T.; Koh, M.; Moriya, T.; Araki, T.; Aoyama, H.; Yamashita, T.; Yamazaki, T.; Furukawa, T.; Itani, T. Tetrafluoroethylene-based

- Fluoropolymers for 157-nm Resist Materials. *J. Photopolym. Sci. Technol.* **2003**, *16*, 607-613.
146. Yamashita, T.; Masamachi, M.; Yoshito, T.; Santillan, J. J.; Toshiro, I. High-sensitivity EUV Resists based on Tetrafluoroethylene Contained Fluoropolymers. *J. Photopolym. Sci. Technol.* **2011**, *24*, 165-172.
147. Crawford, M. K.; Tran, H. V.; Schadt, F. L.; Zumsteg, F. C.; Feiring, A. E.; Fryd, M. Photoresists Comprising Polymers Derived from Fluoroalcohol-Substituted Polycyclic Monomers. U.S. Patent 7,507,522 B2, Mar 24, 2009.
148. Araki, T.; Ishikawa, T.; Koh, M. Fluorine-Containing Polymer, Resist Composition Prepared from Same and Novel Fluorine-Containing Monomer. U.S. Patent 7,511,179, Mar 31, 2009.
149. Toriumi, M.; Yamazaki, T.; Watanabe, H.; Itani, T.; Araki, T.; Koh, M.; Ishikawa, T. Method of Forming Fine Pattern. U.S. Patent 2004/0248042 A1, Dec 9, 2004.
150. Hikita, T.; Tabata, Y.; Oshima, K.; Ishigure, K. Radiation-Induced Copolymerization of Tetrafluoroethylene with Vinyl Ethers. *J. Polym. Sci., Part A: Polym. Chem.* **1972**, *10*, 2941-2949.
151. Hercules, D. A.; Thrasher, J. S. Reactivity Ratios of Poly(TFE-co-VDF). Unpublished Results.

152. Weise, J. K. *Polym. Preprints (American Chemical Society, Division of Polymer Chemistry)* **1971**, 12, 512.

Chapter 2

Development of Academic Tetrafluoroethylene (TFE) Polymerization Facilities

2.1. Introduction

Throughout the history of the use of tetrafluoroethylene (TFE) in the making of fluoropolymers and other materials, one can see that TFE is only ever used in industry due to the inherent safety precautions with the compound (*vide infra*). It is well known that TFE is a deflagrant with the equivalent release of energy of black gunpowder,¹ and therefore the development of barricades has been undertaken by industry in order to be able to work with TFE in safe a manner. On the other hand, industry is in constant downsizing and looking for alternative places to both carry out basic research and develop new products, and thus it is attractive to have access to an academic institution capable of working with TFE in order to carry out research projects at a lower operational cost. Another factor that keeps industrial plants from expanding is that R&D sites were traditionally secluded from major populations, but with the increasing expansion of cities around the industrial sites it has become harder to be secluded from highly populated areas and therefore carrying dangerous procedures becomes more difficult. Industry has invested a huge amount of resources in developing barricades for various uses and processes. The

barricade style that is widely used in industrial setups is compartmentalized into smaller rooms and several rooms are located side-by-side as shown in Figure 2.1.

It can also be observed in Figure 2.1 that the arrangement of rooms allows access from only one side through a steel sliding door. Each room has a reinforced view window opposite the door, in which the operator can see the entirety of the room. The operator would locate the reactor or dangerous equipment inside the room and operate the process from the outside. During the operation, no operator would remain standing at the back of the rooms (where the only entrance is located) in order to avoid the weakest point of the room giving in and exposing the operator to fragments of an explosion.²

There have been other designs of reaction room barricades that include a barrier wall to protect other buildings against flying projectiles. In Figure 2.2 one can observe a sketch of such rooms where an overhanging concrete wall serves as a blast mat in front of an earthen berm. The entrance of each reaction room is at the back of the building (on the earthen berm side), and the front walls of the building are built of reinforced concrete to protect the operators as shown in the schematic in Figure 2.3.³

The disadvantages of the design shown in Figure 2.2 are that it could reflect projectiles that bounce off the earthen berm and that the capital cost of such a development is large and it requires a great area of construction not only to host the development but also to keep away other buildings.

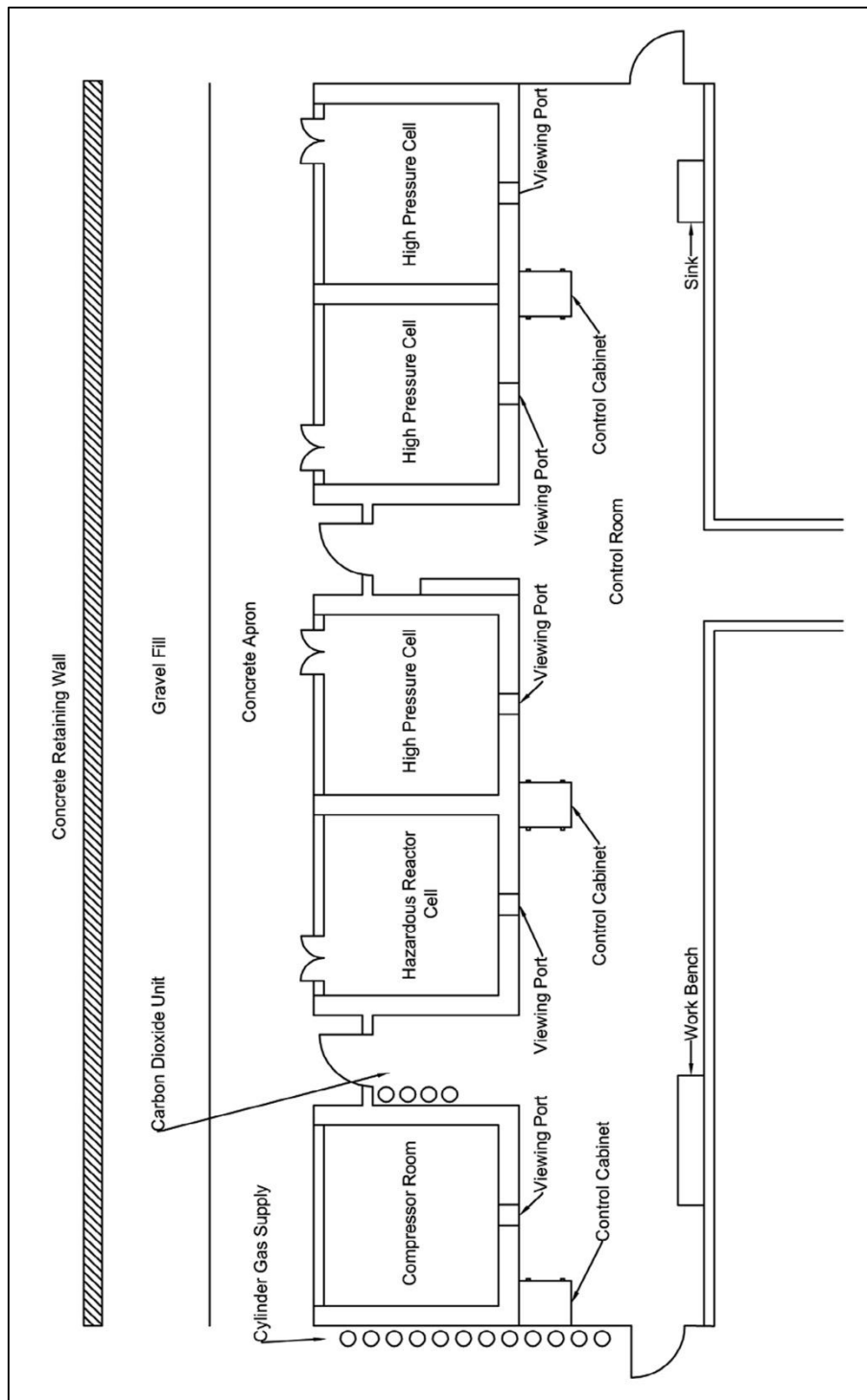


Figure 2.1. Schematic of a barricade setup with its rooms side by side.²

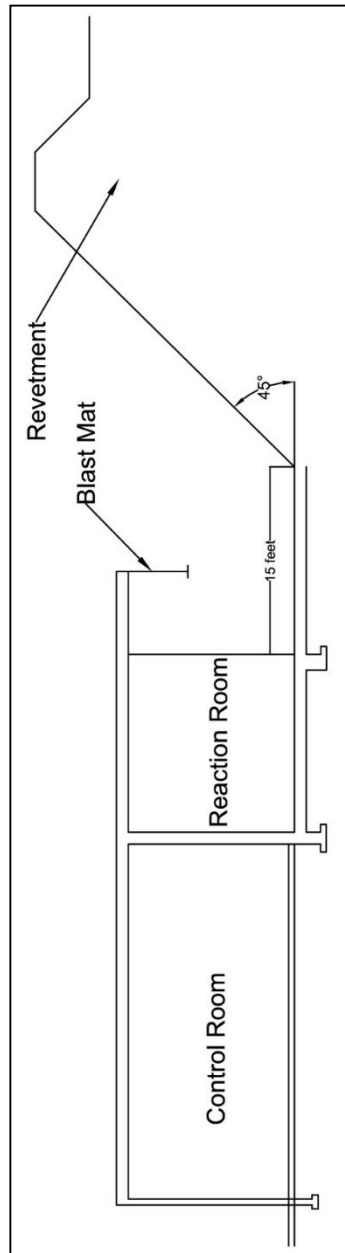


Figure 2.2. Schematic of a reaction cell unit equipped with an earthen berm at the back of the unit.³

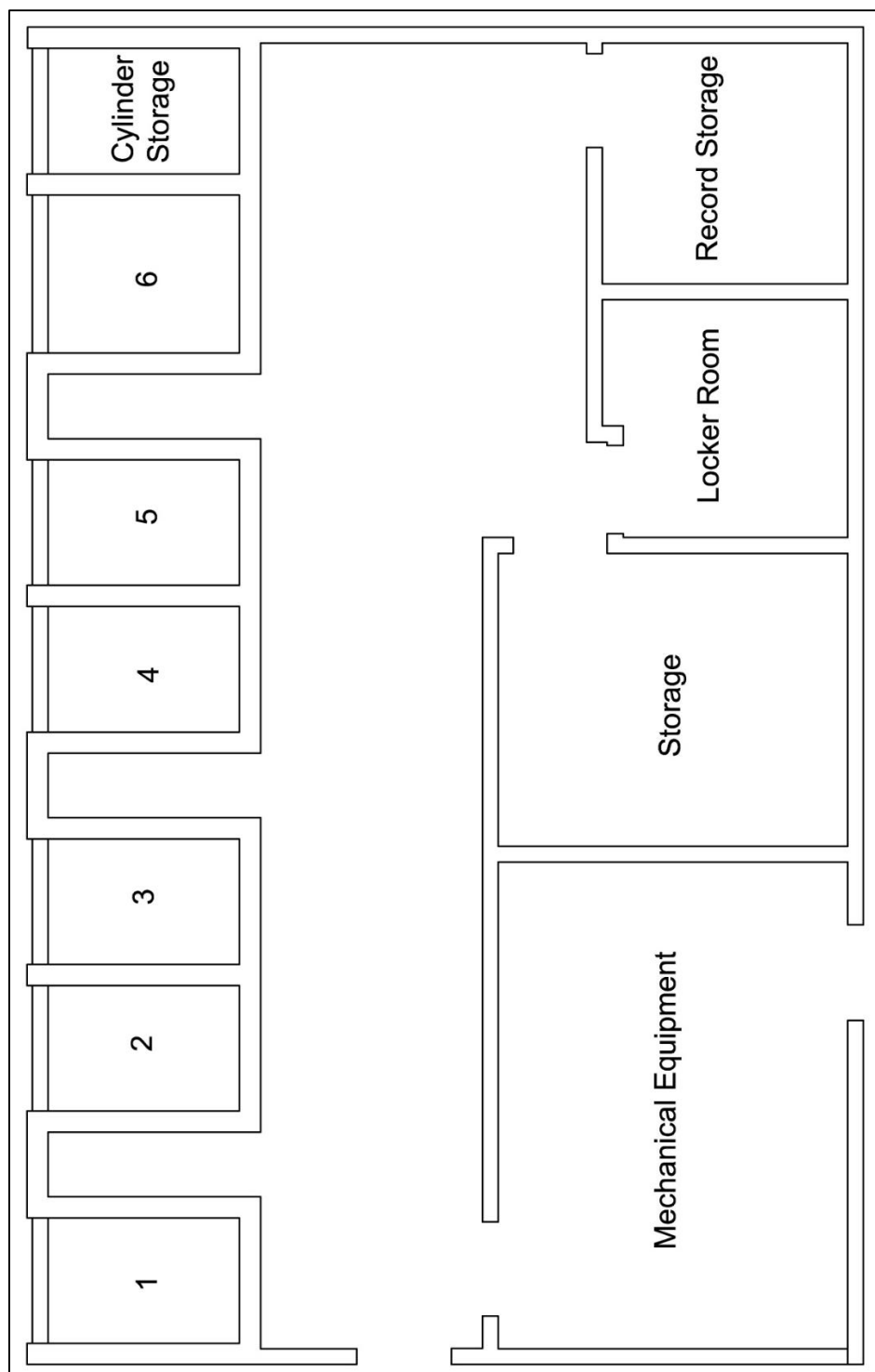


Figure 2.3. Schematic for multi-cell barricade setup. Individual cells are numbered 1 through 6.³

One of the first reported uses of a flanged panel was made in 1957⁴ in the use of pressure reactors inside reaction rooms. The idea behind the blowout panel is to disperse and guide any type of deflagration material in case of an explosion instead of making the walls of the room resist the high pressure of an explosion.

Another option that has been considered is to use a blowout roof system. The main disadvantage is the lack of control of bouncing projectiles in the case of an explosion. Also, if there is an explosion resulting in a high release of pressure onto the roof, it could result in blowing the roof system out of place if it is not properly anchored to the reaction room.⁵

The last strategy industry has developed to reduce building space and increase productivity is to introduce the pressurized reactor into a containment vessel. The vessel is designed in steel and is usually divided in two parts so that one can be lifted exposing the interior for ease of setup and manipulation of the equipment prior to and post reaction. Such containment vessels, as shown in Figure 2.4,² allocate a reinforced glass or polycarbonate window at the front so the operator can look inside the vessel during the reaction. The vessel is rated to safely contain a release of pressure that could occur during an explosion. Notice in Figure 2.4 that the containment vessel has service sleeves in the bottom of the vessel in order to introduce any service gases needed for the reaction, nitrogen, vacuum, water cooling, etc.

In 1984 E. I. du Pont de Nemours and Company patented a containment vessel for high pressure reactions, which include explosive reactions.⁶ The explosiveness rating of such a vessel is reported as the equivalent force generated by a given quantity of

2,4,6-trinitrotoluene (TNT). For the invention, it was reported that a vessel of approximately 4000 lbs in weight is designed to contain an explosive energy equivalent of 340 g of TNT. No information exists on whether the vessel was used in TFE polymerization reactions or how much TFE can be handled in such vessel. A schematic of such a containment vessel is shown in Figure 2.5.⁶

One of the major disadvantages of this design is that the internal space of the vessel is relatively small compared to the size of the vessel and therefore the amount of equipment, or the size of the reactor, is constricted to the amount of space inside the vessel. A 2-gal vertical polymerization reactor is almost 6 feet tall, and one can imagine the large size of a containment vessel needed to allocate such a size reactor.

To the best of my knowledge, very little is known about construction of barricades that are specifically designed to handle TFE polymerization reactions, and therefore a great need for the development of such a facility was a key motivating factor for its construction at Clemson University. One of the major problems of the development of a TFE polymerization facility at an academic institution is that the fluorochemical industry will typically not share detailed plans of their barricades because of the high risk that they imply and liability issues.

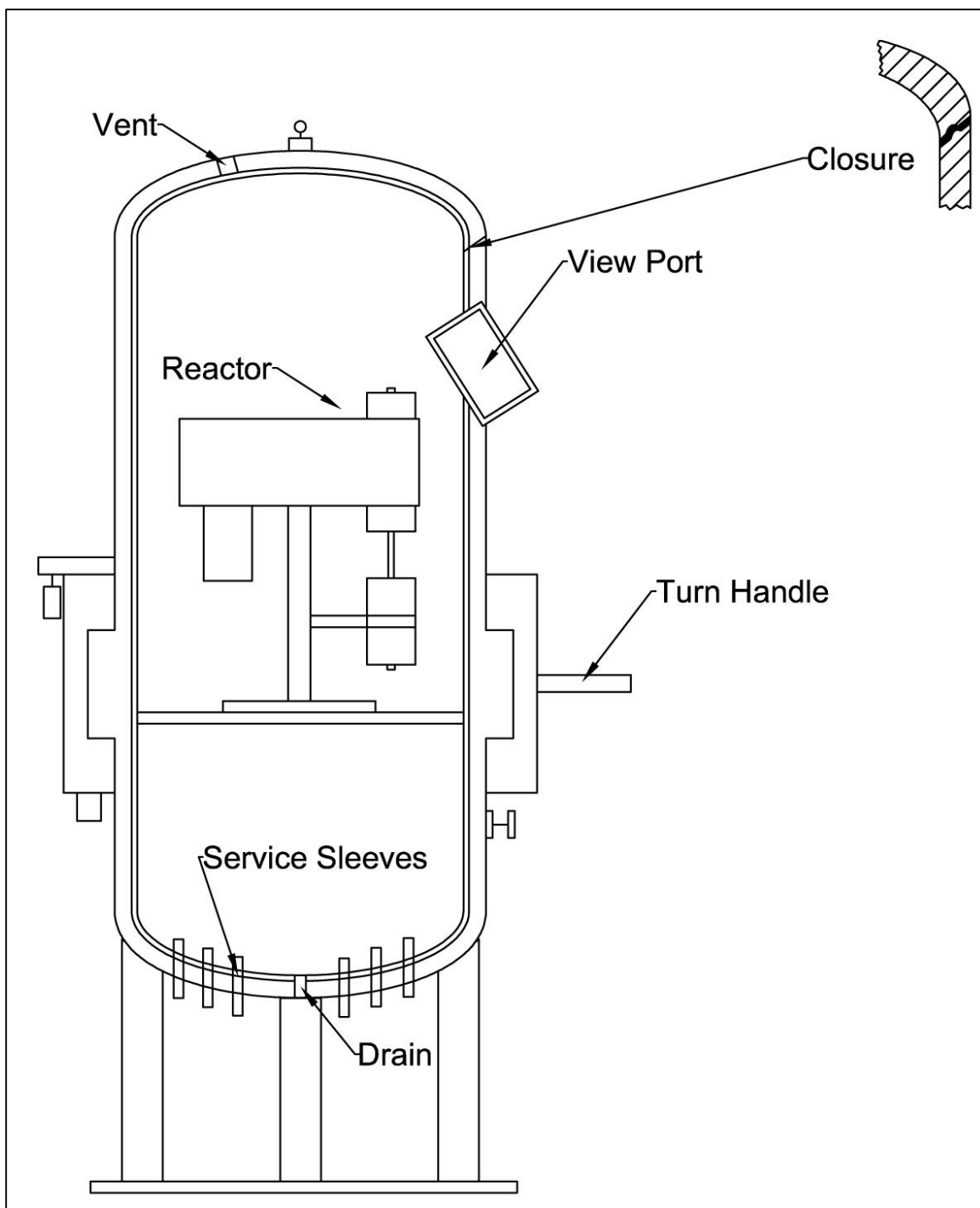


Figure 2.4. Containment vessel equipped with a vertical reactor and a polycarbonate viewing port. Reproduced from the literature.²

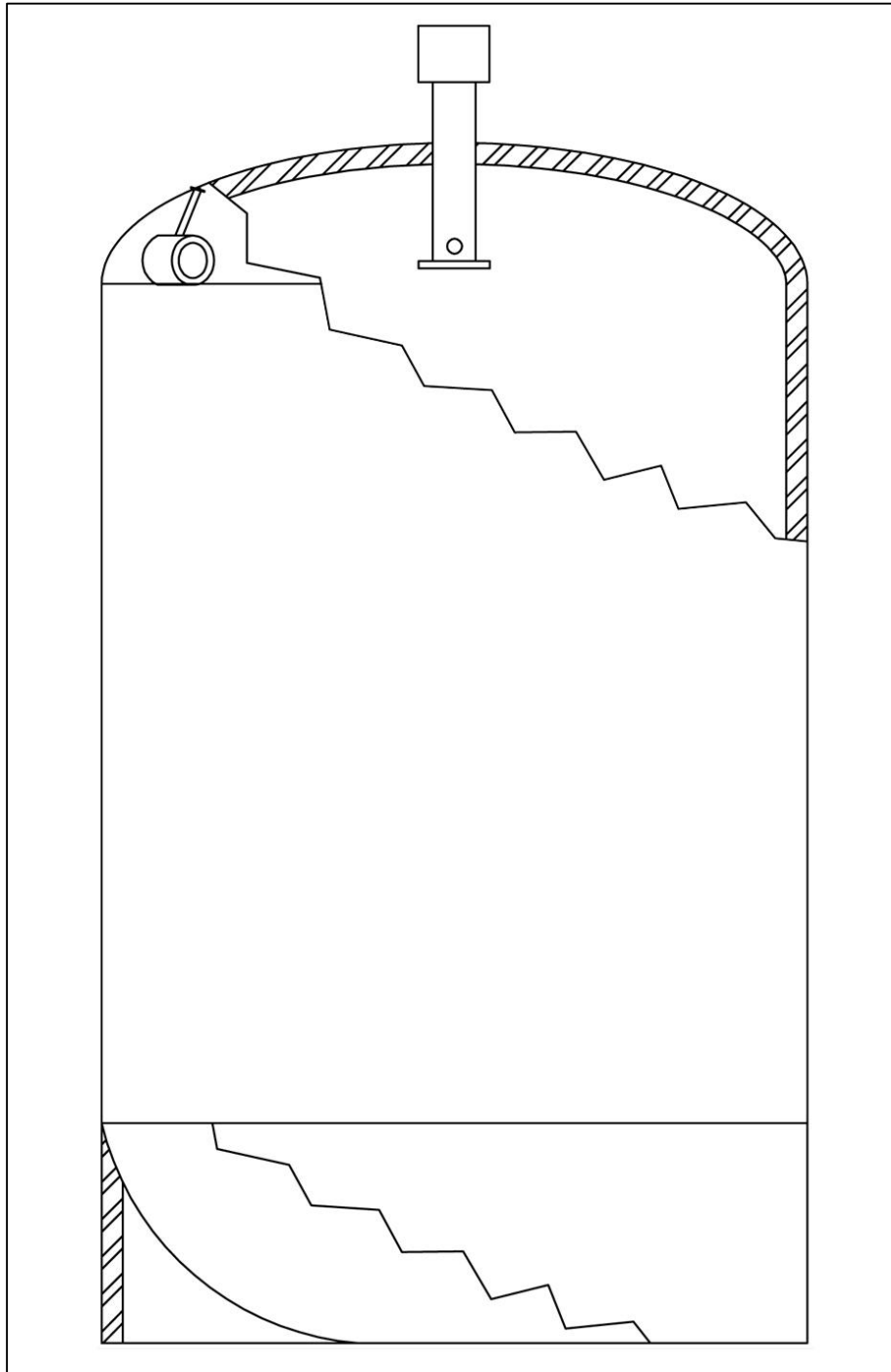


Figure 2.5. Containment Vessel for the use and handling of TNT.⁶

The main goal of this chapter is to document the evolution of academic TFE barricades for the purpose of preparing fluoropolymers based on TFE which, to the best of my knowledge, began close to 30 years ago with a facility at Clemson University's Hunter Laboratories, which will be discussed later in this Chapter. In this account, three facilities are included in this development: an older one at Clemson University, one at the University of Alabama, which has since been decommissioned, and the most recently developed facility at Clemson University as shown in Table 2.1.

Table 2.1. Chronological order of development of TFE polymerization facilities.

Year of Development	Place of Development	Academic person responsible	Amount of TFE handled* (g)
1987	Clemson University	Darryl DesMarteau ⁷	ca. 10
2004	Alabama University	Joseph S. Thrasher ^{8,9}	100
2011	Clemson University	Joseph S. Thrasher ¹⁰	2000

*Amount of TFE handled in one single reaction (maximum amount of TFE used).

As will be explained below, the initial Clemson University barricade was constructed primarily for the storage of TFE cylinders, from which ca. 10 grams of TFE was destabilized at a time and used to prepare the initial perfluorosulfonimide polymer electrolytes in the DesMarteau laboratory.^{11,12}

Approximately ten years ago, another barricade for TFE work was built as part of a new interdisciplinary science building (Shelby Hall) at the University of Alabama in

Tuscaloosa, where Joseph S. Thrasher and co-workers carried out polymerizations with up to 100 grams of TFE per batch.^{8,9} More recently with Dr. Thrasher's return to Clemson, the construction of a new TFE barricade was undertaken at the research laboratories for fluorine chemistry at the remote Clemson University Research Park, in which quantities of up to 1-2 kilograms of TFE per batch polymerization can be used. The aforementioned TFE barricades will be called first-, second-, and third-generation facilities in the remainder of this Chapter.

There are several conditions to avoid while working with TFE, especially if it is not stabilized with either some type of free radical inhibitor (e.g., a terpene like D-limonene) or a diluent known to eliminate or reduce the explosive hazard of TFE (e.g., HCl, CO₂,¹³ HFP¹⁴). As previously mentioned, TFE is a known deflagrant, which means that it is worse than an explosive because a deflagration can back-propagate to the storage cylinder through the gas handling system. One of the most likely causes of accidents when working with TFE is opening a valve too rapidly when a high-pressure differential exists in the tubing/pipeline between the two sides of the valve. Localized heating can arise from an adiabatic compression causing high temperatures in small sections of the gas handling system, which can end up triggering an explosion. The heat released can trigger two possible reactions: the decomposition of TFE into tetrafluoromethane (CF₄) and carbon black or cause its dimerization to octafluorocyclobutane (PFCB) as shown in Equations 1 and 2, respectively.¹⁵⁻¹⁷





The adiabatic compressions can also occur if the rupture disc pipelines (or any other pipelines or tubing in which pressurized TFE is contained) have hard bends instead of prolonged curves. Hard bends in the pipe at the moment of a release of high pressure can provoke shear of the TFE against the walls of the pipe, producing a localized compression, a rise in the temperature and finally a trigger of one or both of the reactions mentioned above in Equations 1 and 2.^{17,18}

In the presence of oxygen TFE decomposes violently, as shown in Equation 3. Thus, great care needs to be taken to eliminate oxygen by ensuring the use of leak free systems as well as the proper evacuation, purging, and degassing of equipment and reagents (e.g., solvents, initiator solutions, co-monomer feeds, etc.).



To the best of my knowledge, no study exists on what type of physical impact on a cylinder of TFE might result in that TFE cylinder exploding. One must take appropriate care in manipulating cylinders with TFE or TFE/CO₂ mixtures in order to avoid hard impacts to the cylinder (dropping the cylinder, potential impact from pieces of equipment, etc). Other aspects of safety for storing and manipulating large amounts of TFE include storing the cylinders properly capped and in a temperature-controlled room to avoid the gases from expanding and contracting with the changing temperature.

2.2 First Generation

A TFE barricade was built on the top/service floor of Hunter Laboratories during its construction in 1987. The architectural drawing shown in Figure 2.6 details the primary features of the barricade, which is made of reinforced concrete. The barricade room has a work area of 39 sq. ft. and is accessed by a heavy duty sliding door. In the event of an explosion, a window located on the top and back of the barricade room serves as a 'weak spot.' This section of the laboratory is primarily used for TFE cylinder storage (kilogram quantities in several size 300 cylinders, where the TFE is stabilized by D-limonene), a nitrogen cylinder for purging and leak checking, and two smaller sampling cylinders for transferring and purifying small amounts of TFE (10-80 g) from the storage cylinders. The remainder of the laboratory (148 sq. ft.) is outfitted with two fume hoods, a gas handling system (combination glass and metal vacuum line), the polymerizer (Parr Instrument stirred reactor), and several pass-through ports between the laboratory and the barricade for the transfer of materials. The schematic of the gas handling system is shown in Figure 2.7, and the overall design and operation of this facility has already been described in a number of publications and dissertations from the DesMarteau group.^{7,19-24}

It may be noted that the initial cylinders of TFE in the first-generation TFE facility at Clemson came from the Bayonne, New Jersey plant of Imperial Chemical Industries PLC (ICI). In 1999, Asahi Glass Co., Ltd. purchased this plant, and in 2007 a decision was made to shut it down, thereby halting the production of fluorochemicals at the site of their American counterpart AGC Chemicals Americas, Inc.²⁵ This is important because TFE is

not available commercially anymore, and industrial companies that produce TFE are not willing to provide the material due to the inherent dangers of its use and the liability associated with it.

Finally, the standard operating procedures (SOPs) for this TFE gas handling system call for the TFE to undergo a number of phase changes while being transferred and purified before going into the polymerization reactor. During a normal reaction, a small amount of TFE is taken out of the storage cylinder and condensed with liquid nitrogen in a smaller collection cylinder by using the vacuum glass line as filling volume to know exactly how much TFE is being transferred. Normally only 5-10 grams of TFE are used per polymerization, and these manipulations are largely done behind the barricade. The TFE is only destabilized immediately before use by passing it through a silica gel column connected directly to one of the ports of the autoclave. The D-limonene scrubbing takes place in the room where the operators and the reactor are, and one wonders if improvements can be made to avoid the operators being in the same room where the reactor and the destabilized TFE are.

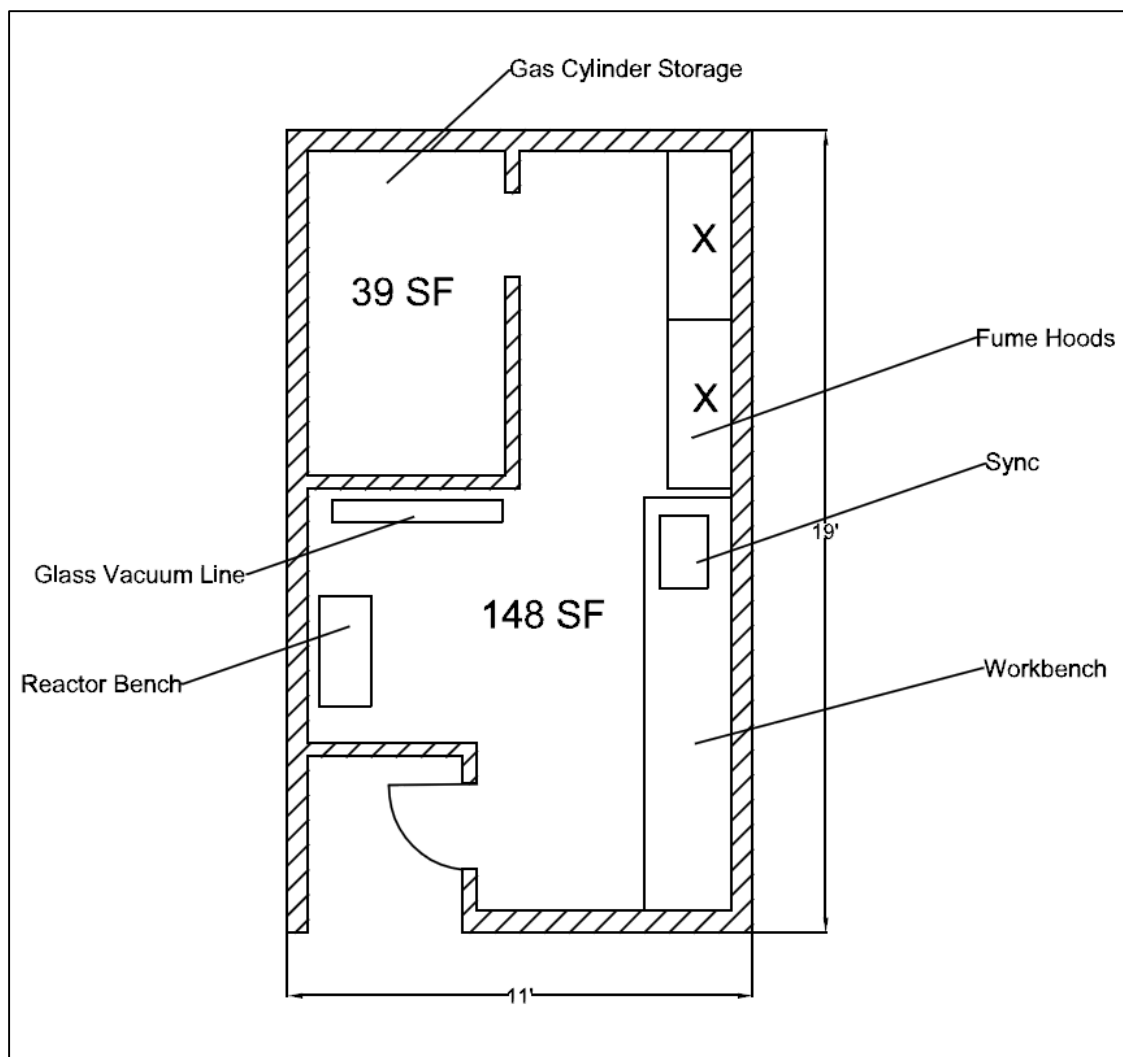


Figure 2.6. Architectural drawing of TFE barricade at Hunter Laboratories.

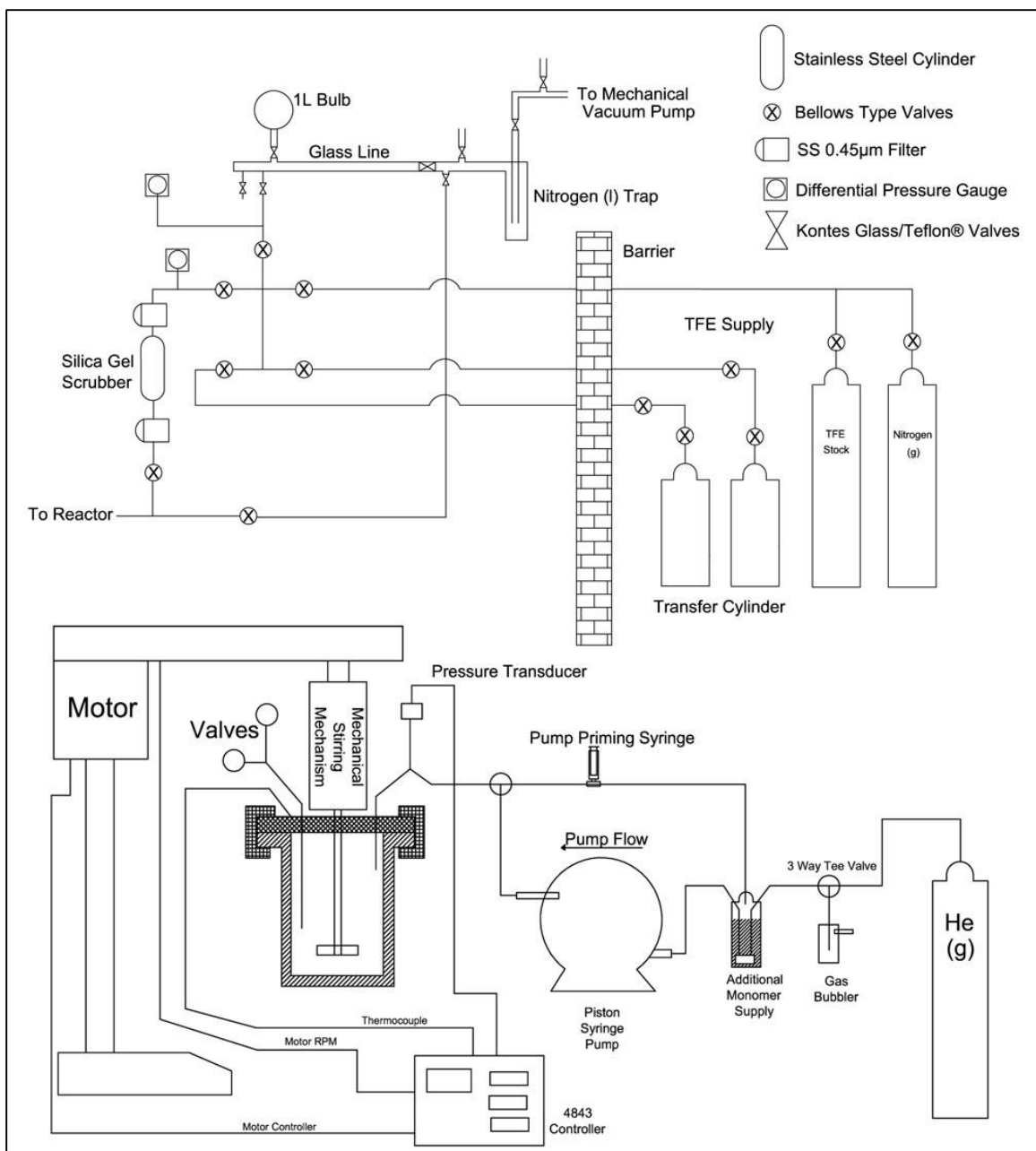


Figure 2.7. Top: Schematic of TFE barricade and gas handling system located in Hunter Laboratories, Bottom: Diagram of the reactor setup.²¹⁻²³

2.3 Second Generation

The barricade at The University of Alabama was installed in the service floor/attic (4th floor) of the chemistry building, which was newly built in 2004. The architectural drawing of the barricade is shown in Figure 2.8, and its interior has three separate sections. Two of these sections are either side of an entrance foyer to the third section, which is located towards the back of the setup. One of the two initial rooms contained a close-looped cooling machine and an ISCO syringe ISCO pump for radical initiator feed as well as an HPLC pump for comonomer feed, while the other room was equipped with a glass vacuum line used in both the preparation of TFE/CO₂ gas mixtures and the evacuation and leak checking of the TFE polymerization system. The back room was used for TFE storage, gas handling, and polymerizations.

The strength of the walls of the rooms was both incorrectly designed (even the original specified reinforced concrete walls) and built, and therefore it was not possible to use the barricade facility for reactions involving up to 225 g of TFE as had been originally intended. Fortunately, patent technology from the DuPont Company came to the rescue, as they had previously discovered that if TFE was kept mixed with 30-mol% or more of carbon dioxide, CO₂, the TFE could not be made to explode even when fusing a Nichrome® wire (1350 °C) in a cylinder test.¹³ Furthermore, DuPont only claimed the liquid composition of TFE/CO₂ in their patent,¹³ and since reactions were generally operated with only gaseous mixtures of TFE and CO₂, it was assumed that these operations

were outside of the scope of this patent, which has recently expired. The gas handling system is shown in Figure 2.9.

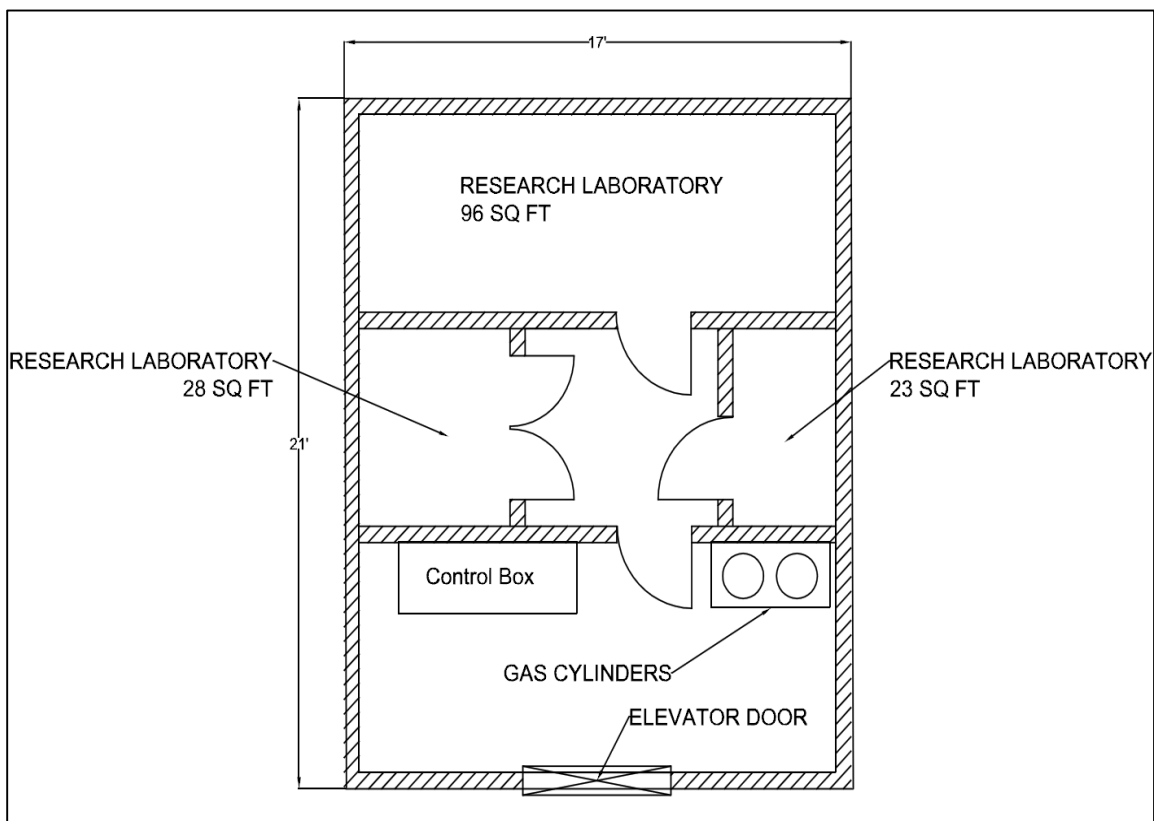
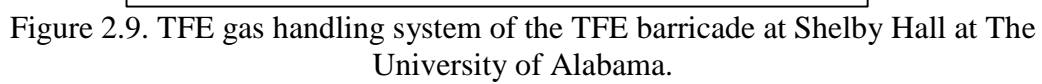
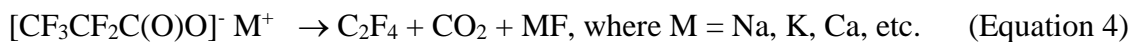


Figure 2.8. Architectural drawing of the TFE barricade at Shelby Hall in University of Alabama.

With a safe supply of TFE conceptually in hand, one then needed to come up with a real way to prepare a mixture of TFE and CO₂. Although improved technology continues to be developed to prepare TFE from waste poly(tetrafluoroethylene) (PTFE),²⁴ this approach does not make sense for an academic laboratory that might not necessarily have waste PTFE for pyrolysis.



Furthermore, this approach, especially on a laboratory scale with normal equipment, yields very impure TFE, with the other primary components being hexafluoropropene (HFP), octafluorocyclobutane (OFCB), and highly toxic perfluoro-*iso*-butylene (PFIB),⁷ and after purification, the TFE would still have to be mixed with CO₂. However, a search of the literature revealed that the 3M Corporation had both patented and published in the early 1950s a procedure for preparing an ca. 50:50-mol% mixture of TFE and CO₂ in 90+% yield from the pyrolysis of pentafluoropropionate salts,^{25,26} as shown in Equation 4.



We have also benefited from the experimental procedure of Kornath and Kaufmann for this reaction, as they rediscovered this process before finding the original literature.^{27,28} Although 3M and Kornath reported a preference for using the sodium salt, far foaming during gas evolution was found with the potassium salt. Accelerating rate calorimetry (ARC) studies on these pentafluoropropionate salts also support the conclusion that gas evolution is preferential with the potassium salt; however, a small exotherm does exist in the vicinity of 175 °C for this salt, so care must be taken not to dry the salts too strongly. On the other hand, the salts must be scrupulously dried prior to pyrolysis in order to minimize the amount of pentafluoroethane, C₂F₅H, that will be formed as a byproduct. This methodology has been used to prepare kilogram quantities of TFE.^{8,9}

Returning to the design of the second-generation TFE barricade and gas handling system, the latter of which is shown in the top of Figure 2.9, a number of safety features

should be pointed out. First, extra shielding in the form of a 1/2-in. thick, plate steel door was added around the open sides of the southeast corner of the back room where the TFE cylinder was stored (Figure 2.8). The control panel for the polymerization system was placed outside of the barricade so that two doors/walls existed between the polymerizer and the operators. The operators were able to both regulate monomer feed rates as well as monitor numerous read-outs for temperature, pressure (vacuum and high pressure), and stirring speed from this panel. With respect to controlling the flow of TFE to the polymerization, both air-actuated valves that fail closed and a backpressure regulator (BPR) were used. Orifices were used after the main TFE cylinder valve and the two TFE air actuated valves (labeled 1TFE and 2TFE in Figure 2.9) to prevent adiabatic compression when the valves were opened as well as any back propagation of a flame front (flame arrestors) were an explosion to occur downstream towards the autoclave; all connections between the components of the gas handling system were made with 1/4-in. stainless steel tubing (0.035 in. wall thickness). The orifices used were basically made from tube reducers (Swagelok®) that had been welded shut and then drilled open with 0.010 in. precision holes. The orifices and BPR allowed for a very controlled flow of gases through the system. Co-polymerizations with TFE, both aqueous emulsion and solution, were found to run in the presence of CO₂; however, the polymerization kinetics were slowed as one might expect.^{8,9} On the other hand, if one desired to carry out polymerizations in the absence of CO₂, this was effectively accomplished by scrubbing out the CO₂ with either Ascarite® or soda lime in an in-line, water-cooled scrubber on the way to the polymerizer. Ascarite® was found to be more effective than soda lime, and in order

to insure that the scrubbing was not too rapid and thereby might increase the risk of creating ‘hot spots,’ a multipoint thermocouple was used to monitor the temperature throughout the length of the Ascarite® bed.^{8,9} Finally, in the instance of an ‘event,’ two ‘crash’ buttons existed, one for closing all of the air actuated valves at the same time and another for shutting off power to the facility.

Because of the time element, a data acquisition system was never added to this facility, and with Thrasher’s move to Clemson, the entire system was decommissioned and disassembled in 2012.

2.4 Third Generation at Clemson University

The details previously discussed reveal how each of the barricade systems led to a new conceptual design as well as an optimal place to build a new generation of TFE barricade for polymerizations that require a large amount (c.a. 1 kg) of TFE in order to bring pilot scale capability to Clemson University. The location had to be as close to the chemical laboratories at the AMRL as possible, but in this case there was not the luxury of a new chemistry building that could include such a barricade like the original designs of both the previous two facilities.

When looking at the literature that describes the different kinds of high-pressure cells/cubicles,^{2,5,26} one finds that the common denominator is a blowout panel or a weak wall that points to the outside or to an earthen berm. A negative point about this is the fact

that projectiles can fly out at high speeds and shock waves can occur in the case of an explosion. Another down side to this approach is the high capital cost, high space requirements and the lack of expansion capability. Some reviews^{5,6,29} suggest that the use of vented containment rooms is more appropriate. It was found that Fluitron, Inc. in Ivyland, Pennsylvania markets containment vessels like those described in the literature.^{30,31} In fact, they appear to have both manufactured and now have for resale some of the same vessels previously used at Exxon Chemical Company (now ExxonMobil Chemical Co., a Division of ExxonMobil) high-pressure laboratory in Allendale, New Jersey.

The high cost of a new vessel exceeded the allowable budget, and therefore an industrial company would have to fabricate and deliver one to the AMRL building. In the meantime the vessel would need a place to go, and the best place for it would have been a space within the AMRL for a hazards laboratory located at the edge of the building as shown in Figure 2.10. For simplicity, Figure 2.10 shows a zoom-in of the section of the AMRL building where the initial considerations for building the containment vessel were initially conceived. The room initially considered is labeled room 154 in Figure 2.10 and was designed to be a waste treatment room. Currently room 154 is being used as a safe room for placing chemical and biological waste from the AMRL. The walls of the room are weaker than the walls of a containment vessel.

No building codes are available for TFE facilities, and therefore an investigation was undertaken to find what building codes would be applicable. The potential use of a vented containment vessel dictated that the boiler code for the State of South Carolina must

be applied.³² The major implication of adopting the boiler code is that the walls of the proposed room within the AMRL to house the containment vessel must have the same or greater strength than the walls of the vessel itself (which means a huge effort to build strong walls after the vessel is installed in place). This meant that part of the structure of the roof had to be removed in order to lower the vessel in place inside the room and also strengthen the walls, which made the potential costs of this operation prohibitive. Another problem with the possibility of using a large containment vessel was the transportation of such vessel through the South Carolina highways. Since the vessel being considered was of large proportions, it had to be transported in a low-bed truck system which would have been also cost prohibitive.

After realizing that a new direction had to be taken, James L. Clark from the Clemson's Office of Research Safety suggested a new conceptual design using commercially available buildings built for storage of chemicals (U.S. Chemical Storage Superloc Model SL1610) and explosive storage [U.S. Explosive Storage Model ML263 (Type II/Outdoor)]. The chemical storage room would be used as the reaction room, and the explosive storage would be used as the control room where the operator would monitor and control the reactions. The reaction room is featured in Figure 2.11 – 2.13 and the control room is featured in Figure 2.14 – 2.15.

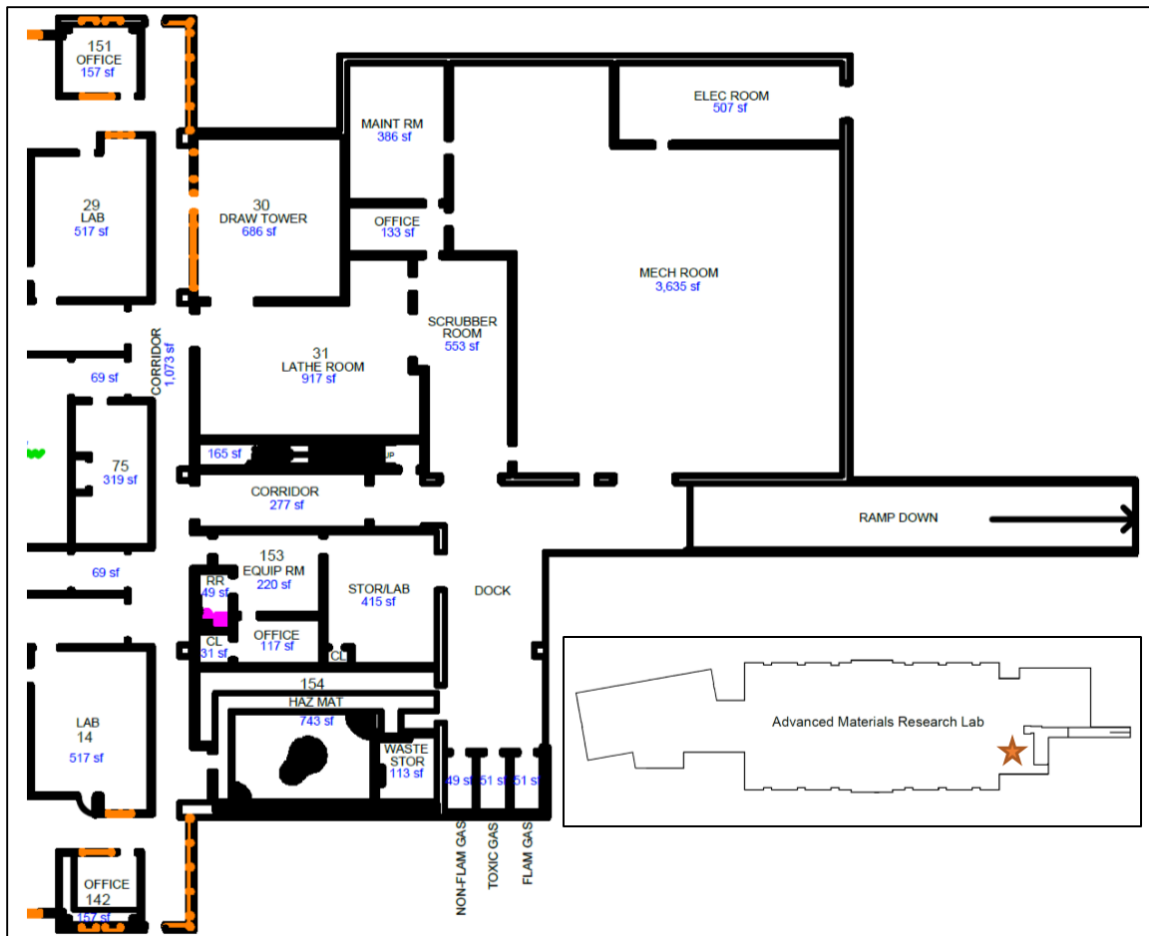


Figure 2.10. Distribution floor plan for the AMRL building section highlighted on the overall outline shown in the bottom right corner of the figure [Drawing provided by Clemson Facilities].

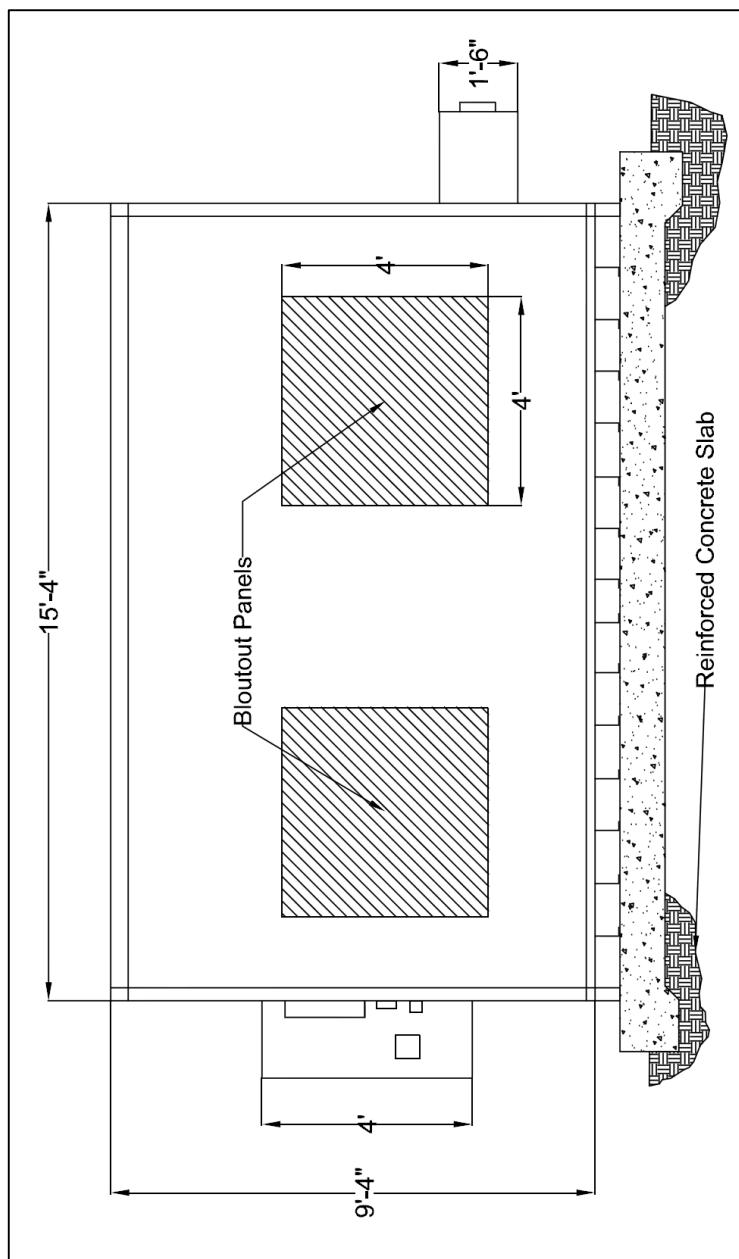


Figure 2.11. Architectural drawing of the back view of the reaction room (reproduced with permission from the manufacturer).

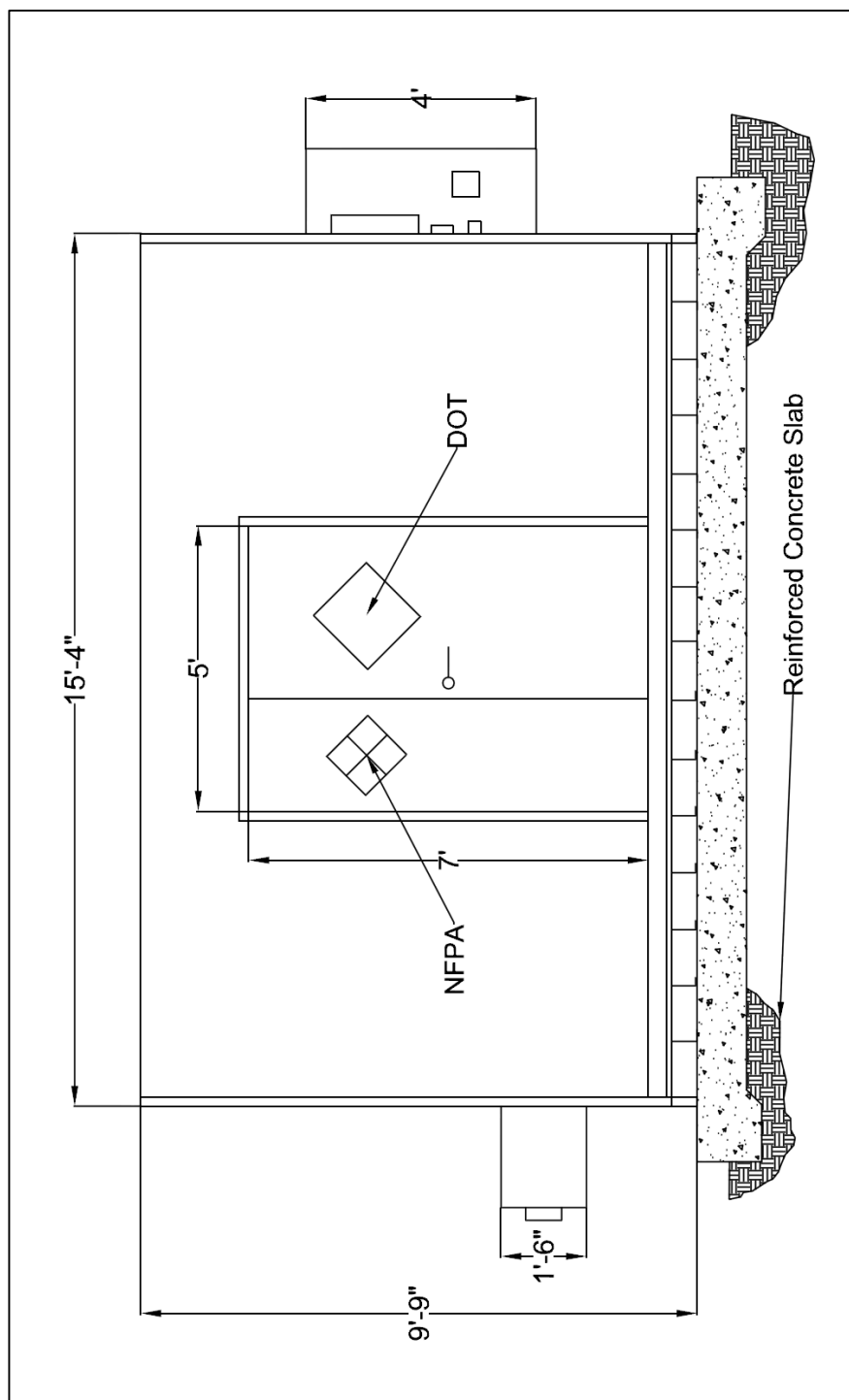


Figure 2.12. Architectural drawing of the front view of the reaction room (reproduced with permission from the manufacturer).

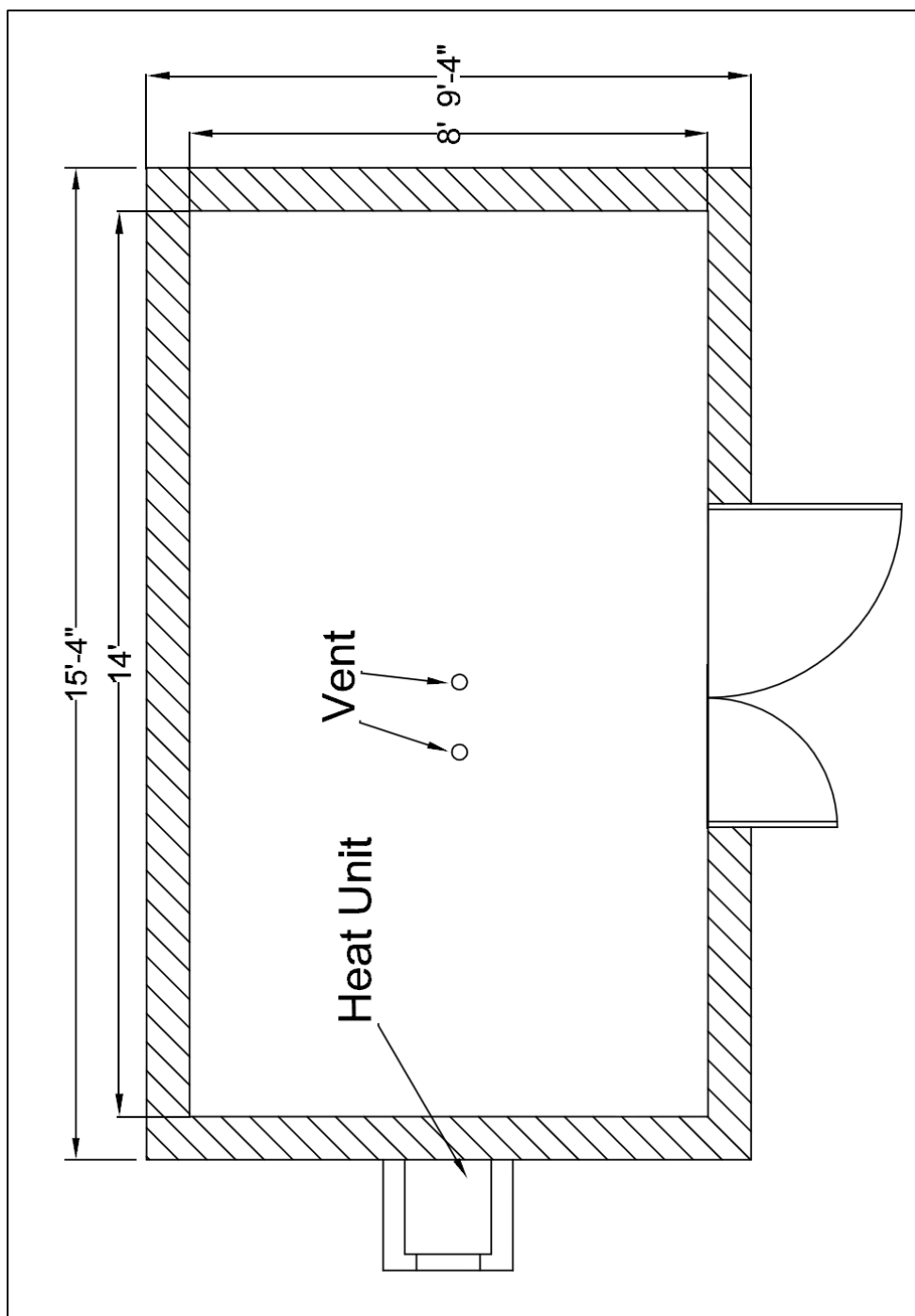


Figure 2.13. Architectural drawing of the top view of the reaction room (reproduced with permission from the manufacturer).

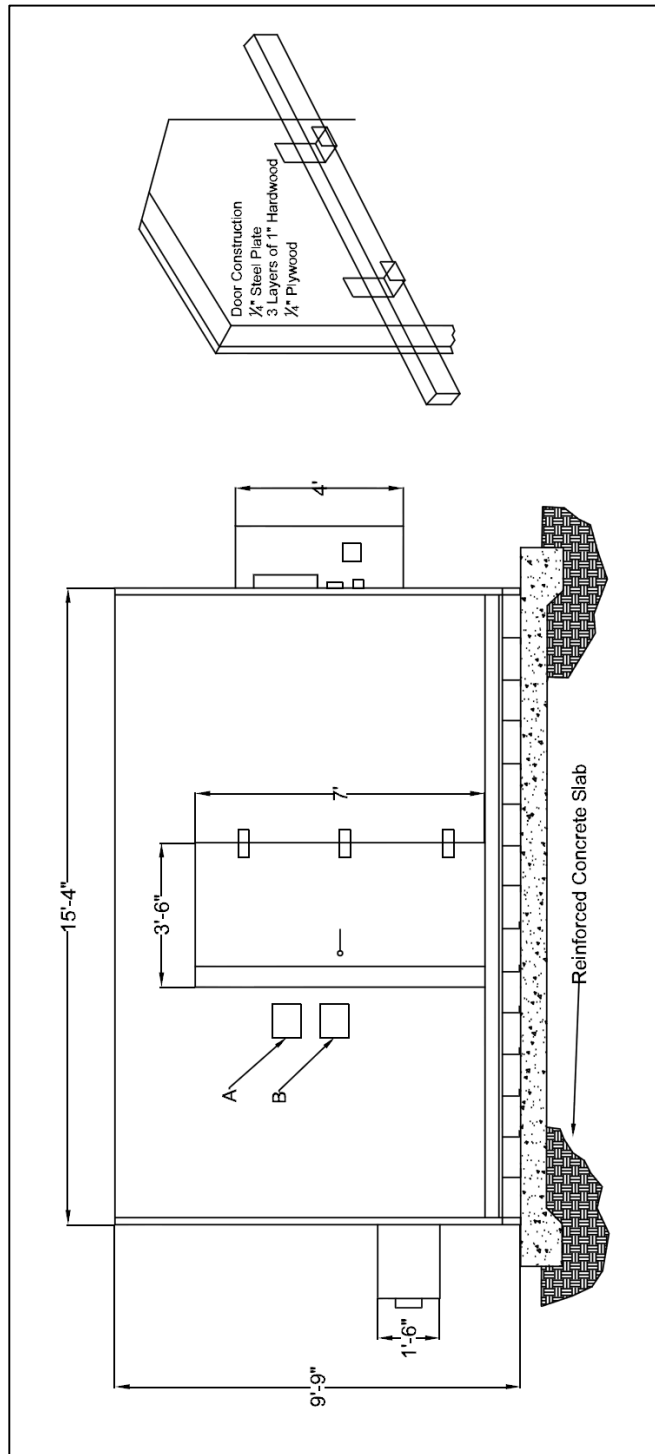


Figure 2.14. Architectural drawing of the control room. Left: Front of the control room, Right: diagram of the door and wall construction (reproduced with permission from the manufacturer).

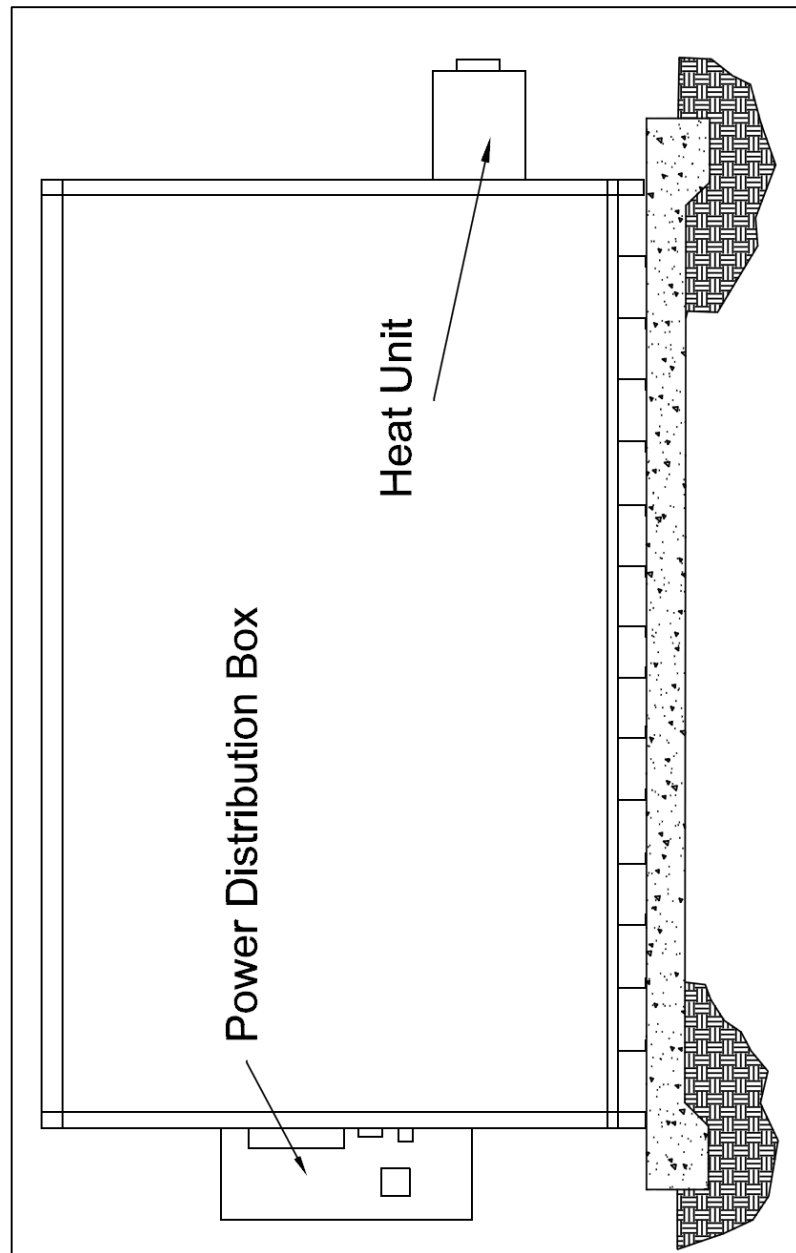


Figure 2.15. Architectural drawing of the back view of the control room (reproduced with permission from the manufacturer).

In other words, the control room is ‘reverse engineered’ in the sense that the reaction will occur in the reaction room while the operators are in the control room and in the case of an explosion outside the control room, the operators will remain safely inside. In Figure 2.16 we can see the two rooms side-by-side.

The location of this facility is a parking lot behind the CETL building, which is approximately 300 yards away from the AMRL laboratories. Originally the parking lot was being used as a ‘bone yard,’ for old high-bay space equipment but after cleaning the space the area was able to fit a concrete pad of 24 x 31-8” ft. that could bear the weight and structural anchoring of the buildings (as shown in Figure 2.16), and it also served as a level surface for their installation. Because of construction codes and safety aspects of construction, the building had to be placed 65 ft. away from the CETL building as well as 60 ft. away from a nearby parking lot and closest roadway. Because of the aforementioned distances, a concrete walkway had to be built in order to have an access ramp to load and unload equipment to and from the CETL building where a high-bay space area [13 ft (W) x 19 ft (L) x 25 ft (H)] serves as support laboratory space for collateral research and/or preparative work. Electrical conduits had to be brought underground from the CETL building to provide electric power and internet lines. A progression of satellite pictures of the AMRL and CETL buildings, the fenced area for the barricade, and the barricade buildings is shown in Figures 2.17-2.19. The distribution plan of the ground floor of the CETL building is shown in Figure 2.20 where a star has been placed on top of the high bay area and a square has been placed in the support room where analytical equipment can be

installed to give support to the research carried, whether in the high-bay area or in the barricade polymerization facility.



Figure 2.16. TFE barricade located at CETL. Left: control room, Right: reaction room.



Figure 2.17. Google Earth picture of AMRL and CETL.



Figure 2.18. Zoom of CETL and fenced area.

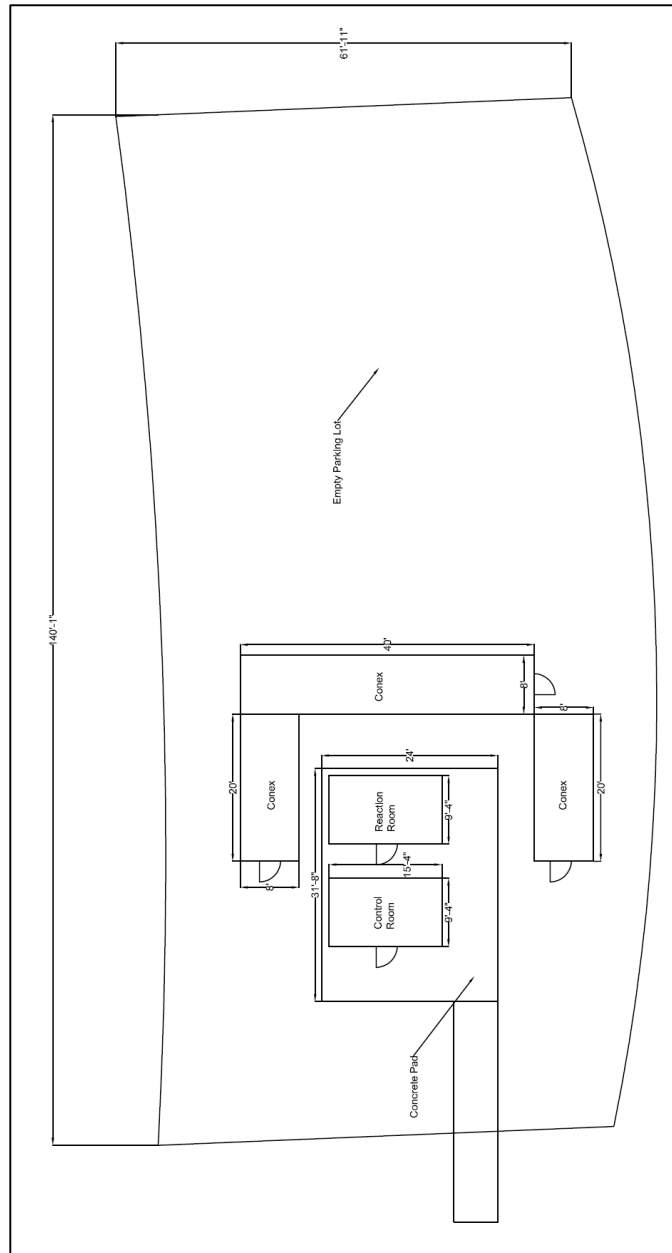


Figure 2.19. Schematic close up of the fenced area in which the barricade is located. The dimensions and overall shape of the parking lot were determined manually at the site. Dimensions are given in feet.

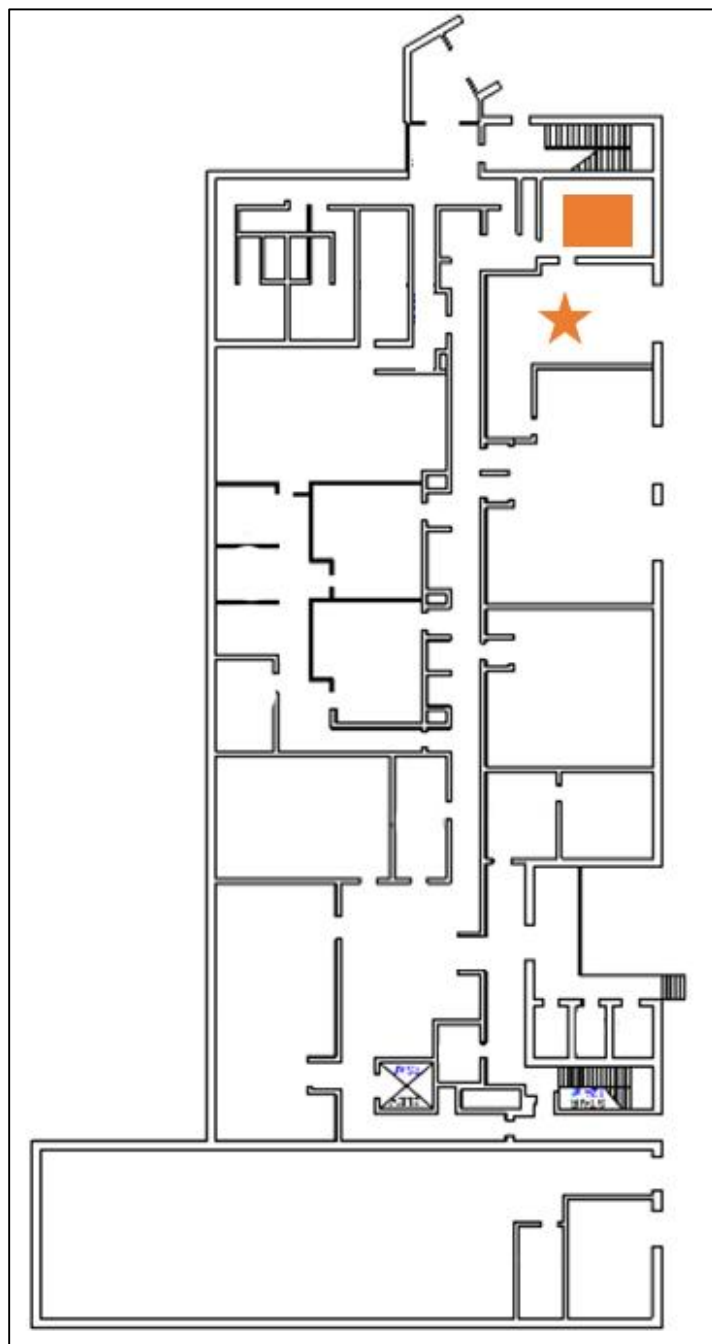


Figure 2.20. Architectural drawing of the first floor of CETL (supplied by Clemson facilities). The room marked with the star is the high bay area while the one marked with the square is the support room for installation of analytical equipment.

Both of the buildings (the control and reaction room), were placed on the concrete pad with the doors facing the CETL building and 10 ft. apart from each other; in the case of the operator having the control room door open, the operator can enter or exit the control room without being in front of the access door of the reaction room. By locating the door of the reaction room towards the CETL building, the blowout panels (rated at 4.7 lb/ft²) are facing away from the building protecting the common areas from any projectiles. To accomplish this pressure rating at the blowout panels, the panels are equipped with M&M Explosion Venting Fasteners, Model RV1 rated at 75 lb/ft² each. With an area of 32 ft² per panel, and two fasteners per panel, the pressure needed to rupture the fasteners and flap out the panel has to be greater than 4.7 lb/ft². The same company offers fasteners rated at 100, 150, 265 and 390 lb/ft² but considering that we desire the panels to be as sensitive as possible, we selected the lower rated ones mentioned above.

Surrounding the reaction room are three Conex shipping modules that are placed in the shape of a U around the rear and sides. These Conex boxes serve as a secondary shield against projectiles behind the blow out panels in case of an explosion. The next safety feature is an earthen berm located in between the barricade facility and the nearest parking lot. The whole facility (the entirety of the parking lot) is surrounded by an 8-ft tall security fence with two gates: a 4-ft wide gate at the concrete walkway/ramp towards the CETL building, and a 12-ft sliding gate at the rear of the yard.

2.4.1. Equipment Installed In The Tetrafluoroethylene Facility.

Each of the storage units is equipped with its own 18,000 BTU heat pump unit and 200-A electrical. The dimensions of each building and other minor specifications are shown in Figures 2.17 and 2.18. The reaction room has a full storage capacity of 56,000 lbs, a building weight of 17,587 lbs, a floor load of 500 psf, a door load of 25 psf, a snow load of 40 psf, seismic rating of zone 4, tie downs of anchor angle at each corner, and a wind load of 130 mph. The walls and roof are built of mineral wool insulation and multiple layers of gypsum wallboard encased between heavy-gauge Galvanneal sheet steel to provide a four (4) hour fire rating.³³

A diagram of the control room is shown in Figure 2.14. The exterior walls and door of this explosive storage magazine are constructed from ¼ in.-thick, ASTM A-36 prime plate steel lined with 3-in. thick hardwood, where the direction of the grain of the hardwood is rotated 90° with every ½-in. thick overlapping pieces of hardwood. The design criteria meet or exceed ATF Type II Outdoor specifications and conform to Article 77 of the Uniform Fire Code (UFC). The control room has nominal dimensions of 16 ft (W) x 8 ft (H) X 8 ft (D), a weight of 14,376 lbs, tie downs of anchor angle at each corner, an open channel construction, and crane lifting lugs.³³

Both the control room and the reaction room are equipped with their own breaker box in which each circuit is isolated by its own breaker. That said, the autoclave stirring motor and heater are the only two pieces of equipment located in the reaction room that are powered from the control room. This is done for safety reasons in case the operator needs

to cut the power from the autoclave without cutting the power from the rest of the equipment located in the reaction room that might be supporting a reaction, such as the cooling machine, the vacuum pump, or the venting fan. The power distribution boxes are sketched in Figure 2.21.

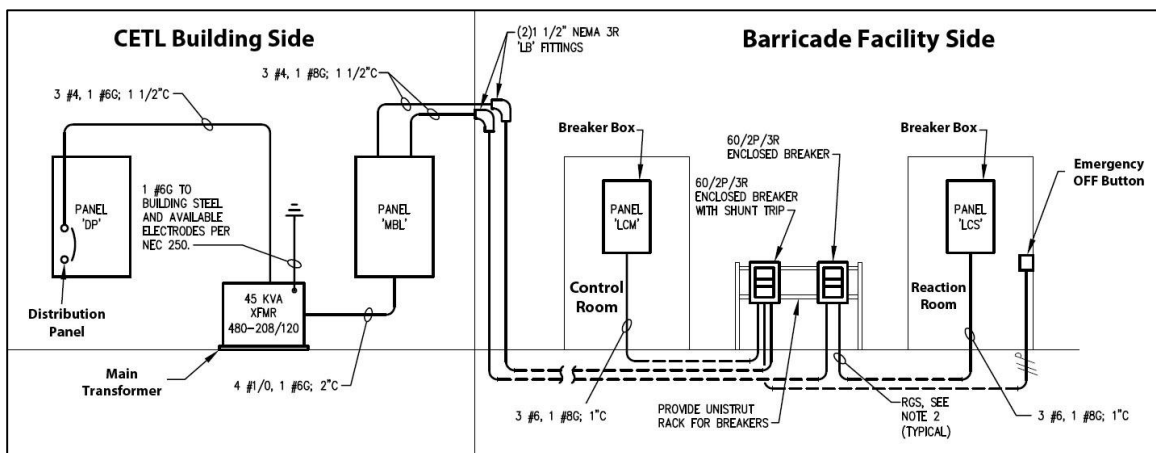


Figure 2.21. Electrical connection diagram. Panel LCM is located on the side of the control room while the Panel LCS is located in the side of the reaction room. The Panel MEL is located inside the support room (aforementioned) inside the CETL facility.

Originally the power distribution boxes were planned to be placed in between the two rooms as shown in Figure 2.21 but later it was decided that a better place would be in front of the control room so the power distribution boxes would not be in the way of the operators, a few feet closer to the CETL and also located on the edge of the concrete pad so that it would ease the installation of the lines. A complete diagram is shown in Figure 2.22 that denotes the path of the power distribution lines in between the CETL building and the power distribution panels in front of the control room at the barricade. In the original plans, the lines were going to be buried underground and brought over to the

reaction room through the side of the parking lot, but later it was considered that moving the distribution boxes in front of the control room would allow a straighter path to the final locations of the distribution boxes from the CETL building, alongside the concrete walk path and into the front side of the control room.

In order to transmit the power in between the control and reaction rooms, the machine shop fabricated a cable tray/raceway from parts bought in McMaster-Carr (catalog numbers: two elbows (8511K21) and 10 ft raceway (8511K17)) as shown in Figure 2.23 (elbows not shown in the picture). The cable tray is 4-in. in diameter and is located on the left sides of the buildings away from the operator's access to either building. This cable tray also hosts the nylon (1/4-in. o.d.) air lines that control the air actuated valves, all the data lines for the Data Acquisition System [including pressure transducers in the gas handling and carbon dioxide scrubber systems, the thermocouple encoder, and the mass flow controllers (MFC)], power and control cables for the 2-gal and smaller autoclaves (e.g., the oven, the thermocouple, the tachometer, the pressure transducer, and the solenoid valve for the internal cooling), the syringe pumps control lines, and the power and signal cables for the video cameras.

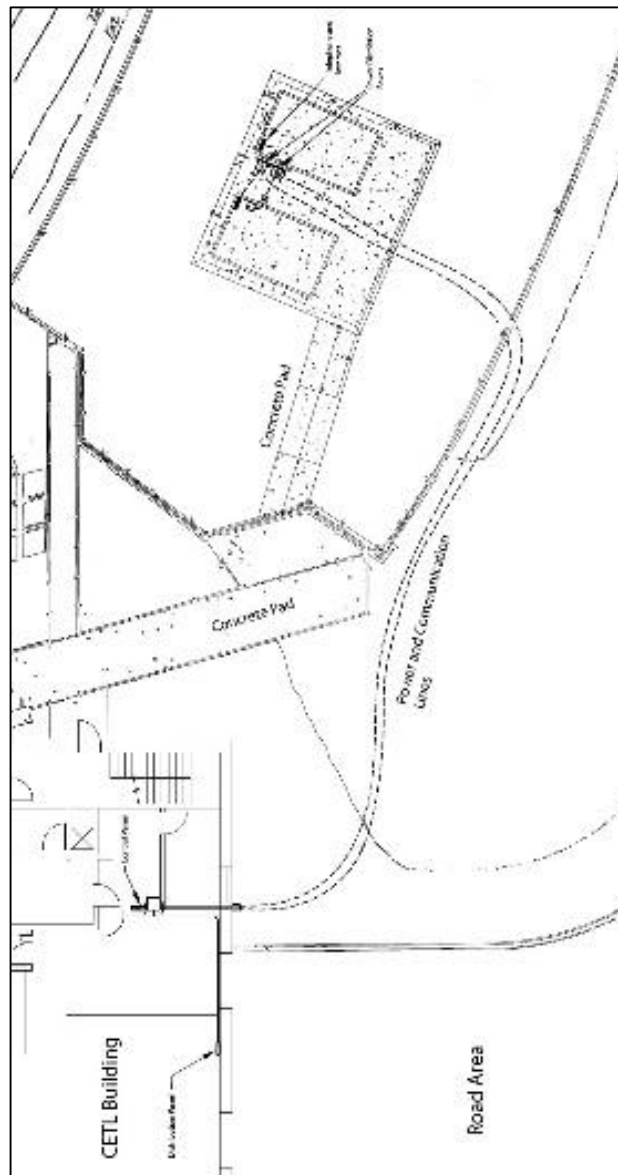


Figure 2.22. Original diagram for tracing the power distribution lines from the CETL building to the barricade facility.



Figure 2.23. Picture of the cable tray between the reaction room (right) and the control room (left).

2.4.2. Safety and Control Section

Both the reaction module and control room are equipped with several features that ease the control and maximize the safety of a TFE polymerization reaction. These features are listed below:

- **Depleted oxygen sensors:** Both the reaction and control room are equipped with a series 1000 depleted oxygen sensor manufactured by Alpha Omega Instruments (Model 1000-232). Each sensor is equipped with a dual LED indicator light that is located outside the room visible to the operators. In case the oxygen level decays below 16%, the LED light will change from green to red. If the oxygen level falls below 14% (11% is the minimum allowed to sustain life), the oxygen sensor will indicate to vacate either room with an audible alarm. In addition, the oxygen sensor

is equipped with an output signal that can be data logged on the data acquisition software (explained later in the Chapter) or used for feedback in a remote application. When in the reaction room, in the case of a leak of a gas monomer, nitrogen, or any other gas, the use of such an oxygen monitor serves as an alarm. A picture of the oxygen sensor is shown in Figure 2.24.



Figure 2.24. Picture of the Model 1000-232 Alpha Omega oxygen sensor installed in the control room.

- **Fail-closed air actuated valves:** The air actuated valves are manufactured by the Swagelok Company, and they are fail-closed in such a way that in the event of a

leak in the air lines that power the valves, each valve will close automatically, preventing from overfeeding a gas into the reactor or the defective part of the line. Most importantly, if the crash valve were to be used (located in the valve control panel), all the air that drives the air actuators will be vent and therefore all the valves will be safely closed to their default position (fail-closed). Also, there are multiple pathways to feed the reactor from the storage cylinders in the case of a blockage or a leak in a section of the gas handling system (explained later in this Chapter). The valves are model (SS-4BK-5C) in which the valve body is constructed of stainless steel, and the actuator is built in cast aluminum. The opening time is 0.5 seconds from fully closed to fully open at 60 psig. The diagram and dimensions of the valve are pictured in Figure 2.25.

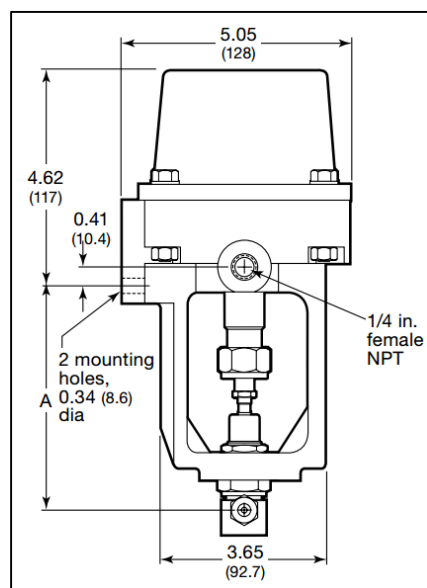


Figure 2.25. Air Actuated valve (Reproduced with permission from Swagelok digital catalog³⁴).

- **Vent Valve:** As with the second-generation TFE barricade, these air-actuated process valves are all fail-closed, and furthermore, since the air supply to all of these valves are plumbed to a master cutoff valve, they can all be closed with a simple 180° turn of one ball valve on the right end of the valve control panel (not in sight in Figure 2.30).
- **Orifices:** Orifices are installed in the gas handling system (after the TFE stem valve and downstream from the TFE1, TFE2, and 1N valves) in order to both minimize a rapid expansion of the gas across a high pressure differential as well as act as flame arrestors were there to be a back propagation of a downstream flame, flash, or explosion. If TFE is expanded rapidly, the adiabatic compression across the pressure differential can cause shear and friction that could potentially provoke an explosion. As mentioned before, TFE is a deflagrant, and therefore the orifices along the line can protect the storage cylinder in the case of a back propagation of a flame in the gas lines. Also, when remotely opening a valve, the orifices help fill the lines at an adequately slow rate minimizing rapid expansions. (Please see Figure 2.32 for the gas handling system details about the location of each orifice.) The orifices are made of stainless steel and manufactured by Swagelok. The basic design of the orifice is a Swagelok tube reducer that has been welded shut in which a 0.0010 inch hole has been drilled in the middle. Figure 2.26 shows a diagram of the orifice. The Clemson University machine shop is also able to manufacture such orifices on demand by welding shut a fitting and drilling a hole to specifications in between 0.0010 to 0.0020 of an inch. In Figure 2.26 the actual blockage where the

orifice is drilled is not shown, but the fitting is welded shut in section E prior to drilling the actual orifice.

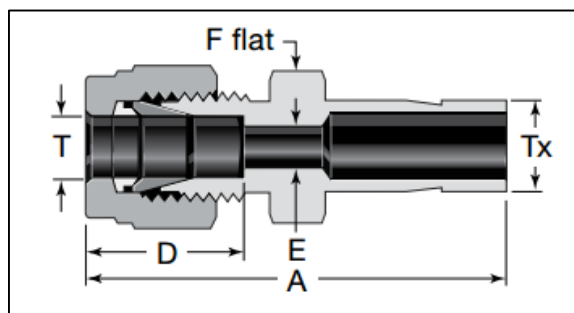


Figure 2.26. Sectional cut of a tube fitting used in the design of an orifice (Reproduced with permission from Swagelok digital catalog³⁴).

- Gas handling system filters:** Each mass flow controller (MFC) has its own filter to prevent the risk of condensation water or fine particulates to travel back through the gas handling system from the reactor and clog the fine capillary sensor of the mass flow controller. Each filter (Swagelok part number SS-FCE) is equipped with its own purge valve that is opened regularly during cleaning to pour any water or debris captured by the filter.
- Mass flow controllers:** The reaction room has two mass flow controllers (MFCs, model HFC-202) installed on each of the gaseous monomer feed lines. The settings of these MFCs are regulated in the control room by a controller (Teledyne Hastings THP-400), which is capable of controlling up to four MFCs at a given time. The controller is capable of visualizing either the total flow of gas that flows through the lines (standard liters per minute “SLM”) or the integrated flow versus time (i.e., totalizer), known as the total gas given in standard liters (SL). The unit is capable

of putting out a TTL signal that can be data logged in the data acquisition system in order to integrate the flows with respect to pressures and temperatures for a more complete set of data for each reaction. The controller is featured in Figure 2.27.



Figure 2.27. Picture of a Teledyne Hastings Mass Flow Controller (Obtained Teledyne Hastings Online Catalog³⁴).

- **Two ISCO syringe pumps:** The reaction room is also equipped with two Teledyne ISCO pumps (Teledyne ISCO 1000D) that are capable of delivering with high precision (down to 0.01 mL/min) a constant flow of a solution of either a liquid monomer, a liquid surfactant, or a radical initiator into the reactor. The initiator line (1/16-in. o.d. stainless steel) is contained inside a 3/8-in. o.d. copper tube that can be cooled down to -50 °C depending on the stability of the radical initiator solution used. By simply turning a 3-way valve, the initiator solution can be delivered either to the large or small reactor as needed. A more detailed schematic of the ISCO pumps is featured in Figure 2.28. The cooling lines are filled with a 50:50 V/V mixture of ethylene glycol and water propelled by an individual cooling machine installed underneath a table holding the syringe pumps. A diagram of the cooling system can be observed in Figure 2.29.



Figure 2.28. Picture of a Teledyne ISCO pump Model 1000D (obtained with permission from Teledyne ISCO online catalog³⁵).

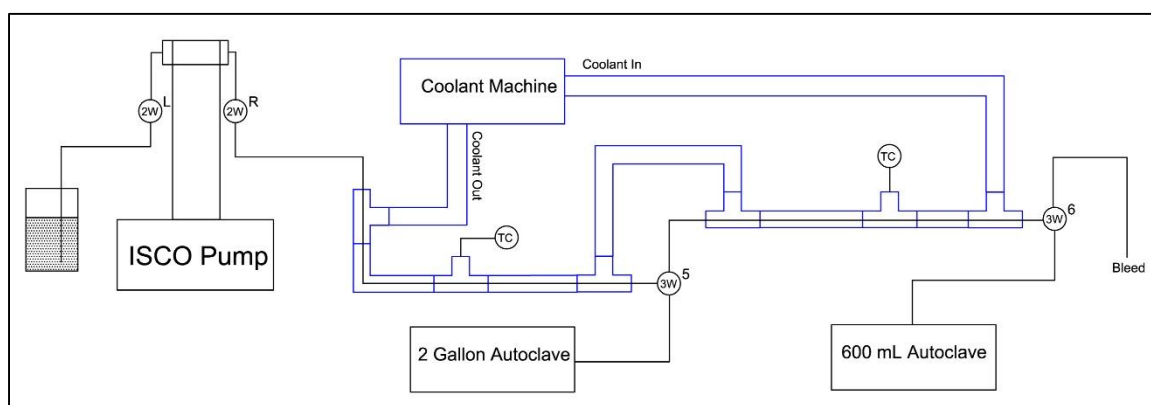


Figure 2.29. Cooling coil diagram for the ISCO Pump used in the feed of radical initiator solution.

- **Standard operational procedures (SOPs):** The control room is equipped with a full set of operational procedures (see Appendix A for a full copy of the existing procedures). The main idea is to have the requirement of checking step-by-step the entire process before each experiment in order to maximize safety and increase the redundancy of each checking point. Normally an operator will remain in the control room assisting with the turning ON and OFF of each valve, while another operator will remain inside the reaction room assisting with the counterpart during the checking phase. Both operators can maintain communication through an internal phone/intercom system.
- **High-definition video control:** The reaction room is equipped with three high-definition (HD) web cameras that are capable of video recording and streaming images or video of the reactor room through the Internet.
- **Fire suppression system:** The reaction room is equipped with a fire suppression system (temperature melt sensors are located in the ceiling), that is activated if the temperature in the room exceeds 375 °F, causing the devices to melt, releasing the tension in the metal steel string they are attached to and triggering the release of dry powder fire suppressant into the room. More recent attempts to get the dry powder replaced by an alternative chemical have been undertaken since dry powder fire suppressant is not intended to be used in rooms with electrical equipment since it can ruin them. Additionally the control room is equipped with a fire extinguisher that is connected to a transmitter and in the event of lifting up the extinguisher from

its wall support, the connector cable will break and trigger a signal to the local fire department to come and help and take control of the event.

- **Air-actuated valve control panel:** The valve control panel shown in Figure 2.30 features all of the control valves for the air-actuated valves as well as the back-pressure regulators (BPRs) in the gas handling system. A full schematic of the valve control panel is shown in Figure 2.31, which shows the full detail of the plumbing of the valves. The valves used for the control panel are brass three-way valves manufactured by Swagelok (part number B-41GXS1). The panel is internally plumbed in ¼-in. o.d. stainless steel tubing and nylon tubing for the leg of the valve that connects to the respective air-actuated valve. The main idea is to have a way to deflect the air flow from either the air cylinder to the valve or from the valve to the atmosphere (venting process). In case any one of the nylon air lines that controls an air-actuator valve was to rupture (lines that are fed from a DOT-300 size cylinder of breathing air installed in the control room), a leak would not be a problem to the operators inside the control room since the gas in question is breathing air. On the other hand, if a nitrogen line that controls the BPRs (operated up at up to 700 psig) develops a leak inside the control room, an alarm from the oxygen deficiency monitor will be activated as previously discussed.

A complete list of the components (valves, actuators, orifices, etc) are detailed in Appendix B where their model numbers and prices are given.



Figure 2.30. Air-actuated valve control panel located in the control room.

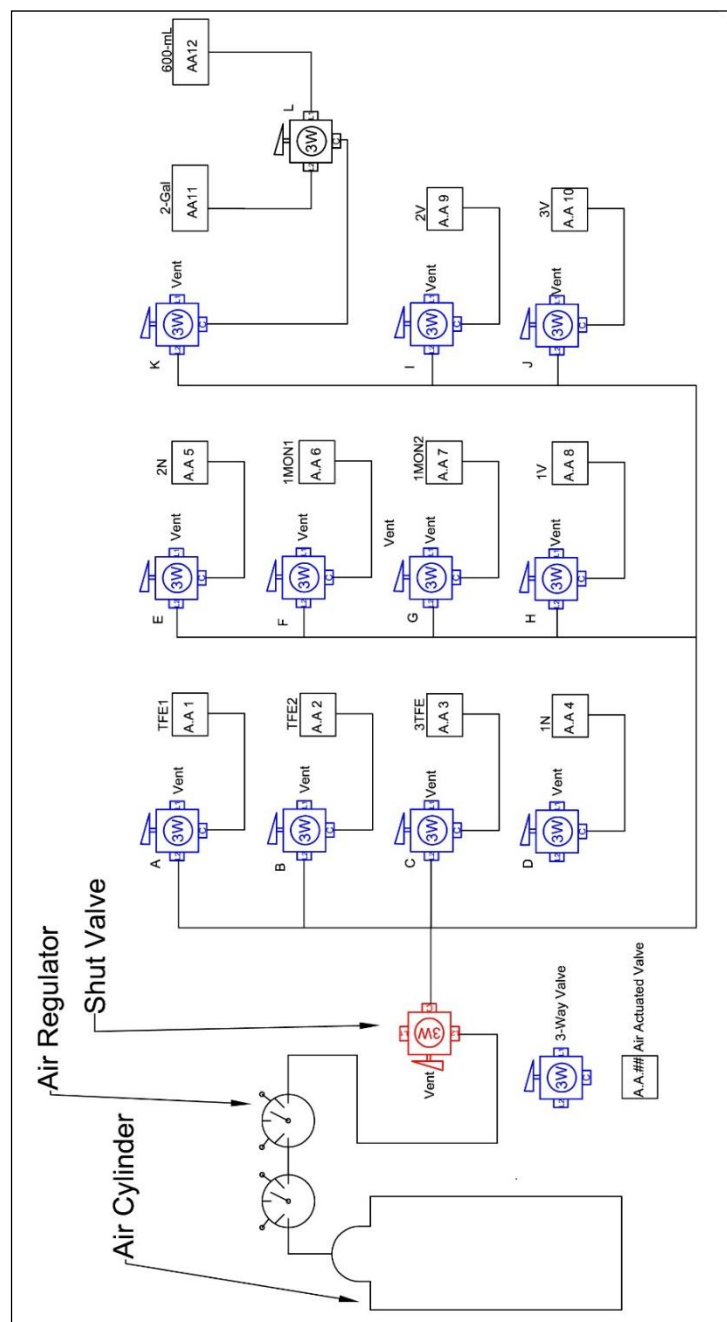


Figure 2.31. Schematic of the valve control panel. The three-way valves labeled A through K are located at the panel in the control room. The air actuators labeled AA 1 through AA 12 are located at the reaction room.

2.4.3. Data Acquisition (DAQ) System

The control room is equipped with a computer hosting the software that communicates with the data acquisition board. The software is widely explained in Appendix C, and the hardware design is discussed in Appendix D. Both software and hardware were designed and built on its entirety by myself.

2.4.4. Gas Handling System

The entirety of the gas handling system is built in stainless steel (type 316) and is detailed in Figure 2.32. A zoomed-in view of the gas handling system is shown in Figure 2.33 and 2.34 where the diagram is split in half at three points marked as A, B, and C. The main idea of the gas handling system is to incorporate TFE into the polymerization reactor from one side of the facility and another gas monomer from the opposite side of the reaction room. Both sides are equipped with a high purity nitrogen cylinder that is meant for leak checking and purging the system from traces of oxygen. Each line (TFE and second monomer) is equipped with a mass flow controller (MFC) with an inline filter before the MFC.

As mentioned above, different configurations of the system allow different parts of the system to be evacuated or purged at any time. In the case of a plug in the line, that part of the system can be isolated just before the reactor and right after the TFE cylinder, and

the lines in between can be evacuated remotely and purged with nitrogen before the operator can repair them. After the repair is made (if a reaction/polymerization needs to take place) the lines can be evacuated and purged several times in order to remove oxygen before opening the TFE cylinder again to continue the reaction/polymerization. The gas handling system (TFE side) also contains a 300-mL ballast volume element to compensate fast pressure fluctuations during a reaction. The system also contains a small (500-mL internal) scrubber to remove small amounts of carbon dioxide from TFE/CO₂ gas mixtures. This is only advised if the reaction or process requires a small amount of neat TFE as the capacity of the scrubber is limited. The scrubber is also equipped with a multi-point thermocouple that can track the heat wave produced as the scrubbing material is consumed along the trap. The operator will know when the scrubbing capacity is near the end by tracking the heat wave as it gets close to the end of the scrubbing cylinder. The scrubber is filled with Ascarite®, which is commercially available in a variety of grain sizes.

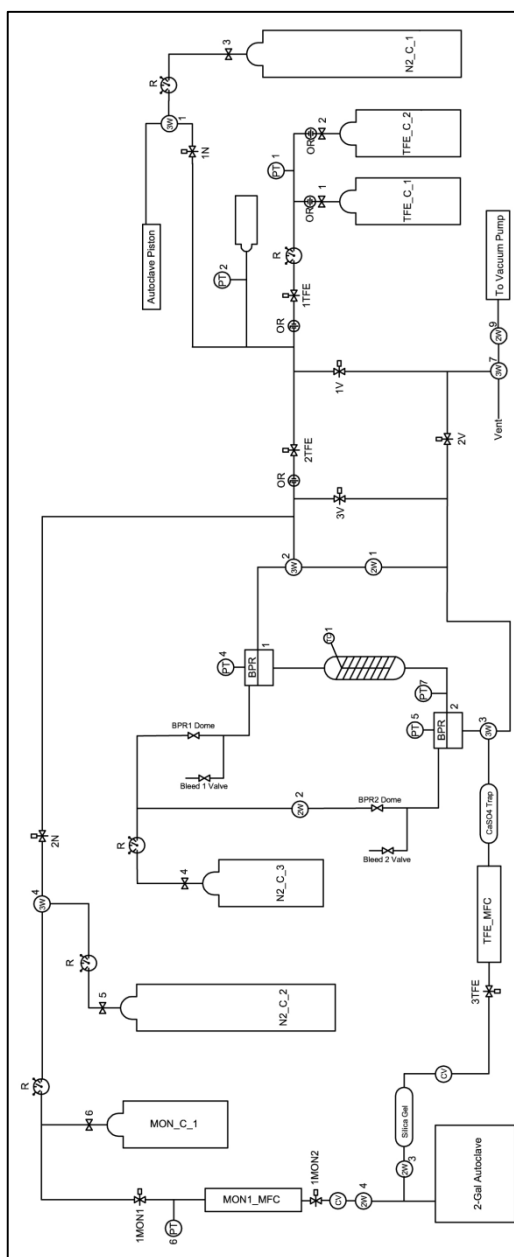


Figure 2.32. Schematic of the gas handling system at TFE barricade in Clemson University.

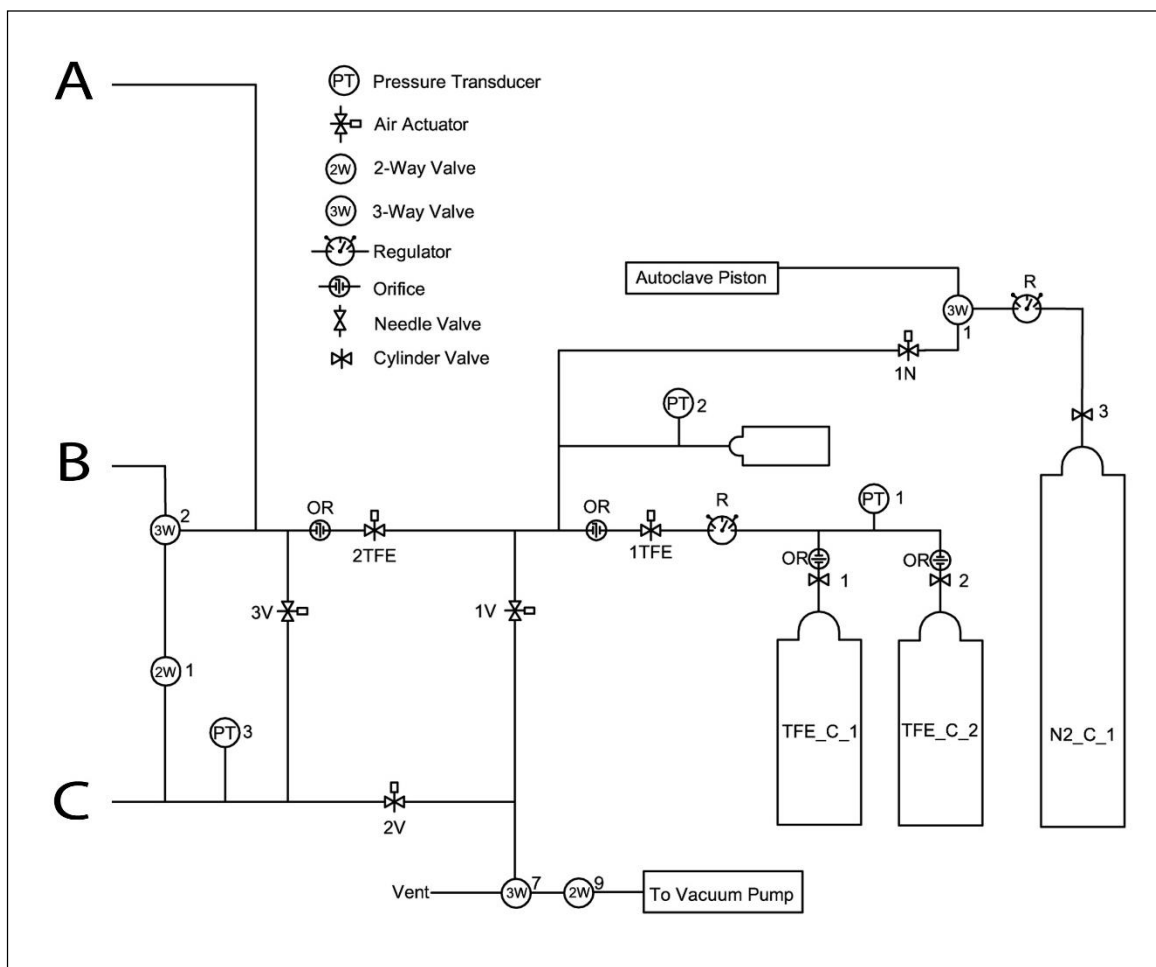


Figure 2.33. Schematic of the gas handling system at TFE barricade in Clemson University. View of the right side of the system (see Figure 2.34 for the counterpart of the figure).

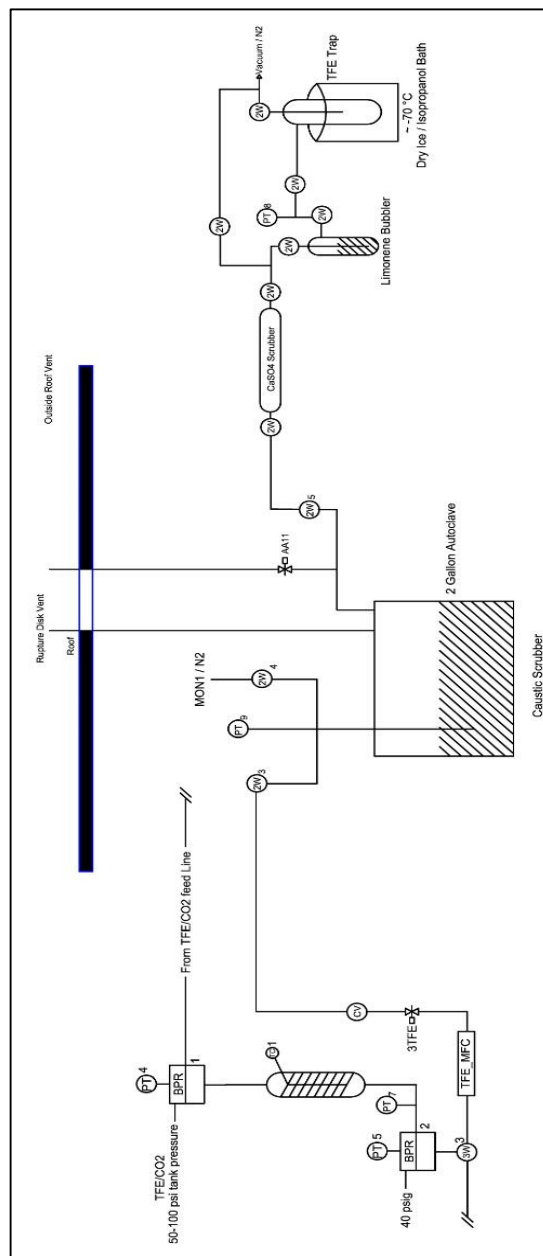


Figure 2.35. TFE scrubbing system.

As an improvement over the previous scrubbing system (University of Alabama) we have added a back pressure regulator (BPR) on the outlet of the scrubber in order to control the downstream pressure. It is important to control the residence time of the TFE/CO₂ mixture in the scrubber in order to guarantee that all the carbon dioxide is being scrubbed out of the mixture. Also by losing 50% of the molar amount of gas, there is a pressure decay along the scrubber and therefore having a higher threshold at the exit of the scrubber helps maintain the mixture inside the scrubber for a longer time. It is important to mention that the controls for the BPRs are located in the main valve panel in the control room as shown at the left side of the panel in Figure 2.30. The diagram of the nitrogen feed into the domes of the BPRs are shown in Figure 2.3.

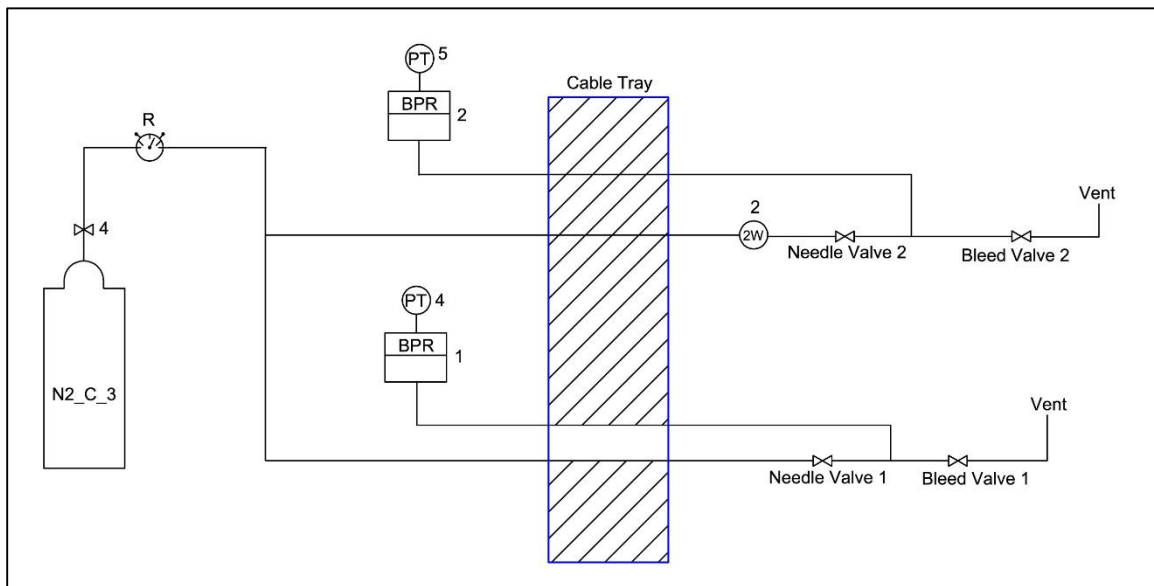


Figure 2.36. BPR valve system connection diagram.

2.4.5. Deoxygenated Water System

Considering that an aqueous TFE polymerization reaction requires oxygen free water as the solvent, a system was developed in which the level of dissolved oxygen can be controlled and minimized. Industrial setups often use a steam out method in which superheated water vapor is introduced in the reactor to displace any oxygen. There is not currently a steam generator at this facility, and therefore the need to find an alternative approach led to one of the labs in the AMRL being equipped with a large container for deionized, deoxygenate water. Our approach is shown schematically in Figure 2.3. A funnel-shaped water tank (Den Hertog IBFD35 Set)³⁷ shown on the left side of the figure is first filled with high quality, deionized water. The water is then sparged with a stream of nitrogen (< 45 psig; the large lid to the Den Hartog tank is not totally leak free, so the over pressure of nitrogen and displaced oxygen can vent here) until the dissolved oxygen level is below 1.0 ppm as measured by a dissolved oxygen meter (YSI ProODO meter²⁵ shown in Figure 2.3). A water line from the bottom of the water reservoir is introduced into a glove bag that is equipped with a balance to measure the amount of water required accurately. By purging the glove bag with nitrogen gas, the glove bag can reach less than 100 ppm of oxygen, which is measured with a vapor oxygen sensor (Vacuum Atmospheres) that samples from the glove bag using an aquarium air pump.

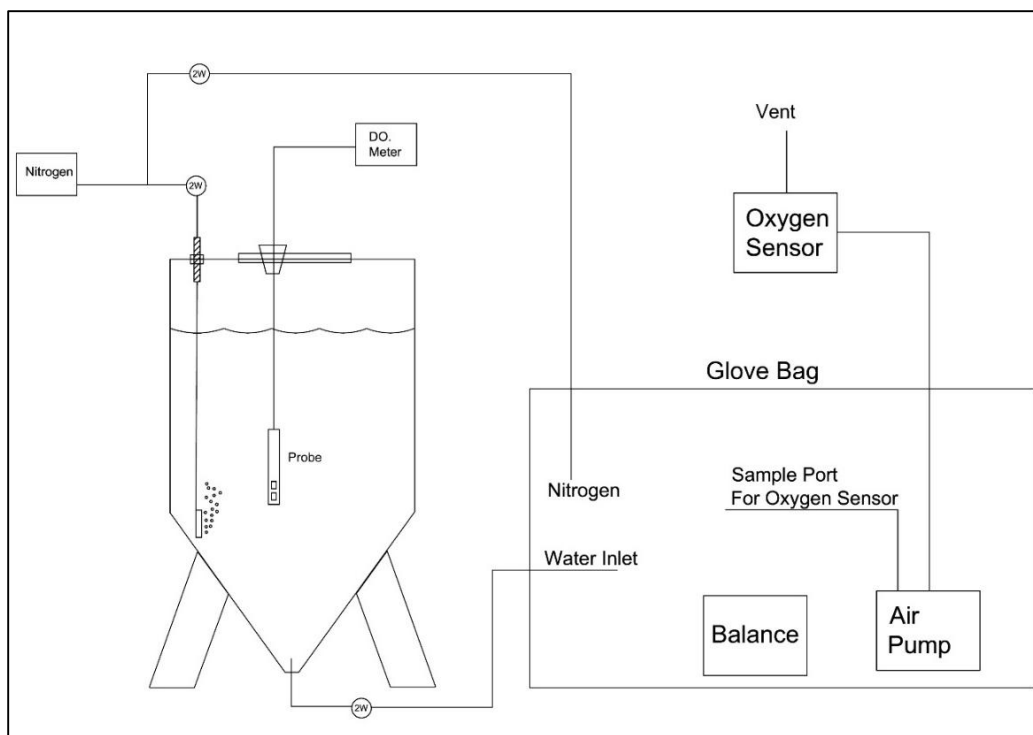


Figure 2.37. Deionized, deoxygenated water and glove bag system installed in lab 3 at the AMRL building.³⁷



Figure 2.38. Dissolved oxygen sensor YSI ProODO meter (Picture taken from YSI online catalog²⁵).

2.4.5. Reactor Setup

The barricade is able to handle autoclaves ranging from 50-mL to 2-gal. The heart of the facility is a 2-gal standing reactor (Parr Instruments) which is shown in Figure 2.3 in full detail. One of the features of the reaction room is its ability to handle different reactors by just changing some electrical and gas connections. The TFE and other monomer gas lines can be connected to the specific reactor to be used as well as the thermocouple (for temperature control), the cooling lines (which are equipped with leak-free quick disconnect fittings), the air line for the air actuated valve that opens the vent port (each reactor is equipped with its own air actuated valve), the tachometer sensor cable line, the stirring motor power line, the pressure transducer signal cable and the radical initiator line. Once the aforementioned connections are made to the specific reactor to be used, one can continue to check the standard operating procedures (SOPs) for instructions on how to continue with a reaction/polymerization. More details and schematics of the reactor (as well as its replacement parts) are included in Appendix B.

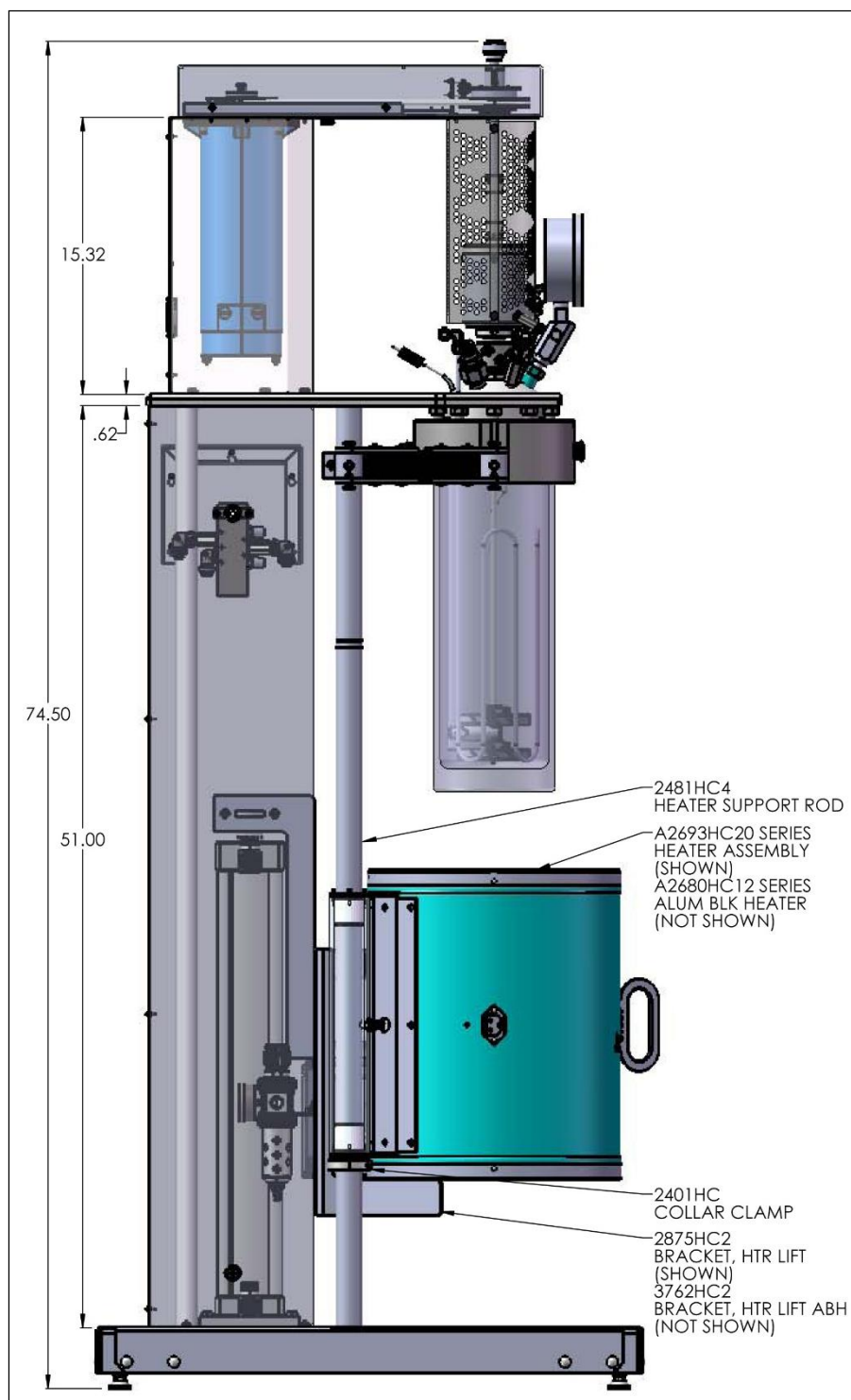


Figure 2.39. Parr Reactor left side view. Reproduced with permission from Parr Industries (April 2016).

The autoclave vent line is connected to outside of the reaction room by a straight 1/4-in. o.d. stainless steel tube, and the vent line is connected to a fail-closed, air-actuated valve that is controlled from the control room. Each autoclave is equipped with its own air actuated valve to minimize the distance between the inside volume of the reactor and the seal of the actuated valve. If only one actuated valve for venting had been located in a common place for both reactor locations, then the volume of the reactor (and therefore the reactor contents) would be exposed in that line creating a risk of a leak and/or an operator bumping into the line. The vent line is piped through a hole in the ceiling of the reaction room to outside of the room, and on the exterior of the reaction room, this line is bent in such way that the end is pointing downwards to avoid liquids from coming back down inside the line.

Another type of vent line inside the reaction room is the one attached to the rupture disc assembly. The 2-gal reactor has plumbing in place for the rupture disc made out of stainless steel tubing of 3/8-in. o.d. An industrial partner advised to try to maintain very soft and prolonged curves on that pipe so that in the case of blowing a rupture disc, the shear will be minimized. The rupture disc pipeline is also passed through the ceiling of the facility to outside of the room. The small autoclave table setup does not contain a fixed pipe for the rupture disc assembly, because in the event of a rupture of the disc on a small autoclave, the amount of material does not represent a major problem to be vented inside the room. Nevertheless, a piece of flexible copper tubing can be connected to the outlet of the burst disc assembly on smaller autoclaves, and that tube can be aimed into a collection bucket in the event of a failure of the rupture disc.

Internal cooling to the respective autoclave is controlled by the autoclave controller (Parr Instruments 4848 type controller). A PID temperature controller is capable of supplying 24 VAC to a solenoid valve that is connected to the cooling loop right outside the output of the cooling machine. In this case, the cooling machine (Thermo Scientific ULT 80) is normally set around at 5-20 °C which is significantly lower than the temperature at which a reaction is typically run (60-130 °C), and the autoclave controller is able to open and close these solenoid valves, letting the coolant inside the loop and thereby controlling the temperature of the reaction. When the cooling coil is open to the autoclave, the active heating is turned off to minimize electric consumption and the hysteresis of the controller is setup to 1 °C for maximum precision on the temperature control. The controller can be tuned (2 hour process) periodically to make sure that the PID settings are the optimal for a given process. Usually before using a new set of conditions, the autoclave is auto-tuned in order to achieve a stable temperature with both cooling and heating for the desired amount of solvent in the reactor, the target temperature inside the vessel and the target temperature inside the cooling coil.

2.5. Summary

The knowledge passed from generation to generation of TFE polymerization facilities has enabled Clemson University to complete the construction of a safe barricade facility. This facility from time to time acquires TFE from the storage cylinders located in main Clemson University campus (first generation facility) and transported safely to the

new polymerization facility for further polymerization. Furthermore, the polymers discussed later in this Dissertation were developed in the facility discussed in detail in this Chapter.

2.6. References

1. Ebnesajjad, S. Fluoroplastics. Volume 1: Non-Melt Processible Fluoroplastics: The Definitive User's Guide and Databook; 2nd ed. Plastics Design Library: Norwich, NY, 2000.
2. Franko-Filipasic, B. R.; Michaelson, R. C. CEP, Chem. Eng. Prog. **1984**, 80, 65-69.
3. Blackburn, D. W.; Reiff, H. E. Ann. N.Y. Acad. Sci. **1967**, 145, 192-203.
4. Stephens, H. R.; Walker, K. E. Safety in Small-Scale High Pressure Experiments. Ind. Eng. Chem. **1957**, 49, 2022-2025.
5. Penninger, J. M. L.; Okazaki, J. K. CEP, Chem. Eng. Prog. **1980**, 76, 65-71.
6. Bodurtha, F. T. J.; Bonifaz, C. Laboratory Barricade. U.S. Patent 4,474,052, Oct 2, 1984.
7. Sharif, I.; Creager, S.; Desmarteau, D. D. "Fluorinated Ionomers and Ionomer Membranes Containing the Bis[(Perfluoroalkyl)sulfonyl]imide Protogenic Group". In Handbook of Fluoropolymer Science and Technology; 1st ed.; Iacono, S. T., Iyer, S. S., Smith, D. W., Eds.; John Wiley & Sons: Hoboken, NJ, USA, 2014, pp 521-544.
8. Sayler, T. S. Preparation of Perfluorinated Ionomers for Fuel Cell Applications. Ph.D. Dissertation, The University of Alabama, Tuscaloosa, AL, 2012.

9. Sayler, T. S.; Tice, K. T.; Beg, M. A.; Fernandez, R. E.; Thrasher, J. S. Preparation of Low Equivalent Weight Perfluorinated Ionomers with Water Insolubility. *Polym. Prepr. (Am. Chem. Soc., Div. Polym. Chem.)* **2012**, 53, 39-40.
10. Hercules, D. A.; Desmarteau, D. D.; Fernandez, R. E.; Clark, J. L.; Thrasher, J. S. "Evolution of Academic Barricades for the Use of Tetrafluoroethylene (TFE) in the Preparation of Fluoropolymers". In *Handbook of Fluoropolymer Science and Technology*; 1st ed.; Iacono, S. T., Iyer, S. S., Smith, D. W., Eds.; John Wiley & Sons: Hoboken, NJ, USA, 2014, pp 415-433.
11. DesMarteau, D. D. Copolymers of Tetrafluoroethylene and Perfluorinated Sulfonyl Monomers and Membranes Made There From. U.S. Patent 5,463,005, Oct 31, 1995.
12. Wainright, J. S.; Savinell, R. F.; Desmarteau, D. D.; Ma, J. J.; Sung, K.; Zhang, L. *Proc. Electrochem. Soc.* **1994**, 94, 265-274.
13. Van Bramer, D. J.; Shiflett, M. B.; Yokozeki, A. Safe Handling of Tetrafluoroethylene. U.S. Patent 5,345,013, Sep 6, 1994.
14. Van Bramer, D. J. Tetrafluoroethylene Shipping/Storage Mixtures. U.S. Patent 5,866,727, Feb 2, 1999.
15. Babenko, Y. I.; Lisochkin, Y. A.; Poznyak, V. I. Explosion of Tetrafluoroethylene During Nonisothermal Polymerization. *Combust. Explos. Shock Waves* **1993**, 29, 603-609.

16. Reza, A.; Christiansen, E. A Case Study of a TFE Explosion in a PTFE Manufacturing Facility. *Process Saf. Prog.* **2007**, 26, 77-82.
17. Ferrero, F.; Meyer, R.; Kluge, M.; Schroder, V.; Spoormaker, T. Self-Ignition of Tetrafluoroethylene Induced by Rapid Valve Opening in Small Diameter Pipes. *Loss Prevent Proc.* **2013**, 26, 177-185.
18. Burch, D. H. Dupont. Private Communication, 2012.
19. Thomas, B. H.; DesMarteau, D. D. Self-Emulsifying Polymerization (SEP) of 3,6-Dioxa- Δ^7 -4-Trifluoromethyl Perfluorooctyl Trifluoromethyl Sulfonimide With Tetrafluoroethylene. *J. Fluorine Chem.* **2005**, 126, 1057-1064.
20. Thomas, B. H.; Shafer, G.; Ma, J. J.; Tu, M. H.; DesMarteau, D. D. Synthesis of 3,6-Dioxa- Δ^7 -4-Trifluoromethyl Perfluorooctyl Trifluoromethyl Sulfonimide: Bis[(Perfluoroalkyl)Sulfonyl] Superacid Monomer and Polymer. *J. Fluorine Chem.* **2004**, 125, 1231-1240.
21. Shafer, G. Chemistry of Perfluoroalkylsulfonyl Methanes. Development of Vinyl Ether Monomers and Their Copolymerization with Tetrafluoroethylene. Ph.D. Dissertation, Clemson University, SC, 2001; pp 26-28.
22. Zhou, S. Synthesis and Characterization of Perfluorinated Sulfonimide Copolymers Electrolyte Membranes. Ph.D. Dissertation, Clemson University, SC, 2002; pp 82-84.

23. Ford, L. A. Novel Semifluorinated Polyaryl Ether Electrolytes Containing the Perfluorocyclobutane Linkage. PhD. Dissertation, Clemson University, Clemson, SC, 2002; pp 18-21.
24. Lu, C.; Kim, J. H.; DesMarteau, D. D. Synthesis of Perfluoro-t-butyl trifluorovinyl ether and its Copolymerization with TFE. *J. Fluorine Chem.* **2010**, 131, 17-20.
25. YSI: A Xylem Brand. ProODO Handheld Optical Dissolved Oxygen Meter. <http://www.ysi.com/productsdetail.php?ProODO-19> (accessed February 21, 2013).
26. Craig, L. E.; Dew, J. E. *Ind. Eng. Res.* **1959**, 51, 1249-1252.
27. Kornath, A.; Kaufmann, A. Ludwig-Maximilians-Universität München, Germany. Private Communication, July 2007.
28. Kauffman, G. B. Teflon – 50 Slippery Years. *Educ. Chem.* **1988**, 25, 173.
29. Livingston, E. H. *CEP, Chem. Eng. Prog.* **1984**, 80, 70-75.
30. Fluitron, Inc. Innovation in Pressure Technology: Containment Cells. <http://catalog.fluitron.com/item/all-categories/containment-cells/item-1007?forward=1> (accessed September 13, 2010).
31. Folawewo, F. Fluitron, Inc. Ivyland, PA. Private communication, 2010.
32. South Carolina Department of Labor, Licensing and Regulation. Boiler Safety Program. Boiler Registration and Inspection Information. Document 200.

- <http://www.llr.state.sc.us/POL/Boilers/Forms/Doc%20200.pdf> (accessed October 8, 2010).
33. U.S. Explosive Storage. Our Strength is Your Security. Outdoor Magazines. http://www.usexplosivestorage.com/index.php?option=com_content&view=article&id=93&Itemid=119 (accessed June 30, 2013).
34. Swagelok Online Catalog. <https://www.swagelok.com/en/Resources/Product-Catalog> (accessed January 04, 2016).
35. Teledyne ISCO Online Catalog. <http://www.isco.com/products/literature.asp>. (accessed January 04, 2016).
36. Hercules, D. A.; Parrish, C. A.; Sayler, T. A.; Tice, K. T.; Williams, S. M.; Lowery, L. E.; Brady, M. E.; Coward, R. B.; Murphy, J. A.; Hey, T. A.; Scabuzzo, A. R.; Rummler, L. M.; Mastnev, A. V.; Thrasher, J. S. Preparation of Tetrafluoroethylene from the Pyrolysis of Pentafluoropropionate Salts. Manuscript in Preparation.
37. Den Hertog Industries, Inc. New 35 & 60 Gallon Full Drain Blow Molded Inductor Tanks and Poly Stand Sets. <http://www.denhartogindustries.com/news/new-35-60-gallon-fulldrain-blow-molded-inductor-tanks-and-poly-stand-sets/> (accessed February 7, 2013).

Chapter 3

Preparation of Tetrafluoroethylene from the Pyrolysis of Pentafluoropropionate

Salts

3.1. Abstract

The synthesis of tetrafluoroethylene (TFE) for use in academic institutions beyond a few millimoles has often been inhibited by the compound's inherent danger and its general lack of commercial availability. On the other hand, TFE is prepared industrially on a rather large scale by a number of major fluorochemical companies via the pyrolysis of chlorodifluoromethane at high temperatures, yielding TFE and HCl. For a few years at The University of Alabama and Clemson University, we have been preparing TFE on a 100⁺-gram scale by the pyrolysis under dynamic vacuum of pentafluoropropionate salts, which can be obtained from the neutralization of pentafluoropropionic acid with a $M(OH)_n$ (where $M = Li, Na, K,$ and Cs for $n = 1$ and $Mg, Ca,$ and Ba for $n = 2$). Additionally, potassium pentafluoropropionate can be prepared from the reaction of potassium trimethylsilanolate and ethyl pentafluoropropionate. The pentafluoropropionate salts and their decomposition products have been characterized by thermogravimetric analysis (TGA), accelerating rate calorimetry (ARC), nuclear magnetic resonance (NMR) spectroscopy, mass spectrometry, Fourier transform-infrared (FTIR) spectrophotometry, scanning electron microscopy (SEM) / energy dispersive spectroscopy (EDAX), X-ray diffraction (XRD), and single-crystal X-ray crystallography, where applicable. Typical yields of TFE obtained from pyrolysis of potassium pentafluoropropionate obtained from

the acid-base neutralization method are > 98% (as seen in Figure 3.1), while yields of TFE from the same salt prepared by the silanolate method from ethyl pentafluoropropionate are ca. 80%.

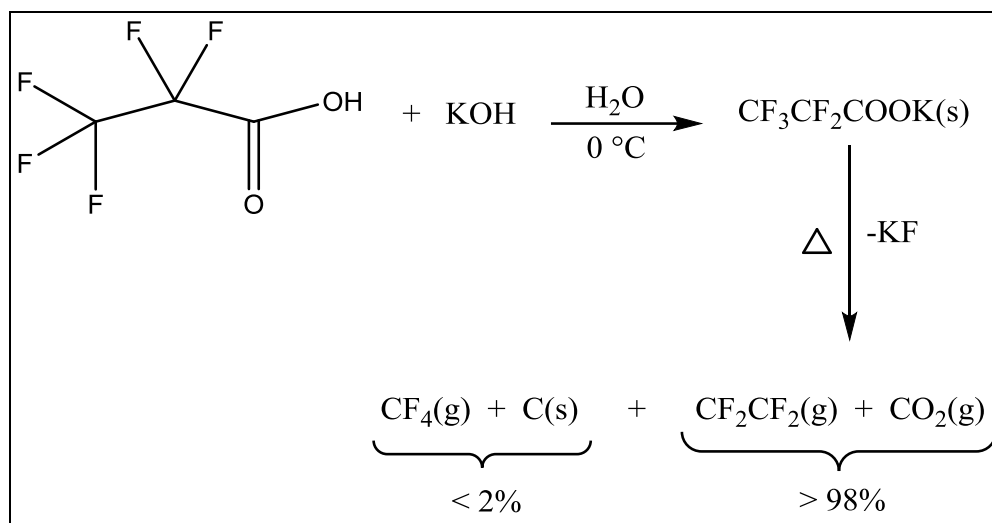


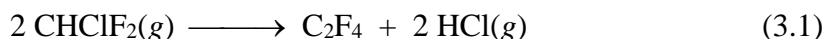
Figure 3.1. Reaction scheme for the preparation of TFE/CO₂ from the pyrolysis of potassium perfluoropropionate.

3.2. Introduction

Since the curious discovery of polytetrafluoroethylene (PTFE) in 1938 by Plunkett,¹⁻³ the interest and use of tetrafluoroethylene (TFE) as a building block for fluoropolymers has increased due to the unique properties of materials that are made from this monomer. Its homopolymer has the advantages of being both chemically and

thermally resistant, which are of great benefit for its use in aeronautics, parts manufacturing, and specialty materials.¹⁻³ Other compositions of matter of great importance can be derived from TFE such as its copolymers with various perfluoroalkyl vinyl ethers to give perfluoroalkoxy resins (PFA), with hexafluoropropylene to give fluorinated ethylene-propylene (FEP) resins, and with ethylene forming poly(ethylene-*co*-tetrafluoroethylene) (ETFE).⁴ Another major use of TFE is in the manufacture of perfluorinated ionomers such as Nafion[®], Aquivion[®], and others for applications in the chlor-alkali industry as well as energy conversion and storage devices.^{5,6}

The fluorochemical industry prepares TFE via the pyrolysis of chlorodifluoromethane (CHClF₂), more commonly known as R22, as shown in equation 3.1. The advantage of this process is the ability to obtain TFE from 99.99% to 99.999% purity, but we have been led to believe that this synthetic method is impractical to be built on a smaller scale for an academic institution due to prohibitive cost and the inherent complications of running a continuous process without interruption.⁷⁻¹²



In addition to being able to prepare adequate quantities of TFE, a facility for the safe handling of TFE represents the other primary hurdle that an academic institution must overcome¹³ when trying to prepare research quantities of TFE-based homo-, co-, and terpolymers. Thus, both at the University of Alabama^{14,15} and more recently at Clemson University, we have constructed special facilities for the safe handling and polymerization

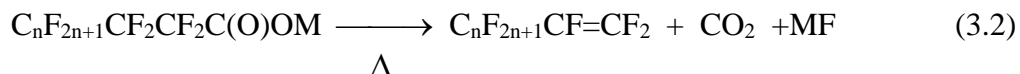
of TFE. Until now, large quantities of TFE have been deemed too unsafe to be handled in an academic institution.¹⁶⁻¹⁸ However, with the use of the aforementioned facilities, especially the most recent and advanced one at Clemson, the ability to handle TFE has been increased to the kilogram scale, while the storage of multi-kilogram quantities of TFE has also been enabled. These facilities, including a former TFE barricade at Clemson that was constructed by DesMarteau, were the subject of a recent review chapter.¹³

For a number of years, TFE has not been commercially available with the exception of small quantities from an occasional catalog chemical company (e.g., ABCR GmbH), and even then the price is prohibitively expensive for the scale being described. Thus, we had to come up with a way to prepare TFE in our own laboratories. A common alternative to the industrial route to TFE is to actually pyrolyze waste PTFE; however, until recently, this method had been fraught with significant quantities of side products including hexafluoropropylene (HFP), octafluorocyclobutane (OFCB), and the extremely toxic perfluoroisobutylene (PFIB).¹⁹⁻²⁶ However, unless one has ready access to waste or scrap PTFE, this method may not be cost effective.

While at the University of Alabama, an additional safety requirement existed due to the fact that the barricade facility there had been both incorrectly designed and built (i.e., too weak walls and floor to contain a deflagration of less than 125 g of TFE). In order to use that facility, we turned to patented technology of the DuPont Company (now Chemours) where Van Bramer, Shiflett, and Yokozeki discovered that TFE could be rendered safe from deflagration when mixed with 30-mol %, or more, carbon dioxide,

CO₂.²⁷ Since this patent claimed only the liquid composition of TFE/CO₂, we made sure to use/store only gaseous mixtures of TFE/CO₂ until the patent expired.

However, even with the additional safety requirement in hand at least theoretically, a source of TFE/CO₂ was still required, as DuPont (now Chemours) only sells its TFE Safe-Supply™ to its commercial partners.²⁸ Interestingly enough, in the early 1950s both 3M and Haszeldine independently discovered that the pyrolysis of either alkali metal or alkaline earth metal pentafluoroalkanoate salts gave terminal perfluoroolefins and carbon dioxide in approximately equimolar mixtures as shown in equation 2.²⁹⁻³³ In their publications, 3M gave the most examples and obtained the best yields (96-99%) for the generation of HFP when n = 1 in equation 3.2. Researchers at 3M and Haszeldine both seemed to favor sodium as the alkali metal of choice for this reaction, and for the preparation of TFE (where n = 0 in equation 3.2), they both obtained ca. 80-90% yield. Likewise, during the process of coming up to speed in terms of



preparing TFE-based fluoropolymers, we learned that Kornath and Kaufmann at the Ludwig-Maximilians-Universität Munich had rediscovered this route to TFE and CO₂, where they too seem to have a preference for the pyrolysis of the sodium salt. Admittedly, we learned and benefitted from their shared procedure.³⁴

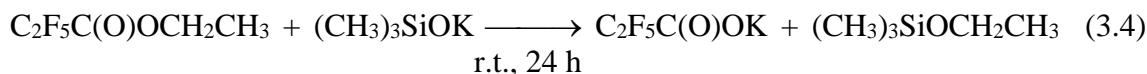
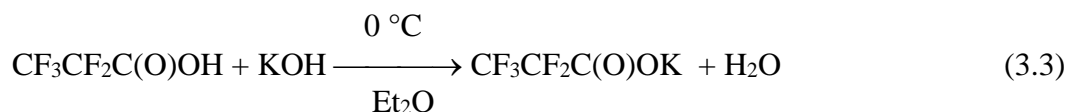
More recently, our laboratory developed a process that demonstrates the importance of equimolar TFE/CO₂ mixtures not only for the preparation of fluoropolymers

but also for small molecule chemistry, in particular for the synthesis of SF₅-containing compounds. Thus, it was found that the 50:50 molar mixture of TFE/CO₂ could be safely converted into pentafluorosulfanyldifluoroacetic acid [SF₅CF₂C(O)OH] over four steps in about 60% overall yield. All earlier known approaches to SF₅CF₂C(O)OH were either significantly lower yielding processes or required the use of dangerous reagents, such as alkyl trifluorovinyl ethers or uninhibited TFE. The use of TFE/CO₂ mixtures allowed us to both prepare SF₅CF₂C(O)OH on a multi-gram scale as well as explore the chemistry of the SF₅CF₂- group in the synthesis of compounds that might be of interest to medicinal and agro chemistry.³⁵

In the present report, support will be provided for the preference of potassium pentafluoropropionate as the starting material of choice for preparing mixtures of TFE and CO₂. The reasons include, among others, (1) an increased overall yields of TFE and CO₂, (2) a more even control of heat and mass transfer during the pyrolysis, and (3) less foaming with the evolution of gases during the pyrolysis. The simple hydrolysis of pentafluoropropionic acid, CF₃CF₂C(O)OH, with potassium hydroxide, KOH, to give potassium pentafluoropropionate will also be preferred over the reaction of the corresponding ethyl ester CF₃CF₂C(O)OCH₂CH₃ with potassium trimethylsilanolate, (CH₃)₃SiOK.^{9,36,37} Evidence for the formation of carbon, C, and tetrafluoromethane, CF₄, as minor byproducts in the formation of TFE and CO₂ in the pyrolysis of potassium pentafluoropropionate will also be presented.

3.3. Results and discussion

We have incorporated former patent technology from both 3M³¹ and DuPont (now Chemours)²⁷ in the preparation and use of TFE-CO₂ mixtures. Two approaches can be used to prepare either alkali or alkaline earth metal pentafluoropropionates: (Method A) the slow neutralization of an aqueous metal hydroxide solution/slurry by pentafluoropropionic acid yielding water and the corresponding alkali or alkali earth metal pentafluoropropionate, as shown in equation 3.3, or (Method B) the corresponding reaction of a pentafluoropropionate ester with a metal silanolate in an organic solvent such as diethyl ether, as shown in equation 3.4. With Method A, pentafluoropropionic acid is added drop wise to a chilled, aqueous solution (or slurry) of base in order to prevent loss of acid due to evaporation from the heat of the reaction. The reaction is also titrated until slightly acidic, as any excess acid can easily be removed during the drying stages,



where that would not be possible for excess base. While it was easy to obtain 98-99% yield of the corresponding metal pentafluoropropionate from the simple acid-base chemistry, we had trouble achieving the 92-93% literature yield^{36,38} of potassium pentafluoropropionate via the silanolate chemistry and only obtained the desired salt in 75-80% yield. Two

possible rationale for the difference in percent yields are the choice of reaction solvent (previous results are reported using either THF, dioxane, diethyl ether, or CH_2Cl_2)³⁶⁻³⁸ and the molar ratio of the reactants used. For example, in a more recent and thorough study, Lovrić and co-workers used 1.2 molar equivalents of silanolate for every mole of ester,³⁷ where we carried out our reactions on an equimolar scale as described by the previous investigators.^{36,38} Furthermore, the silanolate route does not seem to be nearly as cost effective, and as will be described below, the pyrolysis of potassium pentafluoropropionate prepared by this route also gave far lower yields of TFE and CO_2 .

Another important step in the process of obtaining TFE/ CO_2 in high yield and purity is the drying of the pentafluoropropionate salt. First, bulk water is removed using a rotary evaporator, and the resulting material is then ground to a fine powder with a mortar and pestle prior to exhaustive drying at 80 °C and 20 mTorr vacuum until the salts reach a constant weight. (The early literature indicates drying "by heating in air at 100 °C for 8 hours".²⁹) If necessary, the salts can be ground again, but usually just shaking the material within the flask will break up any clumps that may have formed during further drying. The drying stages beyond the removal of bulk water are usually carried out both on the amount of salts that will be used in an upcoming pyrolysis as well as in what will become the pyrolysis flask so as to not have to transfer the material further. As will be shown further when the thermal properties of the pentafluoropropionate salts are discussed, it is extremely important to **not overheat** the salts while drying so as to avoid rapid gas evolution due to an unexpected onset of thermal decomposition. It is crucial to pay attention to this part of the drying process in an academic institution, especially if

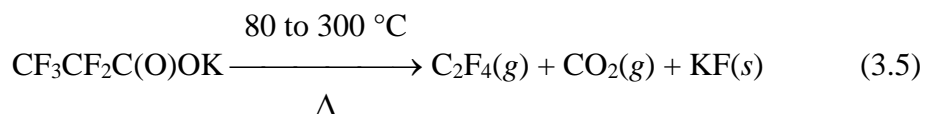
undergraduate students are involved. On the other hand, should residual water remain in the salts, the primary impurity previously found in the pyrolysis products, other than TFE and CO₂, was pentafluoroethane (CF₃CF₂H, HFC-125).^{14,29-31}

The pentafluoropropionate salts, especially the potassium salt, were spectroscopically characterized by multinuclear NMR, infrared, and mass spectrometry. All spectra were as expected, with only the results of the negative ion, electrospray ionization (ESI) mass spectrometry bearing further comment. In the Experimental and Supporting Information sections, one will notice that many of the anion clusters observed in the ESI-mass spectra of potassium pentafluoropropionate have one or more sodium (Na) atoms present. Alkali metal salts are well known for not being metal pure, so perhaps the technical grade KOH used had some sodium contamination, and/or some sodium contamination came during the sample preparation, etc. Furthermore, other researchers have reported that the ESI-mass spectra of lariat ethers with carboxylate arms display a strong selectivity for sodium over potassium.³⁹ Both the thermal and crystal properties of the pentafluoropropionate salts will be discussed below.

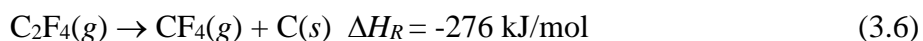
One of the primary reasons for our preference of using potassium pentafluoropropionate over sodium pentafluoropropionate turns out to be the fact that one can routinely prepare a mixture of TFE and CO₂ in 98% yield with the potassium salt, where we and others (3M and Haszeldine)²⁹⁻³³ only achieved about 80-90% yield from the sodium salt. For comparison, it is important to note that researchers at 3M were able to obtain 98-99% yields of hexafluoropropylene (HFP) and CO₂ when pyrolyzing sodium heptafluorobutyrate (see equation 2 for $n = 1$).²⁹⁻³¹ Haszeldine also appeared to carry out

his pyrolysis at 150 Torr, which could have also led to more side products (e.g., perfluorocyclobutane, C₄F₈). Perhaps this outcome is parallel to the observation that less impurities are obtained in the production of TFE when the pyrolysis of PTFE is carried out under more strongly reduced pressure.^{14,15} In our hands, the pyrolysis of potassium pentafluoropropionate under a low heating rate of 1°C per minute from 80 to 300 °C and dynamic vacuum (10⁻³ to 10⁻⁴ Torr, with the gaseous products being collected at liquid nitrogen temperature) gave a mixture of TFE and CO₂ with no discernible impurities by NMR and infrared spectroscopy. On the other hand, although the potassium pentafluoropropionate prepared by the silanolate method appeared spectroscopically to be the same as the potassium salt prepared by the simple neutralization reaction, its thermal decomposition gave TFE and CO₂ in only about 75-80% yield. Overall, it is important to remember that regardless of the choices of metal cation and pyrolysis conditions, one obtains TFE with roughly equimolar amounts of CO₂, which results in a safe gas mixture for handling²⁷ in further research.

We next turned our attention to the identity of the yield-loss products as well as any rationale for why the potassium salt gives higher yields of TFE and CO₂. First, remaining after the pyrolysis of any pentafluoropropionate salt should be the corresponding white, metal fluoride, as shown by way of example for the potassium salt in equation 3.5. However, the salts remaining after



the pyrolysis of potassium pentafluoropropionate prepared by the neutralization reaction appeared to have dark-colored specks throughout them, while the salts remaining after the pyrolysis of either potassium pentafluoropropionate prepared by the silanolate method or sodium pentafluoropropionate appeared tan to light brown in color. Previously, Haszeldine had mentioned in the Experimental section of one of his papers that the pyrolysis of potassium pentafluoropropionate in addition to TFE, CO₂, and KF "gave a small amount of carbon",³³ although no characterization/analytical method was given. As shown in Figure 3.2, we had the salts remaining from a number of pyrolysis experiments examined by scanning electron microscopy (SEM) / energy dispersive spectroscopy (EDAX), and clearly elemental carbon is present. Furthermore, when applying our normal heating rate of 1 °C/min, the amount of carbon found in the remaining salts was around 0.5 to 1.0 wt%, but when applying a more rapid heating rate of 4 °C/min, 1.5 wt% carbon or higher was found. The latter was typically the case for analyses of the salts remaining from the pyrolysis of either potassium pentafluoropropionate prepared by the silanolate method or sodium pentafluoropropionate. When comparing the observations from the EDAX experiments, the most likely source of elemental carbon would be from the well-known, and undesired, disproportionation of TFE as shown in equation 3.6.¹⁶⁻¹⁸ If this is the case, then one should also be able to find evidence for the formation of carbon tetrafluoride.



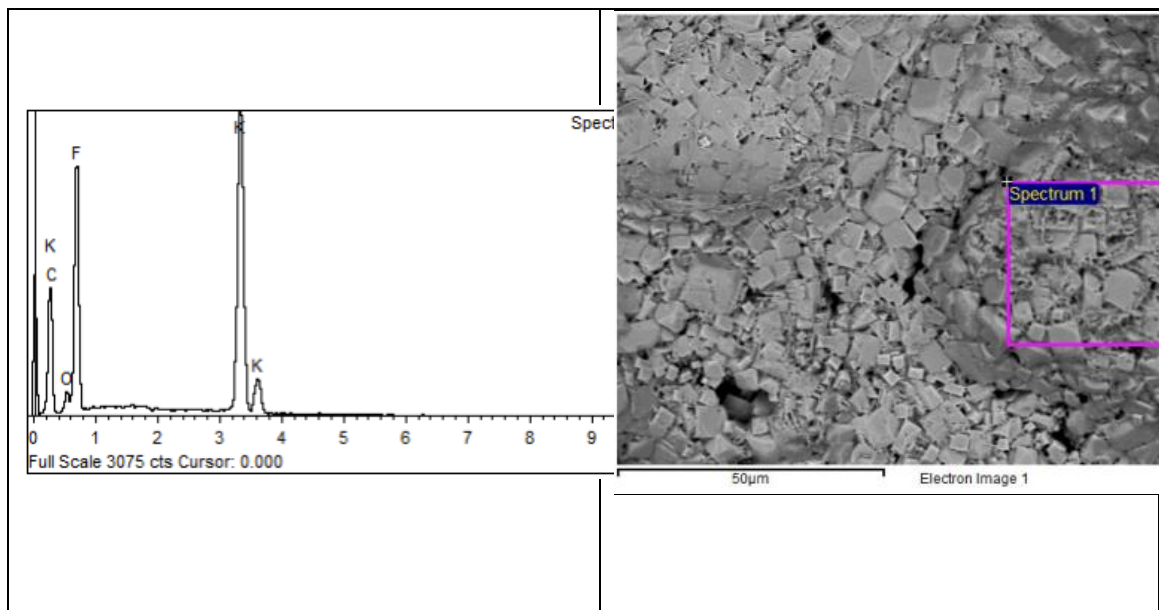


Figure 3.2. Left: X-ray elemental analysis of left over solids after pyrolysis showing the presence of elemental carbon. Right: Electron microscopy image of left over solids after pyrolysis.

In fact, one experimental observation that has not yet been mentioned is that a slight rise in pressure of about 20-30 mTorr is observed during the actual period of thermal decomposition of each pentafluoropropionate salt on a thermocouple gauge tube that is placed between the main vacuum trap (held at -196°C) and the vacuum pump. This can only be indicative of either a small leak in the vacuum system or the generation of a small, but constant amount of a non-condensable gas. In fact, when the pyrolysis of the salts is complete, the reading of the thermocouple vacuum gauge comes back down to whatever the previous ultimate obtainable vacuum level of the system was prior to the pyrolysis. Having ruled out any leaks in the system during numerous experiments, only the generation of a small, but continuous amount of a non-condensable gas can be operative. Furthermore,

CF₄ is known to have a very small residue vapor pressure even at liquid nitrogen temperature.⁴⁰ We expended great effort trying to first obtain infrared spectroscopic evidence for the presence of CF₄ by sampling the gases either coming directly off of the pyrolysis of the salts prior to the liquid nitrogen-cooled collection trap or coming through the liquid nitrogen trap, including warming this trap slightly in order to catch a representative sample of the most volatile products. In no case could we observe convincing evidence for the presence of CF₄; an example of several overlaid FT-IR spectra of gases coming off a pyrolysis versus authentic spectra of samples of TFE and CF₄ is shown in Figure S11 (cf.^{41,42}). Thereafter, we moved to a more sensitive analytical technique, namely GC-mass spectrometry, including the use of selective ion monitoring (SIM). Use of the latter was chosen not only due to the enhanced sensitivity of the SIM mode, but also because a comparison of both literature^{43,44} and experimental mass spectra of CF₄ and TFE reveals a striking difference in the intensity of the 69 m/z peak for CF₃⁺. More specifically, the 69 m/z peak is by far and away the base peak in the mass spectrum of CF₄, while this peak is only about 4-5% relative intensity versus the base peak at 81 m/z for C₂F₃⁺ in TFE (when collecting data above 40 m/z). As shown in a series of mass spectra in the Supporting Information (see Figures D.13-D.15), the 69 m/z peak in the aforementioned gas samples taken during the pyrolysis is approximately twice as intense as it is in an authentic sample of TFE that has been degassed of any residual CF₄. These observations collectively give the best evidence that we have to date for CF₄ being a minor side product, along with carbon, in the thermal decomposition of pentafluoropropionate salts to generate a mixture of TFE and CO₂.

Moving to the thermal properties of the pentafluoropropionate salts, we have already reported results on the accelerating rate calorimetry of the sodium, potassium, and calcium salts (see Figures D.16-D.18);^{14,15} however, an overview of the results bears repeating here. First, the sample of sodium pentafluoropropionate appears to start slowly decomposing around 230 °C and does not finish decomposing until about 100 minutes later at about 260 °C. Meanwhile, the sample of potassium pentafluoropropionate does not start decomposing as evidenced by rapid gas evolution until about 280 °C, and the decomposition is complete within a few minutes before the sample reaches 300 °C. However, a word of caution can be offered here, as a small exotherm, without significant gas evolution, is observed at a temperature as low as 175 °C. This is the reason for the earlier warning of not drying potassium pentafluoropropionate salts at too high of a temperature. The sample of calcium pentafluoropropionate exhibited a small endotherm and pressure increase at about 160 °C, which could have been due to the elimination of water from a small amount of remaining hydrate. However, stronger decomposition and gas evolution did not occur until about 280 °C and continued for ca. 500 minutes to beyond 350 °C. Collectively, the ARC results seem to indicate a preference for potassium pentafluoropropionate over the corresponding sodium and calcium salts.^{14,15} No ARC experiment gave rise to a strong exotherm, which is consistent on one hand with the fact the thermal decomposition of these salts requires constant heat input until their decompositions are complete, i.e., their thermal decompositions are not exothermic enough whereby the heats of reaction generate sufficient energy to keep the decompositions proceeding once started. On the second hand, it is also important to note that the ARC

results are in agreement with the DuPont (now Chemours) technology for 'safe TFE' as no deflagrations were observed under condition up to 400 °C and 350 psig.

In hopes of learning more about the thermal properties of these materials, pentafluoropropionate salts of lithium, sodium, potassium, cesium, magnesium, calcium, and barium were prepared, dried, and studied by thermogravimetric analysis (TGA) even though researchers at 3M had carried out parallel studies back in the 1950s.³⁰ The results are overviewed in Tables 1 and 2 and shown graphically in Figures D.19-D.34. As indicated by fewer ARC experiments, the data further confirm that higher decomposition temperatures are required by each of the divalent metal salts than all of the monovalent salts. On the other hand, no noticeable trends were observed based on cation size within either the alkali metal or the alkaline earth metal series of salts in terms of the concept of stabilization of a complex anion by a bulky cation, i.e., minimization of the lattice energy differences between the metal pentafluoropropionate and its corresponding metal fluoride by using a bulky cation.⁴⁵ Nevertheless, the TGA of potassium pentafluoropropionate displays step-like behavior (with weight loss versus increasing temperature and time) as indicated by an initial maximum rate of decomposition at 196 °C followed later by a second maximum rate of decomposition at 229 °C.

Table 1. Thermogravimetric data analysis (TGA) for $\text{CF}_3\text{CF}_2\text{C}(\text{O})\text{O}^-\text{M}^+$ (where $\text{M} = \text{Li}^+, \text{Na}^+, \text{K}^+, \text{Cs}^+, \text{Mg}^{2+}, \text{Ca}^{2+}, \text{or Ba}^{2+}$).

Sample	Temperature at 10% mass loss ($^{\circ}\text{C}$)	Mass % remaining at end of TGA	Temperature at maximum rate decomposition ($^{\circ}\text{C}$)	Mass percent loss at maximum rate decomposition ($\%/^{\circ}\text{C}$)
$\text{CF}_3\text{CF}_2\text{C}(\text{O})\text{O}^-\text{Li}^+$	258	14.44	281	2.81
$\text{CF}_3\text{CF}_2\text{C}(\text{O})\text{O}^-\text{Na}^+$	227	23.14	243	2.81
$\text{CF}_3\text{CF}_2\text{C}(\text{O})\text{O}^-\text{K}^+$	197*	28.96	196 and 229	1.25 and 3.82
$\text{CF}_3\text{CF}_2\text{C}(\text{O})\text{O}^-\text{Cs}^+$	208**	52.95	205 and 236	1.17 and 3.31
$[\text{CF}_3\text{CF}_2\text{C}(\text{O})\text{O}^-]_2\text{Mg}^{2+}$	298	17.52	331	2.79
$[\text{CF}_3\text{CF}_2\text{C}(\text{O})\text{O}^-]_2\text{Ca}^{2+}$	324	21.83	345	2.77
$[\text{CF}_3\text{CF}_2\text{C}(\text{O})\text{O}^-]_2\text{Ba}^{2+}$	290	33.55	321	2.37

Additionally, potassium pentafluoropropionate shows 3% mass loss at 130 $^{\circ}\text{C}$ and cesium pentafluoropropionate shows a 3% mass loss at 120 $^{\circ}\text{C}$. *At this temperature, the compound is already decomposing rapidly (see SI for the detailed TGA analysis). **At this temperature, the compound is already decomposing rapidly (see SI for the TGA analysis).

Interestingly, during this second decomposition step, the potassium salt shows the fastest rate of decomposition (i.e., gas evolution) at 3.82%/ $^{\circ}\text{C}$ of any of the pentafluoropropionate salts studied. While the cesium salt also displays this step-like decomposition, none of the alkaline earth metal salts did so as might have been expected from the ARC data on the calcium salt.

Table 2. Mass percent of metal fluoride remaining at the end of each TGA – theoretical versus experimental.

Sample		Metal fluoride remaining (theoretical)			Mass % remaining at the end of each TGA (experimental)
Formula	M.W. (g/mol)	Formula	M.W. (g/mol)	Mass %	
$\text{CF}_3\text{CF}_2\text{C}(\text{O})\text{O}^-\text{Li}^+$	169.96	LiF	25.94	15.26	14.44
$\text{CF}_3\text{CF}_2\text{C}(\text{O})\text{O}^-\text{Na}^+$	186.01	NaF	41.99	22.57	23.14
$\text{CF}_3\text{CF}_2\text{C}(\text{O})\text{O}^-\text{K}^+$	202.12	KF	58.10	28.74	28.96
$\text{CF}_3\text{CF}_2\text{C}(\text{O})\text{O}^-\text{Cs}^+$	295.93	CsF	151.91	51.33	52.95
$[\text{CF}_3\text{CF}_2\text{C}(\text{O})\text{O}^-]_2\text{Mg}^{2+}$	350.35	MgF_2	62.30	17.78	17.52
$[\text{CF}_3\text{CF}_2\text{C}(\text{O})\text{O}^-]_2\text{Ca}^{2+}$	366.12	CaF_2	78.07	21.32	21.83
$[\text{CF}_3\text{CF}_2\text{C}(\text{O})\text{O}^-]_2\text{Ba}^{2+}$	463.37	BaF_2	175.33	37.84	33.55

At this point, we were still not satisfied with the existing rationale for why the thermal decomposition of potassium pentafluoropropionate gave better results, so we decided to film the thermal decompositions of bulk quantities of sodium and potassium pentafluoropropionate, which are normally carried out in our barricade facility¹³ and had only been watched momentarily while filling liquid nitrogen baths around product (TFE and CO_2) collection cylinders. Two, time-lapsed videos are provided as part of the supporting information, and they provide clear visual insight as for why potassium pentafluoropropionate should be preferred. First, the sodium salt clearly melts prior to any

significant decomposition, and due to the better heat and mass transfer in a liquid (versus a solid), the reaction is rather rapid and violent. Lots of foaming is observed with the evolution of gases, which was the original reason for using long-necked flasks for the decomposition reactions.³⁴ The foaming is undoubtedly due to the well-known surfactant properties of sodium pentafluoropropionate,⁴⁶⁻⁴⁸ and the corresponding potassium salt would be expected to be an even better surfactant based on the larger cation. The remaining mass in the reaction flask from the thermal decomposition of sodium pentafluoropropionate only solidifies near the end of the thermal decomposition when the bulk material is nominally sodium fluoride; the brownish color, first of the melt and then the solid, is also clearly visible.

In the second video, one clearly sees that the potassium pentafluoropropionate salts never truly melt. Instead, one sees what appears like a 'wetted' or slightly darker band of color move progressively across from the outer walls of the reaction flask toward the center of the flask. Clearly the salts that are in more direct contact with the outer walls of the reaction flask increase in temperature more rapidly than do the salts toward the center of the flask, as they are in closest proximity to the heat source. Even though the TGA and ARC experiments showed a more rapid gas evolution (thermal decomposition) of the potassium salt, these experiments were only done on the scales of milligrams to about a gram. When carried out on the scale of several hundred grams of material, the much poorer heat and mass transfer in a solid bed versus a melt helps mitigate or control the rate of thermal decomposition of potassium pentafluoropropionate. We feel that this situation results in an overall lower reaction pressure when the product gases are being trapped at

liquid nitrogen temperature under dynamic vacuum and thus less unwanted side products are generated and a greater overall yield of TFE and CO₂ is obtained.

In a final attempt to better understand perhaps why no dependence on cation size was found in the thermal studies of the pentafluoropropionate salts, we recently undertook a study of the powder and single crystal X-ray diffraction of these materials. Unfortunately, humid air could not be excluded during the collection of the powder data, so some of the materials undoubtedly absorbed water during the data collection, especially the lithium and magnesium salts.⁴⁹ In terms of growing single crystals, water has so far been the solvent of choice, but we have been fortunate to obtain acceptable data on non-hydrated crystals of both sodium and potassium pentafluoropropionate. Structures of hydrated crystals of magnesium and calcium pentafluoropropionate were also obtained, but these will be reported separately. The molecular structure of sodium pentafluoropropionate is shown below in Figure 3.3. No unusual bond distances or angles were found, and all of the tables of data corresponding to the structure solutions are shown in the Supporting Information. More important is to compare the coordination spheres around both sodium and potassium in the two structures as shown with the ball-and-stick representations in Figure 3.4. As expected due to its smaller size, the sodium atom is six-coordinate, while the larger potassium atom is nine-coordinate (although other eight-, nine-, and ten-coordinate potassium atoms exist in the complex unit cell of this structure; further details will appear separately). It is interesting to note that some of the pentafluoropropionate ligands filling the coordination spheres of the sodium and potassium atoms are not just monodentate but polydentate as well, and the coordination (or close contacts) is not just

via the carboxylate oxygen atoms, but also sometimes through a fluorine atom. In fact, in sodium pentafluoropropionate, the short contacts involving fluorine atoms are always to an α -fluorine atom, while in potassium pentafluoropropionate, these types of short contacts are most often to β -fluorine atoms. Since the mechanism for the generation of TFE and CO_2 from the decomposition of a metal pentafluoropropionate salt would generally be thought of as occurring by a concerted β -elimination, one wonders if these structural differences also play a role in the potassium salt yielding better results.

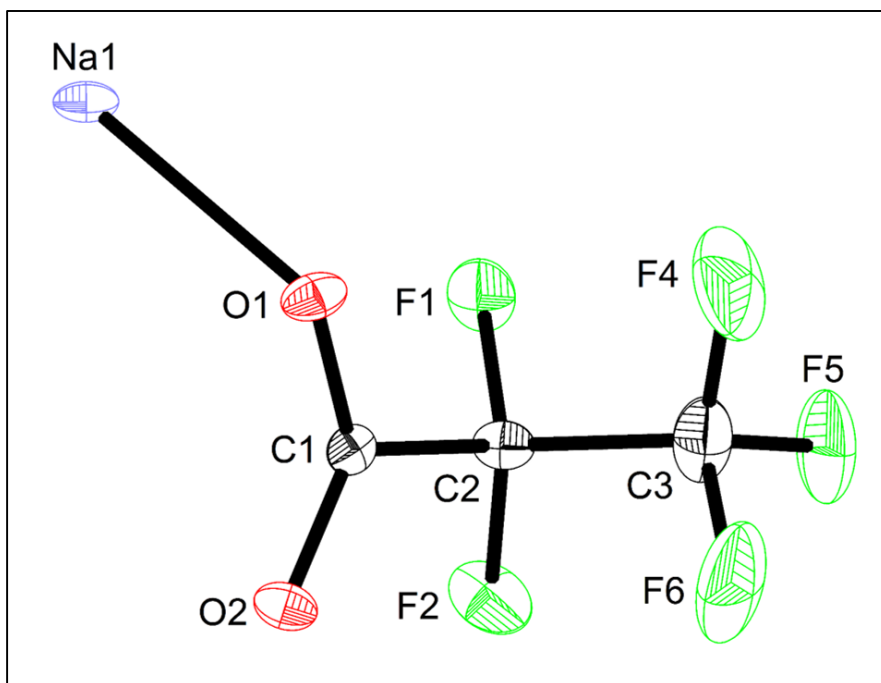


Figure 3.3. ORTEP representation of sodium pentafluoropropionate (50% probability ellipsoids).

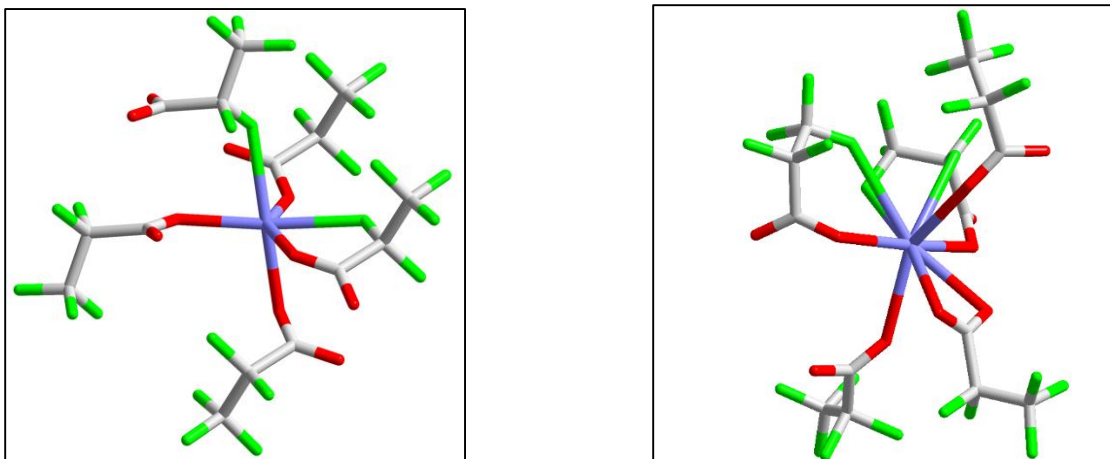


Figure 3.4. Ball-and-stick representations of sodium pentafluoropropionate around the sodium atom (left side) and potassium pentafluoropropionate around the potassium atom (right side), respectively. Gray = carbon atom, green = fluorine atom, red = oxygen atom, and blue = alkali metal cation.

3.4. Conclusions

Herein, we report evidence for why potassium pentafluoropropionate prepared from the simple neutralization of pentafluoropropionic acid and potassium hydroxide is the preferred pentafluoropropionate salt for pyrolysis to prepared TFE/CO₂ mixtures in high yield and purity. These rationale include (1) an increased overall yields of TFE and CO₂, often 98+% yield, (2) a more even control of heat and mass transfer during the pyrolysis, (3) capture of the pyrolysis gases at low temperature under high vacuum, and (4) little to no foaming of the reaction medium with the evolution of gases during the pyrolysis. Both the thermal and coordination properties of potassium pentafluoropropionate help contribute to its advantages as a starting material for this synthetic method. Evidence for the minor-yield byproducts carbon, C, and carbon tetrafluoride, CF₄, is also offered, and

these byproducts almost certainly arise from the unwanted disproportionate reaction of TFE under the harsh reaction conditions used.

3.5. Experimental

Disclaimer: *The authors make no warranties, expressed or implied, and assume no liability in connection with any use of the information presented in this paper. No one but persons having technical skill in this area of fluorine chemistry should attempt or repeat anything presented herein, and then at their own discretion and risk.*

3.5.1. Materials

The following reagents were purchased from the vendors indicated and used as received: $\text{CF}_3\text{CF}_2\text{C}(\text{O})\text{OH}$ (SynQuest Labs or Matrix Scientific), $\text{CF}_3\text{CF}_2\text{C}(\text{O})\text{OCH}_2\text{CH}_3$ (SynQuest Labs), $(\text{Me})_3\text{SiOK}$ (SynQuest Labs). Technical grade potassium hydroxide (90+%), as well as other alkali metal and alkaline earth metal hydroxides, were taken from laboratory stock. Diethyl ether was distilled off of sodium metal prior to use.

3.5.2. Methods

The ^1H -, ^{19}F -, and ^{13}C -NMR spectra were recorded on a JEOL 300-MHz spectrometer using a Young's tube for gaseous samples and normal techniques for solid and liquid samples. ^1H -NMR spectra were recorded for substances that do not even have

protons in order to double check their purities. IR spectra were recorded on a Thermo Scientific Nicolet iS5 spectrophotometer with either the iD1 Transmission or iD5 ATR option, depending on the physical state of the sample. Gaseous mixtures of TFE/CO₂, TFE, and CF₄ were loaded at 40 Torr (sometimes less) into a 10-cm gas cell with silicon windows, while samples of potassium pentafluoropropionate were placed as dry, fine powders on the diamond crystal of the ATR accessory. GC-mass spectra were obtained on all gaseous samples on a Shimadzu GCMS-QP5000 with a 30 m, 0.25 μ m film Rxi-5HT column, while LC-mass spectrometry data on solids (in methanol) were collected on a Bruker HCT Ultra PTM Discovery System using ESI and the negative ion mode.

Thermogravimetric analyses (TGAs) were run on a TA Instruments Model Q500 under a stream of dry nitrogen; as much as possible, samples were further dried on the instrument in a stream of nitrogen at 100 °C prior to acquiring the data. The accelerating rate calorimetry (ARC[®]) experiments were carried in an ARC[®] 2000[™] from Arthur D. Little, Inc. using 1-in. o.d. Hastelloy bombs from Tricor Metals Inc. and ca. 0.5-1.5 g of pentafluoropropionate salt samples. Prior to use, the bombs were washed with acetone and deionized water followed by overnight drying in an oven at 120 °C. The "heat-wait-search" mode of operation was used in which a heating rate of 10 °C/min with 10 °C steps making sure that the self-heating range was lower than 0.02 °C/min. The system was kept adiabatic for both periods of "wait" and "search".⁵⁰ The energy dispersive X-ray analysis (EDAX) were performed on a Hitachi S3400 SEM / Oxford X-Max EDX using a beam energy of 10 kV. Each solid sample was placed in the sample holder with the aid of copper double-sided adhesive tape.

Bulk reaction products were evaluated by powder X-ray diffraction (XRD) using a Rigaku Ultima IV diffractometer. Well-ground samples were analyzed in Bragg-Brentano geometry using Cu K α ($\lambda = 1.5406 \text{ \AA}$) radiation. Data were collected in 0.02-degree increments from 5-50 degrees in 2-theta at a rate of one degree per minute. Single crystal X-ray diffraction experiments of colorless plate-like crystals were performed at 100 K using a Bruker D8 Venture diffractometer. The data were collected using phi and omega scans (0.50° oscillations) with a Mo K α ($\lambda = 0.71073 \text{ \AA}$) microfocus source and Photon 100 detector. Data were processed using the SAINT software program, and corrected for absorption using the SADABS multi-scan technique, both within the Apex III suite.⁵¹ The structures were solved by intrinsic phasing and subsequently refined by full matrix least squares on F^2 using the SHELXTL software package.⁵²

3.5.3. Preparation of CF₃CF₂C(O)O⁻K⁺

(*Method A*): An amount of 164.0 g (1.00 mol) of CF₃CF₂C(O)OH is added drop wise to a solution of 56.1 g (1.00 mol) of KOH (90+% technical grade)⁵³ dissolved in 300.0 mL H₂O cooled in an ice bath. The acid must be added slowly to avoid the mixture warming up rapidly and therefore evaporating away any of the acid. The pH of the resulting solution is tested, and CF₃CF₂C(O)OH is added until the solution becomes slightly acidic. After removal of bulk water with a rotavap, the salt is ground to a fine powder with a mortar and pestle, and then dried until constant weight at 80-100 °C under dynamic vacuum at 20-30 mTorr. A percent yield of 98% was achieved.

(*Method B*): A solution of 50 mmol of $(\text{Me})_3\text{SiO}^-\text{K}^+$ in 25 mL of dry diethyl ether was added drop wise to a solution of 50 mmol of $\text{CF}_3\text{CF}_2\text{C}(\text{O})\text{OCH}_2\text{CH}_3$ dissolved in 300 mL of dry diethyl ether contained in a 1-L, round-bottomed flask under N_2 atmosphere. Once the $(\text{CH}_3)_3\text{SiO}^-\text{K}^+$ was added, the solution was left stirring overnight. The agitation was removed, and the solution was allowed to stand for a period of 48 hours. The solution was then filtered, and the filter cake was washed thoroughly with dry diethyl ether and dried under vacuum at 20-30 mTorr. A percent yield of 77% was achieved.

Potassium pentafluoropropionate: ^{19}F NMR (282 MHz, D_2O , CFCl_3) δ -83.2 (s, 3F), δ -120.9 (s, 2F). ^{13}C NMR (75.46 MHz, D_2O , TMS) δ 107.15 (tq, $J_1 = 262.1$ Hz, $J_2 = 37.7$ Hz, CF_2), δ 118.66 (qt, $J_1 = 284.7$ Hz, $J_2 = 35.1$ Hz, CF_3), δ 163.45 (t, $J_2 = 24.5$ Hz, $\text{C}=\text{O}$). FT-IR: ($\text{C}=\text{O}$) 1674 (m), 1408 (w), 1322 (w), ($\text{C}-\text{F}$) 1204 (m), 1150 (s), 1026 (m) cm^{-1} . Mass spectrum (ESI $^-$, m/z, ion): 119.0 $[\text{CF}_3\text{CF}_2]^-$, 162.9 $[\text{CF}_3\text{CF}_2\text{COO}]^-$, 327.0 $[(\text{CF}_3\text{CF}_2\text{COO})_2 + \text{H}]^-$, 348.9 $[(\text{CF}_3\text{CF}_2\text{COO})_2 + \text{Na}]^-$, 364.9 $[(\text{CF}_3\text{CF}_2\text{COO})_2 + \text{K}]^-$, 534.9 $[(\text{CF}_3\text{CF}_2\text{COO})_3 + 2\text{Na}]^-$, 550.9 $[(\text{CF}_3\text{CF}_2\text{COO})_3 + \text{Na} + \text{K}]^-$, 720.9 $[(\text{CF}_3\text{CF}_2\text{COO})_4 + 3\text{Na}]^-$, 736.8 $[(\text{CF}_3\text{CF}_2\text{COO})_4 + 2\text{Na} + \text{K}]^-$, 752.8 $[(\text{CF}_3\text{CF}_2\text{COO})_4 + \text{Na} + 2\text{K}]^-$.

3.5.4. General method of preparation of $\text{CF}_3\text{CF}_2\text{C}(\text{O})\text{O}^-\text{M}^+$

In a similar way as preparing $\text{CF}_3\text{CF}_2\text{C}(\text{O})\text{O}^-\text{K}^+$ (Method A), other pentafluoropropionate salts can be prepared by neutralizing a solution of the $\text{M}^{n+}(\text{OH})_n$. For the cases of $\text{Ca}(\text{OH})_2$ and $\text{Ba}(\text{OH})_2$ that are slightly soluble, the desired amount of base to be neutralized is placed in a beaker, and acid is added until all the base dissolves and the pH is slightly acidic. After removal of bulk water with a rotavap, the salt is dried at 80-

100 °C for 24 h using a dynamic vacuum at 20-30 mTorr until constant weight. A percent yield of 99% was achieved.

3.5.5. Preparation of tetrafluoroethylene-carbon dioxide (TFE-CO₂) mixture

(Method A- from potassium pentafluoropropionate): An amount 202 g (1.00 mol) of dry and finely grounded CF₃CF₂COO⁻K⁺ salt was placed in a 1-L long-necked, round-bottomed flask. The flask was connected to a 1-Gal Hoke stainless steel cylinder that had been converted into a trap. The outlet port of the cylinder was connected to dynamic vacuum (20-30 mTorr). The flask was heated slowly until reaching 300 °C, during which time a small increase in the vacuum pressure gauge was observed indicating the presence of a non-condensable gas. The heating process was stopped after the pressure in the vacuum gauge once again returned to 20-30 mTorr. The flask was allowed to cool to room temperature again under dynamic vacuum. Often, two or three reaction flasks were connected to a common manifold prior to the collection cylinder/trap. An amount of 141 g of a mixture of TFE/CO₂ was obtained from the pyrolysis of one batch of potassium pentafluoropropionate representing a percent yield of 98%.

Pyrolysis of smaller quantities of potassium pentafluoropropionate prepared by the silanolate method generally produced TFE/CO₂ in only about 75-80% yield. For example, 34.0 g of potassium pentafluoropropionate gave 17.9 g of a mixture of TFE and CO₂.

(Method B – from sodium pentafluoropropionate): An amount 74.4 g (0.400 mol) of dry and finely ground CF₃CF₂C(O)O⁻Na⁺ salt was placed in a 1-L long-necked, round-bottomed flask. The flask was connected to a 500-mL Hoke stainless steel cylinder, which

had been converted into a trap. The outlet port of the cylinder was connected to 20-30 mTorr of dynamic vacuum. The previously dried salts were left overnight at 80 °C under dynamic vacuum for further drying and leak checking of the system. After the salts had been dried scrupulously, the Hoke cylinder was cooled to liquid nitrogen temperature, and the round-bottomed flask was heated slowly at a rate of 1 °C/min until reaching 300 °C. An increase in the vacuum pressure gauge (from a baseline of 30 mTorr to 50 mTorr), by the presence of a non-condensable gas, was observed. The heating process was stopped after the pressure in the vacuum gauge once again returned to 30 mTorr. The flasks were left to reach room temperature again under dynamic vacuum. A total of 52.6 g (0.365 mol each) of TFE/CO₂ were gained in the Hoke trap cylinder, and a total of 21.6 g of primarily NaF were left in the round-bottomed flask. The yield calculated from the TFE/CO₂ produced is 91.3%.

In a separate pyrolysis experiment where the sodium pentafluoropropionate salts were heated considerably quicker to 300 °C, a significant decrease in yield was observed. For example, when 99.0 g (0.532 mol) of sodium pentafluoropropionate were used, a mass of 44.7 g remained in the pyrolysis flask, while 53.9 g (0.374 mol each) of primarily TFE/CO₂ remained in the collection trap. The percent yield of TFE/CO₂ was 70.3%.

Tetrafluoroethylene-carbon dioxide: ¹⁹F-NMR (282 MHz, CCl₃F) δ -137.77 (s, 4F). ¹³C-NMR (75.46 MHz) δ 129.69 (s, CO₂), 143.67 (m, C₂F₄).^{54,55} FT-IR (gas): (O=C=O) 2351 (m), (C-F) 1333 (vs), (C-F) 1194 (vs) cm⁻¹.⁵⁶

3.5.6. Scrubbing of carbon dioxide from tetrafluoroethylene-carbon dioxide (TFE-CO₂) mixture and reinhibition with D-limonene

The experimental setup used for this separation is illustrated in Figure 4. The D-limonene bubbler is a single-ended, 250-mL Hoke cylinder containing approximately 100 g of D-limonene. The calcium sulfate scrubber is a double-ended, 500-mL Hoke cylinder completely filled with calcium sulfate. The whole system is leak checked, evacuated, and purged with nitrogen three times before the following procedure is followed.

Two 1-Gal Hoke cylinders that have been made into trap cylinders are connected to a manifold containing a TFE regulator that is adjusted to 50 psig. Three in-line orifices (0.010" internal diameter) are placed immediately after the cylinder valve of each cylinder and the other one after the regulator in order to control the flow. The contents of one of TFE/CO₂ cylinder at a time is bubbled at a constant rate of 0.3500 SLM through a stainless steel bubbling stone submersed in a 5 L, 40 wt% aqueous solution of KOH that has previously been placed and degassed inside the 2-Gal stainless steel autoclave shown in Figure 4. Agitation of the caustic solution is kept at a constant rate of 800 rpm, while the temperature of the reactor is maintained at 10 °C by the action of the internal cooling coil that is connected to a cooling machine set at 5 °C. As the TFE bubbles to the surface of the solution, it is carried under reduced pressure through a calcium sulfate desiccator and then through a D-limonene bubbler before being collected in a third 1-Gal stainless steel Hoke cylinder being held at -70 °C (dry ice / isopropanol bath). Once the pressure of the source cylinder being scrubbed decreases to about 20 psig, the main cylinder valve is

closed, and the second source cylinder is opened (as observed by an increase of the pressure in the manifold as shown in Figure D.40). For the data featured in the graph shown in Figure D.40, a total of 757 g of gas mixture was taken out of the first cylinder and a total of 738 g of mixture was taken from the second cylinder to give a total of 1495 g of TFE/CO₂ that passed through the scrubber. A total of 1007 g of TFE were collected for a total yield of 97.0%. Further analysis of the TFE by infrared spectroscopy confirms that all the CO₂ has been removed.

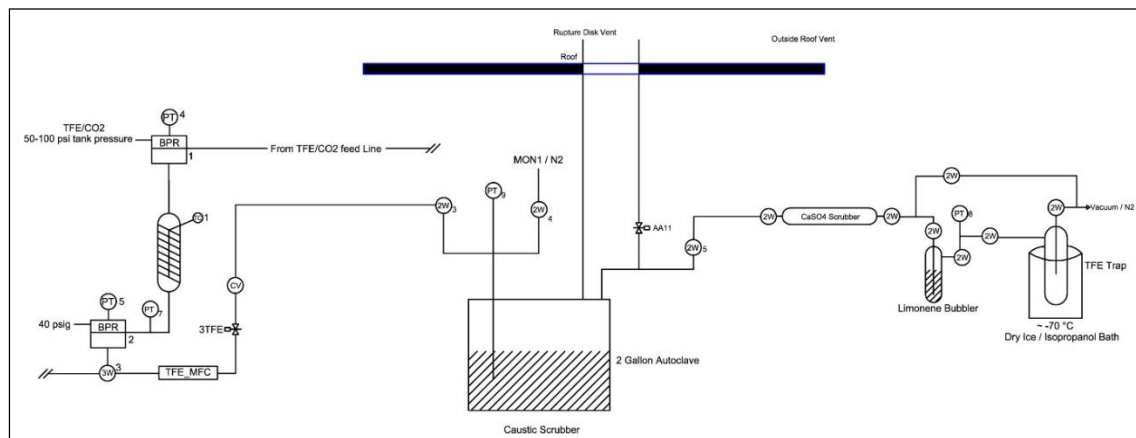


Figure 3.5. Schematic of 2-Gal autoclave converted into a caustic scrubber.¹³

3.5.7. Powder and single crystal X-ray diffraction of pentafluoropropionate salts

Prior to analysis by powder X-ray diffraction, each sample of the pentafluoropropionate salts, where $M^{n+} = Li^+, Na^+, K^+, Cs^+, Mg^{2+}, Ca^{2+}$, was finely ground and dried under vacuum at 20-30 mTorr for 48 hours. Samples were then placed in a conventional aluminum sample holder and carefully flattened against the surface of the

holder in order to provide a flat and level surface. The data collections were performed without the possibility to isolate the samples from humidity, so the most hygroscopic samples (lithium and magnesium salts) will have absorbed some water during the data collection period of ca. 45 minutes.

Crystals of both nonhydrated sodium and potassium pentafluoropropionate suitable for single crystal X-ray analysis were grown from slow evaporation of aqueous solutions, while only hydrated crystals of magnesium and calcium pentafluoropropionate have been obtained by the same method. The structures of the latter will be reported separately, as they have no bearing on adding to the understanding of preparing TFE from the pyrolysis of anhydrous pentafluoropropionate salts.

Sodium Pentafluoropropionate: A specimen of $\text{C}_3\text{F}_5\text{O}_2\text{Na}$, approximate dimensions 0.034 mm x 0.204 mm x 0.210 mm, was used for the X-ray crystallographic analysis. The X-ray intensity data were measured. The integration of the data using a monoclinic unit cell yielded a total of 11740 reflections to a maximum θ angle of 27.00° (0.78 Å resolution), of which 1323 were independent (average redundancy 8.874, completeness = 99.7%, $R_{\text{int}} = 3.15\%$, $R_{\text{sig}} = 1.68\%$) and 1186 (89.64%) were greater than $2\sigma(F^2)$. The final cell constants of $a = 21.9135(13)$ Å, $b = 6.1114(4)$ Å, $c = 9.1313(5)$ Å, $\beta = 94.738(2)^\circ$, volume = $1218.70(13)$ Å³, are based upon the refinement of the XYZ-centroids of reflections above $20 \sigma(I)$. The calculated minimum and maximum transmission coefficients (based on crystal size) are 0.9026 and 1.0000.

The structure was solved and refined using the Bruker SHELXTL Software Package, using the space group $C 1 2/c 1$, with $Z = 8$ for the formula unit, $\text{C}_3\text{F}_5\text{O}_2\text{Na}$. The

final anisotropic full-matrix least-squares refinement on F^2 with 100 variables converged at $R1 = 3.47\%$, for the observed data and $wR2 = 8.31\%$ for all data. The goodness-of-fit was 1.055. The largest peak in the final difference electron density synthesis was $0.395 \text{ e}^-/\text{\AA}^3$ and the largest hole was $-0.401 \text{ e}^-/\text{\AA}^3$ with an RMS deviation of $0.060 \text{ e}^-/\text{\AA}^3$. On the basis of the final model, the calculated density was 2.028 g/cm^3 and $F(000)$, 720 e^- .

Potassium pentafluoropropionate: A specimen of $\text{C}_3\text{F}_5\text{O}_2\text{K}$, approximate dimensions 0.042 mm x 0.102 mm x 0.118 mm, was used for the X-ray crystallographic analysis. The X-ray intensity data were measured. The integration of the data using a monoclinic unit cell yielded a total of 123222 reflections to a maximum θ angle of 26.00° (0.81 \AA resolution), of which 11233 were independent (average redundancy 10.970, completeness = 99.9%, $R_{\text{int}} = 7.34\%$, $R_{\text{sig}} = 3.42\%$) and 8747 (77.87%) were greater than $2\sigma(F^2)$. The final cell constants of $a = 23.4667(16) \text{ \AA}$, $b = 9.9952(6) \text{ \AA}$, $c = 25.5061(18) \text{ \AA}$, $\beta = 107.046(2)^\circ$, volume = $5719.8(7) \text{ \AA}^3$, are based upon the refinement of the XYZ-centroids of reflections above $20 \sigma(I)$. The calculated minimum and maximum transmission coefficients (based on crystal size) are 0.9030 and 0.9640.

The structure was solved and refined using the Bruker SHELXTL Software Package, using the space group $P 1 21/n 1$, with $Z = 36$ for the formula unit, $\text{C}_3\text{F}_5\text{O}_2\text{K}$. The final anisotropic full-matrix least-squares refinement on F^2 with 946 variables converged at $R1 = 7.08\%$, for the observed data and $wR2 = 18.25\%$ for all data. The goodness-of-fit was 1.021. The largest peak in the final difference electron density synthesis was $1.893 \text{ e}^-/\text{\AA}^3$, and the largest hole was $-1.529 \text{ e}^-/\text{\AA}^3$ with an RMS deviation of $0.135 \text{ e}^-/\text{\AA}^3$. On the basis of the final model, the calculated density was 2.113 g/cm^3 and $F(000)$, 3528 e^- .

3.6. Acknowledgements

We acknowledge Prof. Dr. Andreas Kornath and Dr. Alexander Kaufmann (Ludwig-Maximilians-Universität München, München, Germany) for their helpful advice on this project. We also thank Dr. Taghi Darroudi (Clemson University, 91 Technology Drive, Anderson, SC 29625, USA) for his help with conducting the EDAX experiments. We acknowledge the help from Dr. Qiaoli Liang (University of Alabama, Box 870336, Tuscaloosa, AL 35487, USA) for her help with the LC-mass spectrometry experiments. JST acknowledges the National Science Foundation (CHE-1124859) and the U.S. Department of Energy, Basic Energy Sciences (DE-FG02-05ER15718) for financial support. We also thank Dr. Christopher P. Junk for helpful discussions.

3.7. References

1. Plunkett, R. J. "The History of Polytetrafluoroethylene: Discovery and Development". In *High Perform. Polym., Proc. Symp.*; Seymour, R. B., Kirschenbaum, G. S., Eds.; 1986, pp 261-266.
2. Kauffman, G. B. Teflon – 50 Slippery Years. *Educ. Chem.* **1988**, 25, 173.
3. Ebnesajjad, S. *Fluoroplastics. Volume 1: Non-Melt Processible Fluoroplastics: The Definitive User's Guide and Databook*; 2nd ed. Plastics Design Library: Norwich, NY, 2000.
4. Ebnesajjad, S. *Fluoroplastics. Volume 2: Melt Processible Fluoropolymers: The Definitive User's Guide and Databook*; 2nd ed. Plastics Design Library: Norwich, NY, 2003.
5. Okada, D.; Saito, M.; Hayamizu, K. *Perfluorinated Polymer Electrolyte Membranes for Fuel Cells* Nova Science Publishers: New York, 2008.
6. Arcella, V.; Merlo, L.; Pieri, R.; Toniolo, P.; Triulzi, F.; Apostolo, M. "Fluoropolymers for Sustainable Energy". In *Handbook of Fluoropolymer Science and Technology*; Smith, D. W., Iacono, S. T., Iyer, S. S., Eds.; John Wiley & Sons: New York, 2014, pp 393-412.
7. Downing, F. B.; Benning, A. F.; McHarness, R. C. Pyrolysis of Chloro-Fluoro Alkanes. U.S. Patent 4,898,645, May 8, 1951.

8. Voigt, H.; Freudenreich, R. Process for the Production of Pure Tetrafluoroethylene. U.S. Patent 4,898,645, Feb 6, 1990.
9. Chiney, P. B.; Sunavala, P. D. Thermodynamics and Kinetics for the Manufacture of Tetrafluoroethylene by the Pyrolysis of Chlorodifluoromethane. *Ind. Eng. Chem. Res.* **1987**, 26, 1340-1344.
10. Broyer, E.; Bekker, A. Y.; Ritter, A. B. Kinetics of the Pyrolysis of Chlorodifluoromethane. *Eng. Chem. Res.* **1988**, 27, 208-211.
11. Sung, D. J.; Moon, D. J.; Moon, S.; J., K.; Hong, S.-I. Catalytic Pyrolysis of Chlorodifluoromethane Over Metal Fluoride Catalysts to Produce Tetrafluoroethylene. *Appl. Catal. A-Gen.* **2005**, 292, 130-137.
12. Bauer, G. L.; Weigelt, J. D.; Hintzer, K.; Loehr, G.; Schwertfeger, W.; Ponelis, A. A. Process for Manufacturing Fluoroolefins. U.S. Patent 6,919,015, Jul 19, 2005 and references therein.
13. Hercules, D. A.; Desmarteau, D. D.; Fernandez, R. E.; Clark, J. L.; Thrasher, J. S. "Evolution of Academic Barricades for the Use of Tetrafluoroethylene (TFE) in the Preparation of Fluoropolymers". In *Handbook of Fluoropolymer Science and Technology*; 1st ed.; Iacono, S. T., Iyer, S. S., Smith, D. W., Eds.; John Wiley & Sons: Hoboken, NJ, USA, 2014, pp 415-433.
14. Sayler, T. S. Preparation of Perfluorinated Ionomers for Fuel Cell Applications. Ph.D. Dissertation, The University of Alabama, Tuscaloosa, AL, 2012.

15. Sayler, T. S.; Tice, K. T.; Beg, M. A.; Fernandez, R. E.; Thrasher, J. S. Preparation of Low Equivalent Weight Perfluorinated Ionomers with Water Insolubility. *Polym. Prepr. (Am. Chem. Soc., Div. Polym. Chem.)* **2012**, 53, 39-40.
16. Babenko, Y. I.; Lisochkin, Y. A.; Poznyak, V. I. Explosion of Tetrafluoroethylene During Nonisothermal Polymerization. *Combust. Explos. Shock Waves* **1993**, 29, 603-609.
17. Reza, A.; Christiansen, E. A Case Study of a TFE Explosion in a PTFE Manufacturing Facility. *Process Saf. Prog.* **2007**, 26, 77-82.
18. Ferrero, F.; Meyer, R.; Kluge, M.; Schroder, V.; Spoormaker, T. Self-Ignition of Tetrafluoroethylene Induced by Rapid Valve Opening in Small Diameter Pipes. *Loss Prevent Proc.* **2013**, 26, 177-185.
19. Puts, G.; Crouse, P.; Ameduri, B. "Thermal Degradation and Pyrolysis of Polytetrafluoroethylene". In *Handbook of Fluoropolymer Science and Technology*; Smith, D. W., Iacono, S. T., Iyer, S. S., Eds.; John Wiley & Sons, Inc.: Hoboken, NJ, 2014, pp 83-106.
20. Zhu, J.; Wang, B.-H.; Liu, D.-Z. Synthesis of 1,2-Diiodotetrafluoroethane With Pyrolysis Gas of Waste Polytetrafluoroethylene as Raw Material. *Green Chem.* **2013**, 15, 1042-1047.

21. van der Walt, J. I.; Neomagus, J. P.; Nel, J. T.; Bruinsma, O. S. L.; Crouse, P. A. Kinetic Expression for The Pyrolytic Decomposition of Polytetrafluoroethylene. *J. Fluorine Chem.* **2008**, *129*, 314-318.
22. Bhadury, P. S.; Singh, S.; Sharma, M.; Palit, M. Flash Pyrolysis of Polytetrafluoroethylene (Teflon) in a Quartz Assembly. *J. Anal. Appl. Pyrolysis* **2007**, *78*, 288-290.
23. Meissner, E.; Wroblewska, A.; Milchert, E. Technological Parameters of Pyrolysis of Waste Polytetrafluoroethylene. *Polym. Degrad. Stab.* **2004**, *83*, 163-172.
24. Baradie, B.; Shoichet, M. S. Synthesis of Fluorocarbon–Vinyl Acetate Copolymers in Supercritical Carbon Dioxide: Insight into Bulk Properties. *Macromolecules* **2002**, *35*, 3569-3575.
25. Simon, C. M.; Kaminsky, W. Chemical Recycling of Polytetrafluoroethylene by Pyrolysis. *Polym. Degrad. Stab.* **1998**, *62*, 1-7.
26. Hunadi, R. J.; Baum, K. Tetrafluoroethylene: A Convenient Laboratory Preparation. *Synthesis* **1982**, *1982*, 454-454.
27. Van Bramer, D. J.; Shiflett, M. B.; Yokozeki, A. Safe Handling of Tetrafluoroethylene. U.S. Patent 5,345,013, Sep 6, 1994.
28. Chemours Home, FluoroIntermediates, Products & Services, TFE, Tetrafluoroethylene – Safe Supply™,

https://www.chemours.com/FluoroIntermediates/en_US/products/olefin_tfe.html

(accessed June 28, 2016).

29. Hals, L. J.; Reid, T. S.; Smith, G. H. The Preparation of Terminally Unsaturated Perfluoro Olefins by the Decomposition of the Salts of Perfluoro Acids. *J. Am. Chem. Soc.* **1951**, 73, 4054.
30. LaZerte, J. D.; Hals, L. J.; Reid, T. S.; Smith, G. H. Pyrolyses of the Salts of the Perfluoro Carboxylic Acids. *J. Am. Chem. Soc.* **1953**, 75, 4525-4528.
31. Hals, L. J.; Reid, T. S.; Smith, G. H. Process of Making Perfluoro Olefins. U.S. Patent 2,668,864, Feb 9, 1954.
32. Haszeldine, R. N. The Reactions of Metallic Salts of Acids with Halogens. Part III. Some Reactions of Salts of Fluorohalogenoacetates and of Perfluoro-acids. *J. Am. Chem. Soc.* **1952**, 4259-4268.
33. Haszeldine, R. N.; Leedham, K. The Reactions of Fluorocarbon Radicals. Part IX. Synthesis and Reactions of Pentafluoropropionic Acid. *J. Chem. Soc.* **1953**, 1548-1552.
34. Kornath, A.; Kaufmann, A. Ludwig-Maximilians-Universität München, Germany. Private Communication, July 2007.

35. Matsnev, A. V.; Qing, S.-Y.; Stanton, M. A.; Berger, K. A.; Haufe, G.; Thrasher, J. S. Pentafluorosulfanyldifluoroacetic Acid: Rebirth of a Promising Building Block. *Org. Lett.* **2014**, *16*, 2402-2405.
36. Laganis, E. D.; Chenard, B. L. Metal Silanolates: Organic Soluble Equivalenets for O^{2-} . *Tetrahedron Lett.* **1984**, *25*, 5831-5834.
37. Lovrić, M.; Capanec, I.; Litvić, M.; Bartolinčić, A.; Vinković, V. Scope and Limitations of Sodium and Potassium Trimethylsilanolate as Reagents for Conversion of Esters to Carboxylic Acids. *Croat. Chem. Acta* **2007**, *80*, 109-115.
38. Chenard, B. L.; Laganis, E. D. Preparation of Anhydrous Organic Acid Salts. U.S. Patent 4,723,016, Feb 2, 1988.
39. Kempen, E. C.; Brodbelt, J. S.; Bartsch, R. A.; Jang, Y.-C.; Kim, J. S. Investigations of Alkali Metal Cation Selectivities of Lariat Ethers by Electrospray Ionization Mass Spectrometry. *Anal. Chem.* **1999**, *71*, 5493-5500.
40. Matheson Gas Data Handbook, 5th ed.; Matheson Gas, 1971.
41. NIST, National Institute of Standards and Technology. Chemistry WebBook. Tetrafluoromethane. Infrared Spectrum. Gas Phase Spectrum. <http://webbook.nist.gov/cgi/cbook.cgi?ID=C75730&Units=SI&Type=IR-SPEC&Index=1#IR-SPEC> (accessed July 15, 2016).

42. NIST, National Institute of Standards and Technology. Chemistry WebBook. Ethene, tetrafluoro-. Infrared Spectrum. Gas Phase Spectrum. <http://webbook.nist.gov/cgi/cbook.cgi?ID=C116143&Units=SI&Type=IR-SPEC&Index=1#IR-SPEC> (accessed July 15, 2016).
43. NIST, National Institute of Standards and Technology. Chemistry WebBook. Tetrafluoromethane. Mass spectrum (electron ionization). <http://webbook.nist.gov/cgi/cbook.cgi?ID=C75730&Units=SI&Mask=200#Mass-Spec> (accessed July 15, 2016).
44. NIST, National Institute of Standards and Technology. Chemistry WebBook. Ethene, tetrafluoro-. Mass spectrum (electron ionization). <http://webbook.nist.gov/cgi/cbook.cgi?ID=C116143&Units=SI&Mask=200#Mass-Spec> (accessed July 15, 2016).
45. R. Steudel, Chemistry of the Non-Metals; Walter de Gruyter: Berlin, 1977; pp 68-69.
46. Sugihara, G.; Hisatomi, M. Roles of Counterion Binding in the Micelle Formation of Ionic Surfactants in Water. *J. Jpn. Oil Chem. Soc.* **1998**, 47, 661-716.
47. Haque, R. Nuclear Magnetic Resonance Study of Micelle Formation in Sodium Perfluorocaprylate and -propionate. *J. Phys. Chem.* **1968**, 72, 3056-3059.
48. McNamee, C. E.; Matsumoto, M.; Hartley, P. G.; Mulvaney, P.; Tsujii, Y.; Nakahara, M. Interaction Forces and Zeta Potentials of Cationic Polyelectrolyte

- Coated Silica Surfaces in Water and in Ethanol: Effects of Chain Length and Concentration of Perfluorinated Anionic Surfactants on Their Binding to the Surface. *Langmuir* **2001**, *17*, 6220-6227.
49. An accessory for collecting powder XRD data was recently obtained for our new diffractometer, so in the future, where necessary, we will be able to collect powder data on sealed samples in order to exclude moisture.
50. Sun, L.; Waterfeld, A.; Thrasher, J. S. A Modified Accelerating Rate Calorimeter (ARC[®]) with Capabilities for Handling Gaseous Samples Under Vacuum or an Inert Atmosphere. *J. Fluorine Chem.* **2006**, *27*, 1436-1439.
51. Sheldrick, G. M. A Short History of SHELX. *Acta Cryst.* **2008**, *A64*, 112-122.
52. M. Adam, Bruker AXS Announces Next-Generation Platform for X-ray Crystallography, May 12, 2015, <https://www.bruker.com/products/x-ray-diffraction-and-elemental-analysis/news-events-x-rayelemental/news/single-view/article/bruker-axs-announces-next-generation-platform-for-x-ray-crystallography.html> (accessed July 14, 2016).
53. The two main impurities in technical grade KOH are water and K₂CO₃, neither of which has an adverse affect on the yield of potassium pentafluoropropionate. Duda Diesel Material Safety Data Sheets and Standard Certificate of Analysis. Grades of Chemicals. <http://www.dudadiesel.com/sheets.php> (accessed July 15, 2016).

54. Ditchfield, R.; Ellis, P. D. ^{13}C NMR Chemical Shifts for Fluoroethylenes and Fluoroacetylenes. *Chem. Phys. Lett.* **1972**, *17*, 342-344.
55. Kühn-Velten, J. H.; Hägele, G.; Fuss, W.; Hering, P.; Ivarenko, M. M. Carbon Isotopomers of Tetrafluoroethylene: Laser-Induced Synthesis and NMR Spectroscopic Characterization. *Magn. Reson. Chem.* **2002**, *40*, 77-80.
56. Torkington, P.; Thomson, H. W. The Infra-red Spectra of Fluorinated Hydrocarbons. *I. Trans. Faraday Soc.* **1945**, *41*, 236-245.

Chapter 4

Preparation, Characterization, and Relative Reactivity Ratios of Monomers in Poly(VDF-*co*-TFE)

4.1. Introduction

Vinylidene difluoride (VDF) is a monomer that has been widely used commercially, not only to make the homopolymer poly(vinylidene difluoride) (PVDF) but also to prepare copolymers with tetrafluoroethylene (TFE) and other monomers such as chlorotrifluoroethylene (CTFE),¹⁻³ hexafluoropropylene (HFP),⁴⁻⁶ trifluoroethylene (TrFE),⁷⁻⁹ pentafluoropropene,^{10,11} 3,3,3-trifluoropropene, and 1,1,1,2-tetrafluoropropene.¹² Other less-explored compositions that have been reported in the literature are shown in Table 4.1.

Table 4.1. Other monomers that have been copolymerized with VDF.

Monomer	Publication Year
$\text{H}_2\text{C}=\text{CHCF}_2\text{Br}$ and $\text{F}_2\text{C}=\text{CFCF}_2\text{Br}$	1982 ¹³
$\text{H}_2\text{C}=\text{CHC}_2\text{F}_4\text{Br}$	1994 ¹⁴
$\text{H}_2\text{C}=\text{CHC}_6\text{F}_{12}\text{Br}$	2007 ¹⁵
$\text{F}_2\text{C}=\text{CHBr}$	2000 ¹⁶
$\text{F}_2\text{C}=\text{CFBr}$	1984 ¹⁷
$\text{F}_2\text{C}=\text{CFC}_2\text{H}_4\text{Br}$	2005 ¹⁸
$\text{F}_2\text{C}=\text{CFOC}_2\text{F}_4\text{Br}$	1993 ¹⁹

4.2. Synthesis of VDF

Several methods exist by which VDF is prepared commercially. The most common route shown in Figure 4.1 involves the chlorination of 1,1-difluoroethane (HFC-152a) to obtain 1-chloro-1,1-difluoroethane (HCFC-142b) followed by a dehydrochlorination²⁰ at 900 °C using copper catalysts (Method A in Figure 4.1).²¹ However, this method is not the only way to obtain VDF, which can also be prepared from the pyrolysis of 1,1,1-trifluoroethane through a platinum-lined Inconel tube at 1200 °C (Hauptschein process; Method B in Figure 4.1). Alternatively, VDF can be made from the hydrofluorination of 1,1,1-tri-chloroethane (R-140a) to yield 1-chloro-1,1-difluoroethane, which is subsequently dehydrochlorinated (Method C in Figure 4.1).²² Some non-commercial routes have been explored such as the dehydrobromination of 1-bromo-1,1-difluoroethane²³ and the dechlorination of 1,2-dichloro-1,1-difluoroethane.²⁴

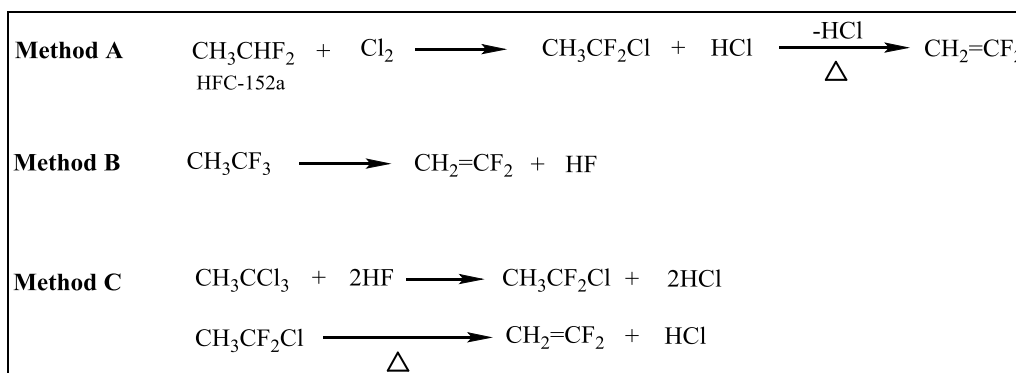


Figure 4.1. Commercial and non-commercial routes for the manufacture of VDF.^{21,22,24}

4.3. Synthesis and Properties of PVDF

Poly(vinylidene fluoride) displays several interesting properties that make it special. One of the most important properties is its piezoelectric character - the ability to generate a voltage when pressure is applied to the material. This behavior was discovered in 1969²⁵ and first reported in 1971.^{26,27} Although PVDF can be found in five distinct crystalline polymorphs (α , β , γ , δ , and ϵ),²⁸⁻³⁰ where the α , β , and γ forms are shown in Figure 4.2, only the beta form of the homopolymer presents enhanced piezoelectric properties due to the alignment of a dipole across the polymer chain (with the positive partial charge being the side with the hydrogen atoms, and the partial negative charge being the side where the fluorine atoms are aligned). A more detailed discussion of the polymorphic phases of PVDF has already been reported in the literature.^{31,32} The piezoelectric behavior has been of great aid in generating a wide range of applications for PVDF. Some of these applications include, but are not limited to, sound wave detectors, oscillators for electronic applications, transducers for microphones or speakers, mechanical actuators, and pressure sensors. Because of its dielectric behavior, PVDF can also be used in lithography drums, as a charge can be placed precisely over a drum and solid pigments (toner) can be adhered and melted into paper by releasing PVDF from the drum by means of inverting its polarity. PVDF can also be used as a component of electrolytes, or binders for electrode materials,³³ or as a separator in lithium ion batteries.³⁴

Water dispersions that can dry at room temperature and can be applied to historical structures such as columns, statues, and other historical features represent another area of

application of PVDF.³⁵ The dispersion is applied at 70 °C and allowed to dry on the structure. The coating helps prevent degradation of the structure where it has been applied from sunlight or other weather factors.

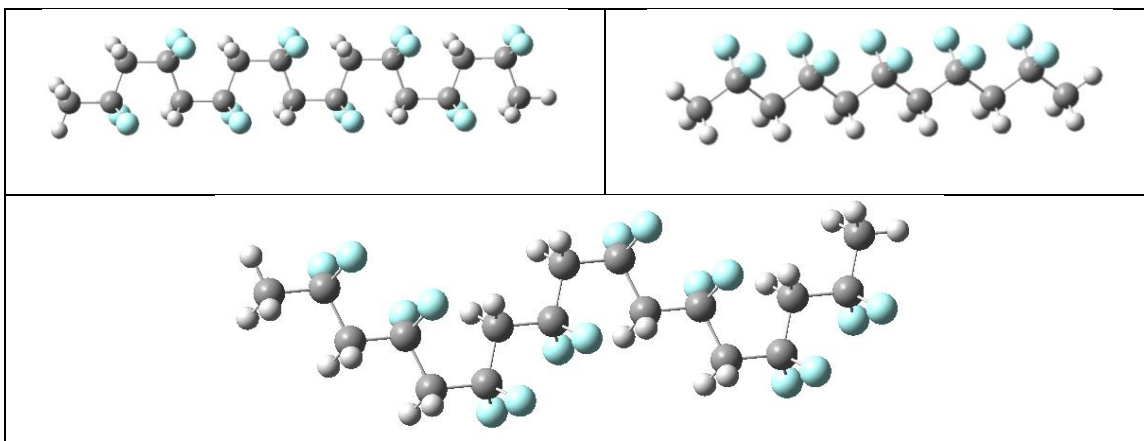


Figure 4.2. Three major polymorphs of PVDF. Top Left: alpha form, Top Right: beta form, Bottom: gamma form.²³

4.4. Synthesis, Uses, and Properties of Poly(VDF-*co*-TFE)

Poly(VDF-*co*-TFE) has previously been prepared by both emulsion³⁶⁻³⁹ and plasma polymerization.⁴⁰ It is well known that PVDF is only 50-70% crystalline³¹ and that poly(tetrafluoroethylene) (PTFE) has a remarkably higher degree of crystallinity.¹⁷ Great efforts have been made to produce poly(VDF-*co*-TFE) with different percentages of TFE to study its crystallinity and other properties. The particular case of poly(VDF-*co*-TFE) has gained great attention since its Curie transitions between ferroelectric and paraelectric states were first pointed out by Lovinger²⁸ in 1983. The composition analyzed was an

experimental grade sample of Kynar 7200 manufactured by Pennwalt Corporation with a composition of 19 and 81 mol% of TFE and VDF, respectively.

Another potential application of poly(VDF-*co*-TFE) includes the manufacture of high electric energy storage capacitors by means of stacking layers of the copolymer with layers of poly(ethylene terephthalate) (PET). Such devices can obtain energy densities up to 16 J/cm³.⁴¹ Over the years, different compositions of co- and ter-polymers of VDF have been made in order to make use of the special ferroelectric characteristics of PVDF⁴²⁻⁴⁴ while maintaining a high energy storage density that can vary from 10 to 25 J/cm³.⁴⁵⁻⁵²

As the content of TFE increases in poly(VDF-*co*-TFE), the degree of crystallinity increases in the copolymer. This can be interpreted as a random distribution of the two monomers throughout the material. Furthermore, the reported product of their reactivity ratios ($r_{\text{VDF}} = 0.23$, $r_{\text{TFE}} = 3.73$) is 0.86 (determined by the Fineman and Ross method),^{17,23} which indicates that the copolymer is a perfectly random distribution of the two monomers. Another set of reactivity ratios for VDF and TFE (determined from the Fineman and Ross method) were reported earlier in 1974 by Naberezhnykh and Sorokinas ($r_{\text{VDF}} = 0.32$, and $r_{\text{TFE}} = 0.28$), with a product $r_{\text{VDF}}r_{\text{TFE}} = 0.09$,³⁹ and this set of data deviates largely from the aforementioned reactivity ratios. Additional reactivity ratios, including the ones mentioned above are listed in Table 4.2. As the product of reactivity ratios tends to zero, the monomers in the copolymer tend to be perfectly alternating. On the other hand, if the product of reactivity ratios tends toward 1, the monomers in the copolymer tend to have a completely random distribution.⁵³

Table 4.2. Reactivity ratios of VDF and TFE in poly(VDF-*co*-TFE).

r_{VDF}	r_{TFE}	$r_{\text{VDF}r_{\text{TFE}}}$	Year Reported
0.23 (F-R)	3.73	0.86	1984 ¹⁷
0.32 (F-R)	0.28	0.09	1974 ³⁹
0.11	1.06	0.12	2001 ³⁸

Note: reactivity ratios determined using the Fineman and Ross method are marked by “F-R”.

The goal for the research reported herein was to reinvestigate the reactivity ratios of VDF and TFE in poly(VDF-*co*-TFE). Additionally, as explained in Chapter 2,⁵⁴ with the development of the TFE polymerization facility at Clemson University, and the inherited knowledge of safely handling TFE in an equimolar mixture with CO₂, we have also investigated the reactivity ratios of TFE and VDF in poly(VDF-*co*-TFE) both when using an equimolar mixture of TFE and CO₂ and when using only a partial pressure of CO₂.

4.5. Experimental Determination of Relative Reactivity Ratios

This section contains a brief explanation of the concepts that lead to the experimental determination of relative reactivity ratios. This content has been previously described in a number of publications as well as text books that will be referenced along the section.^{53,55-61} Radical copolymerization can be modeled by considering that the modelling process depends on the last monomer added to the chain. For a two monomer system, one can have the following four equations that show the addition of either monomer (M₁ or M₂) to the growing end of the polymer chain (R-M₁• and R-M₂•), as shown in Figure 4.3.

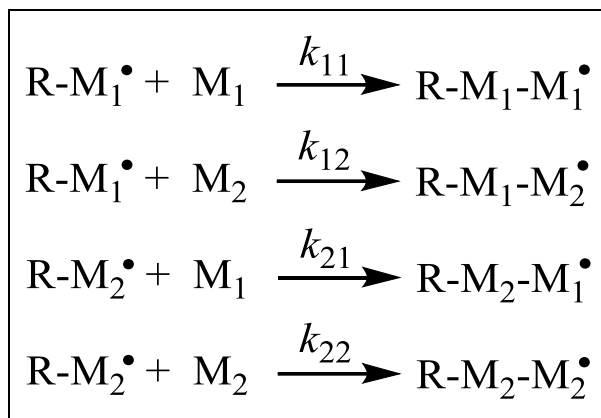


Figure 4.3. Possible radical propagation pathways for chain growth for the radical polymerization of VDF with TFE.⁵⁵

Based in the information from Figure 4.3, the change in monomer composition can be stated as shown in equations 4.1 and 4.2. A ratio of their reaction rates can be drawn as shown in equation 4.3 (which comes from the division of equation 4.1 by equation 4.2), and assuming a steady state of polymerization using equation 4.4 (defined as the equal rate of either monomer radical attacking the other monomer), the final identity of the polymer composition can be established in equation 4.5. The final equation 4.8 comes from substituting equations 4.6 and 4.7 into Equation 4.5. The aforementioned equations are shown below.⁵⁵

$$-\frac{d[M_1]}{dt} = k_{11}[M_1^\bullet][M_1] + k_{21}[M_2^\bullet][M_1] \quad (4.1)$$

$$-\frac{d[M_2]}{dt} = k_{12}[M_1^\bullet][M_2] + k_{22}[M_2^\bullet][M_2] \quad (4.2)$$

$$\frac{d[M_1]}{d[M_2]} = \frac{k_{11}[M_1^*][M_2] + k_{21}[M_2^*][M_1]}{k_{12}[M_1^*][M_2] + k_{22}[M_2^*][M_2]} \quad (4.3)$$

$$k_{12}[M_1^*][M_2] = k_{21}[M_2^*][M_1] \quad (4.4)$$

$$\frac{d[M_1]}{d[M_2]} = \frac{\frac{k_{11}[M_1^*][M_1]}{k_{12}[M_1^*][M_2]} + \frac{k_{21}[M_2^*][M_1]}{k_{21}[M_2^*][M_1]}}{\frac{k_{12}[M_1^*][M_2]}{k_{12}[M_1^*][M_2]} + \frac{k_{22}[M_2^*][M_2]}{k_{21}[M_2^*][M_1]}} \quad (4.5)$$

$$r_1 = \frac{k_{11}}{k_{12}} \quad (4.6)$$

$$r_2 = \frac{k_{22}}{k_{21}} \quad (4.7)$$

$$\frac{d[M_1]}{d[M_2]} = \frac{[M_1](r_1[M_1] + [M_2])}{[M_2](r_2[M_2] + [M_1])} \quad (4.8)$$

When r_1 is less than 1, M_2 will be added more readily than M_1 to $R-M_1^*$, and the opposite is true when r_1 is greater than 1.

Several values are possible for r_1 and r_2 . When $r_1 = r_2 = 0$, both of the propagation reactions denoted by the reaction constants k_{11} and k_{22} will not occur. This means that a polymer chain ending in M_1 will add only M_2 , and a polymer chain ending in M_2 will add only M_1 as the next monomeric unit. In other words, the polymer obtained is a perfect alternating polymer of both units $M_1-M_2-M_1-M_2-M_1$, etc. Subsequently, the polymer obtained will have an equal number of M_1 units and M_2 units. It is important to note that

when this case is present, both monomer units cannot homopolymerize and can copolymerize only when in the presence of each other.

On the other hand, when $r_1 = r_2 = 1$, both of the monomers have the same probability of adding to each other and to themselves. This means that a polymer chain ending in M_1 can equally add another M_1 unit or an M_2 unit. In other words, the four reactions (denoted before by the reaction constants k_{11} , k_{12} , k_{21} , k_{22}) are equally possible. This means that the resulting copolymer has a perfectly random distribution of the two monomers in the polymer chain, and the ending polymer composition is completely identical to the initial ratio of monomer feeds. This is also called the “ideal polymerization”⁵⁶ since the polymerization can be controlled very easily by the ratio of the monomer feeds. Also, since the composition of the ending polymer is the same as the ratio of monomer feeds, this copolymerization is called an azeotropic polymerization.⁵⁵

When $r_1 > 1$ and $r_2 < 1$, the propagation types denoted by the reaction constants k_{11} and k_{21} are preferred over the propagation steps denoted by k_{12} and k_{22} , and this results in a higher probability of M_1 entering the polymer than M_2 . If the ratios differ widely from one another, then the probability of incorporating M_2 decreases until it is very hard for the polymer to incorporate this monomer. This situation can be alleviated by adjusting the monomer feeds and keeping the ratio M_1/M_2 always less than 1.

When $r_1 < 1$ and $r_2 < 1$, the propagation steps denoted by the reaction constants k_{12} and k_{21} are preferred over the ones denoted by k_{11} and k_{22} . This means that the same probability exists for adding M_1 to a growing chain ending with M_2 as for adding M_2 to a growing chain ending with M_1 . In this case, the polymer composition will depend solely

on the values of r_1 , r_2 , and the monomer feed ratio. If both of the values of r_1 and r_2 are equal (and the monomer feed rate is $M_1/M_2 = 1$), then the composition of the final polymer will have equal amounts of M_1 and M_2 , but distributed randomly. In this particular case, the term “azeotropic composition” is also used. For an azeotropic composition one uses the term $N = 0.5$, which means that the distribution of the monomers in the polymer is perfectly alternating. If one changes the values of r_1 and r_2 , then the N term will change as well as a consequence of this change. If $r_1 < r_2$, then the N term will decrease from 0.5, and the opposite will occur when $r_1 > r_2$. It is possible to calculate the azeotropic composition depending on the reactivity ratios using the following equation 4.9.⁵⁵

$$N_1 = \frac{1-r_1}{(2-r_1-r_2)} \quad (4.9)$$

When $r_1 > 1$ and $r_2 > 1$, the polymerization system does not undergo random copolymerization. The system will proceed either as a combination of the two homopolymers or it will form a large sequence of block polymers where a long section of M_1 is followed by a long sequence of M_2 .

When $r_1 = 0$ or $r_2 = 0$, the system results in a copolymer with a particular azeotropic composition. If the mole fraction of the monomer with $r = 0$ is below the azeotropic composition, the product will contain the copolymer of the azeotropic composition and a homopolymer of the comonomer (since the co-monomer is in excess and has a larger reactivity ratio). If the mole fraction of the monomer with $r = 0$ is above the azeotropic composition, the product will contain the azeotropic polymer until the co-monomer is

exhausted from the polymerization system and any excess of the monomer with $r = 0$ will be found unpolymerized. A graphical diagram of the typical plots of compositions of monomer in the feed versus the composition of monomer in the copolymer for each of the combinations of reactivity ratios is shown in Figure 4.4.

After an initial analysis of the polymer is made, the data can be fit to a model. The Fineman and Ross (abbreviated as “F-R”), the Kelen and Tüdös (abbreviated as “K-T”), and the extended Kelen and Tüdös (abbreviated as “E-K-T”) linearization methods are widely used to analyze initial feed ratios and final polymer compositions to obtain relative reactivity ratios. These models are used to analyze polymer systems at low conversion (less than 15%) for a number of reasons, but mostly because of composition drift. Compositional drift is the change over time of the polymer composition due to instantaneous local change in the concentration of the monomer in solution. If the polymer amount is large enough to make the polymer crash out of the solution, then the reactive ends of the polymers that are not in solution do not react with the monomers in solution, and therefore the overall composition changes as well. Therefore, stopping the polymerization at low conversion is key in order to obtain an accurate composition of the polymer that is a true reflection of the reactivity ratios of the monomers and in order to minimize effects that affect the polymer composition over time.

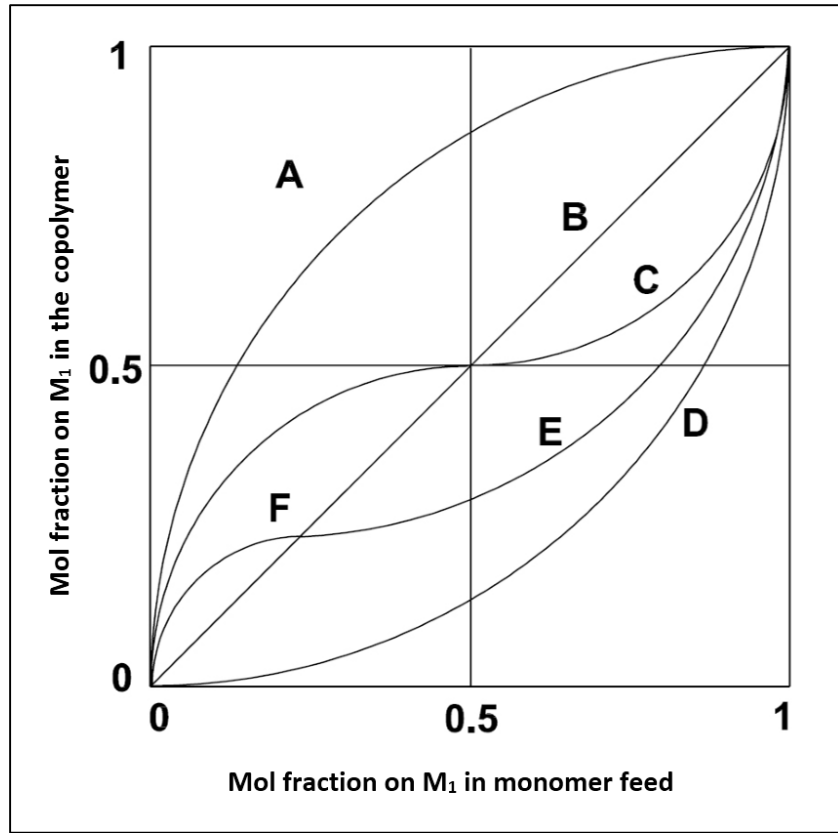


Figure 4.4. Diagram of correlation in between a monomer in the feed mixture to the monomer in the final copolymer formed. A: $r_1 > 1$, $r_2 < 1$, B: $r_1 = r_2 = 1$, C: $r_1 = r_2 < 1$, D: $r_1 < 1$, $r_2 > 1$, E: r_1 and $r_2 < 1$, and $r_1 < r_2$, F: azeotropic point.⁵⁵

The Fineman and Ross method (F-R), which was established in 1950 by Morton Fineman and Sidney D. Ross⁵⁶ (based on previous work),⁵⁷ uses the general equation 4.7, while the K-T method, named after its developers Tibor Kelen and Ferenc Tüdös,⁵⁹⁻⁶¹ uses the general reworked equation derived from the F-R method as indicated in equation 4.10,

$$G = r_1 H + r_2 \quad (4.10)$$

where $G = \frac{X(Y-1)}{Y}$, $H = \frac{X^2}{Y}$ and $X = \frac{f_1}{f_2}$, $Y = \frac{F_1}{F_2}$ and with f as the molar composition on the monomer feed and F as the final molar composition on the copolymer.

If the Fineman and Ross equation (shown in equation 4.10) is further manipulated by the inclusion of two new parameters η and ξ (which are defined below), and the intercept is further normalized by the α parameter (defined below), the resulting equation can be rearranged to form a new expression that is more widely known as the Kelen and Tüdös equation (shown by equation 4.11),

$$\eta = \left(r_1 + \frac{r_2}{\alpha}\right)\xi - \frac{r_2}{\alpha} \quad (4.11)$$

where $\eta = \frac{G}{(\alpha+H)}$, $\xi = \frac{H}{(\alpha+H)}$ and $\alpha = \sqrt{H_m H_M}$, and where H_m and H_M are the minimum and maximum value of H obtained from the experimental data as used for the Fineman and Ross method.

With this foundation already stated, the experimental determination of reactivity ratios is reduced to obtain the final polymer composition (molar fraction of each monomer), as well as the initial monomer composition in the feed (in molar fraction) and evaluate the data with the aforementioned equations.

4.6. Results and Discussion

Polymer samples of poly(VDF-co-TFE) were prepared in the pilot-scale tetrafluoroethylene polymerization facility at Clemson University that has been described

in detail not only in the literature⁵⁴ but also in Chapter Two of this Dissertation. A couple of different methods of preparation were followed: either charging the reactor to the desired reaction pressure with VDF and TFE gas and continuing the reaction feeds of the individual monomers at the desired molar ratio, or using a gaseous mixture of the desired molar composition to drive the polymerization reaction. Both of these polymerization procedures were also repeated either using a small amount of carbon dioxide in the head-space of the autoclave to provide a partial pressure of CO₂ during the reaction, or charging an equimolar mixture of carbon dioxide and TFE as an independent gas feed along with VDF. More details are described in the Experimental section.

The following sections (Section 4.6.1, 4.6.2, 4.6.3, and 4.6.4) include DSC, TGA, XRD, and NMR characterization data for the poly(VDF-*co*-TFE) samples prepared in this study. Most importantly, analyses of the ¹⁹F NMR spectra are useful in determining the final compositions of the various copolymers that were prepared, as this type of information is essential for being able to experimentally determine the relative reactivity ratios of TFE and VDF.

4.6.1. Differential scanning calorimetry (DSC) analyses of samples of poly(VDF-*co*-TFE)

Differential scanning calorimetry (DSC) analyses were carried out on the samples of poly(VDF-*co*-TFE) prepared in both the presence and absence of CO₂. Two trends were

observed that are consistent with what one would think if the content of TFE was increased in the samples of poly(VDF-*co*-TFE), namely that both the T_c and T_m temperatures increased as the content of TFE increased in the polymer. First PVDF has a T_m of 159.4 °C and as the TFE content increases, the T_m decreases. It can be observed in Table 4.3 that such T_m keeps decreasing to about 126 °C (at TFE content of 20 mol%) and then the T_m starts increasing as the TFE content passes the 20 mol% mark. Representative DSC thermograms are included in Figures 4.5, 4.6, and 4.7, and a complete list of the DSC analyses is included in Appendix E. It can also be found in the literature that PVDF has a glass transition temperature (T_g) ranging from -40 to -30 °C and a melting (T_m) temperature ranging from 155 to 192 °C.²³

Table 4.3. Summary of differential scanning calorimetry (DSC) data on samples of PVDF, poly(VDF-*co*-TFE), and PTFE.

Composition (VDF-TFE mol%)	1 st Melting (°C)	2 nd Melting (°C)	1 st Cooling (°C)	2 nd Cooling (°C)
100-0	159.4	163.2	137.0	135.2
90-10 (A)	158.8	158.6	126.7	126.7
90-10-CO ₂ (E)	159.7	158.7	127.5	127.5
80-20 (B*)	126.1 / 154.2	127.1 / 155.9	119.9 / 109.3	119.9 / 109.3
80-20 (B)	117.5	118.8	99.2	99.2
80-20-CO ₂ (F)	118.5	119.0	98.9	98.9
80-20-High Conversion	117.7 / 126.6	129.7	111.8 / 102.7	111.8 / 102.7
70-30 (C)	109.8 / 133.2	131.6	133.1 / 120.5	133.1 / 120.5
70-30-CO ₂ (G)	145.6	146.5	103.4	103.4
60-40 (D)	165.6 / 176.8	165.6 / 176.8	154.5 / 137.9	154.5 / 137.9
60-40-CO ₂ (H)	171.8	174.8	150.8	150.8
0-100	326.0	324.1	313.5	313.5

Note: in the rest of the document the samples are labeled A through H where samples A, B, C, and D present composition of 90, 80, 70, and 60 mol% of VDF, respectively. Samples labeled E, F, G, and H follow the same labeling format. Sample B* is of the same nominal

composition as sample B, but this sample was made in larger blocks as explained in this chapter.

An interesting feature about the DSC results on a couple of samples of poly(VDF-*co*-TFE) both having 20 mol% of TFE that bears further comment. One of the copolymer samples was made from a gaseous mixture of the two monomers, while the other one was made in large blocks by flowing each monomer alternatively into the reactor. The details of their preparations are discussed in the Experimental section. When the sample is prepared from a gaseous mixture, or from very small blocks of homopolymer, one can observe only one set of peaks for each transition (T_c and T_m). This could be interpreted as the sample of polymer being more uniform in the distribution of the two monomers throughout the polymer. When the blocks are made in such a way that larger sections of each monomer end up in the polymer, the DSC thermogram includes two sets of peaks at each transition (T_c and T_m). This on the other hand, can be interpreted as the polymer having distinctive sections with different statistical distributions of each monomer throughout the polymer. Representative examples of both of these behaviors are shown in Figures 4.6 and 4.7. Additional DSC thermograms of the other samples of poly(VDF-*co*-TFE) prepared are included in Appendix E.

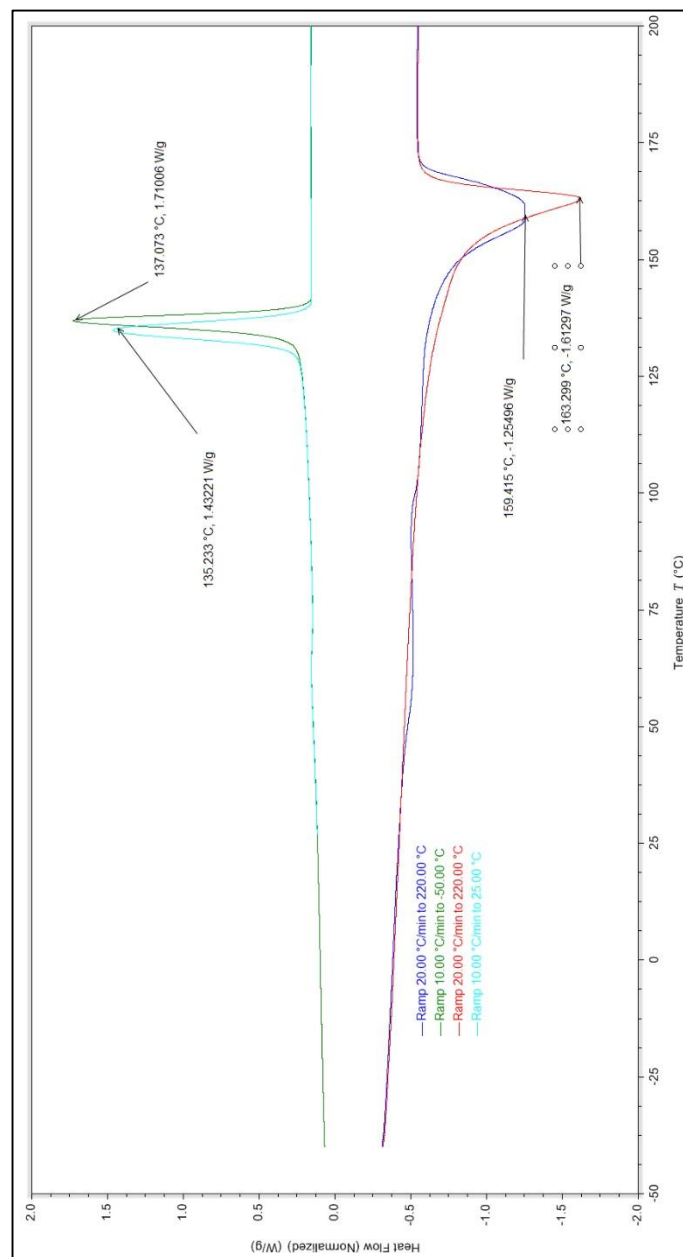


Figure 4.5. Representative DSC thermogram for a sample of PVDF.

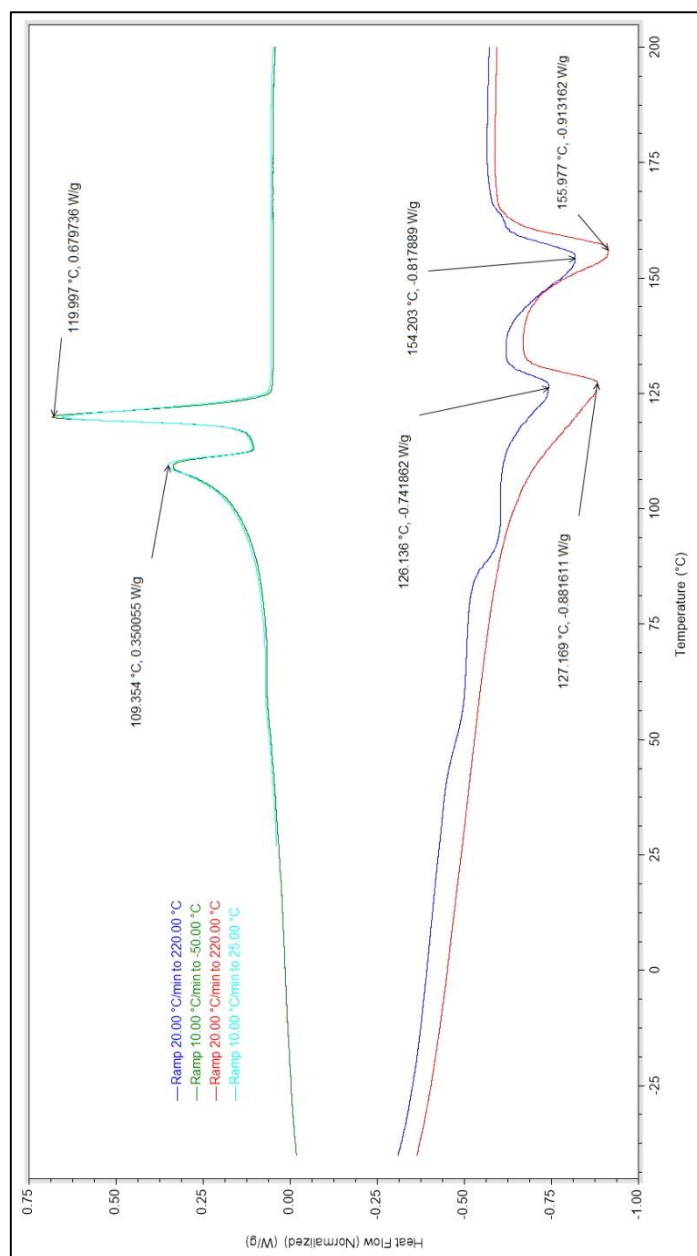


Figure 4.6. Representative DSC thermogram for a sample of poly(VDF-*co*-TFE) of 80 and 20 mol% of VDF and TFE, respectively. Sample prepared using large block technique.

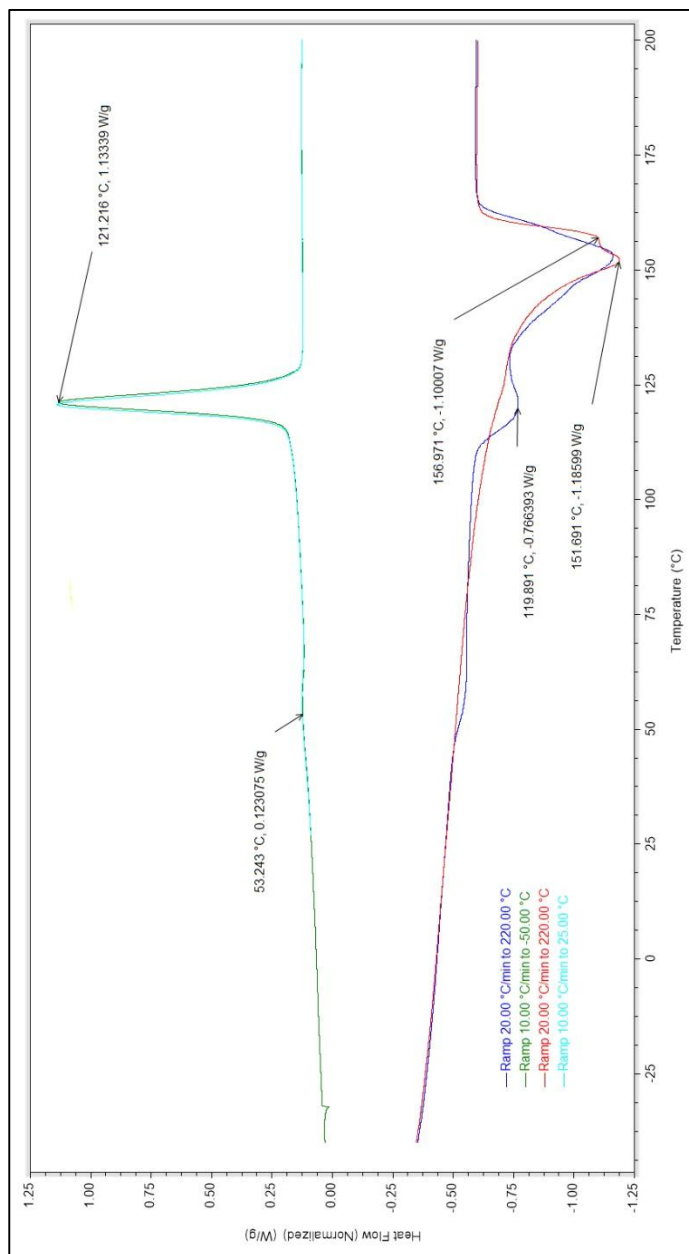


Figure 4.7. Representative DSC thermograph for a sample of poly(VDF-*co*-TFE) of 80 and 20 mol% of VDF and TFE, respectively. Sample prepared using short block technique.

4.6.2. Thermogravimetric analyses (TGA) of samples of poly(VDF-*co*-TFE)

Thermogravimetric analysis (TGA) was used to analyze each of the samples prepared in order to see if the incorporation of TFE in the copolymer had any effect on the decomposition temperature of the polymers or any other characteristic thermal indicators (e.g., 2% and 10% mass loss decomposition temperatures). It is expected that as the content of TFE increases in the copolymer the decomposition temperature of the material would increase as the incorporation of TFE should lead to a stronger backbone chain. An overview of the TGA results for the samples of poly(VDF-*co*-TFE) are included in Table 4.4. As reference, data for 10% mass loss from a larger collection of poly(VDF-*co*-TFE) samples where the polymerizations were run to completion are listed by range of composition in Table 4.5.

Table 4.4. TGA results for the samples of poly(VDF-*co*-TFE) studied.

Composition (VDF-TFE mol%)	VDF (mol%)	TFE (mol%)	Temperature at 10% Loss (°C)
100-0	100	0	430.3
90-10 (A)	88	12	391.2
90-10-CO ₂ (E)	92	8	390.4
80-20 (B)	78	22	393.6
80-20-CO ₂ (F)	81	19	392.1
70-30 (C)	75	25	405.8
70-30-CO ₂ (G)	67	33	405.2
60-40 (D)	65	35	413.3
60-40-CO ₂ (H)	64	36	408.5
0-100	0	100	538.2

Table 4.5. TGA results for the samples of poly(VDF-*co*-TFE) by range of composition.

Sample Range	VDF (mol%)	TFE (mol%)	Temperature at 10% Loss (°C)
0 mol% range of TFE	100	0	395-430*
10 mol% range of TFE	90-95	5-10	390-395*
20 mol% range of TFE	80-90	10-20	360-430*
30 mol% range of TFE	70-80	20-30	405-410*
40 mol% range of TFE	60-70	30-40	400-415*
PTFE	0	100	538**

* The ranges of temperatures are observed for samples taken from reactions that were driven pass the 20% solids mark.

** Sample prepared experimentally at Clemson University.

The 10% mass loss temperature for samples prepared in presence of carbon dioxide are not significantly different than the ones obtained without using carbon dioxide as a diluent for TFE. A trend is observed that an increase in mol% TFE used results in an increased temperature at 10% mass loss in the samples. These results are presented graphically and can be found in Appendix E.

Additional TGA thermograms obtained from representative samples of poly(VDF-*co*-TFE) containing 10-, 20-, 30-, and 40-mol% of TFE where the polymerizations were run to completion are included in Appendix E.

4.6.3. Powder X-ray diffraction (XRD) analyses of samples of poly(VDF-*co*-TFE)

A search of the literature revealed a primary publication that explored the powder X-ray diffraction patterns of poly(VDF-*co*-TFE).¹⁷ Furthermore, we recorded such results to observe if our collected data were in agreement with the data already reported in the literature. A full assembly of the results is shown in Figure 4.8 in order to more easily visualize the morphology of the signals. A full detail of each experimental powder X-ray diffraction pattern recorded is shown in Appendix E. It is easier to observe the degree of crystallinity of the samples when looking only at the data for 2θ angle between 10 to 30°; however, the results are shown in the range of 10 to 50°.

One can observe the high degree of crystallinity of PTFE from X-ray diffraction by studying the ratio of the intensities of the crystalline portion to the amorphous portion. The degree of crystallinity in PTFE is often studied in order to assess the wearability of PTFE.⁶² This could be also applied for copolymers of TFE and VDF, if the copolymer were to be used in an application where wear was an important factor. As observed in Figure 4.8, the increase of TFE in the copolymer increases the overall crystallinity of the polymer. This can be explained on the basis of the isomorphous substitution (substitution of a VDF unit by a TFE unit) of the two comonomers over the full composition of the polymer. This means that for the copolymers, both of the monomer units are present in the crystallite. This could serve as another piece of evidence for the presence of a randomly distributed copolymer and not a block copolymer. The same was observed with the previously reported results.¹⁷

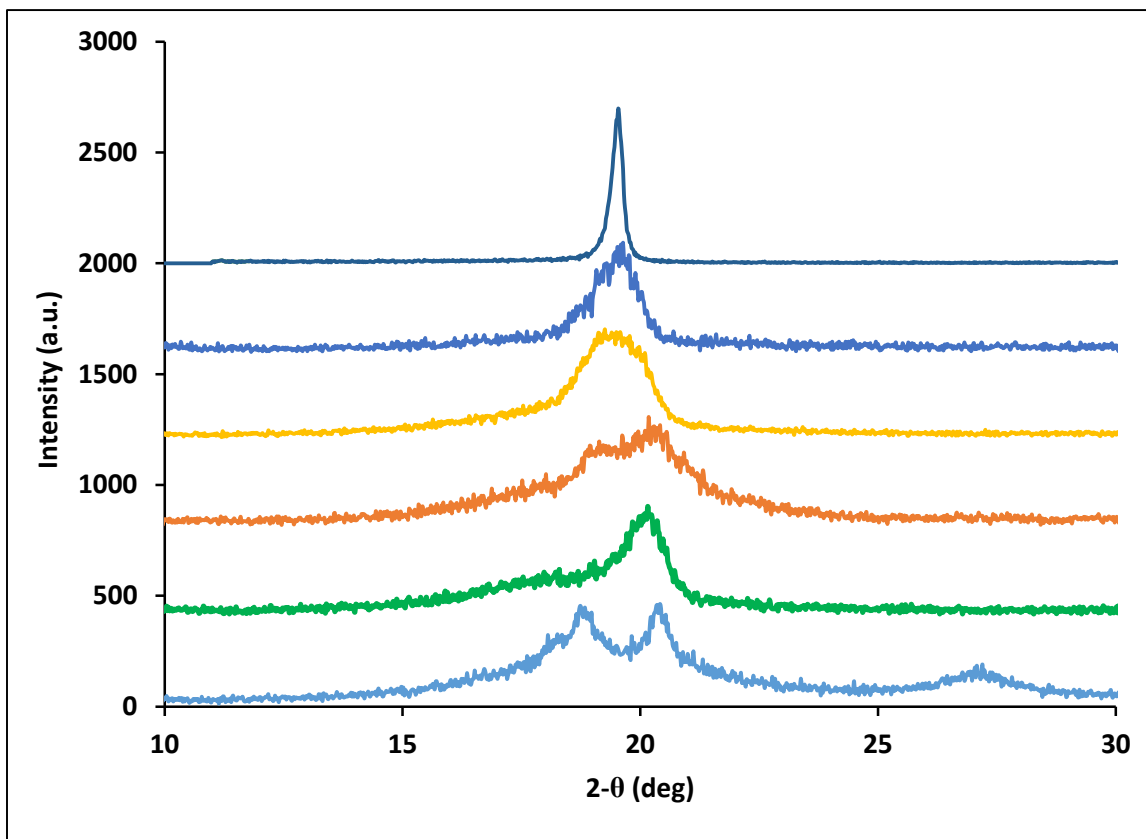


Figure 4.8. Assembly of XRD data for samples of polymers. From top to bottom respectively: PTFE, poly(VDF-*co*-TFE) with 40 mol% TFE, 30 mol% TFE, 20 mol% TFE, 10 mol% TFE, and PVDF (in its α form).

It has to be mentioned that the PTFE XRD results were recorded only for comparison as the PTFE was not prepared using the same reaction conditions. The PTFE sample was obtained from a deposited sample of the homopolymer over a silica wafer and it was only included in the Figure 4.8 as a reference and for comparison between the other samples.

4.6.4. Characterization of poly(VDF-*co*-TFE) using fluorine-19 nuclear magnetic resonance (^{19}F NMR) spectroscopy

It was possible to obtain 1-3% solutions by mass of the samples of poly(VDF-*co*-TFE) in deuterated dimethyl sulfoxide (DMSO- d_6). Other solvents were tested, but DMSO proved to be the best solvent to help dissolve enough of the polymer in order to obtain good quality NMR spectra. The samples were prepared by dissolving enough mass to obtain a clear solution of about 2% in weight of the copolymer in DMSO- d_6 . At about 3-5 wt%, the solution turns very cloudy, and one wonders if all the material is dissolved or if part of the polymer sample does not enter the solution. After filtering higher weight percent solutions, one can observe that the filtered solution is much clearer, hence confirming that at higher weight percent not all the material is soluble. To help with the preparation of the solutions, the polymer samples were finely powdered by using a mortar and pestle. If other methods of sample preparation are used, such as cryo-grinding, the sample is so fine that it is electrostatically attracted to all surfaces and impossible to manipulate (place inside a vial, an NMR sample tube, etc.).

The characterization of poly(VDF-*co*-TFE) has been reported in the literature not only using one-dimensional NMR spectroscopy⁶³ but most recently in 2012 and 2015 by both two- and multidimensional NMR studies, respectively.^{64,65} These latest publications assess the characterization of poly(VDF-*co*-TFE) to an extent that is not necessary for the purpose of our studies; for example, it is only necessary to analyze the sequences of triads to obtain composition information as opposed to analyzing the sequences of pentads and heptads to obtain more detailed information about the polymer such as tacticity, branching,

or statistical distributions of large blocks of either monomer within the polymer. The two- and multidimensional NMR studies of Rinaldi and co-workers on poly(VDF-*co*-TFE) and poly(TFE-*ter*-VDF-*ter*-HFP), respectively,^{64,65} not only give the mol% composition of monomers in these polymers, but they also give other information such as percentages of head-to-head, tail-to-tail, and head-to-tail linkages in these co- or terpolymers. In the present study for the evaluation of relative reactivity ratios, one only needs the composition of the copolymers and not their tacticities, etc. In other words, previous assignments of the signals in the ¹⁹F NMR spectra will be used as means of evaluating the composition of copolymers prepared herein instead of developing such a method from the ground up. With respect to composition, no significant difference exists in the assignments of the ¹⁹F NMR spectra between the original publication appearing in 1981⁶³ and those that appeared in 2012 and 2015.^{64,65} As previously mentioned, the focus of the contents of this Chapter is not the tacticity of poly(VDF-*co*-TFE), but rather an experimental determination of the reactivity ratios of VDF and TFE. The synthetic strategies that favor a head-to-head distribution of monomers over a head-to-tail conformation are well known and have been previously explained by Ying and co-authors.⁶⁶ For example, it has been shown in the literature⁶⁶ that the content of head-to-head in PVDF is directly related to temperature effects and not related to the types of initiators used. The same concept can be applied to poly(VDF-*co*-TFE) in which polymerization temperatures in the range of 50 – 85 °C, were used to favor the head-to-tail configuration. As explained by Ying and co-authors,⁶⁶ who studied the copolymerization of VDF and TFE by keeping all of the conditions of the polymerization the same and only changed the initiator used [diisopropyl

peroxydicarbonate (IPP), dicyclohexyl peroxydicarbonate (DCPD), di-*t*-butyl peroxide (DTBP), and potassium persulfate (PPS)], in all cases the distribution of head-to-head did not change. Even though the radical initiators are different ($\text{SO}_4^{\cdot-}$ is negatively charged and the others are neutral, free radicals $\text{R-CHO}\cdot$), the effect of using one radical initiator to another, only showed a 0.1 – 0.2% variation of structural features (head-to-head, or tail-to-tail). This demonstrates how important temperature is (compared to the type of radical initiator used) during the polymerization reaction.

In order to begin to describe the diad, triad, etc. structures in poly(VDF-*co*-TFE), one should review the nomenclature that has been used in the past. For example, the nomenclature for each type of carbon atom present in the copolymer ($-\text{CH}_2-$ or $-\text{CF}_2-$) can be written as “0” if the carbon atom does not have any fluorine atoms attached to it, or “2” if the carbon atom has two fluorine atoms attached to it. In the same way, the monomer VDF can be represented by the diad term 02, or its reverse unit 20. On the other hand, the monomer TFE can be only represented by the diad term 22, since both of the carbon atoms of the monomer are equivalent to each other. In the same way, small sequences of three carbon atoms are shown in Figure 4.9, while sequences of three (triads), five (pentads), and seven (heptads) carbon atoms can be represented by all possible permutations in the copolymer as listed in Table 4.6.

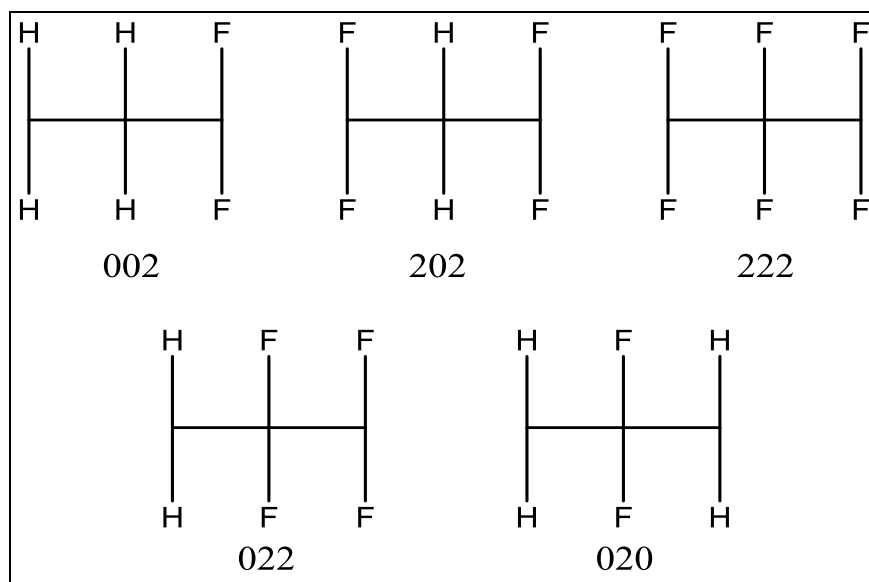


Figure 4.9. Most probable triad diagrams (note that the two reverse representations of 002 and 022 are not displayed).⁶³⁻⁶⁵

One can analyze the different mechanistic routes of the radical polymerization of these two monomers that can produce the different combinations of the monomer in the final copolymer. For example, in Figure 4.10, one can see an illustration of the different pathways by which a radical reacts with either monomer and consequently grows the chain in different fashions. Each radical end on any growing polymer chain can attack either a VDF unit or a TFE unit. When attacking a VDF unit, the reaction can proceed head-to-tail, head-to-head, or tail-to-tail. In a head-to-tail reaction, the $\text{CF}_2\cdot$ end reacts with the CH_2 end of a VDF monomer to form a sequence $-\text{CH}_2\text{CF}_2\text{-CH}_2\text{CF}_2-$, while in a head-to-head mechanism the sequence changes to $-\text{CH}_2\text{CF}_2\text{-CF}_2\text{CH}_2-$, and lastly the tail-to-tail sequence will appear as $-\text{CF}_2\text{CH}_2\text{-CH}_2\text{CF}_2-$ in the copolymer.

The ^{19}F NMR spectrum of poly(VDF-*co*-TFE) can be separated in three well delimited sections depending on the sequence of interest. The region with resonances from 020 sequences appears at around -90 to -100 ppm, while the region with 022/200 sequences goes from -107 to -117 ppm, and the region with 222 sequences goes from -118 to -127 ppm.

Typically, the ^{19}F spectrum of poly(VDF-*co*-TFE) will show multiple different signals in the regions of the 020, 022 and 222 sequences. Each of those signals corresponds to the different environments corresponding to the different possible permutations for each of the triads. As an example, the 020 triad (as shown in Table 4.6) has two different pentads and subsequently three different heptads. The pentads can be easily resolved if the mobility of the polymer is achieved in the solution, but the heptads are more difficult to resolve. A typical ^{19}F NMR spectrum of poly(VDF-*co*-TFE) (70 and 30 mol%, respectively, for VDF and TFE) is shown in Figure 4.11, and one can clearly see the different signals arising for each of the three different ranges of the spectra where the distribution of permutations of the monomers can be found.

Table 4.6. Permutations of triads, pentads, and heptads present in poly(VDF-*co*-TFE).

Triads	Pentads	Heptads
020	20202 20200	0202020 0202022 2202022
022/220	20222 20220 00222 00220	2202220 2202222 0202222 0202220 2002220 2002222 0202202 0202200 2202202 2202200 2002202 2002200
222	22222 22220 02220	2222222 0222222 0222220 2222202 0222202 0222200 2222200 2022202 0022202

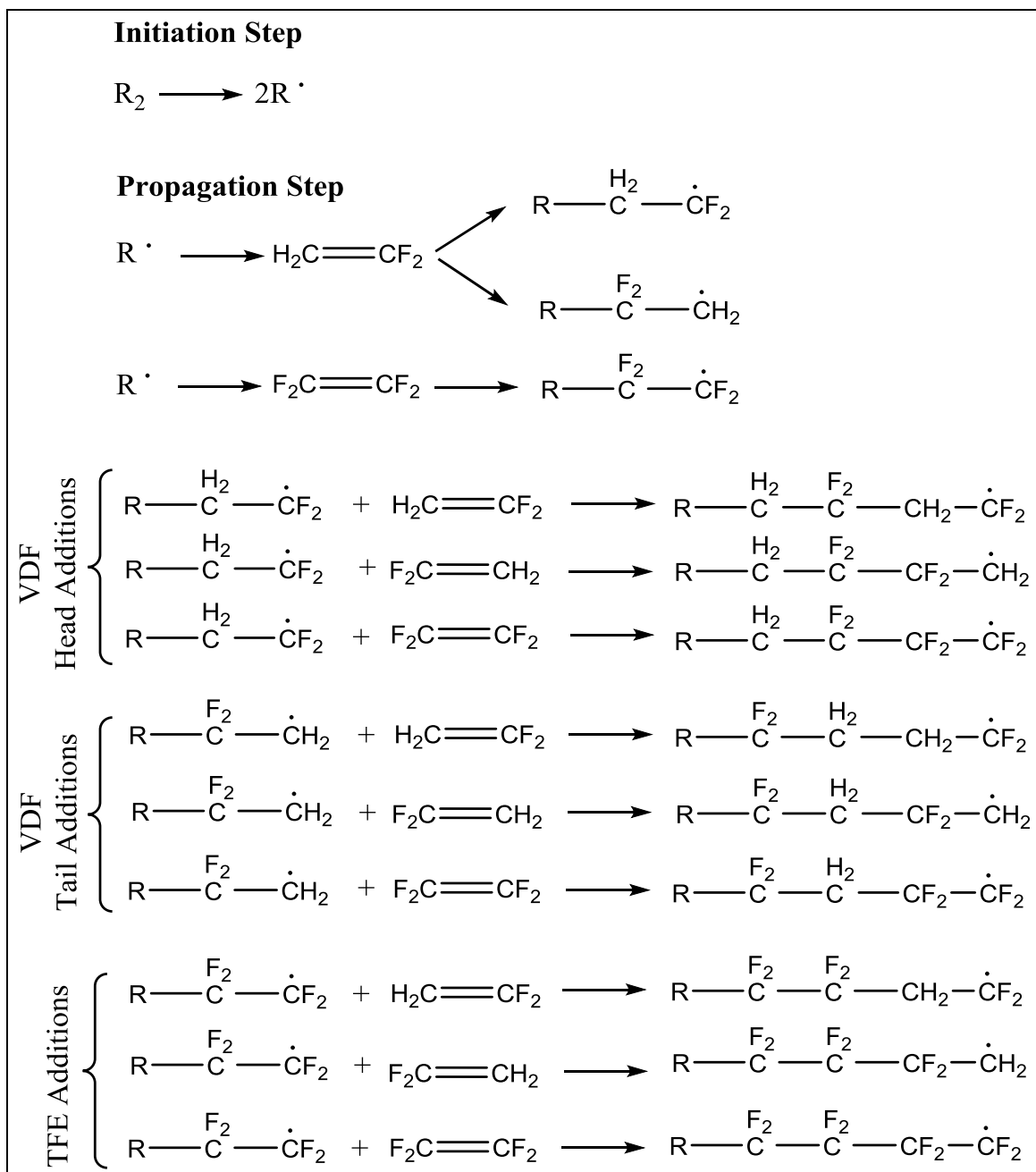


Figure 4.10. Schematic of the different steps of a radical copolymerization of TFE with VDF. Termination steps are not shown.

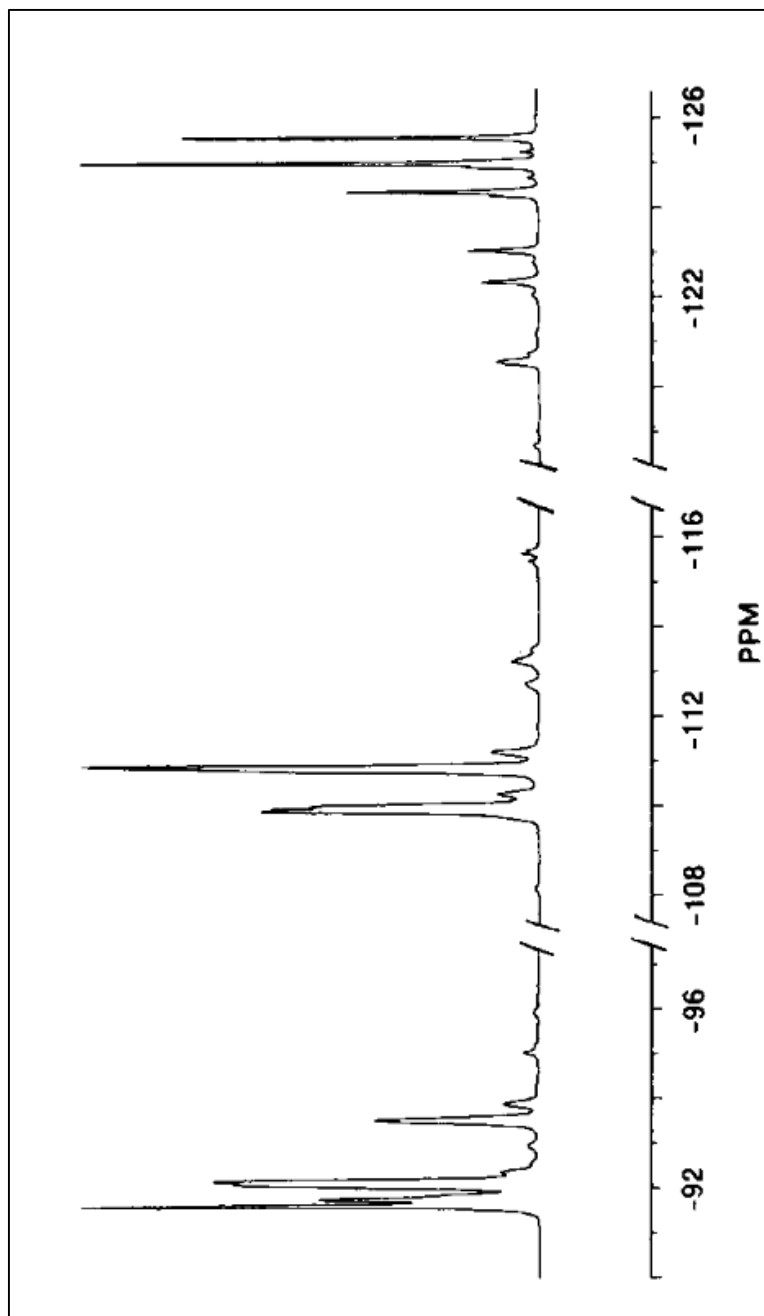


Figure 4.11. Typical distribution of signals in the ^{19}F NMR spectrum of poly(VDF-*co*-TFE). From left to right: sections for signals from 020 (-90 to -96 ppm), 022 (-108 to -116 ppm) and 222 (-117 to -126 ppm) triads.⁶³

The literature⁶⁷⁻⁷¹ has clearly provided sufficient examples of how to use such data not only to accurately characterize poly(VDF-*co*-TFE) but also poly(TFE-*ter*-HFP-*ter*-VDF). Assignments for all of the signals are required to accurately characterize poly(VDF-*co*-TFE). A mathematical relationship can be obtained (equation 4.12) that relates the integrated area of selected signals to the mol% of VDF present in the polymer. The relation of each signal in the equation is shown in Table 4.7. More examples of ¹⁹F NMR spectra of samples of poly(VDF-*co*-TFE) with 10-, 20-, 30-, and 40-mol% of TFE are included in Appendix E.

$$\text{VDF mol\%} = 200 \cdot (2a+b+d+e+f) / (4a+3b+2c+d+e+f) \quad (4.12)$$

Table 4.7. ¹⁹F NMR spectroscopy assignments for the different VDF sequence distributions.⁶³

Key	020	022	222	00202	00222	00220
(ppm)	(-87, -97)	(-106, -116)	(-116, -124)	-94	-112	-115
Assignment	a	b	c	d	e	f

The method of calculating composition of VDF in samples of poly(VDF-*co*-TFE) can be exemplified by using the details in Figure 4.12. By using the equation 4.12, the calculated VDF mol% is 91, and therefore the TFE content is 9 mol% by difference.

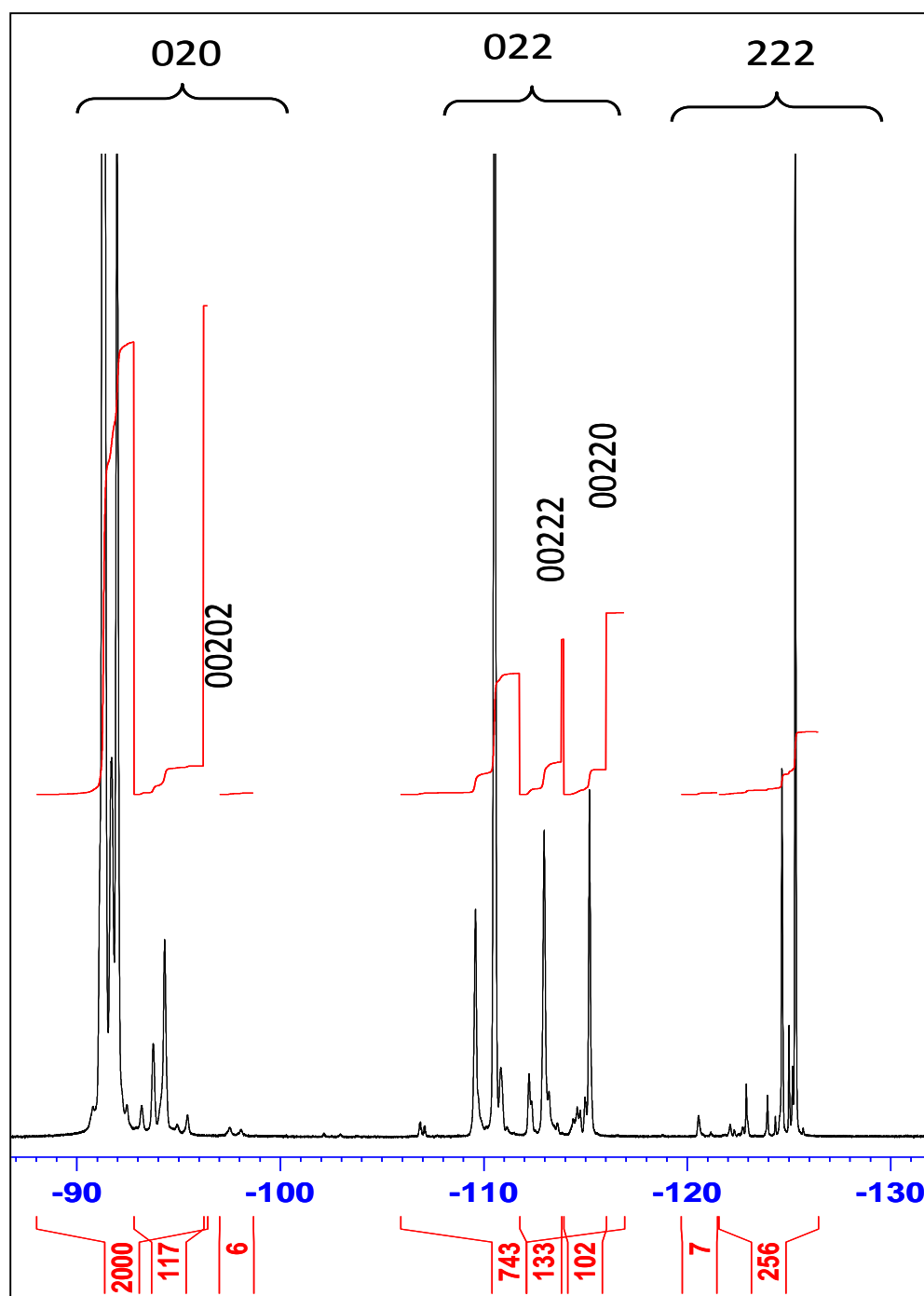


Figure 4.12. ^{19}F NMR spectrum of poly(VDF-co-TFE) of 90-10 mol% composition of VDF and TFE, respectively, with integration (provided by our industrial sponsor).

4.6.5. Experimental Determination of Reactivity Ratios of VDF and TFE in poly(VDF-*co*-TFE)

It is important to note that we have used the same method of signal integration of the ^{19}F NMR spectrum of a sample of poly(VDF-*co*-TFE) of experimental composition of 90 and 10 mol% for VDF and TFE, respectively, in the same manner as our industrial sponsor. Our findings are the same as those of our industrial sponsor, which not only indicates that our integration method compares favorably to the one used by them, but also that the sample preparation and experimental setup is consistent at both the industrial facility and Clemson University. A table of integration values for a set of samples is provided in Appendix E as a guide or template to indicate how such final compositions are determined.

It should also be noted that the NMR spectroscopic method has a precision of $\pm 1\%$ on the obtained signals, and that this is the error bar assigned to the measurements and results obtained from the integration of signals for the experimental samples analyzed. This $\pm 1\%$ comes not from the integration method (as it can be as accurate as $\pm 0.1\%$) but rather from the detection limit of the NMR spectrometer. The uncertainty associated with the experimental determination of reactivity ratios is dictated by all of the uncertainties of the measurements carried out during the polymerization reaction and also during the characterization. The mass flow controllers (MFCs) have a precision of $\pm 1\%$ over their nominal values for flow rate, and therefore they have the same error as the NMR measurements. Overall, the determinations of reactivity ratios are subject to a $\pm 2\%$ error on their determinations as a result of the combined error in both measurements.

The samples obtained by aqueous emulsion polymerization methods were analyzed by ^{19}F NMR spectroscopy, and the results were inserted into the aforementioned equation in order to obtain the samples' compositions. Something important was revealed during the analysis of the NMR data, namely that the final compositions of VDF and TFE varied within 1 mol% when either the latex, the dried latex, or the melt pressed plaque were analyzed.

Not only did these polymerizations, but commonly all the polymerizations, show a lower percentage of incorporation of TFE than the targeted composition. The reactions mentioned above were made by directly feeding the two monomers into the reactor at the same time using MFCs at the desired flow rates in order to maintain the desired composition of the feed. In a typical run, close attention was taken to open and close the MFCs in order to keep the composition as close to the target as possible. For example, for a 80-20 mol% of VDF-TFE, respectively, one would open the VDF mass flow controller and charge eight standard liters (SLs), and then open the TFE mass flow controller to allow two SLs of TFE enter the reactor. The feed was kept at a constant rate until the desired amount of polymer was made. For a typical run that is driven to obtain the maximum amount of polymer, the target is set to a total of 21% solids by mass, but when studying the relative reactivity ratios of TFE and VDF in poly(VDF-*co*-TFE), the polymerization is ran in such a way that less than 15% of solids are obtained.

It was also observed that the introduction of TFE seemed to lower the overall flow of monomers into the reactor. This was observed as the general feed rates (in SL/min) would decrease over time. Some tests were done by charging the reactor with VDF and

starting the reaction with just VDF, once the reaction achieved a constant VDF feed rate of 2.5 SL/min, then the feed would be switched to TFE. In every case, the switch from VDF to TFE (even though the pressure was kept constant) would affect the speed of the reaction, and the uptake of TFE would not be as high as the uptake of VDF before the switch.

Another strategy used was to prepare a mixture beforehand of the two monomers in the desired composition of the final polymer. It was observed that when using a mixture, the uptake of TFE would be at least 10% lower than the target composition.

Using the methods described in Section 4.6.4., the determination of the relative reactivity ratios for the copolymerization of TFE and VDF were determined. Values from both the Fineman and Ross (F-R) and Kelen and Tüdös (K-T) models were calculated for the radical copolymerization of TFE and VDF under aqueous emulsion polymerization conditions both in the presence and absence of CO₂ (included in the feed of TFE). In other words, when CO₂ was introduced in the reactor, it was introduced as an equimolar mixture of TFE and CO₂ obtained from the thermal decomposition of CF₃CF₂C(O)O⁻K⁺, as previously discussed in Chapter 3 of this Dissertation and the literature.⁵⁴

In the following tables (Tables 4.8, 4.9, and 4.10), where results are shown, samples A, B, C, and D, are samples of poly(VDF-*co*-TFE) that were prepared in absence of CO₂, while samples E, F, G, and H, are polymers that were prepared in presence of CO₂. In Table 4.8 the targeted and final polymer compositions are detailed (where the polymer compositions were calculated using the NMR method discussed above). In Table 4.9, the Kelen and Tüdös and the Fineman and Ross evaluated parameters are detailed. Such

parameters were used to determine experimentally the reactivity ratios for VDF and TFE, which are shown in Table 4.10.

Table 4.8. Reaction data: target compositions and final compositions of poly(VDF-co-TFE) in presence (light red) and absence (light blue) of CO₂.

Sample	Targeted Composition (mol %)		Composition Determined Experimentally (mol% \pm 1%)	
	VDF	TFE	VDF	TFE
A	90	10	91	9
E	92	8	92	8
B	80	20	85	15
F	83	17	81	19
C	70	30	82	18
G	71	29	67	33
D	60	40	74	26
H	60	40	64	36

Table 4.9. Parameters evaluated for obtaining reactivity ratios using the Fineman and Ross as well as the Kelen and Tüdös method in presence (light red) and absence (light blue) of CO₂.

Sample	η	ξ	α	X	Y	G	H
A	0.70	0.67	3.73	8.83	10.22	7.96	7.62
E	0.69	0.75	3.82	11.50	11.50	10.50	11.50
B	0.48	0.65	3.73	6.25	5.54	5.12	7.05
F	0.40	0.59	3.82	4.88	4.26	3.74	5.59
C	0.43	0.60	3.73	5.14	4.69	4.04	5.64
G	0.18	0.44	3.82	2.45	2.03	1.24	2.95
D	0.26	0.35	3.73	2.34	2.78	1.50	1.98
H	0.13	0.25	3.82	1.50	1.78	0.66	1.27

The next figure (Figure 4.13) the correlation in between the targeted polymer composition versus the experimentally determined polymer composition is detailed. It is observed that for the runs in which CO₂ was used, the obtained polymer composition is much closer to the targeted one, while for the runs in which CO₂ was not used, the obtained polymer composition deviates the more from the targeted composition as the amount of TFE increases in the copolymer.

In Figures 4.14 and 4.15, graphical representations of the Fineman and Ross method of relative reactivity ratio analyses are shown. First, in Figure 4.14 the data represents the runs in which CO₂ was not used in the polymerization reaction, while in Figure 4.15 the data represents the runs in which CO₂ was used during the polymerization reactions (see Experimental section below). Additionally, in Figures 4.16, and 4.17, the Kelen and Tüdös graphical representations are featured. In Figure 4.16 the data represents the runs in absence of CO₂, while in Figure 4.17 the data represents the runs carried in presence of CO₂.

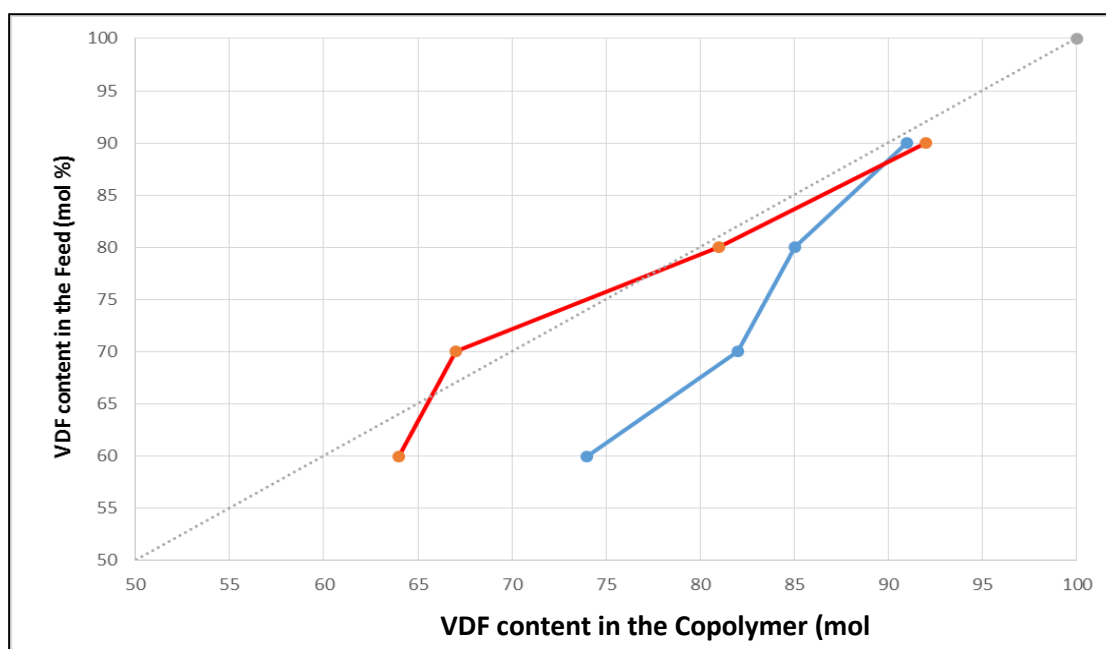


Figure 4.13. Monomer/polymer composition curve for poly(VDF-*co*-TFE) in presence (red line) and absence (blue line) of CO₂. Dotted line is a diagonal for ease of visualization of the data.

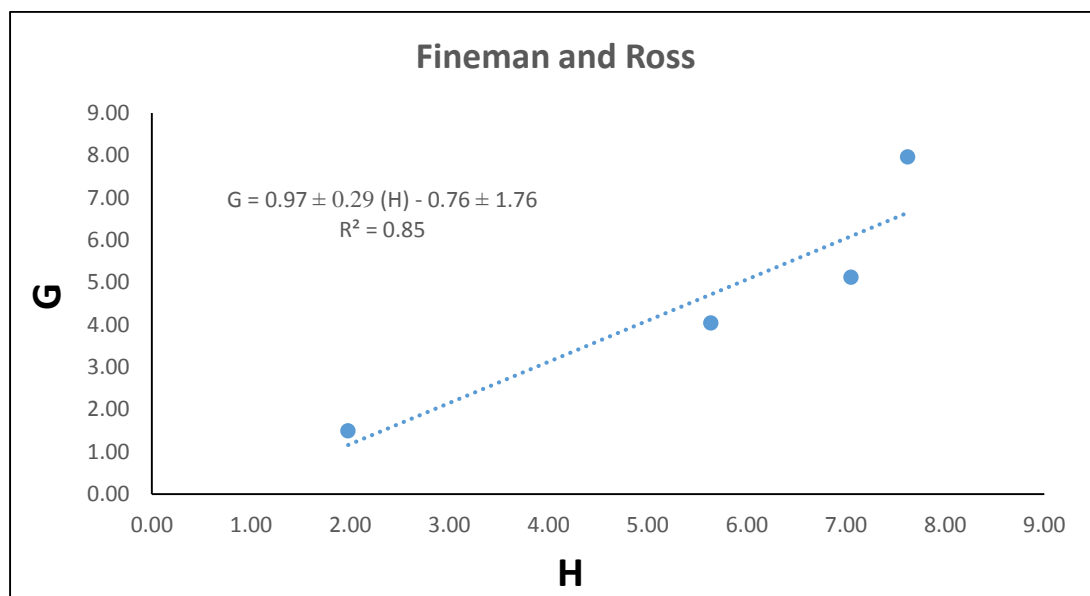


Figure 4.14. Fineman and Ross plot of H and G for poly(VDF-*co*-TFE) in absence of CO₂.

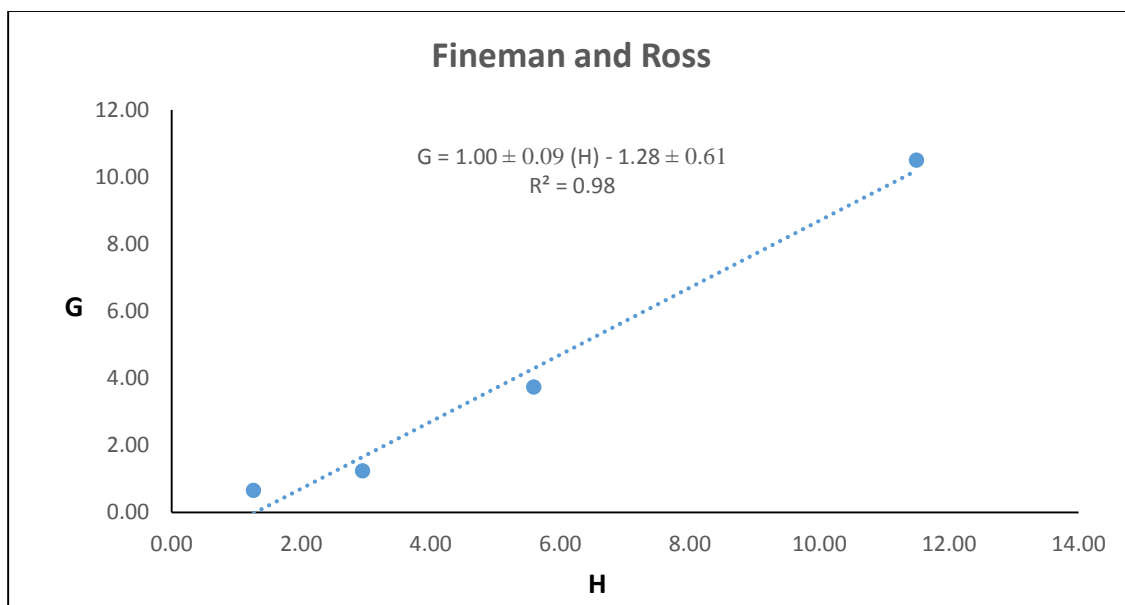


Figure 4.15. Fineman and Ross plot of H and G for poly(VDF-*co*-TFE) in presence of CO₂.

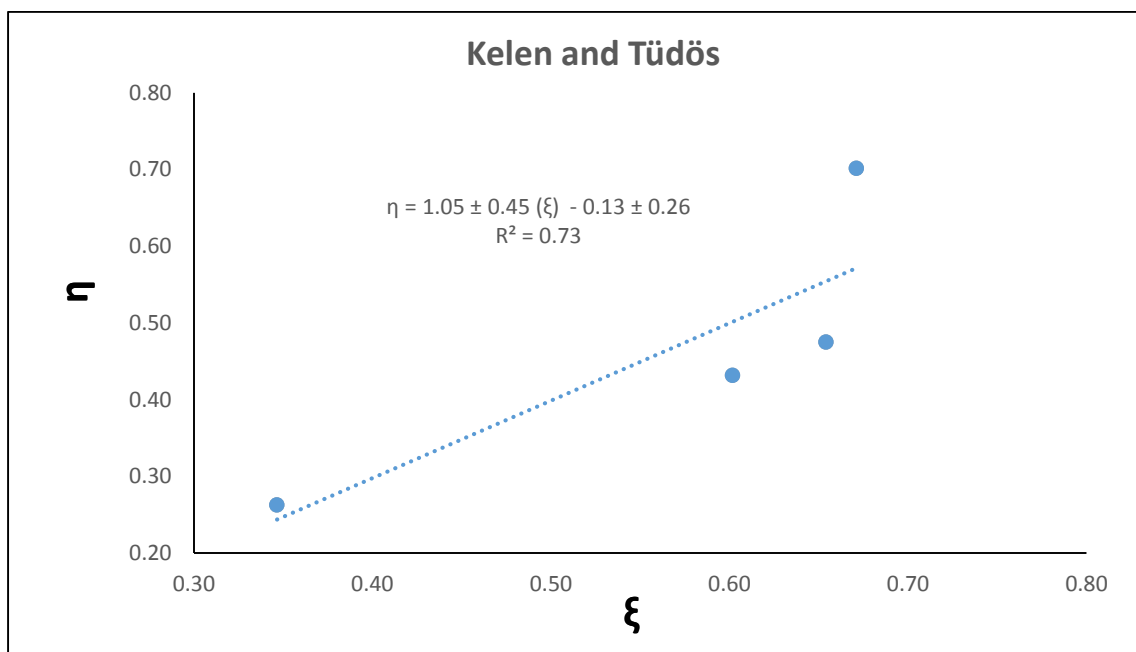


Figure 4.16. Kelen and Tüdös plot of ξ and η for poly(VDF-*co*-TFE) in absence of CO₂.

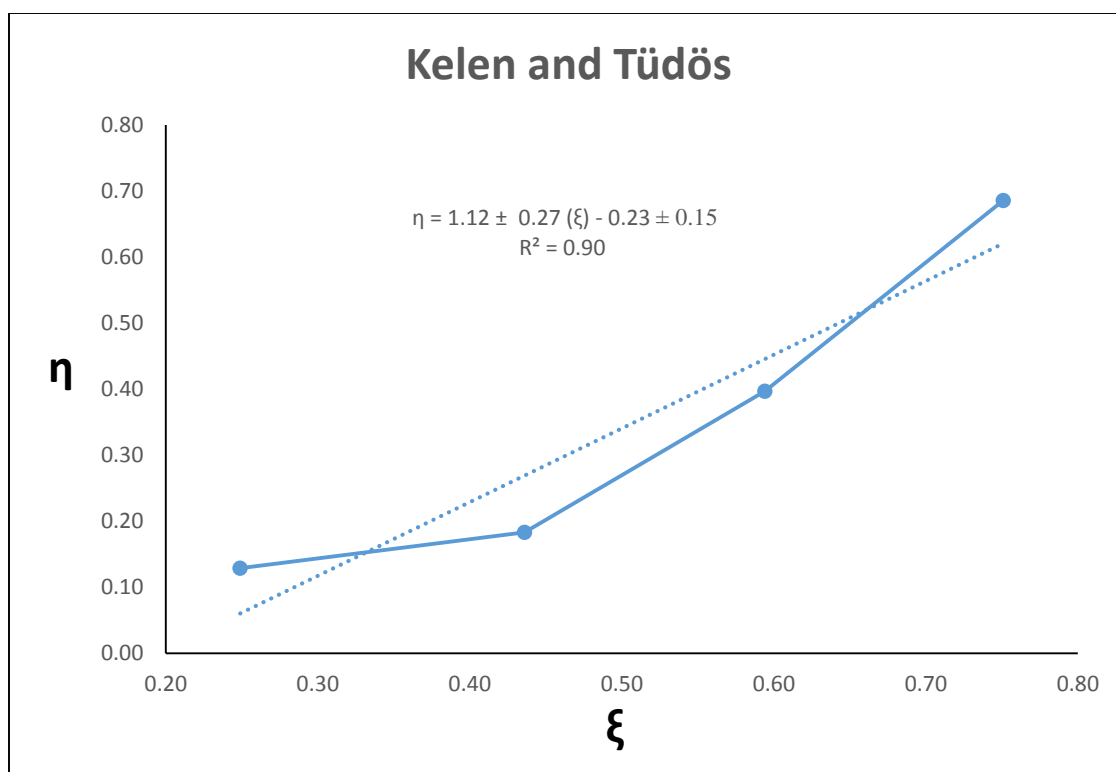


Figure 4.17. Kelen and Tüdös plot of ξ and η for poly(VDF-*co*-TFE) in presence of CO₂.

Table 4.10. Reactivity ratios of VDF and TFE in poly(VDF-*co*-TFE) in the presence and absence of CO₂ at 83 °C.

Samples	Monomer	Kelen - Tüdös	Fineman - Ross
A-D	VDF r_1	3.37 ± 0.45	0.97 ± 0.29
	TFE r_2	0.39 ± 0.26	-0.76 ± 1.74
E-H	VDF r_1	0.87 ± 0.27	1.00 ± 0.09
	TFE r_2	1.03 ± 0.15	-1.28 ± 0.61
B-D*	VDF r_1	0.62 ± 0.06	0.70 ± 0.06
	TFE r_2	0.07 ± 0.06	0.13 ± 0.06

Note: B-D* is the same range of polymer compositions as A-D minus the sample A results. The correlation for the Fineman and Ross, and Kelen and Tüdös reactivity ratios are more in agreement.

The reactivity ratios of VDF and TFE in poly(VDF-*co*-TFE) can be found in the literature, being r_1 (VDF) and r_2 (TFE) with values of 0.23 and 3.73, respectively, for VDF and TFE (determined by the Fineman and Ross method).¹⁷ It is noticeable for the current experiments (A through D, and B-D*) that the reactivity ratio of VDF is larger than that of TFE (when the data is analyzed by the Fineman and Ross method). For the experimental compositions E through H, that the reactivity ratio of TFE is larger than the one for VDF. Also when reducing the range of compositions from A-D to B-D*, the agreement of the reactivity ratios from the two methods is much closer. Reducing the sample range (deleting the point or points that deviate the most in the series) did not help obtain a better agreement for the samples prepared in presence of CO₂ (Samples E-H).

For the Kelen and Tüdös, and Fineman and Ross calculated reactivity ratios, it is observed that the values obtained are opposite to the ones reported in previous literature (except for the samples prepared in presence of CO₂).¹⁷ In the literature, the reactivity ratio of VDF is lower than the one for TFE. For the runs carried in absence of CO₂, it can be observed in Table 4.10 that the values are opposite to the trend already published in the literature. For the runs carried in presence of CO₂, we can see that the trend is inverted and goes in the same direction as the one published in the literature (reactivity ratio of VDF is higher than the one for TFE).¹⁷

This difference can arise not from the polymerization conditions, but from the fact that the Kelen and Tüdös method includes a normalization of the values of H included in the α parameter, which in fact includes a better linearization of the results. For both cases it is observed that the reactivity ratios are larger for VDF than for TFE, which explains why

at larger targeted incorporations of TFE (>20 mol%) the obtained composition is lower in TFE. For the samples in which 30 and 40 mol % of TFE was targeted, the resulting compositions have a larger amount of TFE in them but still not equal to the targeted composition (as opposed to the ones in which TFE is targeted at 10 or 20 mol%). This is not a reflection of an azeotropic composition since more TFE was able to be included in the samples. If we had an azeotropic composition behavior for this polymerization system, we would have not been able to include more than a certain amount of TFE in the experimental samples. The extended Kelen and Tüdös method was not used to analyze the results since the experiments used for this treatment were selected from a reduced list of low conversion reactions in the range of 10-15 %. In our case, (normally the K-T results leave room for error that inherent of the method), the K-T method gives a more accurate result of the reactivity ratios for this polymer all across our experimental range of conditions. This could be due to the fact that the spread of compositions is spread over a good percentage of the total range of compositions possible and also that the differences in the compositions are significantly large to each other. We will see in Chapter 5, that when a short range of compositions is obtained [for poly(TFE-co-PSVE)], the K-T method gives the most error while the F-R remains the more reliable method for determining reactivity ratios.

In regards to the reactivity ratios, r_1 (VDF) is larger than r_2 (TFE) for the Kelen and Tüdös results (including that r_1 is larger than 1). In agreement with the aforementioned theory, the difference in reactivity ratios and the magnitude of r_1 with respect to r_2 indicates that VDF would be more likely to incorporate with either reactive chain radical (polymer-

$M_1\cdot$ or polymer- $M_2\cdot$), expressed by the reaction constants k_{21} and k_{11} with respect to the other two reaction pathways. For the results obtained from the Fineman and Ross linearization method, one can see that the same trend persists: the reactivity ratio of VDF is larger than that of TFE. The only difference is that both values are less than 1. In agreement with the theory, the distribution of the monomers is random (as observed from the variety of signals obtained from the NMR spectroscopy results), and the final composition is dependent on the monomer feed composition. To prove this, the same experimental setup was performed using a higher content of TFE in the monomer feed, but regardless of the polymerization experimental setup, the reaction seemed not to proceed as expected. When increasing the amount of TFE in the mixture, two approaches were taken into consideration: (1) to have the mass flow controller unit feed the monomers at the desired ratio, or (2) to start the polymerization by making a block of either monomer and then feed the co-monomer into the reactor and to alternatively feed each monomer at the desired ratio in blocks small enough to avoid block copolymer bulk properties and obtain a more homogeneous copolymer. Neither strategy seemed to have worked for higher percentages of TFE in the monomer feed. Therefore a change in the experimental conditions is suggested in order to find the optimal conditions for a higher incorporation of TFE into the final composition of the copolymer. It is important to mention that at the beginning of the study, an extensive design of experiments (DOE) analysis was performed in order to find the best conditions to carry out a polymerization that complied with the original desired attributes of the copolymer (high percent solids in the range of 25 to 30%, non-coagulated latex obtained directly from the reactor at the end of the polymerization,

and high molecular weight). The molecular weights of the polymers obtained were never estimated experimentally, since this was not a primary goal for the study. The variables used in the DOE were rate agitation (measured in revolutions per minute, rpm), feed rate of radical initiator solution (measured in mL/min), amount of surfactant used (measured in wt%), amount of chain transfer agent used (measured in wt%, sodium sulfate and ethyl acetate), and the initial slug of radical initiator solution (measured in mL). It is evident that a DOE with this many variables is a time consuming task, and therefore some variables were kept constant in order to save time and effort.

The amounts of chain transfer agent were kept constant at the same wt%, and the amounts were modified in search of obtaining a stable latex (as opposed to coagulum) at the end of the reaction. Another indicator of favorable conditions was the monomer uptake at a given agitation speed. A series of videos was taken using a glass beaker of comparable size to both of our reactor setups (2-gal and 600-mL reaction vessels) in order to determine what agitation speed was most appropriate to induce a residence time of the gaseous monomers to be in contact with the solution in the form of small bubbles. The speed and shape of the blades of the agitator are critical since too low of a rate of agitation does not help the monomer to be incorporated into the bulk of the solution and too high of a rate of agitation induces shear between the blades and the polymer formed, resulting in coagulum (polymer escaping from the solution and precipitating to the bottom of the reactor). The first attempts at making polymer were geared towards the preparation of PVDF to learn more about the homopolymer, which also kept us from using the more expensive TFE monomer. Once the parameters (agitator speed, volume of initial slug of radical initiator,

amounts of surfactant and chain transfer agent) were modified, and a stable latex of 25% solids was obtained, preparations to include the second monomer (TFE) were made.

Further attempts to incorporate TFE in higher percentages than 40 mol% were made. Attempted strategies included making a mixture of monomers of noticeably higher content of TFE (50 or 60 mol%), and then studying the compositions of polymers obtained using the same experimental conditions used for the other compositions. It has also been suggested to reevaluate the experimental conditions using the aforementioned mixture of monomers and evaluate if such changes have an impact on the final composition. If the experimental setup is changed at all, the reactivity ratios have to be re-evaluated using a consistent experimental setup, as the previous values are only valid for the initial set of conditions studied.

It is vital to analyze the results in the presence of carbon dioxide in the initial charge of monomers. Historically, carbon dioxide (CO₂) has been used as a diluent in order to reduce the homopolymerization of TFE inside a storage cylinder, and also to eliminate the risk of a deflagration (as previously discussed in the introduction of this manuscript and other publications where the technology has been discussed).^{54,72-82}

Polymerizations using the same experimental conditions as before were evaluated in the presence of CO₂. The reactor was charged with a given amount of CO₂ equivalent to 20% of the gas contents of the reactor. The rationale to keep the amount of CO₂ constant was to subject all the different reactions to the same partial pressure of carbon dioxide. The amounts of CO₂, VDF, and TFE used in each polymerization are detailed in Appendix E.

One can observe that a different trend was found when reacting VDF with TFE in the presence of CO₂. Even though the experiments were carried out under a reduced partial pressure of TFE (when CO₂ is used, the partial pressure of TFE is reduced to half its original amount) as compared to that of the previous experiments mentioned (in order to study the effect of pressure on the results of the reaction), the reactivity ratio for TFE was found to be slightly higher than for VDF. It can be concluded that the partial pressure of carbon dioxide does affect the polymerization reaction. The yields of polymer obtained were lower than the yields obtained when carbon dioxide was not used as a diluent. Normally, one would obtain about 81 g of copolymer when using a 600-mL reactor as directed in the Experimental section at 150 psig in the presence of carbon dioxide. For sake of simplicity, the polymerizations with carbon dioxide were carried out at a total pressure of 150 psig in order to avoid using an excess of both monomers, as limited quantities of each existed at the time of the experiments.

One potential rationale for the experimental observation that the reactivity ratio of TFE is now greater than that of VDF could be the fact that the carbon dioxide probably changes the pH of the solution in a significant way, which may affect the reactivity of VDF. Where VDF could be more expected to dissolve in water more than TFE, it makes sense that a change in pH would affect the reactivity of VDF without affecting the reactivity of TFE. In Figure 4.13 (above) it can be observed that the samples prepared in presence of carbon dioxide are closer in composition to the perfect diagonal of the graph meaning that the incorporation of TFE is higher and overall closer to the mol % of TFE fed to the reactor.

Another factor to consider when looking at the differences in reactivity ratios when CO₂ was used as compared to when it was not used, is that, if CO₂ affects the solubility of VDF (as is expected that VDF is more soluble in water than TFE), then the results of the calculations are not reflecting what is happening in reality. The calculations are based on lots of assumptions, one of them being the fact that the total amount of the monomer feed is supposed to be in chemical interaction at the moment of the reaction. If VDF is not entering the solution as fast as when CO₂ is not used, then the head space of the reactor has a different composition than the monomer feed and what monomers are in solution. Since it is impossible to obtain information from the current experiments about composition of the monomers in solution, the best approximation is to use the monomer feed. A solution for this problem would be to use a fluorinated solvent (HFC-4310, FC-72, etc.) in order to favor the solubility of both monomers and therefore minimize differences in the composition of the monomers in the head space of the reactor and the solution. This latter idea is not a viable solution, since changing the solvent will change evidently the reactivity ratios and a fluorinated solvent would not be used industrially for preparing this copolymer.

4.7. Conclusions

1. It can be concluded that the experimental conditions used to prepare poly(VDF-*co*-TFE) in the absence of CO₂ produce reactivity ratios for VDF and TFE that have a trend that is opposite to the trend already published in the literature.¹⁷

2. When using CO₂ as part of the gas mixture, the reactivity ratios for VDF and TFE present the opposite trend as to when CO₂ is not used in the reaction (see Table 4.10). It is concluded that CO₂ competes with VDF for solubility in water and therefore affects the ability of VDF to enter the solution and grow the polymer chain.
3. Given the set of experimental conditions explored, further work must be done in order to obtain a set of conditions that might result in a greater incorporation of TFE in the copolymer.
4. Obtaining more agreement in between the K-T and F-R data analysis from a reduced number of sample compositions reveals that there is still variability in the compositions that is expressed in the lack of agreement in the results. A wider range of compositions needs to be studied in order to assess the behavior.

4.8. Experimental section

All experimental procedures are based on the manual of standard operational procedures (SOP) located in the control room of the TFE polymerization facility. A copy of all of these procedures can be found in Appendix A. The TFE monomer was synthesized in the laboratory using the procedures detailed in Chapter Three while the VDF monomer was obtained from our industrial sponsor. The surfactant (denominated ASOAP) was supplied by our industrial sponsor as well. The rest of the chemicals were purchased from a catalog company if not existent in our chemical inventory.

The NMR analyses were performed in a JEOL 300 MHz nuclear magnetic spectrometer and the NMR was analyzed using their proprietary software. The DSC

analyses were carried in a TA Discovery series differential scanning calorimeter and the thermograms were analyzed using their proprietary software named TRIOS. The TGA were performed in a TA Q500 under nitrogen atmosphere.

4.8.1. Preparation of aqueous polymerization solution

The setup shown in Figure 4.19 is used to prepare the aqueous polymerization solution. A glove bag is filled with nitrogen gas until the level of oxygen is lower than 20 ppm. The distilled water contained in a 35-gal container (Den Hertog IBFD35 Set) has been sparged with nitrogen gas to lower the content of dissolved oxygen to less than 1 ppm (as measured with an YSI ProODO dissolved oxygen meter). The desired amounts of chain transfer agent, surfactant, and any other additives are added to a 5-L Jerry Can that has been previously equipped with Swagelok™ fittings and access valves in order to isolate the contents of the container to the atmosphere. After the desired amount of water is then placed inside the Jerry Can, the container is closed and taken out of the glove bag, where the contents from the Jerry Can can be added to the 2-gal autoclave via Schlenk techniques.

When a small reactor (400-mL or 600-mL) is used to carry polymerizations, the reactor vessel and top are brought to the glove bag. The vessel is opened and filled with water (330 mL), directly from the water container, and the reactor is closed while inside the glove bag. The reactor is brought out of the bag and placed in the vise for further tightening of the lock bolts.

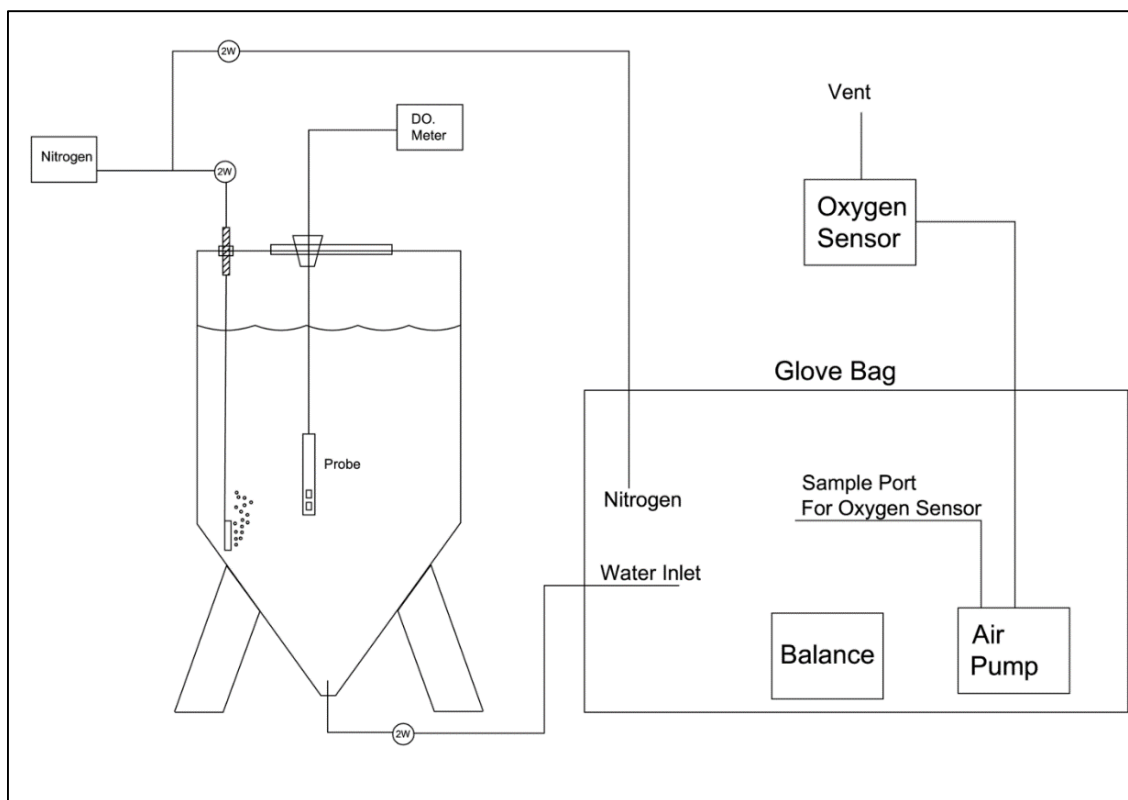


Figure 4.19. Distilled/deoxygenated water setup for preparing polymerization solutions.

4.8.2. Preparation of a gas mixture of TFE and VDF

The reaction room is equipped with a 1-Gal Hoke cylinder made into a trap containing a total of 50 g of D-limonene previously degassed by the freeze/pump/thaw method. The trap cylinder is frozen to liquid nitrogen temperature, and the entire polymerization system is evacuated and back filled with nitrogen three times. The TFE is then flown into the trap cylinder at a constant pressure of 20 psi, and the flow is stopped when the desired amount has been transferred (The amount of TFE can be measured with the mass flow controller when set in totalizer mode). Before the steps are repeated with VDF, the contents of the lines are back-condensed into the main TFE cylinder, and the TFE

source cylinder is closed. Once the transfer of VDF is complete, the trap cylinder is allowed to warm up to room temperature, and a gas sample is taken for ^{19}F NMR spectroscopic analysis. The final weights of all of the cylinders are also recorded in order to double confirm the composition of the mixture. The mixture 60-40 mol% of VDF-TFE has been found to have a vapor pressure of 490 psi at room temperature. A typical amount of 1500 g of mixture is prepared in a 1-Gal Hoke cylinder. This same procedure can be used to prepare other compositions of gas mixtures.

4.8.3 Homopolymerization of VDF by emulsion techniques

The following procedure is designed for when carrying a polymerization reaction to completion (20-25% solids as opposed to <10-15% solids when studying reactivity ratios). A 2-Gal stainless steel autoclave, washed with deionized water, was charged 4000 mL of deionized, deoxygenated water, 1 g of ethyl acetate, and 1.0 g of ASOAP (surfactant of confidential identity). An initiator solution is prepared from 300 mL of deionized deoxygenated water and 15.00 g of potassium persulfate. The reactor is heated to and maintained at 83 °C using a 4848 Parr[®] autoclave controller, an external electrical oven, and an internal cooling loop with a solution of 50% v/v of ethylene glycol and water, which is cooled to 5 °C using a Neslab Model ULT80 circulating bath. The stirring for the reaction is set to 250 rpm. The reactor is then charged with 400 psi of VDF (approximately 65 SL of VDF), a slug of 10.00 mL of initiator solution is fed using an ISCO[®] Model 100DM syringe pump, and then the flow from the syringe pump is re-adjusted to a flow of 0.1 mL/min. The induction period (marked by a steady maximum uptake of VDF monomer

determined by the MFC), of the reaction takes approximately 45 minutes and after which, a flow of 2-3 SLM of VDF is observed. The polymerization is continued until 470 SL of VDF are fed into the reactor (approximately 25% solids), and then the polymerization is stopped by turning off the heat, reducing the stirring speed, and stopping the flow of initiator solution to the reactor. The reactor is allowed to cool to 25 °C by adjusting the temperature controller to that the temperature so that the cooling solution of the internal cooling coil can decrease the temperature of the reactor. After the reactor reaches room temperature, the vessel is vented. The latex is then collected in a plastic 1-gal bottle, and if desired, the contents of that bottle can be dried overnight in a convection oven at 100 °C. Typical yields are 20-25% solids of a white crystalline powder or 1240 g of PVDF.

4.8.4. Copolymerization of TFE and VDF by emulsion techniques using a gas mixture

The following procedure is designed for when carrying a polymerization reaction to completion (20-25% solids as opposed to <10-15% solids when studying reactivity ratios). To a 2-Gal stainless steel autoclave washed with deionized water while scrubbing gently with a cotton rag to avoid scratching the vessel prior to the reaction. A previously mentioned Jerry Can is loaded with 4000 mL of deionized deoxygenated water and 1.0 g of ASOAP (surfactant of confidential identity). The contents are loaded by evacuating the reactor and connecting the Jerry Can to the reactor's loading valve and transferring the contents by differential pressure, i.e., Schlenk techniques. The initiator solution is made with 300 mL of deionized deoxygenated water, 15.0 g of potassium persulfate, and 15.0 g of sodium acetate. The reactor is heated to 83 °C in the same fashion as the previous

procedure. The stirring for the reaction is set to 200 rpm. The reactor is now charged with 400 psi of VDF (approximately 65 SL of VDF), a slug of 10.00 mL of initiator solution is fed using an ISCO® Model 100DM syringe pump, and then the flow from the syringe pump is re-adjusted to a flow of 0.1 mL/min. After the induction period, the VDF feed is stopped, and the mixture of TFE and VDF is fed to the reactor in order to keep the same overall pressure of 400 psi, and the reaction is allowed to continue until the volume of mixture of TFE and VDF flown reaches the overall composition of monomers desired in the polymer. The reaction is stopped as previously discussed, and the product is collected in the same way as in the procedure described above.

When studying reactivity ratios, a 600-mL reactor was used. It was charged with 330 mL of water (as previously detailed in the Experimental procedure 4.8.1), 0.33 g of ethyl acetate and 0.33 g of ASOAP. The stirring speed used was 300 rpm, a 4 mL slug of the same initiator solution is given to the reactor, and continuous feed of the initiator solution is adjusted to 0.05 mL/min. The reaction was quenched by slowly venting the excess pressure of the reactor, and once the reactor was brought to atmospheric pressure, the oven was lowered and the temperature of the reactor was set to 5 °C in order to force the autoclave controller to fully open the cooling lines and bring the reactor rapidly to 5 °C. Since the volume of the reactor is small (compared to the 2-Gal reactor), the final temperature was reached within 2-3 minutes. After the reactor was cooled, the vessel was removed from the reactor table, brought to the control room where the top is unbolted, and the contents of the reactor are poured into a 9 by 11 inch cooking pan. The pan is placed in

a convection oven set at 100 °C for 24 hours. After the polymer is dried, (normally obtained in between 60 to 85 grams) is placed in a Ziploc[®] bag and stored at room temperature.

4.8.5. Emulsion Copolymerization of TFE and VDF using separate gas feeds

The following procedure is designed for when carrying a polymerization reaction to completion (20-25% solids as opposed to <10-15% solids when studying reactivity ratios). Note: depending on how often each monomer gas is switched on or off the reactor, the size of the block produced can be regulated. For larger blocks of each monomer, each gas is allowed to flow for longer periods of time (to allow a larger block to be formed), while for smaller blocks each gas is turned on and off alternatively with faster frequency. The reactor setup used is the same as explained above. The autoclave is charged with VDF to 400 psi and the reaction is started by adding 10 mL of initiator solution to the reactor. The reactor is heated to 83 °C and the agitation is set at 250 rpm. After the induction period has started, and the reaction is showing monomer uptake to about 2-3 SLM, the VDF feed is stopped and the TFE feed is open. The alternating feeds are kept in the molar ratio as previously targeted in the final product. Typically the reaction is carried by feeding two monomers until reaching 25.0% solids. If the reactivity ratios are the purpose of study, then the polymerization is stopped at when the reaction has reached 10 or 15% solids. The product of the reaction is worked up in the same way as explained by the procedure above. When studying reactivity ratios, the same general procedure as detailed in Section 4.8.4 is followed with the exception of the changes made in this procedure (4.8.5) to feed the monomers in separate feeds.

4.8.6. Aqueous emulsion polymerization of TFE and VDF in the presence of carbon dioxide

The reactions using carbon dioxide as a diluent were carried in a 600-mL stainless steel reactor. The reactor was opened inside the glove bag to charge 330 mL of deionized water and 0.33 g of ASOAP surfactant. After the reactor is placed in the polymerization room and all the equipment is attached, the reactor is charged with the desired amount of carbon dioxide. The amount of carbon dioxide is an equimolar amount as the TFE that is needed to be charged in order to fill the reactor with the desired proportion of TFE and VDF before the reaction starts. As an example, if the total pressure is 110 psig, and the reaction is targeted at 90-10 mol% of VDF and TFE respectively, the reactor is then charged with 10 psig of carbon dioxide, 10 psig of TFE and 90 psig of VDF. Typical reactions to study the effect of carbon dioxide were carried at 150 psig total pressure inside the reactor. The reactor is heated to 83 °C and the agitation is set at 250 rpm. The reaction is started by adding 5 mL of an initiator solution of 5 g of potassium persulfate dissolved in 100 mL of deionized water. The alternating feeds are kept in the molar ratio as previously targeted in the final product. Typically the reaction is carried by feeding two monomers until reaching 10 – 15% solids are reached. The product of the reaction is worked up the same way as explained by the procedure above.

4.8.7. DSC characterization

The equipment used is a TA Instruments Discovery that is purged constantly with high purity nitrogen gas at a rate of 20 mL/min. A sample of 2-5 mg of polymer is placed in a previously tared aluminum pan and sealed under pressure using a pan press. The sample is equilibrated at a temperature of -50 °C and then heated at a rate of 10 °C/min to 300 °C and cooled back down to -50 °C to complete the cycle. A total of 2 or 3 cycles are recorded per sample.

4.8.8. TGA characterization

The equipment used is a TA Instruments model Q500 that is purged constantly with high purity nitrogen gas at a rate of 40 mL/min. A sample of 5-10 mg of polymer is placed in a previously tared platinum pan. The sample is equilibrated at 100 °C for 10 minutes before is heated at a rate of 10 °C/min to reach a final temperature of 800 °C. The reported data is the temperature at 10% mass loss.

4.8.9. XRD characterization

Powder XRD was performed in a Bragg-Brentano geometry using a Rigaku Ultima IV diffractometer with Cu K α radiation ($\lambda = 1.5406$ Angstroms). Data were collected from 5 to 50 degrees in 2-theta at a rate of 2 degrees per minute and a sampling width of 0.02 degrees. The samples used were finely powdered and dried in vacuum at 50 mtorr for 24 hours prior to the analyses.

4.8.10. NMR characterization

The sample (that has been previously ground to a fine powder) is placed in a clean NMR tube with 1.0 mL of DMSO- d_6 to which has been previously added 1% by volume of CFCl_3 as internal standard. The tube is placed in a bath at 80 °C for one hour and then sonicated until the sample has dissolved. The samples were recorded at room temperature using a 30° pulse and a relaxation time of three seconds with a total collection of 300 transients for each ^{19}F NMR spectroscopic analysis.

4.9. Sample Calculations

4.9.1. Calculation for NMR polymer composition for poly(VDF-*co*-TFE).

When using the key detailed in Table 4.7 to determine the identity of each integration constant (“a” through “f”), it is possible to use equation 4.12. As an example the integrations constants of a sample of poly(VDF-*co*-TFE) detailed in Figure 4.12 will be used. Such values are a = 2123, b = 978, c = 263, d = 117, e = 133, and f = 102.

$$\text{VDF (mol\%)} = 200 * \frac{(2a + b + d + e + f)}{(4a + 3b + 2c + d + e + f)}$$

$$\text{VDF(mol\%)} = 200 * \frac{(2 * 2123 + 978 + 117 + 133 + 102)}{(4 * 2123 + 3 * 978 + 2 * 263 + 117 + 133 + 102)}$$

$$\text{VDF(mol\%)} = 91$$

$$\text{TFE(mol\%)} = 9$$

4.9.2. Calculation of parameter X, Y, G and H for the determination of reactivity ratios.

For the calculation of X, Y, G, and H, it is necessary to know the final and initial compositions of the polymers being analyzed. For such calculations, the data included in Table 4.11 will be used. The parameters are defined as $X = \frac{f_1}{f_2}$, $Y = \frac{F_1}{F_2}$ where f is the molar composition of the monomer feed and F is the final molar composition of the copolymer. The parameter G is defined as $G = \frac{X(Y-1)}{Y}$ and the parameter H is defined as $H = \frac{X^2}{Y}$.

Table 4.11. Reaction data: target compositions and final compositions of poly(VDF-co-TFE) in presence of CO₂.

Sample	Targeted Composition (mol fraction)		Composition Determined Experimentally (mol fraction)	
	VDF	TFE	VDF	TFE
E	0.92	0.08	0.92	0.08
F	0.83	0.17	0.81	0.19
G	0.71	0.29	0.67	0.33
H	0.60	0.40	0.64	0.36

$$X = \frac{f_1}{f_2} = \frac{0.17}{0.83} = 4.88$$

$$Y = \frac{F_1}{F_2} = \frac{0.81}{0.19} = 4.26$$

$$G = \frac{X(Y-1)}{Y} = \frac{4.88 * (4.26 - 1)}{4.26} = 3.74$$

$$H = \frac{X^2}{Y} = \frac{4.88^2}{4.26} = 5.59$$

4.9.3. Calculation of parameter α for the determination of reactivity ratios.

The parameter alpha (α) is determined from the equation $\alpha = \sqrt{H_m H_M}$. The parameter H_m and H_M are the minimum and maximum value of H obtained from the experimental final compositions of polymers prepared. From Table 4.11, once the values of H are calculated the following values are obtained: 11.50, 5.59, 2.95, and 1.27. Therefore the maximum value of H is 11.50, and the minimum value of H is 1.27.

$$\alpha = \sqrt{H_m H_M}$$

$$\alpha = \sqrt{1.27 * 11.50}$$

$$\alpha = 3.82$$

4.9.4. Calculation of parameter η and ξ for the determination of reactivity ratios.

The parameters η and ξ are calculated from the formulas $\eta = \frac{G}{(\alpha+H)}$ and $\xi = \frac{H}{(\alpha+H)}$, respectively. The value of α , G , and H have been previously calculated, and their values are 3.82, 3.74, and 5.59 respectively (for a sample of initial composition of 0.83 and 0.17 molar fraction of VDF and TFE, respectively, and final composition of 0.81 and 0.19 molar fraction of VDF and TFE respectively).

$$\eta = \frac{G}{(\alpha + H)} = \frac{3.74}{3.82 + 5.59} = 0.40$$

$$\xi = \frac{H}{(\alpha + H)} = \frac{5.59}{3.82 + 5.59} = 0.59$$

4.9.5. Calculation of average of reactivity ratios.

Based on the results from Table 4.10, the average of reactivity ratios are given, and the simple calculation detailed below is applied when calculating an average.

$$r_{VDF} = \frac{(r_1 + r_2)}{2}$$

$$r_{VDF} = \frac{(3.37 + 0.97)}{2}$$

$$r_{VDF} = 2.17$$

4.10. References

1. Mandelkern, L.; Martin, G. M.; Quinn, F. A. Glassy State Transitions of Poly-(Chlorotrifluoroethylene), Poly-(Vinylidene Fluoride), and Their Copolymers. *J. Res. Natl. Bur. Stand.* **1957**, *58*, 137-143.
2. Kalfoglo, J.; Williams, H. L. Mechanical Relaxations of Poly(Vinylidene Fluoride) and some of its Copolymers. *J. Appl. Polym. Sci.* **1973**, *17*, 3367-3373.
3. Wang, Z. M.; Zhang, Z. C.; Chung, T. C. High Dielectric VDF/TrFE/CTFE Terpolymers Prepared by Hydrogenation of VDF/CTFE Copolymers: Synthesis and Characterization. *Macromolecules* **2006**, *39*, 4268-4271.
4. Dixon, S.; Rexford, D. R.; Rugg, J. S. Vinylidene Fluoride-Hexafluoropropylene Copolymer. *Ind. Eng. Chem.* **1957**, *49*, 1687-1690.
5. Lo, E. S. Fluorine-Containing Polymers and Preparation Thereof. U.S. Patent 3,178,399, Aug 10, 1961.
6. Ahmed, T. S.; DeSimone, J. M.; Roberts, G. W. Copolymerization of Vinylidene Fluoride with Hexafluoropropylene in Supercritical Carbon Dioxide. *Macromolecules* **2006**, *39*, 15-18.
7. Yagi, T.; Tatemoto, M. A Fluorine-19 NMR Study of the Microstructure of Vinylidene Fluoride-Trifluoroethylene Copolymers. *Polym. J.* **1979**, *11*, 429-436.

8. Aimi, K.; Ando, S.; Avalle, P.; Harris, R. K. Solid-State ^{19}F MAS and ^1H - ^{19}F CP/MAS NMR Study of the Phase Transition Behavior of Vinylidene Fluoride–Trifluoroethylene Copolymers: 1. Uniaxially Drawn Films of VDF 75% Copolymer. *Polymer* **2004**, *45*, 2281-2290.
9. Yagi, T.; Tatemoto, M.; Sako, J. I. Transition Behavior and Dielectric Properties in Trifluoroethylene and Vinylidene Fluoride Copolymers. *Polym. J.* **1980**, *12*, 209-223.
10. Bolstad, A. N. Polymerization Process for Unsaturated Fluoroolefins. U.S. Patent 3,163,628, Dec 29, 1964.
11. Sianesi, D.; C., B. G.; Regio, A. Copolymers of Vinylidene Fluoride with 1,2,3,3,3-Pentafluoropropylene. U.S. Patent 3,331,823, Apr 01, 1963.
12. Kostov, G.; Ameduri, B.; Brandstadter, S.; Edwards, E. B. Telomer Compositions and Production Processes. U.S. Patent Application 2008/0076892 A1, May 7, 2008.
13. Apotheker, D.; Finlay, J. B.; Krusic, P. J.; Logothesis, A. L. Curing Fluoroelastomers by Peroxides. *Rubber Chem. Technol.* **1982**, *55*, 1004-1018.
14. Kaneko, T.; Sugitani, K.; Saito, M.; Hirai, H. Jp. Patent 0632 9861, 1994.
15. Sauguet, L.; Ameduri, B.; Boutevin, B. Radical Copolymerization of Vinylidene Fluoride with 8-Bromo-1H,1H,2H-perfluorooct-1-ene: Microstructure,

- Crosslinking and Thermal Properties. *Macromol. Chem. Phys.* **2007**, 208, 1061-1072.
16. Akimoto, H.; Saito, S.; Tatsu, H. Jp. Patent Application 07,732, 2000.
 17. Moggi, G.; Bonardelli, P.; Bart, J. C. Copolymers of 1,1-Difluoroethene with Tetrafluoroethene, Chlorotrifluoroethene, and Bromotrifluoroethene. *J. Polym. Sci., Polym. Phys. Edit.* **1984**, 22, 357-365.
 18. Guiot, J.; Neouze, M. A.; Sauguet, L.; Ameduri, B.; Boutevin, B. Synthesis and copolymerization of fluorinated monomers bearing a reactive lateral group. XX. Copolymerization of vinylidene fluoride with 4-bromo-1,1,2-trifluorobut-1-ene. *J. Polym. Sci., Part A: Polym. Chem.* **2005**, 43, 917-935.
 19. Arcella, V.; Albano, M.; Barchiesi, E.; Brinati, G.; Chiodini, G. Development of New Nucleophile Resistant Vinylidene Fluoride Fluorocarbon Elastomers *Rubber World* **1993**, 207, 18-22.
 20. Calfee, J. D.; Florio, P. A. Photochemical Manufacture of 1,1,1-Difluorochloroethane. U.S. Patent 2,499,129, Mar 17, 1948.
 21. Barnhart, W. S.; Mantell, R. M. Selective Dehydrohalogenation of Fluorohaloalkanes Using a Copper Catalyst. U.S. Patent 2,774,799, April 1, 1954.
 22. Meussdoerffer, J. N.; Niederpruem, H. German Patent 2,044,370, 1972.

23. Ameduri, B. From Vinylidene Fluoride (VDF) to the Applications of VDF-Containing Polymers and Copolymers: Recent Developments and Future Trends. *Chem. Rev.* **2009**, *109*, 6632-6686.
24. Hauptschein, A.; Feinberg, A. H. Method for Producing Vinylidene Fluoride. U.S. Patent 3,188,356, Jun 8, 1965.
25. Kawai, H. The Piezoelectricity of Poly (Vinylidene Fluoride). *Jpn. J. Appl. Phys.* **1975**, *8*, 975-976.
26. Bergman, J. G.; McFee, J. H.; Crane, G. R. Pyroelectricity and Optical Second Harmonic Generation in Polyvinylidene Fluoride Films. *Appl. Phys. Lett.* **1971**, *8*, 203-205.
27. Nakamura, K.; Wada, Y. Piezoelectricity, Pyroelectricity, and the Electrostriction Constant of Poly(Vinylidene Fluoride). *J. Polym. Sci. Part A-2: Polym. Phys.* **1971**, *9*, 161-173.
28. Lovinger, A. J. Ferroelectric Transition in a Copolymer of Vinylidene Fluoride and Tetrafluoroethylene. *Macromolecules* **1983**, *16*, 1529-1534.
29. Betz, R. The Advantages of Bioriented Piezo-Electric Film. *Ferroelectrics* **1987**, *75*, 397-404.

30. Perri, C.; Dratz, E. A.; Ke, Y.; Schmidt, V. H.; Kometani, J. M.; Cais, R. E. Ferroelectric Transition in 70/30 VF₂/TrFE Copolymer Studied by Deuteron NMR. *Ferroelectrics* **1989**, *92*, 55-63.
31. Dillon, D. R.; Tenneti, K. K.; Li, C. Y.; Ko, F. K.; Sics, I.; Hsiao, B. S. On the Structure and Morphology of Polyvinylidene Fluoride–Nanoclay Nanocomposites. *Polymer* **2006**, *47*, 1678-1688.
32. Hasegawa, R.; Takahashi, Y.; Chatani, Y. Crystal Structures of Three Crystalline Forms of Poly(vinylidene fluoride). *Polymer J.* **1972**, *3*, 600-610.
33. Sanchez, J. Y. A., F.; Saunier, J. "PVDF Based Polymers for Lithium Batteries". In *Fluorinated Materials for Energy Conversion*; Nakajima, T., Groult, H.: Amsterdam, 2005, pp 305-333.
34. Saunier, J. A., F.; Sanchez, J. Y.; Maniguet, L. Plasticized Microporous Poly(vinylidene fluoride) Separators for Lithium-Ion Batteries. III. Gel Properties and Irreversible Modifications of Poly(vinylidene fluoride) Membranes under Swelling in Liquid Electrolytes. *J. Polym. Sci., Part B: Polym. Phys.* **2004**, *42*, 2308.
35. D'Orazio, L.; Gentile, G.; Mancarella, C.; Martuscelli, E.; Massa, V. Water-Dispersed Polymers for the Conservation and Restoration of Cultural Heritage: A Molecular, Thermal, Structural and Mechanical Characterisation. *Polym. Test.* **2001**, *20*, 227-240.

36. Cais, R. E.; Kometani, J. M. Structural Studies of Vinylidene Fluoride-Tetrafluoroethylene Copolymers by Nuclear Magnetic Resonance Spectroscopy. *Anal. Chim. Acta* **1968**, *189*, 101-116.
37. Loginova, N. N.; Podlesskaya, N. K.; Berezina, G. G. Some Aspects of the Formation and Transformation of Macromolecules During Copolymerization of Fluorine-Containing Monomers. *Plast. Massy* **1990**, 19-25.
38. Yuan, C.-G.; Hu, C.-P.; Xu, X.; Zhang, Q.-L.; Hu, Q. H. Emulsion Copolymerization Kinetics of Gaseous Monomers Containing Fluorine. *Huadong Ligong Daxue Xuebao* **2001**, *27*, 265-268.
39. Naberezhnykh, R. A.; Sorokin, A. D.; Volkova, E. V.; Fokin, A. V. Radiation Copolymerization of Fluoroolefins. *Izv. Akad. Nauk SSSR, Ser. Khim.* **1974**, *23*, 232-233.
40. Golub, M. A.; Wydeven, T. Relative Rates for Plasma Homo- and Copolymerizations of a Homologous Series of Fluorinated Ethylenes. *Plasma Polym.* **1998**, *3*, 35-42.
41. Carr, J. M.; Mackey, M.; Flandin, L.; Schuele, D.; Zhu, L.; Baer, E. Effect of Biaxial Orientation on Dielectric and Breakdown Properties of Poly(ethylene terephthalate)/Poly(vinylidene fluoride-co-tetrafluoroethylene) Multilayer Films. *J. Polym. Sci. Part B: Polym. Phys.* **2013**, *51*, 882-896.

42. Chu, B.; Zhou, X.; Ren, K.; Neese, B.; Lin, M.; Wang, Q.; Bauer, F.; Zhang, Q. M. A Dielectric Polymer with High Electric Energy Density and Fast Discharge Speed. *Science* **2006**, *313*, 334-336.
43. Zhou, X.; Chu, B.; Neese, B.; Lin, M.; Zhang, Q. M. Electrical Energy Density and Discharge Characteristics of a Poly(vinylidene fluoride-chlorotrifluoroethylene) Copolymer. *IEEE Trans. Dielect. Electr. Insul.* **2007**, *14*, 1133-1138.
44. Zhang, Z.; Chung, T. C. M. The Structure-Property Relationship of Poly(vinylidene difluoride)-Based Polymers with Energy Storage and Loss under Applied Electric Fields. *Macromolecules* **2007**, *40*, 9391-9397.
45. Li, J.; Hu, X.; Gao, G.; Ding, S.; Li, H.; Yang, L.; Zhang, Z. Tuning Phase Transition and Ferroelectric Properties of Poly(vinylidene fluoride-co-trifluoroethylene) via Grafting with Desired Poly(methacrylic ester)s as Side Chains. *J. Mater. Chem. C* **2013**, *1*, 1111-1121.
46. Vogelsang, R.; Farr, T.; Frohlich, K. The Effect of Barriers on Electrical Tree Propagation in Composite Insulation Materials. *IEEE Trans. Dielect. Electr. Insul.* **2006**, *13*, 373-382.
47. Murata, Y.; Koizumi, N. Ferroelectric Behavior in Vinylidene Fluoride-Tetrafluoroethylene Copolymers. *Ferroelectrics* **1989**, *92*, 47-54.
48. Liu, Q.; Khatri, I.; Ishikawa, R.; Fujimori, A.; Manabe, K.; Nishiro, H.; Shirai, H. Improved Photovoltaic Performance of Crystalline-Si/Organic Schottky Junction

- Solar Cells Using Ferroelectric Polymers. *Appl. Phys. Lett.* **2013**, *103*, 163503-163507.
49. Ohigashi, H. Piezoelectric Polymers – Materials and Manufacture. *Jap. J. Appl. Phys.* **1985**, *24*, 23-27.
 50. Kim, J. H.; Park, T. K.; Lee, H.; Lee, D. J. Pyroelectricity in Poly(Vinylidene Fluoride) and Poly(Vinylidene Fluoride-co-Tetrafluoroethylene) Synthesized with Various Initiators. *Korea Polym. J.* **1995**, *3*, 101-105.
 51. Kochervinskii, V. V.; Kiselev, D. A.; Malinkovich, M. D.; Pavlov, A. S.; Malyshkina, I. A. Local Piezoelectric Response, Structural and Dynamic Properties of Ferroelectric Copolymers of Vinylidene Fluoride–tetrafluoroethylene. *Colloid Polym. Sci.* **2015**, *293*, 533-543.
 52. Guo, Y.; Hoshino, K.; Hanna, J.; Kokado, H. Charging Characteristics of a Copolymer of Vinylidene Fluoride and Tetrafluoroethylene. *Jpn. J. Appl. Phys.* **1992**, *31*, 1830-1835.
 53. Mayo, F. R.; Walling, C. Copolymerization. *Chem. Rev.* **1950**, *46*, 191-287.
 54. Hercules, D. A.; Desmarreau, D. D.; Fernandez, R. E.; Clark, J. L.; Thrasher, J. S. "Evolution of Academic Barricades for the Use of Tetrafluoroethylene (TFE) in the Preparation of Fluoropolymers". In *Handbook of Fluoropolymer Science and Technology*; 1st ed.; Iacono, S. T., Iyer, S. S., Smith, D. W., Eds.; John Wiley & Sons: Hoboken, NJ, USA, 2014, pp 415-433.

55. Odian, G. *Principles of Polymerization*; 4th ed. John Wiley & Sons: Hoboken, New Jersey, 2004.
56. Fineman, M.; Ross, S. D. Linear Method for Determining Monomer Reactivity Ratios in Copolymerization. *J. Polym. Sci.* **1950**, 2, 259-265.
57. Mayo, F. R.; Lewis, F. M. Copolymerization, I. A Basis for Comparing the Behavior of Monomers in Copolymerization; The Copolymerization of Styrene and Methyl Methacrylate. *J. Am. Chem. Soc.* **1944**, 66, 1594-1601.
58. Young, L. J. Copolymerization Parameters. *Journal of Polymer Science* **1961**, 54, 411-455.
59. Kelen, T.; Tüdös, F. Analysis of the Linear Methods for Determining Copolymerization Reactivity Ratios. A New Improved Linear Graphic Method. *J. Macromol. Sci. Chem.* **1975**, 9, 1-27.
60. Kelen, T.; Tüdös, F.; Turcsanyi, B. Confidence Intervals for Copolymerization Reactivity Ratios Determined by the Kelen-Tüdös Method. *Polym. Bull.* **1980**, 2, 71-76.
61. Tüdös, F.; Kelen, T.; Foldes-Bereznich, T.; Turcsanyi, B. Analysis of Linear Methods for Determining Copolymerization Reactivity Ratios. III. Linear Graphic Method for Evaluating Data Obtained at High Conversion Levels. *J. Macromol. Sci. Chem.* **1976**, 10, 1513-1540.

62. Hu, T. Characterization of the Crystallinity of Polytetrafluoroethylene by X-ray and IR Spectroscopy, Differential Scanning Calorimetry, Viscoelastic Spectroscopy and the Use of a Density Gradient Tube. *Wear* **1982**, 82, 369-376.
63. Murasheva, Y. M.; Shashkov, A. S.; Dontsov, A. A. Analysis of the ^{19}F NMR Spectra of Copolymers of Vinylidene Fluoride with Tetrafluoroethylene, and of Vinylidene Fluoride with Tetrafluoroethylene and Hexafluoropropylene. The Use of an Empirical Additive Scheme and of the Principle of Alternation. *Polym. Sci. U.S.S.R.* **1981**, 23, 711-720.
64. Twum, E. B.; McCord, E. F.; Lyons, D. F.; Rinaldi, P. L. Multidimensional ^{19}F NMR Analyses of Terpolymers from Vinylidene Fluoride (VDF)–Hexafluoropropylene (HFP)–Tetrafluoroethylene (TFE). *Macromolecules* **2015**, 48, 3563-3576.
65. Li, L.; Twum, E. B.; Li, X.; McCord, E. F.; Fox, P. A.; Lyons, D. F.; Rinaldi, P. L. 2D-NMR Characterization of Sequence Distributions in the Backbone of Poly(vinylidene fluoride- co -tetrafluoroethylene). *Macromolecules* **2012**, 45, 9682-9696.
66. Ying, X.; Miaoying, A.; Shanrong, J. Synthesis of Poly(Vinylidene Fluoride) with Low Contents of Head-to-Head Chain. *Polym. Commun.* **1983**, 2, 161-167.

67. Lutringer, G.; Meurer, B.; Weill, G. Microstructure of Vinylidene Fluoride and Tetrafluoroethylene Copolymers by High-Resolution ^{19}F Nuclear Magnetic Resonance. *Polymer* **1992**, *33*, 4920-4928.
68. Pianca, M.; Bonardelli, P.; Tatò, M.; Cirillo, G.; Moggi, G. Composition and Sequence Distribution of Vinylidene Fluoride Copolymer and Terpolymer Fluoroelastomers. Determination by ^{19}F Nuclear Magnetic Resonance Spectroscopy and Correlation with some Properties. *Polymer* **1987**, *28*, 224-230.
69. Russo, S.; Behari, K.; Chenji, S.; Pianca, M.; Barchiesi, E.; Moggi, G. Synthesis and Microstructural Characterization of Low-Molar-Mass Poly(Vinylidene Fluoride). *Polymer* **1993**, *34*, 4777-4781.
70. Wilson, C. W.; Santee, E. R. Polymer Analysis by High-Resolution NMR, with Applications to Poly(Vinylidene Fluoride) and Poly(Vinyl Fluoride). *J. Polym. Sci. Part C: Polym. Symp.* **1965**, *8*, 97-112.
71. Wormad, P.; Ameduri, B.; Harris, R. K.; Hazendonk, P. Fluorine-19 Solid State NMR Study of Vinylidene fluoride Polymers using Selective Relaxation Filters. *Solid State Nucl. Magn. Reson.* **2006**, *30*, 114-123.
72. Van Bramer, D. J.; Shiflett, M. B.; Yokozeki, A. Safe Handling of Tetrafluoroethylene. U.S. Patent 5,345,013, Sep 6, 1994.

73. Haszeldine, R. N.; Leedham, K. The Reactions of Fluorocarbon Radicals. Part IX. Synthesis and Reactions of Pentafluoropropionic Acid. *J. Chem. Soc.* **1953**, 1548-1552.
74. Babenko, Y. I.; Lisochkin, Y. A.; Poznyak, V. I. Explosion of Tetrafluoroethylene During Nonisothermal Polymerization. *Combust. Explos. Shock Waves* **1993**, 29, 603-609.
75. Reza, A.; Christiansen, E. A Case Study of a TFE Explosion in a PTFE Manufacturing Facility. *Process Saf. Prog.* **2007**, 26, 77-82.
76. Ferrero, F.; Meyer, R.; Kluge, M.; Schroder, V.; Spoormaker, T. Self-Ignition of Tetrafluoroethylene Induced by Rapid Valve Opening in Small Diameter Pipes. *Loss Prevent Proc.* **2013**, 26, 177-185.
77. Thomas, B. H.; DesMarteau, D. D. Self-Emulsifying Polymerization (SEP) of 3,6-Dioxa- Δ^7 -4-Trifluoromethyl Perfluorooctyl Trifluoromethyl Sulfonimide With Tetrafluoroethylene. *J. Fluorine Chem.* **2005**, 126, 1057-1064.
78. Thomas, B. H.; Shafer, G.; Ma, J. J.; Tu, M. H.; DesMarteau, D. D. Synthesis of 3,6-Dioxa- Δ^7 -4-Trifluoromethyl Perfluorooctyl Trifluoromethyl Sulfonimide: Bis[(Perfluoroalkyl)Sulfonyl] Superacid Monomer and Polymer. *J. Fluorine Chem.* **2004**, 125, 1231-1240.
79. Molero Meneses, M.; Moreno Beltran, D.; Grau Rios, M. *Libro Actas - Congr. Nac. Med., Hig. Segur. Trab.* **1981**, 9th Conference, 2461-2479.

80. Hals, L. J.; Reid, T. S.; Smith, G. H. The Preparation of Terminally Unsaturated Perfluoro Olefins by the Decomposition of the Salts of Perfluoro Acids. *J. Am. Chem. Soc.* **1951**, 73, 4054.
81. Sayler, T. S. Preparation of Perfluorinated Ionomers for Fuel Cell Applications. Ph.D. Dissertation, The University of Alabama, Tuscaloosa, AL, 2012.
82. Sayler, T. S.; Tice, K. T.; Beg, M. A.; Fernandez, R. E.; Thrasher, J. S. Preparation of Low Equivalent Weight Perfluorinated Ionomers with Water Insolubility. *Polym. Prepr. (Am. Chem. Soc., Div. Polym. Chem.)* **2012**, 53, 39-40.

Chapter 5

Experimental Determination of Relative Reactivity Ratios of TFE, PSEPVE, PSVE, DEVE, and 8-CNVE in poly(TFE-*co*-PSEPVE), poly(TFE-*co*-PSVE), poly(TFE-*co*-DEVE), and poly(TFE-*co*-8CNVE)

5.1. Introduction

The reactivity ratios of PSEPVE, PSVE, DEVE, and 8-CNVE versus TFE are not widely disclosed in the literature. The structures and formulas for the aforementioned monomers are given in Figure 5.1. Such knowledge is often a trade secret within large fluorochemical companies, as no reason exists in publishing such data primarily because either no commercial interest exists in the materials or a huge economical interest exists in the products. In the case of poly(TFE-*co*-PSEPVE), primarily known as Nafion[®], reactivity ratios of the monomers are not largely disclosed in the literature since the material represents a huge economical asset. Two references have appeared in the literature that disclose the reactivity ratios of TFE relative to PSEPVE. In one case the reactivity ratios are reported for solution polymerization in 1,1,2-trichloro-1,2,2-trifluoroethane as $r_{\text{TFE}} = 9$ and $r_{\text{PSEPVE}} = 0.04$,¹ while in the second case, the reactivity ratios in supercritical carbon dioxide (CO₂) as $r_{\text{TFE}} = 7.85$ and $r_{\text{PSEPVE}} = 0.079$.²

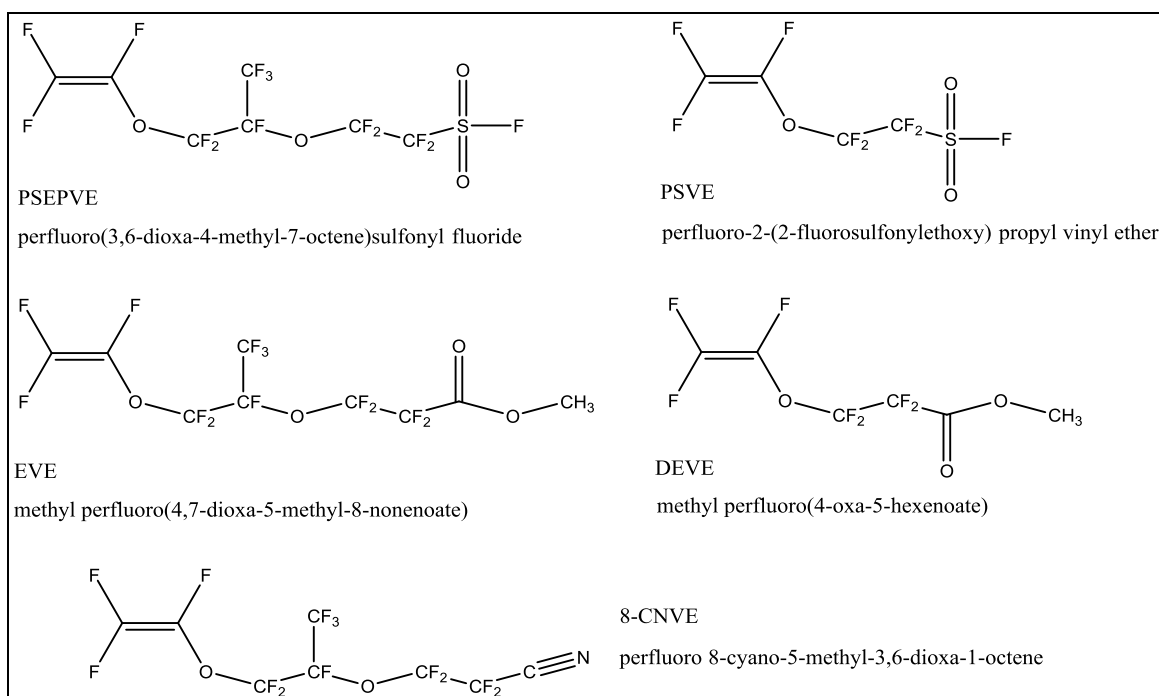


Figure 5.1. Structures and IUPAC names for TFE, PSEPVE, PSVE, DEVE and 8-CNVE.

In the case of poly(TFE-*co*-PSVE) the reactivity ratios are not found in the open literature. One can believe that fluorochemical companies that produce this copolymer keep such information a trade secret.

For poly(TFE-*co*-8CNVE) the relative reactivity ratios of the monomers are not reported in the literature probably because 8-CNVE as a monomer is more often used as a crosslinking component in other terpolymers and not largely explored as a comonomer with just TFE. Such terpolymers in which 8-CNVE is used as a crosslinking agent are known as fluoroelastomers and examples of them include the following: poly(TFE-*ter*-PMVE-*ter*-8CNVE), poly(TFE-*ter*-PEVE-*ter*-8CNVE), and poly(TFE-*ter*-PPVE-*ter*-

8CNVE), where PMVE, PEVE, and PPVE are perfluoromethyl vinyl ether ($\text{CF}_2=\text{CF}-\text{O}-\text{CF}_3$), perfluoroethyl vinyl ether ($\text{CF}_2=\text{CF}-\text{O}-\text{CF}_2\text{CF}_3$), and perfluoropropyl vinyl ether ($\text{CF}_2=\text{CF}-\text{O}-\text{CF}_2\text{CF}_2\text{CF}_3$).³ The most representative product that has been commercially developed is the Kalrez[®] product line developed by DuPont. Kalrez[®] materials are usually a terpolymer of TFE with 8-CNVE and either a perfluoroalkyl vinyl ether or a perfluoroalkoxy vinyl ether.⁴

The goal of the work developed in this Chapter is to report the reactivity ratios of TFE, PSEPVE, PSVE, DEVE, and 8-CNVE in poly(TFE-*co*-PSEPVE), poly(TFE-*co*-PSVE), poly(TFE-*co*-DEVE), and poly(TFE-*co*-8CNVE), by means of solution polymerization, more often than not both in the presence and absence of CO_2 . Using the information from the patent literature, the use of an equimolar mixture of TFE and CO_2 can be beneficial since it represents a safe way to handle TFE while minimizing its explosive character. By using a mixture of TFE and CO_2 , we can see later in this Chapter that the same trends of reactivity ratios are observed while only decreasing the yield of poly(TFE-*co*-PSEPVE) for when CO_2 was used. The other polymers: poly(TFE-*co*-PSVE), poly(TFE-*co*-DEVE), and poly(TFE-*co*-8CNVE) were not studied in the presence of CO_2 to avoid expenditure of the precious monomers.

Due to the more recent environmental discussions about the persistence of perfluorinated surfactants, such as the case of ammonium perfluorooctanoate (PFOA), it is of interest to investigate such reactivity ratios for solution polymerization systems using perfluorinated solvents such as HFC-4310 (2,3-dihydro-decafluoropentane), commercially

known as Vertrel XF[®] (manufactured by Chemours), or other solvents such as DMC (dimethylcarbonate).

5.2. Synthesis of PSEPVE and PSVE

The development of perfluorosulfonyl-terminated monomers was initiated by process in the chlor-alkali industry and more recently with fuel cell membrane technology. The copolymerization of PSEPVE with TFE gives a widely commercialized product under the tradename of Nafion[®]. Other companies such as Asahi Glass Chemical Companies and 3M have similar materials as well. In the particular case of Nafion[®], the product is sold in hydrolyzed membranes with a certain equivalent weight and thickness. Typical nomenclature of commercial membranes, such as N117, denotes that the material is Nafion[®] membrane of equivalent weight (EW: grams of polymer required to neutralize 1 mole of base) of 1100 and a thickness of 7 thousandths of an inch (mils). In the same way, a product denoted by N112 is a Nafion[®] membrane of EW of 1100 and a thickness of 2 mils.

The two major commercial applications of such materials are in fuel cell and the chlor-alkali industries. The former uses thinner membranes since the mechanical strength is not as important as the conductivity, while thicker membranes are preferred in the latter application since the mechanical strength is more valued than the conductivity. Fuel cell membranes of this class are denoted as PEMFCs (polymer electrolyte membrane fuel cells), and they often use hydrogen at the anode (composed of platinum dispersed in a

porous carbon support) to produce protons and electrons. The electrons are used by an external electric circuit, while the protons migrate selectively through the Nafion[®] membrane. At the cathode, oxygen gas flows and combines with the protons and the electrons from the incoming circuit to produce water. The importance of the discovery of Nafion[®] is evident as the material can selectively transport protons through its matrix. Usually larger assemblies use the same aforementioned concept but repeated multiple times in a stack in order to increase the potential. A diagram of a typical fuel cell can be observed in Figure 5.2.

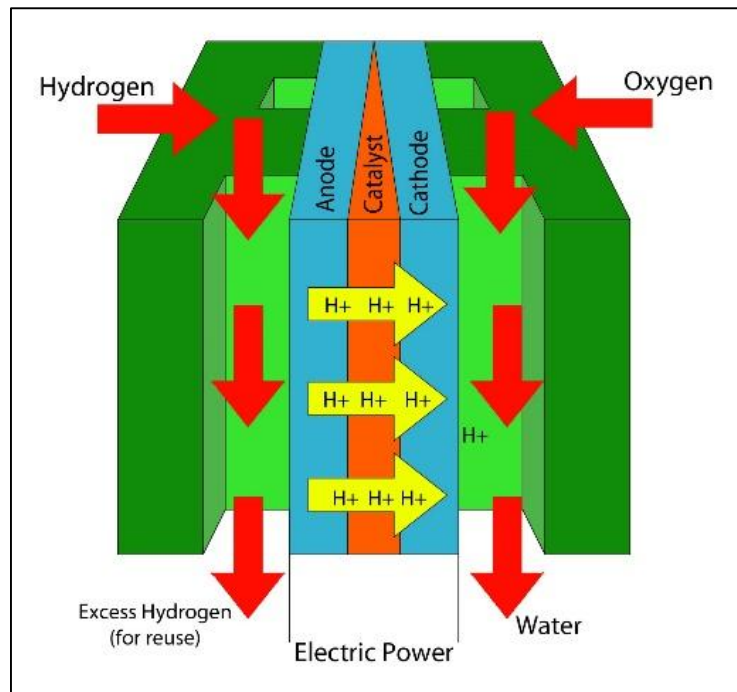


Figure 5.2. General diagram of a hydrogen fuel cell.

One of the key properties based on the equivalent weight of a Nafion[®] membrane is that the lower the equivalent weight, the more soluble the membrane becomes, and

therefore eventually rendering them unusable for fuel cell applications. On the other hand, the higher the equivalent weight, the lower the conductivity. A rationale for the latter could be that the protons have a more hindered path across the membrane in between the anode and the cathode. As an example, it is known in the literature that below the threshold equivalent weight of 700 for the TFE-based copolymer of the 3M monomer [perfluoro-4-(fluorosulfonyl) butyl vinyl ether], the material possesses less crystallinity (i.e., possesses lower mechanical strength), becomes more water soluble, and therefore is not suitable for use in a fuel cell.⁵

“The chlor-alkali process” is the common name for the industrial production of chlorine gas from brine (a concentrated solution of NaCl). The process (diagram shown in Figure 5.3) uses a membrane to separate the two compartments of the cell. Two electrodes are used in the process. The cathode is where hydrogen gas is produced, while chlorine gas is produced at the anode. Both gases are made by means of electrolysis of the solution. At the anode, the main reactant is water and the by-product is sodium hydroxide (where the sodium cation crosses from the cathode chamber to the anode chamber through the membrane). Meanwhile at the anode, the brine solution becomes less and less concentrated in sodium chloride as chlorine gas is produced. The key importance of the use of Nafion[®] as a membrane separator in this cell is that the membrane can withstand the high current needed to start the process, the corrosive character of sodium hydroxide and chlorine generated at the cathode, and also the high conductivity needed to close the circuit in between the two chambers.

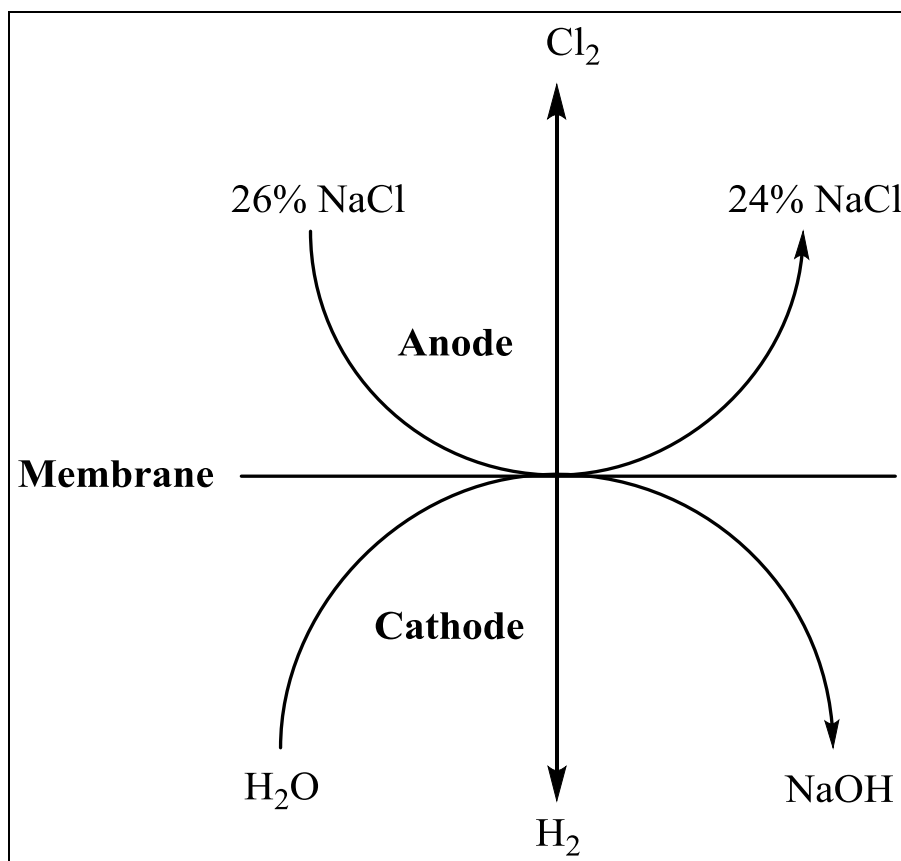


Figure 5.3. Diagram of the Chlor-Alkali process.

Several different designs of cells have been developed at the industrial level, but the point of this Chapter is not to discuss in detail their development other than the importance that this perfluorosulfonyl-terminated ionomer, and other materials developed industrially, have in the process.

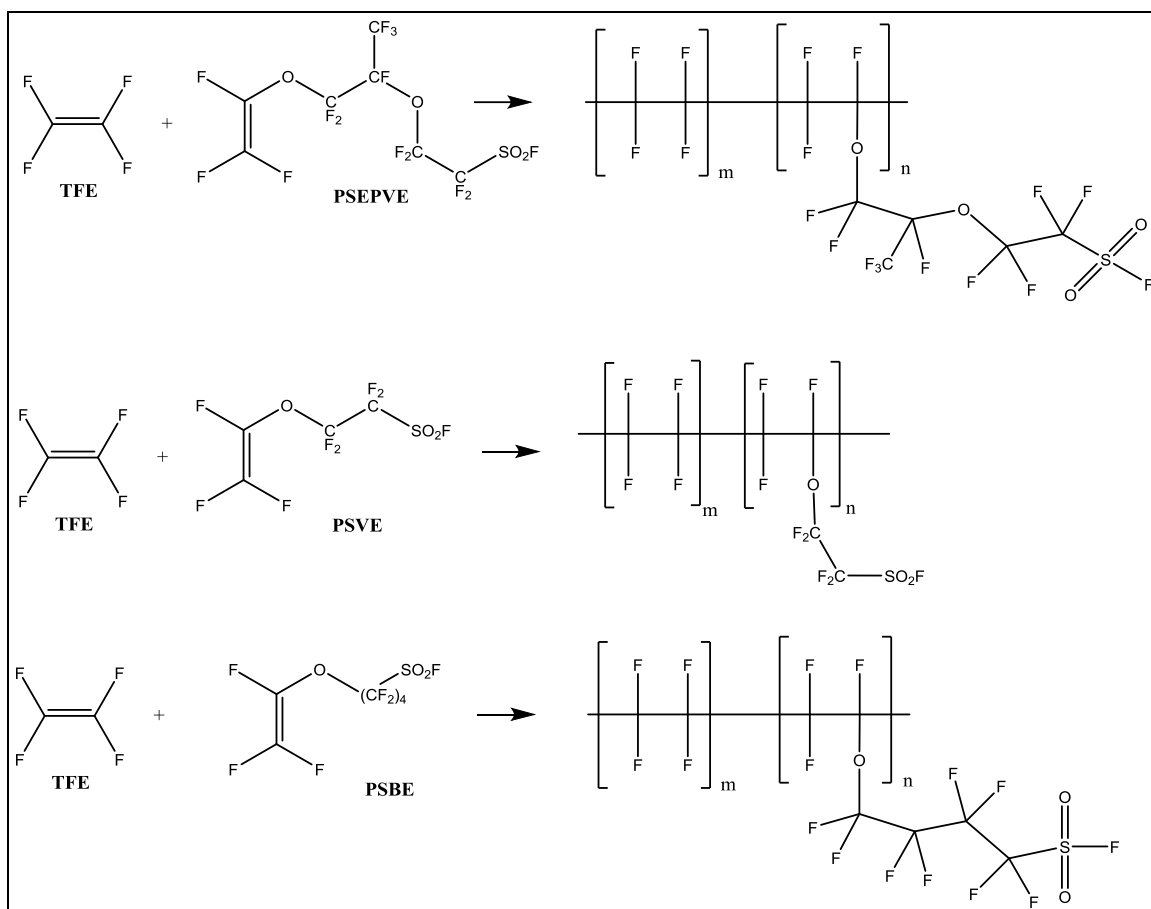


Figure 5.4. Reaction diagrams for the major types of perfluorosulfonyl-terminated ionomer materials that are commercially available.

Nafion[®] (originally developed by DuPont, currently Chemours) has not been the only material that has been developed for this type of application. Another similar material known as Aquivion[®] PFSA and Hyflon Ion[®] has been developed by Solvay Specialty Polymers with monomer structure shown in Figure 5.4. The TFE comonomer in both of the materials mentioned above was initially prepared by DOW Chemical but because of a non-compete deal with DuPont, DOW never commercialized the copolymer of their short

It can be noticed that the reaction requires two subsequent ring-opening polymerizations of hexafluoropropylene oxide (HFPO). More additions of HFPO than the two required to make the adduct of interest cannot be controlled, other than a slow addition of HFPO. The di-adduct is collected by distillation, and the mono-adduct is sent back to the process, making this industrial preparation a flow process. It is important to note that the higher order adducts have no commercial value. The final step of the reaction is the thermal rearrangement of the di-adduct to form the acid fluoride that later rearranges to the final vinyl ether by the addition of sodium carbonate. The final product is distilled as it is being formed under vacuum at 135 °C.

In a similar fashion, the synthesis of perfluoro(3-oxa-4-pentene)sulfonyl fluoride (PSVE and also more widely known as the Dow monomer, being developed by Dow Chemical Company) has been synthesized primarily by two methods. Originally, DuPont developed the synthetic route detailed in Figure 5.6, but due to problems with the cyclic intermediate a new synthetic route was developed, which includes the introduction of a chlorine atom in the acid fluoride to improve selectivity of vinyl ether formation. This improvement is shown in Figure 5.7. Because of the high costs of making the monomer using the aforementioned methods, a new improved method was developed, and it became a more efficient and cheaper way to produce the monomer in high yield as shown in Figure 5.8.⁸⁻¹⁰

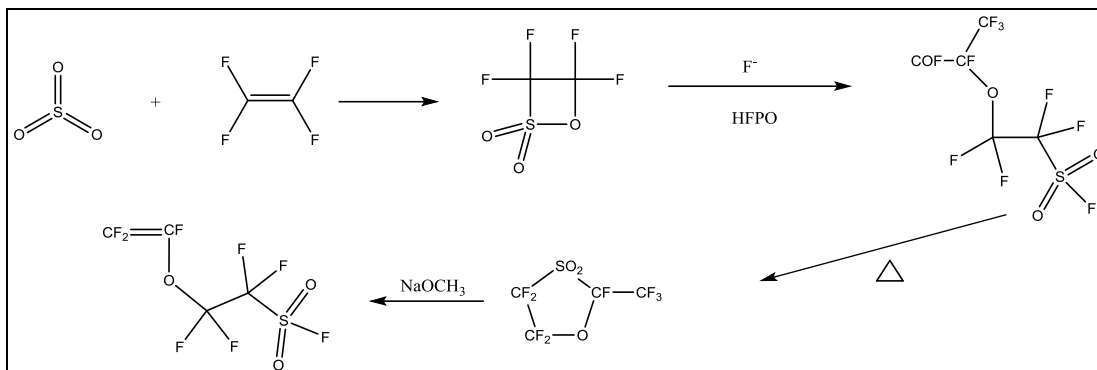


Figure 5.6. Original synthetic method for making PSVE monomer.⁹

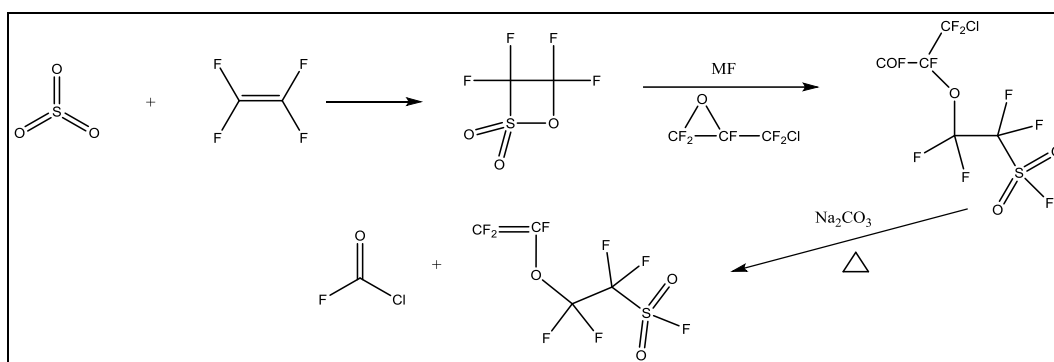


Figure 5.7. Secondary method of preparation of PSVE monomer.¹⁰

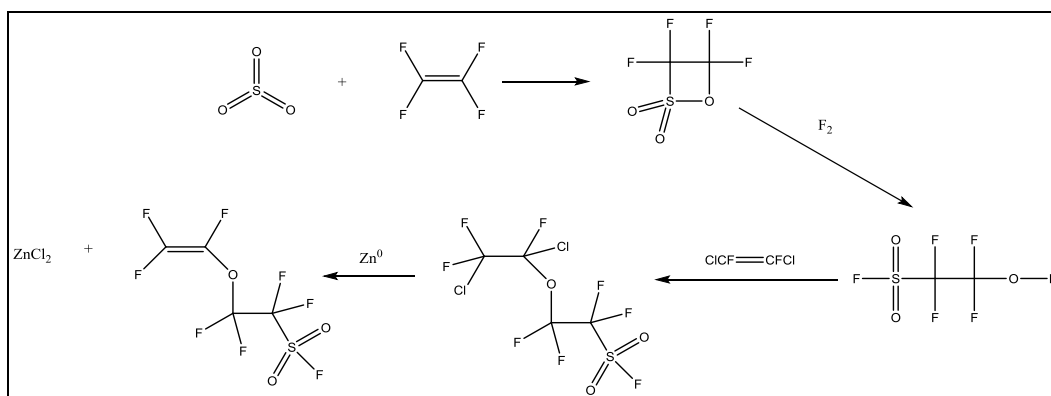


Figure 5.8. Improved reaction scheme for the production of PSVE monomer.⁸

5.3. Synthesis of EVE and DEVE

Another monomer developed for use in the chlor-alkali industry is known as EVE.¹¹⁻¹³ Its chemical name is methyl perfluoro-(5-methyl-4,7-dioxa-8-nonenoate), and its formula is $\text{CF}_2=\text{CFOCF}_2\text{CF}(\text{CF}_3)\text{OCF}_2\text{CF}_2\text{C}(\text{O})\text{OCH}_3$. The patented industrial route is detailed in Figure 5.9, and this route consists of reacting the intermediate 1 (which is prepared from the reaction of 3-methoxytetrafluoropropionic acid first with NaOH and followed by acidification with HCl), with SO_3 to produce compound 2. Compound 2 is then reacted with HFPO (hexafluoropropylene oxide) in the presence of cesium fluoride to produce an oligomer of the repeating unit $(-\text{CF}_2\text{OCF}(\text{CF}_3)-)$, which can be separated into fractions each with a different number of repeat units. The intermediate used further in this reaction is the one with two repeat units (compound 4 in Figure 5.9), which is later pyrolyzed in the presence of sodium phosphate, potassium carbonate, or sodium carbonate to give the final EVE monomer.

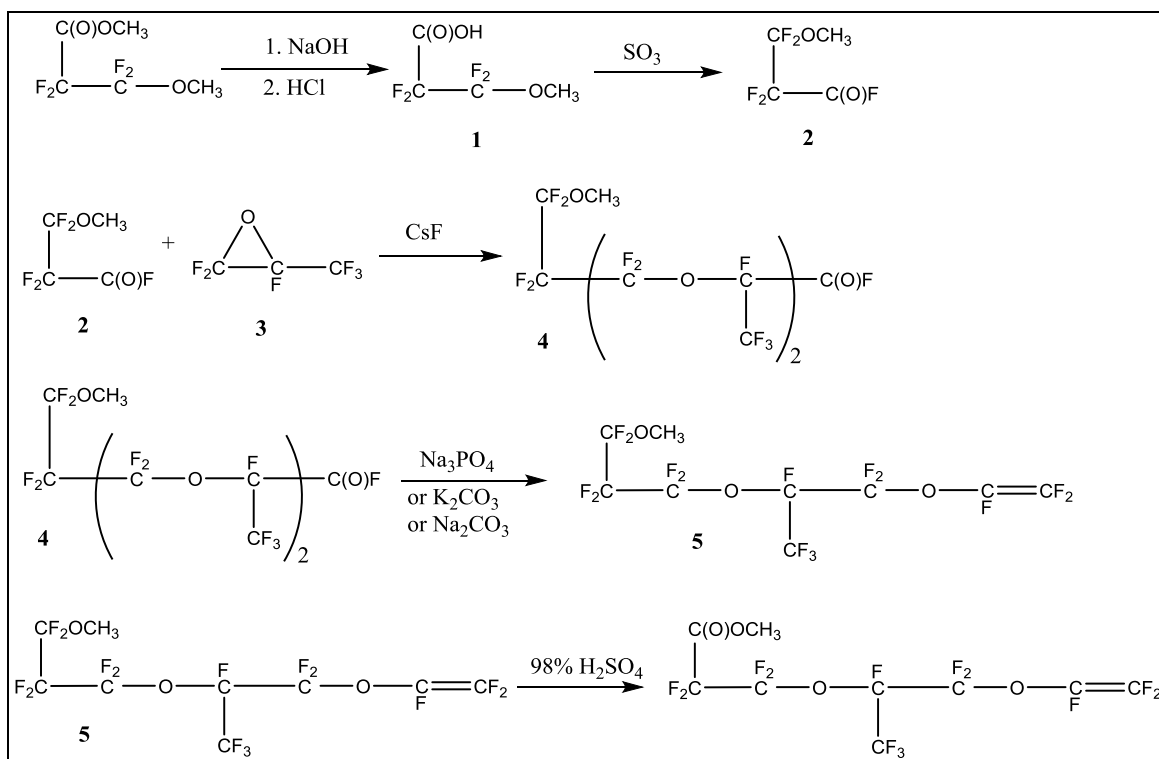


Figure 5.9. Synthetic preparation of EVE monomer.^{13,14}

The short side chain equivalent of EVE is denoted here as the molecular formula being $\text{CF}_2=\text{CFOCF}_2\text{CF}_2\text{C(O)OCH}_3$. Its synthetic preparation is similar in some sense to the preparation of EVE, but it includes some differences worth mentioning. The preparation starts with the reaction of 3-methoxytetrafluoropropionyl fluoride (obtained from the reaction of 3-methoxytetrafluoropropionyl chloride with KF in tetramethylene sulfone) KF in tetraglyme in the presence adiponitrile to produce the respective alkoxide that then ring-opens the epoxide group of an HFPO unit. Although the patent does not explain the role of the tetraglyme and/or the adiponitrile, it is believed that they are used to complex the potassium cation from KF in order the fluoride ion to become more

nucleophilic. The products obtained from this reaction are primarily the addition of two HFPO units or the addition of one HFPO unit. The yields and synthetic sequence are detailed in Figure 5.10. In the case of DEVE, the adduct with the addition of one HFPO unit is flowed slowly through a bed of sodium phosphate at 225 °C to obtain the final monomer. This industrial preparation has been disclosed in the patent literature.¹⁵

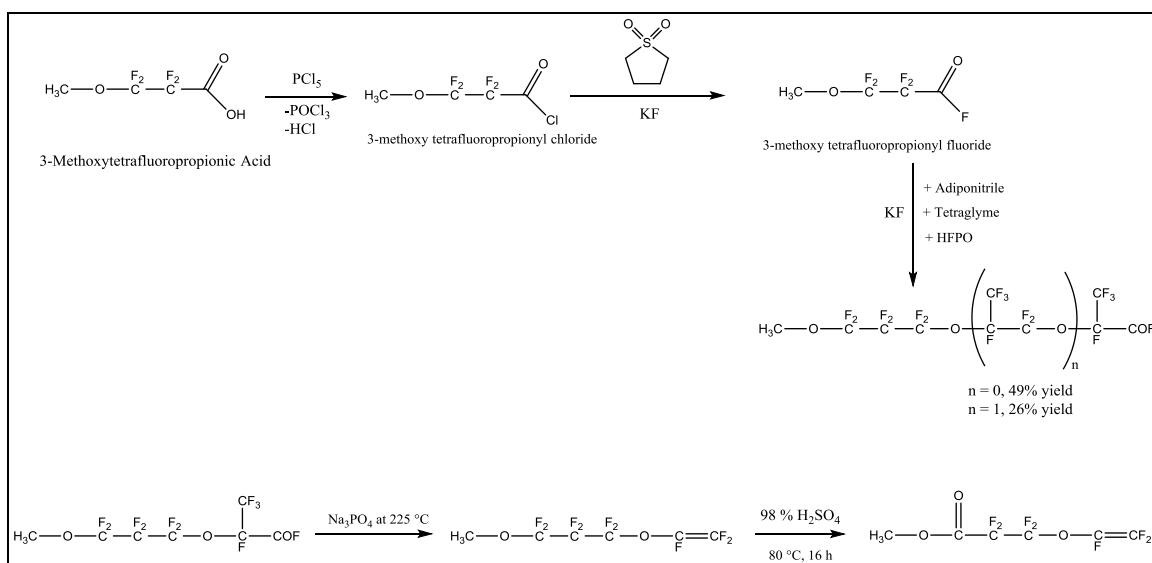


Figure 5.10. Synthetic preparation of DEVE monomer.¹⁵

Uses of poly(TFE-*co*-EVE) are listed in the patent literature as producing alkali metal hydroxides,¹³ electrical insulation, and perm ionic membrane in the chlor-alkali industry,¹⁵ and bubble release agents for ion membrane materials.¹⁶ On the other hand, copolymers of poly(TFE-*co*-DEVE) have not been explored extensively as the long side chain counterpart copolymer poly(TFE-*co*-EVE), and one insight into this might be that

the short side chain materials could still be under development. These materials poly(TFE-*co*-EVE) and poly(TFE-*co*-DEVE) could be used in the same applications as to where poly(TFE-*co*-PSEPVE) and poly(TFE-*co*-PSVE) are used, but being much cheaper to develop makes them interesting for industry to explore. Another factor that might play an important role into their range of applications is the fact that these materials (the DEVE and EVE copolymers of TFE) are not superacids, and therefore their conductivities and proton selectivities are not as high as those of copolymers of PSEPVE and PSVE with TFE.

5.4. Preparation of 8-CNVE

The synthesis of 8-CNVE [perfluoro-(8-cyano-5-methyl-3,6-dioxo-1-octene) or $\text{CF}_2=\text{CFOCF}_2\text{CF}(\text{CF}_3)\text{OCF}_2\text{CF}_2\text{CN}$], as reported in the patent literature,¹⁷ begins with the reaction of EVE [methyl perfluoro-(5-methyl-4,7-dioxo-8-nonenoate) or $\text{CF}_2=\text{CFOCF}_2\text{CF}(\text{CF}_3)\text{OCF}_2\text{CF}_2\text{C}(\text{O})\text{OCH}_3$] with ammonia (as shown in Figure 5.11). After EVE is reacted with ammonia, the excess ammonia is evacuated along with the methanol produced. DMF and pyridine are then added to the reaction followed by the slow addition of trifluoroacetic anhydride as the dehydrating agent while maintaining the temperature in the range of -15 °C to -5 °C. After the reaction, cold water is added, DMF is separated as the top layer, and the bottom layer is evaporated (as it contains the compound of interest). The final product is distilled obtaining it in 98.5% purity and 75 mol% yield based in EVE.

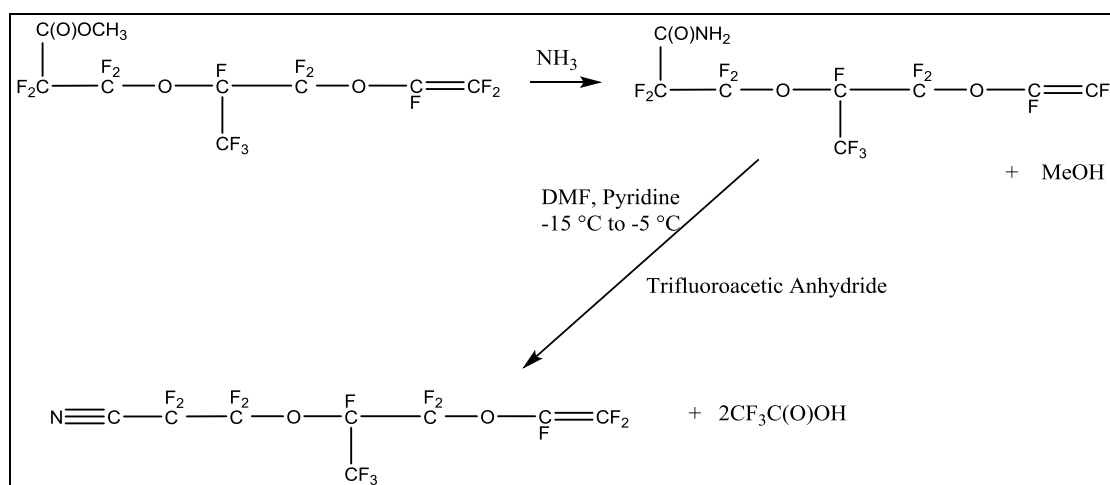


Figure 5.11. Synthetic preparation of 8-CNVE monomer.¹⁷

5.5. Results and Discussion

The polymer samples of poly(TFE-*co*-PSEPVE), poly(TFE-*co*-PSVE), poly(TFE-*co*-DEVE), and poly(TFE-*co*-8CNVE), were prepared at the pilot-scale tetrafluoroethylene polymerization facility at Clemson University. This facility has been previously covered in Chapter 2 of this dissertation and in the open literature.¹⁸ The polymerization technique elected was solution polymerization in HFC-4310 by means of using bis-perfluoropropionyl peroxide (3P) as the radical initiator. The range of temperatures used for these reactions was between 25 and 35 °C at a constant agitation of 450 RPM in a 600-mL stainless steel autoclave.

The basic idea of how to determine the reactivity ratios of the monomers is to first analyze the composition of the copolymers (titration, FT-IR spectroscopy, molten state

NMR spectroscopy, and or elemental analysis). Once the compositions are determined, one can calculate the reactivity ratios of the monomers for each copolymer. Furthermore, a fast and reliable method of analysis can be established using ATR-FTIR that will enable the fast characterization of future polymer samples.

5.5.1. Determination of the composition of poly(TFE-*co*-PSEPVE) by ATR-FTIR

In order to determine the reactivity ratios of the copolymerization of PSEPVE and TFE via solution polymerization, or any other method of polymerization, it is necessary to establish an analytical method to obtain accurate composition of the two monomers in the copolymer. To our advantage, a literature reference exists that has previously established a relationship between the absorbance of the S-F stretching frequencies to the C-F symmetric and asymmetric stretching frequencies of the backbone of the polymer.¹⁹ This is done by means of ATR-FTIR spectroscopy, and to our advantage this gives a fast and easy method to determine the composition of such polymers. It is necessary to evaluate the method against samples of known composition and to draw a more specific correlation between equivalent weight and absorbance due to the great generality (the analytical method can be applied to a wide variety of monomers) of the method.

The samples of poly(TFE-*co*-PSEPVE) can be titrated and evaluated for equivalent weights separately, and the results can be used in correlation to the absorbances of the “S-F” and “C-F” FTIR signals in order to obtain another method of analysis.

Since the samples are prepared from the PSEPVE monomer in the sulfonyl fluoride form, the copolymers obtained contain the “SO₂F” group on the side chain of the polymer. One can thus obtain two different equations that correlate the equivalent weight with the observed absorbances: one equation is between the absorbance of the “S-F” frequency (characteristic of the PSEPVE monomer) and the “CF₂” frequencies, and the second equation is between the “C-O” frequency (characteristic of the ether linkage in the PSEPVE monomer) and the “CF₂” frequencies. As will be explained later, it is indifferent what frequency is used for the “CF₂” signals since both are proportional to each other, but the patent literature gives a preference of the frequency at 1146 cm⁻¹ over the one at 1203 cm⁻¹ (both assigned as the symmetric and asymmetric stretch, respectively, of the “CF₂” bonds in the backbone and polymer side chain).¹

5.5.2. Determination of the composition of poly(TFE-*co*-PSEPVE) by FTIR.

Samples of various known equivalent weights of poly(TFE-*co*-PSEPVE) in the sulfonyl fluoride form were received from DuPont. Equivalent weights of 920, 1000, and 1200 were analyzed using the aforementioned ATR-FTIR method,¹⁹ and by titration of the acid groups (once the polymer is converted to the SO₃H form). Based on the titration information, it is also possible to establish two other methods of characterization as explained above. The assignment of the IR bands has been disclosed in the literature by Ramaswamy et al.²⁰ and such assignments are listed in Table 5.1. Other studies have been

performed on Nafion[®] membranes that support these assignments not only from the experimental determination but also from computational calculations.²¹

The patented analytical method (mentioned throughout the Chapter as the “original method”), is a simple ratio of signals from the C-F bonds to the S-O bonds present in the polymer as indicated in equation 5.1.

Table 5.1. FTIR band assignments of poly(TFE-*co*-PSEPVE).²⁰

Wavenumber (cm ⁻¹)	Assignment
1303	C-C symmetric stretching
1208	CF ₂ asymmetric stretching
1142	CF ₂ symmetric stretching
1059	O=S(O)O symmetric stretching
982	C-O-C ether linkage stretching
969	C-O-C ether linkage stretching

$$R = \frac{4*j(1-S) + S*\sum_{i=1}^m k_i}{h*S} \quad (5.1)$$

In the previous equation, R is the ratio of the absorbance of C-F bonds to that of the S-O bonds. Additionally, S is the molar percentage of monomer B and h is the absorbance of each S-O bond. Also, j is the absorbance of each C-F bond from monomer A, m is the number of C-F bonds in monomer B and k is the absorbance of each C-F bond in monomer B. It is important to notice that monomer A in this case is referring to TFE and monomer B is referring to PSEPVE. Additionally, equation 5.2 can be rearranged to form equation 5.1 shown below.

$$\frac{1}{S} = 1 - \frac{0.25 * \sum_{i=1}^m k_i}{4j} + \frac{h}{4j} * R \quad (5.2)$$

Since the terms k , J and h can be understood as constants, a linear relationship exists between $1/S$ and R . This relationship is shown in Equation 5.3.

$$\frac{1}{S} = -2.70 + 2.88 * R \quad (5.3)$$

Finally, the equivalent weight of the polymers can be found by simply using another equation that converts the molar amount of PSEPVE (S in equation 5.3) to equivalent weight units. This final equation is shown in equation 5.4.

$$EW = 446 + \frac{(1-S)}{S} * 100 \quad (\text{Equation 5.4})$$

The results of these calculations can be observed in Table 5.2 where the equivalent weights of commercial samples of Nafion[®] resin have been analyzed by acid base titration and the aforementioned ATR-FTIR method. An example ATR-FTIR spectra for a sample of poly(TFE-*co*-PSEPVE) are also provided in the Appendix F.

Table 5.2. Results of analysis of commercial samples of Nafion[®] resin using the ATR-FTIR method.

Nominal EW (g/mol)	EW from Titration (g/mol)	EW Method I (g/mol)	EW Method II (g/mol)	EW Method III (g/mol)	EW Original FTIR method ¹⁹ (g/mol)
920	927	942	939	932	926
1000	1020	1001	1002	1009	1033
1200	1181	1186	1185	1183	1235

*Note: The methods for evaluating the equivalent weights from the experimental determination of the ATR-FTIR of the samples are detailed in equations 5.5, 5.6, and 5.7.

It can be observed that the percent error between the determinations of the EW for the samples is not significantly different based upon the method. Therefore, the ATR-FTIR method is suitable for a fast, cost-effective determination of EW of not only Nafion[®] polymers but also for those polymers that come from the polymerization of other sulfonyl fluoride monomers with TFE, such as PSVE, 8-CNVE, or DEVE.

The second set of analytical methods (Method I and Method II), consist of a linear correlation of the intensities of signals obtained from FTIR spectroscopy to the equivalent weights determined experimentally (by titration). The method is similar to the one mentioned above as the “original method” with the only difference that is tailored to only samples of poly(TFE-*co*-PSEPVE). The original method takes into count the absorbance of the S-F signal and if the polymer hydrolyzes, it could be then a problem in the accuracy of the results as the (S-F bond) signal will disappear. Furthermore, the broad signal of the hydroxyl group formed by the hydrolysis of poly(TFE-*co*-PSEPVE) resin is not preferred to be included in calculations, specially since the signal is prone to be affected by hydrogen bonding, humidity, temperature, etc. Therefore, the development of a method that uses the

C-O ether linkage absorbance is more appropriate to analyze resin samples of poly(TFE-*co*-PSEPVE) without the fear of the SO₂F group being hydrolyzed in the meantime while the polymer is analyzed or exposed to air and oxygen.

For reference all the possible regressions have been calculated. Method I comes from the absorbances between the band at 1460 cm⁻¹ and the band at 1202 cm⁻¹. Method II is calculated from the absorbances from the 1460 cm⁻¹ band and the band at 1147 cm⁻¹. Method III is calculated from the absorbances between the band at 1147 cm⁻¹ and the band at 982 cm⁻¹. As mentioned before, Method I and II are subject to error due to hydrolysis of the SO₂F group, while Method III is not.

The three linear relationships are shown in equation 5.5, 5.6, and 5.7. A graphical view of these equations and the data that originated from such graphs is included in Appendix F. A combined view of the three linear relationships is shown in Figure 5.12.

$$\text{Method I} = \text{EW} = 409 \pm 56 (\text{R}) - 229 \pm 177 \quad (5.5)$$

$$\text{Method II} = \text{EW} = 222 \pm 28 (\text{R}) + 148 \pm 115 \quad (5.6)$$

$$\text{Method III} = \text{EW} = 245 \pm 17 (\text{R}) + 213 \pm 58 \quad (5.7)$$

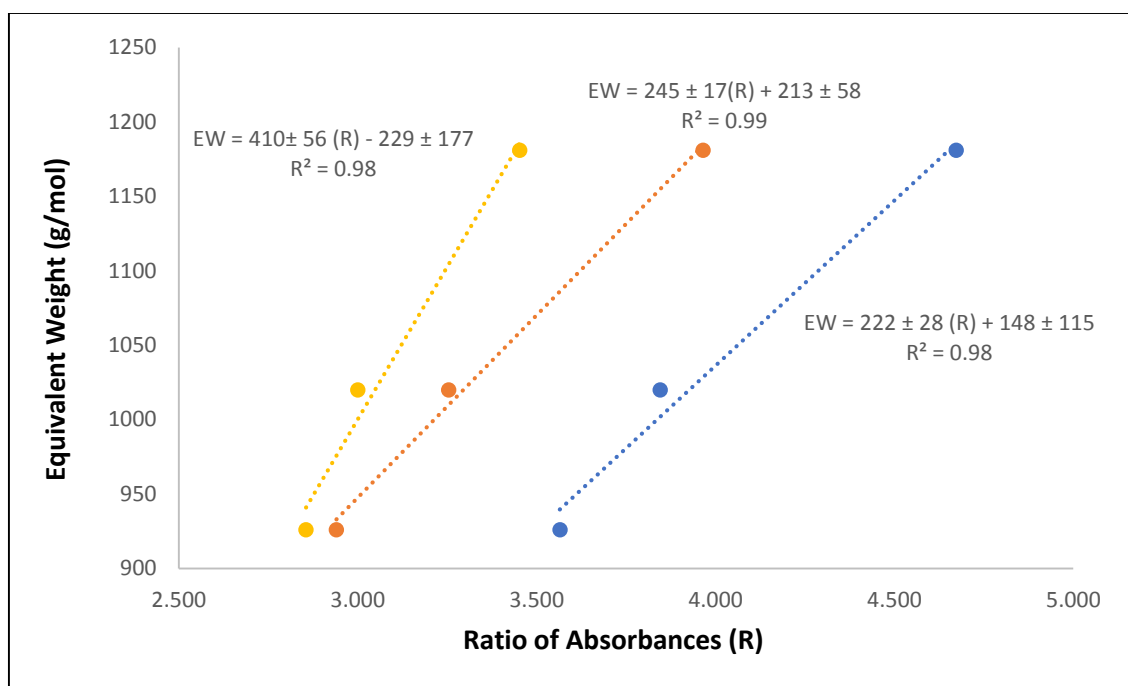


Figure 5.12. Linear relationships between the ratios of absorbances and the equivalent weight of poly(TFE-*co*-PSEPVE). From left to right: Method I, Method III, and Method II.

After evaluating each of the samples (and other experimental samples) of poly(TFE-*co*-PSEPVE), it is clear that all the methods are consistent to each other with great correlation. More details regarding the absorbances for the different samples and the error calculations for each sample are included in Appendix F.

5.5.3. Determination of relative reactivity ratios of TFE and PSEPVE for poly(TFE-*co*-PSEPVE).

Once the analytical methods that permits the experimental determination of equivalent weights for samples of poly(TFE-*co*-PSEPVE) is in place, it is very simple to

calculate the final compositions of the polymer samples using ATR-FTIR methods rather than the conventional titration.

The reactivity ratios of TFE and PSEPVE were determined for samples prepared in presence and absence of CO₂. Therefore, two sets of data are graphed, which include the determination of reactivity ratios using the Kelen and Tüdös method and the Fineman and Ross method for both types of samples (presence and absence of CO₂). In this case, samples prepared in absence of CO₂ are numbered S1 through S5, and samples prepared in presence of CO₂ are named S6 through S10. The complete detail of the calculations can be found in the respective section of Appendix F.

The tables with the detail of the polymer compositions and the determination of the reactivity ratios are included in Appendix F, but a summary of the reactivity ratios is included in Table 5.3. Figures 5.13 and 5.14 contain the graphical representation of the reactivity ratio linear methods for poly(TFE-*co*-PSEPVE) using the Fineman and Ross and Kelen and Tüdös methods, respectively, for when the polymer was made in absence of CO₂. In the same manner, Figure 5.15 and 5.16 contain the Fineman and Ross, and Kelen and Tüdös graphical representations respectively, for samples of poly(TFE-*co*-PSEPVE) when the polymer samples were made in the presence of CO₂. Lastly, a comparisons of the molar composition of PSEPVE supplied in the initial feed are compared to the final composition of the molar fraction of the PSEPVE in the copolymer (both in presence and absence of CO₂) is shown in Figure 5.17.

Table 5.3. Experimental Reactivity Ratios for samples of poly(TFE-*co*-PSEPVE). Samples S1-S5 were prepared in absence of CO₂ while samples S6-S10 were prepared in presence of CO₂.

Sample	Reactivity Ratio	Fineman and Ross	Kelen and Tüdös
S1-S5	r_{TFE}	8.68 ± 1.17	0.23 ± 0.02
	r_{PSEPVE}	0.04 ± 0.05	0.02 ± 0.02
S6-S10	r_{TFE}	10.67 ± 0.87	0.35 ± 0.04
	r_{PSEPVE}	-0.04 ± 0.03	0.02 ± 0.02
Literature 1 ¹	r_{TFE}	9	-
	r_{PSEPVE}	0.04	-
Literature 2 ²	r_{TFE}	7.85	-
	r_{PSEPVE}	0.079	-

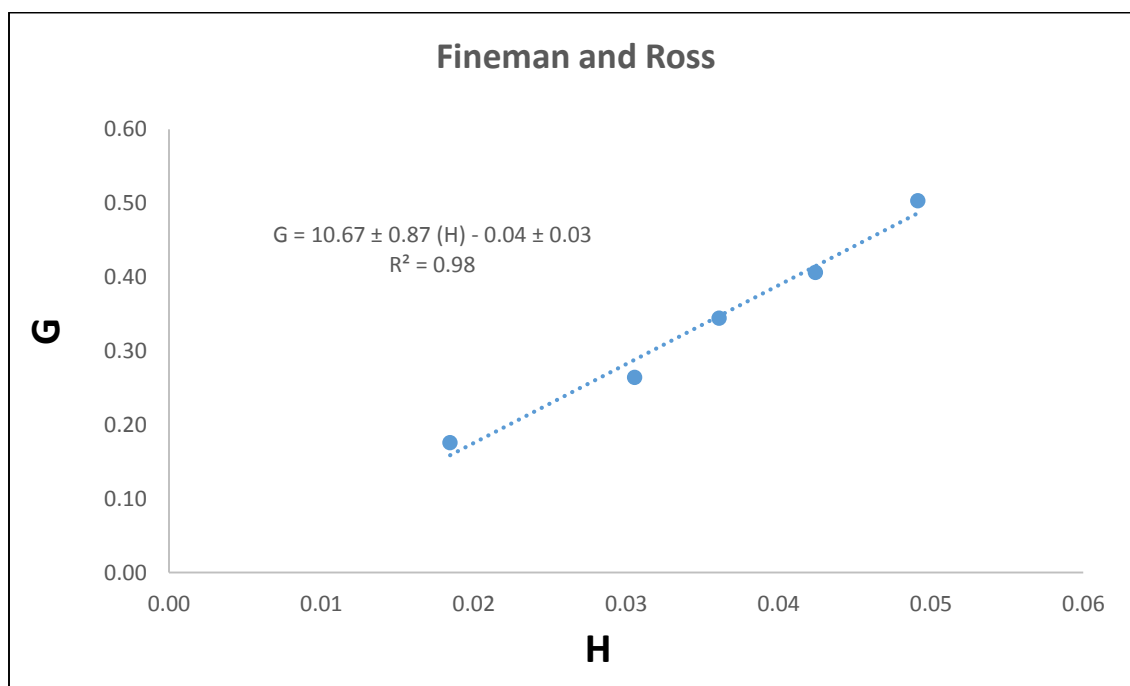


Figure 5.13. Linear Regression of Fineman and Ross method for samples of poly(TFE-*co*-PSEPVE) prepared in absence of CO₂.

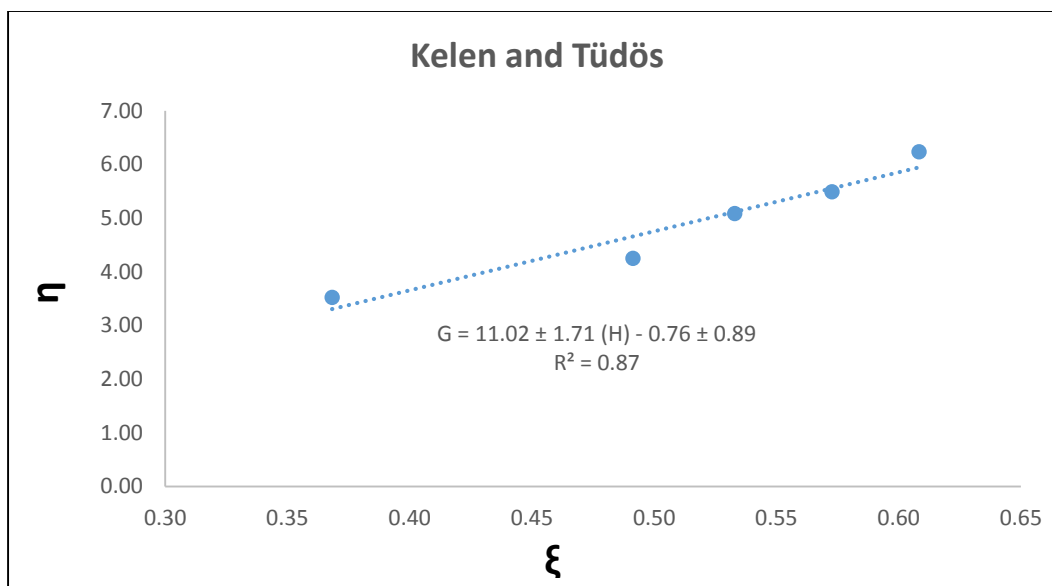


Figure 5.14. Linear Regression of Kelen and Tüdös method for samples of poly(TFE-*co*-PSEPVE) prepared in absence of CO₂.

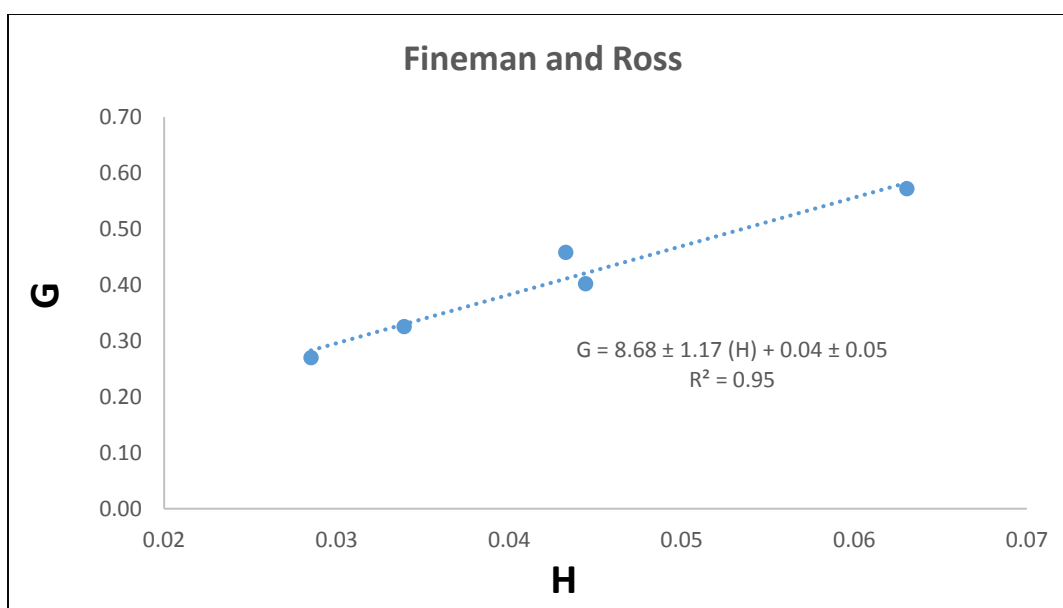


Figure 5.15. Linear Regression of Fineman and Ross method for samples of poly(TFE-*co*-PSEPVE) prepared in presence of CO₂.

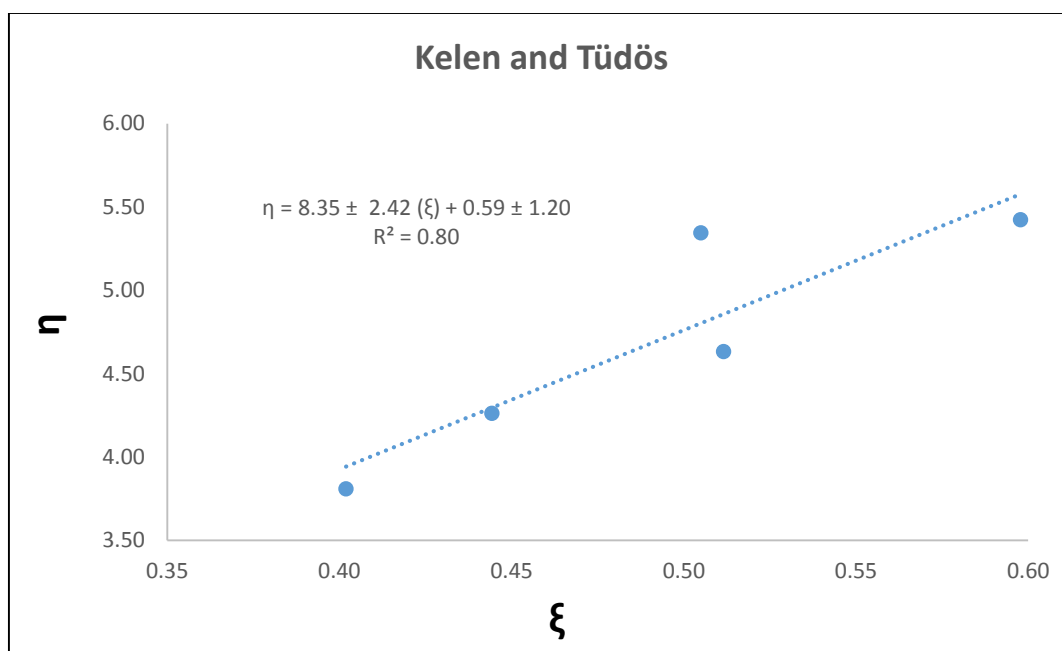


Figure 5.16. Linear Regression of Kelen and Tüdös method for samples of poly(TFE-*co*-PSEPVE) prepared in precense of CO₂.

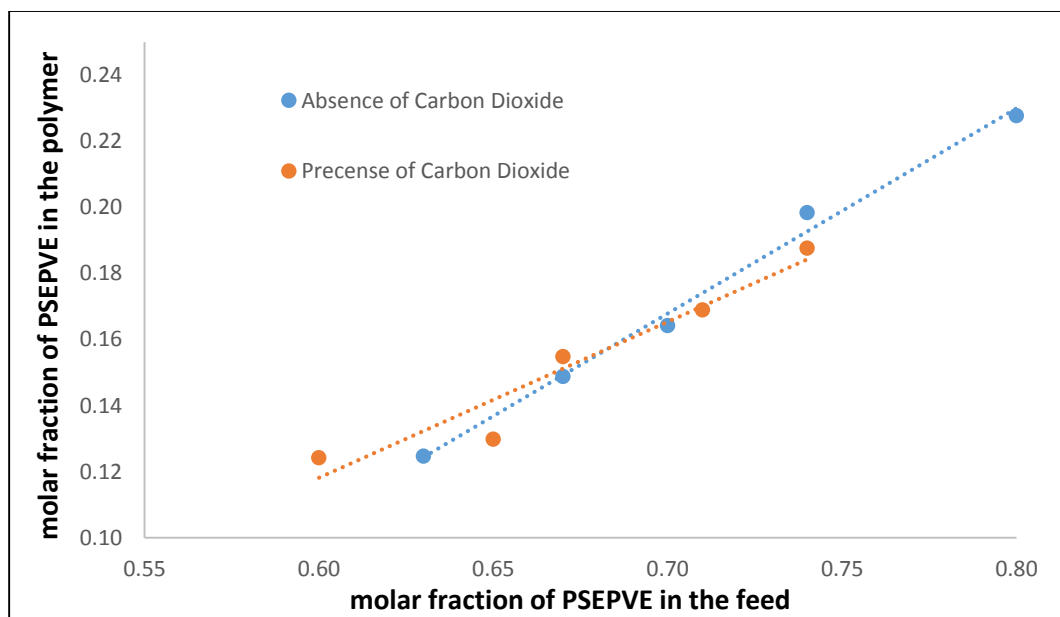


Figure 5.17. Graphical representation of the comparison of the molar fraction of PSEPVE supplied in the monomer feed versus the molar fraction obtained in the copolymer.

In both of the reported values for reactivity ratios of TFE and PSEPVE^{1,2} (as shown in Table 5.3), a trend is observed. The reactivity ratio for TFE is considerably higher than the one for PSEPVE. The values reported in the literature were obtained using the Fineman and Ross linearization method. The values determined experimentally for the samples reported herein show the same trend as well as very similar results to one of the sets reported in the literature.¹ The literature reference determined the ratios in 1,1,2-trichloro-1,2,2-trifluoroethane, while the current determination was made in HFC-4310. The differences could derive from the different solvent used or different set of reaction conditions. The authors of the work¹ used a 200-mL reactor with agitation set at 300 rpm and at 35 °C. One similarity of the current work to theirs is that the pressure of the reaction system was held constant by feeding TFE as it is consumed in both studies. Despite the differences between the experimental conditions used in this study and the literature work, the values of current reactivity ratios are very similar to those reported in the open literature.

Secondly, while observing the reactivity ratios values calculated experimentally in this document, one can see that the trend is maintained when the reaction is carried in presence and absence of CO₂. It is hypothesized that CO₂ does not dissolve considerably in HFC-4310 (solvent used for the polymerization reactions) and therefore does not affect considerably the reaction kinetics as those occur in the solvent and not in the gas phase. The reactivity ratios in presence of CO₂ are slightly larger for TFE and the same for PSEPVE, but not significantly, so this represents a huge advantage since we can prepare the same polymer in presence of CO₂, obtain the same properties of product obtained when

CO₂ is not used in the reaction, and still be safe by using a mixture of TFE and CO₂ to start the reaction and continue the TFE feed with raw TFE as it is consumed. It has been published already in another dissertation from the same research group,²² a method for obtaining poly(TFE-*co*-PSEPVE) using a TFE/CO₂ gas mixture and still obtain comparable polymer as the ones obtained from this work. The only drawback in the previous work was that while using a TFE/CO₂ feed, as TFE is consumed, the partial pressure of CO₂ increased inside the reactor forcing the concentration of TFE in the headspace to become leaner and leaner as time lapsed.

Additionally, the yields obtained in the present study when the reaction was carried in presence of CO₂ were slightly lower than the yields obtained when the reaction was not carried in presence of CO₂ (as can be observed in Table 5.7 in the Experimental section). This last observation serves as a second indicator that the kinetics for the reaction slow down slightly when CO₂ is used as a diluent in the reaction headspace.

Finally, despite the fact that HFC-4310 is a more expensive solvent than water for carrying out a polymerization reaction, the benefits of using it can be appreciated in the sense that a surfactant is not needed (helping the efforts of industry phase out the biopersistent perfluorooctanoate salts), a mixture of TFE/CO₂ can be used to lower the potential risks of using raw TFE, and the equivalent weights of the polymers obtained lay in the range where the polymers can be used in fuel cell membrane technologies and/or other applications.

5.5.4 Experimental Determination of Reactivity Ratios for TFE and PSVE in poly(TFE-*co*-PSVE).

The reactivity ratios of poly(TFE-*co*-PSVE) were determined from the final compositions of polymer samples determined by acid-base titration as explained later in the Experimental section. In Appendix F, a sample of the assembly of the infrared spectra for the experimental samples of poly(TFE-*co*-PSVE) is shown. The characteristic bands for the S-F stretch and C-O-C stretch are too weak (compared to the ones for the CF₂ symmetric and asymmetric stretch) to calculate a ratio of such bands as was done for the samples of poly(TFE-*co*-PSEPVE). The results for the Fineman and Ross reactivity ratios are shown in Table 5.4. The reactivity ratios were not determined from the Kelen and Tüdös are not shown due to large errors in the results, which are probably due to the small distribution of compositions of the polymer samples made and the effect that such a narrow range has on the alpha parameter.

Table 5.4. Experimental reactivity ratios of TFE and PSVE in poly(TFE-*co*-PSVE).

Sample	Reactivity Ratio	Fineman and Ross
A-D	r _{TFE}	4.08 ± 0.32
	r _{PSVE}	0.50 ± 0.07

These experimentally determined reactivity ratios are subject to further analysis. A different set of polymerization reaction conditions shall be investigated in order to consistently obtain a wider range of equivalent weights for the polymer samples in a short period of time that favors the kinetic behavior of the monomers and do not include any

effects from a composition drift. Since the results of the reactivity ratios are obtained from the equivalent weight determinations from acid-base titration (and the error on the titrations was 3%), the error on the reactivity ratios is assigned to 3% of the magnitude of the value determined.

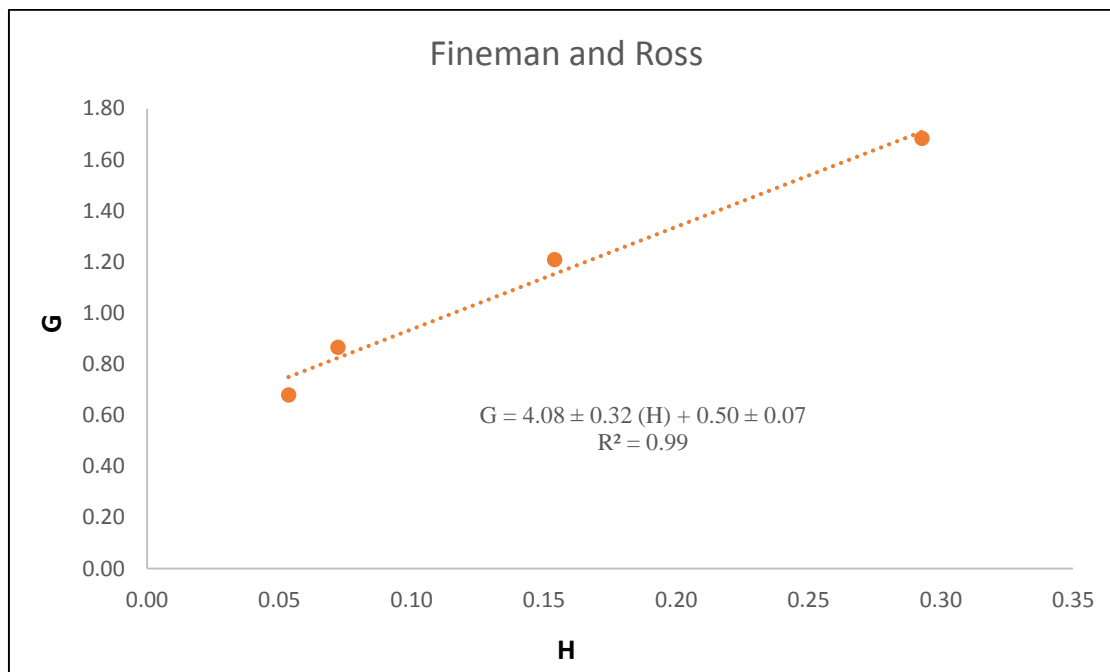


Figure 5.18. Linear Regression of Fineman and Ross method for samples of poly(TFE-*co*-PSVE).

5.5.5. Experimental Determination of Reactivity Ratios for TFE and DEVE in poly(TFE-*co*-DEVE).

Composition analysis of experimental samples of poly(TFE-*co*-DEVE) was obtained via collaboration with Chemours (previously part of DuPont). Chemours is capable of performing NMR spectroscopy analysis on polymer samples at high temperature

which enables the polymer to pass the T_g temperature at which the polymer chains become more mobile, making it possible to acquire a spectra of the polymer as if it was in solution. The fluorine-19 melt NMR spectra was acquired on a Bruker AVIII 400 MHz NMR spectrometer equipped with a 5 mm SEF 400SB ^{19}F - ^1H /D high temperature probe and a BVTE 3900 heater booster. Polymer samples were analyzed in Wilmad 528-PP-8 NMR tubes, using previously acquired thermal data (using TGA and DSC analyses) on each sample as a guide for temperature ramping. Samples were equilibrated for 8-10 minutes when the desired acquisition temperature was reached. All equilibration and acquisition was done with sample spinning at 20 Hz. Few examples are listed in the literature in which this technique has been used to analyze fluoropolymers.²³⁻²⁵

Tables with composition analysis, integration constants for the NMR spectra and images of the experimental NMR results are included in the Appendix F. In Table 5.5 the reactivity ratios for TFE and DEVE in poly(TFE-*co*-DEVE) are included.

Table 5.5. Experimental reactivity ratios of TFE and DEVE in poly(TFE-*co*-DEVE).

Reactivity Ratio	Fineman and Ross
r_{TFE}	8.77 ± 2.74
r_{DEVE}	0.20 ± 0.13

One can notice that the F-R results are in agreement with the expected behavior of a radical copolymerization of TFE with a vinyl ether. Vinyl ethers are known to have

reduced reactivity due to a high mobility of the side chain and also due to lack of ability to stabilize a radical on the ether carbon due to electronic induction from the oxygen.

The graphical representations of the Fineman and Ross analysis method is shown in Figure 5.19 and 5.20, and a final representation of the molar fraction of DEVE supplied in the monomer feed versus the final DEVE molar percentage in the polymer is shown in Figure 5.21.

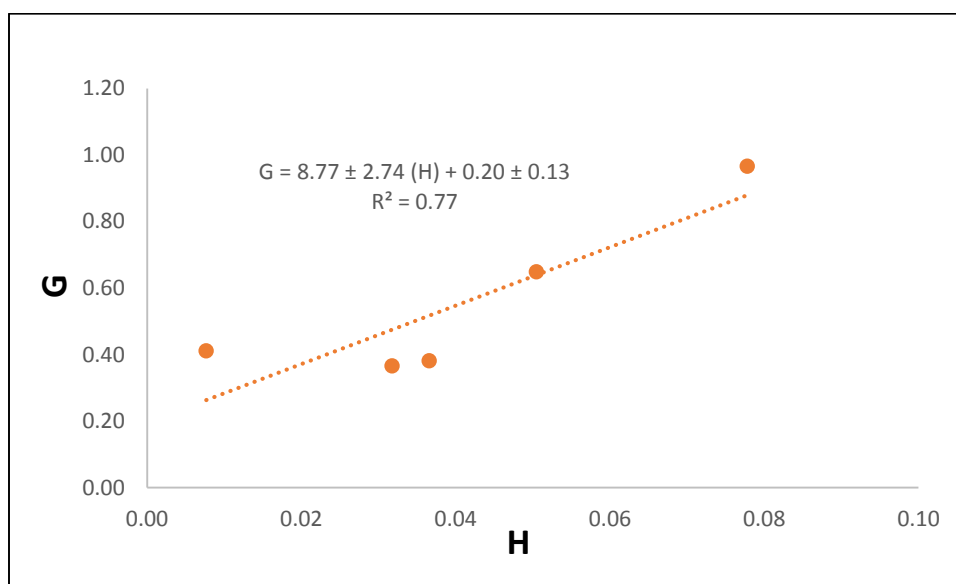


Figure 5.19. Linear Regression of Finemand and Ross method for samples of poly(TFE-co-DEVE).

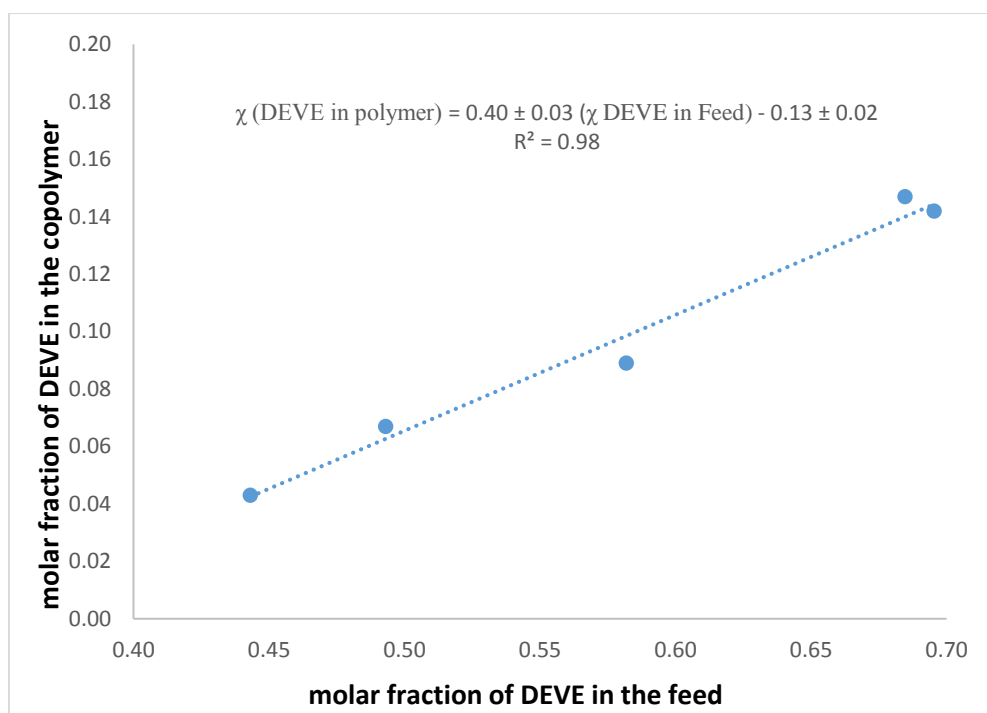


Figure 5.20. Graphical representation of the comparison of the molar fraction of DEVE supplied in the monomer feed versus the molar fraction obtained in the copolymer.

It can be observed that the range of molar fraction of DEVE in the feed ranges from 0.44 to 0.70 and the respective range of DEVE incorporation in the polymer ranges from 0.14 to 0.44. There is a high correlation in between the molar fraction of DEVE in the feed and the DEVE in the copolymer as shown by the trendline in Figure 5.21. Samples 7 and 8 (as seen in Appendix F), were prepared purposely to evaluate final composition reproducibility at the higher content of DEVE. It can be observed that sample 7 has a final composition of 14.2 mol% of DEVE and 85.8 mol% of TFE, while sample 8 has a final composition of 14.7 mol% of DEVE and 85.3 mol% of TFE. This is a good result since it was possible to obtain two compositions that are very similar following the same procedure

in the same conditions. It also evidences the reproducibility on the integration error by the user.

5.6. Experimental section

5.6.1. Preparation of bis-perfluoropropionyl peroxide (3P)

In a similar fashion as the already patented method (U.S. Patent 2,792,423)²⁶ a total of 27.4 g of pentafluoropropionyl chloride is transferred to the small volume element of the glassware equipment shown in Figure 5.25 (marked with a letter A). A total of 100 g of deoxygenated and deionized water is poured into the 1.0-L side of the same apparatus (marked with a letter B in Figure 5.25). The water is cooled to 0 °C and a total of 7.84 g of sodium peroxide is added slowly with stirring over a period of 20 minutes. To the solution, a total of 500 mL of HFC-4310 is added while bubbling nitrogen through the solution to help keep oxygen out, and the resulting mixture is cooled to -5 °C. The glassware equipment is then closed, inverted, and the stopcock separating the two compartments is opened. The perfluoropropionyl chloride is then let flow into the bigger compartment and the equipment is shaken vigorously for a couple of minutes. The resulting mixture is poured into a separatory funnel, and the HFC-4310 layer is then drained into a steel cylinder. The cylinder (Sure/Pac™ 275-mL steel sample cylinder) is then stored to -80 °C. The concentration of the solution after redox titration is 0.110 M with a yield of 75%.

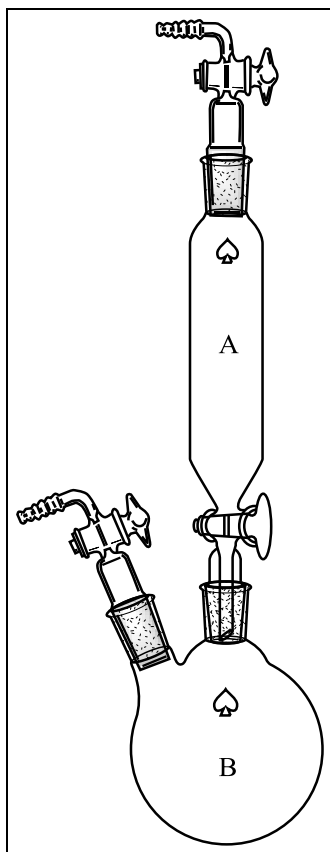


Figure 5.21. Glassware used to prepare a 3P solution in HFC-4310.

5.6.2. Titration of bis-perfluoropropionyl peroxide (3P)

The titration is followed in similar fashion as the already patented method (U.S. Patent 5,021,516).²⁷ A total of 25 mL of glacial acetic acid and 5.0 mL of water is added to a Schlenk flask with 3.0 g of potassium iodide and two pellets (approximately 5 g) of dry ice. A total of 5.0 mL of the 3P initiator solution is added to the flask and allowed to stir for a total of 30 minutes. After such period of time, a total of 100 mL of deoxygenated and deionized water are added. The solution should turn dark orange. From this solution,

5 mL are taken and placed in a small Erlenmeyer. The solution is then titrated with 0.100 M solution of sodium thiosulfate under nitrogen atmosphere to avoid oxygen entering the solution.

5.6.3. Preparation of poly(TFE-*co*-PSEPVE) by solution polymerization

A 600-mL stainless steel Parr Instruments Co. reactor is loaded with 350 g of HFC-4310. Then PSEPVE monomer (see Table 5.7) is charged inside the reactor, the vessel is closed, and its contents degassed by using the freeze/thaw/pump method two times. The reactor is connected to the polymerization system located in the reaction room, and the instructions for carrying out a polymerization are followed as indicated in the respective standard operational procedure (SOP) located in the operations binder in the control room. The temperature of the reactor is adjusted to 35 °C, and the temperature of the cooling system is set to 5 °C. The reactor then charged with TFE to a final pressure of 150 psig, and once the pressure and temperature are stable inside the reactor (and the flow through the mass flow controller is zero), the totalizer is reset to zero and a 5.0 mL slug of 3P initiator solution is feed to the reactor followed by an adjustment of the radical initiator solution feed to 0.02 mL/min. After a period of 30 minutes, the feed of the radical initiator solution is stopped, the radical initiator valve is closed, the TFE valve on the top of the reactor is closed, the heating oven is lowered from the reactor and put aside, and a Dewar flask filled with liquid nitrogen is raise from underneath the reactor to cool the vessel and therefore quench the reaction. After a few minutes (once the reactor is cold), the Dewar is lowered and put away, the reactor vent is opened remotely from the control room, and the

reactor is allowed to warm to room temperature. The reactor is then removed from the system, secured in a vise, and the top of the reactor is removed by unscrewing the locking ring and bolts. The contents of the reactor are poured inside a tared 500-mL round-bottomed flask, and the solvent is evaporated under vacuum. The polymer obtained is then washed twice with 50 mL of HFC-4310, filtered, and dried overnight in a vacuum oven at 90 °C. Typical yields of polymer are detailed in Table 5.7.

Table 5.7. Monomer composition in the preparation of poly(TFE-*co*-PSEPVE).

Run	PSEPVE (g)	TFE (molar fraction)	PSEPVE (molar fraction)	TFE Standard Liters (SL)	Polymer Obtained (g)
S1	5.0	0.20	0.80	1.01	1.20
S2	5.0	0.26	0.74	0.72	0.90
S3	5.0	0.30	0.70	0.58	0.75
S4	5.0	0.33	0.67	0.52	0.70
S5	5.0	0.37	0.63	0.43	0.55
S6	5.0	0.26	0.74	0.72	0.85
S7	5.0	0.29	0.71	0.63	0.75
S8	5.0	0.33	0.67	0.52	0.75
S9	5.0	0.35	0.65	0.47	0.50
S10	5.0	0.40	0.60	0.38	0.45

Note: All the reactions were carried during a period of time of 30 minutes according to the procedure.

Since the calibration curve for the determination of equivalent weights covers the range of equivalent weights in between 900 and 1200 g/mol, the reactions are targeted in the range of molar fractions of PSEPVE between 0.12 and 0.18 approximately.

5.6.4. Preparation of poly(TFE-*co*-PSEPVE) by solution polymerization in the presence of CO₂

The same procedure of preparing poly(TFE-*co*-PSEPVE) in absence of CO₂ is used except that the system is modified so that an extra connection from the reactor is made to an external CO₂ cylinder. The procedure is followed and before charging the TFE into the reactor, a total of 75 psig of CO₂ are introduced into the reactor. Once the pressure of CO₂ is reached, the valve to the CO₂ tank at the top of the reactor is closed. The procedure is followed as indicated before and the reactor pressure was targeted at 150 psig.

5.6.5. Preparation of poly(TFE-*co*-PSVE) by solution polymerization

The procedure is followed in the same fashion as they are listed in Section 5.6.3. The same amount of HFC-4310 is used, and the amounts of PSVE monomer are varied in between 10 to 20 g. During the reaction, TFE is introduced to the reactor (amounts in between 0.9 and 2.2 SL). Typical equivalent weights between 1330 and 1500 g/mol (determined by acid-base titration) are obtained, and a range of polymer in between 0.6 and 1.8 g are isolated from the reaction mixture after the residual monomer and solvent are evaporated.

5.6.6. Preparation of poly(TFE-*co*-DEVE) by solution polymerization

The procedure is followed in the same fashion as procedure 5.6.3. The same amount of HFC-4310 is used and amounts of DEVE monomer are varied in between 60 to 65 g. During the reaction, TFE is introduced to the reactor (amounts in between 2.3 and 6.6 SL).

5.6.7. Preparation of poly(TFE-*co*-8CNVE) by solution polymerization

By the time when this dissertation had to be turned to the graduate school as a requirement for graduation, the final compositions to be determined by melt ^{19}F NMR spectroscopy were not yet determined by our collaborators at Chemours Inc. The procedure is followed in the same fashion as procedure 5.7.3. The same amount of HFC-4310 is used, and the amounts of 8-CNVE monomer are varied in between 5 to 6 g. During the reaction, TFE is introduced to the reactor (amounts in between 0.2 and 2.7 SL).

5.6.8. Titration of poly(TFE-*co*-PSEPVE) or poly(TFE-*co*-PSVE)

A finely particulate sample (1-2 g) of the polymer was placed in a 250-mL Erlenmeyer flask and the polymer was hydrolyzed initially at 60 °C with a solution of 15% KOH, 35% DMSO, and 50% H₂O by weight for two hours. After the initial hydrolysis, washes with distilled water were performed until the decanted liquid is neutral to litmus paper. The material is then preacidified twice with a dilute solution of HNO₃ twice before adding 30 mL of concentrated HNO₃. The samples were left in constant agitation under nitrogen atmosphere at 80 °C for one hour. The samples were washed with distilled water until the decanted liquid is neutral to litmus paper and dried under vacuum in an oven at 100 °C and 50 mtorr for 24 hours. The dried sample is weighed (0.100 – 0.120 g) and placed in a 250-mL Erlenmeyer flask with 30 mL of distilled water, 10 mL of ethanol, and 2 drops of phenolphthalein. A solution of 0.01 M NaOH is added until the equivalence point, and an excess of 2 mL are added beyond such point. The resulting solution is then

titrated with a 0.01 M solution of HCl until the equivalence point always taking care that the procedure is done under nitrogen atmosphere. The resulting equivalent weight in meq/g is calculated using equation 5.8, and the equivalent weight in g/mol (grams of polymer per mol of acid sites) is calculated using equation 5.9.

$$EW \left(\frac{meq}{g} \right) = \frac{(Volume\ of\ NaOH * 0.01\ M) - (Volume\ of\ HCl * 0.01\ M)}{Dried\ polymer\ weight\ (g)} \quad (5.8)$$

$$EW \left(\frac{g}{mol\ of\ H^+} \right) = \frac{mass\ of\ polymer\ (g)}{(Volume\ of\ NaOH * 0.01\ M) - (volume\ of\ HCl * 0.01\ M)} \quad (5.9)$$

5.6.9. Alternate method for titration of poly(TFE-co-PSEPVE) or poly(TFE-co-PSVE)

A finely particulate sample (0.100 to 0.200 g) of the polymer was placed in a 100-mL Erlenmeyer flask and hydrolyzed initially at 80 °C with a solution of 10% KOH in ethanol for 24 hours. The polymer is washed with distilled water until the decanted liquid is neutral to litmus paper and dried under vacuum overnight at 90 °C. Once the polymer is dried, a sample of 0.100 grams are placed in a 100-mL Erlenmeyer flask with 50 mL of distilled water, 10 mL of ethanol and 2 drops of phenolphthalein. The polymer is let under constant agitation for 2 hours before titration with a 0.01 M solution of NaOH until light pink color appears. An excess of 2.00 mL is added, and is allowed to stand overnight. During the titration, enough care is taken to avoid the contact of the sample with air (sample is kept under a nitrogen atmosphere). The polymer is titrated again a final time until light

pink and left under agitation for 5 hours. If the color does not change, it is assumed that the equivalence point is reached. The equivalent weight can be calculated from the equation 5.10. If titration is done slowly enough (and always taking care of keeping CO₂ and oxygen out), there is no need to back titrate with HCl. If back titration is necessary, the equation 5.10 can be modified in the same way as equations 5.8 or 5.9 are listed.

$$EW \left(\frac{g}{mol} \right) = \frac{\text{mass of polymer (g)}}{\text{Volume of NaOH (L)} * \text{Concentration (M)}} \quad (5.10)$$

5.6.10. ATR-FTIR analysis of polymer samples

The FTIR equipment (Nicolet iS5) is equipped with an Attenuated Total Reflection (ATR) accessory. A total of 0.1 – 0.2 g of sample is placed and pressed with the pressure knob after collecting a background of the ATR accessory without sample. Typical conditions of analysis are 50 scans at a resolution of 0.8 cm⁻¹ in the range of 650 to 4000 cm⁻¹. Characteristic IR spectra are supplied in Appendix F.

5.6.11. TGA analysis of polymer samples

A total of 2-8 mg of sample is placed in a clean, previously tared platinum pan under a constant purge of 40 mL/min of nitrogen gas on a TA Instruments Q500 Thermo Gravimetric Analyzer (TGA). The sample is let equilibrate at 100 °C for 10 minutes before ramping from 100 °C to 600 °C at a constant rate of 10 °C/min. Characteristic TGA thermograms are supplied in Appendix F.

5.6.12. DSC analysis of polymer samples

A total of 2-5 mg of sample is placed in a clean, new, and, previously tared aluminum pan. The sample is placed in the auto-sampler of a TA Discovery Series differential scanning calorimeter (DSC). After the appropriate software setup, the sample is first cooled from room temperature to -50 °C and then heat up to 320 °C (or 20 °C lower than the 2% mass loss decomposition temperature: previously obtained by TGA analysis), at a constant rate of 10 °C/min. Other ramp rates can be used such as 5 or 2 °C/min. The cycle is usually repeated 2 times. Characteristic DSC thermograms are supplied in Appendix F.

5.7. References

1. Odínokov, A. S.; Bazanova, O. S.; Sokolov, L. F.; Barabanov, V. G.; Timofeev, S. V. Kinetics of Copolymerization of Tetrafluoroethylene with Perfluoro(3,6-dioxo-4-methyl-7-octen)sulfonyl Fluoride. *Russ. J. Appl. Chem.* **2009**, 82, 112-115.
2. Xu, A.; Zhao, J.; Yuan, W. Z.; Li, H.; Zhang, H.; Wang, L.; Zhang, Y. Tetrafluoroethylene Copolymers with Sulfonyl Fluoride Pendants: Syntheses in Supercritical Carbon Dioxide, Polymerization Behaviors, and Properties. *Macromol. Chem. Phys.* **2011**, 212, 1497-1509.
3. Xu, P.; Hegenbarth, J. High Purity Perfluoroelastomer Composites and a Process to Produce the Same. CA Patent 2,775,760 A1, May 01, 2005.
4. Fukushi, T.; Wellner, S. J. Low Temperature Curable Amorphous Fluoropolymers. W.O. Patent Application 2010/147815, Dec 23, 2010.
5. Yandrasits, M. New Fluorinated Ionomers for Proton Exchange Membranes. In *Advances in Materials for PEMFC Systems*, Asilomar, California, Feb. 2011.
6. Yandrasits, M. A.; Aieta, N.; Stanis, R. J.; Hamrock, S. J.; Cockson, D. J.; Herring, A. M. Dynamics of PFSA Polymer Hydration Measured In Situ by SAXS. *ECS Transactions* **2006**, 3, 915-921.

7. Ebnesajjad, S. *Fluoroplastics. Volume 1: Non-Melt Processible Fluoroplastics: The Definitive User's Guide and Databook*; 2nd ed. Plastics Design Library: Norwich, NY, 2000.
8. Navarrini, W.; Tortelli, V.; Russo, A.; Corti, S. Organic Hypofluorites and their New Role in Industrial Fluorine Chemistry. *J. Fluorine Chem.* **1999**, *95*, 27-39.
9. Yoshitake, M.; Watakabe, A. Perfluorinated Ionic Polymers for PEFCs (Included Supported PFSA). *Adv. Polym. Sci.* **2008**, *215*, 127-155.
10. Novara, A. M.; Perego, G. Direct Fluorination of Fluoro-Beta-Sultones in Order to Produce the Corresponding Fluorooxy-Fluorosulfonyl-Fluoro-Compounds. U.S. Patent 4,962,282, Oct 9, 1990.
11. Korach, M.; Foster, R. Electrolysis of Brine Using Permeable Membranes Comprising Fluorocarbon. U.S. Patent 3,853,720, Oct 24, 1972.
12. Darlington, W.; Foster, R. Process for Electrolysing Brine. U.S. Patent 3,853,721, Oct 24, 1972.
13. Oda, Y.; Suhara, M.; Endo, E. Process of Producing Alkali Metal Hydroxide. U.S. Patent 4,065,366, Oct 17, 1975.
14. Resnick, P. R. Proces for Preparing Ester Fluorinated Ion Exchange Polymer Precursor by Acid Treatment of Ether. U.S. Patent 4,474,899, Dec 12, 1983.

15. Resnick, P. R. Fluorinated Vinyl Ethers, Copolymers Thereof, and Precursors Thereof. U.S. Patent 4,526,948, Dec 12, 1983.
16. Birdwell, F. D. Method for Forming Polymer Films Having Bubble Release Surfaces. U.S. Patent 4,610,762, May 31, 1985.
17. Hung, M. H.; Subramanyam, V. Process of Synthesizing Fluorinated Nitrile Compounds. U.S. Patent 5,637,748, Mar 01, 1995.
18. Hercules, D. A.; Desmarteau, D. D.; Fernandez, R. E.; Clark, J. L.; Thrasher, J. S. "Evolution of Academic Barricades for the Use of Tetrafluoroethylene (TFE) in the Preparation of Fluoropolymers". In *Handbook of Fluoropolymer Science and Technology*; 1st ed.; Iacono, S. T., Iyer, S. S., Smith, D. W., Eds.; John Wiley & Sons: Hoboken, NJ, USA, 2014, pp 415-433.
19. Qin, S.; Gao, Z.; Zhang, C.; Cui, X.; Zhang, Y.; Zhang, H. A Method of Measuring the Perfluoro Sulfonyl Monomer Content. Chinese Patent CN 101,051,024 A, Oct 10, 2007.
20. Ramaswamy, N.; Arruda, T. M.; Wen, W.; Hakim, N.; Saha, M.; Gulla, A.; Mukerjee, S. Enhanced Activity and Interfacial Durability Study of Ultra Low Pt Based Electrocatalysts Prepared by Ion Beam Assisted Deposition (IBAD) Method. *Electrochim. Acta* **2009**, *54*, 6756-6766.

21. Korzeniewski, C.; Snow, E. D.; Basnayake, R. Transmission Infrared Spectroscopy as a Probe of Nafion Film Structure: Analysis of Spectral Regions Fundamental to Understanding Hydration Effects. *Appl. Spectrosc.* **2006**, *60*, 599-604.
22. Sayler, T. S. Preparation of Perfluorinated Ionomers for Fuel Cell Applications. Ph.D. Dissertation, The University of Alabama, Tuscaloosa, AL, 2012.
23. Yonemori, S.; Jitsugiri, Y.; Ogawa, T. Compositional and Microstructural Analysis of Tetrafluoroethylene Copolymers by Molten-State ^{19}F -NMR. *J. Chem. Soc. Jpn.* **1995**, *1*, 30-34.
24. English, A. D.; Garza, O. T. Composition and Microstructure of Fluoropolymers. High-Temperature High-Resolution FT NMR. *Macromolecules* **1979**, *12*, 351-353.
25. Wilson, C. W. Observation of Chemical Shifts in a Bulk Crystalline Polymer. *J. Polym. Sci.* **1962**, *56*, S16-S17.
26. Stoops, W. N.; Young, D. M. Production of Bis(Perfluoroacyl) Peroxides. U.S. Patent Application 2,792,423 A, May 14, 1957.
27. Wheland, R. C. Poly(perfluoroether)acyl Peroxides. U.S. Patent 5,021,516 A, Jun 04, 1991.

APPENDICES

Appendix A

Standard Operational Procedures.

The following document includes all the standard operational procedures (SOP's) that shall be followed prior, and during any task at the AMRL barricade and/or the Hunter barricade. A list of all the procedures is included below and the diagrams and figures for all the procedures are included at the end of the document.

List of procedures:

- A.1. Standard Operational Procedures (SOP) related to a polymerization reaction
 - SOP for initial work to be carried out before any reaction
 - SOP for leak checking the gas handling system
 - SOP for ISCO pump operation
- A.2. SOP for scrubbing carbon dioxide (CO₂) from TFE/CO₂ mixture
- A.3. SOP for leak check in vacuum line in bomb room for transferring TFE from large cylinder to high pressure cylinder through transfer cylinder
- A.4. SOP for transferring TFE from large cylinder to transfer cylinder (500 cm³ volume)
- A.5. SOP for transferring TFE from transfer cylinder to high pressure cylinder (500 cm³ volume)

A.1. SOP Related to a Polymerization Reaction.

A.1.1. SOP for Initial Work to be Carried Out Before any Reaction.

The present SOP must be completed before any reaction or procedure is carried inside the reaction room located in the TFE facility.

1. Verify the mass of all the cylinders to be used and write down the mass either in a file in the computer or the notebook specific for each process and as well in your personal notebook.
2. Make sure that all the connections to the gas cylinders used in the specific procedure are leak free and/or evacuated and/or oxygen and water free. If the connections have to be deoxygenated a normal back fill with nitrogen and vacuum cycle must be repeated at least 3 times to ensure such conditions.
3. At the end of every procedure (unless decided previously), all the cylinders involved must be disconnected and capped with either a stainless steel or brass cap to ensure that the cylinders are closed and unable to develop a major leak.
4. The door of the operating room must be closed at all times during the time in which any procedure is performed in the reaction room.
5. For all the procedures carried in the facility there should be a SOP written electronically and physically inside the control room and such must be followed by all the members of the team involved in the aforementioned process. If there is not a

SOP for a given procedure, the leader of the process can write its own SOP as long as is reviewed and approved by all the members of the team responsible of the facility (Dr. Thrasher and Graduate Students).

6. Any corrections to any of the SOP's must be followed in such way as discussed in the PHR for copolymerizations of TFE. Corrections must be written down in a copy of the SOP in question, presented to members of the team and once consensus is reached, the person in charge of making such corrections will update the file and a new copy of the procedures will be issued.

A.1.2. SOP for Leak Checking the Gas Handling System.

NOTES:

- The controls of the underlined items (for example 3W1) are located in the reaction room as part of the gas handling system, and the controls of the items that are not underlined are located in the control room.
- The Figures listed in these SOPs are listed at the end of the document and will be located in the reaction and control room as well.
- A Table with the location of every part in the system is provided at the end of the document.
- In between runs/reactions only sections that have been broken into (for example autoclaves, monomer feed lines, etc.) should be leak checked.

- The following procedures are divided in sections that can easily be followed by where the components that limit each section are located on the system.

Procedures for section from N2_C_1 to 1TFE, 2TFE, and 1V

1. Make sure that 3W1 (Figure A.1) is closed (vertical position).
2. Make sure that 1N (Figure A.1) is closed and verify that it is closed with the laser indicator on the valve control panel.
3. Open N2_C_1 tank valve (Figure A.1) and adjust regulator to 400 psig.
4. Verify that 1V (Figure A.1), 2V (Figure A.1), and 3V (Figure A.1) are closed, 1TFE (Figure A.1) is closed and 2TFE (Figure A.1) is closed.
5. Open the 3W1 (Figure A.1) valve connecting N2_C_1 (Figure A.1) and 1N (Figure A.1).
6. Open 1N (Figure A.1) and verify with the laser indicator. The PT2 (Figure A.1) should read 400 psig.
7. Close 1N (Figure A.1), wait 10 minutes and monitor the pressure on PT2 (Figure A.1). If the pressure holds then the specified section is considered leak free.

Procedures for section from N2_C_3 and N2_C_1 to BPR1, and BPR2

8. Verify that BPR1 DOME, BPR2 DOME, BLEED 1 and BLEED 2 are closed.

9. Verify 2W2 (Figure A.1) is open.
10. Reopen 1N (Figure A.1)
11. Open N2_C_3 tank valve (Figure A.1) and adjust regulator to 350 psig.
12. Open 2TFE (Figure A.1) and 3V (Figure A.1), and turn 3W2 (Figure A.1) toward BPR1 inlet and open 3W3 towards 3V and watch PT3 rise to 400 psig.
13. Open BPR1 DOME valve and BPR2 DOME valve and watch PT4 (Figure A.1) and PT5 (Figure A.1) get to 350 psig.
14. Close N2_C_3 tank valve (Figure A.1) and 1N then wait for ten minutes. If the pressure holds on PT3, PT4, and PT5 then the specified section is considered leak free.

Procedures for section from BPR1 and BPR2, to Small Autoclave

15. Verify 1V (Figure A.1), 2V (Figure A.1), 1TFE (Figure A.1), 2N (Figure A.1), 2W1 (Figure A.1), and 2W6 are closed.
16. Make sure that 3W2 (Figure A.1) is connecting the 2TFE (Figure A.1) and BPR1 (Figure A.1).
17. Make sure that 3TFE (Figure A.1) is closed.
18. Reopen N2_C_3 (Figure A.1).
19. Make sure that 3W3 (Figure A.1) is open connecting BPR2 (Figure A.1) and the CaSO₄ trap (Figure A.1).

20. Make sure that the TFE MFC (Figure A.1) (mass flow controller for the TFE line) is open.
21. Open 2W1 (Figure A.1)
22. Open 3TFE (Figure A.1)
23. Open 1N (Figure A.1), verify pressure on PT2 (Figure A.1) and PT3 (Figure A.1) are equal.
24. Close 1N (Figure A.1), monitor for 10 minutes. If the pressure holds then the specified section is considered leak free.

**Procedures for section from N2_C_2 and MON_C_1 cylinder, to Small Autoclave
(2W7)**

25. Make sure that the regulator on MON_C_1 (Figure A.1) is closed.
26. Make sure that 3W4 (Figure A.1) is open between N2_C_2 (Figure A.1) and MON_C_1 (Figure A.1) cylinder.
27. Open N2_C_2 tank valve and adjust regulator to 410 psig.
28. Close 2W7 (Figure A.1)
29. Make sure that the MON1_MFC (Figure A.1) is open.
30. Open 1MON1 (Figure A.1) and 1MON2 (Figure A.1) and verify with the laser indicators that these valves are open (green - at the valve control panel).
31. Monitor the pressure (LED and computer) on PT6 (Figure A.1).

32. Close 3W4 (Figure A.1) and follow the pressure (LED and computer) for 10 minutes on PT6 (Figure A.1).

SOP for Leak Checking the Small Autoclave (600-mL) from MON1 Direction

33. Make sure that the feed lines for MON1, TFE, and initiator (3W5 is turned away from the large autoclave) are connected as well as the electronics for the autoclave's pressure transducer, thermocouple, tachometer, stirring motor, and oven.
34. Make sure that 3TFE (Figure A.1), 2N (Figure A.1), and 1N (Figure A.1) are closed.
35. Make sure that 3W4 (Figure A.1) is connecting the N2_C_2 (Figure A.1) cylinder in the direction of the autoclave.
36. Make sure the vent valve AA11 (Figures A.1, A.2) on the large autoclave (2-gal) is closed. To do this, turn 3WL (Figure A.4) in the direction of the large autoclave (AA11) and vent 3WK (Figure A.4).
37. Make sure that 2W6 (Figure A.1), 2W7 (Figure A.1), 2W8 (Figure A.1), and AA12 (Figure A.2) are closed; the latter is done by making sure that valve 3WL (Figure A.4) is vented in the direction of AA12 (Figure A.2) and by venting 3WK (Figure A.4).
38. Make sure that the radical initiator line is closed. This is done by turning 3W6 (Figure A.3) to the closed position.
39. Make sure that the MON1_MFC (Figure A.1) is open.
40. Make sure that the control box of the autoclave is turned ON.

41. Open 2W7 (Figure A.1).
42. Watch the PT (Figure A.1) on the autoclave control box come up.
43. Close 1MON2 (Figure A.1).
44. Monitor the pressure on the autoclave control box for 10 minutes. If the pressure holds, then the specified section is considered leak free.
45. Open vent (AA12) (Figure A.2) on the autoclave by applying air back to 3WK (Figure A.2) (in the Control Room) and monitor the pressure drop on the autoclave control box; close AA12 as soon as possible.

SOP for Polymerizations – Small Autoclave

46. Follow the procedural steps suggested by the sponsor as well as the specifics outlined in the Run Sheet for the specific run.
47. Prepare the radical initiator solution and load the syringe pump (See SOP for loading the ISCO pump).
48. Open the bleed 3W6 (Figure A.3) valve of the radical initiator line and place the bleed line in a 20 cc vial (provided). Start the pump and wait until the solution is coming out of the bleed end of the line and add a test strip to the vial. Bleed until the flow is uniform and bubble free and changes the test strip to a dark purple color.
49. Stop the ISCO pump and close the bleed 3W6 (Figure A.3).
50. Start the data acquisition system (See SOP for data acquisition system start up).
51. Make sure that 1MON2 (Figure A.1) and 3TFE (Figure A.1) are closed.

52. Heat the reactor to 83 °C by adjusting the temperature on the Autoclave control box located in the control room.
53. Start the stirring on the reactor to the rpm specified on the run sheet.
54. Open AA12 (Figure A.1, A2) to drop the pressure of the reactor to atmospheric pressure.
55. Close AA12 (Figure A.1, A2).
56. Open 2W7 (Figure A.1, A2).
57. Open initiator feed line 3W6 (Figure A.3) towards the small autoclave.
58. Make sure that 1MON1 (Figure A.1) and 1MON2 (Figure A.1) are closed.
59. Open MON_C_1 (Figure A.1) valve and adjust regulator so that PT6 reads 400 psig.
60. Open 2W6 (Figure A.1, A2).
61. Make sure that 1TFE (Figure A.1) and 2TFE2 and 3TFE (Figure A.1) are closed.
62. Open TFE_C_1 (Figure A.1) valve and adjust regulator so that PT1 reads 400 psig.
63. Walk out of the reaction module, lock the reaction module and place the red shade on the Status Lamp outside the reaction room to indicate that there is a reaction running.
64. Put up the yellow safety chain and signage blocking egress through the main gate to the facility and go inside the control room and close the door.
65. Set the MON1_MFC (Figure A.1) feed rate to 1 SLM and change display to totalizer SL.
66. Open 1MON1 (Figure A.1) and 1MON2 (Figure A.1).

67. Monitor PT on the autoclave (Figure A2) until 200 psig is reached and then close 1MON2.
68. If the pressure drops then the water inside the autoclave is not saturated with the MON1 (Figure A.1) gas. If this is the case, open 1MON2 (Figure A.1) to bring the pressure up to 200 psig.
69. Once the pressure inside the vessel is stable, we know that the water has been saturated with monomer.
70. Set the TFE MFC (Figure A.1) feed rate to 1SLPM and change display to totalizer SL.
71. Open 1TFE (Figure A.1) and 2TFE and then 3TFE (Figure A.1).
72. The pressures of PT1 (Figure A.1) and the PT (Figure A.2) on the autoclave control box should both read 400 psig after a few minutes.
73. Close 3TFE (Figure A.1) and observe the pressure. If the pressure drops then the water inside the autoclave is not saturated with the TFE C 1 (Figure A.1) gas. If this is the case, open 3TFE (Figure A.1) and wait for few more minutes.
74. Once the pressure inside the vessel is stable, we know that the water has been saturated with monomer.
75. Open 1MON2 and 3TFE (Figure A.1) and observe little to no flow on both MFCs before proceeding.
76. Add the initial charge of radical initiator from the ISCO pump controller and then set the feed to the desired feed rate of initiator for the remainder of the polymerization.

77. Follow the totalizer on MON1 MFC controller until standard liters of MON1 have been fed as specified on the run sheet. Follow the totalizer on TFE MFC and record the value upon shutdown. Then proceed to SOP for Shut Down.

SOP for Shut Down (Small Autoclave).

78. Turn OFF the heat from the autoclave control box (SEE SOP for operating the Autoclave Control box).
79. Close 1MON1, 1MON2, 1TFE, 2TFE and 3TFE.
80. Stop initiator feed from ISCO pump.
81. Let the reactor cool to less than 50 °C.
82. Let the reactor reach an internal pressure of ideally less than 150 psig. If 150 psig is not reached in a reasonable time proceed to next step.
83. Vent the reactor using AA12 (Figure A.2) for the 600-mL reactor.
84. Turn off stirring.
85. Reaction Module is now safe to enter.

SOP for collecting Latex (Small Autoclave).

86. Drop the heater.
87. Close 2W7 (Figure A2), 2W8 (Figure A.2), 3W6 (Figure A.3).

88. Disconnect monomer feed lines, vent line, initiator feed line, stirring motor, PT, and thermocouple.
89. Physically carry reactor into CETL.
90. Place reactor in vice.
91. Open the reactor, drop the vessel and take a picture or pictures of the inside.
92. Execute the latex stability test (see SOP for taking a latex stability test).
93. Take 2 samples of 1-2 mL of the latex and take them to AMRL for further testing (% solids, etc.).

SOP for Purging the MON1 Line.

94. Close the MON1 cylinder regulator and valve.
95. Make sure that 2N is closed and 3W4 is open from the N2_C_2 to the MON1 line.
96. Open N2_C_2.
97. Walk out of the reaction module and close the reactor module door and walk into Control Room.
98. Open 1MON1 and 1MON2 and flush the line for 5 minutes with nitrogen.
99. Close 1MON1 and 1MON2.
100. Follow SOP for Idle Conditions

SOP for Purging the TFE Line.

101. Close the TFE_C_1 cylinder regulator and valve.
102. Make sure that 1N is closed and 3W1 is open from the N2_C_1 to the TFE_C_1 cylinder line.
103. Open N2_C_1.
104. Walk out of the reaction module and close the reactor module door and walk into Control Room.
105. Open 1TFE, 2TFE and 3TFE and flush the line for 5 minutes with nitrogen.
106. Close 1TFE, 2TFE and 3TFE.
107. Follow SOP for Idle Conditions

Table A.1. List of all the components located in the diagrams for the gas handling system and reaction room.

Part Code	Description	Location on Facility	Location on Drawing	Idle Condition
N2_C_1	Nitrogen Cylinder Tank	Reaction Room	Figure A.1	Closed
N2_C_2	Nitrogen Cylinder Tank	Reaction Room	Figure A.1	Closed
N2_C_3	Nitrogen Cylinder Tank	Reaction Room	Figure A.1	Closed
TFE_C_1	Nitrogen Cylinder Tank	Reaction Room	Figure A.1	Closed
TFE_C_2	Nitrogen Cylinder Tank	Reaction Room	Figure A.1	Closed
MON_C_1	Nitrogen Cylinder Tank	Reaction Room	Figure A.1	Closed
Autoclave Piston	Pneumatic Piston	Reaction Room	Figure A.1	N/A
Autoclave Vessel	Autoclave Vessel	Reaction Room	Figure A.1	Open
TFE_MFC	Mass Flow Controller	Reaction Room	Figure A.1	OFF
MON1_MFC	Mass Flow Controller	Reaction Room	Figure A.1	OFF
3W1-3W4	Three Way Valve	Reaction Room	Figure A.1	Closed
3W5-3W6	Three Way Valve	Reaction Room	Figure A.3	Closed
2W1, 2W3, 2W4	Two Way Valve	Reaction Room	Figure A.1	Closed
2W2	Two Way Valve	Control Room	Figure A.1	Closed
1V-3V	Air Actuated Valve	Reaction Room	Figure A.1	Closed
1TFE-3TFE	Air Actuated Valve	Reaction Room	Figure A.1	Closed
1MON1-1MON2	Air Actuated Valve	Reaction Room	Figure A.1	Closed
CaSO4 Trap	Calcium Sulfate Trap	Reaction Room	Figure A.1	N/A

Table A.1 Continued. List of all the components located in the diagrams for the gas handling system and reaction room.

BPR1-BPR2	Back Pressure Regulator	Reaction Room	Figure A.1	N/A
BPR1 DOME Valve	Needle Valve	Control Room	Figure A.1	Open
BPR2 DOME Valve	Needle Valve	Control Room	Figure A.1	Open
Bleed 1 Valve	Needle Valve	Control Room	Figure A.1	Open
Bleed 2 Valve	Needle Valve	Control Room	Figure A.1	Open
PT1-PT6	Pressure Transducer	Reaction Room	Figure A.1	N/A
1N-2N	Air Actuated Valve	Reaction Room	Figure A.1	Closed
2WL, 2WR	Two Way Valve	Reaction Room	Figure A.3	Closed
ISCO Pump	ISCO Syringe Pump	Reaction Room	Figure A.3	OFF
3W7	Three Way Valve	Reaction Room	Figure A.1	Closed
2W5-2W8	Two Way Valve	Reaction Room	Figure A.2	Closed
AA11, AA12	Two Way Valve	Reaction Room	Figure A.2	Closed
3WK	Three Way Valve	Control Room	Figure A.4	Vent
3WL	Three Way Valve	Control Room	Figure A.4	Back and Forth*
2W9	Two Way Valve	Reaction Room	Figure A.1	Closed

Note: 3WL has to be placed in Idle position after 3WK is set to the idle position.

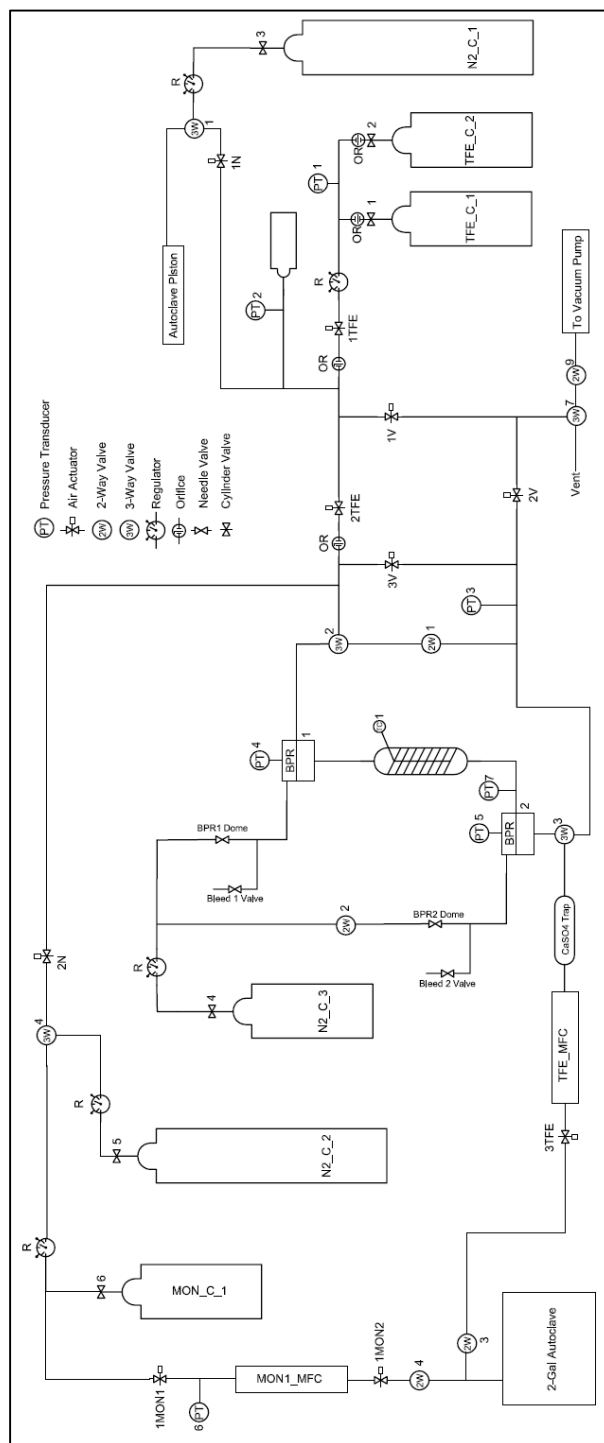


Figure A.1. Gas handling system schematic diagram. A larger format image is included in Appendix B.

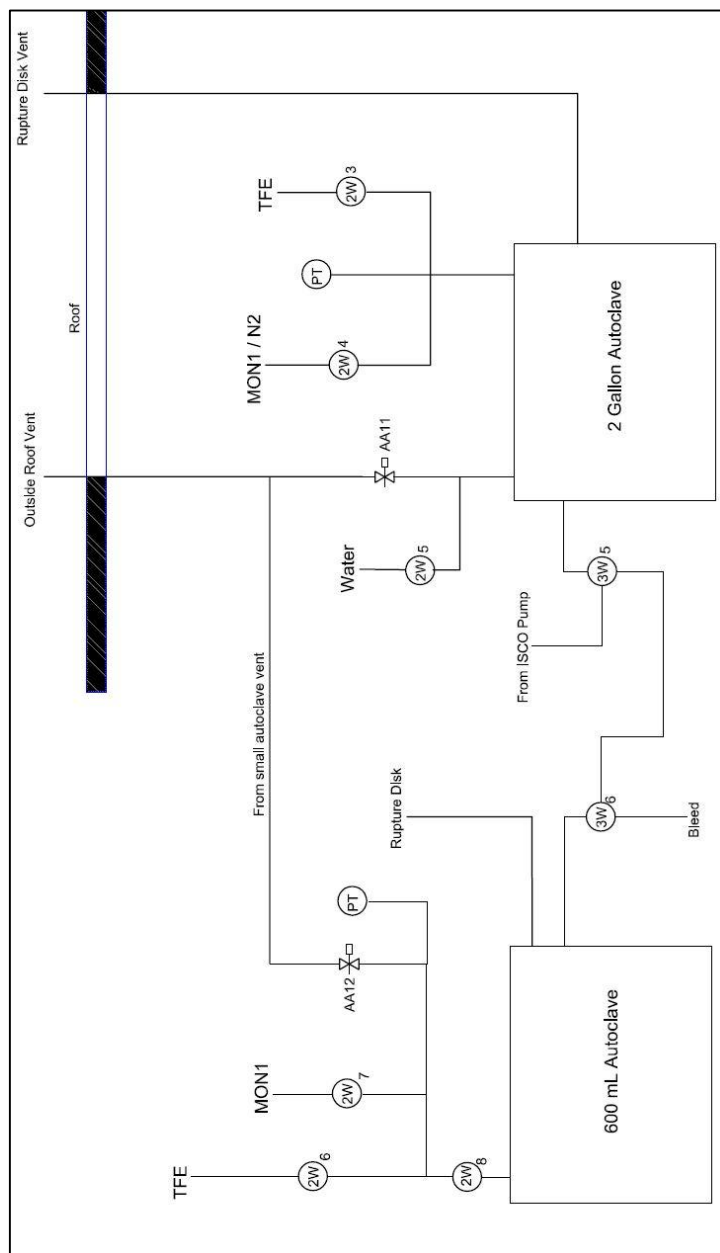


Figure A.2. Schematic of valves at autoclave heads.

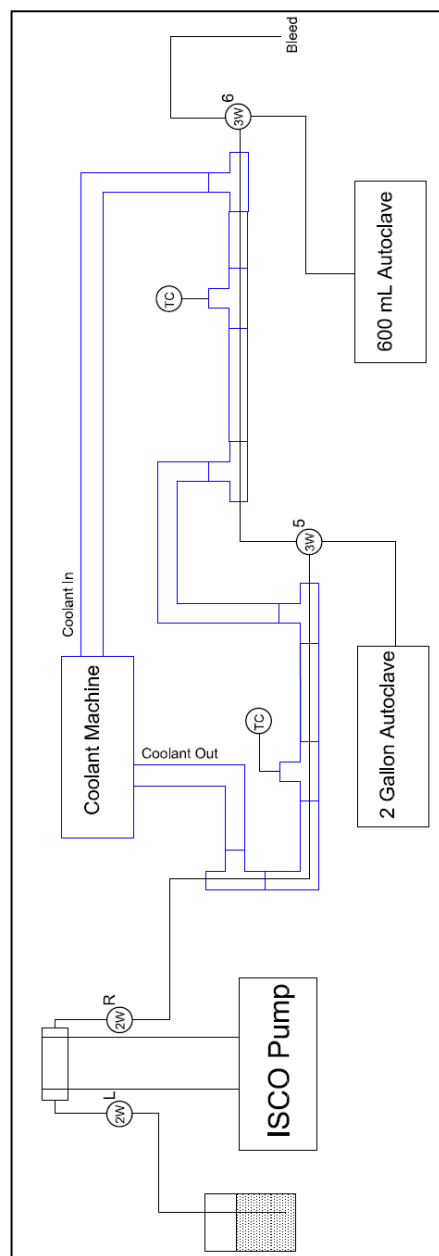


Figure A.3. Schematic for ISCO pump system.

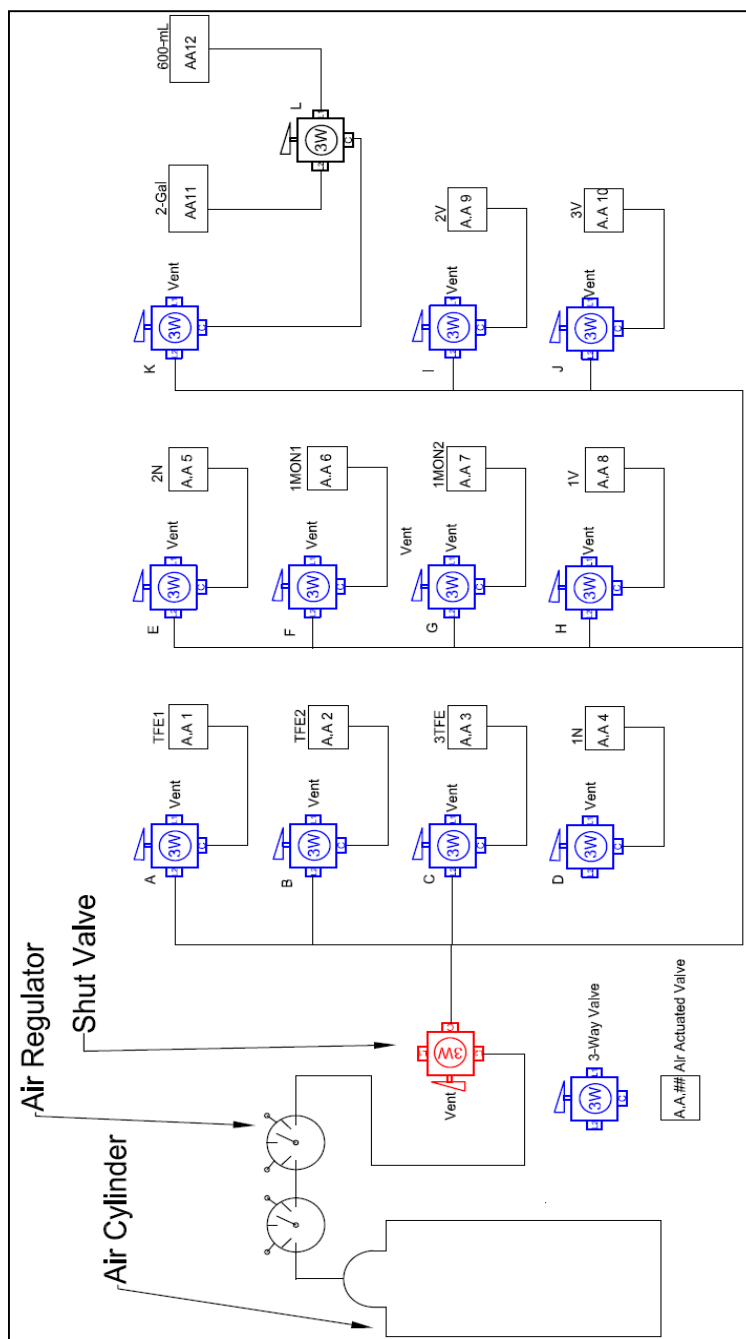


Figure A.4. Connection layout for air actuated valves. The Valve colored in black is located in the reaction room while the ones colored in red are the ones located in the control room.

A.1.3. SOP for ISCO Pump Operation.

1. Make sure, that there is sufficient amount of the initiator solution in the "Inlet Fluid" container (recommended to have approximately 50 mL more than required for current reaction) and inlet tube immersed all way down to the bottom of the container.
2. Turn power switches on ISCO pump (in reaction module) and on ISCO pump controller (in the control room) ON
3. Make sure that ISCO pump is empty (if NOT empty it following "bleeding step" SOP for leak-check).
4. Make sure that 2WR on ISCO pump is closed and then open 2WL.
5. Press "Refill" button on the ISCO pump controller and wait until pump will be filled with solvent (it will be done automatically).
6. Close 2WL and open 2WR.
7. Bleed air (follow "bleeding step" SOP for leak-check)
8. To set up flow rate, press "CONST FLOW" button on the pump controller, then set up required flow rate and press "ENTER". Pump is ready.
9. To start delivery of the initiator solution, press "RUN".
10. After required amount of the initiator is delivered, press "STOP" on the Pump Controller.
11. After the reaction is completed, flush pump with deoxygenated DI water 3-4 times, empty pump and turn power switches OFF on both pump and controller.

A.2. SOP for Scrubbing Carbon Dioxide (CO₂) from TFE/CO₂ Mixture.

NOTES:

- The controls of the underlined items (for example 3W1) are located in the reaction room as part of the gas handling system, and the controls of the items that are not underlined are located in the control room.
 - Prior to evacuating any section of the gas handling system with the vacuum line, the pressure in that section should be reduced to less than 40 psig, if at possible. If not possible and one is suspicious of high pressure in the section, then vent pressure through 3W7 prior to slowly opening 2W9.
 - When evacuating a section of the gas handling system with the vacuum line, the evacuation should continue for 15-20 minutes after the best vacuum level is reached in order to insure sufficient removal of oxygen.
 - When carrying out evacuation-refill with nitrogen steps, the procedure should be carried out three (3) or more times in order to insure sufficient removal of oxygen.
1. As described in the following steps, first prepare the individual components of the CO₂ Scrubbing System shown in Figure A5 that will be used for scrubbing CO₂ from the TFE/CO₂ mix, which will take advantage of as much remote control from the Control Room as possible with the system for scrubbing CO₂ being set-up in the Reaction Module.

2. Replace the internal dip-leg on the 2-gallon autoclave on what will be the TFE/CO₂ inlet (2W3, see Figure A5), as the large autoclave will be used to contain the aqueous caustic solution that will be used to scrub the CO₂. Connect the TFE/CO₂ feed line (flex hose after 3TFE air-actuated valve) to the inlet valve 2W3 (on the dip-leg) of the autoclave (Caustic Scrubber). Make sure that 2W3, 2W4, and 2W5 are closed.
3. Make sure that the TFE gas handling system (through 1TFE, 2TFE, BPR1, BPR2, etc.) from TFE_C_1 and TFE_C_2 to 3TFE is oxygen and leak free. To do this, first carry out the following steps to evacuate and leak-check the system from 1TFE back to TFE_C_1 and TFE_C_2. Make sure that 1N, 1TFE, 2TFE, and 3TFE are closed, and open 1V. In case of high pressure in the system (PT2), first vent through 3W7, and then open 3W7 toward vacuum and slowly open 2W9 to evacuate the gas-handling system back to 1TFE. Once this section is evacuated and leak-checked, open 1TFE and dial in the diaphragm on the in-line TFE regulator. This should allow the system to be pumped out back to TFE_C_1 and TFE_C_2. Close 2W9, 3W7, 1TFE, and dial back the diaphragm on the in-line TFE regulator. Then follow steps 1-24 in the SOP entitled Leak Checking the Gas Handling System for the large autoclave. This will leave 400 psig of N₂ pressure up to 3TFE; open 1TFE to also pressurize the section of the system back to TFE_C_1 and TFE_C_2 with nitrogen. 1N will be closed once step 24 is completed.
4. Cap off the vent line to the small autoclave, which will typically not be in place when this procedure is being carried out. Open 1N, 3TFE, and 2W3 to pressurize the autoclave with 400 psig of nitrogen and leak check the autoclave. Close 2W3, and

vent the autoclave by opening AA11 and monitoring the pressure transducer on the autoclave. Close AA11, open 2W3, and re-pressurize the autoclave with nitrogen, followed by venting again. Do this several times to flush out the gas handling system and the autoclave with nitrogen. Make sure that both 2W3 and AA11 are closed.

5. While lowering the remaining pressure in the gas handling system and the autoclave not more than 20 psig, adjust the N₂ pressure to ca. 20 psig on the regulator on N2_C_1; close 1N.
6. Since this step will be done at AMRL, it can be done in advance of steps 1-5. In the glove bag in AMRL Lab 3, prepare 5,000 mL of a 45-wt% solution of KOH (1.456 g/mL) from ca. 4,004 g of deionized, deoxygenated water and ca. 3,276 g (58.4 mol) of KOH flakes/pellets. Since the balance in the glove bag does not have a sufficiently high weight range, the caustic solution will have to be made up in aliquots in a large beaker, and each aliquot poured into the Jerry Can after weighing. Four (4) aliquots each of ca. 1,000 g of water and ca. 820 g of KOH should work.
Caution: Carefully add the KOH flakes/pellets into the water in the beaker, as the dissolving of KOH will be very exothermic; some external cooling with an ice bath may be necessary. (Note: The KOH flakes/pellets may contain some included air, so it may become necessary to do addition degassing of the caustic solution with nitrogen gas within the glove bag. The gaseous oxygen sensor should give an indication of whether or not this is necessary.) This should give ca. 5,000 mL of a 45-wt% solution of KOH (1.456 g/mL) for use in the large autoclave, which will make it nominally two-thirds full. This should be enough KOH to scrub at least

14.6 moles of CO₂ (two-fold excess of base) by the reaction $2 \text{KOH} + \text{CO}_2 \rightarrow \text{K}_2\text{CO}_3 + \text{H}_2\text{O}$, and all of the K₂CO₃ formed should still be soluble even if all of the KOH is consumed.

7. Connect the Jerry Can with the aqueous caustic solution to the large autoclave at 2W5 (water inlet valve for suspension polymerizations) via a section of Tygon tubing. Connect the autoclave to the vacuum line through 2W4 and another section of Tygon tubing. Evacuate first the Tygon tubing to valve 2W4, then open 2W4 to evacuate the autoclave, and finally open 2W5 to evacuate the piece of Tygon tubing making the connection to the Jerry Can. Make sure that these connections are leak free, and if necessary back fill with 15-20 psig of nitrogen from the gas handling system through 2W3, re-evacuate, and repeat the process two to three times to make sure that the system is oxygen free.
8. Once the system is leak free and evacuated, make sure that 2W3 and 2W4 are closed. Open the valve at the bottom of the Jerry Can and allow the caustic solution to flow into the large autoclave. When the bulk of the contents of the Jerry Can have emptied, close the valve at the bottom of the Jerry Can and valve 2W5. Remove the Jerry Can and the connecting piece of Tygon tubing.
9. Turn on the cooling machine connected to the internal cooling coil of the large autoclave, adjust the set point to 0 °C, and start cooling the bath (ethylene glycol/water) the set point. Adjust the autoclave controller so that the solenoid valve to the cooling machine opens in order to start cooling the caustic solution to 0 °C.

10. This step should be done in advance of steps 1-9. Load a 500-mL double-ended cylinder with CaSO_4 (Drierite without indicator, 8 mesh). This should take about 500 grams of Drierite with a loading density of ca. 50% of the density of CaSO_4 (2.96 g/mL). Attach this cylinder to a vacuum line and heat to 180 °C overnight to completely dry the Drierite. Then allow the CaSO_4 scrubber to cool to RT under vacuum, make sure that it is leak free, and then close the inlet- and outlet-valves.
11. Connect the inlet of the CaSO_4 scrubber to the outlet of 2W5.
12. This step should be done in advance of steps 1-9. Load a 150-mL trap cylinder with ca. 100 mL (84.11 g) of D-limonene, replace valve/dip-leg assembly, and take through several freeze-pump-thaw cycles to remove all dissolved air. Close both cylinder valves.
13. This step should also be done in advance of steps 1-9. Assemble the TFE Collection Trap after having added ca. 50 g of D-limonene in the cylinder, go through several freeze-thaw-pump cycles in order to evacuate the cylinder and degas the D-limonene. Check to make sure that the cylinder is leak free. Close all cylinder valves.
14. Assemble the CO_2 Scrubbing System as outlined in Figure A5. Connect the system to the vacuum line after the TFE Collection Trap as shown. Cool the bottom of the collection trap with liquid N_2 in order to keep the Limonene from pumping away (D-limonene: b.p. = 176 °C; m.p. = -74 °C). Pull a vacuum on the cooled TFE Collection Trap, the connection between TFE Collection Trap and the Limonene Bubbler, the connection between the Limonene Bubbler and the CaSO_4 Scrubber, the CaSO_4 Scrubber, and the connection between the CaSO_4 scrubber and the Caustic

Scrubber. Make sure that these sections are leak free, and after having evacuated them all with vacuum, back fill with high purity nitrogen up to 14.7 psia (0.0 psig) by use of the vacuum system (i.e., close 2TFE, 2V, 3W7, 2W9, and the main stopcock on the vacuum manifold to the ‘muck trap’; open 1V, followed by 3W7, the stopcock on the vacuum manifold that connects the gas handling system to the vacuum line, and then slowly open 2W9 while watching the test gauge pressure come toward 760 Torr). Leave the system under vacuum after several pump-purge cycles.

15. Prepare the cold bath TFE Collection Trap shown in Figure A5. The cold bath (isopropanol/Dry Ice) around the TFE Collection Trap should be ca. -70 °C (several inches of solid pieces of Dry Ice in the bottom of the Dewar should be sufficient to maintain -70 °C).
16. Once the cold baths are in place and at temperature and the CO₂ Scrubbing System has been assembled and made oxygen and leak free, open the inlet and outlet valves of the limonene bubbler at the same time, and then open the inlet and outlet valves of the Caustic Scrubber at the same time. This is to prevent any suck-back in case the pressure is different on either leg of these two trap cylinders.

The system should now be about ready to start the CO₂ scrubbing process, and a decision needs to be made by the Team whether to use the BPRs or not. If not, two methods exist to not use the BPRs: (A) leave BPR1 DOME and BPR2 DOME at atmospheric pressure, so they will basically act like open valves when inlet pressures above atmospheric are applied, or (B) by-pass them by turning 3W2 towards 2W1,

opening 2W1, and turning 3W3 towards 2W1. If Method A is chosen, then bleed the Dome pressures off the BPRs, and if Method B is chosen, then some of the following steps with respect to the BPRs will not apply.

17. Verify that BPR1 DOME, BPR2 DOME, BLEED 1 and BLEED 2 valves are closed.
18. Verify 2W2 (Figure A.1) is open.
19. Make sure that 1TFE, 2TFE, and 3TFE are closed. Slowly open the cylinder valve of either TFE C 1 or TFE C 2 and observe the pressure of the TFE/CO₂ mix on PT1. Adjust the in-line TFE regulator delivery pressure to 40 psig.
20. Open N2_C_3 tank valve (Figure A.1) and adjust the regulator to 150 psig.
21. Adjust the pressure on the regulator of N2_C_1 to ca. 40 psig.
22. Open 2W3 and 2W5 to the Caustic Scrubber, i.e., the TFE/CO₂ feed line and scrubbed-TFE exit line. Close door to Reaction Module and go to Control Room and close door.
23. Open BPR1 DOME and BPR2 DOME valves to allow pressures of 150 psig on PT4 and PT5. Close BPR1 DOME and BPR2 DOME valves. Close 2W2.
24. Open 1TFE and observe TFE/CO₂ pressure on PT2.
25. Open 2TFE and monitor pressure on PT2, which should increase to ca. 40 psig. Close 2TFE.
26. Close BPR1 DOME valve, and decrease the pressure on BPR1 DOME by slowly opening BLEED 1 valve. Allow the pressure on PT4 to decrease to within a few psig

(more or less) of the pressure on PT2. This should allow a slow flow of TFE/CO₂ through BPR1.

27. Observe the pressure increase on PT7.
28. Open TFE MFC (to a slow flow rate – to be determined) and 3TFE to allow flow of TFE/CO₂ mix to the CO₂ Scrubber System.
29. Close BPR2 DOME valve, and by using the BLEED 2 valve for BPR2, slowly lower the pressure on BPR2 DOME (PT5) to allow flow of TFE/CO₂ toward 3TFE at a pressure of about 20-40 psig; use the PT on the large autoclave (caustic scrubber) to monitor this.
30. By opening and closing 2TFE and adjusting the BLEED 1 and BLEED 2 valves to control the pressure on BPR1 DOME (PT4) and BPR2 DOME (PT5), respectively, control the flow of TFE/CO₂ to the CO₂ Scrubber System. Should the flow become too fast, then open BPR1 DOME valve and/or BPR2 DOME valve and 2W2, as necessary, to either slow or stop the flow of TFE/CO₂ toward the CO₂ Scrubber System or simply close 3TFE. Also, continually monitor the pressure on the PT8 on the TFE Collection Trap, as the pressure of TFE at -70 °C should be ca. 19-20 psi.
31. As the TFE/CO₂ tank pressure (PT1) drops, BLEED 1 valve will have to be controlled in order to allow flow across BPR1 (and perhaps BLEED 2 valve for BPR2). When the pressures on PT1, PT2, and PT7 approach atmospheric, then the bulk of the TFE/CO₂ mix has passed through the system. This should also be indicated by the cessation of flow across TFE MFC, too. Close 1TFE, 2TFE, and 3TFE.

32. Enter the Reaction Module and close the cylinder valves on the TFE Collection Trap. Then close the exit valve of the Limonene Bubbler and disconnect the TFE Collection Trap (cap/plug the valves to this cylinder).
33. Open 1N, 1TFE, 2TFE, and 3TFE and allow approximately 40 psig of nitrogen pressure to flow into and pressurize the system.
34. Enter the Reaction Module and slowly open the exit valve on the Limonene Trap allowing nitrogen to purge through the system. Exit the Reaction Module during the purging procedure.
35. After 15-30 minutes of nitrogen purge, re-enter the reaction module and close the exit valve of the Limonene Trap.
36. Close 1N, 1TFE, 2TFE, 3TFE, and the valve to TFE C 1 and TFE C 2. The tare weights of the TFE/CO₂ feed cylinders should be checked to verify that all of the mixture has been fed through the caustic scrubber system. It should now be safe to disassemble the system and prepare the components for future use.

A.3. SOP for Leak Check in Vacuum Line in the Reaction Room for Transferring TFE from a Large Cylinder to High Pressure Cylinder Through Transfer Cylinder.

Usually a pressure of 40-50 psi of nitrogen gas shown on digital pressure gauge DPG1 is left in the metal line system with VL2, V1, V3, and V4 valves closed to the pump. Be sure that Nitrogen gas cylinder valve and TFE high-pressure valve is closed, Nitrogen trap down and vacuum pump off. Also the heating mantle on diffusion oil trap must be off.

1. Start the vacuum pump and put liquid nitrogen tarp and switch on heating mantle on diffusion oil trap.
2. Open VL2, V2, V1, V3, and V4 valves and let the nitrogen evacuate through the vacuum pump.
3. Open VM, VB1, VB2, VB3 to create vacuum in glass line as well. Wait till it pulls the vacuum to at least 10-15 microns.
4. Close VL2, V1, VM, VB3 valves, and open valve on nitrogen gas cylinder.
5. Open V1 valve slowly to have a pressure of about 50 psi in the line, See pressure reading on digital pressure gauge DPG 1. Close V1 valve. Now slowly open VM valve to have a pressure of 760 mmHg (Torr) shown on digital pressure gauge DPG2 in glass line and in bulb.
6. Close Nitrogen cylinder valve and close VM valve. Check the pressure on DPG1 and DPG2 for 15 minutes that it stays same.
7. Open VL2 and let nitrogen gas evacuate, then open VB3 valve to evacuate nitrogen gas from glass line. Wait till vacuum is 10-15 microns.

8. Repeat step 5-8 to be sure that there is no oxygen (air) in system.
9. Evacuate till vacuum is 10-15 micron

A.4. SOP for Transferring TFE from a Large Cylinder to a Small Transfer Cylinder (500 cm³ volume).

1. Put liquid nitrogen Dewar under transfer cylinder and evacuate it opening V4, V2, VL2, VL1.
2. Be sure that N₂ cylinder valve is closed. Close V1, V2, V3, V4, VM and VB3. Be sure VB1, VB2 open.
3. Open Large TFE cylinder valve slowly, and then open next valve to it slowly.
4. Open V1 slowly only to 20° and then open slowly VM valve slowly to fill bulb (1 liter) at 760 mmHg shown on digital pressure gauge DPG2, which reads as 0.760.
5. When reached to 760 mm Hg pressure close V1 valves. Open V4 valve slowly to transfer TFE from bulb to transfer cylinder. In last open VM valve fully. Keep putting liquid nitrogen in Dewar for transfer cylinder.
6. When all TFE is transferred, check pressure on digital transducer to be nearly 0.00-0.02 mm Hg
7. Close V4 and VM. Repeat steps 4-6 for 10 times. After transferring the last TFE segment into transfer cylinder, Close valve on TFE big cylinder and open V1 valve and V4 valve and transfer TFE in line into the transfer cylinder. After filling transfer cylinder, put some more liquid nitrogen in transfer cylinder Dewar and evacuate it

and close the valve. It will transfer about 80 g of TFE and perfluorocyclobutane to transfer cylinder. Perfluorocyclobutane is only 2-3% in TFE.

A.5. SOP for Transferring TFE From a Transfer Cylinder to a High Pressure Cylinder (500 cm³ volume).

1. Remove liquid nitrogen from transfer cylinder and put a slush of pentane and liquid nitrogen to have a temperature of about -80 to -100 °C, so that when TFE transferred to high pressure cylinder, perfluorocyclobutane stays in transfer cylinder.
2. Put liquid nitrogen under high pressure cylinder, and evacuate it through V3, V2, VL2, and VL1. Be sure V1, V4, and VM are closed.
3. Close V3, V2. Open V4 slowly and then open VM to fill TFE from transfer cylinder to the bulb till it reads 760 mmHg on digital pressure gauge DPG2. Close V4.
4. Open V3 to transfer TFE from bulb to high pressure cylinder. Keep putting liquid nitrogen in Dewar of high-pressure cylinder.
5. Repeat steps 3 and 4, ten times to transfer 80 gm of TFE to high-pressure cylinder. This will give a pressure of about 400-500 psi in high pressure cylinder.
6. Keep an eye on transfer cylinder temperature that it does not exceed higher than -80°C.
7. After transferring last portion of TFE, close valve on transfer cylinder. Open V3 and V4 and transfer TFE in line into high-pressure cylinder and evacuate high-pressure cylinder under liquid nitrogen Dewar, and put liquid nitrogen under transfer cylinder as well and evacuate it by opening its valve and close both cylinders and remove

liquid nitrogen traps in both cylinders. Do not close too hard. They are needle valve and can easily damage by a little wrestling.

8. After pulling vacuum on line about 10-15 microns, close V1, VL2, V3, V4. VM, and VB3. Open nitrogen gas valve. Then open V1 to add nitrogen gas into metal line up to pressure of 30-40 psi, read on digital pressure gauge DPG1. Close nitrogen gas cylinder valve. Drop liquid nitrogen trap and let highly volatiles go to pump. Give air to pump by opening valve in liquid nitrogen trap and switch off the pump, and leave the room. Switch off lights before you leave.

Do not forget to evacuate the lines before and using them to avoid traces of oxygen. Open TFE valves slowly. The heat of friction of the gas against the walls of the tubes is enough to make TFE deflagrate. Evacuate the entire system before using. Purge the entire system at least 3 times with high purity nitrogen before using the gas handling system or after breaking a tight connection. After using the vacuum line, please remove the liquid nitrogen Dewar and vent the mug trap.

A.6. SOP for Transferring TFE at Hunter Barricade.

Stages of the process

1. Initial state and leak check
2. Evacuation of the system and fill with nitrogen (several times)
3. Transferring of TFE
4. Condensing the TFE in the line after the transfer is done.
5. Purge
6. Transportation of TFE to storage location outside campus

A.6.1. Preparation before hand

1. Make sure that the TFE collection cylinder is leak free beforehand and that 50 g of R-Limonene are added to it. Please record all the tare weights with limonene and the empty cylinder as well.
2. Prepare the Digital pressure transducer to use in the process. This includes the software, hardware and power supply.
3. Prepare the flex hoses that are going to be used
4. Collect enough liquid nitrogen or dry ice
5. Make sure that the MFC is opening and closing appropriately and that the cable is long enough to operate it from outside the barricade.

A.6.2. Initial State and Leak Check.

1. Make sure that V1, V2, V3, V4, V5, V6 and R1 and R2 are closed and that MFC_TFE is open.
2. At any step forward, no TFE will be involved in the process but if a leak is found please proceed to tight up the connections involved in order to solve the leak.
3. Open V3 until vacuum reaches its maximum. Confirm the reading with the vacuum gauge located on top of the glass manifold outside the barricade.
4. Make sure the Valve on the TFE main cylinder (V1) is closed and proceed to open V3 until vacuum is reached.
5. Procedure to dial in the regulator on the TFE cylinder in order to open the path across the regulator and evacuate the space in between the regulator and the steam valve (V1).
6. Dial out the regulator on the TFE Cylinder all the way out and close V2.
7. Open V5 and dial in the regulator (R2) on the Nitrogen cylinder in order to open the path across the regulator and evacuate the space in between the regulator and the steam valve (V6).
8. Freeze the TFE collection cylinder in liquid nitrogen or dry ice and wait until the cylinder is frozen.
9. Dial out the regulator on the Nitrogen Cylinder all the way out and close V5.
10. Proceed to open V4 in order to evacuate the cylinder. Double check with the gauge previously described.

11. Close V4 and wait. No change in the vacuum gauge should be detected.
12. Make sure all the valves are closed at this point.
13. The system is now leak free.

A.6.3. Evacuating the System and Fill Back with Nitrogen.

1. Make sure that V1-V6 are closed and that MFC is open.
2. Open V6 and adjust the pressure on R2 to about 20 psi.
3. Open V2 and Dial in the Regulator on TFE Cylinder (R1) and wait until the pressure in the regulator reaches the same pressure on the regulator at the Nitrogen tank.
4. Wait until the flow across the MFC has stopped.
5. Close V5 to cut the nitrogen feed
6. Open V3 slowly to evacuate the system until maximum vacuum is reached.
7. Repeat steps 1 through 6 at least 3 times and move to step 8.
8. After repeating at least 3 times the procedure in steps 1-6, make sure all the valves are closed.

A.6.4. Transfer The TFE.

*During the process, make sure that the cylinder has enough dry ice or nitrogen to keep it under the right temperature

1. Make sure all the valves are closed.
2. Make sure that the TFE collection cylinder is frozen.
3. Reset the Totalizer on the MFC and close the MFC.
4. Make sure the regulator on the TFE cylinder is dialed out
5. Open V1 slowly and wait until the pressure comes up on the regulator of the TFE cylinder.
6. Dial in around 20 psi on the TFE regulator and slowly open V2. Double check the pressure with PT1.
7. Open V4
8. Move to the outside of the barricade and open the MFC and record the flow and the pressure every 5 minutes.
9. When the pressure of the tank reaches the 20 psi threshold of the regulator, its optional to dial back the regulator to about 10 psi to continue to transfer more material.
10. After all the transferring is done, close V1 and dial in the regulator of the TFE all the way in to get all the TFE in between the regulator and the steam valve.
11. Check the pressure with PT1, it should go negative under this conditions when all the TFE is transferred to the TFE collection cylinder.
12. Close V4.
13. At this point, no TFE is on the line and is safe to Open V5 and charge the line with nitrogen to dilute any TFE remaining on the line.
14. Close V5 and open V3 to evacuate the lines.
15. Close V3.

A.6.5. Transportation Back to AMRL Laboratories.

1. Make sure that the cylinder is still frozen
2. Move carefully the cylinder to the vehicle and make sure that the Dewar and the cylinder are secured in place.
3. Make sure that it has enough dry ice or nitrogen on the Dewar.
4. Proceed to drive to Perimeter Road, then Cherry Road and then use the back route to get to the CETL.
5. Locate the TFE collection cylinder inside the barricade and turn the IN USE light.

Appendix B

List of Necessary Components Used in the Construction of the TFE Barricade.

B.1. Parts Used in the Control and Reaction Room.

Table B.1. List of components, manufacturers and prices used in the Control and Reaction Room.

Item	Manufacturer / Supplier	Model / Catalog #	Unit Price (\$)	Date Inquired	Units Used
Reaction Room	U.S. Chemical Storage	SUPERLoc Model SL1610	45750.00	12/6/2010	1
Control Room	U.S. Explosive	Model ML263	28750.00	12/6/2010	1
Oxygen Sensors	Alpha Omega	Model 1000-B	1776.00	2/28/2013	2
LED Indicator Lights	Loftek	50 W RGB Exterior Light	66.99	4/16/2016	2
Power Supply	EVGA	1000 W	129.99	4/16/2016	1
Control Panels	Square D	Lowes Item # 67611	38.65	4/16/2016	3
Alarm Horns	ELK	30 W Alarm Horn	19.99	4/16/2016	2
Electrical Receptacles Installation (control room and reaction room)	Quality Electric Construction Inc.	NA	2499.00	8/9/2012	1
Autoclave Cooling Machine	Thermo Scientific	ULT-80	14262.50	4/6/2011	1
Vacuum Pump	Welch	Model 1402	2226.71	5/30/2012	1
2-Gal PARR Vertical Autoclave	Parr Instrument Company	4554-T-HD-SS-230-VS.50-2000-SC-BDV-4848-HCM-PDM-SVM-A1925E4-SpecView	37740.00	3/30/2011	1
1-Gal Conversion parts for the 2-Gal autoclave	Parr Instrument Company	NA	6055.00	3/30/2011	1

B.2. Parts Used in the Gas Handling System.

Table B.2. List of components, manufacturers and prices used in the gas handling system located in the reaction room.

Item	Manufacturer / Supplier	Model / Catalog #	Unit Price (\$)	Date Inquired	Units Used
Air Actuated Valve	Swagelok	SS-4BK-5C	555.35	4/20/2016	10
Orifice	Swagelok	SS-400-6PD-E-010	25.35	4/20/2016	4
1/4" SS tubing	Swagelok	SS-T4-S-035-20	4.38	4/18/2016	200
1/4" Swagelok M to 1/4" NPT F (Pressure Transducer)	Swagelok	SS-400-1-4	7.10	4/16/2016	6
1/4" Swagelok M to 1/4" NPT F (Air Actuators)	Swagelok	B-400-1-4	2.90	4/16/2016	10
Pressure Transducer Model G17M0215CD1000	Ashcroft	Grainger 5LRX6	196.50	4/16/2016	6
Mass Flow Controllers	Teledyne Hastings	HFC-202	1539.00	4/27/2016	2
1/4" Swagelok M to 1/4" NPT M (MFC)	Swagelok	B-400-1-2	3.10	4/16/2016	4
Reactor Vent Actuator	Swagelok	SS-HBS4-C	326.50	4/16/2016	2
Three Way Valve	Swagelok	SS-42GXS4	87.00	4/16/2016	4
Shut Valve	Swagelok	SS-42GS4	72.90	4/16/2016	4
Ballast Cylinder 300 mL single ended	Swagelok	304L-05SF4-300	218.00	4/16/2016	1
1/4" Stainless Steel Tee	Swagelok	A-400-3	16.20	4/16/2016	13
VDF Cylinder Regulator	Air Gas	Y12-N145G	626.30	4/16/2016	1
TFE Cylinder Regulator	Air Gas	Y11-N145G	396.00	4/16/2016	1
Stainless Steel In-Line Filter	Swagelok	SS-FCB	297.80	4/16/2016	2

B.3. Parts Used in the Valve Control Panel.

Table B.3. List of components, manufacturers and prices used in the air actuated valve panel located in the reaction room.

Item	Manufacturer / Supplier	Model / Catalog #	Unit Price (\$)	Date Inquired	Units Used
Shut Valve	Swagelok	SS-42GS4	72.90	4/16/2016	4
Three Way Valve	Swagelok	B-42XS4	49.60	4/16/2016	14
1/4" Swagelok Brass cross	Swagelok	B-400-4	14.00	4/16/2016	2
1/4" Swagelok Brass Elbow	Swagelok	B-400-6	6.60	4/16/2016	6
1/4" Swagelok Brass Tee	Swagelok	B-400-3T	15.10	4/16/2016	7
Control Panel Box	General Electric	Lowes Item #39399	149.00	4/16/2016	1
Air Regulator	Fisher Scientific	10-575-125	725.60	4/16/2016	1
1/4" Swagelok Male Union	Swagelok	SS-400-6	11.10	4/16/2016	6
Plastic Wall Cable Tray	Lowes	Monosystems Inc. CH512-KTW	2.31 / ft	4/12/2016	36
Three Way Valve Stainless Steel	Swagelok	SS-42GXS4	87.00	4/16/2016	1
1/4" Nylon Tubbing	Grainger	4HM08	64.50 / 100 ft	4/16/2016	1000 ft

B.4. Parts Used in the Radical Initiator and Cooling Lines.

Table B.4. List of components, manufacturers and prices used in the radical initiator solution feed line system.

Item	Manufacturer / Supplier	Model / Catalog #	Unit Price (\$)	Date Inquired	Units Used
3/8" Swagelok Tee for Thermocouple	Swagelok	B-600-3TTF	14.30	4/16/2016	2
3/8" Swagelok Tee	Swagelok	B-600-3TFT	14.30	4/16/2016	4
1/4" NPT M to 1/16" Swagelok M	Swagelok	SS-400-1-4	7.10	4/16/2016	4
1/4" NPT M to 1/8" Swagelok M	Swagelok	SS-400-1-2	6.90	4/16/2016	2
3/8" Tubbing Cu	Mueller Streamline	Lowes Item # 4182	58.90 / 50 ft	4/16/2016	40 ft
1/16" Tubbing SS	Swagelok	SS-T1-S-016-20-3P	17.25 / ft	4/16/2016	42 ft
ISCO Pump	Teledyne ISCO	100DM	15895.38	2/14/2012	2
K thermocouple 1/8"	Omega	CAIN-18(E)-12	32.00	4/16/2016	2
ISCO Pump Cooling Machine Model RTE 740	Thermo Scientific	TH-NERTE7	1995.00	4/27/2016	2
Three Way Valve 1/16"	Swagelok	SS-41GXS1	94.00	4/16/2016	2

B.5. Parts Used in the BPR Array.

Table B.5. List of components, manufacturers and prices used in the BPR Array.

Item	Manufacturer / Supplier	Model / Catalog #	Unit Price (\$)	Date Inquired	Units Used
Back Pressure Regulator - Hastelloy C	Core Laboratories LP	BP-50-HC	3892.00	3/30/2012	1
Back Pressure Regulator - Stainless Steel	Core Laboratories LP	BP-50-SS	3307.00	3/30/2012	1
Ascarite® Scrubbing Column	Sigma Aldrich	223913-100G	165.00 / 100 g	4/16/2016	1
1/4" Bulk Head Male Fitting	Swagelok	B-400-61	6.30	4/16/2016	4
1/4" Swagelok M to 1/4" NPT M (BPR)	Swagelok	B-400-1-2	3.10	4/16/2016	2
Calcium Sulfate Trap 500 mL double ended Cyl	Swagelok	316L-50DF4-500	343.60	4/16/2016	1
1/4" Swagelok union	Swagelok	SS-400-6	11.10	4/16/2016	18
Nitrogen Regulator	Victor	Model SR4F-680	1026.00	4/16/2016	1
1/4" SS tubing	Swagelok	SS-T4-S-035-20	4.38	4/18/2016	250 ft
Needle Valve	Swagelok	SS-4BMRG	423.10	4/16/2016	4
Shut Valve	Swagelok	SS-42GS4	72.90	4/16/2016	2

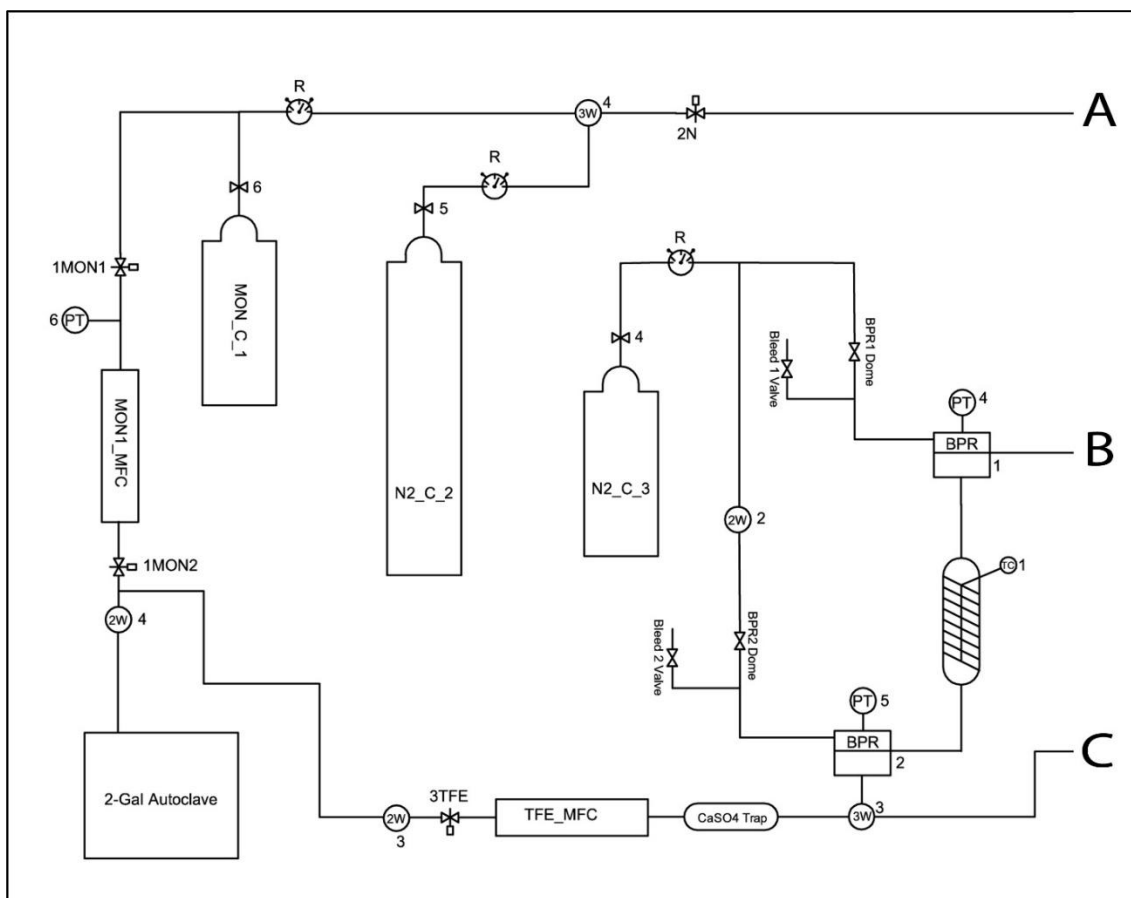


Figure B.1. Diagram of the left side of the gas handling line.

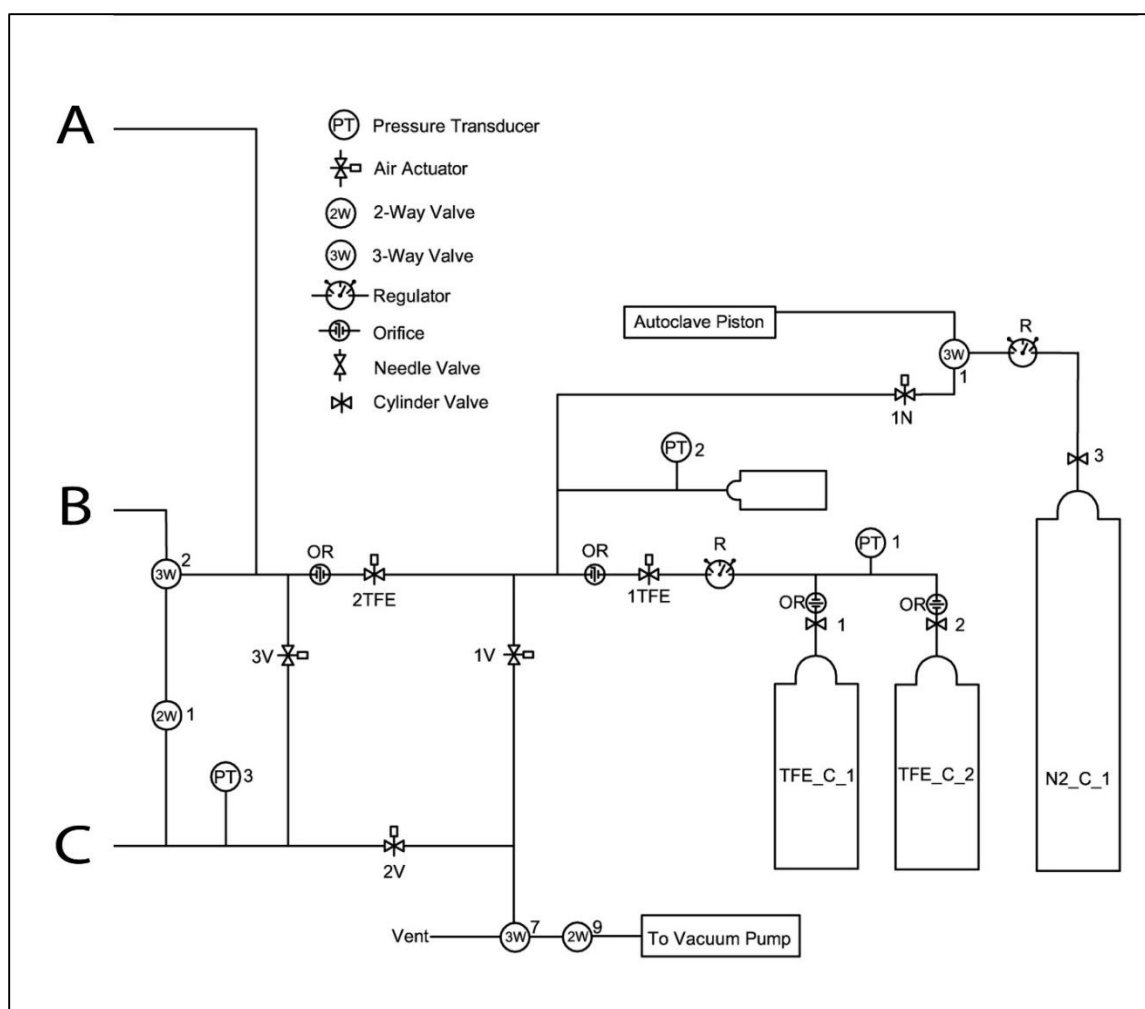


Figure B.2. Diagram of the right side of the gas handling line.

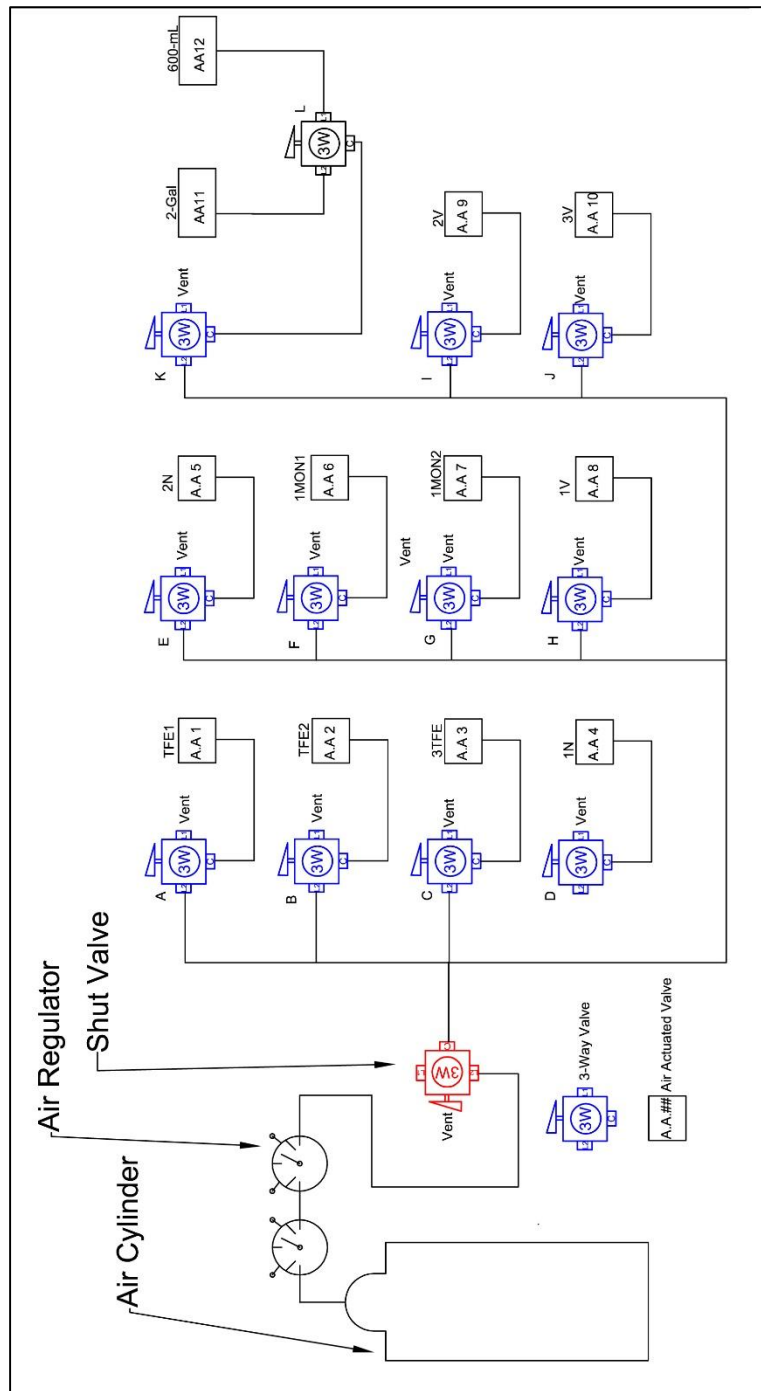


Figure B.3. Diagram of the valve panel.

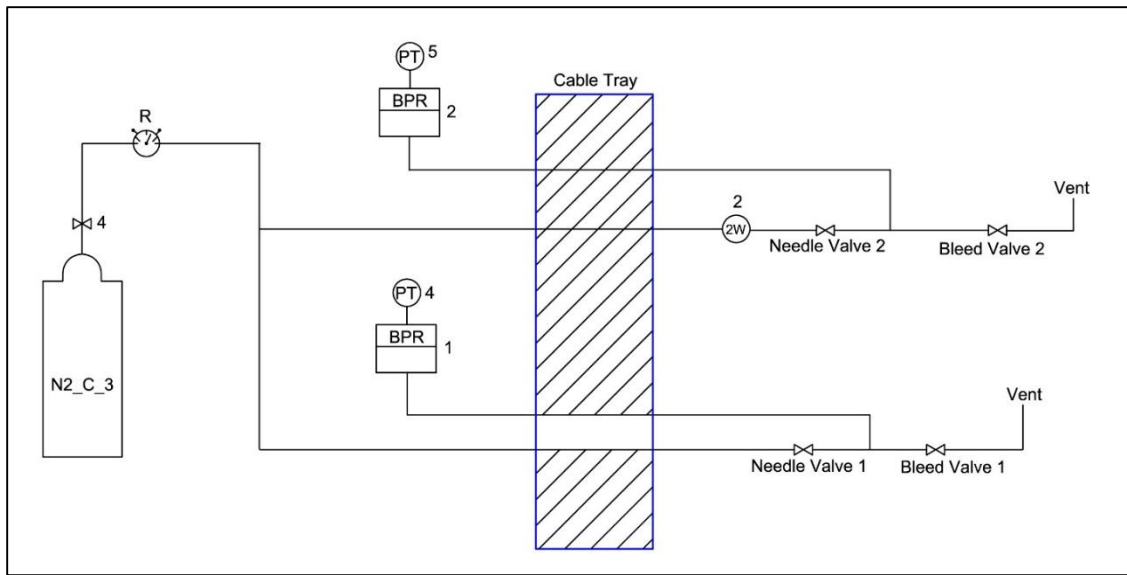


Figure B.4. Diagram of the BPR array.

B.6. Parr Instruments Inc. Reactor System.

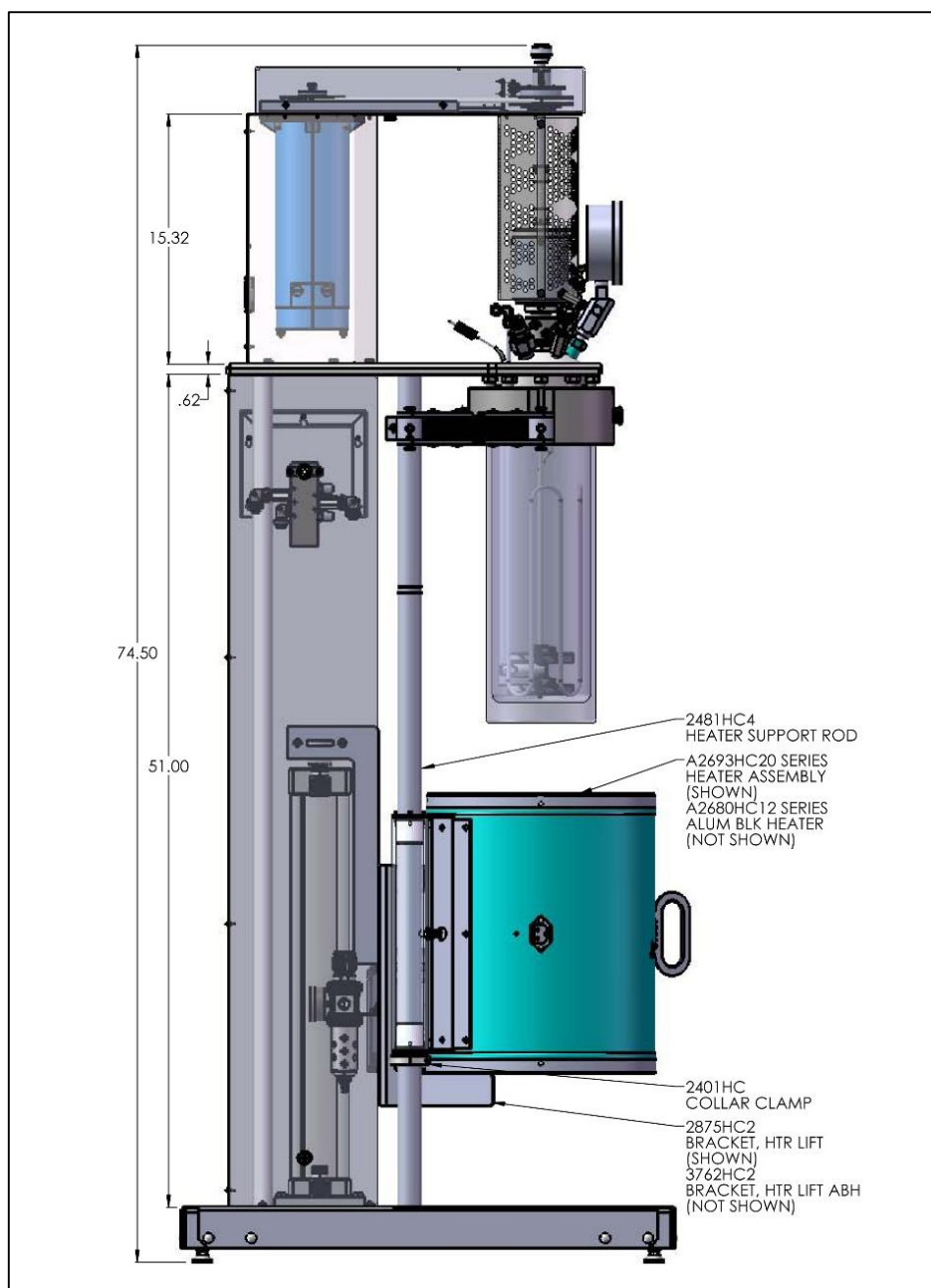


Figure B.5. Reactor side view (reproduced with permission from Parr Instruments Inc.).

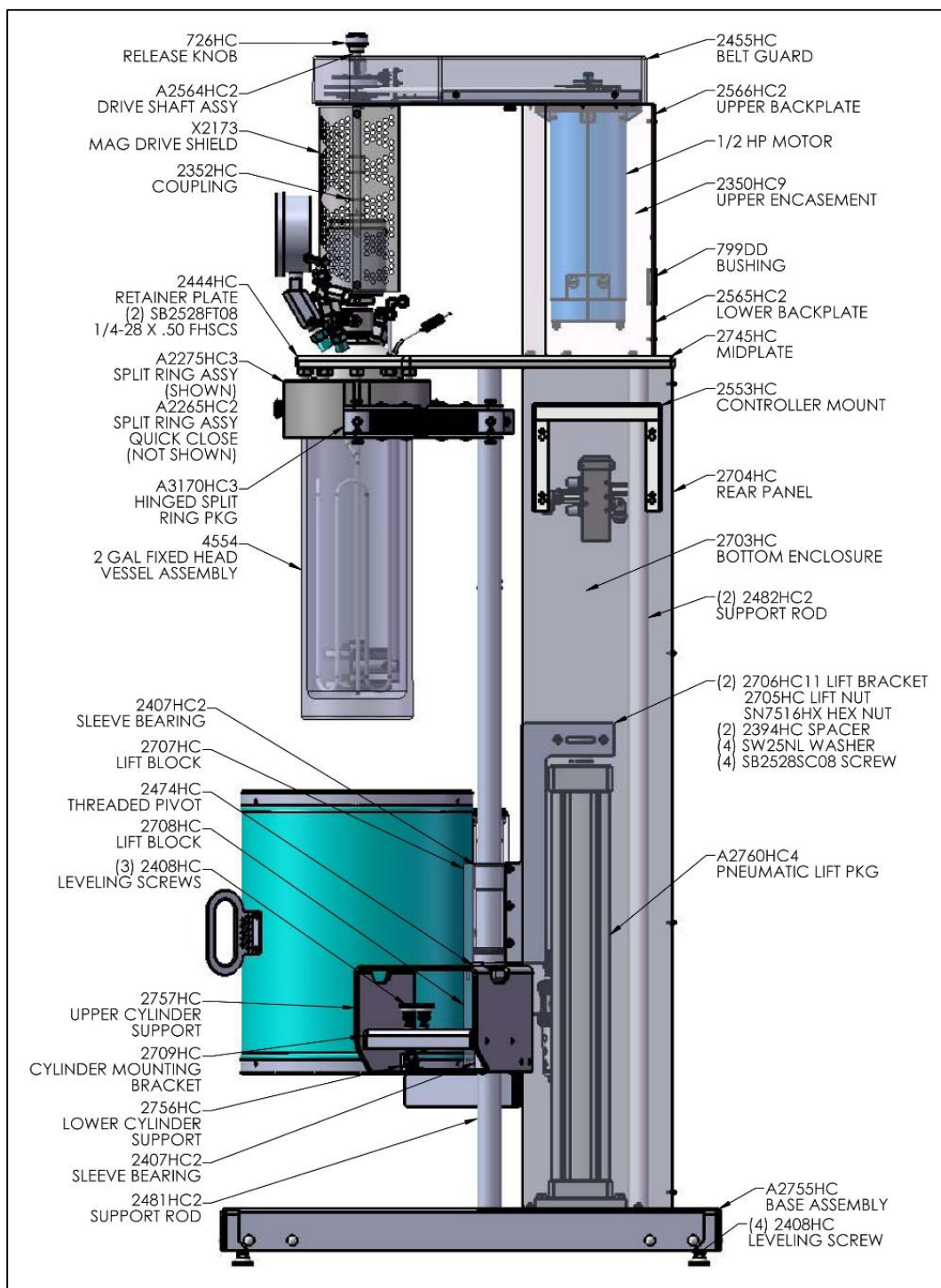


Figure B.6. Reactor side view (reproduced with permission from Parr Instruments Inc.).

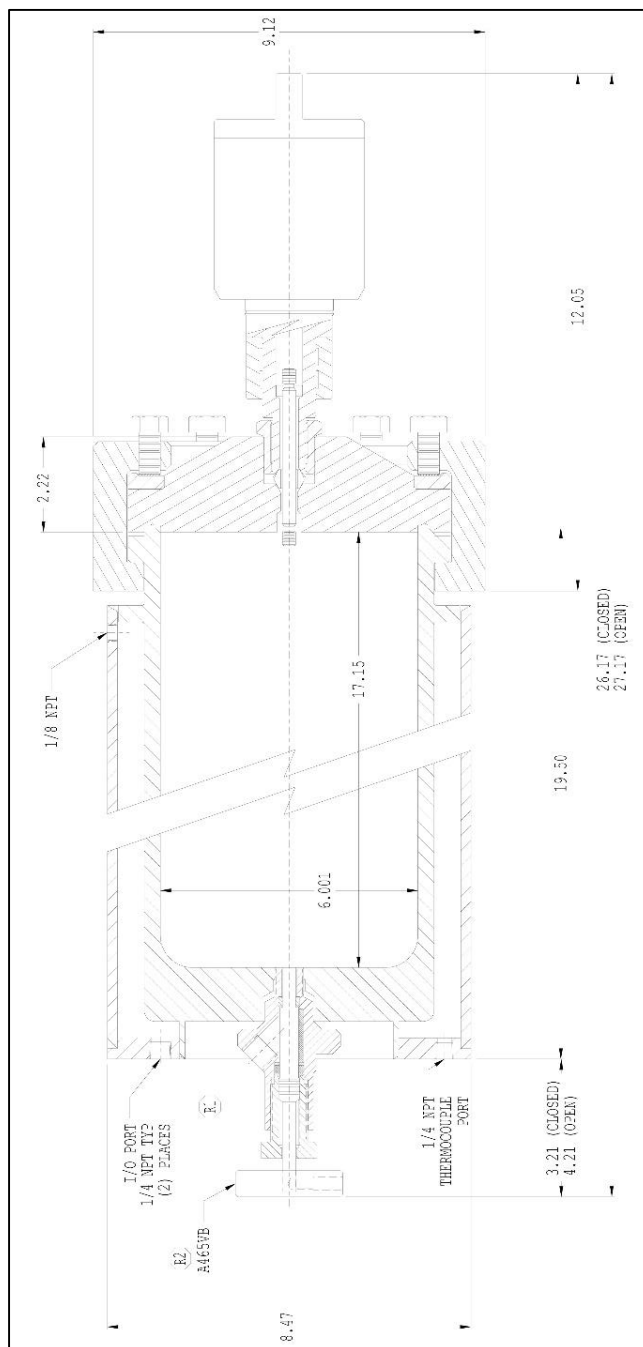


Figure B.7. Reactor vessel side view (reproduced with permission from Parr Instruments Inc.).

Appendix C

Data Acquisition Software Code Reference.

The data acquisition software is designed in Visual Studio 2010 ® which is a software development platform designed by Microsoft ® that uses the .NET language structure. The advantage of using Visual Basic ® as the development language is that it is easier to relate to external components (outside the computer) since the language is object oriented and is easier to deploy than other languages such as ASP.NET or C#.net. For simplicity, all the components used in Visual Studio 2010® are also included in Visual Studio 2010 Express Edition ® which is freely available for universities and academic institutions.

This software contains two form windows, one for introduction to the software and one that contains all the components used by the software. All the components of the software are shown in Figure C.1 on the solution explorer. Inside the Resources folder there are two images shown during the software initialization to honor the microcontroller of the brand ATMEL (the ATMEGA® 32) and EXCEL ® which is the end structured data file that can display the data collected. The solution explorer clearly shows two forms (Form1.vb and Intro.vb) which will be explained in detail in the current appendix.

This appendix contains three sections. Section C.1 contains the objects and code details for the Form1.vb form, Section C.2 contains the code and details for the Intro.vb form, and Section C.3 contains the full code detail for the entire solution.

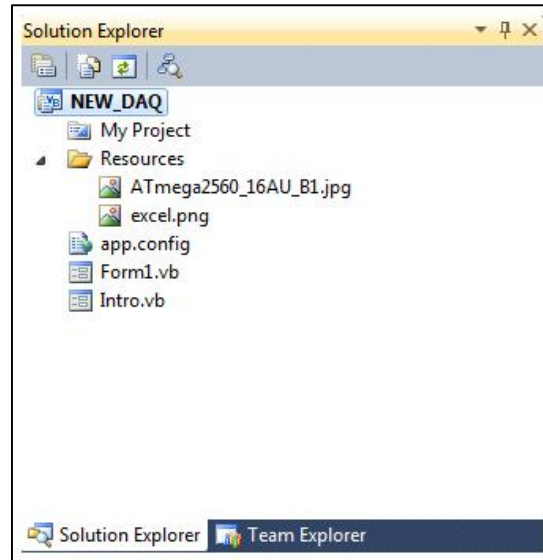


Figure C.1. Visual Studio solution explorer showing the components of the project.

C.1. Form1.vb Code and Form Details.

The additional components for Form1.vb are shown in Figure C.2: a Status Strip, a Timer, an Open File Dialog Window and a Folder Browser Dialog.

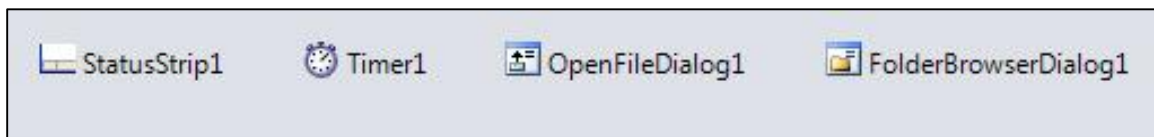


Figure C.2. Form 1 active components. Arranged from left to right: StatusStrip containing a label called Status_Label, a timer, a open file dialog box and a folder browse dialog box.

The code for both the “OpenFileDialog1” and “FolderBrowserDialog1” is included below. This code sets the path of where the Access[®] database file (streamed data) is located and also where the exported Excel[®] file will be saved. The data is originally stored in a structure data file. The software used for this purpose is Access[®] because it is already existent in computers in which Microsoft Office[®] products are installed and also because it gives the ability to the software to store data at high rates. By using a file format (.accdb) that is able to capture and store large amounts of data and a multithread approach from the code in the software, the data acquisition application can acquire and store data as fast as 10 samples/second for the 16 channels continuously without any compromise in performance.

```
Private Sub OpenFileDialog1_FileOk(ByVal sender As System.Object, ByVal e As  
System.ComponentModel.CancelEventArgs) Handles OpenFileDialog1.FileOk  
    DB_SelectFile.Text = OpenFileDialog1.FileName
```

```

DBPATHPATH = OpenFileDialog1.FileName
End Sub

```

```

Private Sub FolderBrowserDialog1_HelpRequest(ByVal sender As System.Object, ByVal e As System.EventArgs) Handles FolderBrowserDialog1.Disposed
    DB_ExportFile.Text = FolderBrowserDialog1.SelectedPath
End Sub

```

The software contains an array of Tab Pages that are able to compress every single part of the operation in sections in order to minimize space in the window. Figure C.3 and Table C.1 show the distribution and names of the components used in the main window.

Table C.1. Component names and function for Form 1 as shown in Figure C.3.

Number	Component Name	Component Function	Visible Name
1	Status_Strip1	Hold other components	NA
2	T0 – T15	Text Box to show values	NA
3	TabControl1	Hold Tab Pages	NA
A	TabPage4	Hold form components	Port Configuration
B	TabPage1	Hold form components	Channel Names
C	TabPage2	Hold form components	Channel ON / OFF
D	TabPage3	Hold form components	Calibration Parameters
E	TabPage5	Hold form components	Data Logging
F	TabPage6	Hold form components	Other Options
G	TabPage7	Hold form components	Processed Data

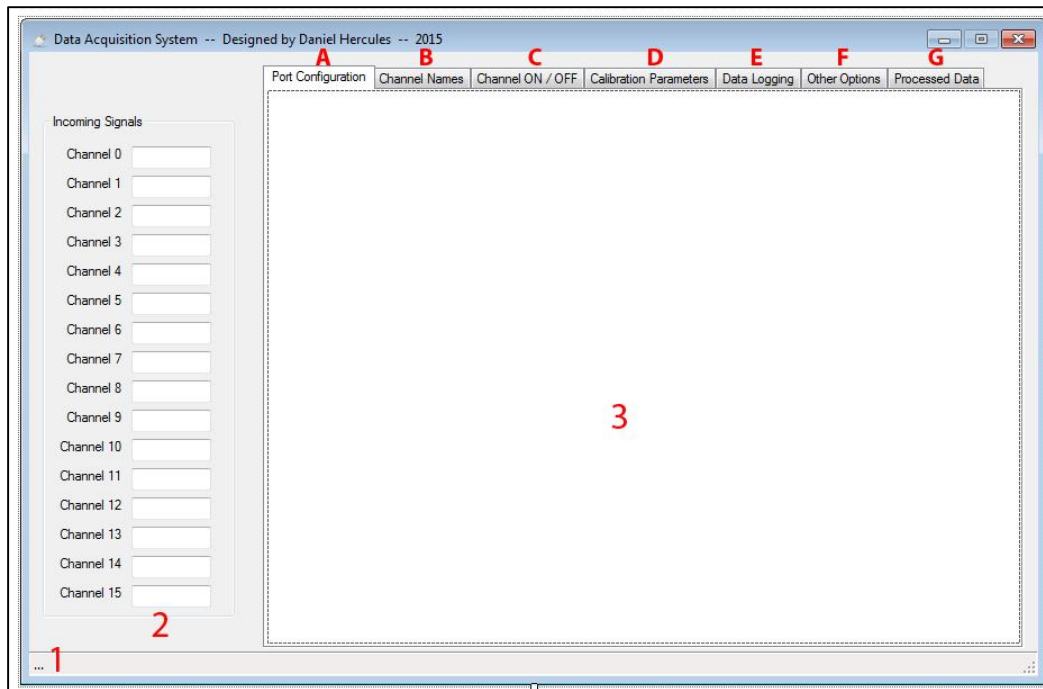


Figure C.3. Form1 main component layout.

The first tab page called “Port Configuration” includes the necessary components to find the available communication ports in the computer and once a port is selected, to connect or disconnect such port. The first task is to find all the COM ports that the computer can see at any given moment.

```
Private Sub Button35_Click(ByVal sender As System.Object, ByVal e As
System.EventArgs) Handles Button35.Click
    Dim nameArray() As String
    nameArray = SerialPort.GetPortNames
    Array.Sort(nameArray)
    cmbPorts.DataSource = nameArray
    cmbPorts.DropDownStyle = ComboBoxStyle.DropDownList
End Sub
```

Once a port is selected it is necessary to connect to it in order to acquire data. The instruction to connect to the port is shown below.

```
Private Sub Button34_Click(ByVal sender As System.Object, ByVal e As
System.EventArgs) Handles Button34.Click
    Dim SELECTED_PORT As String = cmbPorts.Text
    If String.IsNullOrEmpty(SELECTED_PORT) Then
        MsgBox("Please Select A Port")
        Exit Sub
    Else
        cmbPorts.Enabled = False
        Try
            objSerial.PortName = SELECTED_PORT
            objSerial.BaudRate = 57600
            objSerial.Open()
        Catch ex As Exception
            MsgBox(ex.ToString)
            Exit Sub
        End Try
    End If
End Sub
```

If one desires to disconnect from the selected port at any given moment, it can be done by executing the following code:

```
Private Sub Button33_Click(ByVal sender As System.Object, ByVal e As
System.EventArgs) Handles Button33.Click
    Try
        objSerial.Close()
        cmbPorts.Enabled = True
    Catch ex As Exception
        MsgBox(ex.ToString)
    End Try
Exit Sub
End Sub
```

Any of the “Connect” or “Disconnect” functions could indicate an exception to the procedure by displaying a message box stated by the syntax “MsgBox(ex.ToString)”. If such an exception is triggered, the instruction will end and no action will be performed.

When the Form1.vb loads there are some instructions triggered as shown by the “mybase.load” instruction below.

```
Private Sub Form1_Load(ByVal sender As System.Object, ByVal e As
System.EventArgs) Handles MyBase.Load
    DB_FileName.Text = "Data_" & Today.Month & "-" & Today.Day & "-" &
Today.Year
    Dim nameArray() As String
    nameArray = SerialPort.GetPortNames
    Array.Sort(nameArray)
    cmbPorts.DataSource = nameArray
    cmbPorts.DropDownStyle = ComboBoxStyle.DropDownList
    LOAD_CHANNEL_NAMES()
End Sub
```

The function LOAD_CHANNEL_NAMES() is executed every time the form loads and is in charge of populating all the personalized names for each channel that the user gives. How to add the names to each channel will be explained in another section of this appendix and the code can be found at the end of this document. Each name for each channel is stored in the local registry at the address “HKEY_CURRENT_USER\HerculesSoft\DAQ” and each channel has two string properties called “CH##” and “Units###” where the “##” is the number of the channel respectively from “00” to “15” (a total of 16 channels).

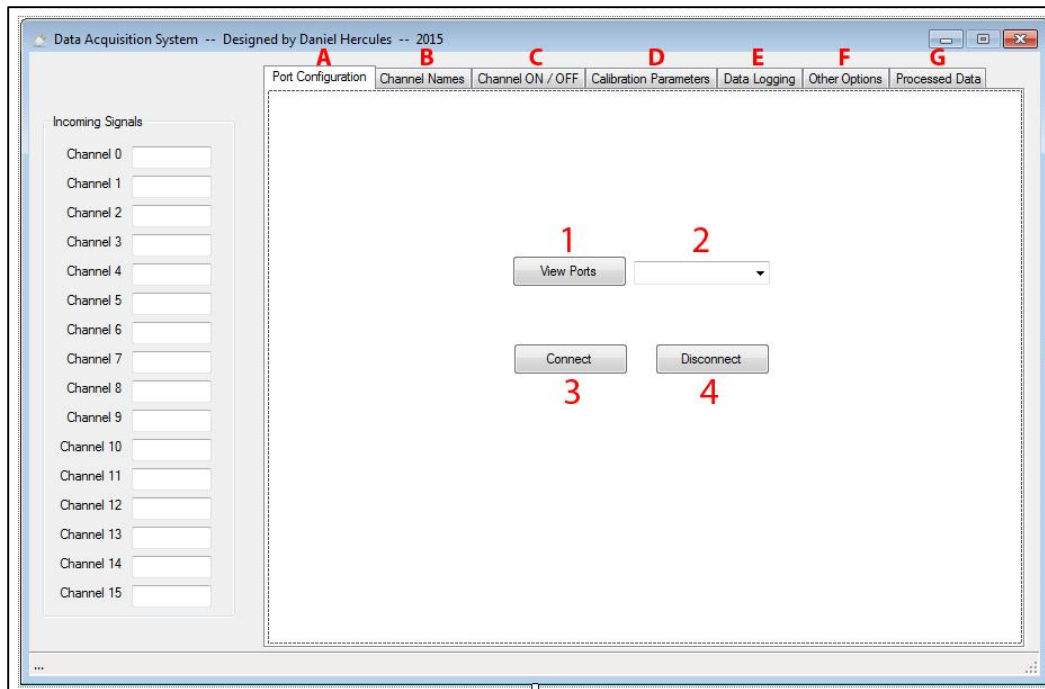


Figure C.4. Layout of components inside the “Port Configuration” tab labeled as “A”

Table C.2. Component names and function for the “Port Configuration” tab as shown in Figure C.4.

Number	Component Name	Component Function	Visible Name
1	Button35	Perform a click	View Ports
2	cmbPorts	Show multiple options	NA
3	Button34	Perform a click	Connect
4	Button33	Perform a click	Disconnect

The “Channel Names” tab contains a collection of text boxes in which the user can set up the specific name of each channel for easy reading and reference to which signal is coming into which channel. This is useful when looking at a log file because it clarifies what channel is assigned to each signal. The reference code is shown below.

```

Private Sub Button1_Click(ByVal sender As System.Object, ByVal e As
System.EventArgs) Handles Button1.Click
    Dim SSString, Variable_Name As String
    SSString = "HKEY_CURRENT_USER\HerculesSoft\DAQ"
    Variable_Name = Channel_Name_00.Text
    My.Computer.Registry.SetValue(SSString, "CH00", Variable_Name)
    Dim Units_Name As String = Units00.Text
    My.Computer.Registry.SetValue(SSString, "Units00", Units_Name)
    LOAD_CHANNEL_NAMES()
End Sub

```

Every time a channel name is saved, the “LOAD_CHANNEL_NAMES()” function is called to refresh the names of the channels immediately. This affects the log file as it is being saved and also refreshes the rest of the views in which the name of the channel is shown. A sample of the code declaring the variables and one function is shown below. The figure showing a view of the tab and the table containing the names of the objects used are in Figure C.5 and Table C.3 respectively.

```

Private Sub LOAD_CHANNEL_NAMES()
Dim regKey As RegistryKey
    Dim path As String = "HerculesSoft\DAQ"
    regKey = Registry.CurrentUser.OpenSubKey(path, True)

    Try
        Name_A_00.Text = regKey.GetValue("CH00").ToString
        Name_B_00.Text = regKey.GetValue("CH00").ToString
        Channel_Name_00.Text = regKey.GetValue("CH00").ToString
        Processed_Name_00.Text = regKey.GetValue("CH00").ToString
    Catch ex As Exception
        Exit Try
    End Try
End Sub

```

Table C.3. Component names and function for the “Channel Names” tab as shown in Figure C.5.

Number	Component Name	Component Function	Visible Name
1	Channel_Name_00 - Channel_Name_15	Display a text	NA
2	Units00 – Units15	Display a text	NA
3	Button1 – Button16	Perform Click	Save
4	Button36	Perform Click	Refresh Names

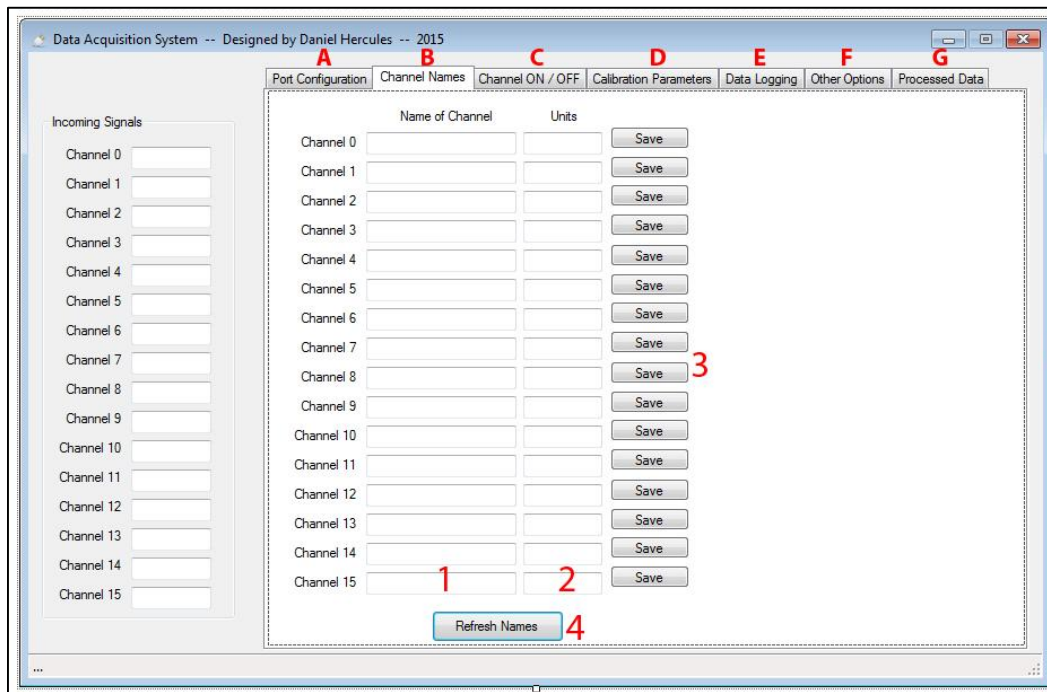


Figure C.5. Layout of components inside the “Channel Names” tab labeled as “B”

The next tab is called “Channel ON / OFF” and as the name indicates, the tab contains a collection of check boxes in which the user can turn each channel on or off depending of the desired log output. This is particularly useful when only a few channels are used since it increases the performance of the software by saving time when storing the data in the database file. If a check box is selected for a given channel, the channel value will be stored. By default all the channels are set to “ON” which means that all channels

will be stored when recording. The view of this tab and a table containing the objects are shown in Figure C.6 and Table C.4 respectively.

Table C.4. Component names and function for the “Channel ON / OFF” tab as shown in Figure C.6.

Number	Component Name	Component Function	Visible Name
1	Name_B_00 – Name_B_15	Display a text	NA
2	Check_CH00 – Check_CH15	Accept a mark as check or unchecked	Channel ON (Store)

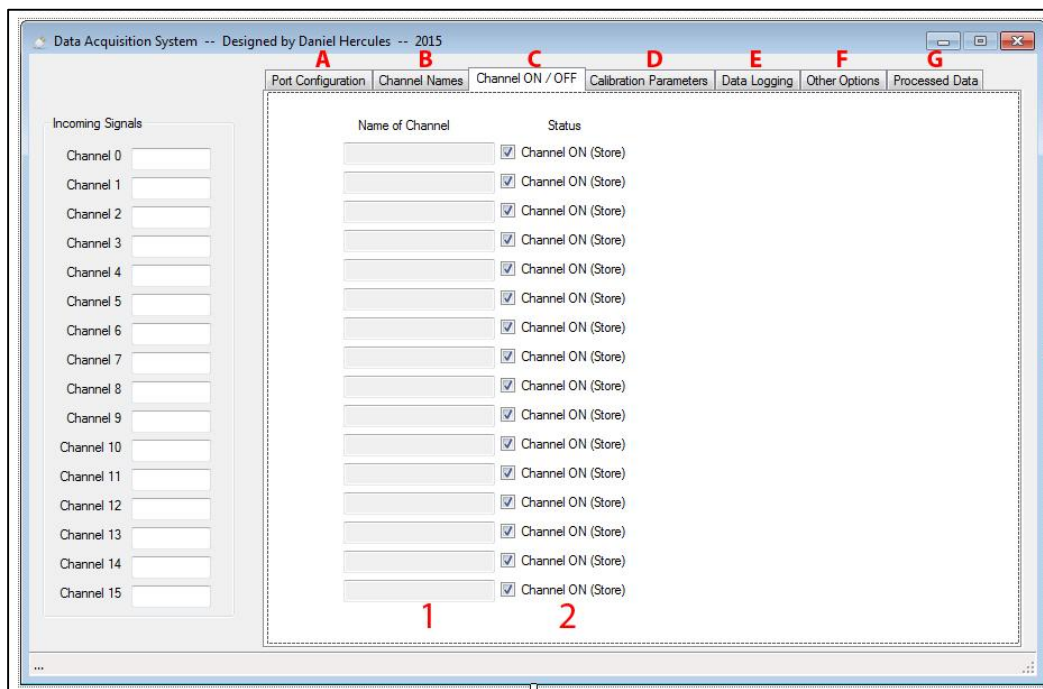


Figure C.6. Layout of components inside the “Channel ON / OFF” tab labeled as “C”

Since this software is intended to serve as a platform for multiple types of sensors and applications, each channel is thought to have variable input values. These input values are destined to be a voltage in between 0-5 V DC for when the device is used in 10-bit

resolution (reference voltage is the internal MCU operational voltage) or 0-4.096 V when the AREF (analog reference voltage value) is set to the output of a LM4040 reference voltage regulator as shown in Schematic 1. When the AREF is set to the output voltage of the LM4040, a resistor of 560 ohm is required to limit the current coming into the AREF pin of the MCU to a value greater than 100 micro amperes (μA) and lower than 15 mili amperes (mA).

Taking into account that all signals coming into the microcontroller are subject to either a pre-amplification or a simple voltage division (achieved by a set of two resistors in series) and are linear, a post treatment of the signal that can compensate for such conversions and an external calibration, plays an important role. The software is equipped (as shown in Figure C.8) with a tab called “Calibration Parameters” in which each channel is subject to a linear calibration curve. A simple calculation and calibration can be performed to each channel to find the slope (m value) and intercept (b value) of the linear model correlation line and therefore obtain a new value that is representative of the full range of the sensor in the units that the sensor is intended to measure.

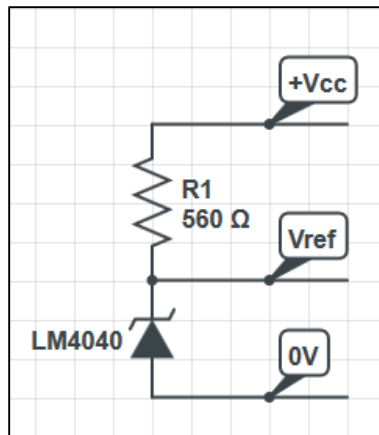


Figure C.7. Schematic of LM4040 reference circuit

Other methods can be used in order to reduce the noise in the signal or smooth the sensor output as it comes to the analog channel. The signal can be averaged in between 5 to 20 times before exporting the value to the data streamed to the computer. Additionally, a PID (although used for control algorithms, it can be used for extrapolating a signal that is subject to noise) algorithm can be used to reduce the noise of the output signal from each sensor while the signal change. This is particularly useful when sudden changes in the signals are often, or when large changes in the signal are expected. If the changes of the signal occur within the refresh rate of the readings done in the microcontroller (in our case 20 Hz), there is no need then to use a filter for sudden changes as they will happen within the refresh rate of the signal.

Each of these parameters (slope and intercept) can be saved (one at a time) in the registry of the computer for each channel.

Every time the thread process calls on an update of the values (triggered by a new signal coming into the computer) then the following function is called and the values are

updated. The same operation is repeated to all the channels as the new values come in one at a time.

```
Public Sub UpdateCH0_Box(ByVal CH0 As String)
    T0.Text = CH0
    New_Value_00.Text = Val(T0.Text) * Val(m00.Text) + Val(b00.Text)
    Processed_Input_00.Text = CH0
    Value_Processed_00.Text = New_Value_00.Text
End Sub
```

Table C.5. Component names and function for the “Calibration Parameters” tab, shown in Figure C.8.

Number	Component Name	Component Function	Visible Name
1	Name_A_00	Display a text	NA
2	m00 – m15	Display a text	NA
3	b00 – b15	Display a text	NA
4	Button17 – Button32	Perform Click	Save
5	New_Value_00 – New_Value_15	Display a text	NA
6	Units_Cal_00 – Units_Cal_15	Display a text	NA

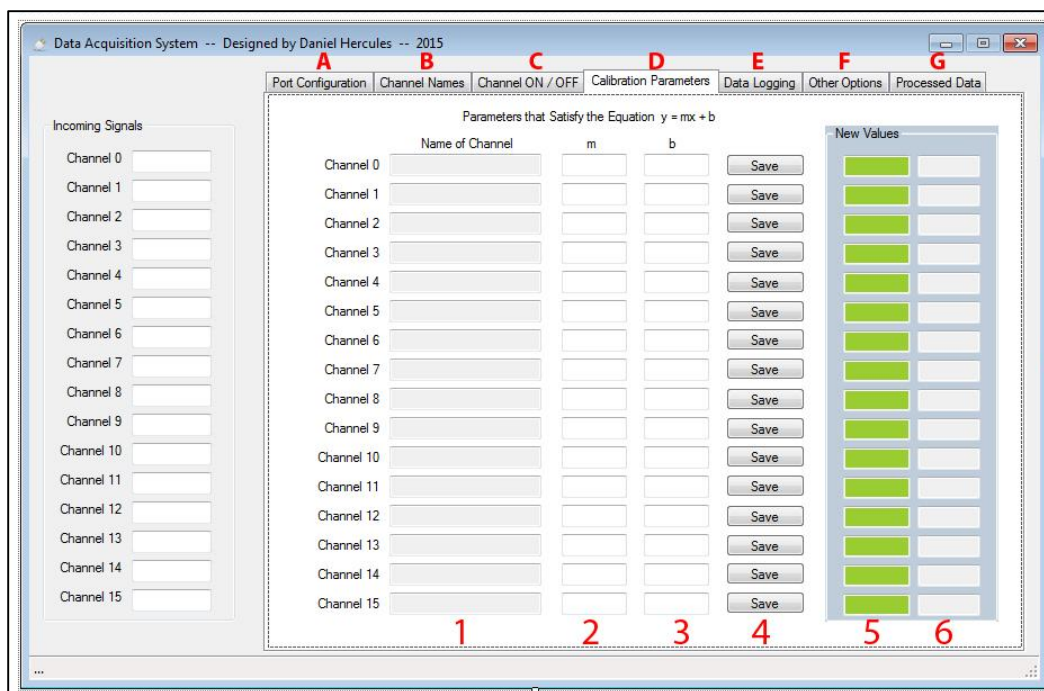


Figure C.8. Layout of components inside the “Calibration Parameters” tab labeled as “D”

The next tab included in the software is called “Data Logging” and contains objects that trigger the procedures to store the data as well as to start and stop recording. A list of objects can be found in Table 8.

Table C.6. Component names and function for the “Data Logging” tab as shown in Figure C.9.

Number	Component Name	Component Function	Visible Name
1	DB_FileName	Display a text	NA
2	DB_CreateFile	Perform Click	Create File
3	Combobox1	Select From Different Options	Sample Rate
4	Button41	Perform Click	Start Recording
5	Button40	Perform Click	Stop Recording
6	Indicator1	Turn green when recording and turn red when stopped	NA
7	DB_SelectFileName	Perform Click	Select
8	DB_SelectFile	Display a text	NA
9	DB_SaveDestination	Perform Click	Pick Destination
10	DB_ExportFile	Display a text	NA
11	DB_Export	Perform Click	Export the Data

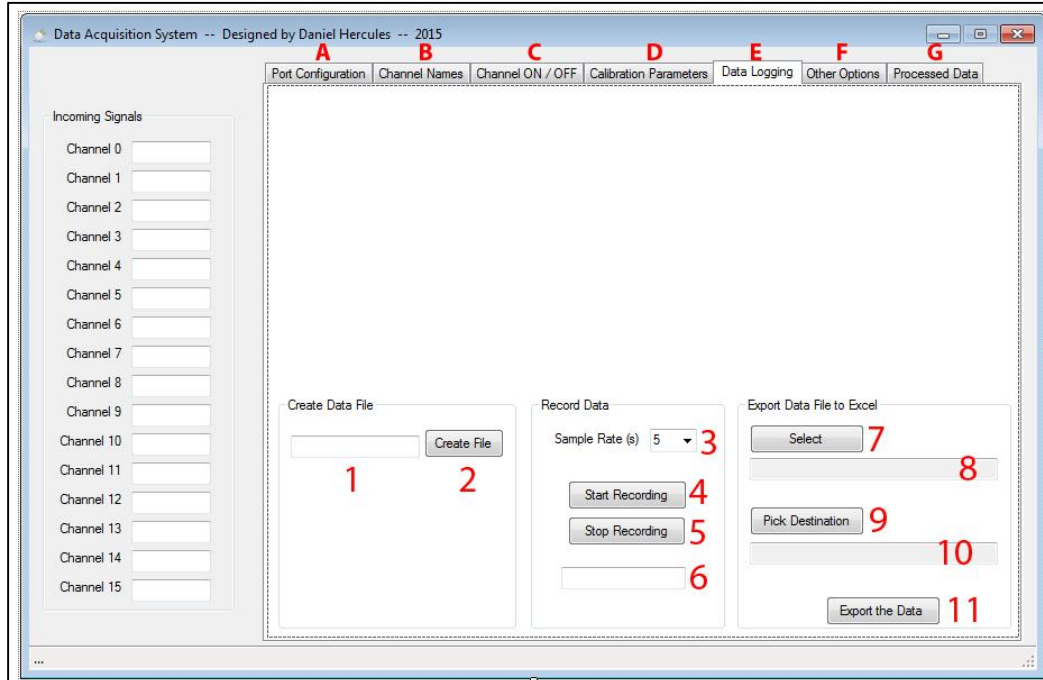


Figure C.9. Layout of components inside the “Data Logging” tab labeled as “E”

The system starts the recording by calling a different thread process that is completely independent from the one that handles receiving the data and updating the channel information. This code is shown below.

```
Private Sub Button41_Click(ByVal sender As System.Object, ByVal e As
System.EventArgs) Handles Button41.Click
    DB_FileName.Enabled = False
    trd = New Thread(AddressOf ThreadTask)
    trd.IsBackground = True
    trd.Start()
    Indicator1.BackColor = Color.Green
    Indicator1.Text = "Recording"
End Sub
```

The same way, the process can be stopped when the following instruction is called. Notice that there is an indicator element that helps the user notice what the status of the process is by displaying a red or green flag in the case of the software being in recording or idle state, respectively.

```
Private Sub Button40_Click(ByVal sender As System.Object, ByVal e As
System.EventArgs) Handles Button40.Click
    trd.Abort()
    DB_FileName.Enabled = True

    MsgBox("Recording Stopped", MsgBoxStyle.OkOnly, "Data Log")
    Indicator1.BackColor = Color.Red
    Indicator1.Text = "Stopped"
End Sub
```

The user can create a file name if desired to store the data. The code to programmatically create such a database file with all the correct structure to save the data

is demonstrated below. Notice that the entirety of the file is created in one single state and an error handling “Try / Catch” method is used.

```

Private Sub DBCreateFile_Click(ByVal sender As System.Object, ByVal e As
System.EventArgs) Handles DB_CreateFile.Click
    If String.IsNullOrEmpty(DB_FileName.Text) Then
        MsgBox("The file must be Named", MsgBoxStyle.OkOnly, "Error on File Name")
        Exit Sub
    End If
    'C:\Data_Acquisition_System\
    NameName = DB_FileName.Text

    If (Not System.IO.Directory.Exists("C:\Data_Acquisition_System\")) Then
        System.IO.Directory.CreateDirectory("C:\Data_Acquisition_System\")
    End If

    Try
        Dim AccessDatabaseEngine As New
Microsoft.Office.Interop.Access.Dao.DBEngine
        Dim AccessDatabase As Microsoft.Office.Interop.Access.Dao.Database

        AccessDatabase =
AccessDatabaseEngine.CreateDatabase("C:\Data_Acquisition_System\" & NameName &
".accdb", LanguageConstants.dbLangGeneral, DatabaseTypeEnum.dbVersion120)
        AccessDatabase.Close()
    Catch ex As Exception
        MsgBox(ex.ToString, MsgBoxStyle.OkOnly, "ERROR CREATING FILE")
    Exit Sub
    End Try

    Try
        Using conn As New
OleDb.OleDbConnection("Provider=Microsoft.ACE.OLEDB.12.0;" & _
        "Data Source=C:\Data_Acquisition_System\" & NameName & ".accdb;")
            Using cmd As New OleDb.OleDbCommand("CREATE TABLE DataAcquired
( " & _
                "AutoId int identity," & _
                "Time_Sample NVarchar(50)," & _
                "CH0 NVarchar(50)," & _
                "CH1 NVarchar(50)," & _
                "CH2 NVarchar(50)," & _

```

"CH3 NVarchar(50)," & _
"CH4 NVarchar(50)," & _
"CH5 NVarchar(50)," & _
"CH6 NVarchar(50)," & _
"CH7 NVarchar(50)," & _
"CH8 NVarchar(50)," & _
"CH9 NVarchar(50)," & _
"CH10 NVarchar(50)," & _
"CH11 NVarchar(50)," & _
"CH12 NVarchar(50)," & _
"CH13 NVarchar(50)," & _
"CH14 NVarchar(50)," & _
"CH15 NVarchar(50)," & _
"M0 NVarchar(50)," & _
"M1 NVarchar(50)," & _
"M2 NVarchar(50)," & _
"M3 NVarchar(50)," & _
"M4 NVarchar(50)," & _
"M5 NVarchar(50)," & _
"M6 NVarchar(50)," & _
"M7 NVarchar(50)," & _
"M8 NVarchar(50)," & _
"M9 NVarchar(50)," & _
"M10 NVarchar(50)," & _
"M11 NVarchar(50)," & _
"M12 NVarchar(50)," & _
"M13 NVarchar(50)," & _
"M14 NVarchar(50)," & _
"M15 NVarchar(50)," & _
"B0 NVarchar(50)," & _
"B1 NVarchar(50)," & _
"B2 NVarchar(50)," & _
"B3 NVarchar(50)," & _
"B4 NVarchar(50)," & _
"B5 NVarchar(50)," & _
"B6 NVarchar(50)," & _
"B7 NVarchar(50)," & _
"B8 NVarchar(50)," & _
"B9 NVarchar(50)," & _
"B10 NVarchar(50)," & _
"B11 NVarchar(50)," & _
"B12 NVarchar(50)," & _
"B13 NVarchar(50)," & _
"B14 NVarchar(50)," & _

```

"B15 NVarchar(50)," & _
"Value0 NVarchar(50)," & _
"Value1 NVarchar(50)," & _
"Value2 NVarchar(50)," & _
"Value3 NVarchar(50)," & _
"Value4 NVarchar(50)," & _
"Value5 NVarchar(50)," & _
"Value6 NVarchar(50)," & _
"Value7 NVarchar(50)," & _
"Value8 NVarchar(50)," & _
"Value9 NVarchar(50)," & _
"Value10 NVarchar(50)," & _
"Value11 NVarchar(50)," & _
"Value12 NVarchar(50)," & _
"Value13 NVarchar(50)," & _
"Value14 NVarchar(50)," & _
"Value15 NVarchar(50)," & _
"Units0 NVarchar(50)," & _
"Units1 NVarchar(50)," & _
"Units2 NVarchar(50)," & _
"Units3 NVarchar(50)," & _
"Units4 NVarchar(50)," & _
"Units5 NVarchar(50)," & _
"Units6 NVarchar(50)," & _
"Units7 NVarchar(50)," & _
"Units8 NVarchar(50)," & _
"Units9 NVarchar(50)," & _
"Units10 NVarchar(50)," & _
"Units11 NVarchar(50)," & _
"Units12 NVarchar(50)," & _
"Units13 NVarchar(50)," & _
"Units14 NVarchar(50)," & _
"Units15 NVarchar(50)," & _
"CONSTRAINT [pk_AutoId] PRIMARY KEY (AutoId)) ", conn)
conn.Open()
Try
    cmd.ExecuteNonQuery()
Catch ex As Exception
    MsgBox(ex.ToString)
Exit Sub
End Try
End Using
End Using
Catch ex As Exception

```

```
MsgBox("Error with the DB File. File might be already created or in use",  
MsgBoxStyle.OkOnly, "Error with DB File")  
End Try  
End Sub
```

In order to visualize the data that is being stored (or to verify that it is being stored correctly), the user can view the existing data by accessing the “Other Options” tab in which four different buttons are located. The “Load Data” button loads the data onto the DataGridView1 object and the data that is saved after the content is accessed is not visualized. For further verification of the data, the user must load the data again. The “Incoming” button helps trim the columns to show only the ones that contain the data as it comes from the microcontroller into the computer. The button labeled “Calibrated” shows the columns of the data that is being transformed by the calibration parameters and finally the button labeled “Parameters” displays only the calibration parameters. The window as it looks in the software is listed in Figure C.10 and the objects are listed in Table C.7. The code that performs the actions can be found in the general code section of this appendix.

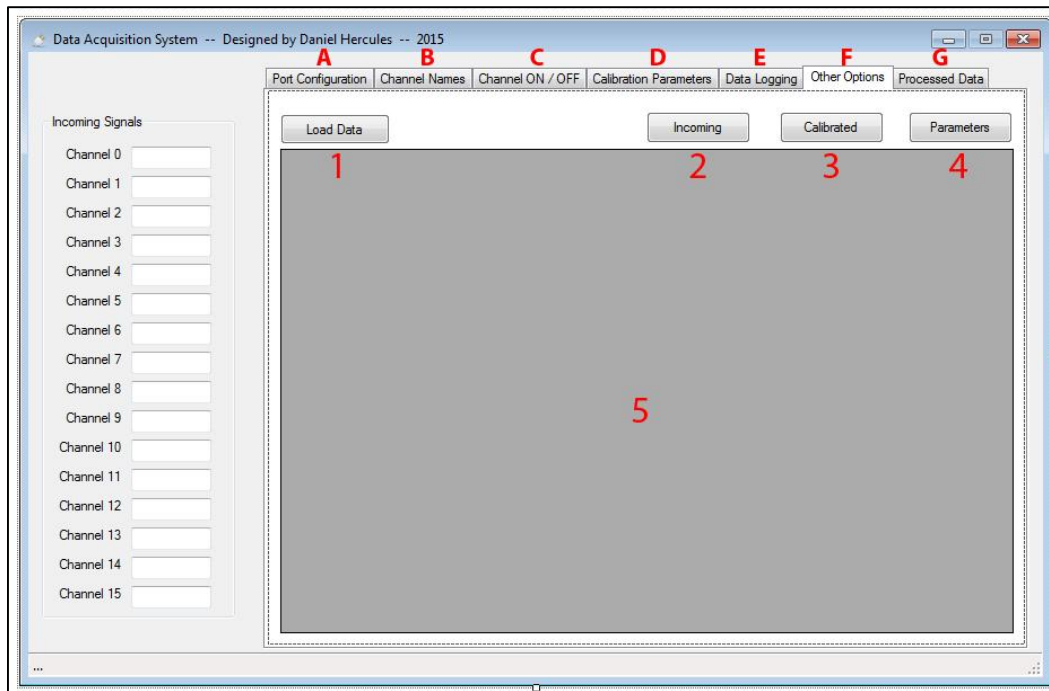


Figure C.10. Layout of components inside the “Other Options” tab labeled as “F”.

Table C.7. Component names and function for the “Other Options” tab as shown in Figure C.10

Number	Component Name	Component Function	Visible Name
1	Button44	Perform Click	Load Data
2	Button37	Perform Click	Incoming
3	Button42	Perform Click	Calibrated
4	Button43	Perform Click	Parameters
5	DataGridView1	Visualize Data from the Database	NA

The final tab is called “Processed Data” and it contains a quick view of all the data as it comes from the microcontroller unit, the new processed values once the calibration parameters have been applied, the units in which each channel is being measured and the name of each channel with respect to the part of the process where the data is coming from.

The objects for this tab are specified in Table C.8 and the view of the tab is shown in Figure C.11.

Table C.8. Component names and function for the “Processed Data” tab as shown in Figure C.11

Number	Component Name	Component Function	Visible Name
1	Processed_Name_00 – Processed_Name_15	Display a text	NA
2	Processed_Input_00 – Processed_Input_15	Display a text	NA
3	Value_Processed_00 – Value_Processed_15	Display a text	NA
4	Units_00 – Units_15	Display a text	NA

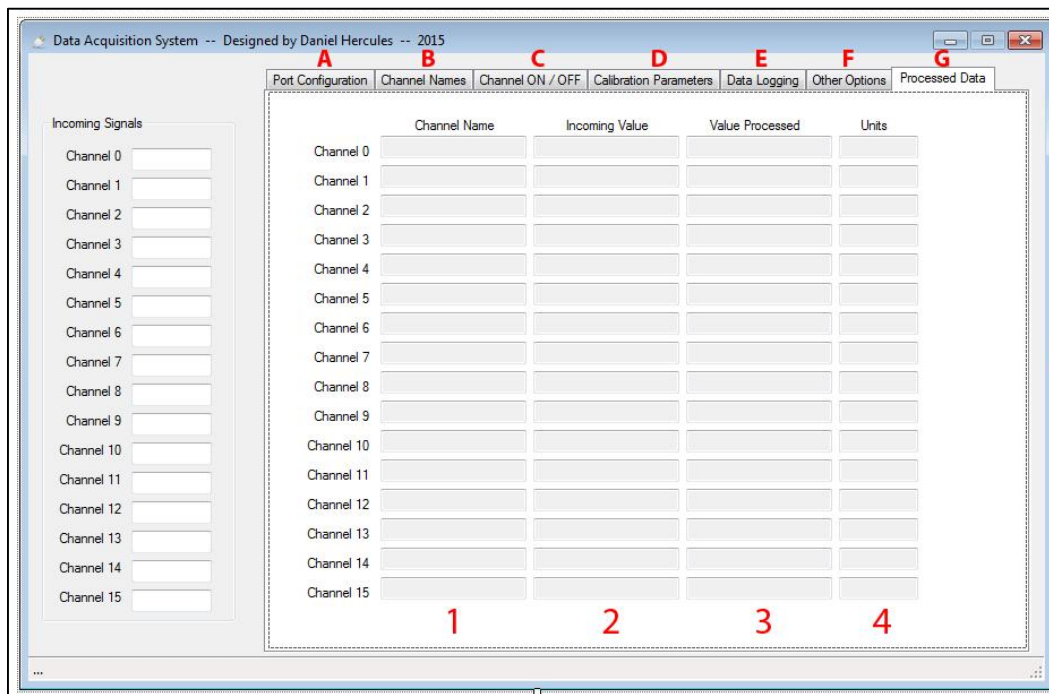


Figure C.11. Layout of components inside the “Processed Data” tab labeled as “E”

The complete code description as it is included in the software is described in the next section titled “Form1 Code” as the form that contains the objects for this section of the software is named “Form1”.

C.2. Intro.vb Code and Form Details.

The Intro.vb form contains a couple of images and shows first when the software is initialized. It contains a timer (Timer1) that is initialized when the MyBase.Load function is called. Once the timer is executed the Timer1 will enable, show the Form1.vb and close the Intro.vb form. The code included altogether inside Intro.vb is shown below.

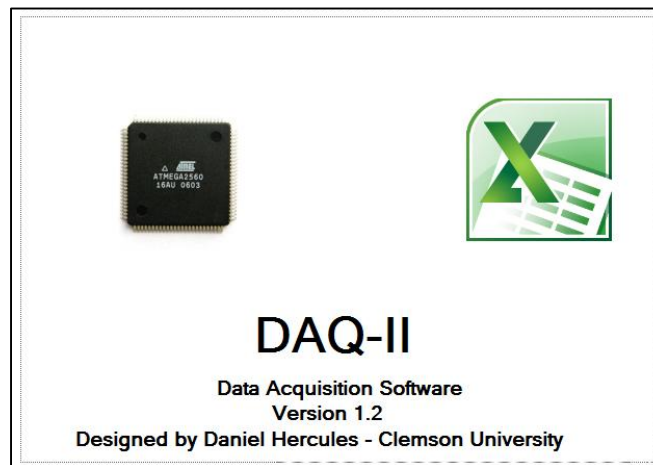


Figure C.12. Introduction form layout.

Table C.9. Properties for the component called “Timer1.”

Property	Value
Enabled	False
Interval	2000
Modifiers	Friend
Name	Timer1

Code

Public Class Intro

```
Private Sub Timer1_Tick(ByVal sender As System.Object, ByVal e As  
System.EventArgs) Handles Timer1.Tick  
    Timer1.Enabled = False  
    Me.Hide()  
    Form1.Show()  
End Sub
```

```
Private Sub Intro_Load(ByVal sender As System.Object, ByVal e As System.EventArgs)  
Handles MyBase.Load  
    Timer1.Enabled = True  
End Sub
```

End Class

C.3. Complete Programming Code Reference.

C.3.1. Form1 Complete Code Reference

```
Imports System.IO.Ports  
Imports Microsoft.Win32  
Imports Excel = Microsoft.Office.Interop.Excel  
Imports System.Threading
```

```
Imports System.Data.SqlClient  
Imports System.Data.OleDb  
Imports System.Data  
Imports System.Xml
```

```
Imports Microsoft.Office.Interop.Access.Dao
```

Public Class Form1

```
Dim xlApp As New Excel.Application  
Dim xlWorkBook As Excel.Workbook  
Dim xlWorkSheet As Excel.Worksheet
```

```

Private WithEvents objSerial As New System.IO.Ports.SerialPort("COM4")

#Region "Channel Declarations"
Private Channel0 As Double
Private Channel1 As Double
Private Channel2 As Double
Private Channel3 As Double
Private Channel4 As Double
Private Channel5 As Double
Private Channel6 As Double
Private Channel7 As Double
Private Channel8 As Double
Private Channel9 As Double
Private Channel10 As Double
Private Channel11 As Double
Private Channel12 As Double
Private Channel13 As Double
Private Channel14 As Double
Private Channel15 As Double
Private Channel16 As Double
#End Region

Private Sub objSerial_DataReceived(ByVal sender As Object, ByVal e As
System.IO.Ports.SerialDataReceivedEventArgs) Handles objSerial.DataReceived
    Dim s As String = objSerial.ReadLine
    Try
        If s.Contains("CHA0") Then
            s = s.Replace("CHA0 = ", "")
            If IsNumeric(s) Then
                Channel0 = CDb1(s)
                T0.Invoke(New UpdateCH0(AddressOf UpdateCH0_Box),
Channel0.ToString)
            End If

            ElseIf s.Contains("CHA1") Then
                s = s.Replace("CHA1 = ", "")
                If IsNumeric(s) Then
                    Channel1 = CDb1(s)
                    T1.Invoke(New UpdateCH1(AddressOf UpdateCH1_Box),
Channel1.ToString)
                End If
            End If
        End Try
    End Sub

```

```

ElseIf s.Contains("CHA2") Then
    s = s.Replace("CHA2 = ", "")
    If IsNumeric(s) Then
        Channel2 = CDb1(s)
        T2.Invoke(New UpdateCH2(AddressOf UpdateCH2_Box),
Channel2.ToString)
    End If

ElseIf s.Contains("CHA3") Then
    s = s.Replace("CHA3 = ", "")
    If IsNumeric(s) Then
        Channel3 = CDb1(s)
        T3.Invoke(New UpdateCH3(AddressOf UpdateCH3_Box),
Channel3.ToString)
    End If

ElseIf s.Contains("CHA4") Then
    s = s.Replace("CHA4 = ", "")
    If IsNumeric(s) Then
        Channel4 = CDb1(s)
        T4.Invoke(New UpdateCH4(AddressOf UpdateCH4_Box),
Channel4.ToString)
    End If

ElseIf s.Contains("CHA5") Then
    s = s.Replace("CHA5 = ", "")
    If IsNumeric(s) Then
        Channel5 = CDb1(s)
        T5.Invoke(New UpdateCH5(AddressOf UpdateCH5_Box),
Channel5.ToString)
    End If

ElseIf s.Contains("CHA6") Then
    s = s.Replace("CHA6 = ", "")
    If IsNumeric(s) Then
        Channel6 = CDb1(s)
        T6.Invoke(New UpdateCH6(AddressOf UpdateCH6_Box),
Channel6.ToString)
    End If

ElseIf s.Contains("CHA7") Then
    s = s.Replace("CHA7 = ", "")
    If IsNumeric(s) Then

```

```

        Channel7 = CDb1(s)
        T7.Invoke(New UpdateCH7(AddressOf UpdateCH7_Box),
Channel7.ToString)
    End If

    ElseIf s.Contains("CHB8") Then
        s = s.Replace("CHB8 = ", "")
        If IsNumeric(s) Then
            Channel8 = CDb1(s)
            T8.Invoke(New UpdateCH8(AddressOf UpdateCH8_Box),
Channel8.ToString)
        End If

    ElseIf s.Contains("CHB9") Then
        s = s.Replace("CHB9 = ", "")
        If IsNumeric(s) Then
            Channel9 = CDb1(s)
            T9.Invoke(New UpdateCH9(AddressOf UpdateCH9_Box),
Channel9.ToString)
        End If

    ElseIf s.Contains("CHB10") Then
        s = s.Replace("CHB10 = ", "")
        If IsNumeric(s) Then
            Channel10 = CDb1(s)
            T10.Invoke(New UpdateCH10(AddressOf UpdateCH10_Box),
Channel10.ToString)
        End If

    ElseIf s.Contains("CHB11") Then
        s = s.Replace("CHB11 = ", "")
        If IsNumeric(s) Then
            Channel11 = CDb1(s)
            T11.Invoke(New UpdateCH11(AddressOf UpdateCH11_Box),
Channel11.ToString)
        End If

    ElseIf s.Contains("CHB12") Then
        s = s.Replace("CHB12 = ", "")
        If IsNumeric(s) Then
            Channel12 = CDb1(s)
            T12.Invoke(New UpdateCH12(AddressOf UpdateCH12_Box),
Channel12.ToString)
        End If

```

```

ElseIf s.Contains("CHB13") Then
    s = s.Replace("CHB13 = ", "")
    If IsNumeric(s) Then
        Channel13 = CDb1(s)
        T13.Invoke(New UpdateCH13(AddressOf UpdateCH13_Box),
Channel13.ToString)
    End If

ElseIf s.Contains("CHB14") Then
    s = s.Replace("CHB14 = ", "")
    If IsNumeric(s) Then
        Channel14 = CDb1(s)
        T14.Invoke(New UpdateCH14(AddressOf UpdateCH14_Box),
Channel14.ToString)
    End If

ElseIf s.Contains("CHB15") Then
    s = s.Replace("CHB15 = ", "")
    If IsNumeric(s) Then
        Channel15 = CDb1(s)
        T15.Invoke(New UpdateCH15(AddressOf UpdateCH15_Box),
Channel15.ToString)
    End If

End If
Catch ex As Exception
    MsgBox(ex.ToString, MsgBoxStyle.OkOnly, "Data Log Error")
End Try

End Sub

#Region "Delegate Procedures"
Delegate Sub UpdateCH0(ByVal CH0 As String)
Delegate Sub UpdateCH1(ByVal CH1 As String)
Delegate Sub UpdateCH2(ByVal CH2 As String)
Delegate Sub UpdateCH3(ByVal CH3 As String)
Delegate Sub UpdateCH4(ByVal CH4 As String)
Delegate Sub UpdateCH5(ByVal CH5 As String)
Delegate Sub UpdateCH6(ByVal CH6 As String)
Delegate Sub UpdateCH7(ByVal CH7 As String)
Delegate Sub UpdateCH8(ByVal CH8 As String)
Delegate Sub UpdateCH9(ByVal CH9 As String)

```

```

Delegate Sub UpdateCH10(ByVal CH10 As String)
Delegate Sub UpdateCH11(ByVal CH11 As String)
Delegate Sub UpdateCH12(ByVal CH12 As String)
Delegate Sub UpdateCH13(ByVal CH13 As String)
Delegate Sub UpdateCH14(ByVal CH14 As String)
Delegate Sub UpdateCH15(ByVal CH15 As String)
#End Region

#Region "Update the Text Boxes"

Public Sub UpdateCH0_Box(ByVal CH0 As String)
    T0.Text = CH0
    New_Value_00.Text = Val(T0.Text) * Val(m00.Text) + Val(b00.Text)
    Processed_Input_00.Text = CH0
    Value_Processed_00.Text = New_Value_00.Text
End Sub

Public Sub UpdateCH1_Box(ByVal CH1 As String)
    T1.Text = CH1
    New_Value_01.Text = Val(T1.Text) * Val(m01.Text) + Val(b01.Text)
    Processed_Input_01.Text = CH1
    Value_Processed_01.Text = New_Value_01.Text
End Sub

Public Sub UpdateCH2_Box(ByVal CH2 As String)
    T2.Text = CH2
    New_Value_02.Text = Val(T2.Text) * Val(m02.Text) + Val(b02.Text)
    Processed_Input_02.Text = CH2
    Value_Processed_02.Text = New_Value_02.Text
End Sub

Public Sub UpdateCH3_Box(ByVal CH3 As String)
    T3.Text = CH3
    New_Value_03.Text = Val(T3.Text) * Val(m03.Text) + Val(b03.Text)
    Processed_Input_03.Text = CH3
    Value_Processed_03.Text = New_Value_03.Text
End Sub

Public Sub UpdateCH4_Box(ByVal CH4 As String)
    T4.Text = CH4
    New_Value_04.Text = Val(T4.Text) * Val(m04.Text) + Val(b04.Text)
    Processed_Input_04.Text = CH4
    Value_Processed_04.Text = New_Value_04.Text
End Sub

```



```

Public Sub UpdateCH5_Box(ByVal CH5 As String)
    T5.Text = CH5
    New_Value_05.Text = Val(T5.Text) * Val(m05.Text) + Val(b05.Text)
    Processed_Input_05.Text = CH5
    Value_Processed_05.Text = New_Value_05.Text
End Sub

```

```

Public Sub UpdateCH6_Box(ByVal CH6 As String)
    T6.Text = CH6
    New_Value_06.Text = Val(T6.Text) * Val(m06.Text) + Val(b06.Text)
    Processed_Input_06.Text = CH6
    Value_Processed_06.Text = New_Value_06.Text
End Sub

```

```

Public Sub UpdateCH7_Box(ByVal CH7 As String)
    T7.Text = CH7
    New_Value_07.Text = Val(T7.Text) * Val(m07.Text) + Val(b07.Text)
    Processed_Input_07.Text = CH7
    Value_Processed_07.Text = New_Value_07.Text
End Sub

```

```

Public Sub UpdateCH8_Box(ByVal CH8 As String)
    T8.Text = CH8
    New_Value_08.Text = Val(T8.Text) * Val(m08.Text) + Val(b08.Text)
    Processed_Input_08.Text = CH8
    Value_Processed_08.Text = New_Value_08.Text
End Sub

```

```

Public Sub UpdateCH9_Box(ByVal CH9 As String)
    T9.Text = CH9
    New_Value_09.Text = Val(T9.Text) * Val(m09.Text) + Val(b09.Text)
    Processed_Input_09.Text = CH9
    Value_Processed_09.Text = New_Value_09.Text
End Sub

```

```

Public Sub UpdateCH10_Box(ByVal CH10 As String)
    T10.Text = CH10
    New_Value_10.Text = Val(T10.Text) * Val(m10.Text) + Val(b10.Text)
    Processed_Input_10.Text = CH10
    Value_Processed_10.Text = New_Value_10.Text
End Sub

```

```

Public Sub UpdateCH11_Box(ByVal CH11 As String)

```

```

    T11.Text = CH11
    New_Value_11.Text = Val(T11.Text) * Val(m11.Text) + Val(b11.Text)
    Processed_Input_11.Text = CH11
    Value_Processed_11.Text = New_Value_11.Text
End Sub

Public Sub UpdateCH12_Box(ByVal CH12 As String)
    T12.Text = CH12
    New_Value_12.Text = Val(T12.Text) * Val(m12.Text) + Val(b12.Text)
    Processed_Input_12.Text = CH12
    Value_Processed_12.Text = New_Value_12.Text
End Sub

Public Sub UpdateCH13_Box(ByVal CH13 As String)
    T13.Text = CH13
    New_Value_13.Text = Val(T13.Text) * Val(m13.Text) + Val(b13.Text)
    Processed_Input_13.Text = CH13
    Value_Processed_13.Text = New_Value_13.Text
End Sub

Public Sub UpdateCH14_Box(ByVal CH14 As String)
    T14.Text = CH14
    New_Value_14.Text = Val(T14.Text) * Val(m14.Text) + Val(b14.Text)
    Processed_Input_14.Text = CH14
    Value_Processed_14.Text = New_Value_14.Text
End Sub

Public Sub UpdateCH15_Box(ByVal CH15 As String)
    T15.Text = CH15
    New_Value_15.Text = Val(T15.Text) * Val(m15.Text) + Val(b15.Text)
    Processed_Input_15.Text = CH15
    Value_Processed_15.Text = New_Value_15.Text
End Sub
#End Region

Private Sub Form1_Load(ByVal sender As System.Object, ByVal e As
System.EventArgs) Handles MyBase.Load
    DB_FileName.Text = "Data_" & Today.Month & "-" & Today.Day & "-" &
Today.Year
    Dim nameArray() As String
    nameArray = SerialPort.GetPortNames
    Array.Sort(nameArray)
    cmbPorts.DataSource = nameArray
    cmbPorts.DropDownStyle = ComboBoxStyle.DropDownList

```

```
LOAD_CHANNEL_NAMES()  
End Sub
```

```
Private Sub LOAD_CHANNEL_NAMES()
```

```
    Dim regKey As RegistryKey  
    Dim path As String = "HerculesSoft\DAQ"  
    regKey = Registry.CurrentUser.OpenSubKey(path, True)
```

```
    Try  
        Name_A_00.Text = regKey.GetValue("CH00").ToString  
        Name_B_00.Text = regKey.GetValue("CH00").ToString  
        Channel_Name_00.Text = regKey.GetValue("CH00").ToString  
        Processed_Name_00.Text = regKey.GetValue("CH00").ToString  
    Catch ex As Exception  
        Exit Try  
    End Try
```

```
    Try  
        Name_A_01.Text = regKey.GetValue("CH01").ToString  
        Name_B_01.Text = regKey.GetValue("CH01").ToString  
        Channel_Name_01.Text = regKey.GetValue("CH01").ToString  
        Processed_Name_01.Text = regKey.GetValue("CH01").ToString  
    Catch ex As Exception  
        Exit Try  
    End Try
```

```
    Try  
        Name_A_02.Text = regKey.GetValue("CH02").ToString  
        Name_B_02.Text = regKey.GetValue("CH02").ToString  
        Channel_Name_02.Text = regKey.GetValue("CH02").ToString  
        Processed_Name_02.Text = regKey.GetValue("CH02").ToString  
    Catch ex As Exception  
        Exit Try  
    End Try
```

```
    Try  
        Name_A_03.Text = regKey.GetValue("CH03").ToString  
        Name_B_03.Text = regKey.GetValue("CH03").ToString  
        Channel_Name_03.Text = regKey.GetValue("CH03").ToString  
        Processed_Name_03.Text = regKey.GetValue("CH03").ToString  
    Catch ex As Exception  
        Exit Try
```

End Try

Try

```
Name_A_04.Text = regKey.GetValue("CH04").ToString  
Name_B_04.Text = regKey.GetValue("CH04").ToString  
Channel_Name_04.Text = regKey.GetValue("CH04").ToString  
Processed_Name_04.Text = regKey.GetValue("CH04").ToString
```

Catch ex As Exception

Exit Try

End Try

Try

```
Name_A_05.Text = regKey.GetValue("CH05").ToString  
Name_B_05.Text = regKey.GetValue("CH05").ToString  
Channel_Name_05.Text = regKey.GetValue("CH05").ToString  
Processed_Name_05.Text = regKey.GetValue("CH05").ToString
```

Catch ex As Exception

Exit Try

End Try

Try

```
Name_A_06.Text = regKey.GetValue("CH06").ToString  
Name_B_06.Text = regKey.GetValue("CH06").ToString  
Channel_Name_06.Text = regKey.GetValue("CH06").ToString  
Processed_Name_06.Text = regKey.GetValue("CH06").ToString
```

Catch ex As Exception

Exit Try

End Try

Try

```
Name_A_07.Text = regKey.GetValue("CH07").ToString  
Name_B_07.Text = regKey.GetValue("CH07").ToString  
Channel_Name_07.Text = regKey.GetValue("CH07").ToString  
Processed_Name_07.Text = regKey.GetValue("CH07").ToString
```

Catch ex As Exception

Exit Try

End Try

Try

```
Name_A_08.Text = regKey.GetValue("CH08").ToString  
Name_B_08.Text = regKey.GetValue("CH08").ToString  
Channel_Name_08.Text = regKey.GetValue("CH08").ToString  
Processed_Name_08.Text = regKey.GetValue("CH08").ToString
```

Catch ex As Exception

```
Exit Try
End Try
```

```
Try
    Name_A_09.Text = regKey.GetValue("CH09").ToString
    Name_B_09.Text = regKey.GetValue("CH09").ToString
    Channel_Name_09.Text = regKey.GetValue("CH09").ToString
    Processed_Name_09.Text = regKey.GetValue("CH09").ToString
Catch ex As Exception
    Exit Try
End Try
```

```
Try
    Name_A_10.Text = regKey.GetValue("CH10").ToString
    Name_B_10.Text = regKey.GetValue("CH10").ToString
    Channel_Name_10.Text = regKey.GetValue("CH10").ToString
    Processed_Name_10.Text = regKey.GetValue("CH10").ToString
Catch ex As Exception
    Exit Try
End Try
```

```
Try
    Name_A_11.Text = regKey.GetValue("CH11").ToString
    Name_B_11.Text = regKey.GetValue("CH11").ToString
    Channel_Name_11.Text = regKey.GetValue("CH11").ToString
    Processed_Name_11.Text = regKey.GetValue("CH11").ToString
Catch ex As Exception
    Exit Try
End Try
```

```
Try
    Name_A_12.Text = regKey.GetValue("CH12").ToString
    Name_B_12.Text = regKey.GetValue("CH12").ToString
    Channel_Name_12.Text = regKey.GetValue("CH12").ToString
    Processed_Name_12.Text = regKey.GetValue("CH12").ToString
Catch ex As Exception
    Exit Try
End Try
```

```
Try
    Name_A_13.Text = regKey.GetValue("CH13").ToString
    Name_B_13.Text = regKey.GetValue("CH13").ToString
    Channel_Name_13.Text = regKey.GetValue("CH13").ToString
    Processed_Name_13.Text = regKey.GetValue("CH13").ToString
```

```

    Catch ex As Exception
        Exit Try
End Try

Try
    Name_A_14.Text = regKey.GetValue("CH14").ToString
    Name_B_14.Text = regKey.GetValue("CH14").ToString
    Channel_Name_14.Text = regKey.GetValue("CH14").ToString
    Processed_Name_14.Text = regKey.GetValue("CH14").ToString
    Catch ex As Exception
        Exit Try
End Try

Try
    Name_A_15.Text = regKey.GetValue("CH15").ToString
    Name_B_15.Text = regKey.GetValue("CH15").ToString
    Channel_Name_15.Text = regKey.GetValue("CH15").ToString
    Processed_Name_15.Text = regKey.GetValue("CH15").ToString
    Catch ex As Exception
        Exit Try
End Try

Try
    m00.Text = regKey.GetValue("m00").ToString
    b00.Text = regKey.GetValue("b00").ToString
    Catch ex As Exception
        Exit Try
End Try

Try
    m01.Text = regKey.GetValue("m01").ToString
    b01.Text = regKey.GetValue("b01").ToString
    Catch ex As Exception
        Exit Try
End Try

Try
    m02.Text = regKey.GetValue("m02").ToString
    b02.Text = regKey.GetValue("b02").ToString
    Catch ex As Exception
        Exit Try
End Try

Try
    m03.Text = regKey.GetValue("m03").ToString

```

```

        b03.Text = regKey.GetValue("b03").ToString
    Catch ex As Exception
        Exit Try
    End Try

    Try
        m04.Text = regKey.GetValue("m04").ToString
        b04.Text = regKey.GetValue("b04").ToString
    Catch ex As Exception
        Exit Try
    End Try

    Try
        m05.Text = regKey.GetValue("m05").ToString
        b05.Text = regKey.GetValue("b05").ToString
    Catch ex As Exception
        Exit Try
    End Try

    Try
        m06.Text = regKey.GetValue("m06").ToString
        b06.Text = regKey.GetValue("b06").ToString
    Catch ex As Exception
        Exit Try
    End Try

    Try
        m07.Text = regKey.GetValue("m07").ToString
        b07.Text = regKey.GetValue("b07").ToString
    Catch ex As Exception
        Exit Try
    End Try

    Try
        m08.Text = regKey.GetValue("m08").ToString
        b08.Text = regKey.GetValue("b08").ToString
    Catch ex As Exception
        Exit Try
    End Try

    Try
        m09.Text = regKey.GetValue("m09").ToString
        b09.Text = regKey.GetValue("b09").ToString
    Catch ex As Exception

```

```

Exit Try
End Try

Try
    m10.Text = regKey.GetValue("m10").ToString
    b10.Text = regKey.GetValue("b10").ToString
Catch ex As Exception
    Exit Try
End Try

Try
    m11.Text = regKey.GetValue("m11").ToString
    b11.Text = regKey.GetValue("b11").ToString
Catch ex As Exception
    Exit Try
End Try

Try
    m12.Text = regKey.GetValue("m12").ToString
    b12.Text = regKey.GetValue("b12").ToString
Catch ex As Exception
    Exit Try
End Try

Try
    m13.Text = regKey.GetValue("m13").ToString
    b13.Text = regKey.GetValue("b13").ToString
Catch ex As Exception
    Exit Try
End Try

Try
    m14.Text = regKey.GetValue("m14").ToString
    b14.Text = regKey.GetValue("b14").ToString
Catch ex As Exception
    Exit Try
End Try

Try
    m15.Text = regKey.GetValue("m15").ToString
    b15.Text = regKey.GetValue("b15").ToString
Catch ex As Exception
    Exit Try
End Try

```



```

Try
    Units00.Text = regKey.GetValue("Units00").ToString
    Units_00.Text = regKey.GetValue("Units00").ToString
    Units_Cal_00.Text = regKey.GetValue("Units00").ToString
Catch ex As Exception
    Exit Try
End Try

```

```

Try
    Units01.Text = regKey.GetValue("Units01").ToString
    Units_01.Text = regKey.GetValue("Units01").ToString
    Units_Cal_01.Text = regKey.GetValue("Units01").ToString
Catch ex As Exception
    Exit Try
End Try

```

```

Try
    Units02.Text = regKey.GetValue("Units02").ToString
    Units_02.Text = regKey.GetValue("Units02").ToString
    Units_Cal_02.Text = regKey.GetValue("Units02").ToString
Catch ex As Exception
    Exit Try
End Try

```

```

Try
    Units03.Text = regKey.GetValue("Units03").ToString
    Units_03.Text = regKey.GetValue("Units03").ToString
    Units_Cal_03.Text = regKey.GetValue("Units03").ToString
Catch ex As Exception
    Exit Try
End Try

```

```

Try
    Units04.Text = regKey.GetValue("Units04").ToString
    Units_04.Text = regKey.GetValue("Units04").ToString
    Units_Cal_04.Text = regKey.GetValue("Units04").ToString
Catch ex As Exception
    Exit Try
End Try

```

```

Try
    Units05.Text = regKey.GetValue("Units05").ToString
    Units_05.Text = regKey.GetValue("Units05").ToString

```

```

        Units_Cal_05.Text = regKey.GetValue("Units05").ToString
    Catch ex As Exception
        Exit Try
    End Try

```

```

    Try
        Units06.Text = regKey.GetValue("Units06").ToString
        Units_06.Text = regKey.GetValue("Units06").ToString
        Units_Cal_06.Text = regKey.GetValue("Units06").ToString
    Catch ex As Exception
        Exit Try
    End Try

```

```

    Try
        Units07.Text = regKey.GetValue("Units07").ToString
        Units_07.Text = regKey.GetValue("Units07").ToString
        Units_Cal_07.Text = regKey.GetValue("Units07").ToString
    Catch ex As Exception
        Exit Try
    End Try

```

```

    Try
        Units08.Text = regKey.GetValue("Units08").ToString
        Units_08.Text = regKey.GetValue("Units08").ToString
        Units_Cal_08.Text = regKey.GetValue("Units08").ToString
    Catch ex As Exception
        Exit Try
    End Try

```

```

    Try
        Units09.Text = regKey.GetValue("Units09").ToString
        Units_09.Text = regKey.GetValue("Units09").ToString
        Units_Cal_09.Text = regKey.GetValue("Units09").ToString
    Catch ex As Exception
        Exit Try
    End Try

```

```

    Try
        Units10.Text = regKey.GetValue("Units10").ToString
        Units_10.Text = regKey.GetValue("Units10").ToString
        Units_Cal_10.Text = regKey.GetValue("Units10").ToString
    Catch ex As Exception
        Exit Try
    End Try

```

```

Try
    Units11.Text = regKey.GetValue("Units11").ToString
    Units_11.Text = regKey.GetValue("Units11").ToString
    Units_Cal_11.Text = regKey.GetValue("Units11").ToString
Catch ex As Exception
    Exit Try
End Try

```

```

Try
    Units12.Text = regKey.GetValue("Units12").ToString
    Units_12.Text = regKey.GetValue("Units12").ToString
    Units_Cal_12.Text = regKey.GetValue("Units12").ToString
Catch ex As Exception
    Exit Try
End Try

```

```

Try
    Units13.Text = regKey.GetValue("Units13").ToString
    Units_13.Text = regKey.GetValue("Units13").ToString
    Units_Cal_13.Text = regKey.GetValue("Units13").ToString
Catch ex As Exception
    Exit Try
End Try

```

```

Try
    Units14.Text = regKey.GetValue("Units14").ToString
    Units_14.Text = regKey.GetValue("Units14").ToString
    Units_Cal_14.Text = regKey.GetValue("Units14").ToString
Catch ex As Exception
    Exit Try
End Try

```

```

Try
    Units15.Text = regKey.GetValue("Units15").ToString
    Units_15.Text = regKey.GetValue("Units15").ToString
    Units_Cal_15.Text = regKey.GetValue("Units15").ToString
Catch ex As Exception
    Exit Try
End Try
End Sub

```

```

Private Sub Button33_Click(ByVal sender As System.Object, ByVal e As
System.EventArgs) Handles Button33.Click

```

```

    Try
        objSerial.Close()
        cmbPorts.Enabled = True
    Catch ex As Exception
        Exit Sub
    End Try
End Sub

Private Sub Button34_Click(ByVal sender As System.Object, ByVal e As
System.EventArgs) Handles Button34.Click

    Dim SELECTED_PORT As String = cmbPorts.Text

    If String.IsNullOrEmpty(SELECTED_PORT) Then
        MsgBox("Please Select A Port")
        Exit Sub
    Else
        cmbPorts.Enabled = False
        Try
            objSerial.PortName = SELECTED_PORT
            objSerial.BaudRate = 57600
            objSerial.Open()
        Catch ex As Exception
            MsgBox(ex.ToString)
        End Try
    End If

End Sub

Private Sub Button36_Click(ByVal sender As System.Object, ByVal e As
System.EventArgs) Handles Button36.Click
    LOAD_CHANNEL_NAMES()
End Sub

#Region "Set Up Names for Channels"

Private Sub Button1_Click(ByVal sender As System.Object, ByVal e As
System.EventArgs) Handles Button1.Click
    Dim SSString, Variable_Name As String
    SSString = "HKEY_CURRENT_USER\HerculesSoft\DAQ"
    Variable_Name = Channel_Name_00.Text
    My.Computer.Registry.SetValue(SSString, "CH00", Variable_Name)

```

```

    Dim Units_Name As String = Units00.Text
    My.Computer.Registry.SetValue(SSString, "Units00", Units_Name)
    LOAD_CHANNEL_NAMES()
End Sub

Private Sub Button2_Click(ByVal sender As System.Object, ByVal e As
System.EventArgs) Handles Button2.Click
    Dim SSString, Variable_Name As String
    SSString = "HKEY_CURRENT_USER\HerculesSoft\DAQ"
    Variable_Name = Channel_Name_01.Text
    My.Computer.Registry.SetValue(SSString, "CH01", Variable_Name)
    Dim Units_Name As String = Units01.Text
    My.Computer.Registry.SetValue(SSString, "Units01", Units_Name)
    LOAD_CHANNEL_NAMES()
End Sub

Private Sub Button4_Click(ByVal sender As System.Object, ByVal e As
System.EventArgs) Handles Button4.Click
    Dim SSString, Variable_Name As String
    SSString = "HKEY_CURRENT_USER\HerculesSoft\DAQ"
    Variable_Name = Channel_Name_02.Text
    My.Computer.Registry.SetValue(SSString, "CH02", Variable_Name)
    Dim Units_Name As String = Units02.Text
    My.Computer.Registry.SetValue(SSString, "Units02", Units_Name)
    LOAD_CHANNEL_NAMES()
End Sub

Private Sub Button3_Click(ByVal sender As System.Object, ByVal e As
System.EventArgs) Handles Button3.Click
    Dim SSString, Variable_Name As String
    SSString = "HKEY_CURRENT_USER\HerculesSoft\DAQ"
    Variable_Name = Channel_Name_03.Text
    My.Computer.Registry.SetValue(SSString, "CH03", Variable_Name)
    Dim Units_Name As String = Units03.Text
    My.Computer.Registry.SetValue(SSString, "Units03", Units_Name)
    LOAD_CHANNEL_NAMES()
End Sub

Private Sub Button8_Click(ByVal sender As System.Object, ByVal e As
System.EventArgs) Handles Button8.Click
    Dim SSString, Variable_Name As String
    SSString = "HKEY_CURRENT_USER\HerculesSoft\DAQ"
    Variable_Name = Channel_Name_04.Text
    My.Computer.Registry.SetValue(SSString, "CH04", Variable_Name)

```

```

    Dim Units_Name As String = Units04.Text
    My.Computer.Registry.SetValue(SSString, "Units04", Units_Name)
    LOAD_CHANNEL_NAMES()
End Sub

Private Sub Button7_Click(ByVal sender As System.Object, ByVal e As
System.EventArgs) Handles Button7.Click
    Dim SSString, Variable_Name As String
    SSString = "HKEY_CURRENT_USER\HerculesSoft\DAQ"
    Variable_Name = Channel_Name_05.Text
    My.Computer.Registry.SetValue(SSString, "CH05", Variable_Name)
    Dim Units_Name As String = Units05.Text
    My.Computer.Registry.SetValue(SSString, "Units05", Units_Name)
    LOAD_CHANNEL_NAMES()
End Sub

Private Sub Button6_Click(ByVal sender As System.Object, ByVal e As
System.EventArgs) Handles Button6.Click
    Dim SSString, Variable_Name As String
    SSString = "HKEY_CURRENT_USER\HerculesSoft\DAQ"
    Variable_Name = Channel_Name_06.Text
    My.Computer.Registry.SetValue(SSString, "CH06", Variable_Name)
    Dim Units_Name As String = Units06.Text
    My.Computer.Registry.SetValue(SSString, "Units06", Units_Name)
    LOAD_CHANNEL_NAMES()
End Sub

Private Sub Button5_Click(ByVal sender As System.Object, ByVal e As
System.EventArgs) Handles Button5.Click
    Dim SSString, Variable_Name As String
    SSString = "HKEY_CURRENT_USER\HerculesSoft\DAQ"
    Variable_Name = Channel_Name_07.Text
    My.Computer.Registry.SetValue(SSString, "CH07", Variable_Name)
    Dim Units_Name As String = Units07.Text
    My.Computer.Registry.SetValue(SSString, "Units07", Units_Name)
    LOAD_CHANNEL_NAMES()
End Sub

Private Sub Button16_Click(ByVal sender As System.Object, ByVal e As
System.EventArgs) Handles Button16.Click
    Dim SSString, Variable_Name As String
    SSString = "HKEY_CURRENT_USER\HerculesSoft\DAQ"
    Variable_Name = Channel_Name_08.Text
    My.Computer.Registry.SetValue(SSString, "CH08", Variable_Name)

```

```

    Dim Units_Name As String = Units08.Text
    My.Computer.Registry.SetValue(SSString, "Units08", Units_Name)
    LOAD_CHANNEL_NAMES()
End Sub

Private Sub Button15_Click(ByVal sender As System.Object, ByVal e As
System.EventArgs) Handles Button15.Click
    Dim SSString, Variable_Name As String
    SSString = "HKEY_CURRENT_USER\HerculesSoft\DAQ"
    Variable_Name = Channel_Name_09.Text
    My.Computer.Registry.SetValue(SSString, "CH09", Variable_Name)
    Dim Units_Name As String = Units09.Text
    My.Computer.Registry.SetValue(SSString, "Units09", Units_Name)
    LOAD_CHANNEL_NAMES()
End Sub

Private Sub Button14_Click(ByVal sender As System.Object, ByVal e As
System.EventArgs) Handles Button14.Click
    Dim SSString, Variable_Name As String
    SSString = "HKEY_CURRENT_USER\HerculesSoft\DAQ"
    Variable_Name = Channel_Name_10.Text
    My.Computer.Registry.SetValue(SSString, "CH10", Variable_Name)
    Dim Units_Name As String = Units10.Text
    My.Computer.Registry.SetValue(SSString, "Units10", Units_Name)
    LOAD_CHANNEL_NAMES()
End Sub

Private Sub Button13_Click(ByVal sender As System.Object, ByVal e As
System.EventArgs) Handles Button13.Click
    Dim SSString, Variable_Name As String
    SSString = "HKEY_CURRENT_USER\HerculesSoft\DAQ"
    Variable_Name = Channel_Name_11.Text
    My.Computer.Registry.SetValue(SSString, "CH11", Variable_Name)
    Dim Units_Name As String = Units11.Text
    My.Computer.Registry.SetValue(SSString, "Units11", Units_Name)
    LOAD_CHANNEL_NAMES()
End Sub

Private Sub Button12_Click(ByVal sender As System.Object, ByVal e As
System.EventArgs) Handles Button12.Click
    Dim SSString, Variable_Name As String
    SSString = "HKEY_CURRENT_USER\HerculesSoft\DAQ"
    Variable_Name = Channel_Name_12.Text
    My.Computer.Registry.SetValue(SSString, "CH12", Variable_Name)

```

```

    Dim Units_Name As String = Units12.Text
    My.Computer.Registry.SetValue(SSString, "Units12", Units_Name)
    LOAD_CHANNEL_NAMES()
End Sub

Private Sub Button11_Click(ByVal sender As System.Object, ByVal e As
System.EventArgs) Handles Button11.Click
    Dim SSString, Variable_Name As String
    SSString = "HKEY_CURRENT_USER\HerculesSoft\DAQ"
    Variable_Name = Channel_Name_13.Text
    My.Computer.Registry.SetValue(SSString, "CH13", Variable_Name)
    Dim Units_Name As String = Units13.Text
    My.Computer.Registry.SetValue(SSString, "Units13", Units_Name)
    LOAD_CHANNEL_NAMES()
End Sub

Private Sub Button10_Click(ByVal sender As System.Object, ByVal e As
System.EventArgs) Handles Button10.Click
    Dim SSString, Variable_Name As String
    SSString = "HKEY_CURRENT_USER\HerculesSoft\DAQ"
    Variable_Name = Channel_Name_14.Text
    My.Computer.Registry.SetValue(SSString, "CH14", Variable_Name)
    Dim Units_Name As String = Units14.Text
    My.Computer.Registry.SetValue(SSString, "Units14", Units_Name)
    LOAD_CHANNEL_NAMES()
End Sub

Private Sub Button9_Click(ByVal sender As System.Object, ByVal e As
System.EventArgs) Handles Button9.Click
    Dim SSString, Variable_Name As String
    SSString = "HKEY_CURRENT_USER\HerculesSoft\DAQ"
    Variable_Name = Channel_Name_15.Text
    My.Computer.Registry.SetValue(SSString, "CH15", Variable_Name)
    Dim Units_Name As String = Units15.Text
    My.Computer.Registry.SetValue(SSString, "Units15", Units_Name)
    LOAD_CHANNEL_NAMES()
End Sub
#End Region

#Region "Setup Calibration Parameters"
Private Sub Button32_Click(ByVal sender As System.Object, ByVal e As
System.EventArgs) Handles Button32.Click
    Dim SSString, Variable_Name, Intercept As String

```



```

SSString = "HKEY_CURRENT_USER\HerculesSoft\DAQ"
Variable_Name = m00.Text
Intercept = b00.Text
My.Computer.Registry.SetValue(SSString, "m00", Variable_Name)
My.Computer.Registry.SetValue(SSString, "b00", Intercept)

```

End Sub

```

Private Sub Button31_Click(ByVal sender As System.Object, ByVal e As
System.EventArgs) Handles Button31.Click
    Dim SSString, Variable_Name, Intercept As String
    SSString = "HKEY_CURRENT_USER\HerculesSoft\DAQ"
    Variable_Name = m01.Text
    Intercept = b01.Text
    My.Computer.Registry.SetValue(SSString, "m01", Variable_Name)
    My.Computer.Registry.SetValue(SSString, "b01", Intercept)

```

End Sub

```

Private Sub Button30_Click(ByVal sender As System.Object, ByVal e As
System.EventArgs) Handles Button30.Click
    Dim SSString, Variable_Name, Intercept As String
    SSString = "HKEY_CURRENT_USER\HerculesSoft\DAQ"
    Variable_Name = m02.Text
    Intercept = b02.Text
    My.Computer.Registry.SetValue(SSString, "m02", Variable_Name)
    My.Computer.Registry.SetValue(SSString, "b02", Intercept)

```

End Sub

```

Private Sub Button29_Click(ByVal sender As System.Object, ByVal e As
System.EventArgs) Handles Button29.Click
    Dim SSString, Variable_Name, Intercept As String
    SSString = "HKEY_CURRENT_USER\HerculesSoft\DAQ"
    Variable_Name = m03.Text
    Intercept = b03.Text
    My.Computer.Registry.SetValue(SSString, "m03", Variable_Name)
    My.Computer.Registry.SetValue(SSString, "b03", Intercept)

```

End Sub

```

Private Sub Button28_Click(ByVal sender As System.Object, ByVal e As
System.EventArgs) Handles Button28.Click
    Dim SSString, Variable_Name, Intercept As String
    SSString = "HKEY_CURRENT_USER\HerculesSoft\DAQ"
    Variable_Name = m04.Text
    Intercept = b04.Text

```

```

        My.Computer.Registry.SetValue(SSString, "m04", Variable_Name)
        My.Computer.Registry.SetValue(SSString, "b04", Intercept)
End Sub

Private Sub Button27_Click(ByVal sender As System.Object, ByVal e As
System.EventArgs) Handles Button27.Click
    Dim SSString, Variable_Name, Intercept As String
    SSString = "HKEY_CURRENT_USER\HerculesSoft\DAQ"
    Variable_Name = m05.Text
    Intercept = b05.Text
    My.Computer.Registry.SetValue(SSString, "m05", Variable_Name)
    My.Computer.Registry.SetValue(SSString, "b05", Intercept)
End Sub

Private Sub Button26_Click(ByVal sender As System.Object, ByVal e As
System.EventArgs) Handles Button26.Click
    Dim SSString, Variable_Name, Intercept As String
    SSString = "HKEY_CURRENT_USER\HerculesSoft\DAQ"
    Variable_Name = m06.Text
    Intercept = b06.Text
    My.Computer.Registry.SetValue(SSString, "m06", Variable_Name)
    My.Computer.Registry.SetValue(SSString, "b06", Intercept)
End Sub

Private Sub Button25_Click(ByVal sender As System.Object, ByVal e As
System.EventArgs) Handles Button25.Click
    Dim SSString, Variable_Name, Intercept As String
    SSString = "HKEY_CURRENT_USER\HerculesSoft\DAQ"
    Variable_Name = m07.Text
    Intercept = b07.Text
    My.Computer.Registry.SetValue(SSString, "m07", Variable_Name)
    My.Computer.Registry.SetValue(SSString, "b07", Intercept)
End Sub

Private Sub Button24_Click(ByVal sender As System.Object, ByVal e As
System.EventArgs) Handles Button24.Click
    Dim SSString, Variable_Name, Intercept As String
    SSString = "HKEY_CURRENT_USER\HerculesSoft\DAQ"
    Variable_Name = m08.Text
    Intercept = b08.Text
    My.Computer.Registry.SetValue(SSString, "m08", Variable_Name)
    My.Computer.Registry.SetValue(SSString, "b08", Intercept)
End Sub

```

```

Private Sub Button23_Click(ByVal sender As System.Object, ByVal e As
System.EventArgs) Handles Button23.Click
    Dim SSString, Variable_Name, Intercept As String
    SSString = "HKEY_CURRENT_USER\HerculesSoft\DAQ"
    Variable_Name = m09.Text
    Intercept = b09.Text
    My.Computer.Registry.SetValue(SSString, "m09", Variable_Name)
    My.Computer.Registry.SetValue(SSString, "b09", Intercept)
End Sub

```

```

Private Sub Button22_Click(ByVal sender As System.Object, ByVal e As
System.EventArgs) Handles Button22.Click
    Dim SSString, Variable_Name, Intercept As String
    SSString = "HKEY_CURRENT_USER\HerculesSoft\DAQ"
    Variable_Name = m10.Text
    Intercept = b10.Text
    My.Computer.Registry.SetValue(SSString, "m10", Variable_Name)
    My.Computer.Registry.SetValue(SSString, "b10", Intercept)
End Sub

```

```

Private Sub Button21_Click(ByVal sender As System.Object, ByVal e As
System.EventArgs) Handles Button21.Click
    Dim SSString, Variable_Name, Intercept As String
    SSString = "HKEY_CURRENT_USER\HerculesSoft\DAQ"
    Variable_Name = m11.Text
    Intercept = b11.Text
    My.Computer.Registry.SetValue(SSString, "m11", Variable_Name)
    My.Computer.Registry.SetValue(SSString, "b11", Intercept)
End Sub

```

```

Private Sub Button20_Click(ByVal sender As System.Object, ByVal e As
System.EventArgs) Handles Button20.Click
    Dim SSString, Variable_Name, Intercept As String
    SSString = "HKEY_CURRENT_USER\HerculesSoft\DAQ"
    Variable_Name = m12.Text
    Intercept = b12.Text
    My.Computer.Registry.SetValue(SSString, "m12", Variable_Name)
    My.Computer.Registry.SetValue(SSString, "b12", Intercept)
End Sub

```

```

Private Sub Button19_Click(ByVal sender As System.Object, ByVal e As
System.EventArgs) Handles Button19.Click
    Dim SSString, Variable_Name, Intercept As String
    SSString = "HKEY_CURRENT_USER\HerculesSoft\DAQ"

```

```

    Variable_Name = m13.Text
    Intercept = b13.Text
    My.Computer.Registry.SetValue(SSString, "m13", Variable_Name)
    My.Computer.Registry.SetValue(SSString, "b13", Intercept)
End Sub

Private Sub Button18_Click(ByVal sender As System.Object, ByVal e As
System.EventArgs) Handles Button18.Click
    Dim SSString, Variable_Name, Intercept As String
    SSString = "HKEY_CURRENT_USER\HerculesSoft\DAQ"
    Variable_Name = m14.Text
    Intercept = b14.Text
    My.Computer.Registry.SetValue(SSString, "m14", Variable_Name)
    My.Computer.Registry.SetValue(SSString, "b14", Intercept)
End Sub

Private Sub Button17_Click(ByVal sender As System.Object, ByVal e As
System.EventArgs) Handles Button17.Click
    Dim SSString, Variable_Name, Intercept As String
    SSString = "HKEY_CURRENT_USER\HerculesSoft\DAQ"
    Variable_Name = m15.Text
    Intercept = b15.Text
    My.Computer.Registry.SetValue(SSString, "m15", Variable_Name)
    My.Computer.Registry.SetValue(SSString, "b15", Intercept)
End Sub
#End Region

#Region "EXCEL METHODS"

Private Sub releaseObject(ByVal obj As Object)
    Try
        System.Runtime.InteropServices.Marshal.ReleaseComObject(obj)
        obj = Nothing
    Catch ex As Exception
        obj = Nothing
    Finally
        GC.Collect()
    End Try
End Sub

Private Sub Button39_Click(ByVal sender As System.Object, ByVal e As
System.EventArgs) Handles Automatic.Click
    Dim TDLAY As Double = TDelay.Text
    Timer1.Interval = TDLAY * 1000

```

```

Select Case Timer1.Enabled
    Case True
        Timer1.Enabled = False
        Status_Label.Text = "Automatic Mode Set Off"
        Automatic.BackColor = Color.Red
    Case False
        Timer1.Enabled = True
        Status_Label.Text = "Automatic Mode Set On"
        Automatic.BackColor = Color.Green
End Select
End Sub
#End Region

Private trd As Thread
Private Sub Button38_Click(ByVal sender As System.Object, ByVal e As
System.EventArgs) Handles Button38.Click
    trd = New Thread(AddressOf ThreadTask)
    trd.IsBackground = True
    trd.Start()
    Button38.Text = "Recording"
    Save_Status.BackColor = Color.Green
End Sub

Dim tdelaydelay As String

Delegate Sub Time_Delay(ByVal TimeTime As Integer)

Private Sub SetText(ByVal text As String)
    If TDelay.InvokeRequired Then
        TDelay.Invoke(New Action(Of Integer)(AddressOf SetText), text)
        tdelaydelay = text
    Else
        TDelay.Text = text
        tdelaydelay = text
    End If
End Sub

Private Sub ThreadTask()
    Do
        Save_All_Data()
        Thread.Sleep(5000)
    Loop
End Sub

```

```

Private Sub Button39_Click_1(ByVal sender As System.Object, ByVal e As
System.EventArgs) Handles Button39.Click
    trd.Abort()
    MsgBox("Recording Stopped", MsgBoxStyle.OkOnly, "Data Log")
End Sub
    Dim NameName As String
    Private Sub DBCreateFile_Click(ByVal sender As System.Object, ByVal e As
System.EventArgs) Handles DB_CreateFile.Click
        If String.IsNullOrEmpty(DB_FileName.Text) Then
            MsgBox("The file must be Named", MsgBoxStyle.OkOnly, "Error on File
Name")
        Exit Sub
    End If

    NameName = DB_FileName.Text

    If (Not System.IO.Directory.Exists("C:\Data_Acquisition_System\")) Then
        System.IO.Directory.CreateDirectory("C:\Data_Acquisition_System\")
    End If
    Try
        Dim AccessDatabaseEngine As New
Microsoft.Office.Interop.Access.Dao.DBEngine
        Dim AccessDatabase As Microsoft.Office.Interop.Access.Dao.Database

        AccessDatabase =
AccessDatabaseEngine.CreateDatabase("C:\Data_Acquisition_System\" & NameName
& ".accdb", LanguageConstants.dbLangGeneral, DatabaseTypeEnum.dbVersion120)
        AccessDatabase.Close()
    Catch ex As Exception
        MsgBox(ex.ToString, MsgBoxStyle.OkOnly, "ERROR CREATING FILE")
    Exit Sub
    End Try
    Try
        Using conn As New
OleDb.OleDbConnection("Provider=Microsoft.ACE.OLEDB.12.0;" & _
        "Data Source=C:\Data_Acquisition_System\" & NameName & ".accdb;")
            Using cmd As New OleDb.OleDbCommand("CREATE TABLE DataAcquired
( " & _
                "AutoId int identity," & _
                "Time_Sample NVarchar(50)," & _
                "CH0 NVarchar(50)," & _
                "CH1 NVarchar(50)," & _

```

"CH2 NVarchar(50)," & _
"CH3 NVarchar(50)," & _
"CH4 NVarchar(50)," & _
"CH5 NVarchar(50)," & _
"CH6 NVarchar(50)," & _
"CH7 NVarchar(50)," & _
"CH8 NVarchar(50)," & _
"CH9 NVarchar(50)," & _
"CH10 NVarchar(50)," & _
"CH11 NVarchar(50)," & _
"CH12 NVarchar(50)," & _
"CH13 NVarchar(50)," & _
"CH14 NVarchar(50)," & _
"CH15 NVarchar(50)," & _
"M0 NVarchar(50)," & _
"M1 NVarchar(50)," & _
"M2 NVarchar(50)," & _
"M3 NVarchar(50)," & _
"M4 NVarchar(50)," & _
"M5 NVarchar(50)," & _
"M6 NVarchar(50)," & _
"M7 NVarchar(50)," & _
"M8 NVarchar(50)," & _
"M9 NVarchar(50)," & _
"M10 NVarchar(50)," & _
"M11 NVarchar(50)," & _
"M12 NVarchar(50)," & _
"M13 NVarchar(50)," & _
"M14 NVarchar(50)," & _
"M15 NVarchar(50)," & _
"B0 NVarchar(50)," & _
"B1 NVarchar(50)," & _
"B2 NVarchar(50)," & _
"B3 NVarchar(50)," & _
"B4 NVarchar(50)," & _
"B5 NVarchar(50)," & _
"B6 NVarchar(50)," & _
"B7 NVarchar(50)," & _
"B8 NVarchar(50)," & _
"B9 NVarchar(50)," & _
"B10 NVarchar(50)," & _
"B11 NVarchar(50)," & _
"B12 NVarchar(50)," & _
"B13 NVarchar(50)," & _

```

"B14 NVarchar(50)," & _
"B15 NVarchar(50)," & _
"Value0 NVarchar(50)," & _
"Value1 NVarchar(50)," & _
"Value2 NVarchar(50)," & _
"Value3 NVarchar(50)," & _
"Value4 NVarchar(50)," & _
"Value5 NVarchar(50)," & _
"Value6 NVarchar(50)," & _
"Value7 NVarchar(50)," & _
"Value8 NVarchar(50)," & _
"Value9 NVarchar(50)," & _
"Value10 NVarchar(50)," & _
"Value11 NVarchar(50)," & _
"Value12 NVarchar(50)," & _
"Value13 NVarchar(50)," & _
"Value14 NVarchar(50)," & _
"Value15 NVarchar(50)," & _
"Units0 NVarchar(50)," & _
"Units1 NVarchar(50)," & _
"Units2 NVarchar(50)," & _
"Units3 NVarchar(50)," & _
"Units4 NVarchar(50)," & _
"Units5 NVarchar(50)," & _
"Units6 NVarchar(50)," & _
"Units7 NVarchar(50)," & _
"Units8 NVarchar(50)," & _
"Units9 NVarchar(50)," & _
"Units10 NVarchar(50)," & _
"Units11 NVarchar(50)," & _
"Units12 NVarchar(50)," & _
"Units13 NVarchar(50)," & _
"Units14 NVarchar(50)," & _
"Units15 NVarchar(50)," & _
"CONSTRAINT [pk_AutoId] PRIMARY KEY (AutoId)) ", conn)
conn.Open()
Try
    cmd.ExecuteNonQuery()
Catch ex As Exception
    MsgBox(ex.ToString)
Exit Sub
End Try
End Using
End Using

```



```

        Catch ex As Exception
            MsgBox("Error with the DB File. File might be already created or in use",
MsgBoxStyle.OkOnly, "Error with DB File")
        End Try
    End Sub

```

```

Private Sub Button41_Click(ByVal sender As System.Object, ByVal e As
System.EventArgs) Handles Button41.Click
    DB_FileName.Enabled = False
    trd = New Thread(AddressOf ThreadTask)
    trd.IsBackground = True
    trd.Start()
    Indicator1.BackColor = Color.Green
    Indicator1.Text = "Recording"
End Sub

```

```

Private Sub Save_All_Data()
    Dim CONN As New OleDb.OleDbConnection
    Dim DBProvider As String
    Dim DBSource As String
    Dim ds As New DataSet
    Dim da As OleDb.OleDbDataAdapter
    Dim sql As String
    Dim datedate As String = Today.Month & "/" & Today.Day & "/" & Today.Year
    Dim NameName As String = DB_FileName.Text
    DBProvider = "Provider=microsoft.ace.oledb.12.0;"
    DBSource = "Data Source = C:\Data_Acquisition_System\" & NameName &
".accdb"
    CONN.ConnectionString = DBProvider & DBSource
    CONN.Open()
    sql = "SELECT * FROM DataAcquired"
    da = New OleDb.OleDbDataAdapter(sql, CONN)
    da.Fill(ds, "Data_Saved")
    CONN.Close()

    Try
        Dim CB As New OleDb.OleDbCommandBuilder(da)
        Dim dsnewrow As DataRow
        dsnewrow = ds.Tables("Data_Saved").NewRow
        dsnewrow.Item(1) = Now.TimeOfDay.ToString

        dsnewrow.Item(2) = T0.Text
        dsnewrow.Item(3) = T1.Text
        dsnewrow.Item(4) = T2.Text
    End Try

```

dsnewrow.Item(5) = T3.Text
dsnewrow.Item(6) = T4.Text
dsnewrow.Item(7) = T5.Text
dsnewrow.Item(8) = T6.Text
dsnewrow.Item(9) = T7.Text
dsnewrow.Item(10) = T8.Text
dsnewrow.Item(11) = T9.Text
dsnewrow.Item(12) = T10.Text
dsnewrow.Item(13) = T11.Text
dsnewrow.Item(14) = T12.Text
dsnewrow.Item(15) = T13.Text
dsnewrow.Item(16) = T14.Text
dsnewrow.Item(17) = T15.Text

dsnewrow.Item(18) = m00.Text
dsnewrow.Item(19) = m01.Text
dsnewrow.Item(20) = m02.Text
dsnewrow.Item(21) = m03.Text
dsnewrow.Item(22) = m04.Text
dsnewrow.Item(23) = m05.Text
dsnewrow.Item(24) = m06.Text
dsnewrow.Item(25) = m07.Text
dsnewrow.Item(26) = m08.Text
dsnewrow.Item(27) = m09.Text
dsnewrow.Item(28) = m10.Text
dsnewrow.Item(29) = m11.Text
dsnewrow.Item(30) = m12.Text
dsnewrow.Item(31) = m13.Text
dsnewrow.Item(32) = m14.Text
dsnewrow.Item(33) = m15.Text

dsnewrow.Item(34) = b00.Text
dsnewrow.Item(35) = b01.Text
dsnewrow.Item(36) = b02.Text
dsnewrow.Item(37) = b03.Text
dsnewrow.Item(38) = b04.Text
dsnewrow.Item(39) = b05.Text
dsnewrow.Item(40) = b06.Text
dsnewrow.Item(41) = b07.Text
dsnewrow.Item(42) = b08.Text
dsnewrow.Item(43) = b09.Text
dsnewrow.Item(44) = b10.Text
dsnewrow.Item(45) = b11.Text
dsnewrow.Item(46) = b12.Text

```

dsnewrow.Item(47) = b13.Text
dsnewrow.Item(48) = b14.Text
dsnewrow.Item(49) = b15.Text

dsnewrow.Item(50) = New_Value_00.Text
dsnewrow.Item(51) = New_Value_01.Text
dsnewrow.Item(52) = New_Value_02.Text
dsnewrow.Item(53) = New_Value_03.Text
dsnewrow.Item(54) = New_Value_04.Text
dsnewrow.Item(55) = New_Value_05.Text
dsnewrow.Item(56) = New_Value_06.Text
dsnewrow.Item(57) = New_Value_07.Text
dsnewrow.Item(58) = New_Value_08.Text
dsnewrow.Item(59) = New_Value_09.Text
dsnewrow.Item(60) = New_Value_10.Text
dsnewrow.Item(61) = New_Value_11.Text
dsnewrow.Item(62) = New_Value_12.Text
dsnewrow.Item(63) = New_Value_13.Text
dsnewrow.Item(64) = New_Value_14.Text
dsnewrow.Item(65) = New_Value_15.Text

dsnewrow.Item(66) = Units_00.Text
dsnewrow.Item(67) = Units_01.Text
dsnewrow.Item(68) = Units_02.Text
dsnewrow.Item(69) = Units_03.Text
dsnewrow.Item(70) = Units_04.Text
dsnewrow.Item(71) = Units_05.Text
dsnewrow.Item(72) = Units_06.Text
dsnewrow.Item(73) = Units_07.Text
dsnewrow.Item(74) = Units_08.Text
dsnewrow.Item(75) = Units_09.Text
dsnewrow.Item(76) = Units_10.Text
dsnewrow.Item(77) = Units_11.Text
dsnewrow.Item(78) = Units_12.Text
dsnewrow.Item(79) = Units_13.Text
dsnewrow.Item(80) = Units_14.Text
dsnewrow.Item(81) = Units_15.Text

ds.Tables("Data_Saved").Rows.Add(dsnewrow)
da.Update(ds, "Data_Saved")
Status_Label.Text = "Data Saved at " & Now.TimeOfDay.ToString
Catch ex As Exception
MsgBox(ex.ToString)
Exit Sub

```

```
End Try
End Sub
```

```
Private Sub Button40_Click(ByVal sender As System.Object, ByVal e As
System.EventArgs) Handles Button40.Click
    trd.Abort()
    DB_FileName.Enabled = True

    MsgBox("Recording Stopped", MsgBoxStyle.OkOnly, "Data Log")
    Indicator1.BackColor = Color.Red
    Indicator1.Text = "Stopped"
End Sub
```

```
Private Sub Button35_Click(ByVal sender As System.Object, ByVal e As
System.EventArgs) Handles Button35.Click
    Dim nameArray() As String
    nameArray = SerialPort.GetPortNames
    Array.Sort(nameArray)
    cmbPorts.DataSource = nameArray
    cmbPorts.DropDownStyle = ComboBoxStyle.DropDownList
End Sub
```

```
Private Sub Button37_Click(sender As System.Object, e As System.EventArgs)
If (Not System.IO.Directory.Exists("C:\Data_Acquisition_System\")) Then
    System.IO.Directory.CreateDirectory("C:\Data_Acquisition_System\")
    MsgBox("not Created")
Else
    MsgBox("Already Created")
End If
End Sub
```

```
Dim DBPATHPATH As String
Dim EXPORTPATH As String
```

```
Private Sub DBSelectFileName_Click(ByVal sender As System.Object, ByVal e As
System.EventArgs) Handles DB_SelectFileName.Click
    OpenFileDialog1.InitialDirectory = "C:\\"
    OpenFileDialog1.Title = "Import the Data Acquired File"
    OpenFileDialog1.Filter = "Access DataBase Files|*.accdb"
    OpenFileDialog1.ShowDialog()
End Sub
```

```
Private Sub DBSaveDestination_Click(ByVal sender As System.Object, ByVal e As
System.EventArgs) Handles DB_SaveDestination.Click
```

```

If EXPORTPATH = "" Then
    Dim dialog As New FolderBrowserDialog()
    dialog.RootFolder = Environment.SpecialFolder.Desktop
    dialog.SelectedPath = "C:\\"
    dialog.Description = "Select Export File Path"
    If dialog.ShowDialog() = Windows.Forms.DialogResult.OK Then
        EXPORTPATH = dialog.SelectedPath
    End If
    DB_ExportFile.Text = EXPORTPATH
End If
EXPORTPATH = ""
End Sub

Private Sub DBExport_Click(ByVal sender As System.Object, ByVal e As
System.EventArgs) Handles DB_Export.Click
    Using AccessConn As New
System.Data.OleDb.OleDbConnection("Provider=Microsoft.ACE.OLEDB.12.0;Data
Source = " & DBPATHPATH & ";")

        Try
            AccessConn.Open()
            Dim AccessCommand As New
System.Data.OleDb.OleDbCommand("SELECT * INTO [Excel 12.0
Xml;DATABASE=" & EXPORTPATH & "\DAQ.xlsx;HDR=Yes;].[DataAcquired]
from [DataAcquired]", AccessConn)
            AccessCommand.ExecuteNonQuery()
            AccessConn.Close()
            MsgBox("Export Done", MsgBoxStyle.OkOnly, "Export / Import Window")
        Catch ex As Exception
            MsgBox(ex.ToString())
        End Try
    End Using
End Sub

Private Sub OpenFileDialog1_FileOk(ByVal sender As System.Object, ByVal e As
System.ComponentModel.CancelEventArgs) Handles OpenFileDialog1.FileOk
    DB_SelectFile.Text = OpenFileDialog1.FileName
    DBPATHPATH = OpenFileDialog1.FileName
End Sub

Private Sub FolderBrowserDialog1_HelpRequest(ByVal sender As System.Object,
ByVal e As System.EventArgs) Handles FolderBrowserDialog1.Disposed
    DB_ExportFile.Text = FolderBrowserDialog1.SelectedPath
End Sub

```

```
Private Sub Button44_Click(sender As System.Object, e As System.EventArgs) Handles  
Button44.Click
```

```
    Dim Connection As New OleDb.OleDbConnection  
    Dim PROVIDER As String  
    Dim SOURCE As String  
    Dim DataSet As New DataSet  
    Dim DataAdapter As OleDb.OleDbDataAdapter  
    Dim SQL_STRING As String
```

```
    NameName = DB_FileName.Text
```

```
    Try  
        PROVIDER = "Provider=microsoft.ace.oledb.12.0;"  
        SOURCE = "Data Source=C:\Data_Acquisition_System\" & NameName &  
        ".accdB"  
        Connection.ConnectionString = PROVIDER & SOURCE  
        Connection.Open()  
        Catch ex As Exception  
            MsgBox("Problem Loading the Database", MsgBoxStyle.OkOnly, "Loading  
Error")  
        End Try
```

```
    SQL_STRING = "SELECT * FROM DataAcquired"
```

```
    Try  
        DataAdapter = New OleDb.OleDbDataAdapter(SQL_STRING, Connection)  
        DataAdapter.Fill(DataSet, "FoundCustomers")  
        Connection.Close()
```

```
    Catch exa As Exception  
        MsgBox(exa.ToString, MsgBoxStyle.OkOnly)  
        GoTo Final
```

```
End Try
```

```
    Try  
        DataGridView1.DataSource = DataSet.Tables("FoundCustomers").DefaultView  
        DataGridView1.Columns(0).Visible = False
```

```
    Catch EXX As Exception  
        MsgBox(EXX.ToString, MsgBoxStyle.OkOnly)  
        GoTo FINAL
```

```
End Try
```

```
FINAL:
```

```
    Try
```

```

        DataGridView1.AutoSizeColumns()

        Catch ex As Exception
            Exit Try
        End Try

    End Sub

Private Sub Button37_Click_1(sender As System.Object, e As System.EventArgs)
    Handles Button37.Click
        DataGridView1.Columns(2).Visible = True
        DataGridView1.Columns(3).Visible = True
        DataGridView1.Columns(4).Visible = True
        DataGridView1.Columns(5).Visible = True
        DataGridView1.Columns(6).Visible = True
        DataGridView1.Columns(7).Visible = True
        DataGridView1.Columns(8).Visible = True
        DataGridView1.Columns(9).Visible = True
        DataGridView1.Columns(10).Visible = True
        DataGridView1.Columns(11).Visible = True
        DataGridView1.Columns(12).Visible = True
        DataGridView1.Columns(13).Visible = True
        DataGridView1.Columns(14).Visible = True
        DataGridView1.Columns(15).Visible = True
        DataGridView1.Columns(16).Visible = True
        DataGridView1.Columns(17).Visible = True

        'm
        DataGridView1.Columns(18).Visible = False
        DataGridView1.Columns(19).Visible = False
        DataGridView1.Columns(20).Visible = False
        DataGridView1.Columns(21).Visible = False
        DataGridView1.Columns(22).Visible = False
        DataGridView1.Columns(23).Visible = False
        DataGridView1.Columns(24).Visible = False
        DataGridView1.Columns(25).Visible = False
        DataGridView1.Columns(26).Visible = False
        DataGridView1.Columns(27).Visible = False
        DataGridView1.Columns(28).Visible = False
        DataGridView1.Columns(29).Visible = False
        DataGridView1.Columns(30).Visible = False
        DataGridView1.Columns(31).Visible = False
        DataGridView1.Columns(32).Visible = False
        DataGridView1.Columns(33).Visible = False

```

'b

```
DataGridView1.Columns(34).Visible = False
DataGridView1.Columns(35).Visible = False
DataGridView1.Columns(36).Visible = False
DataGridView1.Columns(37).Visible = False
DataGridView1.Columns(38).Visible = False
DataGridView1.Columns(39).Visible = False
DataGridView1.Columns(40).Visible = False
DataGridView1.Columns(41).Visible = False
DataGridView1.Columns(42).Visible = False
DataGridView1.Columns(43).Visible = False
DataGridView1.Columns(44).Visible = False
DataGridView1.Columns(45).Visible = False
DataGridView1.Columns(46).Visible = False
DataGridView1.Columns(47).Visible = False
DataGridView1.Columns(48).Visible = False
DataGridView1.Columns(49).Visible = False
```

'out

```
DataGridView1.Columns(50).Visible = False
DataGridView1.Columns(51).Visible = False
DataGridView1.Columns(52).Visible = False
DataGridView1.Columns(53).Visible = False
DataGridView1.Columns(54).Visible = False
DataGridView1.Columns(55).Visible = False
DataGridView1.Columns(56).Visible = False
DataGridView1.Columns(57).Visible = False
DataGridView1.Columns(58).Visible = False
DataGridView1.Columns(59).Visible = False
DataGridView1.Columns(60).Visible = False
DataGridView1.Columns(61).Visible = False
DataGridView1.Columns(62).Visible = False
DataGridView1.Columns(63).Visible = False
DataGridView1.Columns(64).Visible = False
DataGridView1.Columns(65).Visible = False
```

'units

```
DataGridView1.Columns(66).Visible = False
DataGridView1.Columns(67).Visible = False
DataGridView1.Columns(68).Visible = False
DataGridView1.Columns(69).Visible = False
DataGridView1.Columns(70).Visible = False
DataGridView1.Columns(71).Visible = False
```



```
DataGridView1.Columns(72).Visible = False
DataGridView1.Columns(73).Visible = False
DataGridView1.Columns(74).Visible = False
DataGridView1.Columns(75).Visible = False
DataGridView1.Columns(76).Visible = False
DataGridView1.Columns(77).Visible = False
DataGridView1.Columns(78).Visible = False
DataGridView1.Columns(79).Visible = False
DataGridView1.Columns(80).Visible = False
DataGridView1.Columns(81).Visible = False
```

End Sub

Private Sub Button42_Click(sender As System.Object, e As System.EventArgs) Handles Button42.Click

```
DataGridView1.Columns(2).Visible = False
DataGridView1.Columns(3).Visible = False
DataGridView1.Columns(4).Visible = False
DataGridView1.Columns(5).Visible = False
DataGridView1.Columns(6).Visible = False
DataGridView1.Columns(7).Visible = False
DataGridView1.Columns(8).Visible = False
DataGridView1.Columns(9).Visible = False
DataGridView1.Columns(10).Visible = False
DataGridView1.Columns(11).Visible = False
DataGridView1.Columns(12).Visible = False
DataGridView1.Columns(13).Visible = False
DataGridView1.Columns(14).Visible = False
DataGridView1.Columns(15).Visible = False
DataGridView1.Columns(16).Visible = False
DataGridView1.Columns(17).Visible = False
```

'm

```
DataGridView1.Columns(18).Visible = False
DataGridView1.Columns(19).Visible = False
DataGridView1.Columns(20).Visible = False
DataGridView1.Columns(21).Visible = False
DataGridView1.Columns(22).Visible = False
DataGridView1.Columns(23).Visible = False
DataGridView1.Columns(24).Visible = False
DataGridView1.Columns(25).Visible = False
DataGridView1.Columns(26).Visible = False
DataGridView1.Columns(27).Visible = False
DataGridView1.Columns(28).Visible = False
```

```
DataGridView1.Columns(29).Visible = False
DataGridView1.Columns(30).Visible = False
DataGridView1.Columns(31).Visible = False
DataGridView1.Columns(32).Visible = False
DataGridView1.Columns(33).Visible = False
```

'b

```
DataGridView1.Columns(34).Visible = False
DataGridView1.Columns(35).Visible = False
DataGridView1.Columns(36).Visible = False
DataGridView1.Columns(37).Visible = False
DataGridView1.Columns(38).Visible = False
DataGridView1.Columns(39).Visible = False
DataGridView1.Columns(40).Visible = False
DataGridView1.Columns(41).Visible = False
DataGridView1.Columns(42).Visible = False
DataGridView1.Columns(43).Visible = False
DataGridView1.Columns(44).Visible = False
DataGridView1.Columns(45).Visible = False
DataGridView1.Columns(46).Visible = False
DataGridView1.Columns(47).Visible = False
DataGridView1.Columns(48).Visible = False
DataGridView1.Columns(49).Visible = False
```

'out

```
DataGridView1.Columns(50).Visible = True
DataGridView1.Columns(51).Visible = True
DataGridView1.Columns(52).Visible = True
DataGridView1.Columns(53).Visible = True
DataGridView1.Columns(54).Visible = True
DataGridView1.Columns(55).Visible = True
DataGridView1.Columns(56).Visible = True
DataGridView1.Columns(57).Visible = True
DataGridView1.Columns(58).Visible = True
DataGridView1.Columns(59).Visible = True
DataGridView1.Columns(60).Visible = True
DataGridView1.Columns(61).Visible = True
DataGridView1.Columns(62).Visible = True
DataGridView1.Columns(63).Visible = True
DataGridView1.Columns(64).Visible = True
DataGridView1.Columns(65).Visible = True
```

'units

```
DataGridView1.Columns(66).Visible = False
DataGridView1.Columns(67).Visible = False
```

```
DataGridView1.Columns(68).Visible = False
DataGridView1.Columns(69).Visible = False
DataGridView1.Columns(70).Visible = False
DataGridView1.Columns(71).Visible = False
DataGridView1.Columns(72).Visible = False
DataGridView1.Columns(73).Visible = False
DataGridView1.Columns(74).Visible = False
DataGridView1.Columns(75).Visible = False
DataGridView1.Columns(76).Visible = False
DataGridView1.Columns(77).Visible = False
DataGridView1.Columns(78).Visible = False
DataGridView1.Columns(79).Visible = False
DataGridView1.Columns(80).Visible = False
DataGridView1.Columns(81).Visible = False
```

End Sub

Private Sub Button43_Click(sender As System.Object, e As System.EventArgs) Handles
Button43.Click

```
DataGridView1.Columns(2).Visible = False
DataGridView1.Columns(3).Visible = False
DataGridView1.Columns(4).Visible = False
DataGridView1.Columns(5).Visible = False
DataGridView1.Columns(6).Visible = False
DataGridView1.Columns(7).Visible = False
DataGridView1.Columns(8).Visible = False
DataGridView1.Columns(9).Visible = False
DataGridView1.Columns(10).Visible = False
DataGridView1.Columns(11).Visible = False
DataGridView1.Columns(12).Visible = False
DataGridView1.Columns(13).Visible = False
DataGridView1.Columns(14).Visible = False
DataGridView1.Columns(15).Visible = False
DataGridView1.Columns(16).Visible = False
DataGridView1.Columns(17).Visible = False
```

'm

```
DataGridView1.Columns(18).Visible = True
DataGridView1.Columns(19).Visible = True
DataGridView1.Columns(20).Visible = True
DataGridView1.Columns(21).Visible = True
DataGridView1.Columns(22).Visible = True
DataGridView1.Columns(23).Visible = True
DataGridView1.Columns(24).Visible = True
DataGridView1.Columns(25).Visible = True
```

```
DataGridView1.Columns(26).Visible = True
DataGridView1.Columns(27).Visible = True
DataGridView1.Columns(28).Visible = True
DataGridView1.Columns(29).Visible = True
DataGridView1.Columns(30).Visible = True
DataGridView1.Columns(31).Visible = True
DataGridView1.Columns(32).Visible = True
DataGridView1.Columns(33).Visible = True
```

'b

```
DataGridView1.Columns(34).Visible = True
DataGridView1.Columns(35).Visible = True
DataGridView1.Columns(36).Visible = True
DataGridView1.Columns(37).Visible = True
DataGridView1.Columns(38).Visible = True
DataGridView1.Columns(39).Visible = True
DataGridView1.Columns(40).Visible = True
DataGridView1.Columns(41).Visible = True
DataGridView1.Columns(42).Visible = True
DataGridView1.Columns(43).Visible = True
DataGridView1.Columns(44).Visible = True
DataGridView1.Columns(45).Visible = True
DataGridView1.Columns(46).Visible = True
DataGridView1.Columns(47).Visible = True
DataGridView1.Columns(48).Visible = True
DataGridView1.Columns(49).Visible = True
```

'out

```
DataGridView1.Columns(50).Visible = False
DataGridView1.Columns(51).Visible = False
DataGridView1.Columns(52).Visible = False
DataGridView1.Columns(53).Visible = False
DataGridView1.Columns(54).Visible = False
DataGridView1.Columns(55).Visible = False
DataGridView1.Columns(56).Visible = False
DataGridView1.Columns(57).Visible = False
DataGridView1.Columns(58).Visible = False
DataGridView1.Columns(59).Visible = False
DataGridView1.Columns(60).Visible = False
DataGridView1.Columns(61).Visible = False
DataGridView1.Columns(62).Visible = False
DataGridView1.Columns(63).Visible = False
DataGridView1.Columns(64).Visible = False
DataGridView1.Columns(65).Visible = False
```

```
'units
    DataGridView1.Columns(66).Visible = False
    DataGridView1.Columns(67).Visible = False
    DataGridView1.Columns(68).Visible = False
    DataGridView1.Columns(69).Visible = False
    DataGridView1.Columns(70).Visible = False
    DataGridView1.Columns(71).Visible = False
    DataGridView1.Columns(72).Visible = False
    DataGridView1.Columns(73).Visible = False
    DataGridView1.Columns(74).Visible = False
    DataGridView1.Columns(75).Visible = False
    DataGridView1.Columns(76).Visible = False
    DataGridView1.Columns(77).Visible = False
    DataGridView1.Columns(78).Visible = False
    DataGridView1.Columns(79).Visible = False
    DataGridView1.Columns(80).Visible = False
    DataGridView1.Columns(81).Visible = False
End Sub

End Class
```

Appendix D

Supplementary Information for Chapter 3.

List of Contents

Multinuclear NMR Spectra

Infrared Spectra

Mass Spectra

Accelerating Rate Calorimetry (ARC)

Thermogravimetric Analyses

Powder X-Ray Diffraction

Single Crystal X-Ray Diffraction

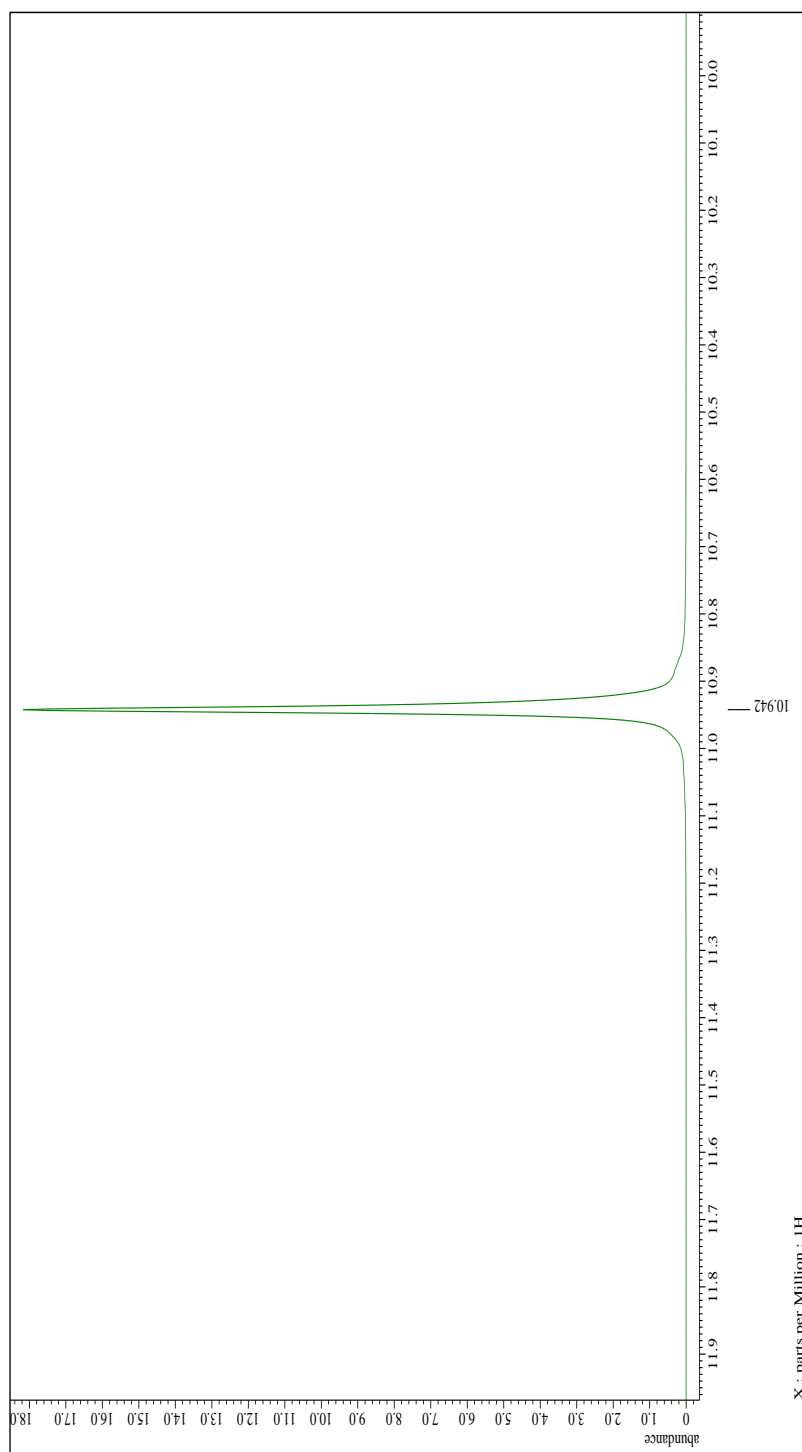


Figure D.1. ^1H NMR spectrum of $\text{CF}_3\text{CF}_2\text{C}(\text{O})\text{OH}$ (CD_3CN): δ 10.94 (s) ppm.

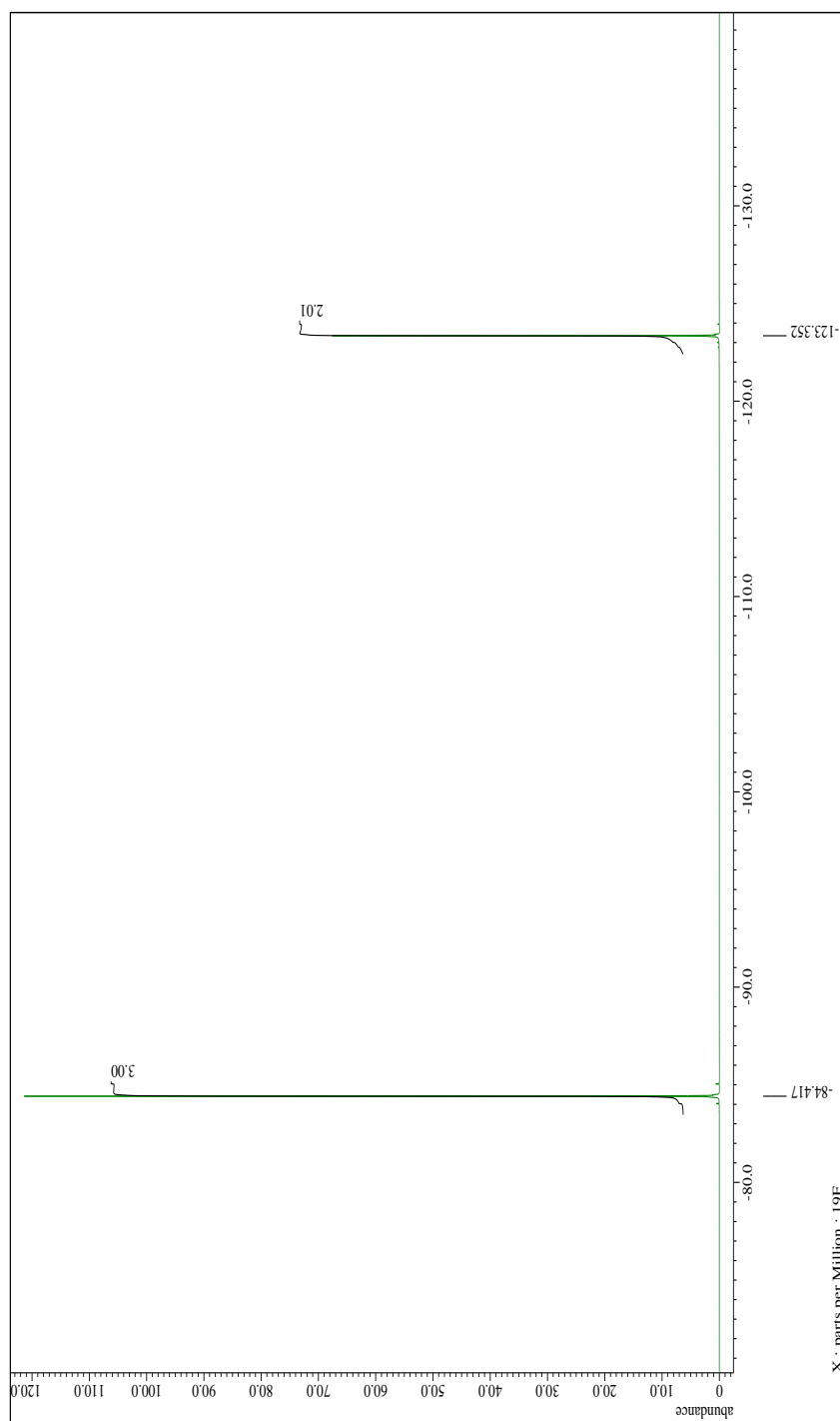


Figure D.2. ^{19}F NMR spectrum of $\text{CF}_3\text{CF}_2\text{C}(\text{O})\text{OH}$ (CD_3CN): δCF_3 -84.42 (s), CF_2 -123.35 (s) ppm.

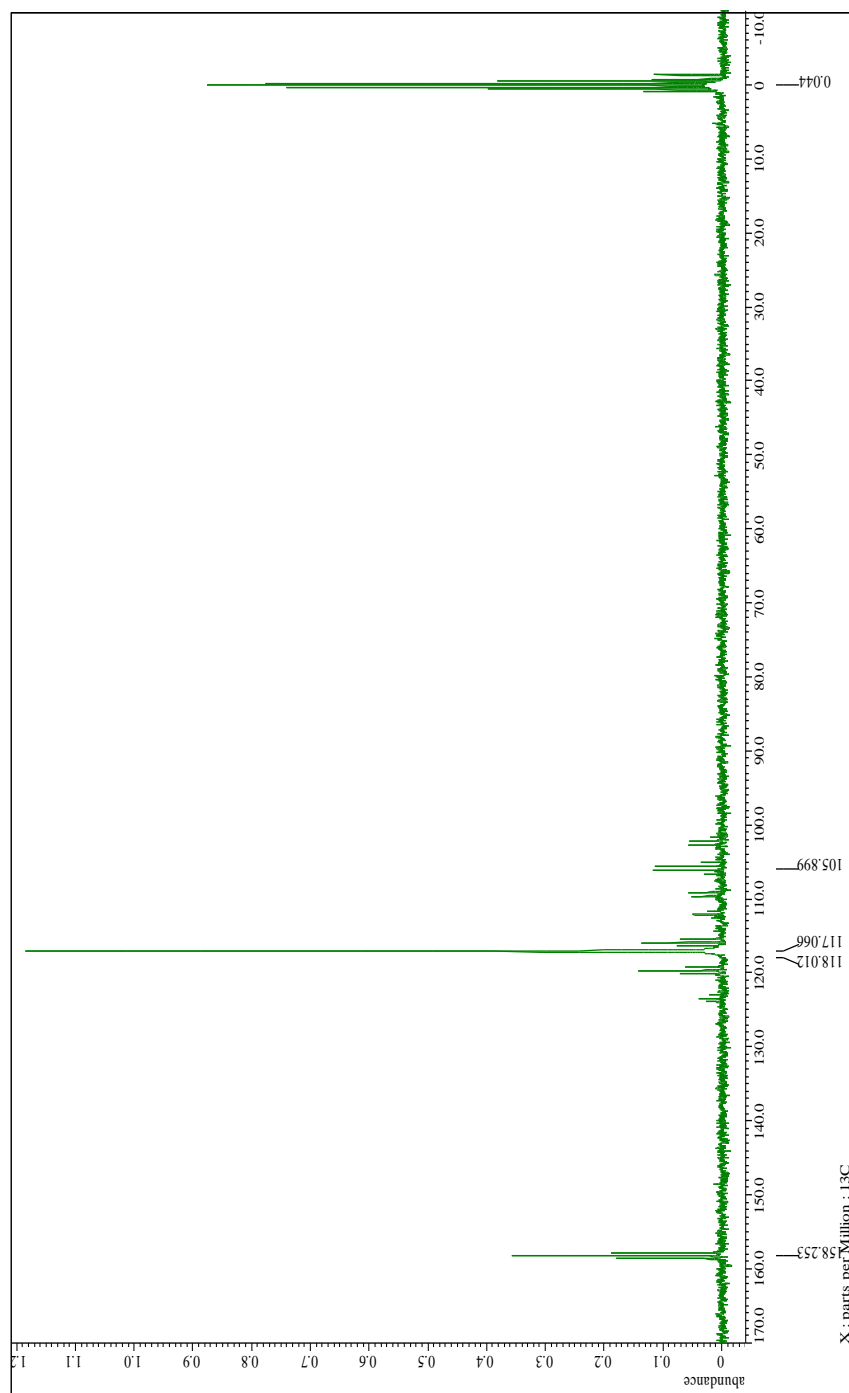


Figure D.3. ^{13}C NMR spectrum of $\text{CF}_3\text{CF}_2\text{C}(\text{O})\text{OH}$ (CD_3CN): δ C(O) 158.25 (t, $J_2 = 28.8$ Hz), CF_3 118.01 (qt, $J_1 = 285.2$ Hz, $J_2 = 33.9$ Hz), CF_2 105.90 (tq, $J_1 = 262.7$ Hz, $J_2 = 39.7$ Hz) ppm.

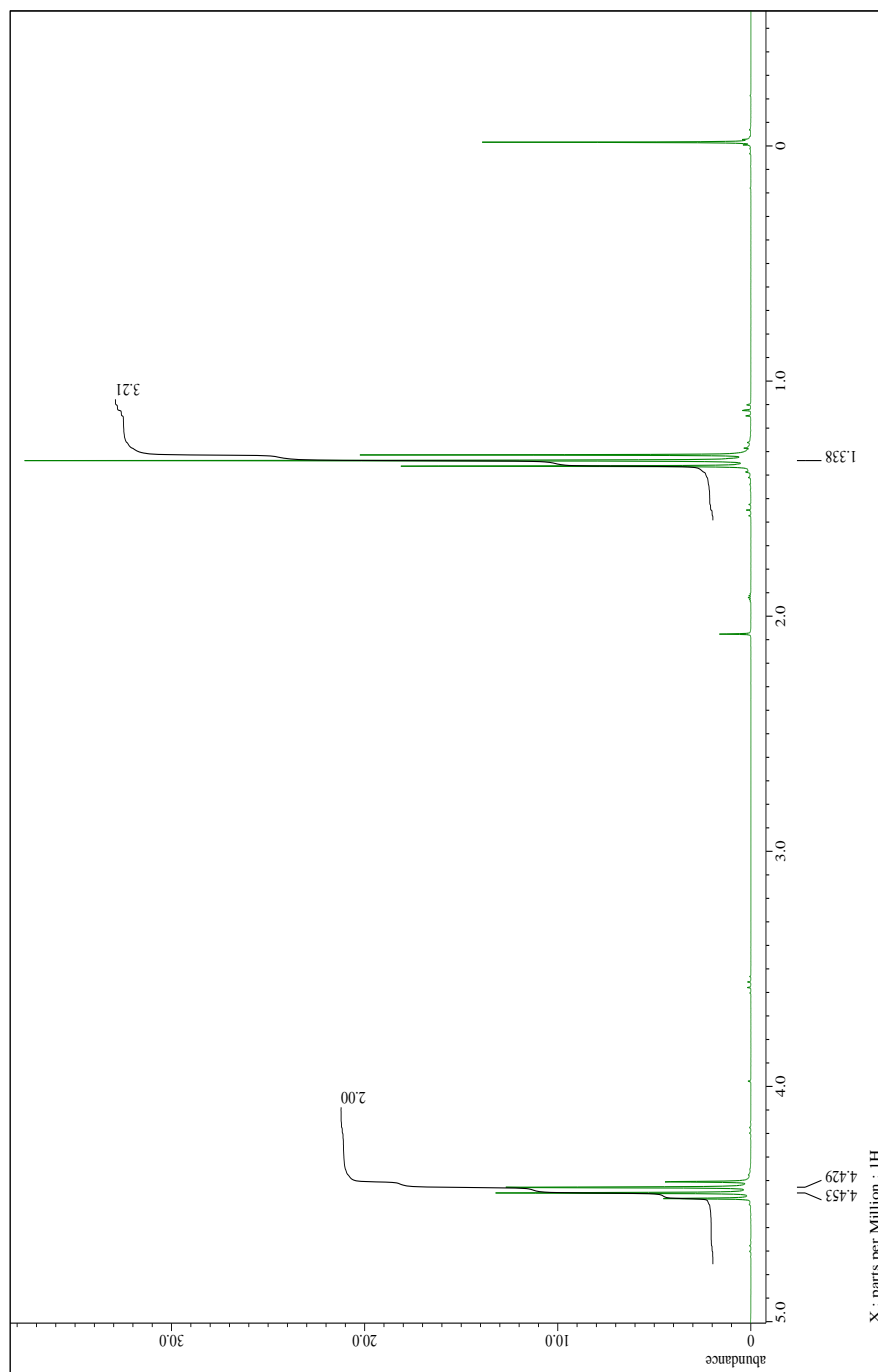


Figure D.4. ^1H NMR spectrum of $\text{CF}_3\text{CF}_2\text{C}(\text{O})\text{OCH}_2\text{CH}_3$ (CD_3CN): δ CH_2 4.44 (q, $J_2 = 7.2$ Hz), CH_3 1.34 (t, $J_2 = 7.2$ Hz) ppm.

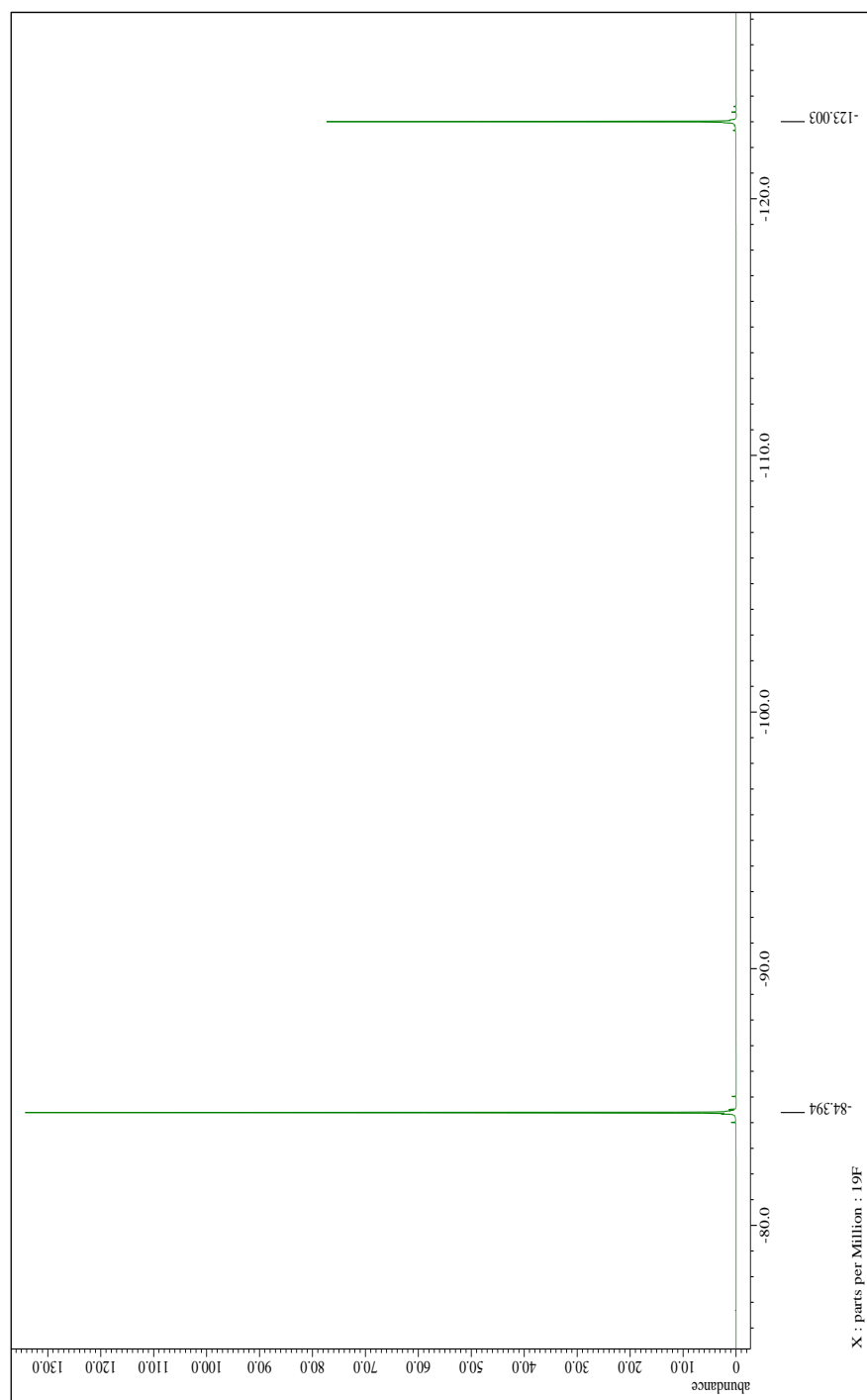


Figure D.5. ^{19}F NMR spectrum of $\text{CF}_3\text{CF}_2\text{C}(\text{O})\text{OCH}_2\text{CH}_3$ (CD_3CN): δ CF_3 -84.39 (s), CF_2 123.00 (s) ppm.

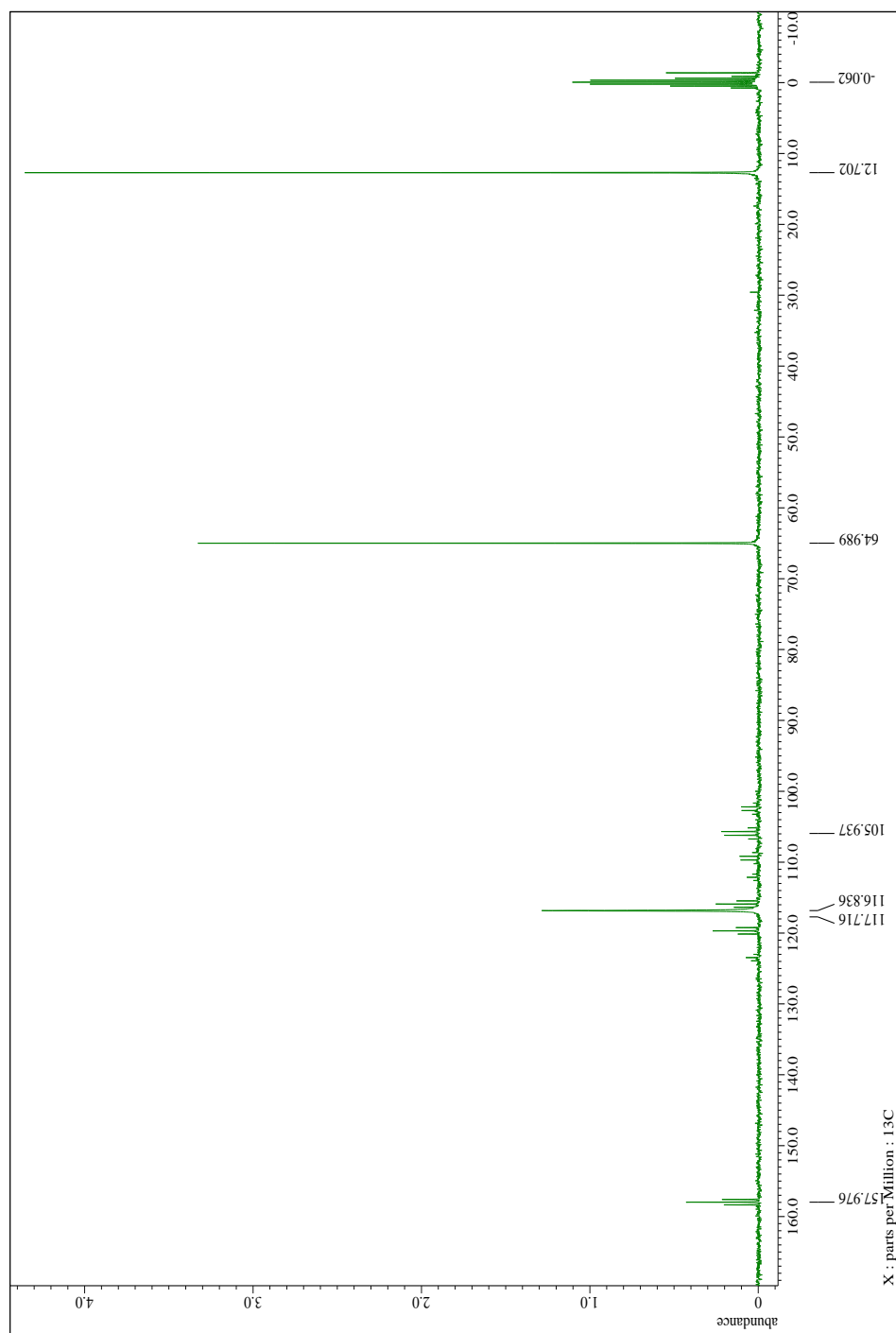


Figure D.6. ^{13}C NMR spectrum of $\text{CF}_3\text{CF}_2\text{C}(\text{O})\text{OCH}_2\text{CH}_3$ (CD_3CN): δ -157.98 $\text{C}(\text{O})$ (t, $J_2 = 28.8$ Hz), 117.80 CF_3 (qt, $J_1 = 285.2$ Hz, $J_2 = 33.9$ Hz), 105.94 CF_2 (tq, $J_1 = 262.7$ Hz, $J_2 = 39.7$ Hz), 64.99 OCH_2 (s), CH_3 12.70 (s) ppm.

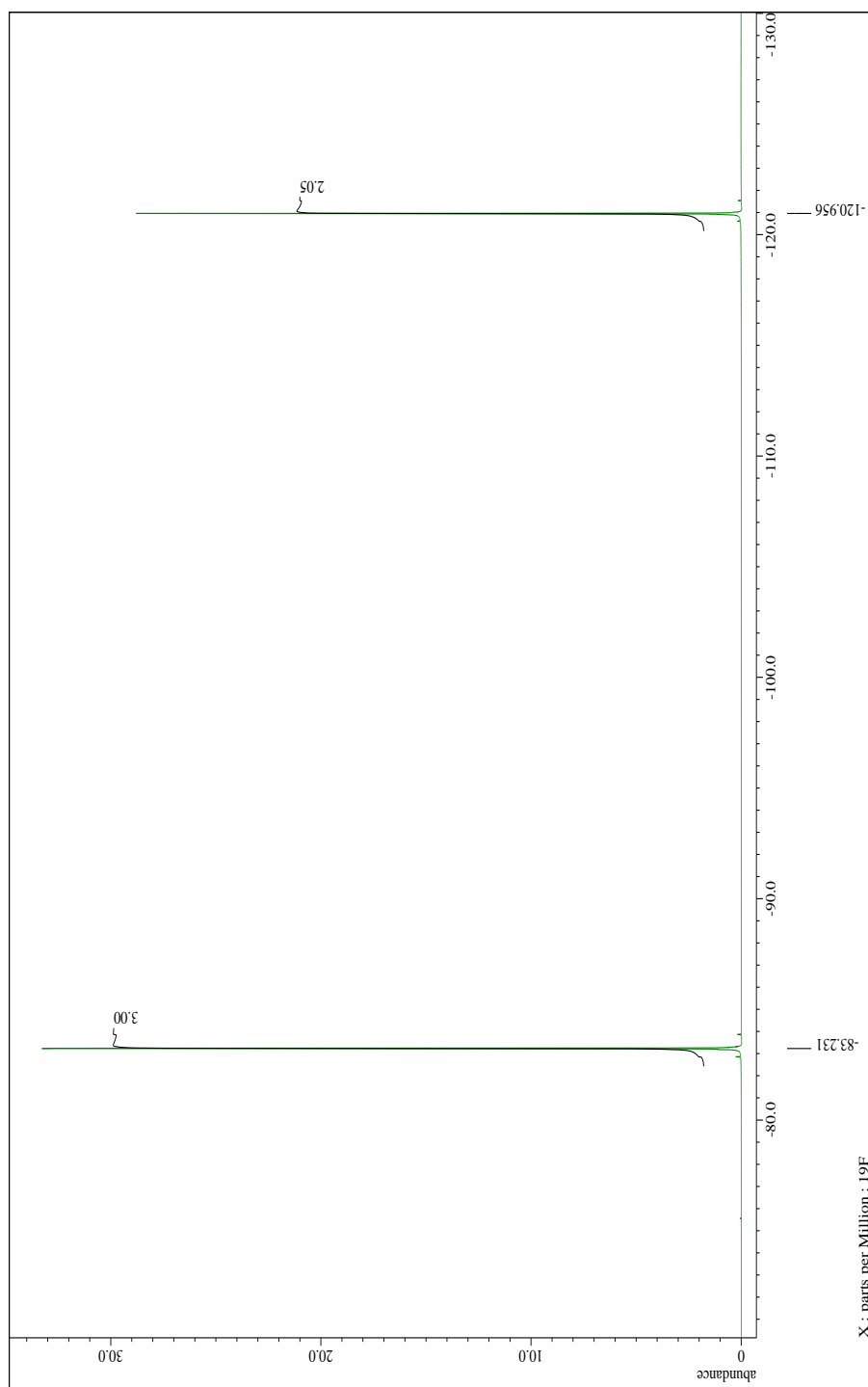


Figure D.7. ^{19}F NMR spectrum of $\text{CF}_3\text{CF}_2\text{C}(\text{O})\text{OK}$ (D_2O): δ -83.23 CF_3 (s), CF_2 -120.96 (s) ppm.

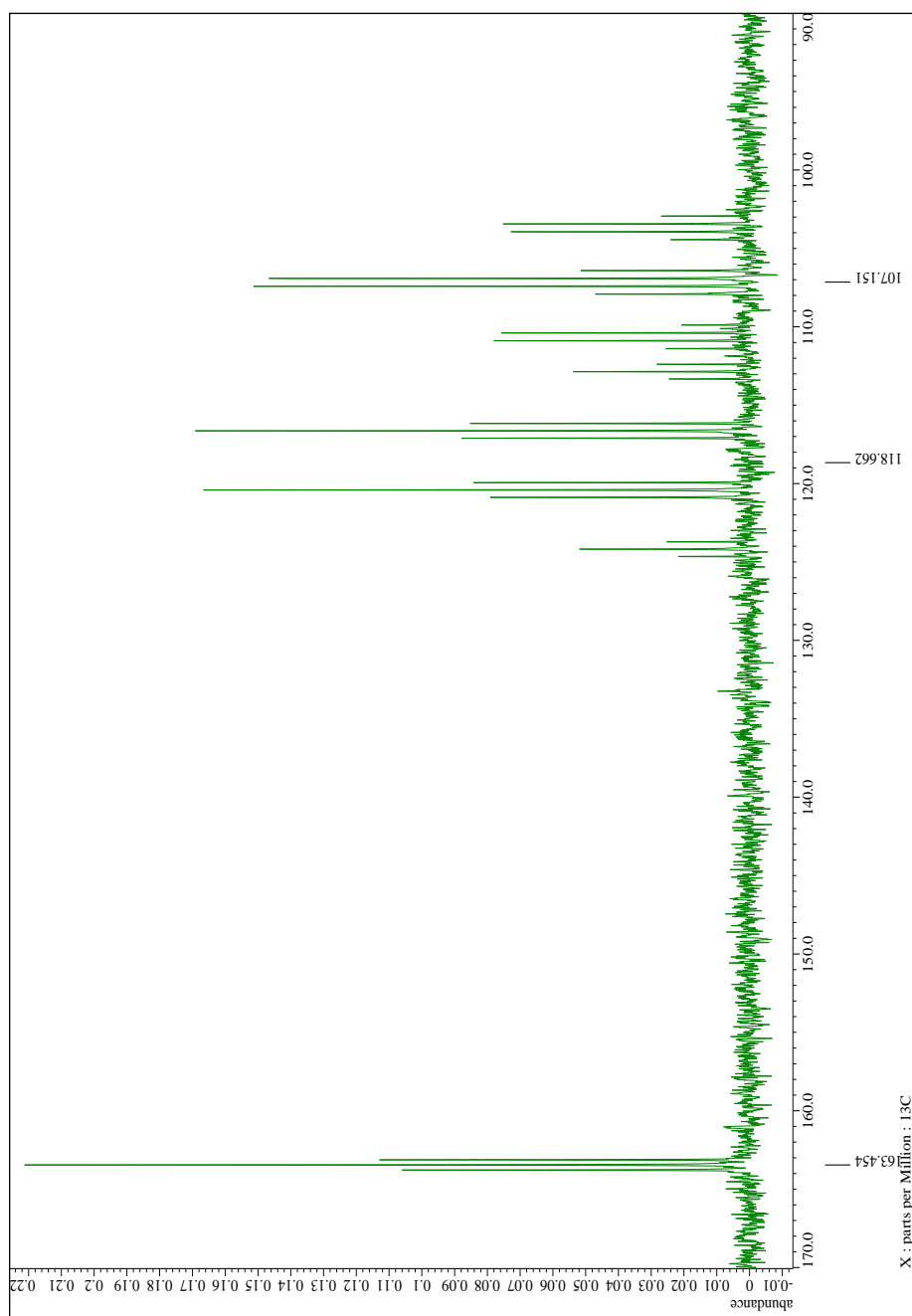


Figure D.8. ^{13}C NMR spectrum of $\text{CF}_3\text{CF}_2\text{C}(\text{O})\text{OK}$ (D_2O): δ 163.45 $\text{C}(\text{O})$ (t, $J_2 = 24.5$ Hz), CF_3 118.66 (qt, $J_1 = 286.3$ Hz, $J_2 = 35.3$ Hz), CF_2 107.15 (tq, $J_1 = 262.7$ Hz, $J_2 = 38.3$ Hz) ppm.

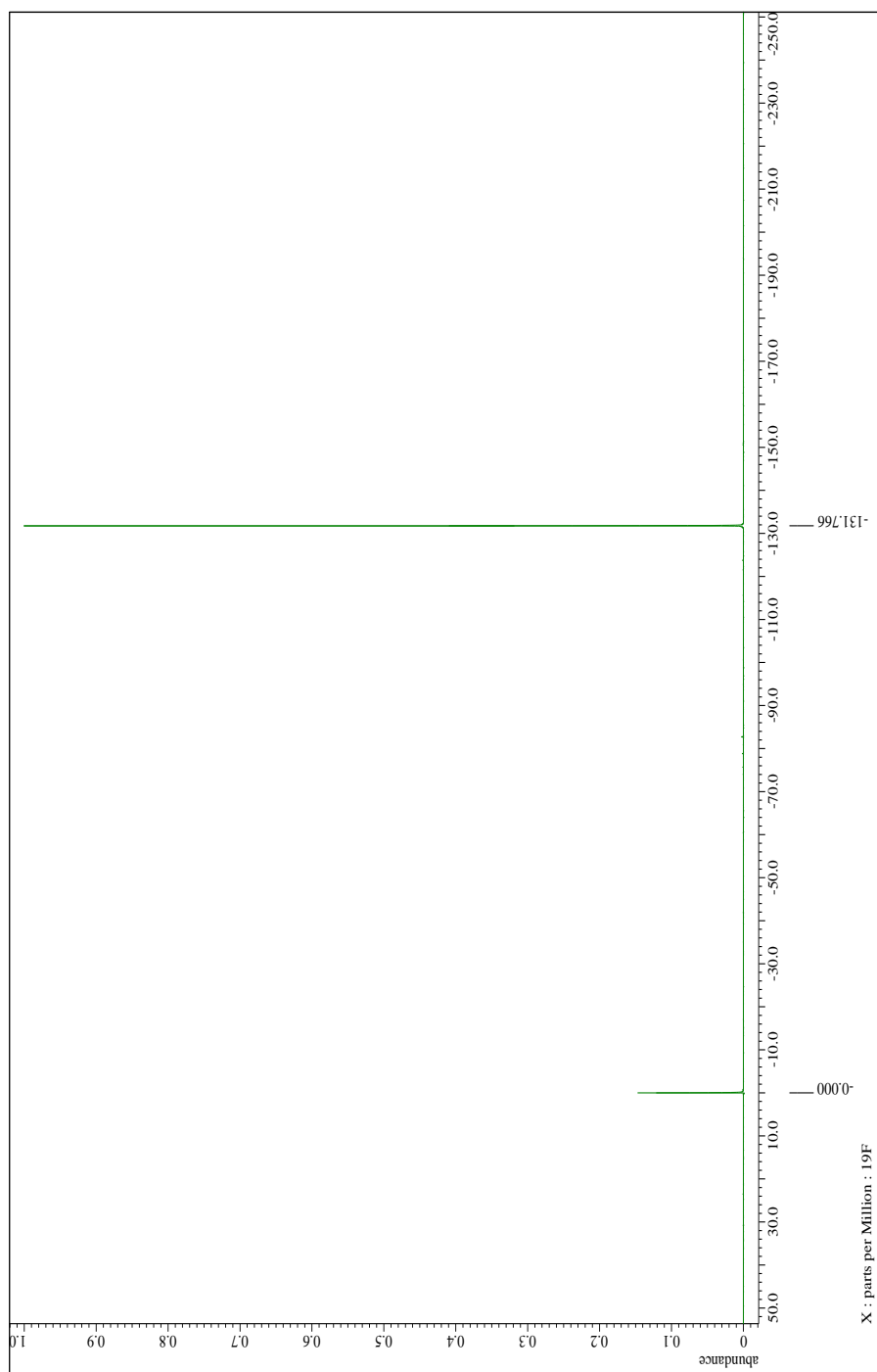


Figure D.9. ^{19}F NMR spectrum of $\text{CF}_2=\text{CF}_2/\text{CO}_2$ (CD_3CN): δ -131.77 (s) ppm.

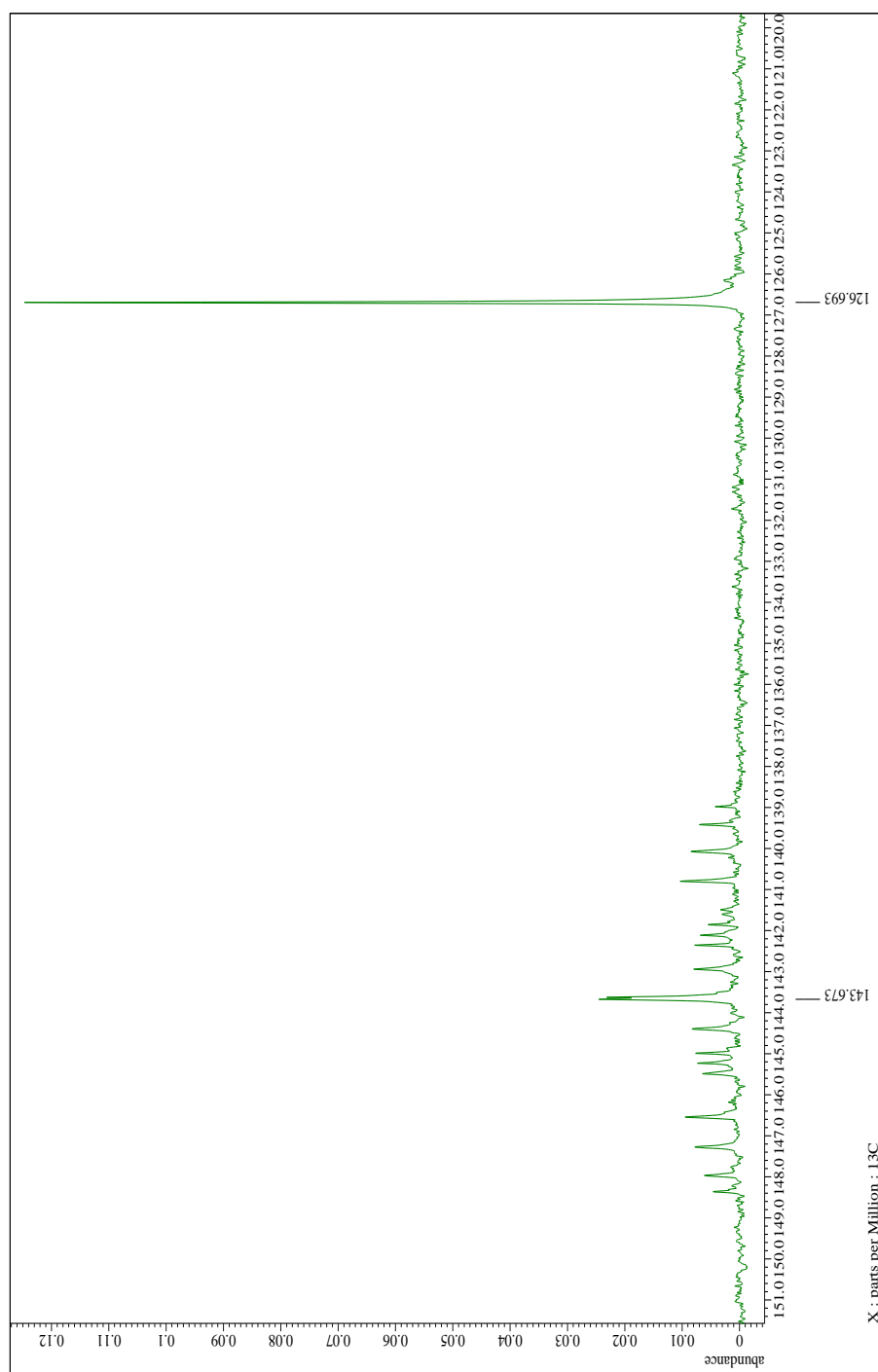


Figure D.10. ^{13}C NMR spectrum of $\text{CF}_2=\text{CF}_2/\text{CO}_2$ (gas): δ 143.67 $\text{CF}_2=\text{CF}_2$ (m), 126.69 CO_2 (s) ppm.

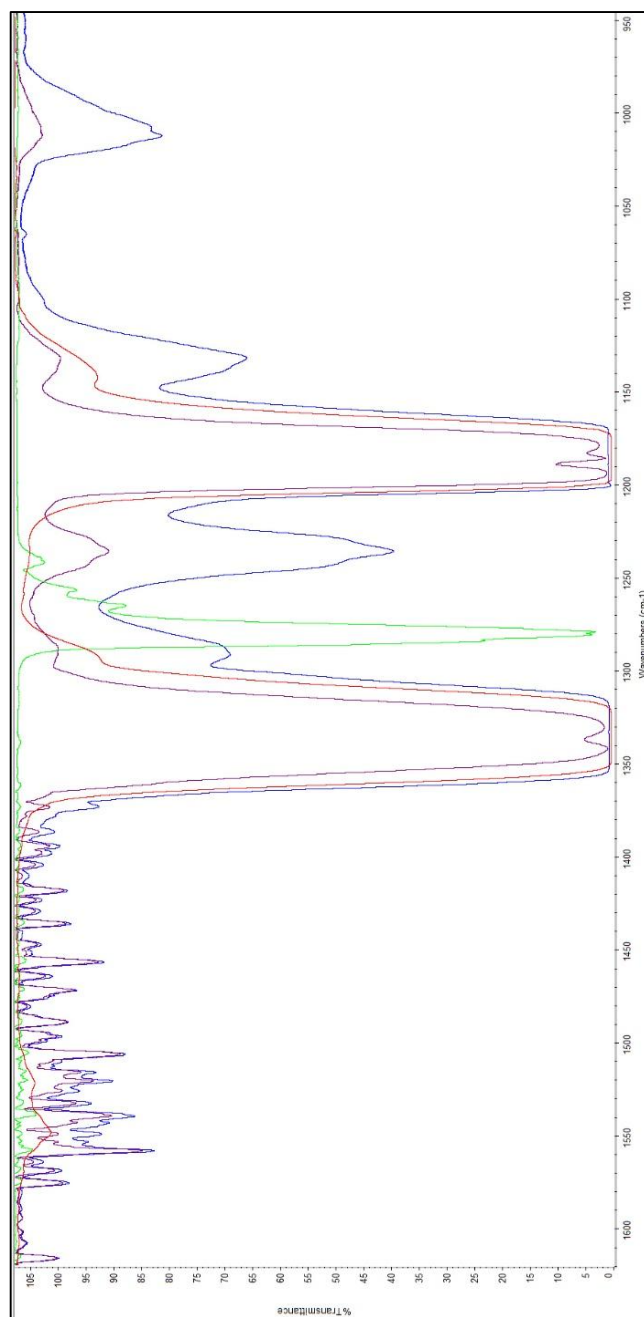


Figure D.11. FTIR spectra of TFE taken from a stream of gas from the pyrolysis of sodium pentafluoropropionate at 50 Torr (blue line) and 5 Torr (purple line), superimposed with a spectra of TFE (red line) that has been evacuated from all the non-condensable gases, and a spectra of a standard sample of CF_4 collected at 5 Torr (green line).

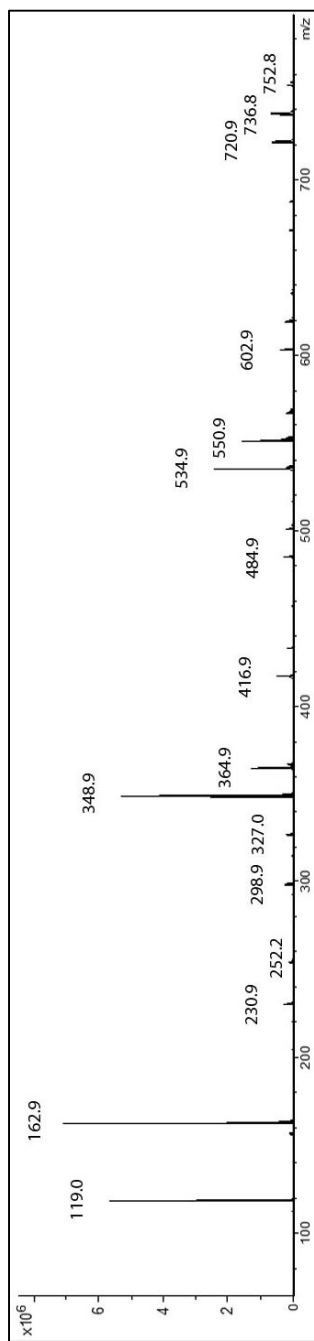


Figure D.12. LC-mass spectrum (ESI, negative ion mode) of potassium pentafluoropropionate.

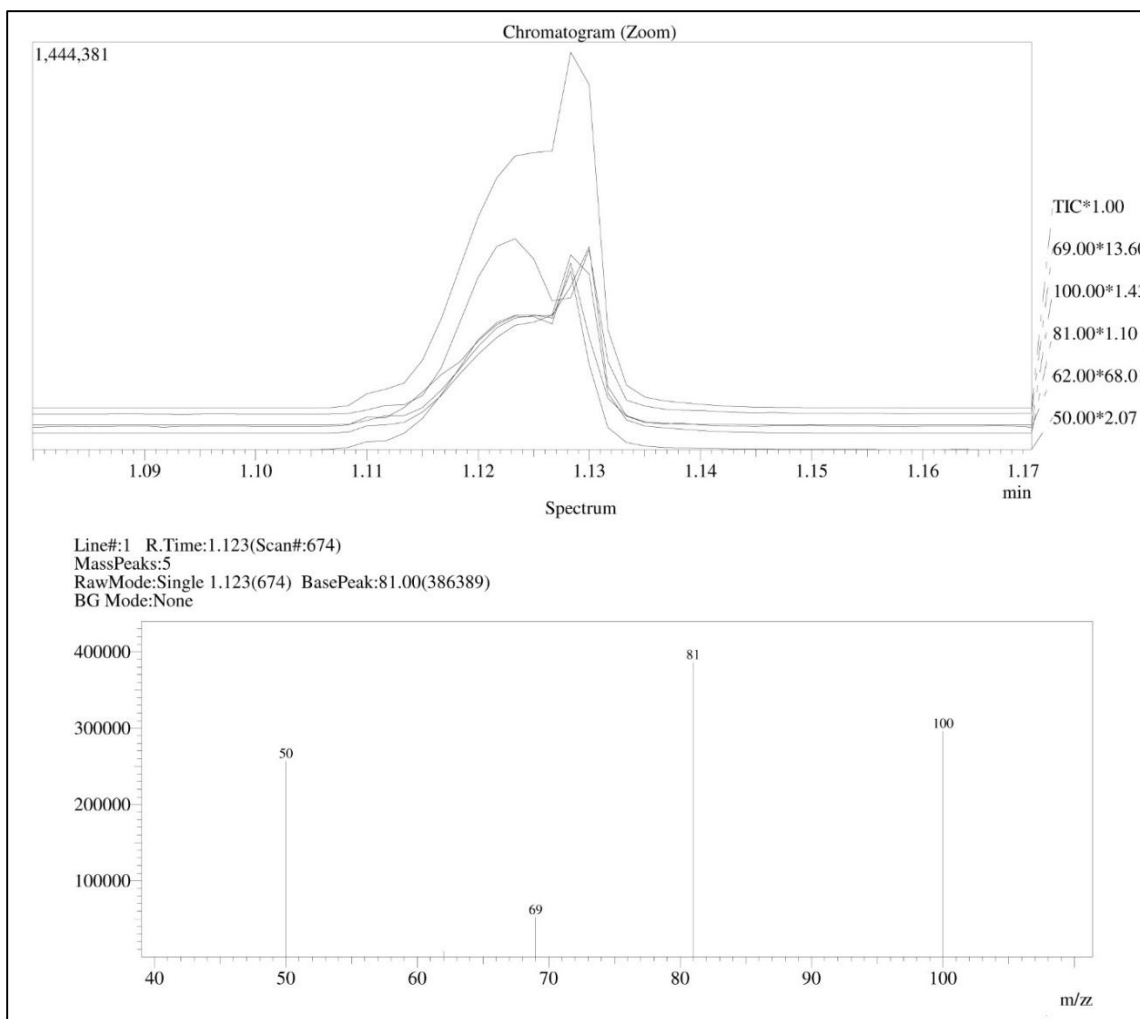


Figure D.13. GC-MS spectrum (selective ion mode, SIM) of a sample of the most volatile gases from a pyrolysis of sodium pentafluoropropionate collected under static vacuum. The ions featured are $C_2F_4^+$ (100 m/z), $C_2F_3^+$ (81 m/z), CF_3^+ (69 m/z), $C_2F_2^+$ (62 m/z) and CF_2^+ (50 m/z). The sum of all the areas is labeled as “TIC”. The large bump on the leading edge of the signal is attributed to the CF_3^+ ion characteristic of CF_4 . Notice that the normalization factor for the peak at 69 m/z at 13.60 is about one-half of what it is in Figure S14, indicating that the presents of another species, other than TFE, is giving rise to a more intense peak for CF_3^+ . As shown in Figure S15, 69 m/z or CF_3^+ is the base peak in the mass spectrum of CF_4 .

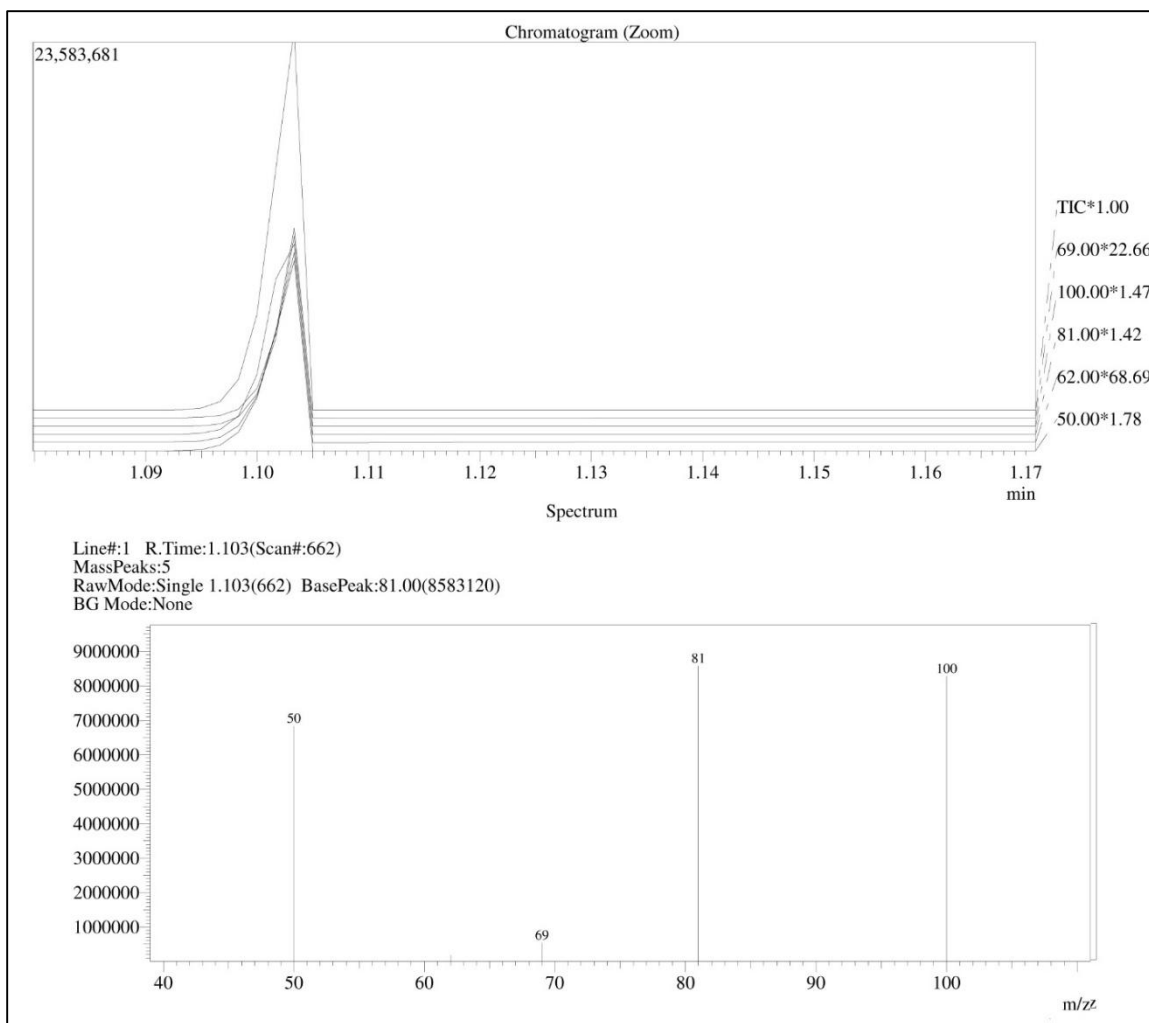


Figure D.14. GC-MS spectrum (selective ion mode, SIM) of a sample of gas from a totally degassed collection cylinder of TFE/CO₂ as the products of a pyrolysis of sodium pentafluoropropionate. The ions featured are C₂F₄⁺ (100 m/z), C₂F₃⁺ (81 m/z), CF₃⁺ (69 m/z), C₂F₂⁺ (62 m/z) and CF₂⁺ (50 m/z). The sum of all the areas is labeled as “TIC”.

Notice that the normalization factor for the peak at 69 m/z for CF₃⁺ at 22.66 is now almost double what it is in Figure D.13.

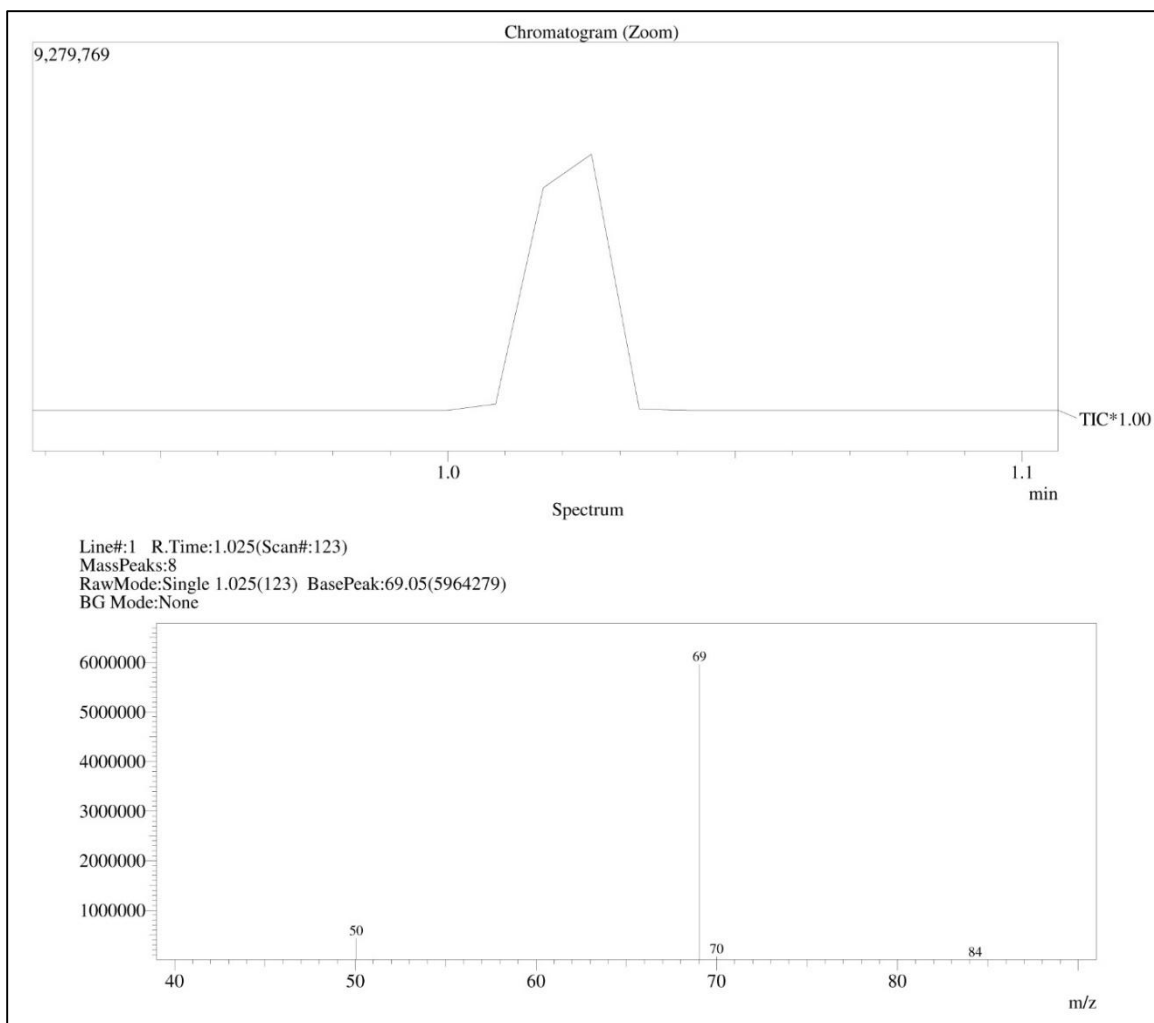


Figure D.15. GC-MS spectrum of a standard sample of CF_4 . The CF_3^+ signal at m/z 69 is the clearly the base peak. The GC-MS spectra shown in Figures S13-S15 were taken on a 30 m, Rxi-5HT column, which is not made for separating permanent gases; small variations in retention times are probably due to differences between manual injections.

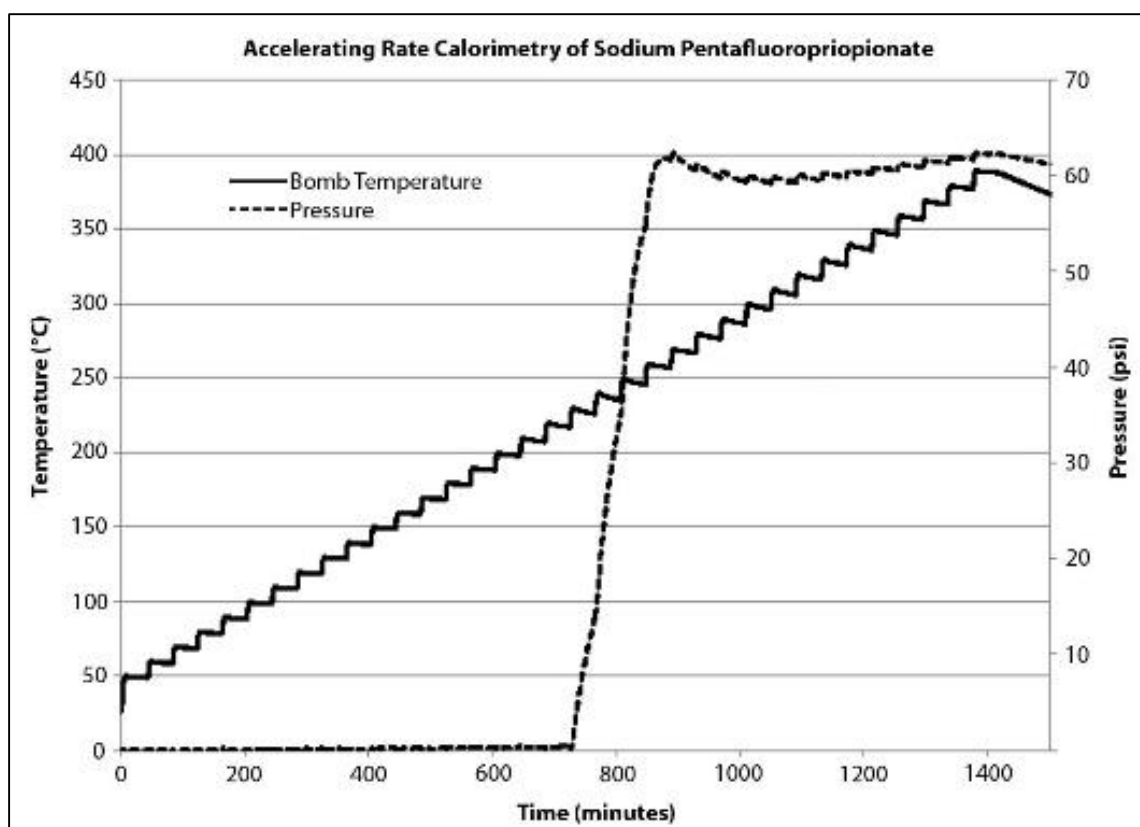


Figure D.16. Accelerating rate calorimetry (ARC) thermogram of sodium pentafluoropropionate.

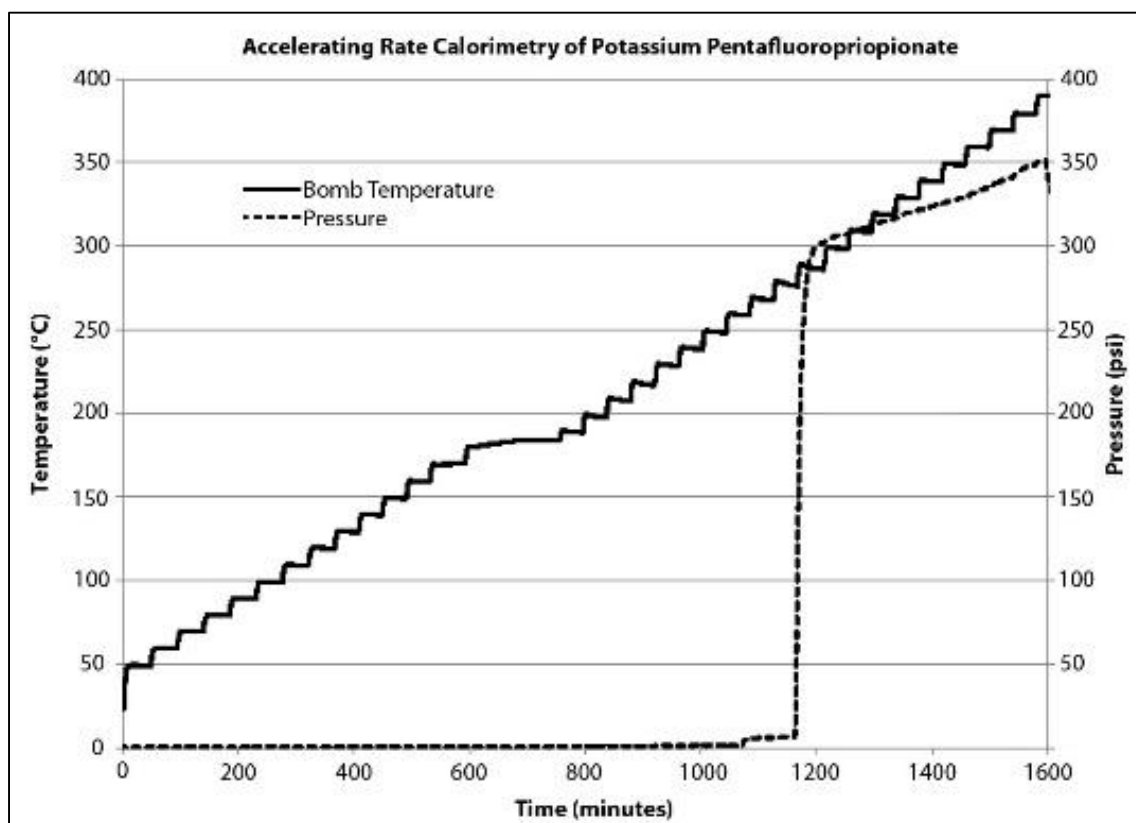


Figure D.17. Accelerating rate calorimetry (ARC) thermogram of potassium pentafluoropropionate.

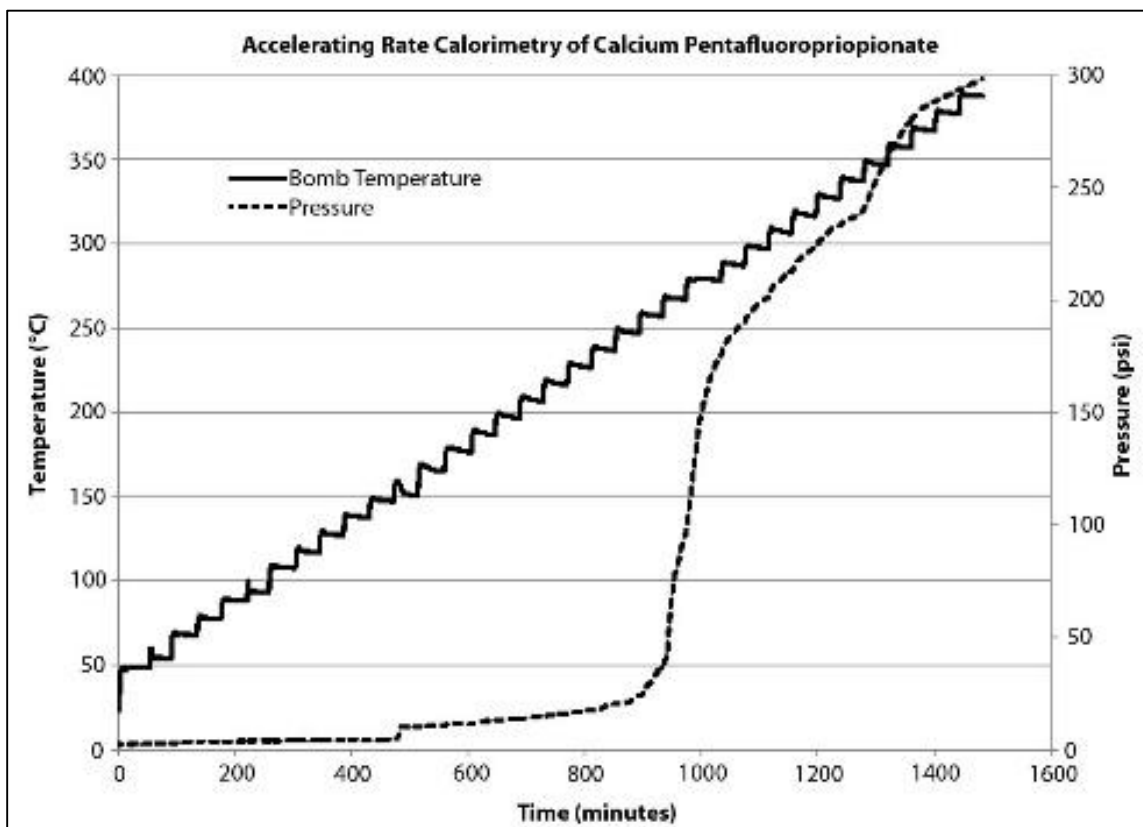


Figure D.18. Accelerating rate calorimetry (ARC) thermogram of calcium pentafluoropropionate.

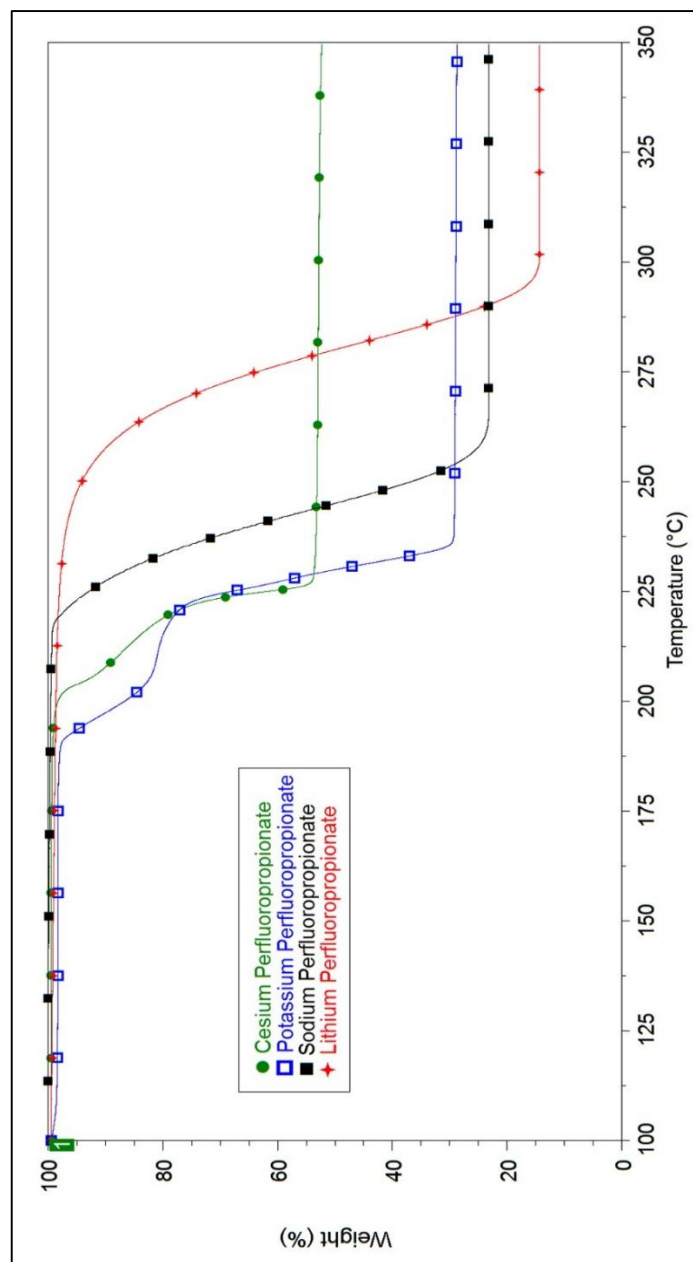


Figure D.19. TGA thermograms of monovalent pentafluoropropionates. Red line: lithium pentafluoropropionate; black line: sodium pentafluoropropionate; blue line: potassium pentafluoropropionate; and green line: cesium pentafluoropropionate. A metal fluoride is left at the end in each case (from top to bottom): cesium fluoride, potassium fluoride, sodium fluoride, and lithium fluoride.

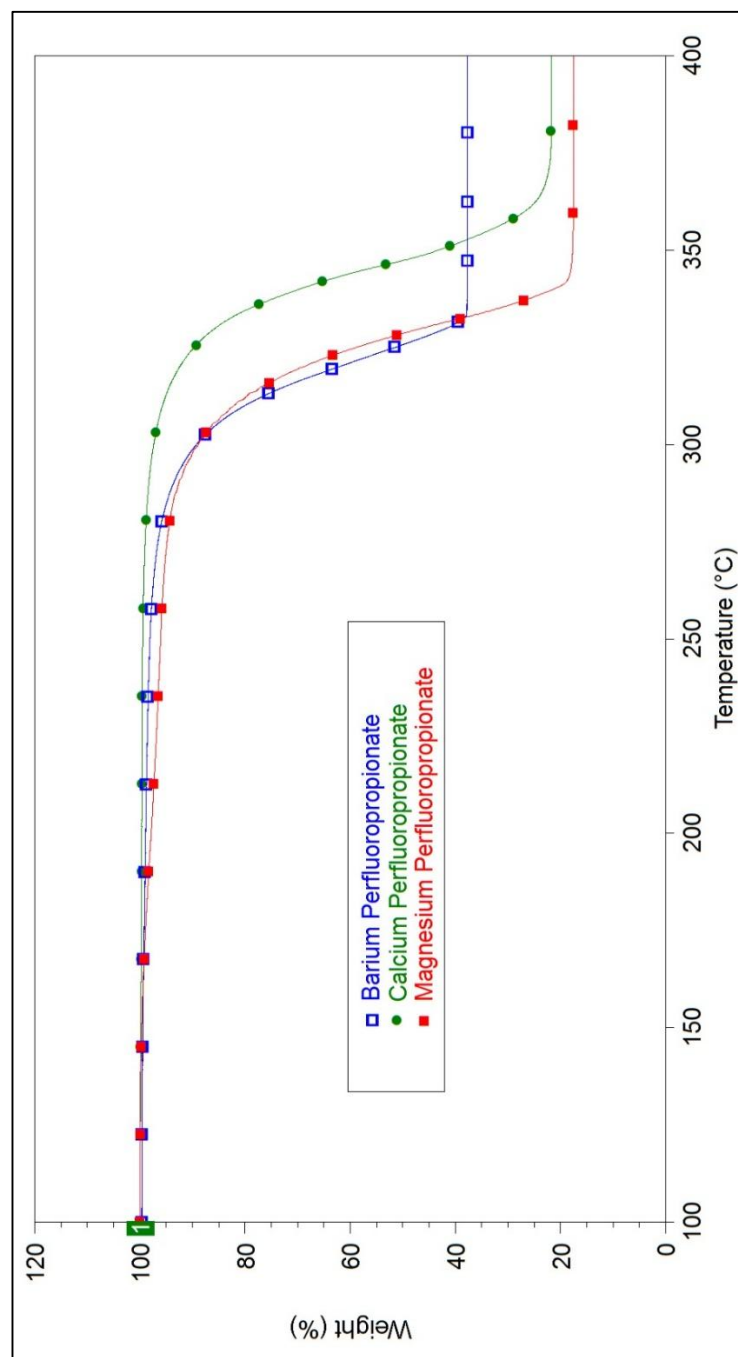


Figure D.20. TGA thermograms of the divalent pentafluoropropionates. Red line: magnesium pentafluoropropionate; blue line: barium pentafluoropropionate; and green line: calcium pentafluoropropionate. A metal fluoride is left at the end in each case (from top to bottom): barium fluoride, calcium fluoride, and magnesium fluoride.

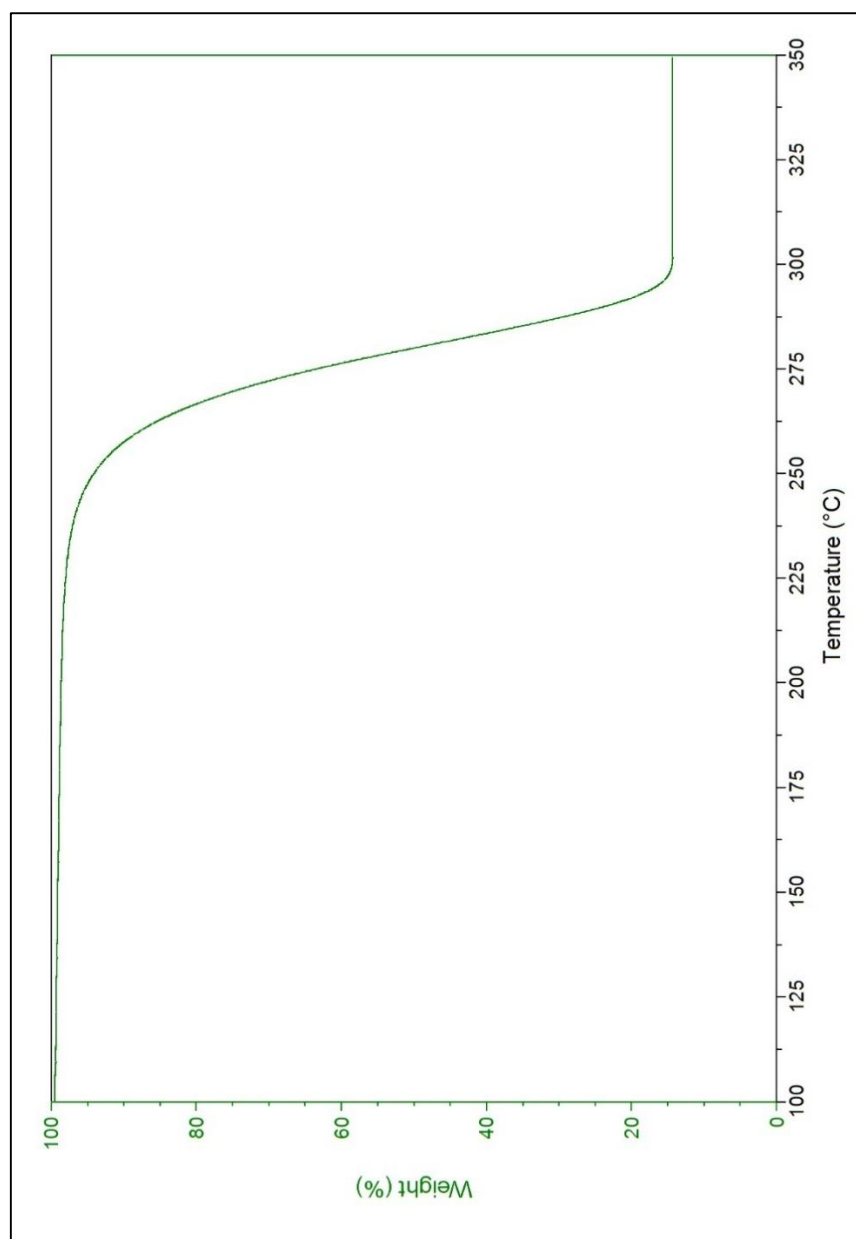


Figure D.21. Thermogravimetric analysis of lithium pentafluoropropionate.

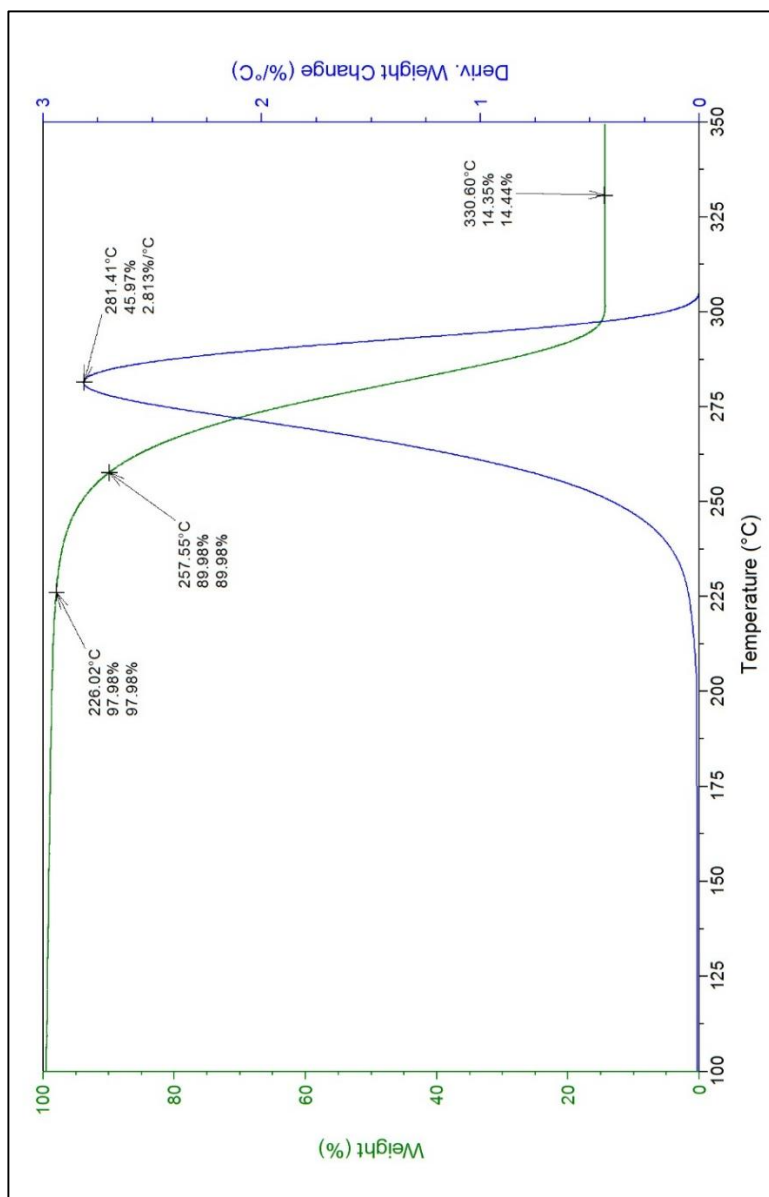


Figure D.22. Thermogravimetric analysis for lithium pentafluoropropionate with detailed information.

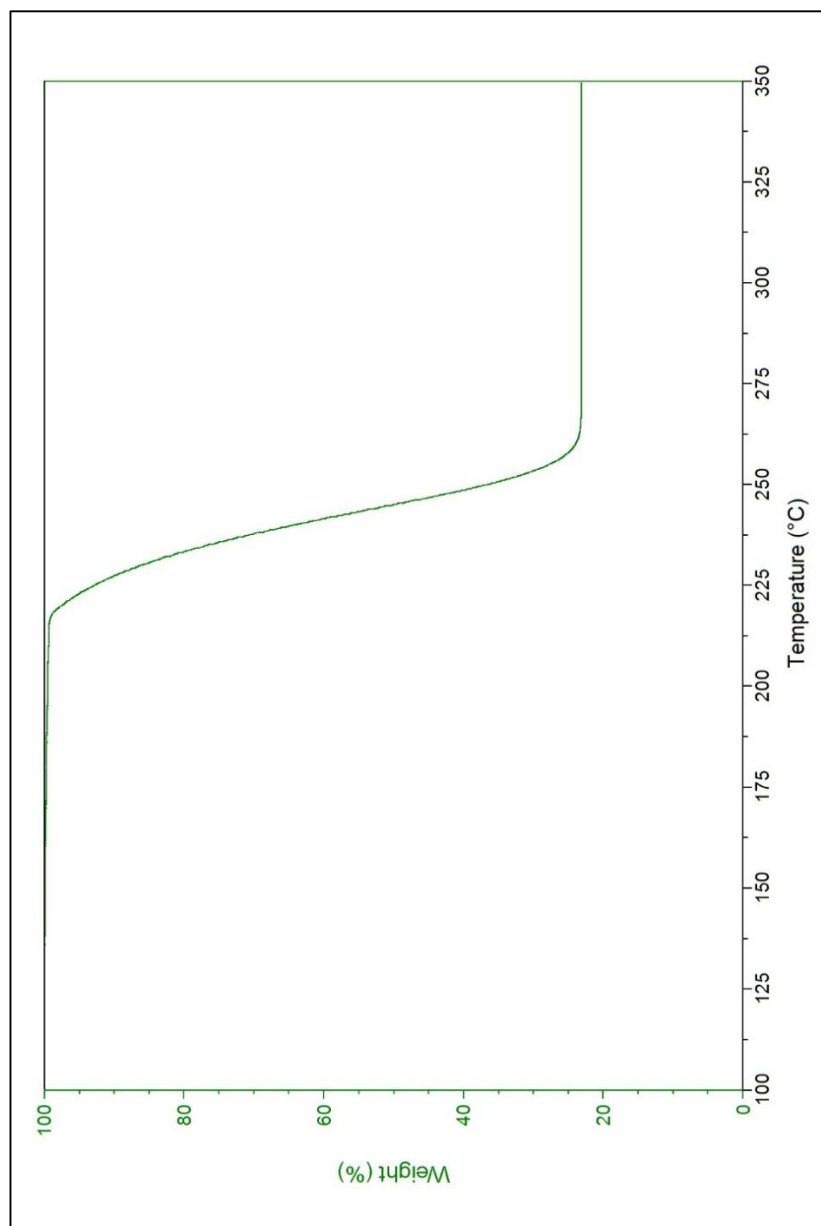


Figure D.23. Thermogravimetric analysis of sodium pentafluoropropionate.

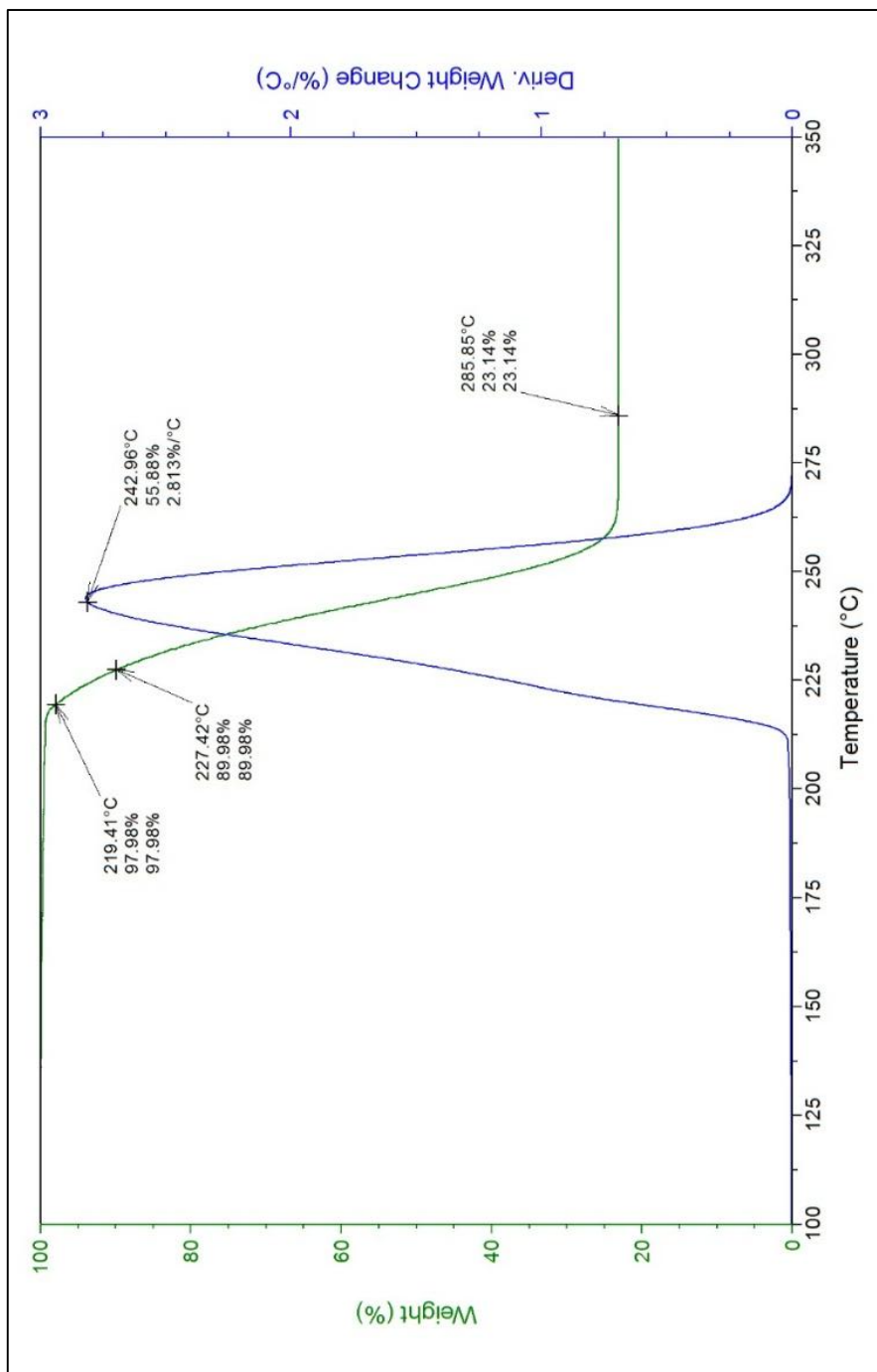


Figure D.24. Thermogravimetric analysis for sodium pentafluoropropionate with detailed information.

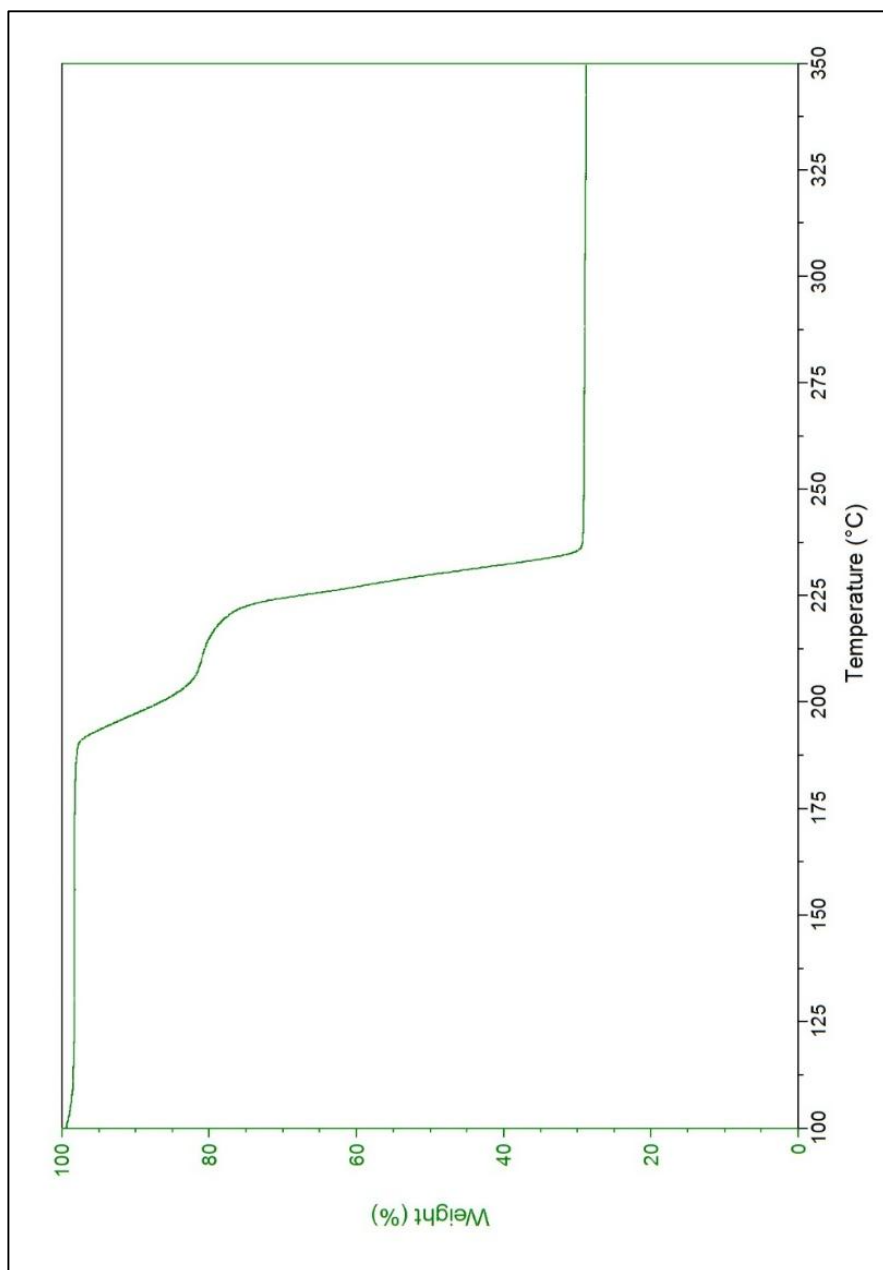


Figure D.25. Thermogravimetric analysis of potassium pentafluoropropionate.

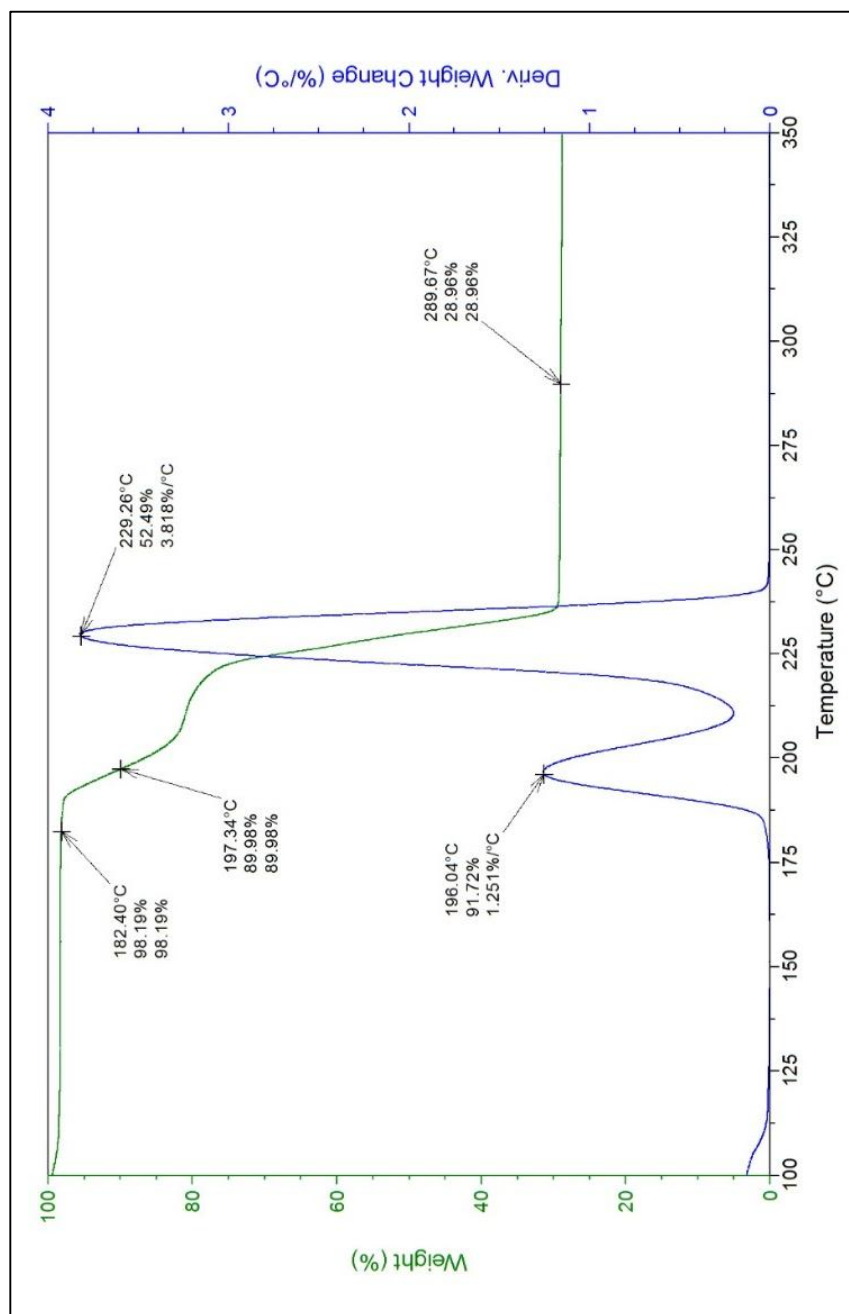


Figure D.26. Thermogravimetric analysis for potassium pentafluoropropionate with detailed information.

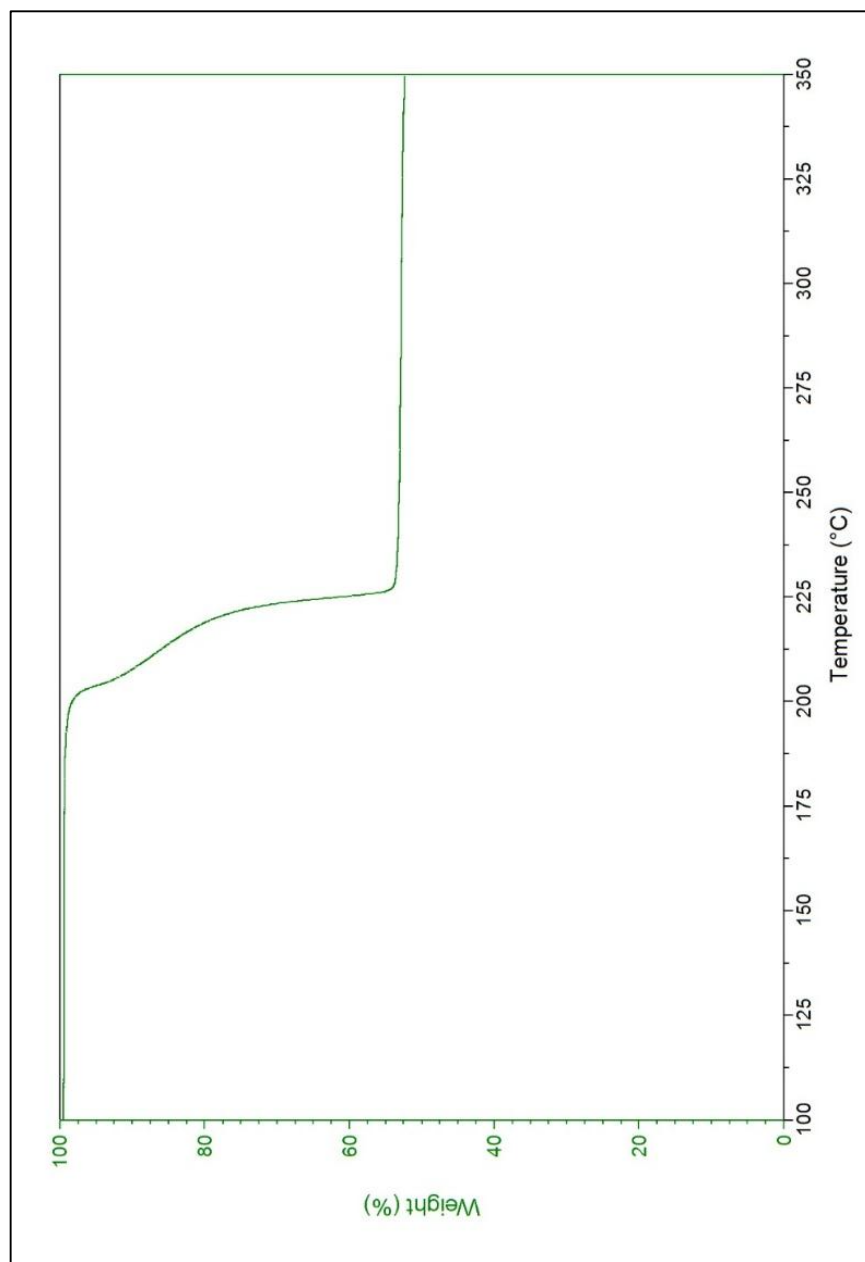


Figure D.27. Thermogravimetric analysis of cesium pentafluoropropionate.

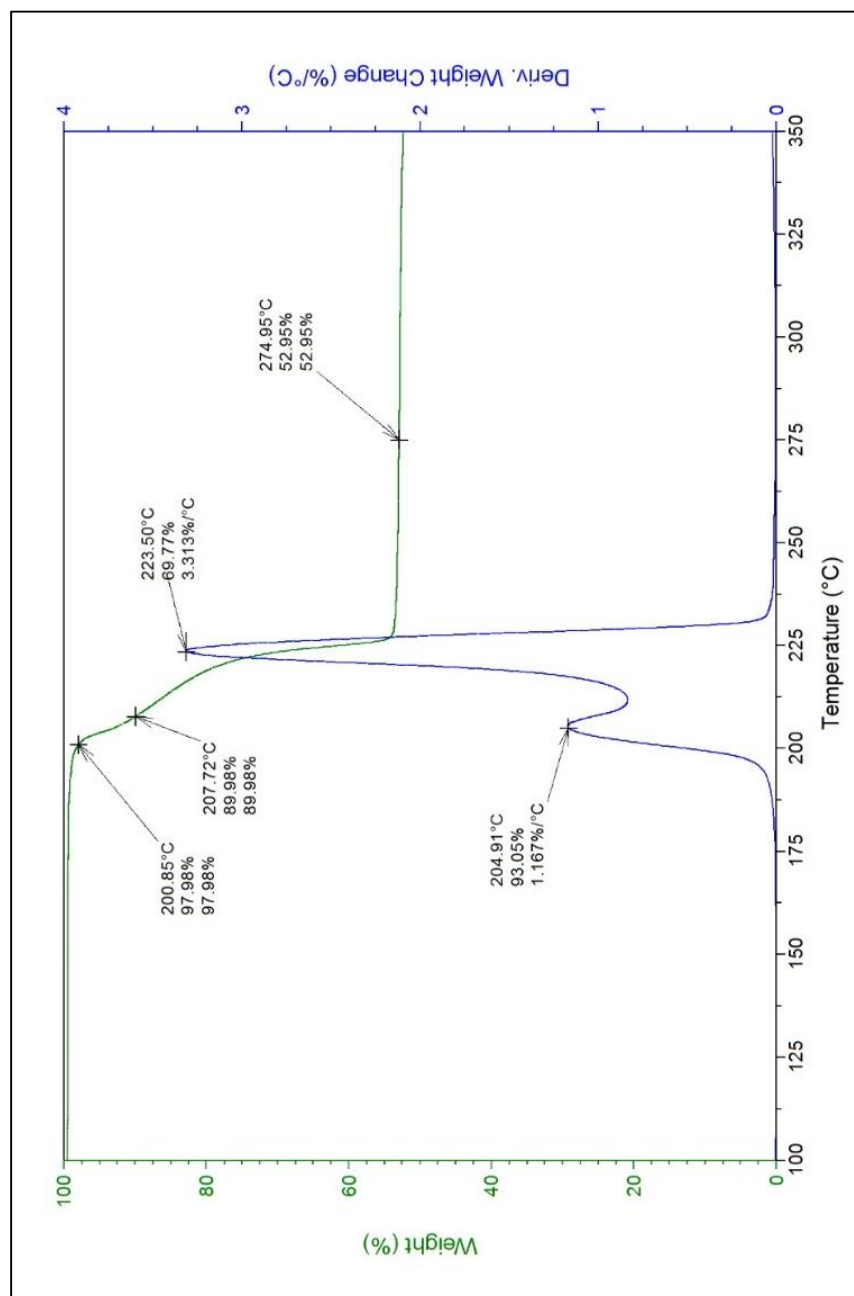


Figure D.28. Thermogravimetric analysis for cesium pentafluoropropionate with detailed information.

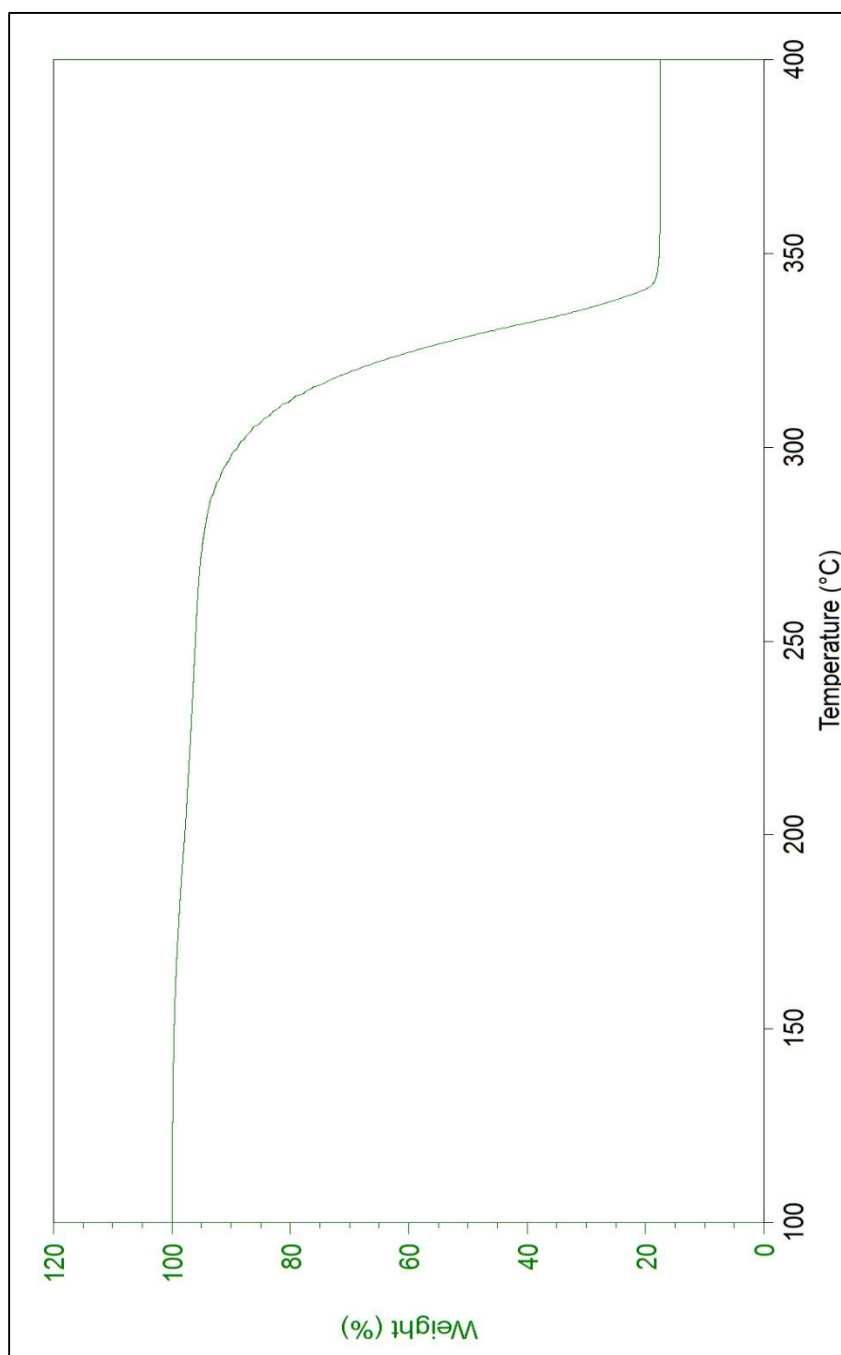


Figure D.29. Thermogravimetric analysis of magnesium pentafluoropropionate.

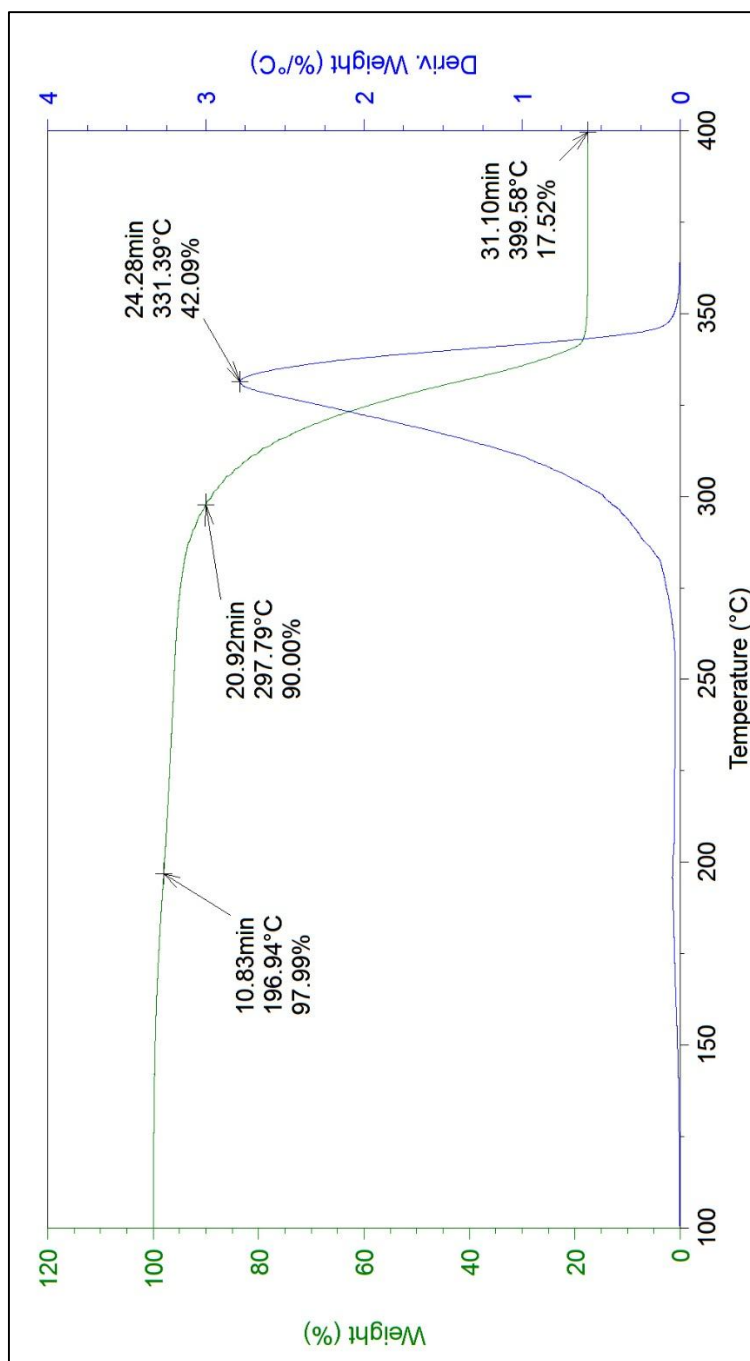


Figure D.30. Thermogravimetric analysis for magnesium pentafluoropropionate with detailed information.

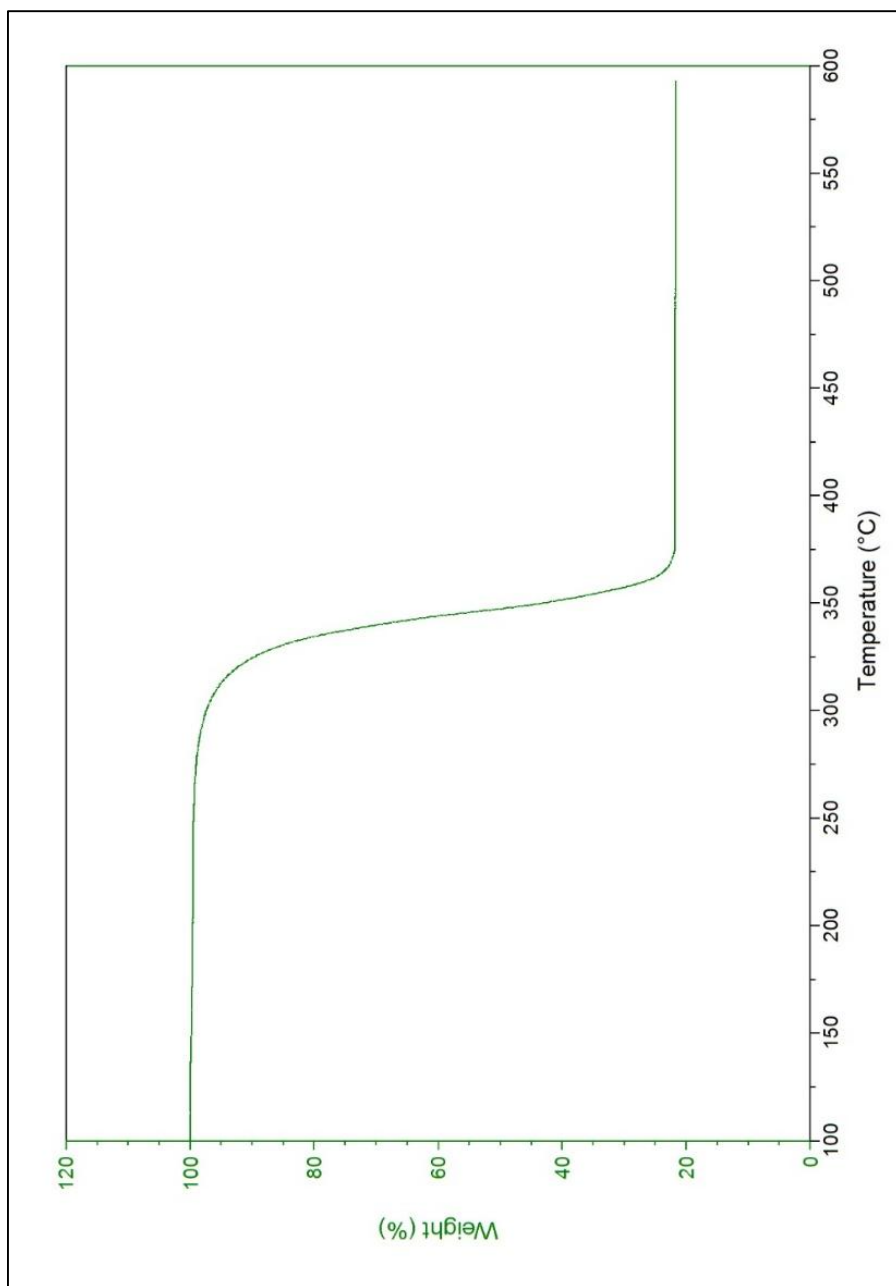


Figure D.31. Thermogravimetric analysis of calcium pentafluoropropionate.

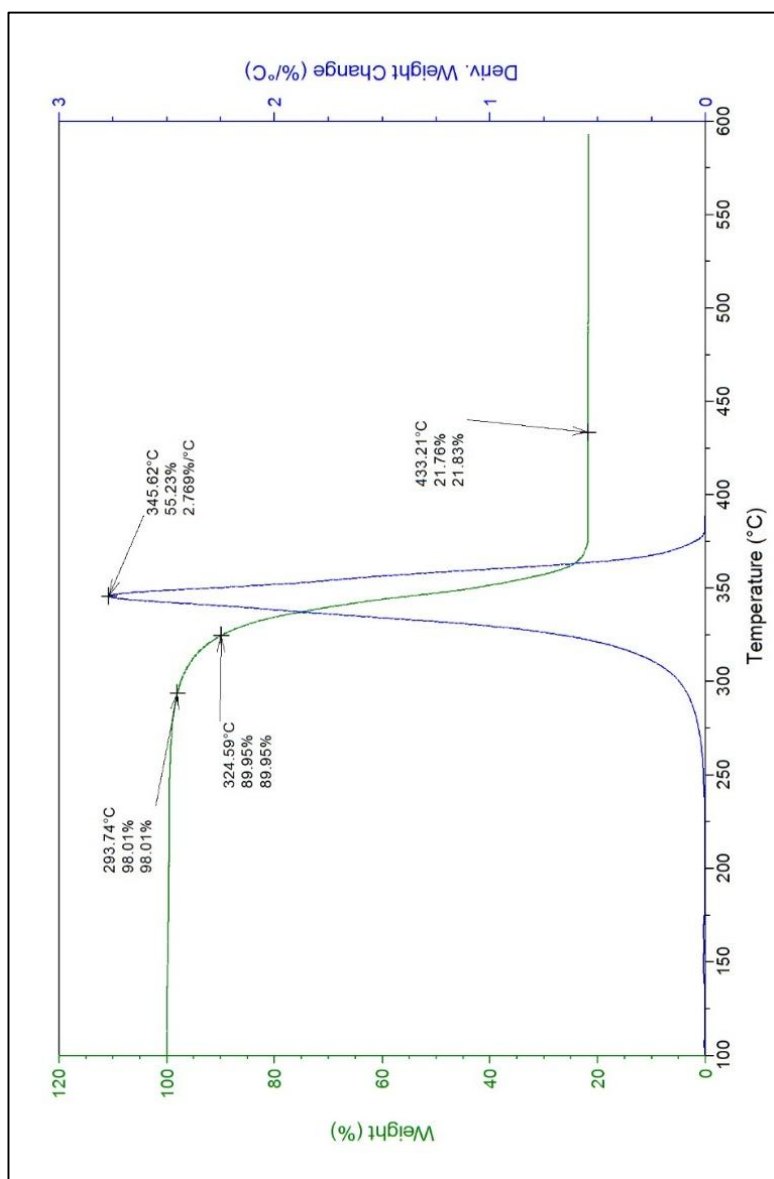


Figure D.32. Thermogravimetric analysis for calcium pentafluoropropionate with detailed information.

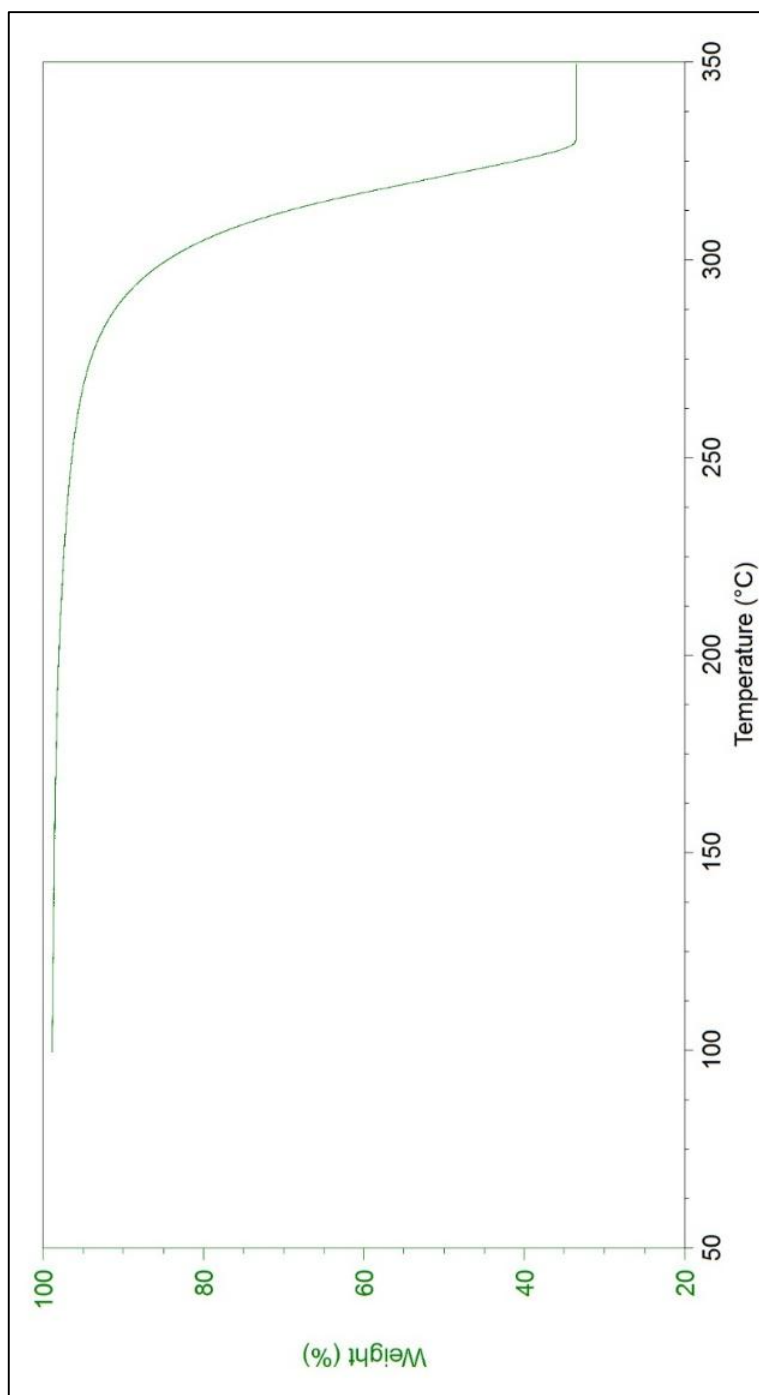


Figure D.33. Thermogravimetric analysis of barium pentafluoropropionate.

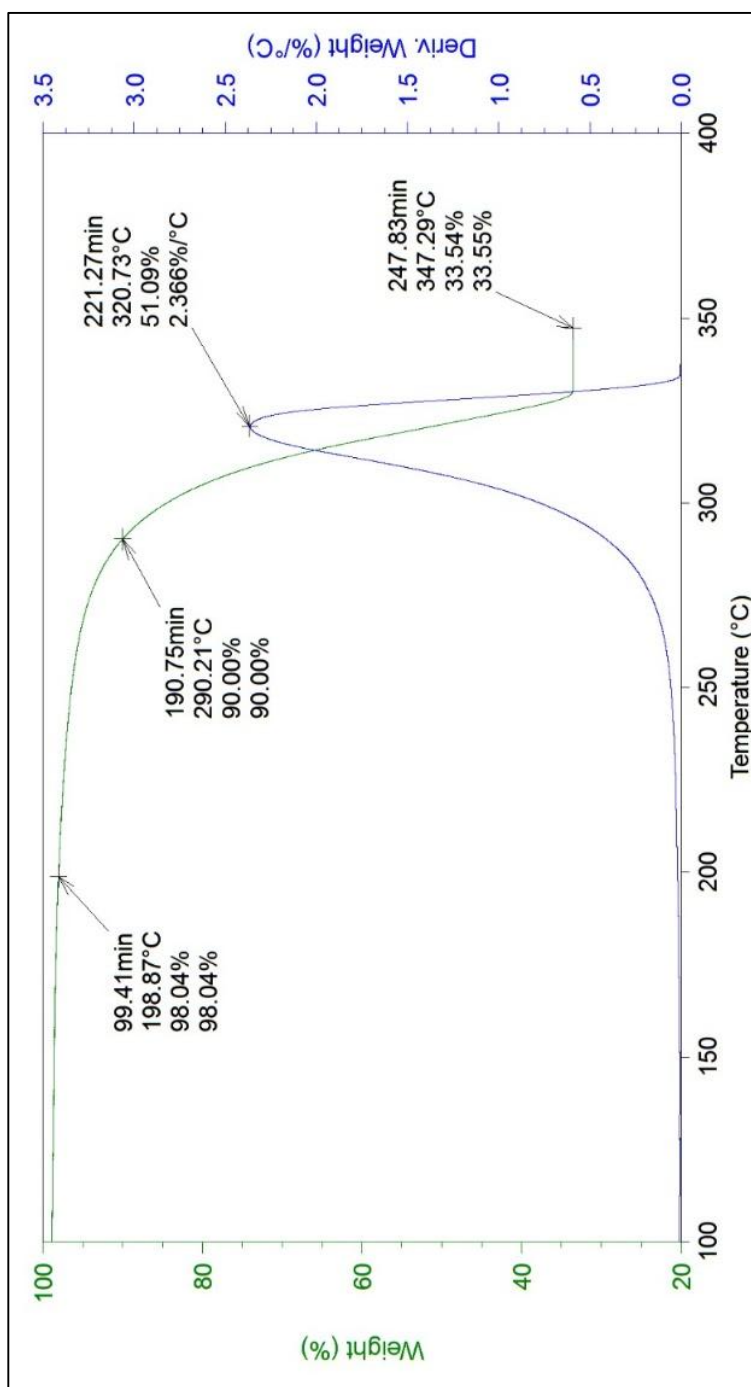


Figure D.34. Thermogravimetric analysis for barium pentafluoropropionate with with detailed information.

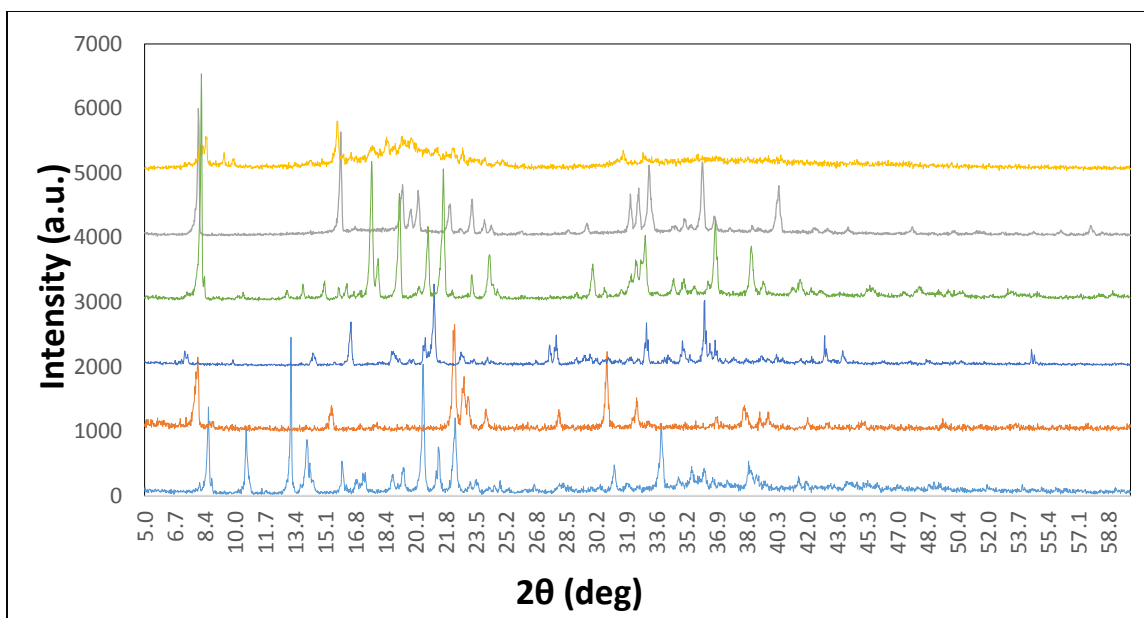


Figure D.35. Powder X-ray diffraction data for pentafluoropropionate salts. From top to bottom: magnesium, lithium, sodium, potassium, cesium, and calcium pentafluoropropionate.

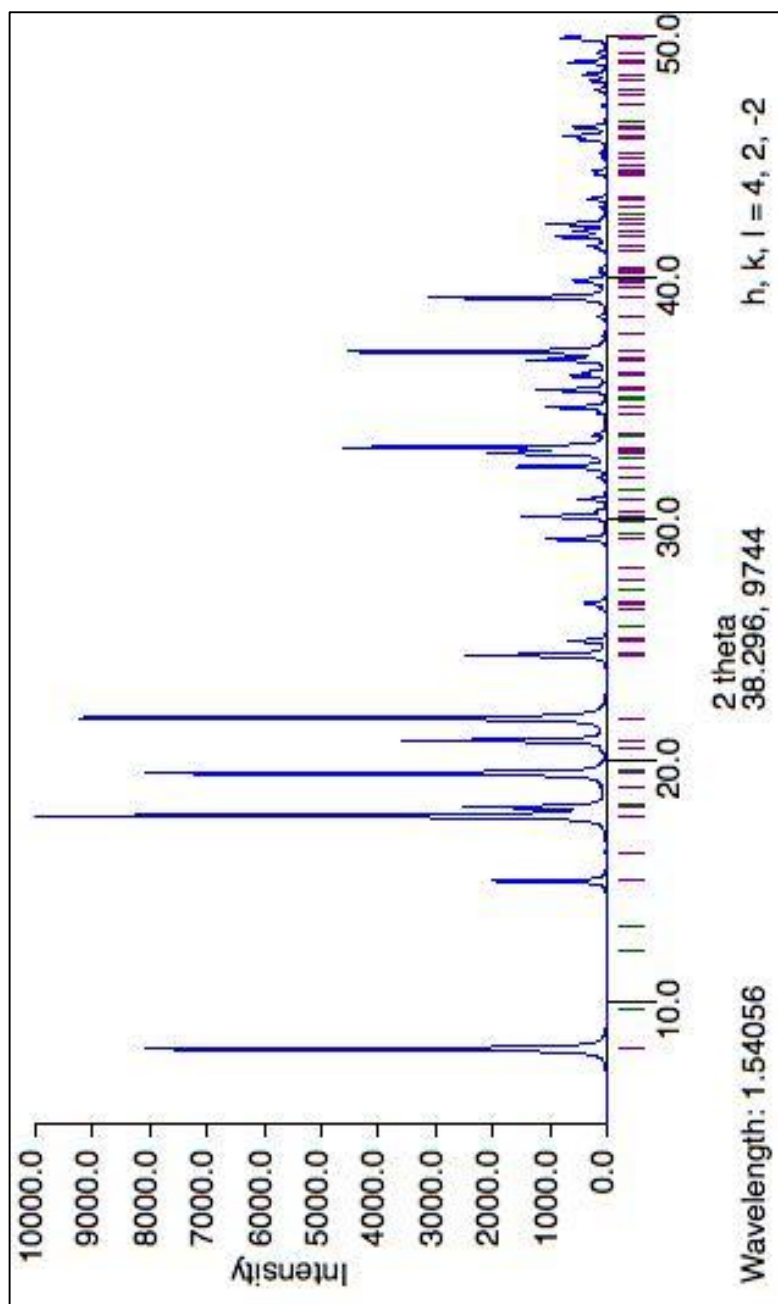


Figure D.36. Calculated powder X-ray diffraction pattern for sodium pentafluoropropionate from the single crystal X-ray diffraction data using Mercury and the .cif file.

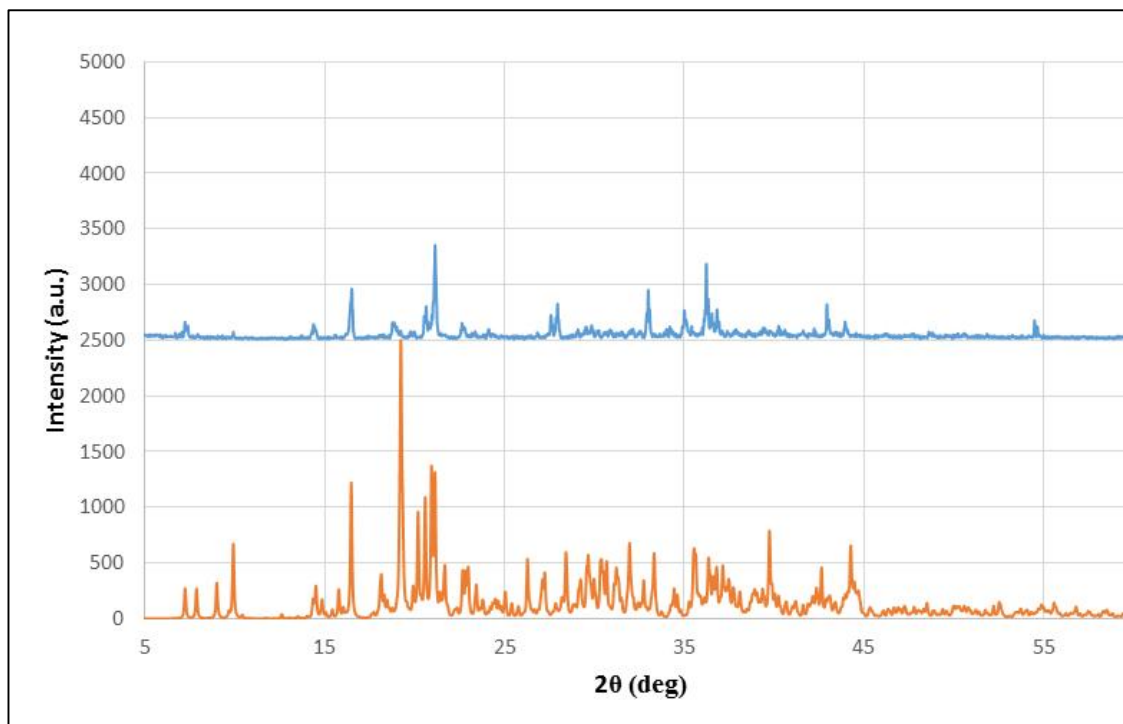


Figure D.37. A comparison of the experimental powder X-ray diffraction pattern (blue) and calculated powder X-ray diffraction pattern (from single crystal data) for potassium pentafluoropropionate.

Table D.1. Sample and crystal data for sodium pentafluoropropionate.

Identification code	D8_0351_WNa	
Chemical formula	$\text{C}_3\text{F}_5\text{NaO}_2$	
Formula weight	186.02 g/mol	
Temperature	100(2) K	
Wavelength	0.71073 Å	
Crystal size	0.034 x 0.204 x 0.210 mm	
Crystal system	monoclinic	
Space group	C 1 2/c 1	
Unit cell dimensions	a = 21.9135(13) Å	$\alpha = 90^\circ$
	b = 6.1114(4) Å	$\beta = 94.738(2)^\circ$
	c = 9.1313(5) Å	$\gamma = 90^\circ$
Volume	1218.70(13) Å ³	
Z	8	
Density (calculated)	2.028 g/cm ³	
Absorption coefficient	0.310 mm ⁻¹	
F(000)	720	

Table D.2. Data collection and structure refinement for sodium pentafluoropropionate.

Theta range for data collection	3.46 to 27.00°	
Index ranges	-27<=h<=27, -7<=k<=7, -11<=l<=11	
Reflections collected	11740	
Independent reflections	1323 [R(int) = 0.0315]	
Max. and min. transmission	1.0000 and 0.9026	
Structure solution technique	direct methods	
Structure solution program	SHELXT-2014 (Sheldrick 2014)	
Refinement method	Full-matrix least-squares on F ²	
Refinement program	SHELXL-2014 (Sheldrick 2014)	
Function minimized	$\Sigma w(F_o^2 - F_c^2)^2$	
Data / restraints / parameters	1323 / 0 / 100	
Goodness-of-fit on F²	1.055	
Δ/σ_{\max}	0.001	
Final R indices	1186 data; I>2σ(I)	R1 = 0.0347, wR2 = 0.0804
	all data	R1 = 0.0392, wR2 = 0.0831
Weighting scheme	w=1/[σ ² (F _o ²)+(0.0356P) ² +2.4010P] where P=(F _o ² +2F _c ²)/3	
Largest diff. peak and hole	0.395 and -0.401 eÅ ⁻³	
R.M.S. deviation from mean	0.060 eÅ ⁻³	

Table D.3. Atomic coordinates and equivalent isotropic atomic displacement parameters (\AA^2) for sodium pentafluoropropionate. $U(\text{eq})$ is defined as one third of the trace of the orthogonalized U_{ij} tensor.

	x/a	y/b	z/c	U(eq)
Na1	0.72406(3)	0.87142(10)	0.64789(7)	0.01462(18)
F1	0.64615(5)	0.3029(2)	0.30750(10)	0.0256(3)
F2	0.64462(5)	0.02988(17)	0.45930(13)	0.0309(3)
O2	0.71305(5)	0.24700(18)	0.65615(12)	0.0153(3)
O1	0.70242(5)	0.55495(18)	0.52223(13)	0.0165(3)
F5	0.53370(5)	0.2028(3)	0.39714(15)	0.0447(4)
F4	0.56575(6)	0.5242(2)	0.4615(2)	0.0537(4)
F6	0.56649(6)	0.2660(3)	0.62063(15)	0.0579(5)
C1	0.69046(7)	0.3625(3)	0.55344(16)	0.0119(3)
C2	0.63993(7)	0.2510(3)	0.44996(18)	0.0164(4)
C3	0.57474(8)	0.3120(4)	0.4830(2)	0.0295(4)

Table D.4. Bond lengths (Å) for sodium pentafluoropropionate.

Na1-O1	2.2787(13)	Na1-O2	2.2961(12)
Na1-O2	2.3098(12)	Na1-O1	2.3718(13)
Na1-F2	2.5375(13)	Na1-F1	2.5661(12)
Na1-Na1	3.3611(12)	Na1-Na1	3.7090(7)
Na1-Na1	3.7090(7)	F1-C2	1.3567(19)
F1-Na1	2.5660(12)	F2-C2	1.3577(19)
F2-Na1	2.5375(13)	O2-C1	1.2436(19)
O2-Na1	2.2960(12)	O2-Na1	2.3099(12)
O1-C1	1.243(2)	O1-Na1	2.3718(13)
F5-C3	1.324(2)	F4-C3	1.324(3)
F6-C3	1.315(2)	C1-C2	1.553(2)
C2-C3	1.530(2)		

Table D.5. Bond angles (°) for sodium pentafluoropropionate.

O1-Na1-O2	101.41(5)	O1-Na1-O2	147.34(5)
O2-Na1-O2	111.18(4)	O1-Na1-O1	87.46(5)
O2-Na1-O1	100.18(5)	O2-Na1-O1	84.91(4)
O1-Na1-F2	83.08(4)	O2-Na1-F2	171.60(5)
O2-Na1-F2	64.86(4)	O1-Na1-F2	87.03(5)
O1-Na1-F1	79.23(4)	O2-Na1-F1	78.73(4)
O2-Na1-F1	108.53(5)	O1-Na1-F1	166.08(5)
F2-Na1-F1	95.31(4)	O1-Na1-Na1	44.83(3)
O2-Na1-Na1	105.01(4)	O2-Na1-Na1	120.54(4)
O1-Na1-Na1	42.63(3)	F2-Na1-Na1	83.21(4)
F1-Na1-Na1	123.93(4)	O1-Na1-Na1	174.18(5)
O2-Na1-Na1	75.03(4)	O2-Na1-Na1	36.24(3)
O1-Na1-Na1	88.65(4)	F2-Na1-Na1	101.03(3)
F1-Na1-Na1	104.31(4)	Na1-Na1-Na1	131.13(4)
O1-Na1-Na1	66.19(3)	O2-Na1-Na1	36.49(3)
O2-Na1-Na1	146.18(4)	O1-Na1-Na1	106.80(4)
F2-Na1-Na1	145.11(4)	F1-Na1-Na1	64.10(3)
Na1-Na1-Na1	86.00(2)	Na1-Na1-Na1	110.95(3)
C2-F1-Na1	124.89(10)	C2-F2-Na1	117.82(10)
C1-O2-Na1	125.14(10)	C1-O2-Na1	125.16(10)
Na1-O2-Na1	107.27(5)	C1-O1-Na1	136.60(10)
C1-O1-Na1	119.81(10)	Na1-O1-Na1	92.54(5)
O1-C1-O2	129.19(15)	O1-C1-C2	115.40(14)
O2-C1-C2	115.42(14)	F1-C2-F2	106.24(13)

F1-C2-C3	107.56(14)	F2-C2-C3	107.27(15)
F1-C2-C1	110.97(13)	F2-C2-C1	110.62(13)
C3-C2-C1	113.82(14)	F6-C3-F5	108.55(17)
F6-C3-F4	108.69(19)	F5-C3-F4	108.70(17)
F6-C3-C2	109.92(16)	F5-C3-C2	111.11(16)
F4-C3-C2	109.82(16)		

Table D.6. Anisotropic atomic displacement parameters (\AA^2) for sodium pentafluoropropionate. The anisotropic atomic displacement factor exponent takes the form: $-2\pi^2[h^2a^{*2}U_{11} + \dots + 2hka^*b^*U_{12}]$

	U ₁₁	U ₂₂	U ₃₃	U ₂₃	U ₁₃	U ₁₂
Na1	0.0234(3)	0.0083(3)	0.0123(3)	0.0010(2)	0.0019(2)	0.0001(2)
F1	0.0251(5)	0.0385(6)	0.0127(5)	-0.0004(5)	-0.0003(4)	0.0006(5)
F2	0.0371(6)	0.0123(5)	0.0405(7)	-0.0045(5)	-0.0146(5)	-0.0028(4)
O2	0.0218(6)	0.0111(6)	0.0126(6)	-0.0005(4)	-0.0003(4)	0.0026(4)
O1	0.0238(6)	0.0089(5)	0.0177(6)	-0.0005(4)	0.0063(5)	-0.0013(4)
F5	0.0187(6)	0.0651(9)	0.0485(8)	-0.0122(7)	-0.0082(5)	-0.0075(6)
F4	0.0281(7)	0.0410(8)	0.0920(12)	-0.0081(8)	0.0050(7)	0.0161(6)
F6	0.0269(7)	0.1178(15)	0.0306(7)	0.0016(8)	0.0119(5)	-0.0117(8)
C1	0.0135(7)	0.0106(7)	0.0123(7)	-0.0027(6)	0.0052(5)	0.0014(6)
C2	0.0211(8)	0.0135(8)	0.0146(8)	0.0011(6)	0.0007(6)	0.0000(6)
C3	0.0191(9)	0.0412(12)	0.0280(10)	-0.0041(9)	0.0019(7)	-0.0029(8)

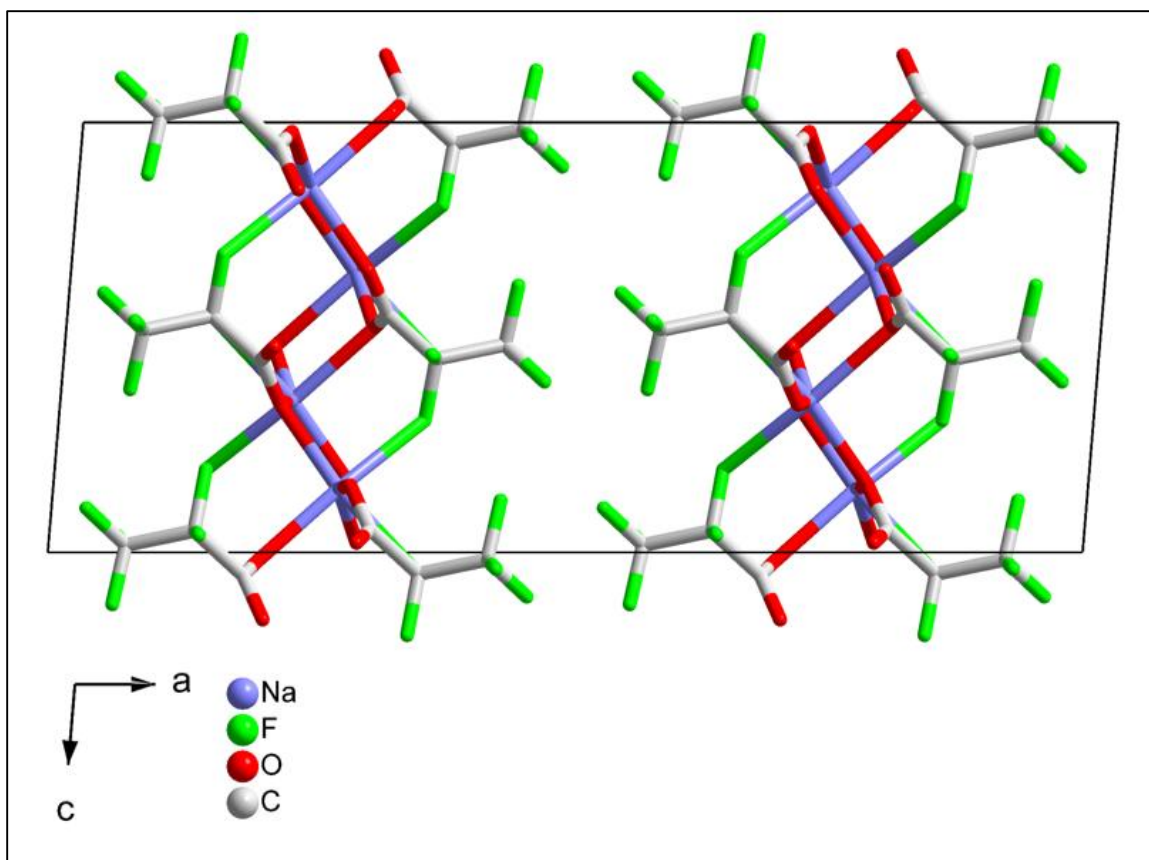


Figure D.38. Unit cell representation of sodium pentafluoropropionate.

Table D.7. Sample and crystal data for potassium pentafluoropropionate.

Identification code	D8_0456_WK	
Chemical formula	$\text{C}_3\text{F}_5\text{KO}_2$	
Formula weight	202.13 g/mol	
Temperature	100(2) K	
Wavelength	0.71073 Å	
Crystal size	0.042 x 0.102 x 0.118 mm	
Crystal system	monoclinic	
Space group	P 1 21/n 1	
Unit cell dimensions	a = 23.4667(16) Å	$\alpha = 90^\circ$
	b = 9.9952(6) Å	$\beta = 107.046(2)^\circ$
	c = 25.5061(18) Å	$\gamma = 90^\circ$
Volume	5719.8(7) Å ³	
Z	36	
Density (calculated)	2.113 g/cm ³	
Absorption coefficient	0.886 mm ⁻¹	
F(000)	3528	

Table D.8. Data collection and structure refinement for potassium pentafluoropropionate.

Theta range for data collection	2.08 to 26.00°	
Index ranges	-28<=h<=28, -12<=k<=12, -31<=l<=27	
Reflections collected	123222	
Independent reflections	11233 [R(int) = 0.0734]	
Max. and min. transmission	0.9640 and 0.9030	
Structure solution technique	direct methods	
Structure solution program	XT, VERSION 2014/4	
Refinement method	Full-matrix least-squares on F ²	
Refinement program	SHELXL-2014/7 (Sheldrick, 2014)	
Function minimized	$\sum w(F_o^2 - F_c^2)^2$	
Data / restraints / parameters	11233 / 16 / 946	
Goodness-of-fit on F²	1.021	
Final R indices	8747 data; I>2σ(I)	R1 = 0.0708, wR2 = 0.1650
	all data	R1 = 0.0936, wR2 = 0.1825
Weighting scheme	w=1/[σ ² (F _o ²)+(0.0668P) ² +53.4283P] where P=(F _o ² +2F _c ²)/3	

Largest diff. peak and hole	1.893 and -1.529 eÅ ⁻³
R.M.S. deviation from mean	0.135 eÅ ⁻³

Table D.9. Atomic coordinates and equivalent isotropic atomic displacement parameters (Å²) for potassium pentafluoropropionate. U(eq) is defined as one third of the trace of the orthogonalized U_{ij} tensor.

	x/a	y/b	z/c	U(eq)
K1	0.72002(5)	0.02709(10)	0.29458(4)	0.0148(2)
K4	0.29462(5)	0.26894(11)	0.34424(4)	0.0165(2)
K8	0.79359(5)	0.70528(10)	0.34572(5)	0.0161(2)
K5	0.21452(5)	0.58982(11)	0.29167(5)	0.0159(2)
K3	0.35765(5)	0.74300(12)	0.27697(5)	0.0198(3)
K6	0.99787(5)	0.39231(12)	0.24708(5)	0.0186(2)
K9	0.86357(5)	0.15995(12)	0.27010(5)	0.0200(3)
K7	0.01527(5)	0.19026(12)	0.38047(5)	0.0207(3)
K2	0.50834(5)	0.73539(14)	0.39455(5)	0.0257(3)
F26	0.23089(15)	0.2985(4)	0.42819(14)	0.0357(9)
F41	0.86776(17)	0.8334(3)	0.45015(13)	0.0334(8)
F42	0.95644(14)	0.9129(4)	0.46099(14)	0.0322(8)
O11	0.17988(15)	0.3632(4)	0.32507(15)	0.0179(8)

F6	0.71343(17)	0.7311(3)	0.12614(14)	0.0355(9)
O3	0.75312(17)	0.7876(4)	0.23167(14)	0.0198(8)
O10	0.26114(16)	0.3514(3)	0.23218(14)	0.0184(8)
O1	0.67919(15)	0.8006(4)	0.32761(14)	0.0174(7)
O9	0.27707(15)	0.5687(3)	0.21776(14)	0.0166(7)
O18	0.83007(15)	0.9594(3)	0.35575(14)	0.0180(8)
O4	0.77399(15)	0.0001(3)	0.21382(15)	0.0176(8)
O8	0.32223(16)	0.5311(4)	0.35833(15)	0.0236(8)
F43	0.91051(17)	0.9959(4)	0.53866(13)	0.0369(9)
O14	0.05695(16)	0.4398(4)	0.17326(15)	0.0217(8)
F44	0.91663(19)	0.1589(4)	0.48597(15)	0.0414(10)
F2	0.72829(16)	0.7431(4)	0.43228(15)	0.0409(10)
O5	0.46757(16)	0.6447(4)	0.28814(16)	0.0235(8)
F7	0.7066(2)	0.9449(4)	0.10799(15)	0.0483(11)
F45	0.83187(17)	0.0695(5)	0.47908(15)	0.0479(11)
O6	0.51896(17)	0.6202(4)	0.22719(16)	0.0233(8)
O17	0.91456(18)	0.0789(4)	0.37519(16)	0.0282(9)
O12	0.09013(16)	0.3252(4)	0.33653(16)	0.0260(9)
O13	0.13693(17)	0.5730(4)	0.18803(16)	0.0287(9)
F16	0.3666(2)	0.3950(4)	0.44921(16)	0.0539(12)
F23	0.3529(2)	0.2851(4)	0.1712(2)	0.0568(12)
F21	0.2353(2)	0.3082(4)	0.12340(17)	0.0524(12)

O2	0.58916(17)	0.7964(5)	0.34129(17)	0.0362(11)
F1	0.64150(19)	0.7295(5)	0.44522(16)	0.0562(13)
O7	0.39709(19)	0.6790(4)	0.38394(17)	0.0316(10)
F8	0.8339(2)	0.7475(5)	0.1503(2)	0.0586(13)
F22	0.2464(2)	0.5216(4)	0.10932(16)	0.0545(12)
F3	0.7121(3)	0.0134(5)	0.41518(18)	0.0668(15)
F27	0.1469(2)	0.2392(6)	0.43714(18)	0.0792(19)
F24	0.3657(2)	0.4957(4)	0.1589(2)	0.0677(15)
F4	0.7111(3)	0.9412(6)	0.49497(17)	0.0746(16)
F28	0.2000(2)	0.4567(6)	0.49709(17)	0.0742(17)
F9	0.7782(3)	0.8015(5)	0.06521(19)	0.0776(18)
F32	0.0667(3)	0.7593(5)	0.1191(2)	0.0711(15)
F10	0.8254(3)	0.9548(5)	0.1249(3)	0.086(2)
C25	0.8788(2)	0.9995(5)	0.38556(19)	0.0134(10)
F5	0.6296(3)	0.9965(7)	0.4356(2)	0.097(2)
C16	0.1445(2)	0.3399(5)	0.3521(2)	0.0157(10)
F33	0.1271(3)	0.5974(6)	0.0717(2)	0.0821(18)
C1	0.6439(2)	0.7970(5)	0.3558(2)	0.0175(11)
C4	0.7591(3)	0.8815(5)	0.2021(2)	0.0205(11)
C10	0.3668(2)	0.5817(5)	0.3906(2)	0.0174(11)
C13	0.2705(2)	0.4486(5)	0.2058(2)	0.0201(11)
C26	0.8984(2)	0.9459(5)	0.4454(2)	0.0172(11)

C7	0.4963(3)	0.5824(6)	0.2627(2)	0.0240(12)
C19	0.0870(2)	0.5311(6)	0.1623(2)	0.0219(12)
C27	0.8889(2)	0.0449(6)	0.4876(2)	0.0230(12)
F12	0.5362(3)	0.4200(7)	0.3349(2)	0.095(2)
F11	0.4417(3)	0.3715(6)	0.2759(2)	0.098(2)
C17	0.1731(2)	0.3322(6)	0.4151(2)	0.0222(12)
F25	0.3248(4)	0.3654(5)	0.0862(3)	0.121(3)
C2	0.6734(2)	0.7991(6)	0.4184(2)	0.0236(12)
F17	0.4502(2)	0.4949(8)	0.4580(3)	0.111(3)
F18	0.4020(4)	0.5332(7)	0.54130(18)	0.130(3)
C5	0.7427(3)	0.8486(6)	0.1388(3)	0.0327(14)
F29	0.1944(5)	0.5586(5)	0.4215(3)	0.168(5)
C11	0.3909(3)	0.5162(7)	0.4474(3)	0.0370(16)
F34	0.0373(4)	0.6623(9)	0.0200(3)	0.208(6)
C3	0.6815(3)	0.9416(9)	0.4418(3)	0.0466(19)
C14	0.2707(4)	0.4169(6)	0.1450(3)	0.0467(19)
F31	0.9925(3)	0.6258(10)	0.1013(3)	0.149(4)
C6	0.7967(5)	0.8401(8)	0.1186(4)	0.060(3)
F30	0.1165(4)	0.4932(13)	0.4395(3)	0.213(7)
F35	0.0521(5)	0.4560(6)	0.0546(3)	0.183(6)
C15	0.3311(5)	0.3892(8)	0.1397(4)	0.065(3)
C20	0.0571(3)	0.6073(10)	0.1082(4)	0.073(3)

C18	0.1712(4)	0.4642(11)	0.4440(3)	0.066(3)
F19	0.3256(6)	0.6177(12)	0.4846(4)	0.184(6)
C8	0.5055(5)	0.4321(10)	0.2785(5)	0.076(3)
C21	0.0760(6)	0.5746(10)	0.0604(4)	0.087(4)
O15	0.93272(16)	0.3760(4)	0.31914(16)	0.0214(8)
C22	0.9096(2)	0.4793(5)	0.3301(2)	0.0166(10)
O16	0.86165(16)	0.5323(4)	0.30646(16)	0.0267(9)
F20	0.4117(7)	0.7070(7)	0.4995(3)	0.245(8)
C12	0.3803(6)	0.5975(9)	0.4942(3)	0.098(5)
C9	0.5255(8)	0.3362(10)	0.2433(6)	0.236(16)
F14	0.4837(4)	0.3497(7)	0.1959(4)	0.159(4)
F15	0.5205(6)	0.2137(7)	0.2676(5)	0.242(8)
F13	0.5797(3)	0.3909(10)	0.2615(6)	0.228(8)
C23	0.9492(3)	0.5603(8)	0.3802(3)	0.056(3)
F36A	0.9794(5)	0.4488(13)	0.4169(4)	0.053(3)
F37A	0.9094(3)	0.5904(10)	0.4130(3)	0.042(2)
C24A	0.9861(5)	0.6524(13)	0.3790(5)	0.043(4)
F38A	0.0183(5)	0.6069(12)	0.3478(6)	0.052(4)
F40A	0.9540(4)	0.7555(8)	0.3553(5)	0.056(3)
F39A	0.0225(4)	0.6899(11)	0.4263(5)	0.083(4)
F36B	0.9290(3)	0.7008(7)	0.3707(3)	0.0297(16)
F37B	0.0048(4)	0.5891(12)	0.3660(5)	0.033(2)

C24B	0.9617(5)	0.5297(12)	0.4332(5)	0.040(3)
F38B	0.9967(4)	0.6166(8)	0.4672(3)	0.053(2)
F39B	0.9884(6)	0.4123(9)	0.4393(4)	0.049(3)
F40B	0.9100(4)	0.5212(12)	0.4426(4)	0.062(3)

Table D.10. Bond lengths (Å) for potassium pentafluoropropionate.

K1-O18	2.683(4)	K1-O1	2.688(4)
K1-O16	2.724(4)	K1-O4	2.729(4)
K1-O3	2.806(4)	K1-F6	2.972(4)
K1-F8	3.079(5)	K1-O3	3.105(4)
K1-C4	3.130(5)	K1-F3	3.138(5)
K1-K8	3.7024(15)	K1-K9	3.8387(15)
K4-O8	2.698(4)	K4-O11	2.758(4)
K4-O9	2.788(4)	K4-O13	2.805(4)
K4-O10	2.855(4)	K4-F33	2.933(6)
K4-F26	2.964(4)	K4-F16	2.993(4)
K4-F22	3.018(4)	K4-F32	3.112(6)
K4-K5	3.7602(15)	K4-K5	3.8513(16)
K8-O18	2.669(4)	K8-O16	2.735(4)
K8-O1	2.757(4)	K8-O4	2.760(4)
K8-F7	2.858(4)	K8-O3	2.902(4)
K8-F37A	2.986(8)	K8-F41	3.008(4)
K8-F36B	3.053(8)	K8-F2	3.058(4)
K8-C25	3.533(5)	K8-K1	3.7024(15)
K5-O11	2.631(4)	K5-O8	2.665(4)
K5-O9	2.716(4)	K5-O13	2.740(4)
K5-O10	2.781(4)	K5-F23	2.844(4)

K5-F21	3.058(5)	K5-O10	3.186(4)
K5-C13	3.194(5)	K5-K3	3.8083(15)
K5-K4	3.8513(15)	K3-O9	2.686(4)
K3-O7	2.689(4)	K3-O5	2.696(4)
K3-O11	2.766(4)	K3-O14	2.829(4)
K3-O10	2.936(4)	K3-O8	3.239(4)
K3-C10	3.269(5)	K3-C19	3.347(6)
K3-O13	3.410(4)	K3-C16	3.417(5)
K6-O14	2.688(4)	K6-O15	2.718(4)
K6-O12	2.729(4)	K6-O2	2.733(4)
K6-O5	2.832(4)	K6-O6	2.852(4)
K6-C7	3.114(6)	K6-F15	3.249(7)
K6-F38A	3.272(13)	K6-C22	3.479(5)
K6-K7	3.8737(16)	K6-K2	3.9016(17)
K9-O4	2.695(4)	K9-O17	2.719(4)
K9-O6	2.766(4)	K9-O15	2.770(4)
K9-O1	2.780(4)	K9-O3	3.009(4)
K9-F13	3.206(9)	K9-O18	3.227(4)
K9-C25	3.280(5)	K9-C1	3.448(5)
K9-K7	3.8490(16)	K7-O17	2.580(4)
K7-O12	2.704(4)	K7-O6	2.717(4)
K7-O15	2.805(4)	K7-F39B	2.851(10)

K7-F43	2.940(4)	K7-F36A	2.952(12)
K7-F27	3.042(5)	K7-K9	3.8490(16)
K2-O7	2.606(4)	K2-O2	2.706(4)
K2-O5	2.753(4)	K2-O14	2.821(4)
K2-F1	3.012(4)	K2-F35	3.105(8)
K2-F34	3.235(6)	K2-F17	3.399(7)
K2-K6	3.9017(17)	F26-C17	1.340(6)
F41-C26	1.360(6)	F42-C26	1.343(6)
O11-C16	1.246(6)	O11-K3	2.766(4)
F6-C5	1.352(7)	F6-K1	2.972(4)
O3-C4	1.239(6)	O3-K1	2.805(4)
O3-K8	2.902(4)	O3-K9	3.009(4)
O10-C13	1.237(6)	O10-K5	2.781(4)
O10-K3	2.936(4)	O1-C1	1.246(6)
O1-K8	2.757(4)	O1-K9	2.780(4)
O9-C13	1.238(6)	O9-K4	2.788(4)
O18-C25	1.239(6)	O18-K1	2.683(3)
O18-K9	3.227(4)	O4-C4	1.247(6)
O4-K8	2.760(4)	O8-C10	1.235(6)
F43-C27	1.344(6)	F43-K7	2.940(4)
O14-C19	1.236(7)	O14-K2	2.821(4)
O14-K3	2.829(4)	F44-C27	1.319(7)

F2-C2	1.353(6)	F2-K8	3.058(4)
O5-C7	1.234(7)	O5-K6	2.832(4)
F7-C5	1.369(7)	F7-K8	2.858(4)
F45-C27	1.314(7)	O6-C7	1.235(7)
O6-K7	2.717(4)	O6-K9	2.766(4)
O6-K6	2.852(4)	O17-C25	1.239(6)
O17-K9	2.719(4)	O12-C16	1.229(6)
O13-C19	1.235(7)	O13-K4	2.805(4)
O13-K3	3.410(4)	F16-C11	1.346(7)
F23-C15	1.324(10)	F23-K5	2.844(4)
F21-C14	1.380(8)	F21-K5	3.058(5)
O2-C1	1.229(6)	O2-K6	2.733(4)
F1-C2	1.346(7)	O7-C10	1.245(6)
F8-C6	1.363(11)	F8-K1	3.079(5)
F22-C14	1.394(8)	F22-K4	3.018(4)
F3-C3	1.332(9)	F27-C17	1.327(7)
F24-C15	1.342(10)	F4-C3	1.331(8)
F28-C18	1.327(8)	F9-C6	1.358(10)
F32-C20	1.550(11)	F32-K4	3.112(6)
F10-C6	1.315(9)	C25-C26	1.554(7)
C25-K9	3.280(5)	F5-C3	1.303(9)
C16-C17	1.553(7)	C16-K3	3.417(5)

F33-C21	1.170(14)	F33-K4	2.933(6)
C1-C2	1.543(7)	C1-K9	3.448(5)
C4-C5	1.579(8)	C10-C11	1.538(8)
C13-C14	1.584(9)	C26-C27	1.526(7)
C7-C8	1.554(10)	C7-K6	3.114(6)
C19-C20	1.552(9)	C19-K3	3.347(6)
F12-C8	1.413(12)	F11-C8	1.598(13)
C17-C18	1.518(10)	F25-C15	1.349(10)
C2-C3	1.534(10)	F17-C11	1.356(9)
F18-C12	1.326(10)	C5-C6	1.504(11)
F29-C18	1.304(14)	C11-C12	1.522(12)
F34-C21	1.451(13)	F34-K2	3.235(6)
C14-C15	1.488(12)	F31-C20	1.486(11)
F30-C18	1.287(11)	F35-C21	1.301(11)
F35-K2	3.105(8)	C20-C21	1.453(16)
F19-C12	1.250(13)	C8-C9	1.480(17)
O15-C22	1.236(6)	O15-K9	2.770(4)
C22-O16	1.229(6)	C22-C23	1.568(8)
O16-K1	2.724(4)	O16-K8	2.735(4)
F20-C12	1.304(10)	C9-F14	1.322(13)
C9-F13	1.337(16)	C9-F15	1.392(13)
F15-K6	3.249(7)	F13-K9	3.206(9)

C23-C24A	1.270(16)	C23-C24B	1.332(15)
C23-F37A	1.455(9)	C23-F36B	1.479(9)
C23-F37B	1.482(11)	C23-F36A	1.494(11)
F37A-K8	2.986(8)	C24A-F39A	1.312(13)
C24A-F40A	1.314(14)	C24A-F38A	1.328(14)
F36B-K8	3.053(8)	C24B-F40B	1.306(14)
C24B-F39B	1.318(14)	C24B-F38B	1.328(12)

Table D.11. Bond angles (°) for potassium pentafluoropropionate.

O18-K1-O1	88.64(11)	O18-K1-O16	147.69(13)
O1-K1-O16	95.51(12)	O18-K1-O4	80.41(11)
O1-K1-O4	116.11(11)	O16-K1-O4	68.98(11)
O18-K1-O3	97.32(11)	O1-K1-O3	169.11(11)
O16-K1-O3	84.34(12)	O4-K1-O3	74.04(11)
O18-K1-F6	63.45(10)	O1-K1-F6	121.94(11)
O16-K1-F6	135.58(12)	O4-K1-F6	108.28(11)

O3-K1-F6	54.25(10)	O18-K1-F8	111.66(12)
O1-K1-F8	103.15(11)	O16-K1-F8	98.59(13)
O4-K1-F8	139.41(11)	O3-K1-F8	66.18(11)
F6-K1-F8	53.31(11)	O18-K1-O3	76.24(10)
O1-K1-O3	71.26(10)	O16-K1-O3	74.87(12)
O4-K1-O3	44.93(10)	O3-K1-O3	118.97(4)
F6-K1-O3	136.00(11)	F8-K1-O3	170.60(12)
O18-K1-C4	82.88(13)	O1-K1-C4	93.16(13)
O16-K1-C4	64.93(14)	O4-K1-C4	23.30(13)
O3-K1-C4	96.62(13)	F6-K1-C4	128.31(13)
F8-K1-C4	158.10(13)	O3-K1-C4	22.92(12)
O18-K1-F3	75.07(14)	O1-K1-F3	61.78(11)
O16-K1-F3	134.49(14)	O4-K1-F3	155.39(14)
O3-K1-F3	110.88(11)	F6-K1-F3	62.18(11)
F8-K1-F3	55.46(13)	O3-K1-F3	124.64(12)
C4-K1-F3	146.43(14)	O18-K1-K8	46.07(8)
O1-K1-K8	47.95(8)	O16-K1-K8	118.42(10)
O4-K1-K8	84.74(8)	O3-K1-K8	140.90(9)
F6-K1-K8	104.98(7)	F8-K1-K8	132.25(9)
O3-K1-K8	49.51(7)	C4-K1-K8	69.65(10)
F3-K1-K8	76.83(10)	O18-K1-K9	56.00(8)
O1-K1-K9	138.83(8)	O16-K1-K9	104.30(9)

O4-K1-K9	44.59(8)	O3-K1-K9	51.01(8)
F6-K1-K9	64.03(8)	F8-K1-K9	108.94(9)
O3-K1-K9	79.53(7)	C4-K1-K9	64.71(11)
F3-K1-K9	118.77(10)	K8-K1-K9	90.98(3)
O8-K4-O11	82.86(11)	O8-K4-O9	148.65(11)
O11-K4-O9	75.48(11)	O8-K4-O13	125.54(13)
O11-K4-O13	143.12(12)	O9-K4-O13	68.58(11)
O8-K4-O10	80.67(11)	O11-K4-O10	75.88(11)
O9-K4-O10	72.31(10)	O13-K4-O10	85.47(11)
O8-K4-F33	113.32(14)	O11-K4-F33	134.33(16)
O9-K4-F33	98.02(13)	O13-K4-F33	61.11(16)
O10-K4-F33	146.15(16)	O8-K4-F26	87.68(12)
O11-K4-F26	54.62(10)	O9-K4-F26	97.63(11)
O13-K4-F26	137.31(12)	O10-K4-F26	130.21(10)
F33-K4-F26	82.54(16)	O8-K4-F16	54.66(11)
O11-K4-F16	106.29(13)	O9-K4-F16	153.88(11)
O13-K4-F16	109.56(13)	O10-K4-F16	133.76(11)
F33-K4-F16	61.55(14)	F26-K4-F16	65.41(12)
O8-K4-F22	146.62(12)	O11-K4-F22	86.68(12)
O9-K4-F22	54.96(10)	O13-K4-F22	79.60(13)
O10-K4-F22	127.12(11)	F33-K4-F22	55.78(15)
F26-K4-F22	60.75(12)	F16-K4-F22	98.92(11)

O8-K4-F32	78.51(13)	O11-K4-F32	160.77(13)
O9-K4-F32	123.51(12)	O13-K4-F32	55.15(12)
O10-K4-F32	105.46(12)	F33-K4-F32	52.18(17)
F26-K4-F32	119.36(11)	F16-K4-F32	58.52(13)
F22-K4-F32	106.41(14)	O8-K4-K5	45.13(8)
O11-K4-K5	44.39(8)	O9-K4-K5	104.74(8)
O13-K4-K5	139.49(9)	O10-K4-K5	55.58(7)
F33-K4-K5	154.12(12)	F26-K4-K5	82.38(8)
F16-K4-K5	92.98(9)	F22-K4-K5	130.91(10)
F32-K4-K5	120.18(11)	O8-K4-K5	121.28(9)
O11-K4-K5	101.85(8)	O9-K4-K5	44.83(7)
O13-K4-K5	45.33(8)	O10-K4-K5	46.10(7)
F33-K4-K5	104.13(13)	F26-K4-K5	142.16(8)
F16-K4-K5	150.32(11)	F22-K4-K5	91.86(8)
F32-K4-K5	91.93(9)	K5-K4-K5	100.69(3)
O18-K8-O16	115.56(12)	O18-K8-O1	87.50(11)
O16-K8-O1	143.28(11)	O18-K8-O4	151.23(11)
O16-K8-O4	68.40(11)	O1-K8-O4	77.90(11)
O18-K8-F7	150.03(11)	O16-K8-F7	69.35(13)
O1-K8-F7	105.35(13)	O4-K8-F7	58.70(11)
O18-K8-O3	80.09(11)	O16-K8-O3	82.35(11)
O1-K8-O3	73.60(11)	O4-K8-O3	72.09(11)

F7-K8-O3	129.23(11)	O18-K8-F37A	95.7(2)
O16-K8-F37A	55.68(15)	O1-K8-F37A	155.07(18)
O4-K8-F37A	108.04(19)	F7-K8-F37A	61.6(2)
O3-K8-F37A	131.32(18)	O18-K8-F41	54.81(10)
O16-K8-F41	110.17(11)	O1-K8-F41	106.47(11)
O4-K8-F41	153.36(10)	F7-K8-F41	95.30(10)
O3-K8-F41	134.54(10)	F37A-K8-F41	57.45(16)
O18-K8-F36B	73.07(15)	O16-K8-F36B	51.93(15)
O1-K8-F36B	160.54(15)	O4-K8-F36B	119.95(15)
F7-K8-F36B	91.59(17)	O3-K8-F36B	103.20(16)
F41-K8-F36B	61.60(15)	O18-K8-F2	91.59(12)
O16-K8-F2	144.34(12)	O1-K8-F2	53.76(10)
O4-K8-F2	99.23(11)	F7-K8-F2	75.67(12)
O3-K8-F2	127.07(10)	F37A-K8-F2	101.37(17)
F41-K8-F2	65.82(10)	F36B-K8-F2	124.21(16)
O18-K8-C25	16.62(11)	O16-K8-C25	106.83(12)
O1-K8-C25	101.63(11)	O4-K8-C25	164.19(11)
F7-K8-C25	135.08(11)	O3-K8-C25	92.51(11)
F37A-K8-C25	79.2(2)	F41-K8-C25	42.20(10)
F36B-K8-C25	59.04(15)	F2-K8-C25	92.90(11)

O18-K8-K1	46.39(8)	O16-K8-K1	133.02(10)
O1-K8-K1	46.38(8)	O4-K8-K1	108.57(8)
F7-K8-K1	151.59(11)	O3-K8-K1	54.47(7)
F37A-K8-K1	142.05(19)	F41-K8-K1	91.78(7)
F36B-K8-K1	115.83(14)	F2-K8-K1	82.32(7)
C25-K8-K1	62.90(8)	O11-K5-O8	85.94(12)
O11-K5-O9	116.05(11)	O8-K5-O9	79.71(12)
O11-K5-O13	94.51(12)	O8-K5-O13	147.09(13)
O9-K5-O13	70.55(11)	O11-K5-O10	169.35(11)
O8-K5-O10	97.43(12)	O9-K5-O10	74.55(10)
O13-K5-O10	88.14(12)	O11-K5-F23	103.18(12)
O8-K5-F23	117.07(14)	O9-K5-F23	138.68(12)
O13-K5-F23	94.91(14)	O10-K5-F23	66.28(11)
O11-K5-F21	118.46(12)	O8-K5-F21	66.98(11)
O9-K5-F21	111.90(12)	O13-K5-F21	137.40(12)
O10-K5-F21	54.74(10)	F23-K5-F21	53.89(13)
O11-K5-O10	72.07(10)	O8-K5-O10	75.25(11)
O9-K5-O10	43.98(10)	O13-K5-O10	73.65(12)
O10-K5-O10	118.54(5)	F23-K5-O10	166.91(13)
F21-K5-O10	139.18(11)	O11-K5-C13	93.99(12)
O8-K5-C13	80.59(13)	O9-K5-C13	22.35(12)
O13-K5-C13	66.54(14)	O10-K5-C13	96.52(12)

F23-K5-C13	155.83(14)	F21-K5-C13	130.62(14)
O10-K5-C13	22.36(11)	O11-K5-K4	47.15(8)
O8-K5-K4	45.84(8)	O9-K5-K4	82.30(8)
O13-K5-K4	114.39(10)	O10-K5-K4	140.05(8)
F23-K5-K4	137.35(10)	F21-K5-K4	107.93(8)
O10-K5-K4	47.65(7)	C13-K5-K4	66.70(10)
O11-K5-K3	138.00(9)	O8-K5-K3	56.80(9)
O9-K5-K3	44.86(8)	O13-K5-K3	106.58(9)
O10-K5-K3	49.98(8)	F23-K5-K3	110.48(9)
F21-K5-K3	67.37(9)	O10-K5-K3	79.51(7)
C13-K5-K3	63.80(10)	K4-K5-K3	90.86(3)
O11-K5-K4	138.64(9)	O8-K5-K4	117.95(9)
O9-K5-K4	46.37(8)	O13-K5-K4	46.71(9)
O10-K5-K4	47.69(8)	F23-K5-K4	95.21(10)
F21-K5-K4	102.36(8)	O10-K5-K4	81.68(7)
C13-K5-K4	60.92(10)	K4-K5-K4	127.42(3)
K3-K5-K4	62.77(3)	O9-K3-O7	113.11(12)
O9-K3-O5	108.48(12)	O7-K3-O5	76.82(13)
O9-K3-O11	77.01(11)	O7-K3-O11	168.01(13)
O5-K3-O11	106.77(11)	O9-K3-O14	172.88(12)
O7-K3-O14	73.87(12)	O5-K3-O14	71.10(11)
O11-K3-O14	96.22(11)	O9-K3-O10	72.48(10)

O7-K3-O10	101.82(12)	O5-K3-O10	178.55(12)
O11-K3-O10	74.44(10)	O14-K3-O10	108.08(11)
O9-K3-O8	70.47(10)	O7-K3-O8	43.21(11)
O5-K3-O8	96.38(11)	O11-K3-O8	144.70(10)
O14-K3-O8	116.62(11)	O10-K3-O8	82.89(10)
O9-K3-C10	91.80(12)	O7-K3-C10	21.42(12)
O5-K3-C10	85.08(12)	O11-K3-C10	165.69(12)
O14-K3-C10	95.22(12)	O10-K3-C10	93.83(12)
O8-K3-C10	21.87(11)	O9-K3-C19	158.72(13)
O7-K3-C19	76.31(14)	O5-K3-C19	92.04(13)
O11-K3-C19	92.02(13)	O14-K3-C19	21.01(12)
O10-K3-C19	87.11(12)	O8-K3-C19	113.79(12)
C10-K3-C19	95.61(14)	O9-K3-O13	137.78(10)
O7-K3-O13	89.37(12)	O5-K3-O13	111.34(11)
O11-K3-O13	78.65(10)	O14-K3-O13	40.79(10)
O10-K3-O13	68.01(10)	O8-K3-O13	117.49(10)
C10-K3-O13	104.90(12)	C19-K3-O13	21.05(11)
O9-K3-C16	80.39(12)	O7-K3-C16	161.50(13)
O5-K3-C16	87.06(12)	O11-K3-C16	19.90(11)
O14-K3-C16	92.50(12)	O10-K3-C16	94.20(11)
O8-K3-C16	150.25(11)	C10-K3-C16	166.57(13)
C19-K3-C16	95.53(13)	O13-K3-C16	88.10(11)

O9-K3-K5	45.48(8)	O7-K3-K5	81.70(9)
O5-K3-K5	133.40(9)	O11-K3-K5	102.74(8)
O14-K3-K5	139.86(8)	O10-K3-K5	46.52(7)
O8-K3-K5	43.52(7)	C10-K3-K5	62.95(9)
C19-K3-K5	122.27(10)	O13-K3-K5	109.23(8)
C16-K3-K5	116.38(9)	O14-K6-O15	172.81(12)
O14-K6-O12	100.57(12)	O15-K6-O12	83.43(12)
O14-K6-O2	84.16(12)	O15-K6-O2	95.98(12)
O12-K6-O2	145.19(15)	O14-K6-O5	71.19(11)
O15-K6-O5	115.61(11)	O12-K6-O5	79.60(12)
O2-K6-O5	69.28(13)	O14-K6-O6	117.66(12)
O15-K6-O6	69.15(11)	O12-K6-O6	72.69(12)
O2-K6-O6	74.64(14)	O5-K6-O6	46.48(11)
O14-K6-C7	94.37(13)	O15-K6-C7	92.33(13)
O12-K6-C7	77.27(14)	O2-K6-C7	67.97(15)
O5-K6-C7	23.34(13)	O6-K6-C7	23.37(13)
O14-K6-F15	79.8(3)	O15-K6-F15	93.2(3)
O12-K6-F15	112.7(2)	O2-K6-F15	102.1(2)
O5-K6-F15	150.3(3)	O6-K6-F15	161.2(3)
C7-K6-F15	169.1(2)	O14-K6-F38A	116.6(2)

O15-K6-F38A	59.4(2)	O12-K6-F38A	66.9(3)
O2-K6-F38A	141.2(2)	O5-K6-F38A	146.3(3)
O6-K6-F38A	116.3(3)	C7-K6-F38A	135.6(3)
F15-K6-F38A	55.0(4)	O14-K6-C22	154.66(12)
O15-K6-C22	18.23(12)	O12-K6-C22	91.19(12)
O2-K6-C22	98.92(12)	O5-K6-C22	133.52(12)
O6-K6-C22	87.19(12)	C7-K6-C22	110.18(14)
F15-K6-C22	74.9(3)	F38A-K6-C22	48.32(19)
O14-K6-K7	139.83(9)	O15-K6-K7	46.40(8)
O12-K6-K7	44.27(8)	O2-K6-K7	113.73(11)
O5-K6-K7	81.76(8)	O6-K6-K7	44.51(8)
C7-K6-K7	63.62(11)	F15-K6-K7	126.4(3)
F38A-K6-K7	72.5(3)	C22-K6-K7	61.58(9)
O14-K6-K2	46.31(9)	O15-K6-K2	136.57(9)
O12-K6-K2	118.71(10)	O2-K6-K2	43.90(9)
O5-K6-K2	44.87(8)	O6-K6-K2	81.93(8)
C7-K6-K2	61.11(11)	F15-K6-K2	108.9(3)
F38A-K6-K2	161.3(2)	C22-K6-K2	142.81(9)
K7-K6-K2	124.70(4)	O4-K9-O17	113.43(12)
O4-K9-O6	122.98(12)	O17-K9-O6	77.60(12)

O4-K9-O15	164.80(12)	O17-K9-O15	75.92(12)
O6-K9-O15	69.69(11)	O4-K9-O1	78.59(11)
O17-K9-O1	166.74(12)	O6-K9-O1	100.97(11)
O15-K9-O1	91.16(11)	O4-K9-O3	71.27(10)
O17-K9-O3	106.06(12)	O6-K9-O3	163.17(12)
O15-K9-O3	94.96(11)	O1-K9-O3	71.60(10)
O4-K9-F13	71.66(15)	O17-K9-F13	84.4(3)
O6-K9-F13	53.26(18)	O15-K9-F13	122.41(16)
O1-K9-F13	105.5(3)	O3-K9-F13	142.62(16)
O4-K9-O18	71.67(10)	O17-K9-O18	43.26(10)
O6-K9-O18	109.43(11)	O15-K9-O18	113.91(11)
O1-K9-O18	145.63(10)	O3-K9-O18	82.66(10)
F13-K9-O18	81.4(3)	O4-K9-C25	92.92(12)
O17-K9-C25	21.33(12)	O6-K9-C25	93.56(12)
O15-K9-C25	94.63(12)	O1-K9-C25	165.45(12)
O3-K9-C25	94.57(11)	F13-K9-C25	82.6(3)
O18-K9-C25	21.94(10)	O4-K9-C1	85.44(12)
O17-K9-C1	157.54(12)	O6-K9-C1	81.88(12)
O15-K9-C1	88.51(12)	O1-K9-C1	19.56(11)
O3-K9-C1	91.14(11)	F13-K9-C1	90.6(3)
O18-K9-C1	157.09(11)	C25-K9-C1	173.22(12)
O4-K9-K1	45.32(8)	O17-K9-K1	83.69(9)

O6-K9-K1	149.55(9)	O15-K9-K1	128.48(9)
O1-K9-K1	102.56(8)	O3-K9-K1	46.44(7)
F13-K9-K1	101.5(2)	O18-K9-K1	43.57(6)
C25-K9-K1	63.54(9)	C1-K9-K1	118.77(9)
O4-K9-K7	147.78(9)	O17-K9-K7	42.01(8)
O6-K9-K7	44.90(8)	O15-K9-K7	46.73(8)
O1-K9-K7	129.00(8)	O3-K9-K7	128.33(8)
F13-K9-K7	83.49(15)	O18-K9-K7	84.86(7)
C25-K9-K7	63.12(9)	C1-K9-K7	115.70(9)
K1-K9-K7	125.16(4)	O17-K7-O12	152.85(13)
O17-K7-O6	80.86(12)	O12-K7-O6	75.23(12)
O17-K7-O15	77.53(12)	O12-K7-O15	82.25(12)
O6-K7-O15	69.86(11)	O17-K7-F39B	91.3(3)
O12-K7-F39B	95.8(3)	O6-K7-F39B	133.4(2)
O15-K7-F39B	63.6(2)	O17-K7-F43	96.25(13)
O12-K7-F43	106.44(12)	O6-K7-F43	119.01(12)
O15-K7-F43	168.60(11)	F39B-K7-F43	107.5(2)
O17-K7-F36A	93.0(3)	O12-K7-F36A	88.5(3)
O6-K7-F36A	121.1(2)	O15-K7-F36A	51.83(19)

F43-K7-F36A	119.88(19)	O17-K7-F27	151.81(13)
O12-K7-F27	54.85(11)	O6-K7-F27	118.68(13)
O15-K7-F27	126.70(14)	F39B-K7-F27	88.6(3)
F43-K7-F27	57.19(12)	F36A-K7-F27	93.1(3)
O17-K7-K9	44.86(9)	O12-K7-K9	108.06(9)
O6-K7-K9	45.93(8)	O15-K7-K9	45.96(8)
F39B-K7-K9	98.4(2)	F43-K7-K9	133.95(9)
F36A-K7-K9	90.6(2)	F27-K7-K9	162.34(9)
O17-K7-K6	108.66(10)	O12-K7-K6	44.78(8)
O6-K7-K6	47.38(9)	O15-K7-K6	44.56(8)
F39B-K7-K6	94.2(2)	F43-K7-K6	146.55(8)
F36A-K7-K6	81.6(2)	F27-K7-K6	99.46(8)
K9-K7-K6	64.02(3)	O7-K2-O2	145.55(13)
O7-K2-O5	77.20(12)	O2-K2-O5	70.83(12)
O7-K2-O14	75.25(13)	O2-K2-O14	82.16(13)
O5-K2-O14	70.42(11)	O7-K2-F1	157.23(13)
O2-K2-F1	55.12(11)	O5-K2-F1	115.69(12)
O14-K2-F1	125.87(12)	O7-K2-F35	68.3(2)
O2-K2-F35	121.5(2)	O5-K2-F35	125.21(14)
O14-K2-F35	60.61(15)	F1-K2-F35	112.2(2)

O7-K2-F34	94.9(2)	O2-K2-F34	116.7(3)
O5-K2-F34	172.0(2)	O14-K2-F34	107.24(16)
F1-K2-F34	72.0(2)	F35-K2-F34	49.59(15)
O7-K2-F17	50.73(13)	O2-K2-F17	146.78(18)
O5-K2-F17	99.48(15)	O14-K2-F17	125.62(12)
F1-K2-F17	107.01(11)	F35-K2-F17	90.4(2)
F34-K2-F17	75.5(3)	O7-K2-K6	103.09(10)
O2-K2-K6	44.45(9)	O5-K2-K6	46.51(9)
O14-K2-K6	43.54(8)	F1-K2-K6	99.07(8)
F35-K2-K6	101.76(15)	F34-K2-K6	136.8(2)
F17-K2-K6	144.49(11)	O7-K2-K3	43.23(10)
O2-K2-K3	102.71(9)	O5-K2-K3	43.58(8)
O14-K2-K3	46.30(8)	F1-K2-K3	157.05(9)
F35-K2-K3	83.42(13)	F34-K2-K3	129.28(15)
F17-K2-K3	88.86(8)	K6-K2-K3	60.14(3)
C17-F26-K4	122.2(3)	C26-F41-K8	117.2(3)
C16-O11-K5	131.2(3)	C16-O11-K4	127.7(3)
K5-O11-K4	88.47(11)	C16-O11-K3	111.0(3)
K5-O11-K3	96.47(12)	K4-O11-K3	92.49(11)
C5-F6-K1	107.7(3)	C4-O3-K1	119.0(3)
C4-O3-K8	139.8(3)	K1-O3-K8	86.90(10)
C4-O3-K9	125.3(3)	K1-O3-K9	82.55(10)

K8-O3-K9	85.64(10)	C4-O3-K1	79.7(3)
K1-O3-K1	161.20(13)	K8-O3-K1	76.02(9)
K9-O3-K1	88.29(10)	C13-O10-K5	122.6(3)
C13-O10-K4	136.9(3)	K5-O10-K4	86.20(10)
C13-O10-K3	124.2(3)	K5-O10-K3	83.50(10)
K4-O10-K3	87.09(10)	C13-O10-K5	79.2(3)
K5-O10-K5	158.20(13)	K4-O10-K5	76.78(9)
K3-O10-K5	82.14(9)	C1-O1-K1	124.3(3)
C1-O1-K8	132.2(3)	K1-O1-K8	85.68(10)
C1-O1-K9	112.1(3)	K1-O1-K9	102.31(12)
K8-O1-K9	93.05(11)	C13-O9-K3	141.6(4)
C13-O9-K5	101.1(3)	K3-O9-K5	89.66(11)
C13-O9-K4	123.1(3)	K3-O9-K4	93.54(11)
K5-O9-K4	88.80(10)	C25-O18-K8	125.4(3)
C25-O18-K1	146.4(3)	K8-O18-K1	87.54(10)
C25-O18-K9	81.4(3)	K8-O18-K9	131.39(13)
K1-O18-K9	80.43(9)	C4-O4-K9	144.2(3)
C4-O4-K1	96.7(3)	K9-O4-K1	90.09(11)
C4-O4-K8	120.0(3)	K9-O4-K8	94.89(11)
K1-O4-K8	91.31(11)	C10-O8-K5	142.7(3)
C10-O8-K4	127.6(3)	K5-O8-K4	89.02(11)
C10-O8-K3	80.4(3)	K5-O8-K3	79.68(10)

K4-O8-K3	130.27(14)	C27-F43-K7	152.7(3)
C19-O14-K6	137.4(4)	C19-O14-K2	129.8(4)
K6-O14-K2	90.16(11)	C19-O14-K3	103.8(3)
K6-O14-K3	90.34(11)	K2-O14-K3	87.57(11)
C2-F2-K8	120.2(3)	C7-O5-K3	141.5(4)
C7-O5-K2	126.8(4)	K3-O5-K2	91.68(12)
C7-O5-K6	91.3(3)	K3-O5-K6	90.11(12)
K2-O5-K6	88.62(12)	C5-F7-K8	118.6(3)
C7-O6-K7	139.1(4)	C7-O6-K9	131.7(4)
K7-O6-K9	89.17(11)	C7-O6-K6	90.3(3)
K7-O6-K6	88.11(12)	K9-O6-K6	93.54(12)
C25-O17-K7	158.9(4)	C25-O17-K9	105.8(3)
K7-O17-K9	93.13(12)	C16-O12-K7	131.7(3)
C16-O12-K6	137.2(3)	K7-O12-K6	90.95(11)
C19-O13-K5	142.4(4)	C19-O13-K4	128.0(4)
K5-O13-K4	87.97(11)	C19-O13-K3	76.6(3)
K5-O13-K3	80.99(11)	K4-O13-K3	140.49(15)
C11-F16-K4	118.8(3)	C15-F23-K5	125.9(5)
C14-F21-K5	102.6(4)	C1-O2-K2	132.4(4)
C1-O2-K6	135.2(4)	K2-O2-K6	91.65(12)
C2-F1-K2	115.7(3)	C10-O7-K2	138.5(4)
C10-O7-K3	106.5(3)	K2-O7-K3	95.18(13)

C6-F8-K1	118.6(4)	C14-F22-K4	118.4(4)
C3-F3-K1	135.9(4)	C17-F27-K7	116.4(3)
C20-F32-K4	99.7(4)	O18-C25-O17	129.6(5)
O18-C25-C26	116.5(4)	O17-C25-C26	113.9(4)
O18-C25-K9	76.6(3)	O17-C25-K9	52.9(3)
C26-C25-K9	166.7(3)	O18-C25-K8	38.0(2)
O17-C25-K8	146.5(3)	C26-C25-K8	88.6(3)
K9-C25-K8	104.20(13)	O12-C16-O11	129.9(5)
O12-C16-C17	114.9(4)	O11-C16-C17	115.2(4)
O12-C16-K3	86.3(3)	O11-C16-K3	49.1(3)
C17-C16-K3	149.7(3)	C21-F33-K4	132.1(7)
O2-C1-O1	129.7(5)	O2-C1-C2	115.1(5)
O1-C1-C2	115.2(4)	O2-C1-K9	87.4(3)
O1-C1-K9	48.3(3)	C2-C1-K9	148.7(3)
O3-C4-O4	130.4(5)	O3-C4-C5	115.3(5)
O4-C4-C5	114.3(5)	O3-C4-K1	77.4(3)
O4-C4-K1	60.0(3)	C5-C4-K1	146.0(4)
O8-C10-O7	129.4(5)	O8-C10-C11	117.3(5)
O7-C10-C11	113.3(5)	O8-C10-K3	77.7(3)

O7-C10-K3	52.1(3)	C11-C10-K3	162.9(4)
O10-C13-O9	131.1(5)	O10-C13-C14	115.3(5)
O9-C13-C14	113.5(5)	O10-C13-K5	78.5(3)
O9-C13-K5	56.5(3)	C14-C13-K5	151.6(4)
F42-C26-F41	106.7(4)	F42-C26-C27	107.2(4)
F41-C26-C27	106.4(4)	F42-C26-C25	111.0(4)
F41-C26-C25	111.1(4)	C27-C26-C25	114.0(4)
O5-C7-O6	130.5(5)	O5-C7-C8	113.9(6)
O6-C7-C8	115.5(6)	O5-C7-K6	65.4(3)
O6-C7-K6	66.3(3)	C8-C7-K6	167.6(6)
O13-C19-O14	130.2(5)	O13-C19-C20	114.7(5)
O14-C19-C20	115.1(5)	O13-C19-K3	82.3(3)
O14-C19-K3	55.2(3)	C20-C19-K3	147.9(5)
F45-C27-F44	108.7(5)	F45-C27-F43	107.8(5)
F44-C27-F43	107.2(5)	F45-C27-C26	111.0(5)
F44-C27-C26	111.2(5)	F43-C27-C26	110.8(5)

F27-C17-F26	106.2(5)	F27-C17-C18	108.6(6)
F26-C17-C18	105.7(5)	F27-C17-C16	111.1(5)
F26-C17-C16	111.7(4)	C18-C17-C16	113.2(5)
F1-C2-F2	106.4(5)	F1-C2-C3	107.9(5)
F2-C2-C3	106.4(5)	F1-C2-C1	111.8(5)
F2-C2-C1	111.6(4)	C3-C2-C1	112.4(5)
C11-F17-K2	109.0(4)	F6-C5-F7	106.7(5)
F6-C5-C6	106.8(5)	F7-C5-C6	106.5(6)
F6-C5-C4	112.4(5)	F7-C5-C4	111.4(5)
C6-C5-C4	112.6(6)	F16-C11-F17	105.8(6)
F16-C11-C12	106.6(6)	F17-C11-C12	108.7(7)
F16-C11-C10	111.9(5)	F17-C11-C10	109.1(6)
C12-C11-C10	114.3(6)	C21-F34-K2	143.1(10)
F5-C3-F4	108.4(6)	F5-C3-F3	109.6(7)
F4-C3-F3	108.8(7)	F5-C3-C2	109.8(6)
F4-C3-C2	111.2(7)	F3-C3-C2	109.1(5)
F21-C14-F22	104.4(6)	F21-C14-C15	107.2(6)

F22-C14-C15	107.3(6)	F21-C14-C13	112.0(5)
F22-C14-C13	111.8(5)	C15-C14-C13	113.7(7)
F10-C6-F9	111.9(7)	F10-C6-F8	107.6(8)
F9-C6-F8	111.3(6)	F10-C6-C5	111.1(6)
F9-C6-C5	107.9(8)	F8-C6-C5	107.0(6)
C21-F35-K2	146.6(8)	F23-C15-F24	108.4(9)
F23-C15-F25	112.5(7)	F24-C15-F25	112.6(6)
F23-C15-C14	107.5(6)	F24-C15-C14	108.1(6)
F25-C15-C14	107.5(9)	C21-C20-F31	118.8(8)
C21-C20-F32	107.8(6)	F31-C20-F32	89.4(8)
C21-C20-C19	117.8(9)	F31-C20-C19	110.3(6)
F32-C20-C19	108.5(6)	F30-C18-F29	109.4(10)
F30-C18-F28	107.5(8)	F29-C18-F28	109.7(9)
F30-C18-C17	108.9(9)	F29-C18-C17	109.8(7)
F28-C18-C17	111.5(7)	F12-C8-C9	113.9(9)

F12-C8-C7	109.7(8)	C9-C8-C7	120.8(8)
F12-C8-F11	101.6(6)	C9-C8-F11	100.9(10)
C7-C8-F11	107.4(7)	F33-C21-F35	125.6(13)
F33-C21-F34	116.1(9)	F35-C21-F34	108.1(9)
F33-C21-C20	107.0(8)	F35-C21-C20	94.1(10)
F34-C21-C20	100.3(11)	C22-O15-K6	118.3(3)
C22-O15-K9	121.0(3)	K6-O15-K9	96.46(12)
C22-O15-K7	134.8(3)	K6-O15-K7	89.05(11)
K9-O15-K7	87.32(11)	O16-C22-O15	130.5(5)
O16-C22-C23	114.6(5)	O15-C22-C23	114.9(5)
O16-C22-K6	115.6(3)	O15-C22-K6	43.5(2)
C23-C22-K6	108.0(3)	C22-O16-K1	138.1(3)
C22-O16-K8	129.9(3)	K1-O16-K8	91.95(11)
F19-C12-F20	113.7(13)	F19-C12-F18	110.8(10)
F20-C12-F18	104.9(9)	F19-C12-C11	109.1(8)
F20-C12-C11	108.2(9)	F18-C12-C11	110.1(9)
F14-C9-F13	130.6(15)	F14-C9-F15	111.2(12)

F13-C9-F15	113.6(12)	F14-C9-C8	102.0(12)
F13-C9-C8	87.9(11)	F15-C9-C8	102.5(13)
C9-F15-K6	147.6(10)	C9-F13-K9	132.8(7)
C24A-C23-F37A	114.9(9)	C24B-C23-F36B	110.4(7)
C24B-C23-F37B	110.2(8)	F36B-C23-F37B	92.2(8)
C24A-C23-F36A	110.8(9)	F37A-C23-F36A	93.4(8)
C24A-C23-C22	126.8(9)	C24B-C23-C22	127.6(8)
F37A-C23-C22	104.4(6)	F36B-C23-C22	105.8(5)
F37B-C23-C22	104.8(6)	F36A-C23-C22	100.6(7)
C23-F36A-K7	125.6(6)	C23-F37A-K8	112.2(5)
C23-C24A-F39A	116.6(13)	C23-C24A-F40A	106.1(10)
F39A-C24A-F40A	109.3(11)	C23-C24A-F38A	106.2(10)
F39A-C24A-F38A	108.5(12)	F40A-C24A-F38A	110.1(13)
C24A-F38A-K6	135.7(8)	C23-F36B-K8	108.2(5)

F40B-C24B-F39B	110.9(12)	F40B-C24B-F38B	110.7(12)
F39B-C24B-F38B	108.9(10)	F40B-C24B-C23	105.2(10)
F39B-C24B-C23	106.2(11)	F38B-C24B-C23	114.9(11)
C24B-F39B-K7	143.4(8)		

Table D.12. Anisotropic atomic displacement parameters (\AA^2) for potassium pentafluoropropionate. The anisotropic atomic displacement factor exponent takes the form: $-2\pi^2[h^2a^{*2}U_{11} + \dots + 2hka^*b^*U_{12}]$

	U_{11}	U_{22}	U_{33}	U_{23}	U_{13}	U_{12}
K1	0.0139(5)	0.0132(5)	0.0166(5)	0.0010(4)	0.0034(4)	-0.0011(4)
K4	0.0147(5)	0.0143(5)	0.0193(6)	-0.0019(4)	0.0032(4)	0.0017(4)
K8	0.0134(5)	0.0124(5)	0.0205(6)	-0.0033(4)	0.0017(4)	0.0008(4)
K5	0.0157(5)	0.0126(5)	0.0195(6)	0.0021(4)	0.0054(4)	-0.0008(4)
K3	0.0141(5)	0.0234(6)	0.0204(6)	-0.0013(5)	0.0026(4)	-0.0044(4)
K6	0.0160(5)	0.0208(6)	0.0212(6)	0.0012(4)	0.0086(5)	0.0006(4)
K9	0.0137(5)	0.0236(6)	0.0201(6)	0.0034(5)	0.0010(4)	-0.0043(4)
K7	0.0138(5)	0.0265(6)	0.0208(6)	0.0060(5)	0.0036(4)	-0.0021(5)
K2	0.0156(6)	0.0394(7)	0.0226(6)	0.0044(5)	0.0065(5)	-0.0013(5)
F26	0.0237(18)	0.055(2)	0.0249(18)	0.0024(17)	0.0021(14)	0.0174(17)

	U ₁₁	U ₂₂	U ₃₃	U ₂₃	U ₁₃	U ₁₂
F41	0.053(2)	0.0232(18)	0.0222(17)	0.0050(14)	0.0087(16)	-0.0144(16)
F42	0.0207(17)	0.040(2)	0.0286(18)	-0.0018(15)	-0.0041(14)	0.0140(15)
O11	0.0166(18)	0.0192(18)	0.0210(19)	0.0024(15)	0.0104(15)	-0.0005(14)
F6	0.049(2)	0.0269(18)	0.0302(19)	-0.0052(15)	0.0114(17)	-0.0139(16)
O3	0.028(2)	0.0153(18)	0.0161(18)	0.0019(15)	0.0066(16)	0.0012(15)
O10	0.024(2)	0.0137(17)	0.0195(19)	0.0014(14)	0.0096(16)	-0.0010(15)
O1	0.0170(18)	0.0184(18)	0.0193(18)	-0.0008(15)	0.0092(15)	-0.0026(14)
O9	0.0170(18)	0.0128(18)	0.0202(18)	-0.0001(14)	0.0057(15)	-0.0008(14)
O18	0.0139(18)	0.0161(18)	0.0188(19)	-0.0024(14)	-0.0032(15)	-0.0008(14)
O4	0.0170(18)	0.0133(18)	0.0221(19)	-0.0008(14)	0.0050(15)	0.0004(14)
O8	0.0189(19)	0.023(2)	0.023(2)	-0.0059(16)	-0.0019(16)	-0.0003(16)
F43	0.051(2)	0.043(2)	0.0115(16)	0.0029(15)	0.0017(15)	0.0075(18)
O14	0.021(2)	0.0205(19)	0.026(2)	0.0032(16)	0.0109(16)	-0.0008(16)
F44	0.069(3)	0.0222(18)	0.0291(19)	-0.0068(15)	0.0084(19)	-0.0034(18)

	U ₁₁	U ₂₂	U ₃₃	U ₂₃	U ₁₃	U ₁₂
F2	0.030(2)	0.057(3)	0.030(2)	0.0139(18)	0.0000(16)	0.0196(18)
O5	0.0196(19)	0.027(2)	0.026(2)	-0.0038(17)	0.0111(17)	0.0003(16)
F7	0.080(3)	0.030(2)	0.0256(19)	0.0029(16)	0.001(2)	0.022(2)
F45	0.034(2)	0.085(3)	0.0256(19)	-0.006(2)	0.0099(16)	0.025(2)
O6	0.021(2)	0.026(2)	0.026(2)	-0.0007(16)	0.0116(17)	0.0017(16)
O17	0.027(2)	0.034(2)	0.026(2)	0.0042(18)	0.0122(18)	-0.0137(18)
O12	0.0125(19)	0.040(2)	0.025(2)	0.0064(18)	0.0033(16)	-0.0052(17)
O13	0.017(2)	0.038(2)	0.027(2)	0.0015(18)	0.0002(17)	-0.0072(17)
F16	0.093(4)	0.028(2)	0.030(2)	0.0071(17)	0.001(2)	-0.016(2)
F23	0.077(3)	0.024(2)	0.085(3)	0.009(2)	0.048(3)	0.002(2)
F21	0.079(3)	0.035(2)	0.040(2)	-0.0156(18)	0.012(2)	-0.022(2)
O2	0.014(2)	0.068(3)	0.026(2)	0.004(2)	0.0044(17)	-0.002(2)
F1	0.048(3)	0.089(3)	0.035(2)	0.031(2)	0.0160(19)	-0.017(2)
O7	0.031(2)	0.038(2)	0.030(2)	-0.0026(19)	0.0148(19)	-0.0186(19)
F8	0.049(3)	0.057(3)	0.075(3)	-0.021(3)	0.025(2)	0.009(2)
F22	0.095(4)	0.037(2)	0.025(2)	0.0035(17)	0.008(2)	0.002(2)
F3	0.106(4)	0.041(3)	0.042(3)	-0.004(2)	0.004(3)	-0.031(3)
F27	0.064(3)	0.127(5)	0.035(2)	0.041(3)	-0.004(2)	-0.054(3)

	U ₁₁	U ₂₂	U ₃₃	U ₂₃	U ₁₃	U ₁₂
F24	0.082(4)	0.030(2)	0.107(4)	0.004(2)	0.051(3)	-0.017(2)
F4	0.093(4)	0.100(4)	0.022(2)	-0.019(2)	0.004(2)	-0.006(3)
F28	0.076(3)	0.105(4)	0.024(2)	-0.028(2)	-0.012(2)	0.044(3)
F9	0.168(6)	0.047(3)	0.042(3)	-0.010(2)	0.069(3)	-0.009(3)
F32	0.098(4)	0.069(3)	0.055(3)	0.009(3)	0.035(3)	-0.019(3)
F10	0.118(5)	0.049(3)	0.129(5)	-0.028(3)	0.097(4)	-0.043(3)
C25	0.014(2)	0.015(2)	0.012(2)	-0.0010(19)	0.005(2)	0.0025(19)
F5	0.091(4)	0.105(5)	0.083(4)	-0.046(4)	0.007(3)	0.057(4)
C16	0.017(3)	0.014(2)	0.017(3)	0.000(2)	0.007(2)	0.000(2)
F33	0.087(4)	0.075(4)	0.053(3)	-0.005(3)	-0.026(3)	0.005(3)
C1	0.018(3)	0.014(2)	0.020(3)	0.001(2)	0.005(2)	-0.002(2)
C4	0.027(3)	0.018(3)	0.018(3)	0.001(2)	0.009(2)	0.004(2)
C10	0.019(3)	0.020(3)	0.016(3)	-0.002(2)	0.010(2)	0.000(2)
C13	0.026(3)	0.014(3)	0.024(3)	0.000(2)	0.013(2)	0.000(2)
C26	0.014(2)	0.018(3)	0.017(3)	0.000(2)	0.000(2)	-0.002(2)
C7	0.023(3)	0.024(3)	0.026(3)	0.000(2)	0.010(2)	0.001(2)
C19	0.014(3)	0.024(3)	0.026(3)	0.005(2)	0.004(2)	0.002(2)
C27	0.026(3)	0.028(3)	0.014(3)	0.002(2)	0.003(2)	0.004(2)
F12	0.079(4)	0.113(5)	0.076(4)	0.053(4)	-0.003(3)	-0.003(4)
F11	0.160(6)	0.060(4)	0.066(4)	-0.001(3)	0.019(4)	-0.046(4)

	U ₁₁	U ₂₂	U ₃₃	U ₂₃	U ₁₃	U ₁₂
C17	0.017(3)	0.029(3)	0.022(3)	0.006(2)	0.006(2)	0.000(2)
F25	0.279(10)	0.051(3)	0.095(4)	-0.020(3)	0.151(6)	-0.033(4)
C2	0.019(3)	0.032(3)	0.022(3)	0.009(2)	0.009(2)	0.004(2)
F17	0.045(3)	0.160(7)	0.091(4)	0.041(4)	-0.038(3)	0.009(4)
F18	0.245(9)	0.117(5)	0.013(2)	-0.002(3)	0.016(4)	-0.099(6)
C5	0.050(4)	0.016(3)	0.033(3)	0.003(2)	0.014(3)	0.004(3)
F29	0.363(15)	0.024(3)	0.051(4)	-0.011(3)	-0.039(6)	0.012(5)
C11	0.044(4)	0.031(3)	0.024(3)	0.003(3)	-0.007(3)	-0.013(3)
F34	0.216(9)	0.203(9)	0.099(5)	0.123(6)	-0.119(6)	-0.159(8)
C3	0.048(4)	0.067(5)	0.019(3)	-0.016(3)	0.001(3)	0.011(4)
C14	0.086(6)	0.015(3)	0.046(4)	0.006(3)	0.030(4)	-0.003(3)
F31	0.048(3)	0.207(9)	0.155(7)	0.123(7)	-0.025(4)	-0.041(4)
C6	0.105(7)	0.033(4)	0.062(5)	-0.012(4)	0.057(5)	-0.019(5)
F30	0.131(6)	0.369(15)	0.085(5)	-0.125(7)	-0.051(5)	0.187(9)
F35	0.316(12)	0.041(3)	0.090(5)	0.026(3)	-0.101(6)	-0.076(5)
C15	0.114(8)	0.033(4)	0.079(6)	0.001(4)	0.076(6)	-0.004(5)
C20	0.035(4)	0.093(7)	0.065(6)	0.051(5)	-0.023(4)	-0.045(4)
C18	0.072(6)	0.084(7)	0.027(4)	-0.017(4)	-0.011(4)	0.047(5)
F19	0.275(13)	0.227(12)	0.101(6)	0.019(6)	0.136(8)	0.133(10)
C8	0.114(9)	0.053(5)	0.088(7)	0.027(5)	0.070(7)	0.029(6)

	U ₁₁	U ₂₂	U ₃₃	U ₂₃	U ₁₃	U ₁₂
C21	0.137(11)	0.060(6)	0.035(5)	0.012(4)	-0.019(6)	-0.039(7)
O15	0.0191(19)	0.0187(19)	0.028(2)	-0.0024(16)	0.0086(16)	0.0003(15)
C22	0.015(3)	0.017(3)	0.019(3)	-0.002(2)	0.007(2)	-0.002(2)
O16	0.0139(19)	0.038(2)	0.023(2)	-0.0059(18)	0.0021(16)	0.0091(17)
F20	0.62(2)	0.087(5)	0.070(4)	-0.058(4)	0.163(9)	-0.191(9)
C12	0.235(16)	0.043(5)	0.022(4)	-0.014(4)	0.046(7)	-0.048(8)
C9	0.53(5)	0.027(6)	0.106(12)	-0.014(7)	0.03(2)	0.079(15)
F14	0.192(9)	0.070(5)	0.134(7)	-0.014(5)	-0.078(6)	-0.022(5)
F15	0.262(13)	0.027(3)	0.321(15)	0.040(6)	-0.097(11)	-0.019(5)
F13	0.067(5)	0.134(8)	0.397(19)	0.153(10)	-0.067(7)	-0.011(5)
C23	0.030(4)	0.076(6)	0.047(5)	-0.042(4)	-0.015(3)	0.029(4)
F36A	0.058(6)	0.065(8)	0.022(6)	0.000(5)	-0.008(5)	0.034(6)
F37A	0.035(4)	0.065(6)	0.024(4)	-0.021(4)	0.006(4)	0.017(4)
C24A	0.014(7)	0.032(8)	0.076(11)	-0.036(8)	0.002(7)	-0.003(6)
F38A	0.017(5)	0.036(6)	0.111(12)	-0.031(7)	0.033(5)	-0.013(4)
F40A	0.045(5)	0.021(4)	0.099(8)	-0.015(5)	0.015(5)	-0.001(4)
F39A	0.027(5)	0.070(7)	0.122(10)	-0.073(7)	-0.023(5)	0.005(4)
F36B	0.034(4)	0.017(4)	0.033(4)	-0.002(3)	0.002(3)	0.006(3)
F37B	0.013(6)	0.034(5)	0.054(6)	0.004(4)	0.012(4)	-0.006(4)
C24B	0.050(9)	0.030(7)	0.031(8)	-0.009(6)	-0.003(7)	-0.003(7)

	U₁₁	U₂₂	U₃₃	U₂₃	U₁₃	U₁₂
F38B	0.063(6)	0.042(5)	0.034(4)	-0.021(4)	-0.018(4)	0.000(4)
F39B	0.086(8)	0.020(5)	0.029(6)	0.003(4)	0.000(6)	0.013(5)
F40B	0.060(6)	0.089(8)	0.044(6)	-0.015(6)	0.028(5)	-0.016(6)

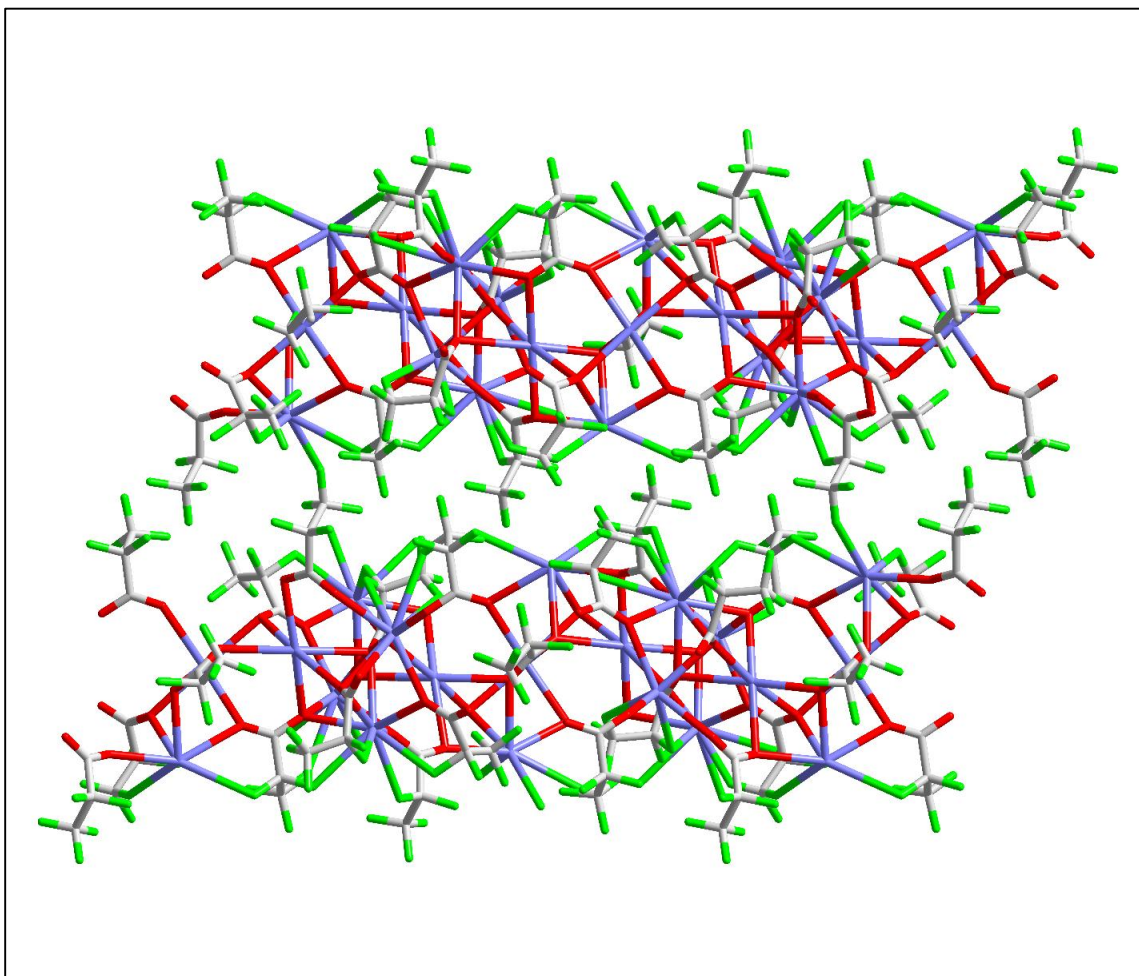


Figure D.39. Unit cell representation of potassium pentafluoropropionate.

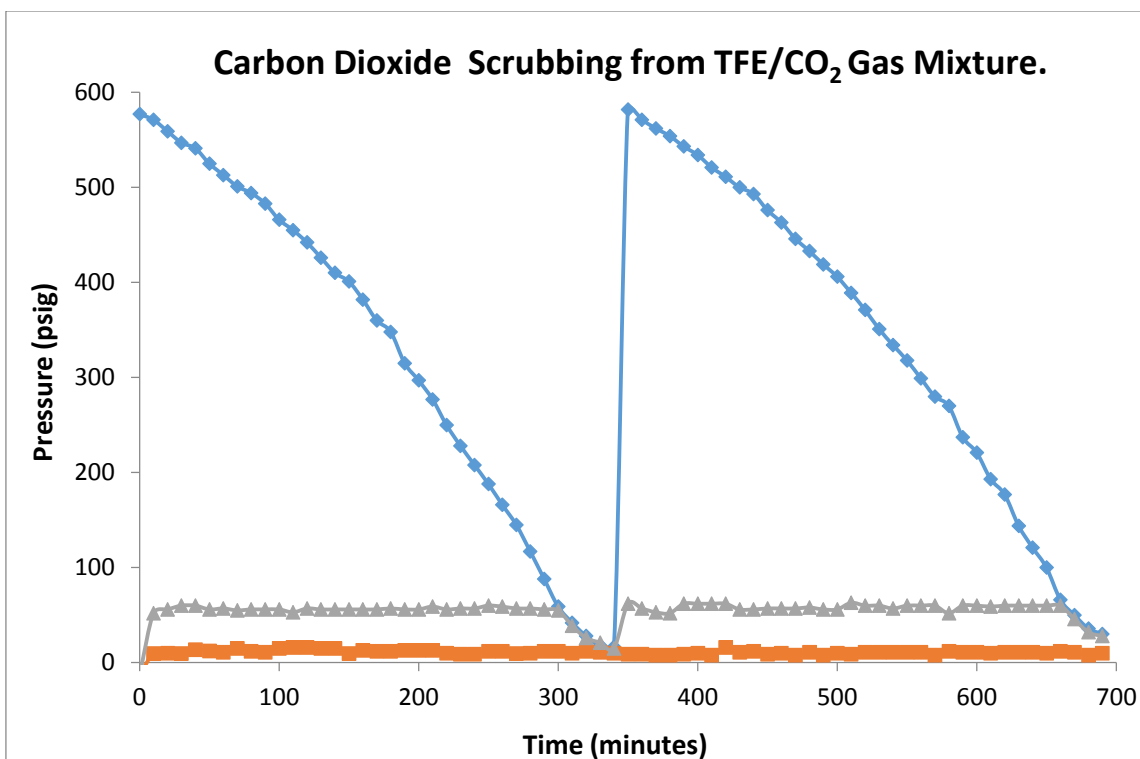


Figure D.40. Plot of pressure versus time from a procedure for scrubbing CO₂ from TFE.

The blue line represents the pressure of a manifold to which two TFE/CO₂ source cylinders are connected, but where only one is used as a feed cylinder at a time. The gray

line represents the pressure downstream of a regulator (kept constant at 50 psig) connected to the manifold with the TFE source cylinders, and the orange line represents the pressure of the TFE collection cylinder after the CO₂ has been scrubbed and the TFE has passed through a D-limonene bubbler.

Appendix E

Supplementary Information for Chapter 4.

The following appendix contains details of analysis performed on samples of poly(VDF-*co*-TFE). Analysis include DSC, TGA, XRD, and NMR results in addition to composition tables, graphs and other important information.

E.1. Differential scanning calorimetry (DSC) Information.

The sample results included below were analyzed on a TA Discovery differential scanning calorimeter. The sample (1-3 mg) was placed in an aluminum pan previously weighed and a reference pan of the same material was used. For the majority of the samples a cooling rate of 10 °C/min to -50 °C was applied, followed by a heating to 300 °C at the same rate. The cycle was completed two times. In some samples the heating was applied first followed by the cooling. The results are summarized in Table E.1 below.

Table E.1. Summary of differential scanning calorimetry (DSC) data on samples of PVDF, poly(VDF-*co*-TFE), and PTFE.

Composition (VDF-TFE mol%)	1 st Melting (°C)	2 nd Melting (°C)	1 st Cooling (°C)	2 nd Cooling (°C)
100-0	159.4	163.2	137.0	135.2
90-10 (A)	158.8	158.6	126.7	126.7
90-10-CO ₂ (E)	159.7	158.7	127.5	127.5
80-20 (B*)	126.1 / 154.2	127.1 / 155.9	119.9 / 109.3	119.9 / 109.3
80-20 (B)	117.5	118.8	99.2	99.2
80-20-CO ₂ (F)	118.5	119.0	98.9	98.9
80-20-High Conversion	117.7 / 126.6	129.7	111.8 / 102.7	111.8 / 102.7
70-30 (C)	109.8 / 133.2	131.6	133.1 / 120.5	133.1 / 120.5
70-30-CO ₂ (G)	145.6	146.5	103.4	103.4
60-40 (D)	165.6 / 176.8	165.6 / 176.8	154.5 / 137.9	154.5 / 137.9
60-40-CO ₂ (H)	171.8	174.8	150.8	150.8
0-100	326.0	324.1	313.5	313.5

Note: in the rest of the document the samples are labeled A through H where samples A, B, C, and D present composition of 90, 80, 70, and 30 mol% of VDF respectively. Samples labeled E, F, G, and H follow the same labeling format. Sample B* is of the same nominal composition as sample B, but this sample was made in larger blocks as explained in Chapter 4.

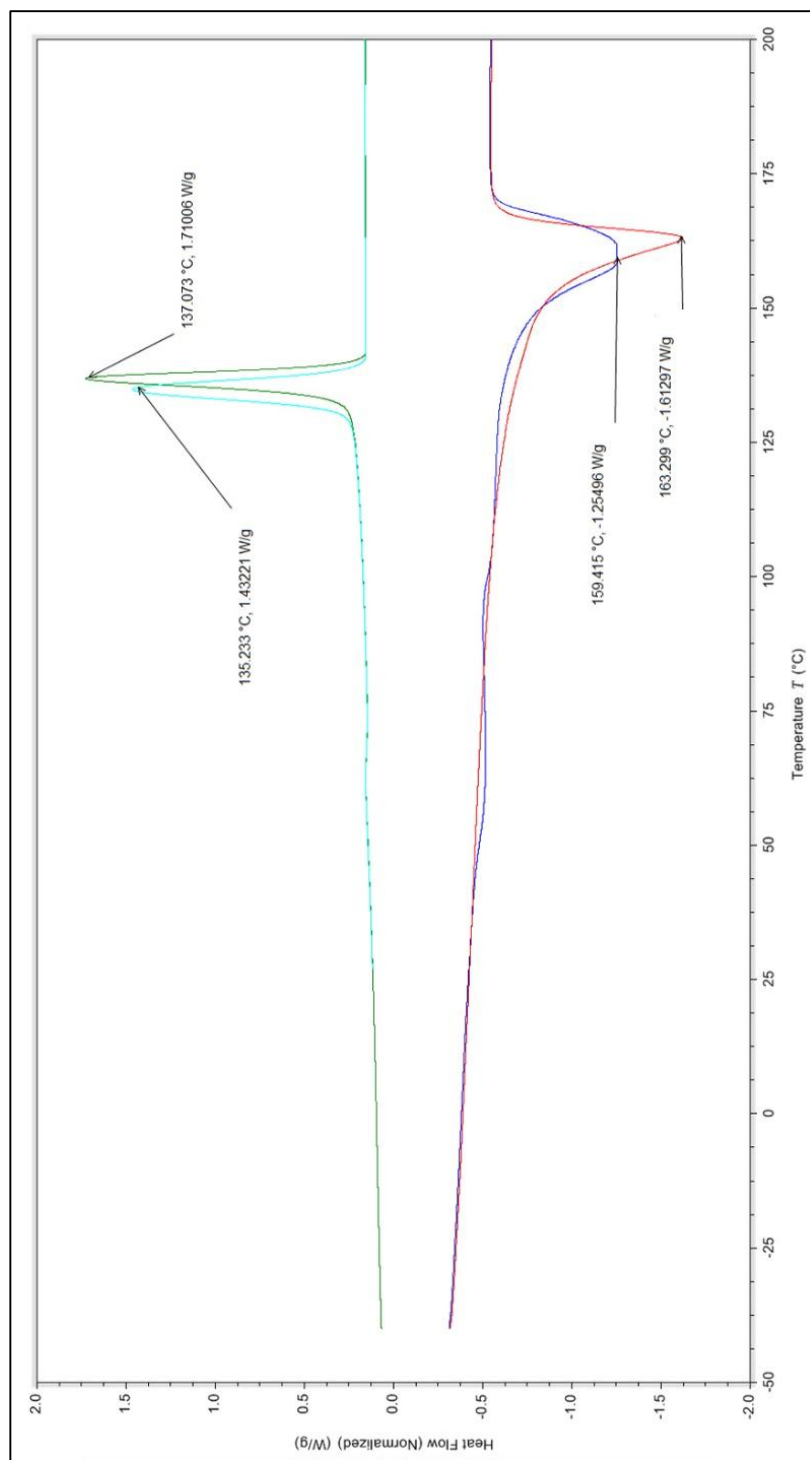


Figure E.1. Representative DSC thermogram for a sample of poly(VDF). Sample was prepared in absence of CO₂.

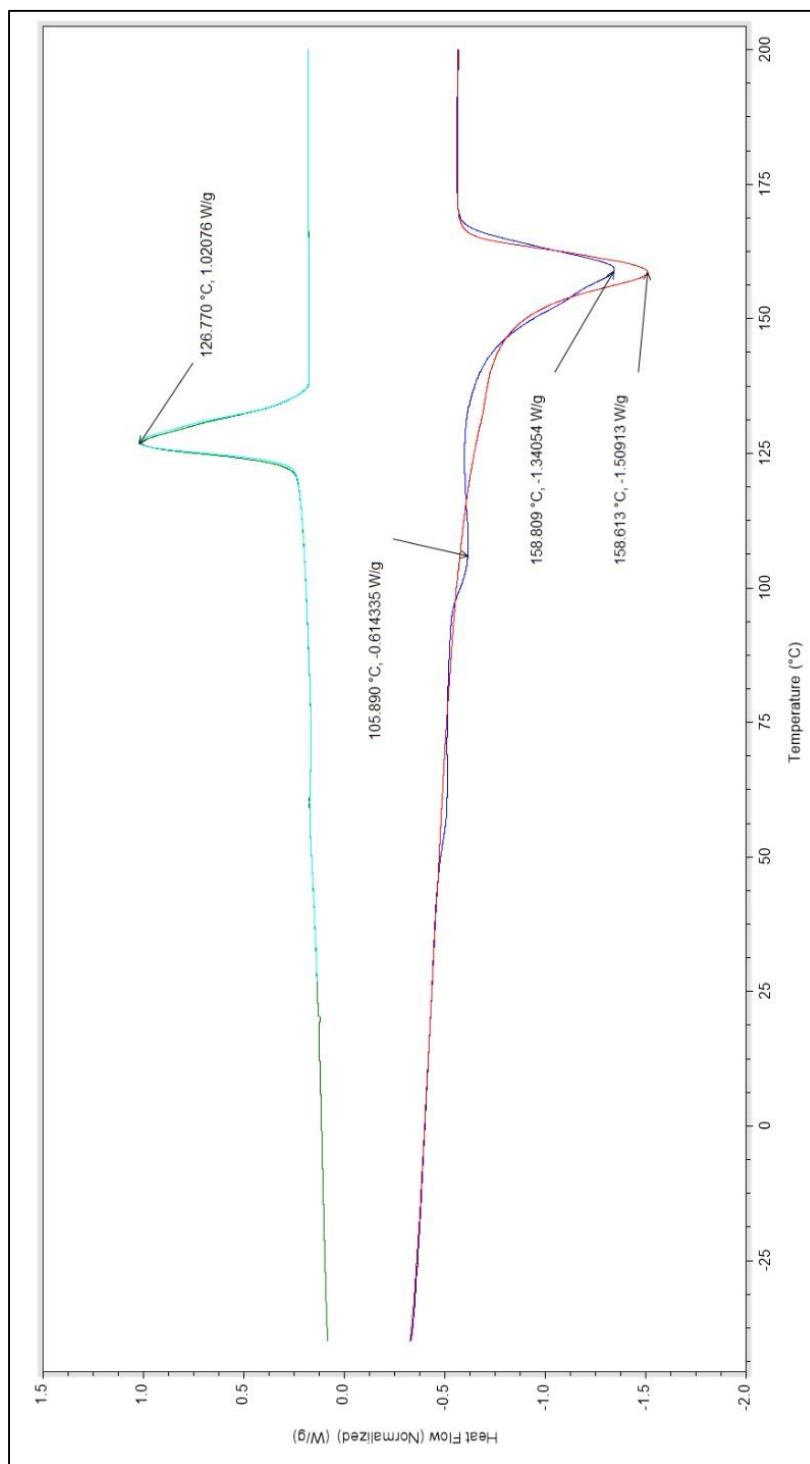


Figure E.2. Representative DSC thermogram for a sample A of poly(VDF-*co*-TFE) containing 90 mol% VDF and 10 mol% TFE. Sample was prepared in absence of CO₂.

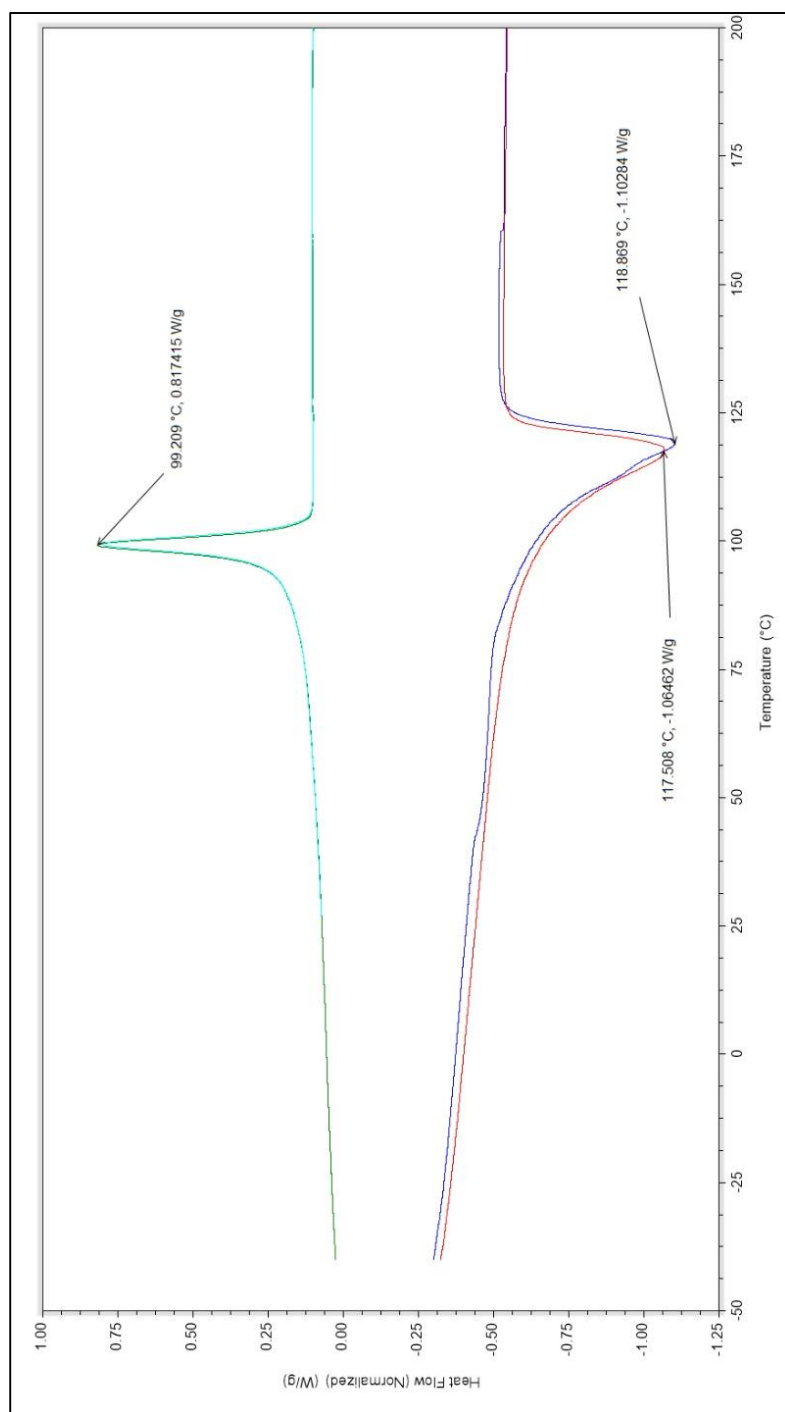


Figure E.3. Representative DSC thermogram for a sample B of poly(VDF-*co*-TFE) containing 80 mol% VDF and 20 mol% TFE. Sample was prepared using short block copolymerization techniques. Sample was prepared in absence of CO₂.

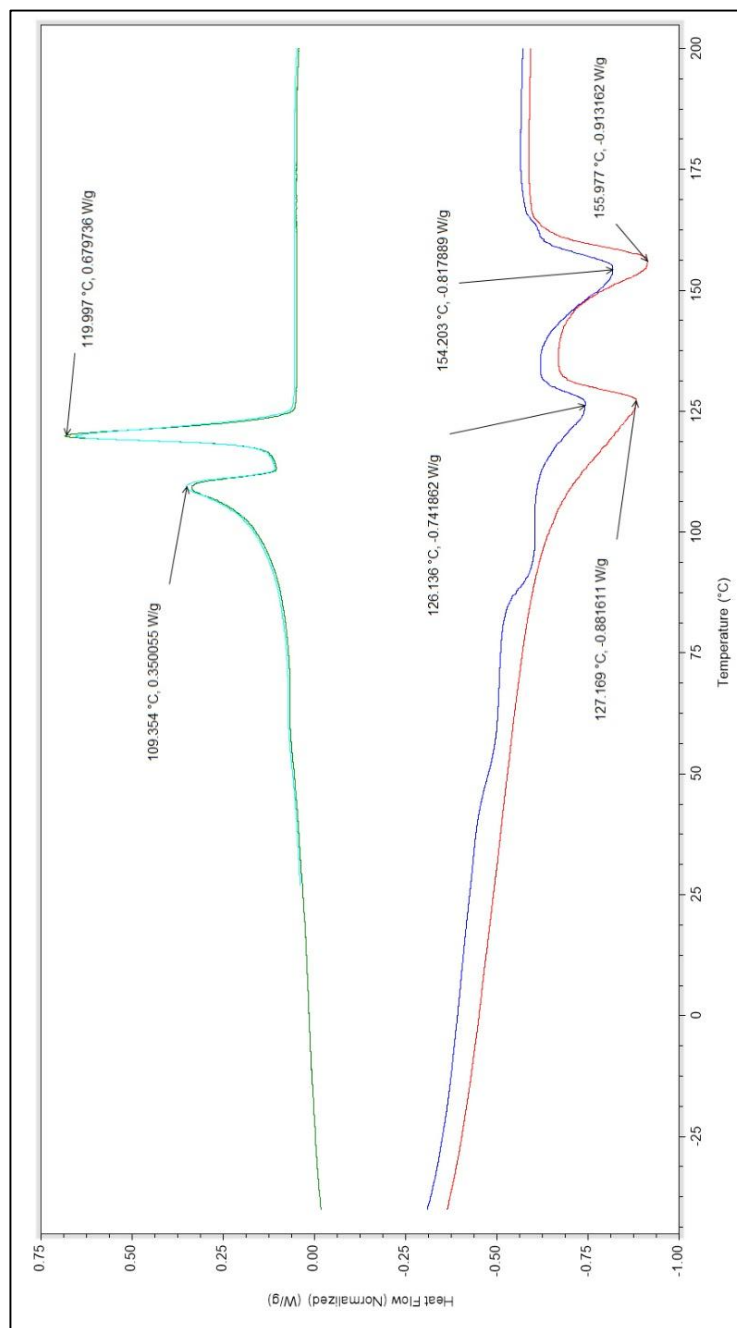


Figure E.4. Representative DSC thermogram for a sample B of poly(VDF-*co*-TFE) containing 80 mol% VDF and 20 mol% TFE. Sample was prepared using large block copolymerization techniques. Sample was prepared in absence of CO₂.

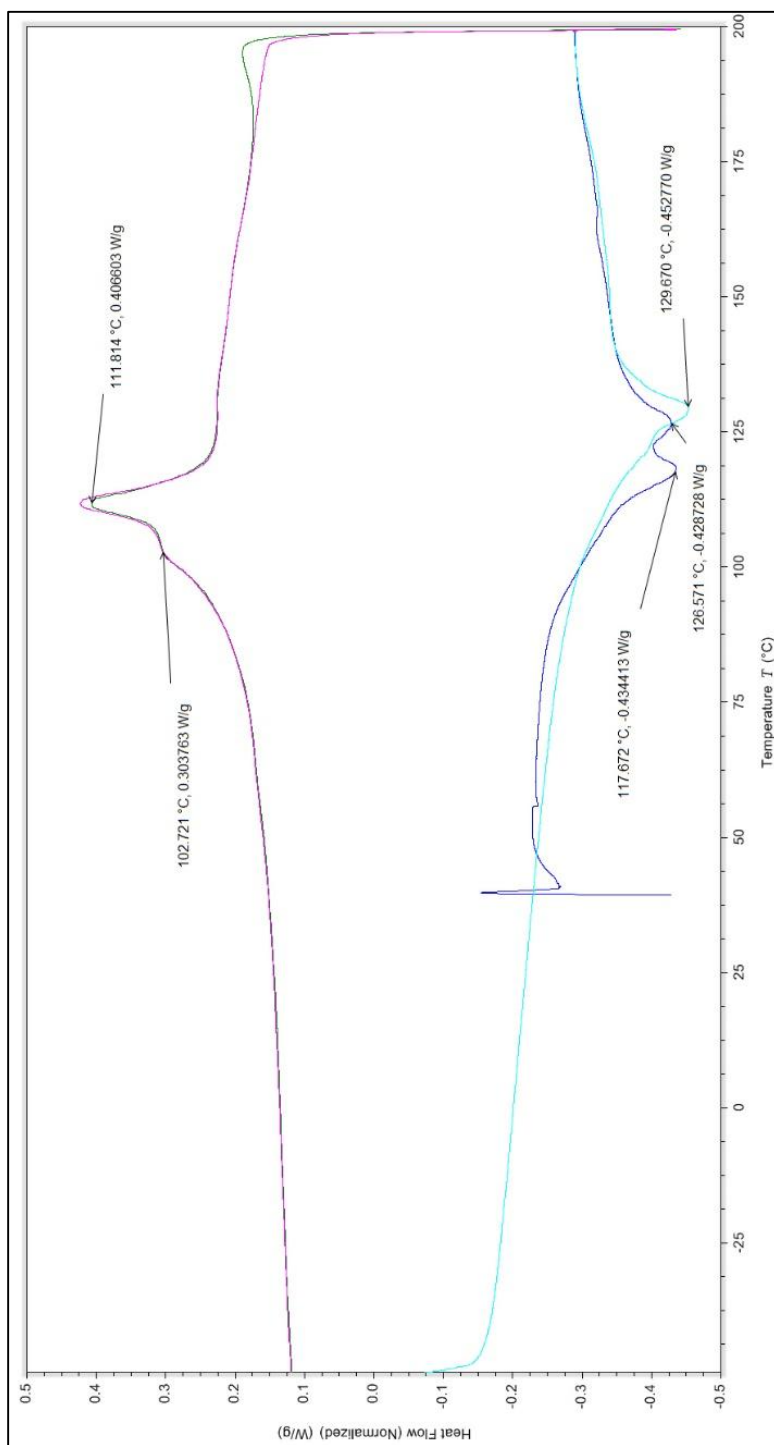


Figure E.5. Representative DSC thermogram for a sample of poly(VDF-*co*-TFE) containing 80 mol% VDF and 20 mol% TFE. Sample was dried from a high conversion polymerization.

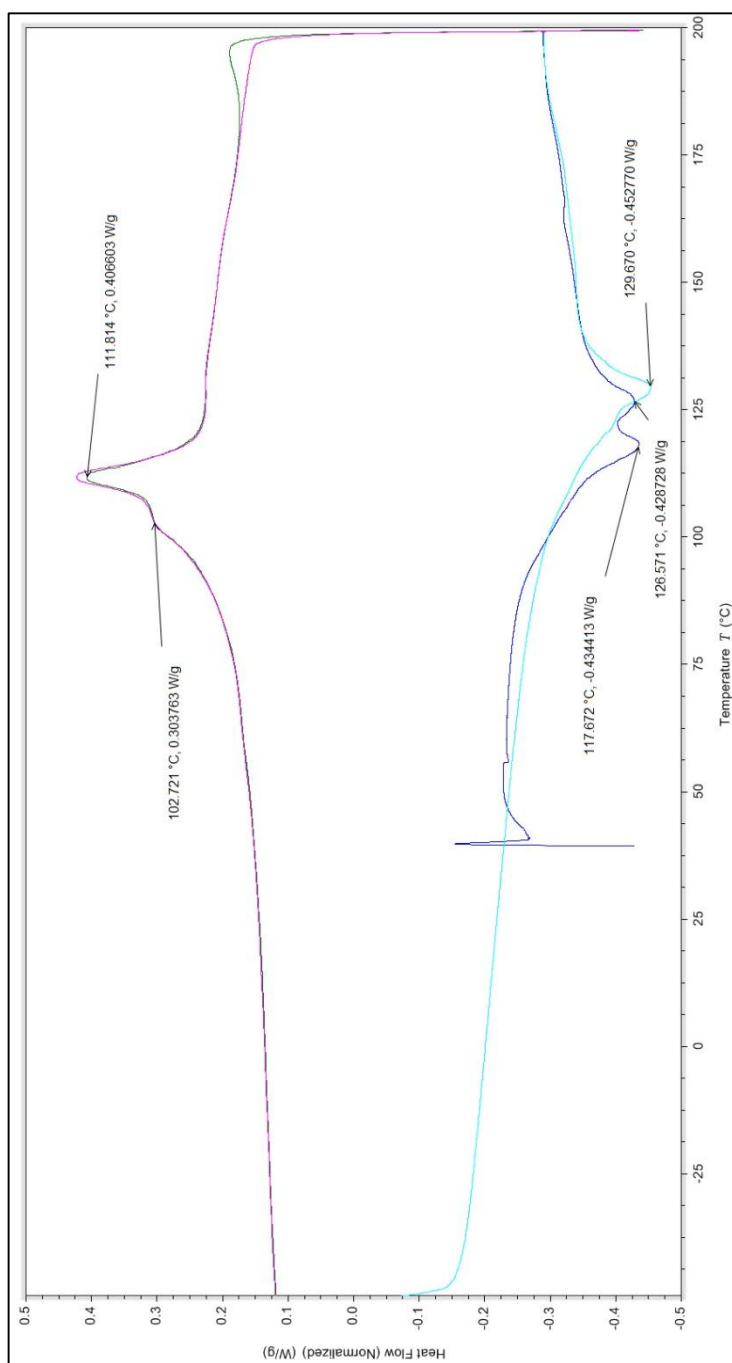


Figure E.6. Representative DSC thermogram for a sample C of poly(VDF-*co*-TFE) containing 70 mol% VDF and 30 mol% TFE. Sample was prepared in absence of CO_2 .

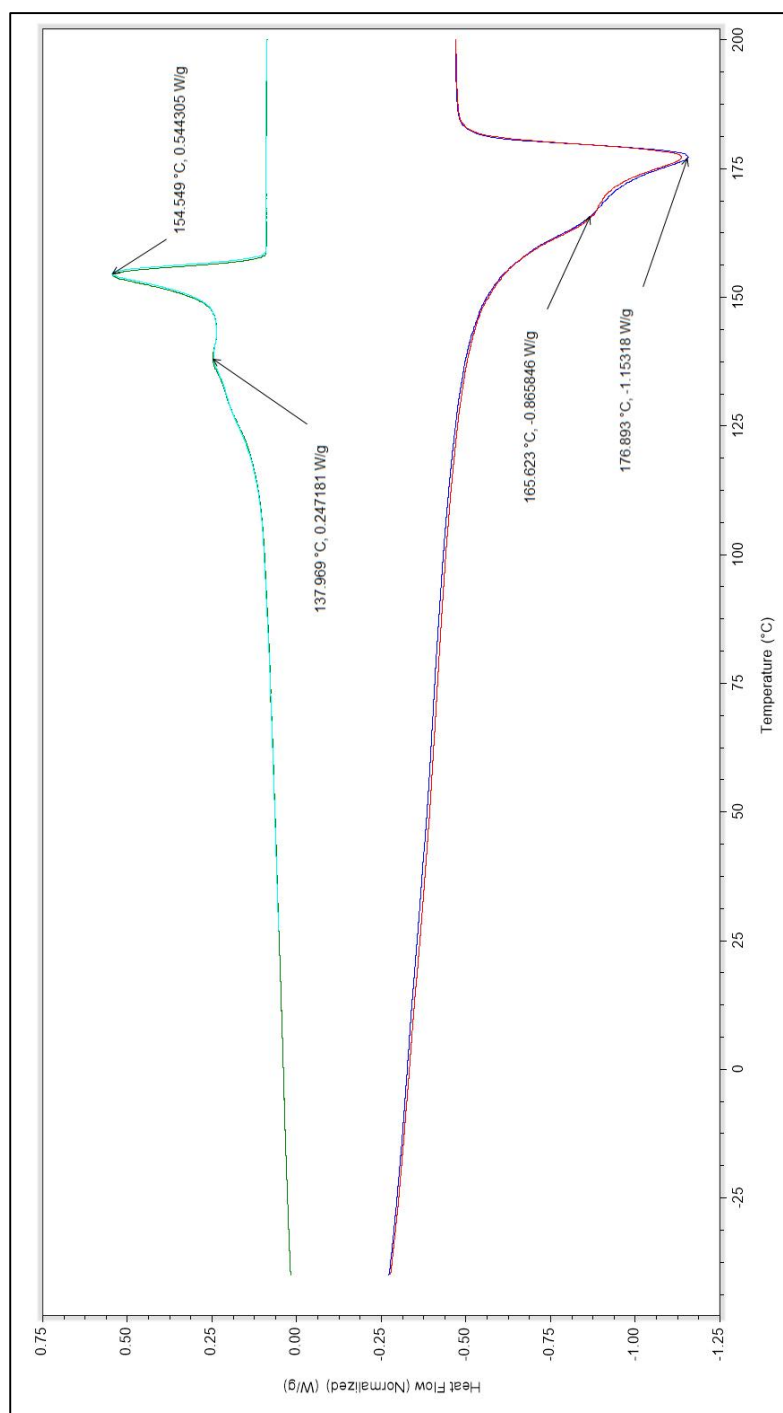


Figure E.7. Representative DSC thermogram for a sample D of poly(VDF-*co*-TFE) containing 60 mol% VDF and 40 mol% TFE. Sample was prepared in absence of CO₂.

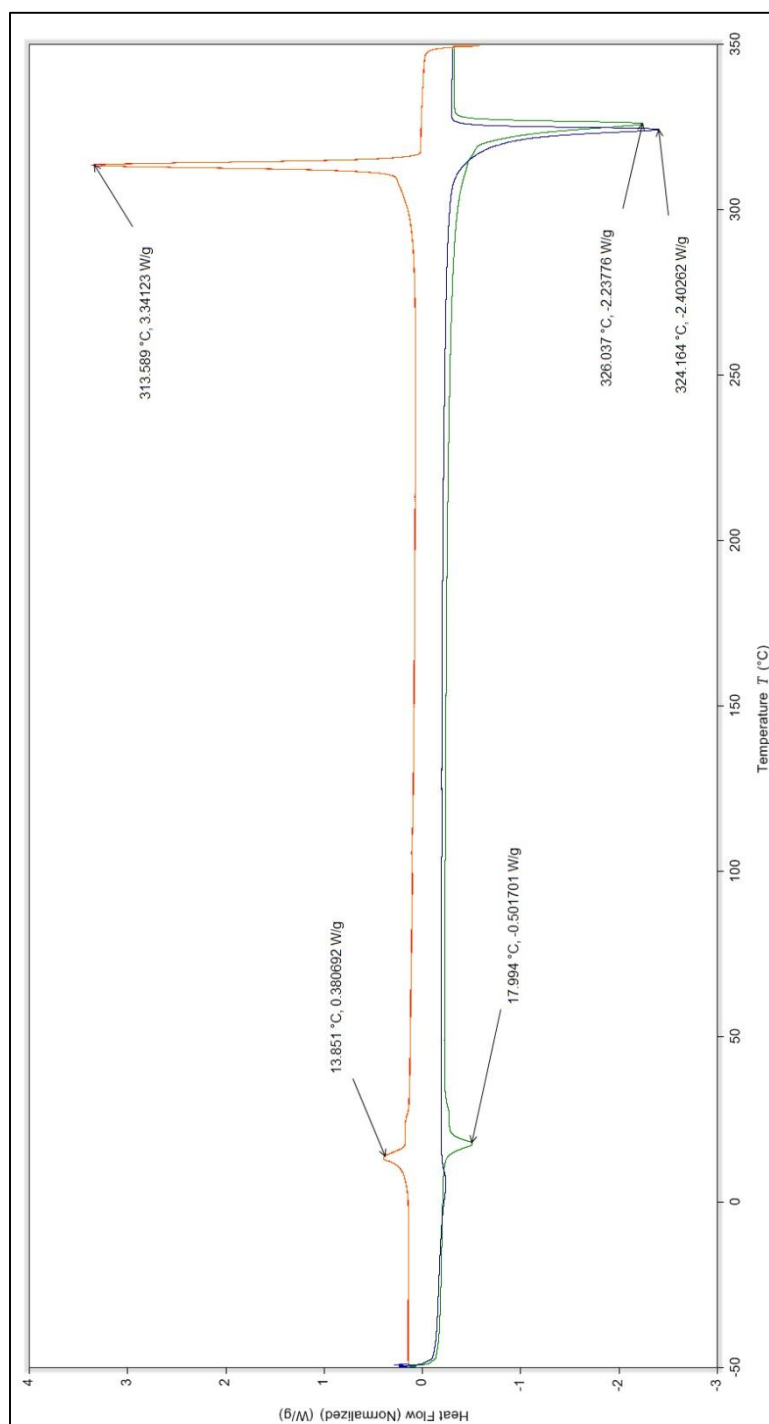


Figure E.8. Representative DSC thermogram for a sample of PTFE.

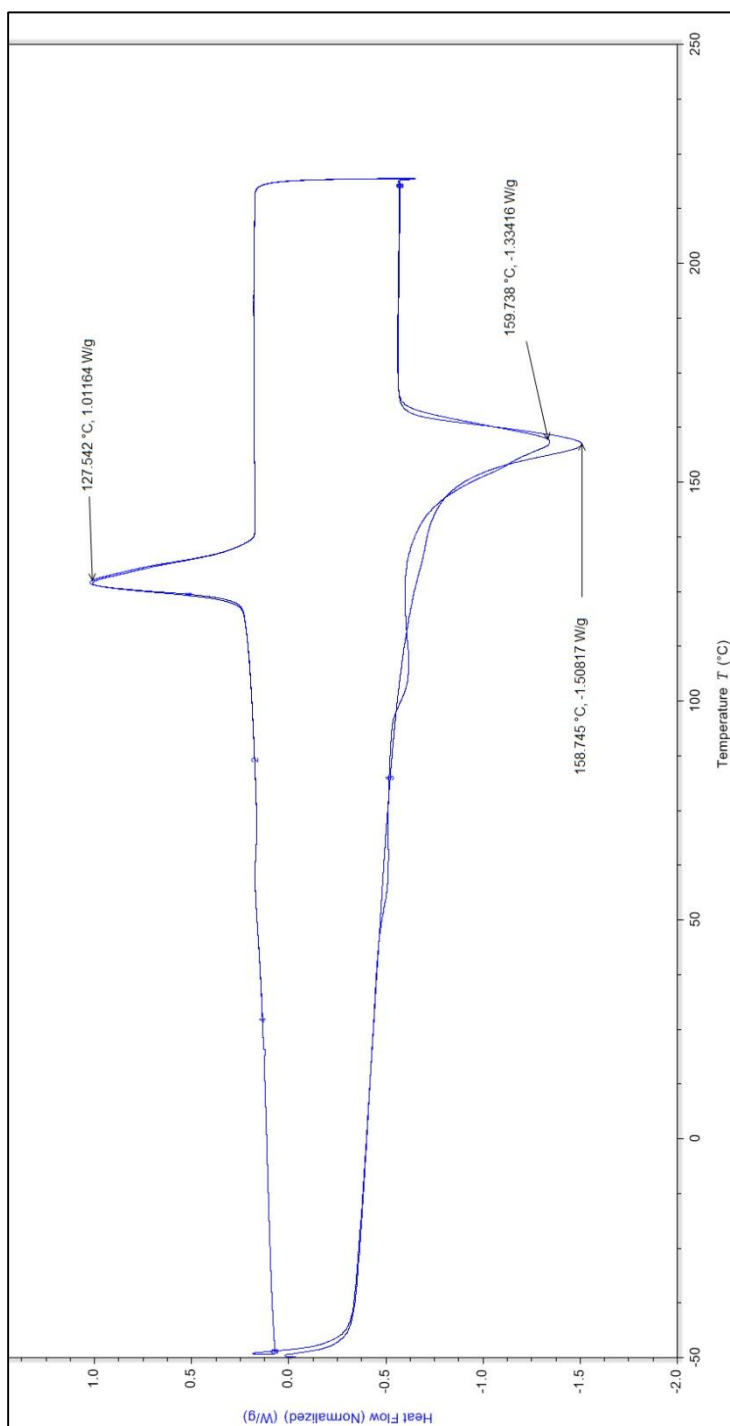


Figure E.9. Representative DSC thermogram for a sample E of poly(VDF-*co*-TFE) containing 90 mol% VDF and 10 mol% TFE. Sample was prepared in presence of CO₂.

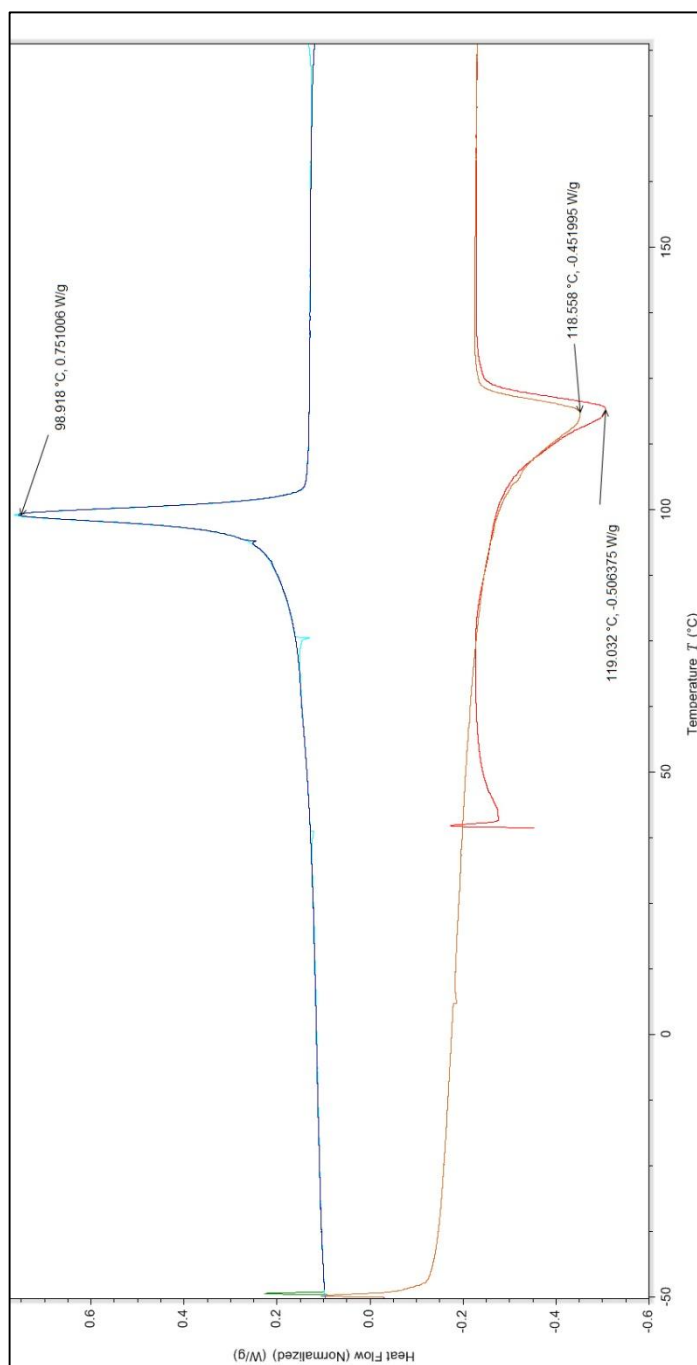


Figure E.10. Representative DSC thermogram for a sample F of poly(VDF-*co*-TFE) containing 80 mol% VDF and 20 mol% TFE. Sample was prepared in presence of CO₂.

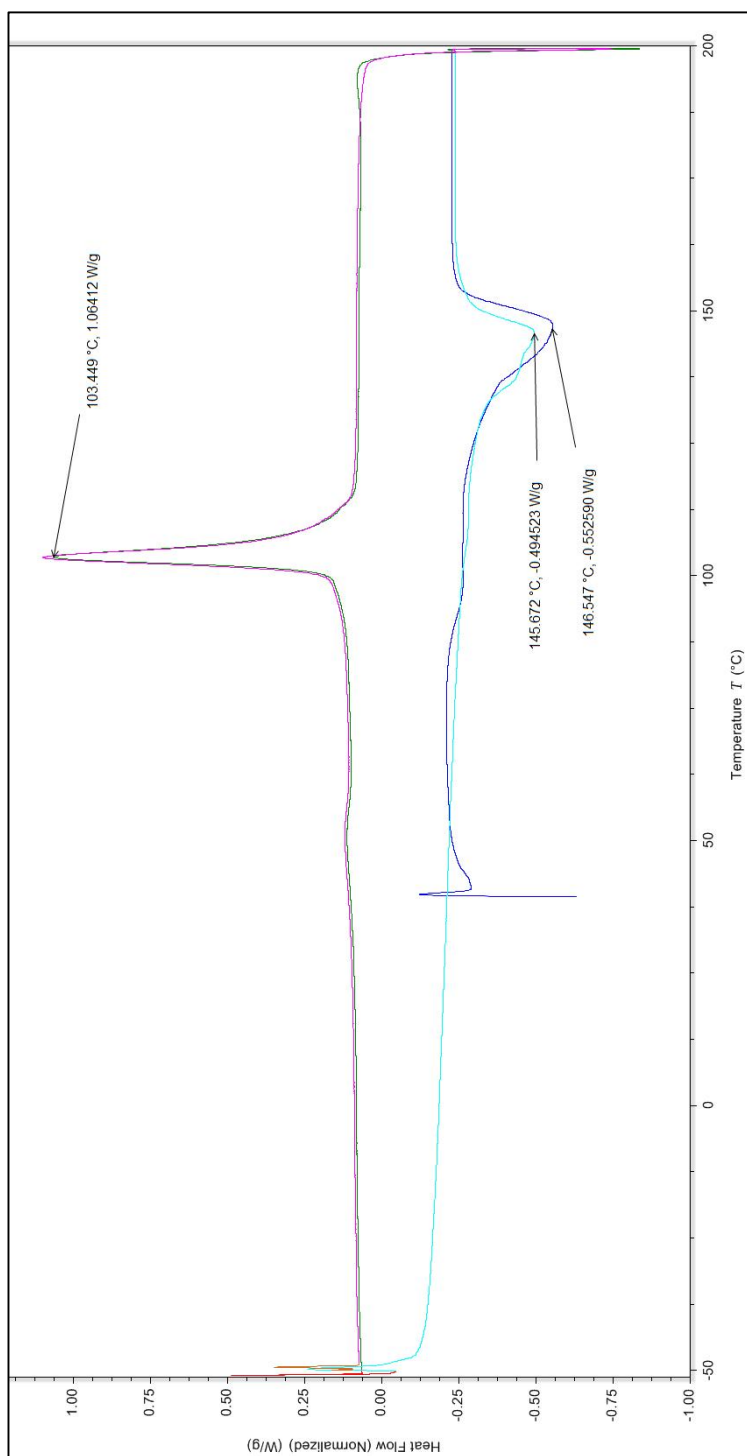


Figure E.11. Representative DSC thermogram for a sample G of poly(VDF-*co*-TFE) containing 70 mol% VDF and 30 mol% TFE. Sample was prepared in presence of CO₂.

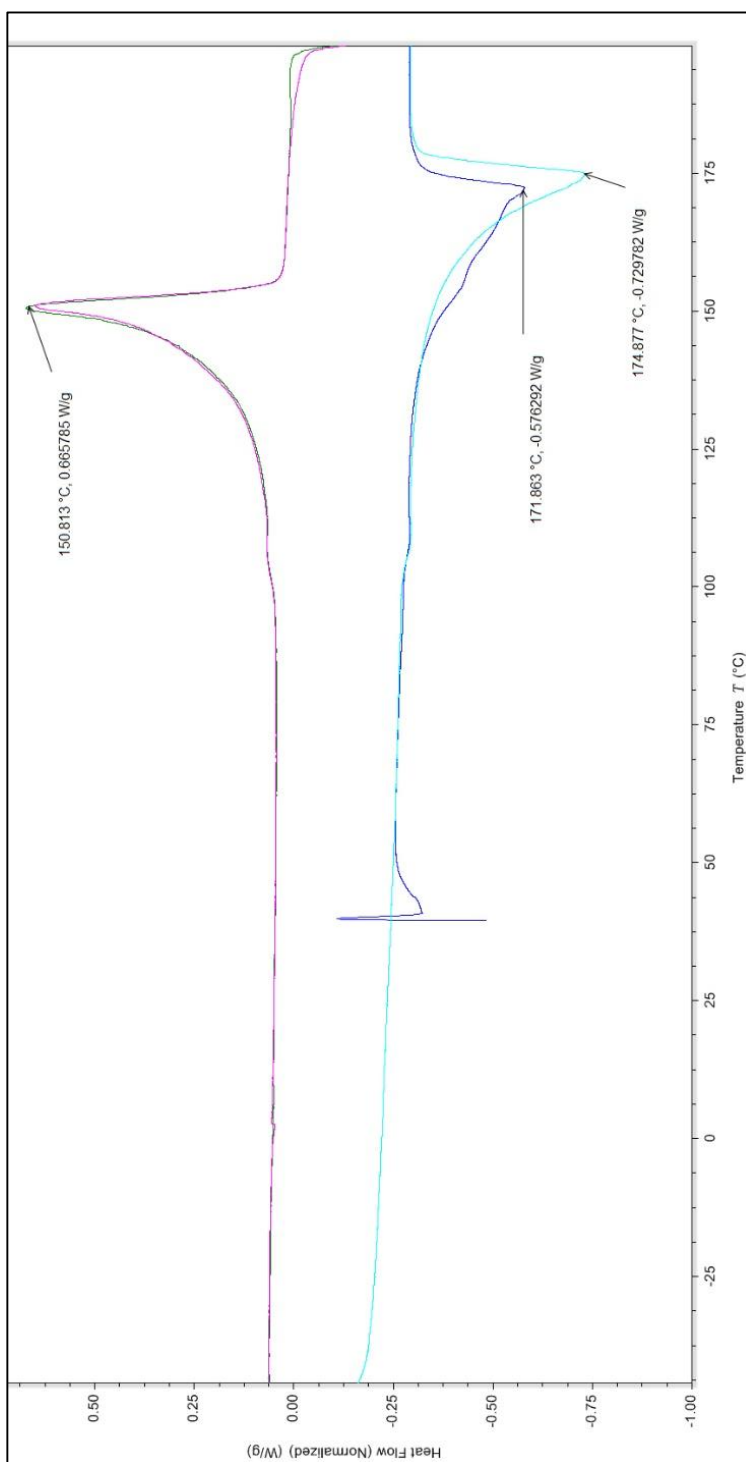


Figure E.12. Representative DSC thermogram for a sample H of poly(VDF-*co*-TFE) containing 60 mol% VDF and 40 mol% TFE. Sample was prepared in presence of CO₂.

E.2. Thermo Gravimetric Analysis (TGA) Information.

The samples were analyzed on a TA Q500 TGA equipment. The sample 2-8 mg was placed in a platinum pan previously weighed. The samples were let equilibrate at 100 °C for 10 minutes followed by a heating ramp of 10 °C/min to 400 °C under nitrogen atmosphere. The results are summarized in Table E.2 below.

Table E.2. TGA results for the samples of poly(VDF-*co*-TFE) studied.

Composition (VDF-TFE mol%)	VDF (mol%)	TFE (mol%)	Temperature at 10% Loss (°C)
100-0	100	0	430.3
90-10 (A)	88	12	391.2
90-10-CO ₂ (E)	92	8	390.4
80-20 (B)	78	22	393.6
80-20-CO ₂ (F)	81	19	392.1
70-30 (C)	75	25	405.8
70-30-CO ₂ (G)	67	33	405.2
60-40 (D)	65	35	413.3
60-40-CO ₂ (H)	64	36	408.5
0-100	0	100	538.2

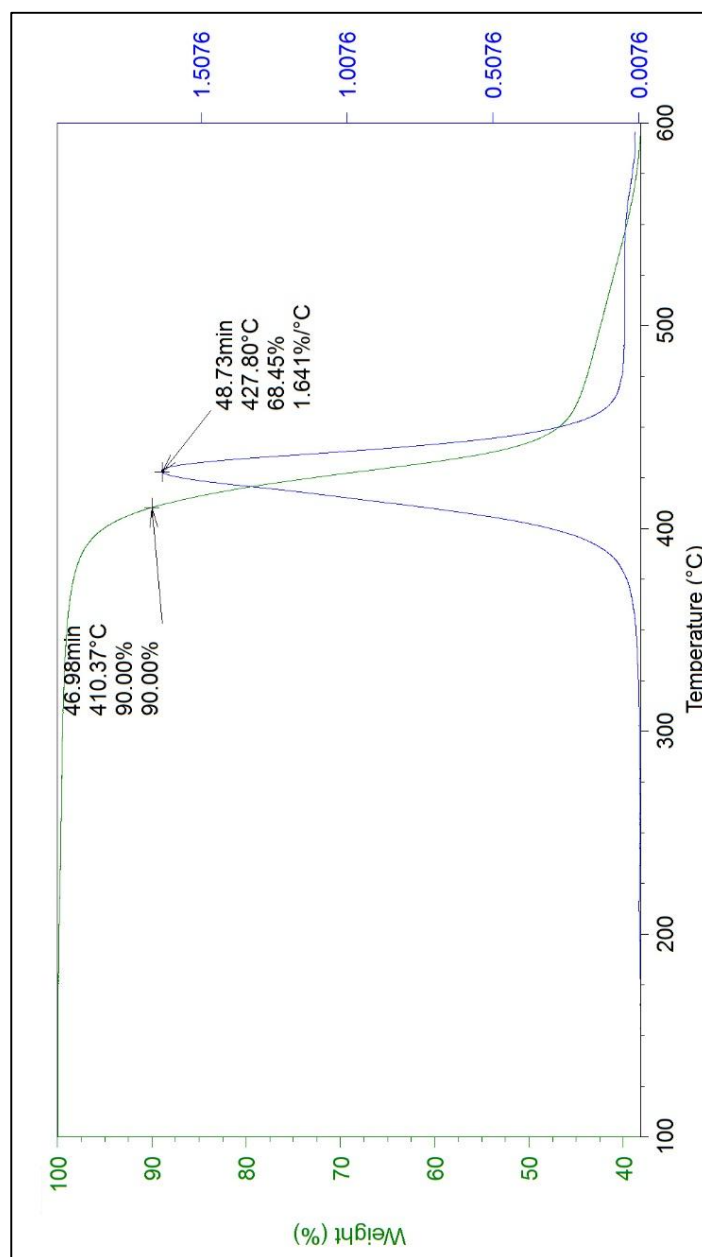


Figure E.13. Representative TGA thermogram for a sample of PVDF.

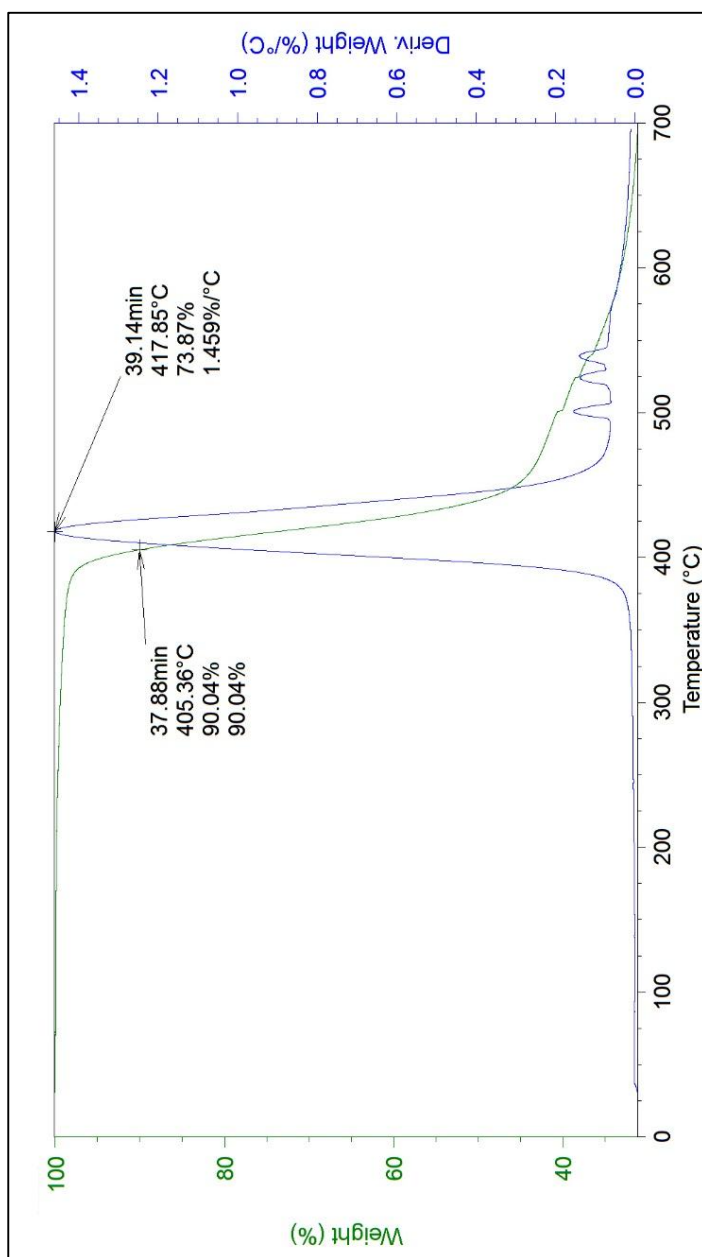


Figure E.14. Representative TGA thermogram for a sample A of poly(VDF-*co*-TFE) of 90 and 10 mol% of TFE and VDF respectively. Sample was prepared in absence of CO₂.

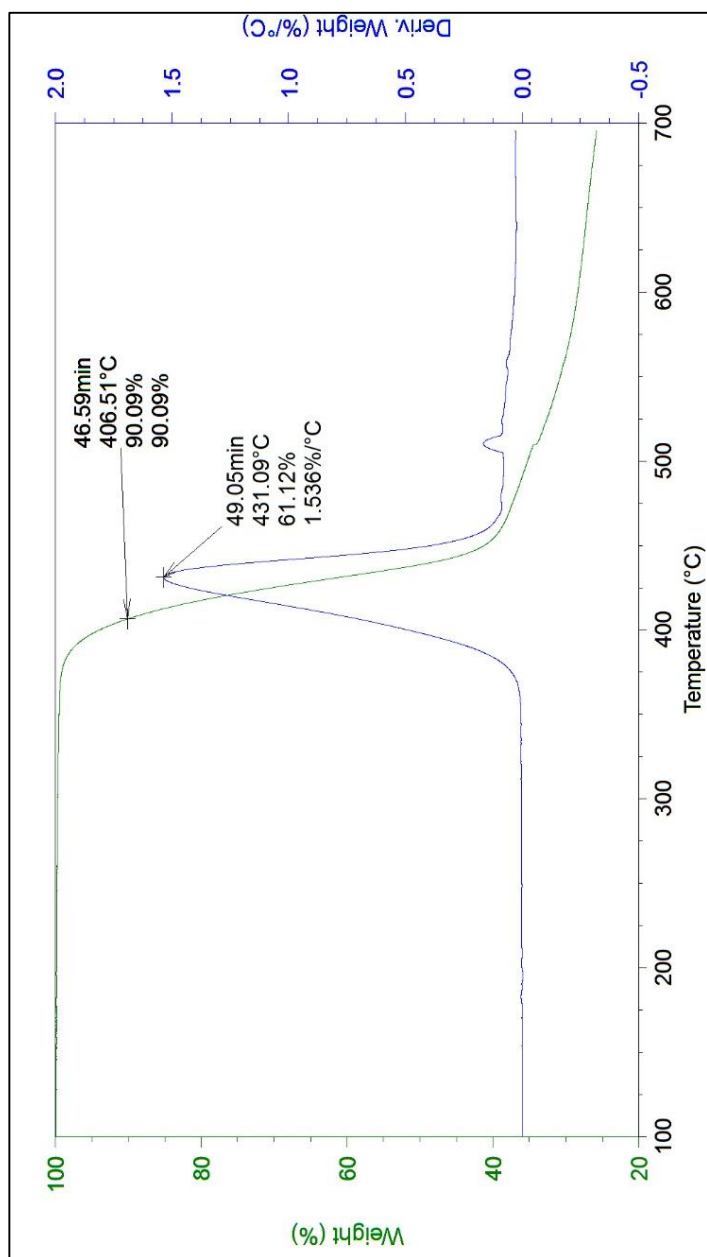


Figure E.15. Representative TGA thermogram for a sample of poly(VDF-*co*-TFE) of 80 and 20 mol% of TFE and VDF respectively. Sample was prepared in absence of CO₂ and short block techniques.

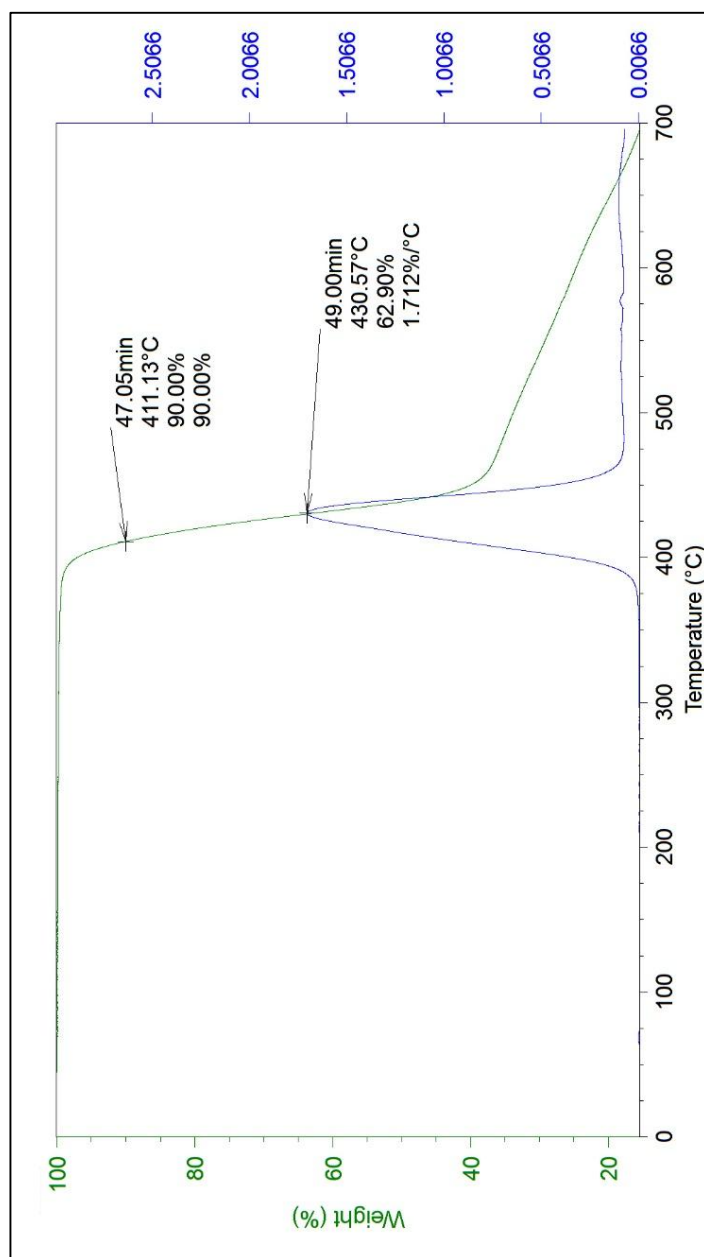


Figure E.16. Representative TGA thermogram for a sample of poly(VDF-*co*-TFE) of 80 and 20 mol% of TFE and VDF respectively. Sample was prepared in absence of CO₂ and large block techniques.

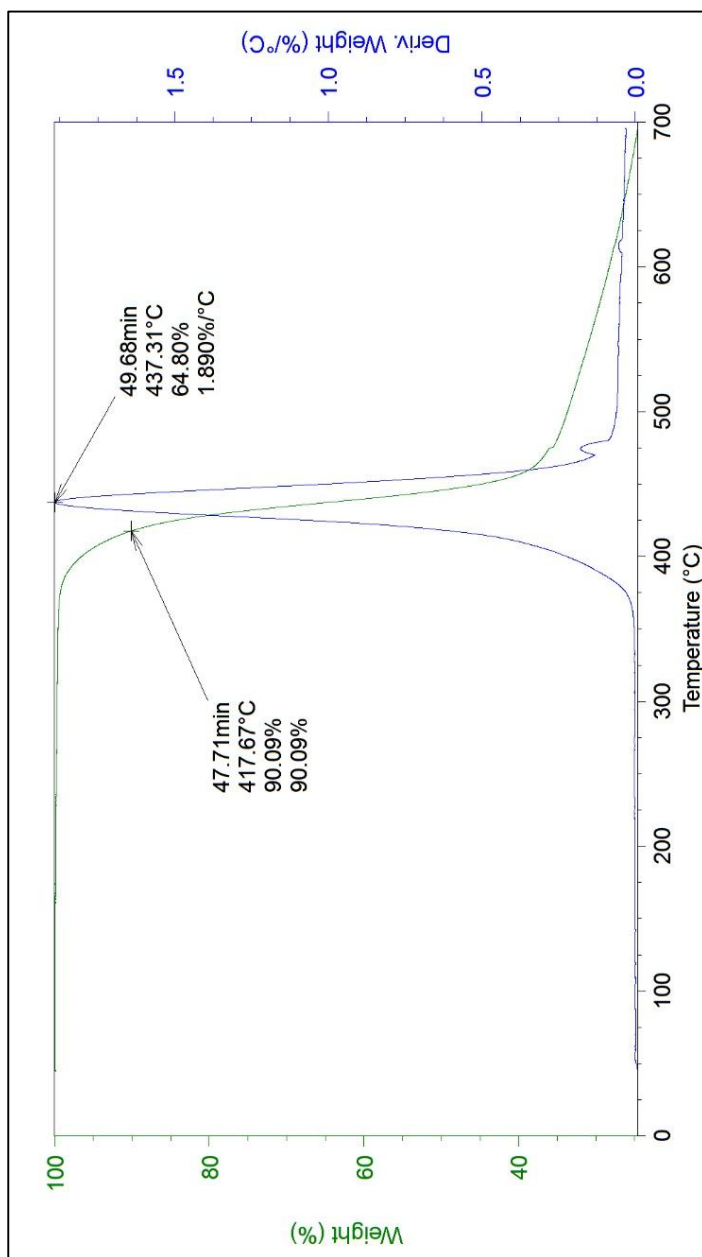


Figure E.17. Representative TGA thermogram for a sample of poly(VDF-*co*-TFE) of 70 and 30 mol% of TFE and VDF respectively. Sample was prepared in absence of CO₂.

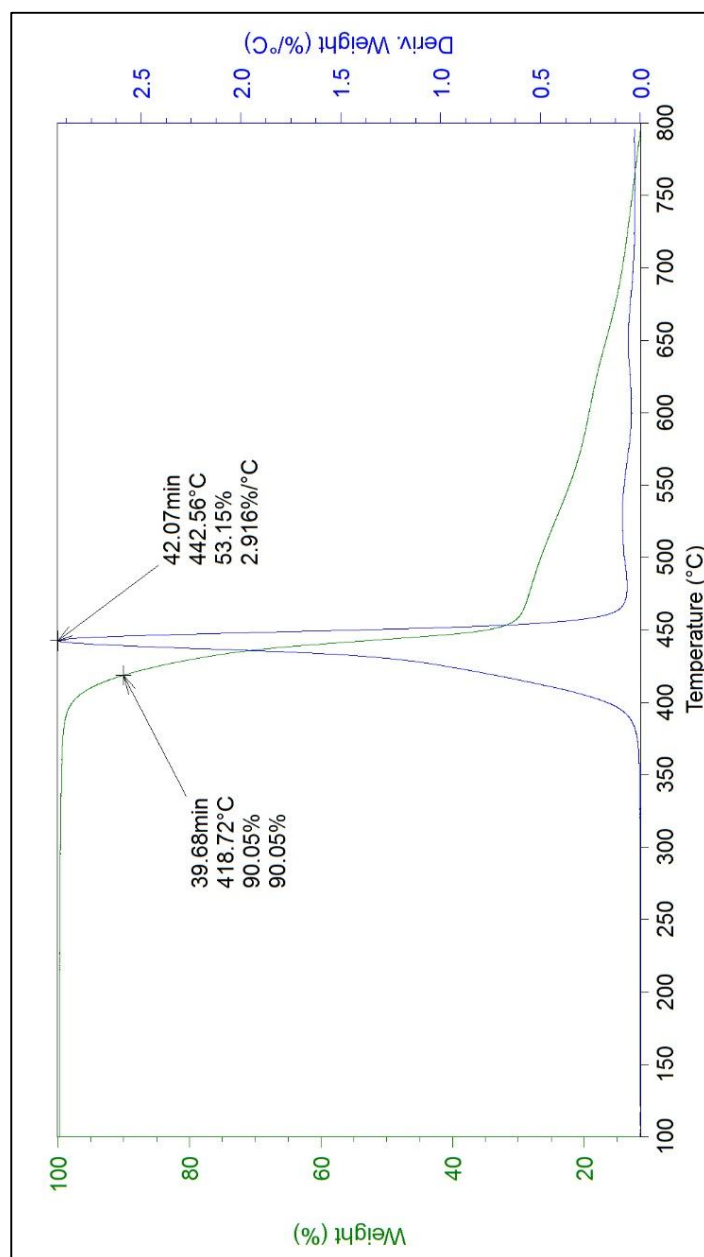


Figure E.18. Representative TGA thermogram for a sample of poly(VDF-*co*-TFE) of 60 and 40 mol% of TFE and VDF respectively. Sample was prepared in absence of CO₂.

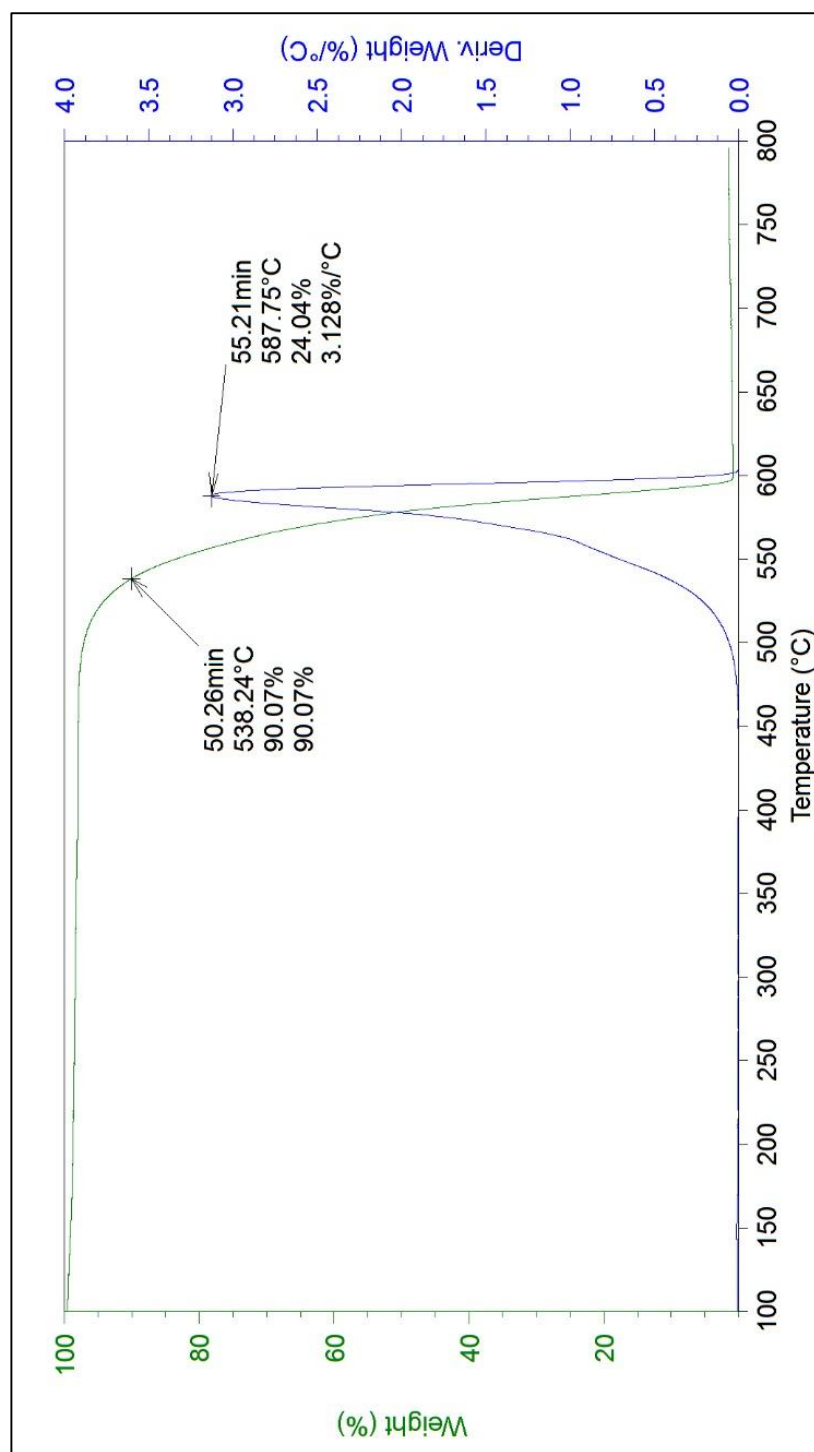


Figure E.19. Representative TGA thermogram for a sample of PTFE.

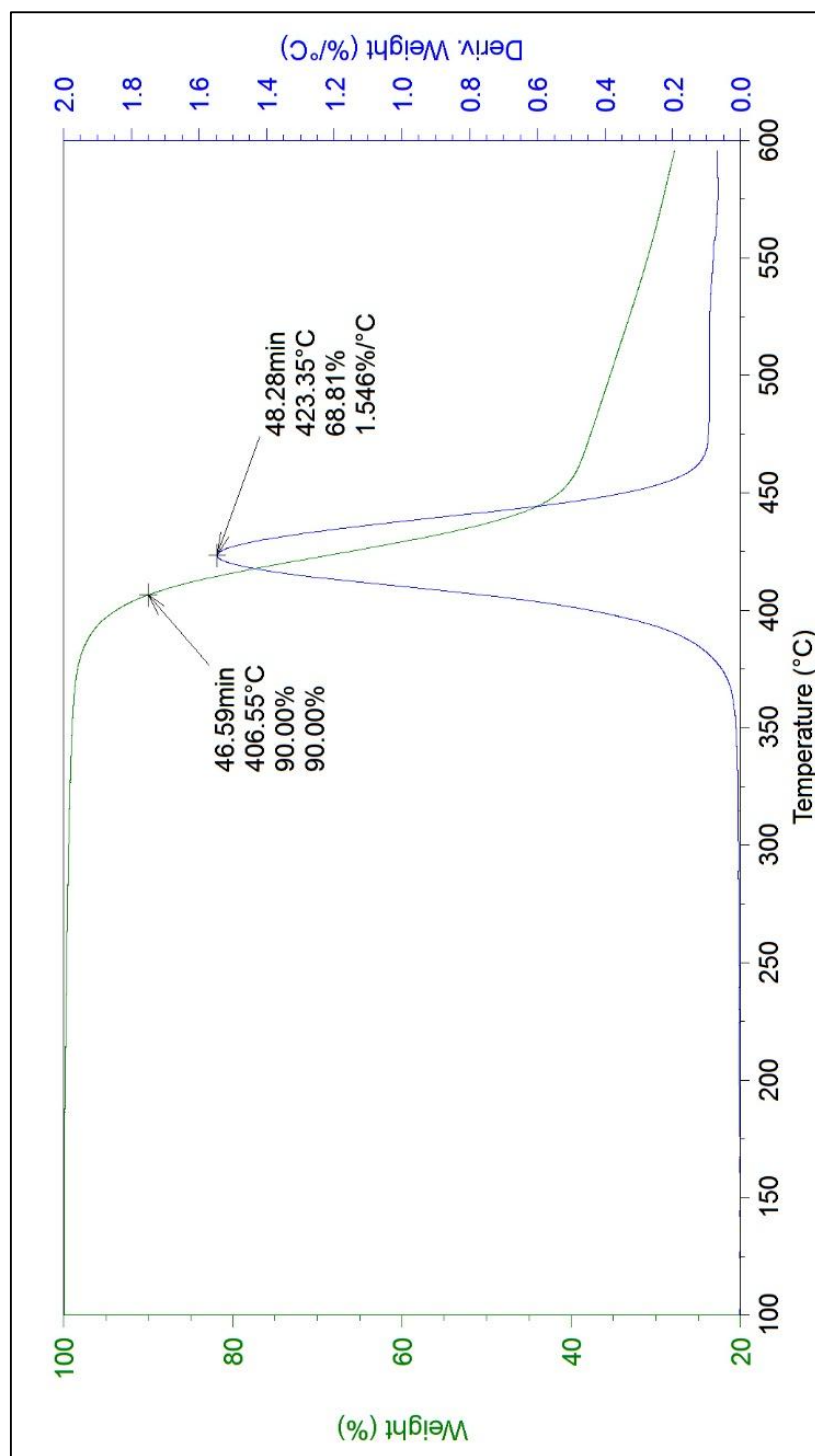


Figure E.20. Representative TGA thermogram for a sample of poly(VDF-*co*-TFE) of 90 and 10 mol% of TFE and VDF respectively. Sample was prepared in presence of CO₂.

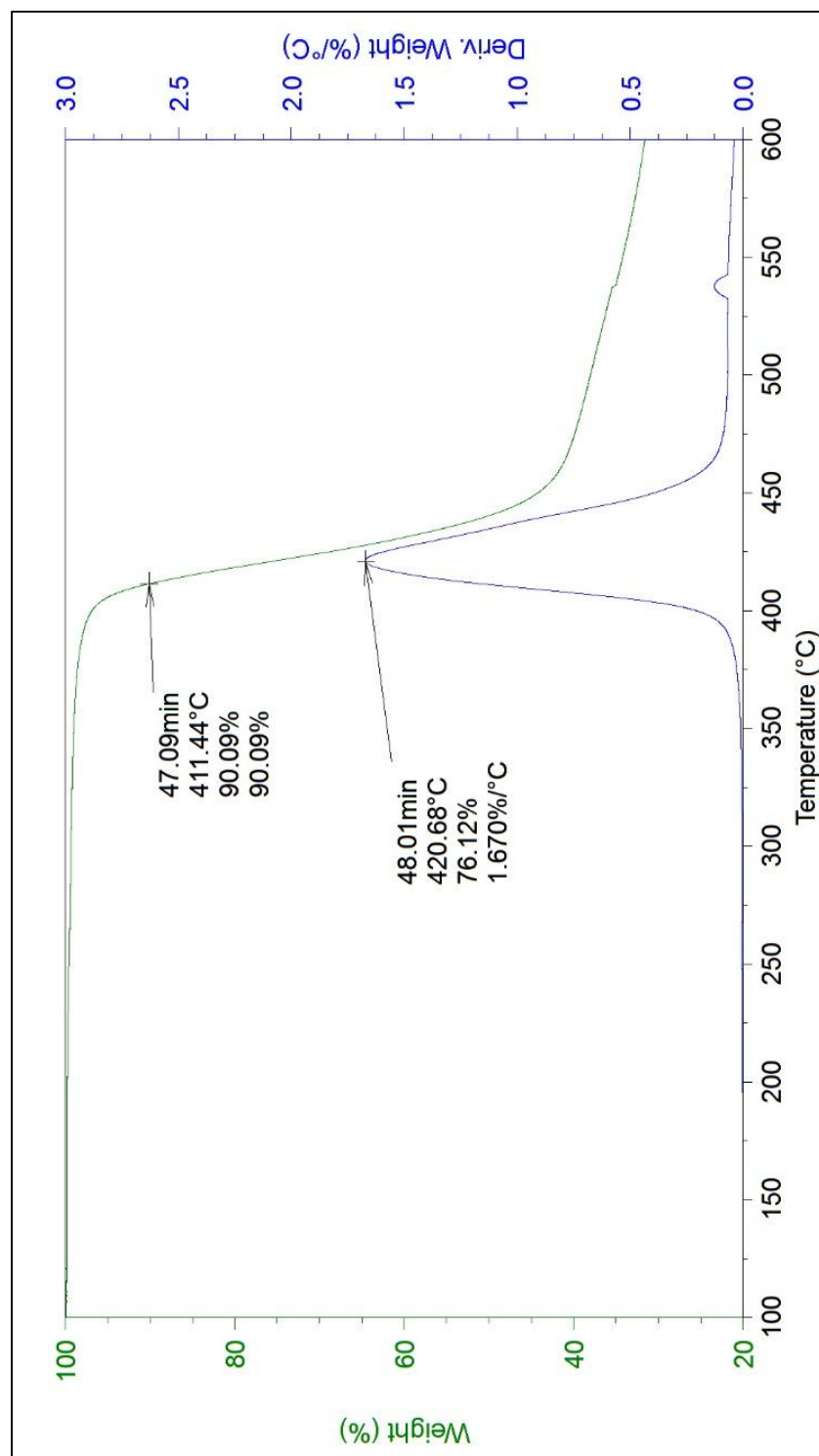


Figure E.21. Representative TGA thermogram for a sample of poly(VDF-*co*-TFE) of 80 and 20 mol% of TFE and VDF respectively. Sample was prepared in presence of CO₂.

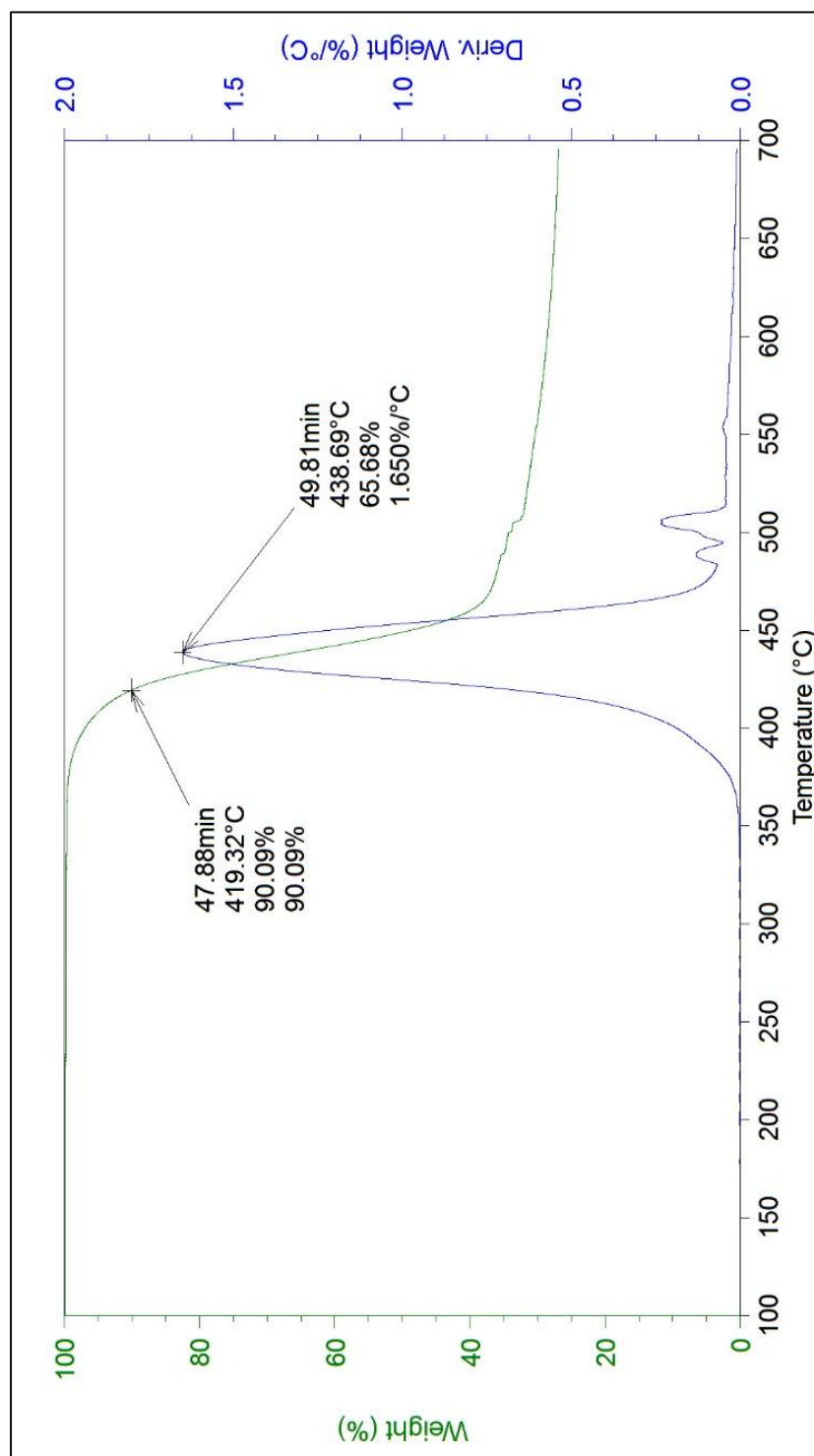


Figure E.22. Representative TGA thermogram for a sample of poly(VDF-*co*-TFE) of 70 and 30 mol% of TFE and VDF respectively. Sample was prepared in presence of CO₂.

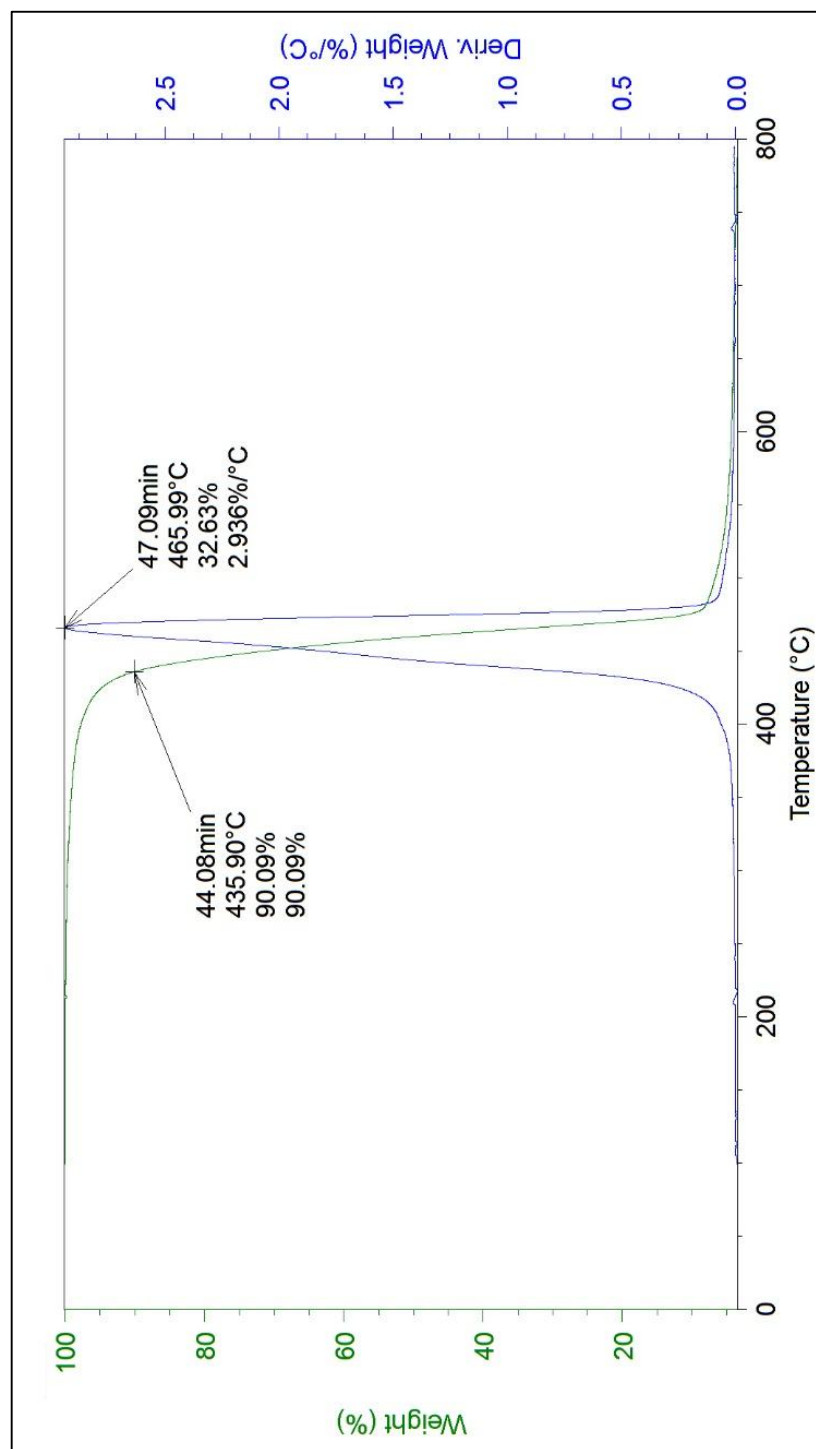


Figure E.23. Representative TGA thermogram for a sample of poly(VDF-*co*-TFE) of 60 and 40 mol% of TFE and VDF respectively. Sample was prepared in presence of CO₂.

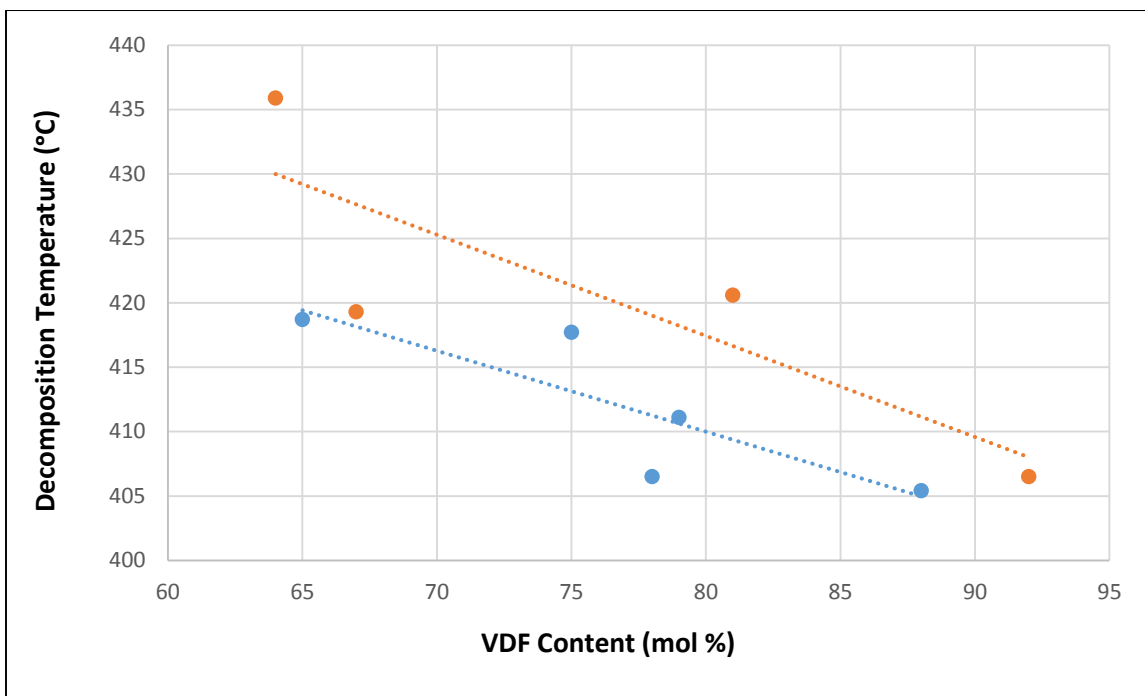


Figure E.24. Relation of 10% mass loss temperature determined by TGA and TFE content in poly(VDF-*co*-TFE) in absence (blue line) and presence (orange line) of CO₂.

E.3. Powder X-ray Diffraction (XRD) analysis of samples of poly(VDF-*co*-TFE).

Powder X-ray diffraction data (XRD) was performed in Bragg-Brentano geometry using a Rigaku Ultima IV diffractometer with Cu K α radiation ($\lambda = 1.5406$ Angstroms). Data was collected from 5 to 50 degrees in 2-theta at a rate of 2 degrees per minute and a sampling width of 0.02 degrees. The samples used were finely powdered and dried in vacuum at 50 mtorr for 24 hours at 100 °C.

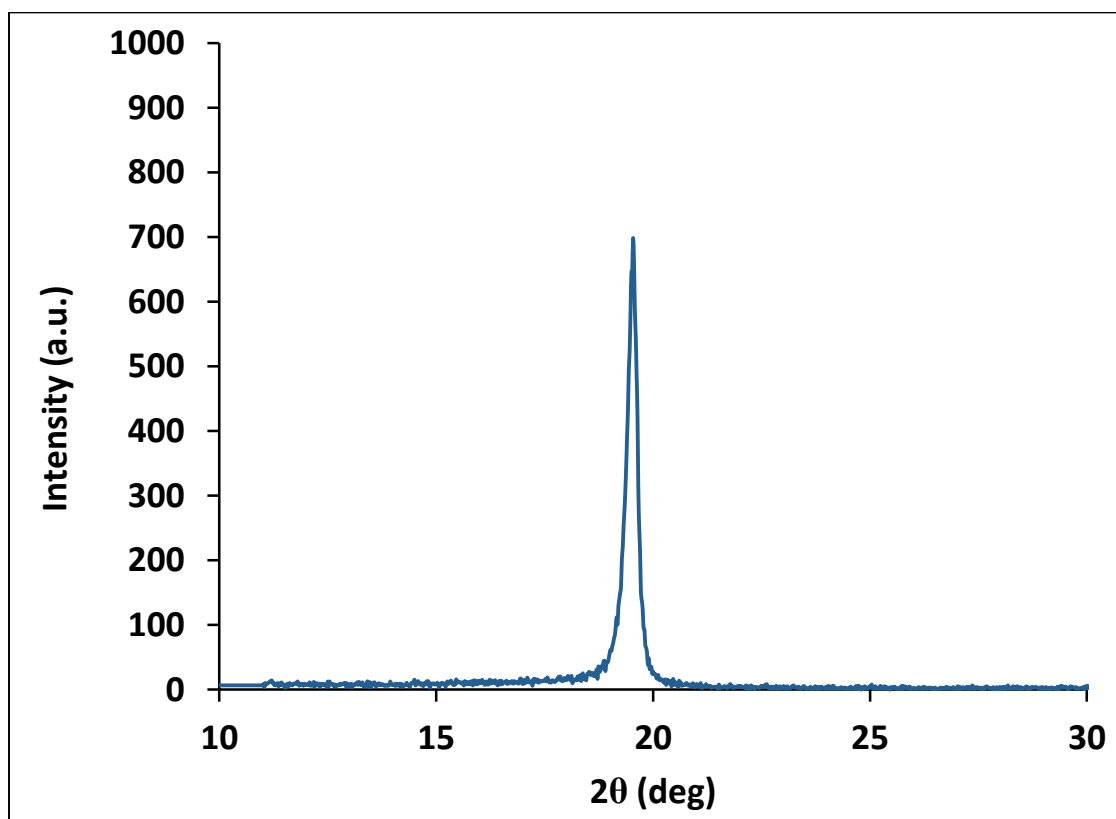


Figure E.25. Powder X-ray diffraction patterns of a sample of PTFE. The analysis was performed on a sample of PTFE deposited on a silicon wafer. This data is only used for comparison and reference.

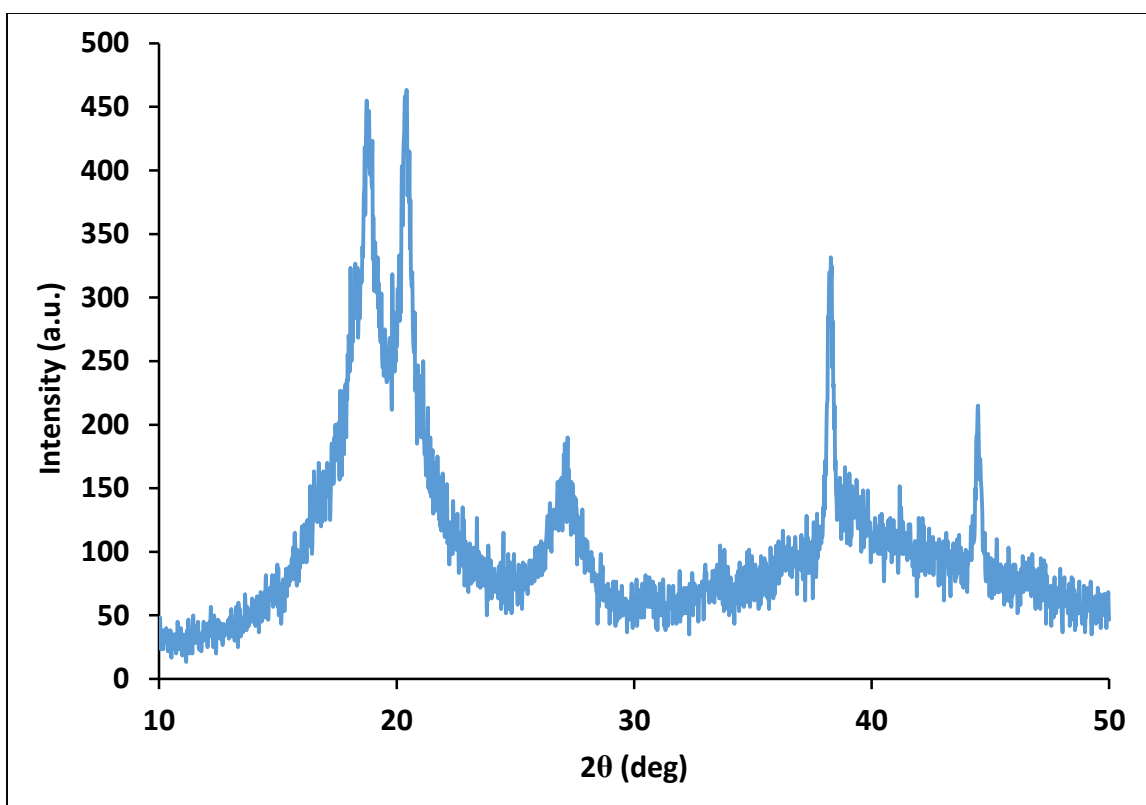


Figure E.26. Powder X-ray diffraction patterns of a sample of PVDF.

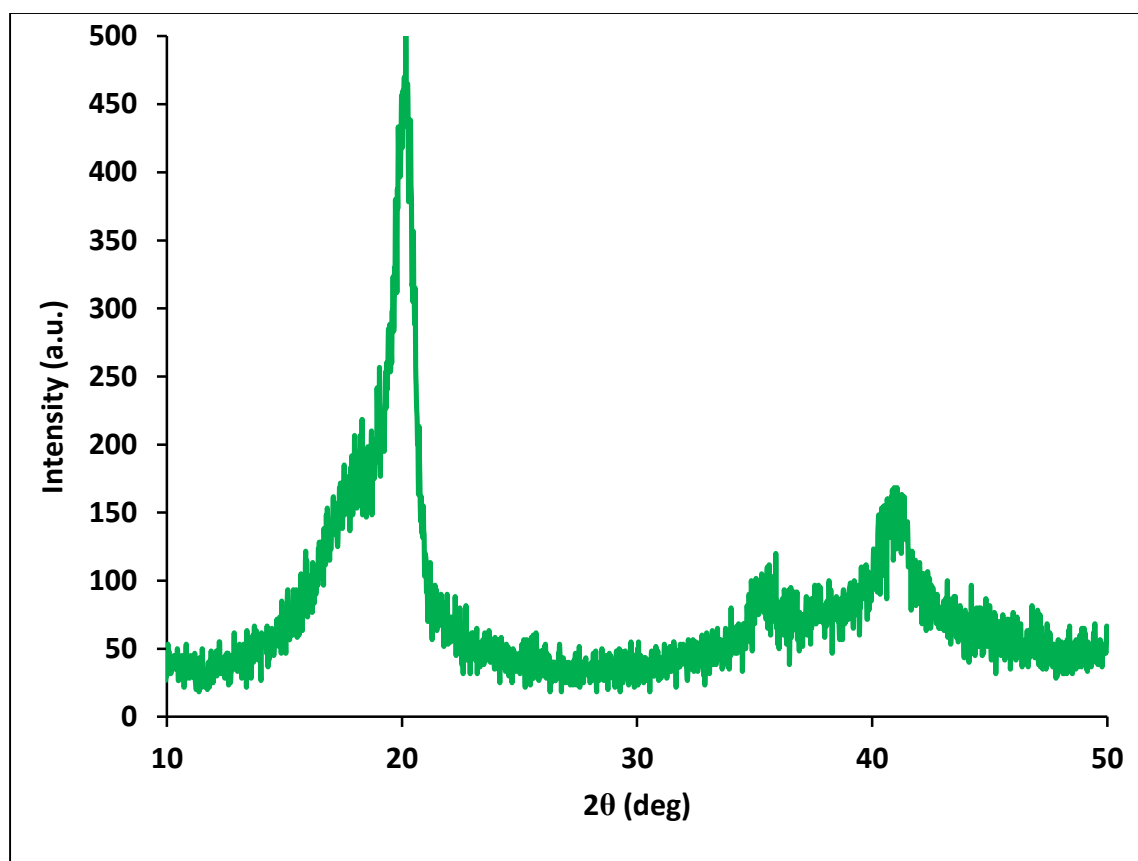


Figure E.27. Powder X-ray diffraction patterns of a sample of poly(VDF-*co*-TFE) of composition 90-10 mol% of VDF and TFE, respectively.

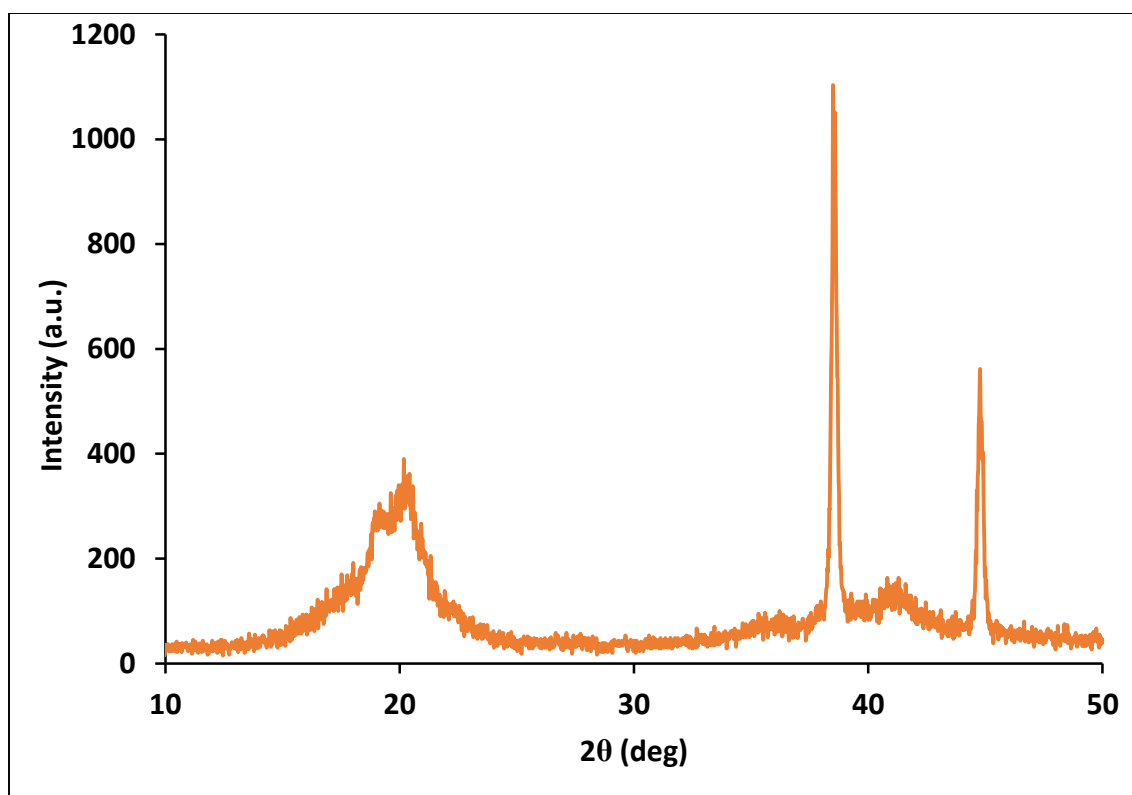


Figure E.28. Powder X-ray diffraction patterns of a sample of poly(VDF-*co*-TFE) of composition 80-20 mol% of VDF and TFE, respectively. Note: the sharp peaks at 38.5 and 44.7 deg are characteristic of the aluminum pan.

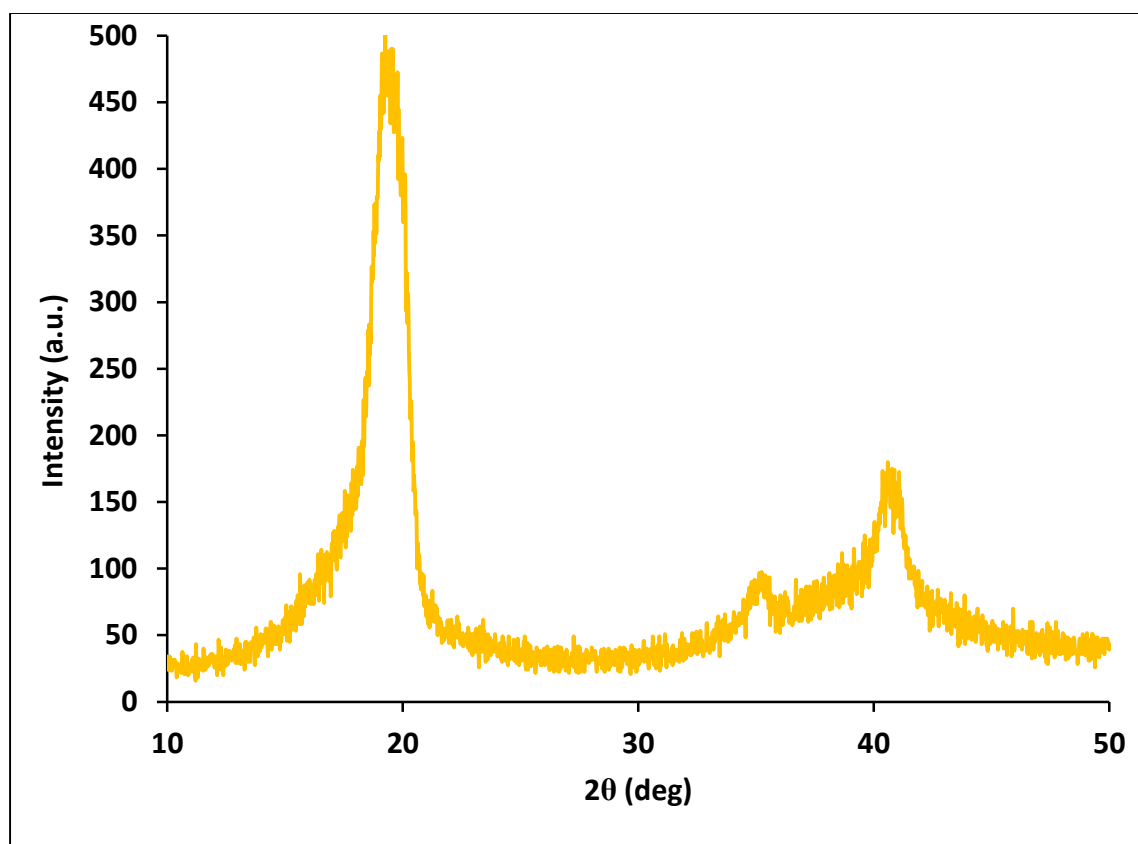


Figure E.29. Powder X-ray diffraction patterns of a sample of poly(VDF-*co*-TFE) of composition 70-30 mol% of VDF and TFE, respectively.

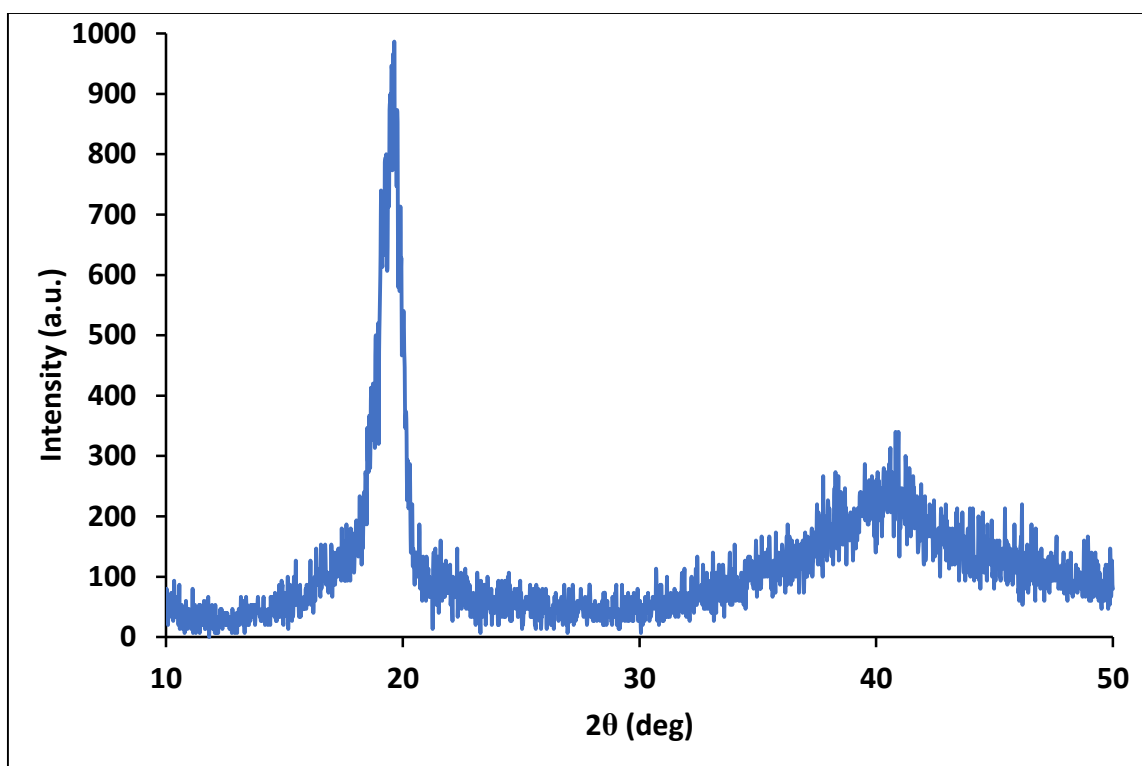


Figure E.30. Powder X-ray diffraction patterns of a sample of poly(VDF-*co*-TFE) of composition 60-40 mol% of VDF and TFE, respectively.

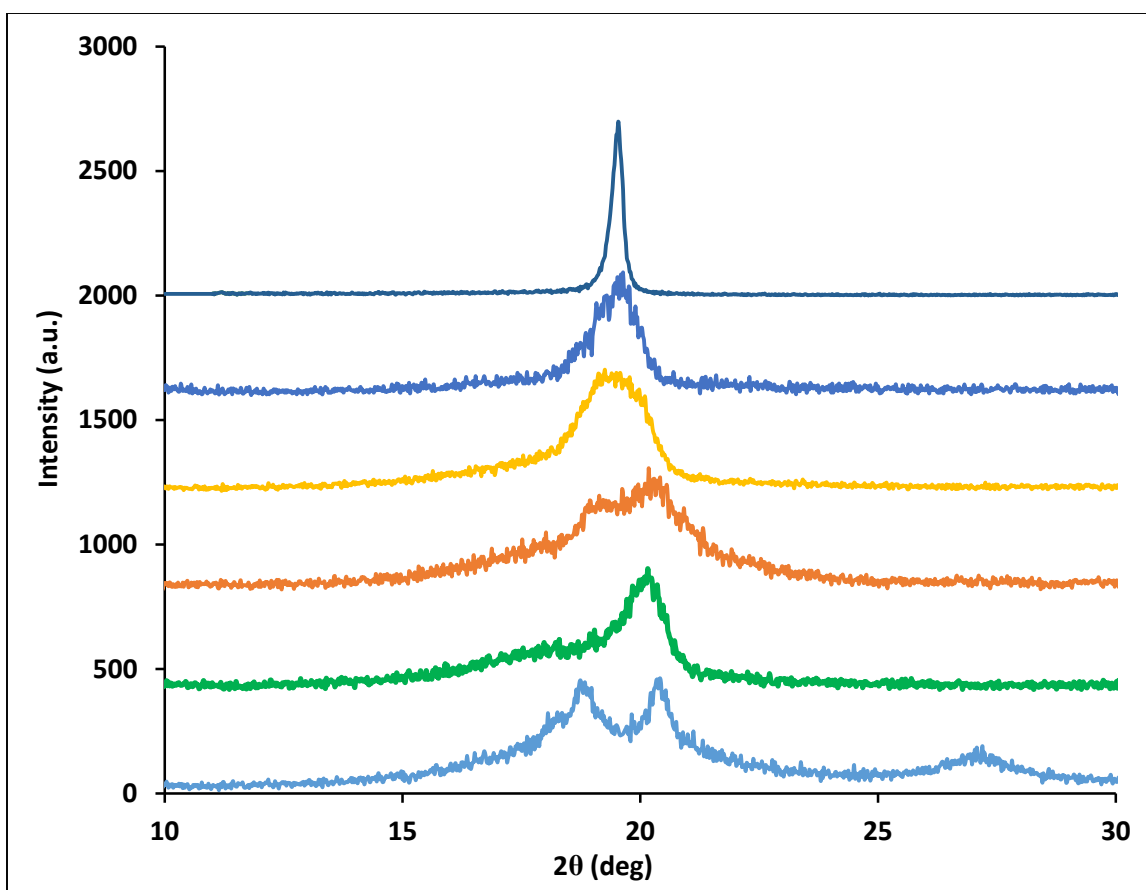


Figure E.31. Assembly of powder X-ray diffraction patterns of polymer samples. From top to bottom respectively: PTFE, poly(VDF-*co*-TFE) with 40 mol% TFE, 30 mol% TFE, 20 mol% TFE, 10 mol% TFE, and PVDF.

E.4. Characterization of poly(VDF-*co*-TFE) using fluorine-19 nuclear magnetic Resonance (¹⁹F NMR) spectroscopy

The fluorine-19 NMR spectroscopy analysis of samples of poly(VDF-*co*-TFE) were carried on a JEOL 300 MHz NMR. The samples were prepared by preparing 3-5 % m/v samples of the copolymer in DMSO-*d*6. In several cases, the aid of a heat gun at 80 °C and sonication were used to help the solution process. The samples produced were clear, but when a cloudy sample solution was obtained, the sample was prepared again by using less amount of copolymer in the same amount of solvent. A summary of the compositions found by NMR are included in Table E.3.

Table E.3. Reaction data: target compositions and final compositions of poly(VDF-*co*-TFE) in presence (light red) and absence (light blue) of CO₂.

Sample	Targeted Composition (mol %)		Composition Determined Experimentally (mol% ± 1%)	
	VDF	TFE	VDF	TFE
A	90	10	91	9
E	90	10	92	8
B	80	20	85	15
F	80	20	81	19
C	70	30	82	18
G	70	30	67	33
D	60	40	74	26
H	60	40	64	36

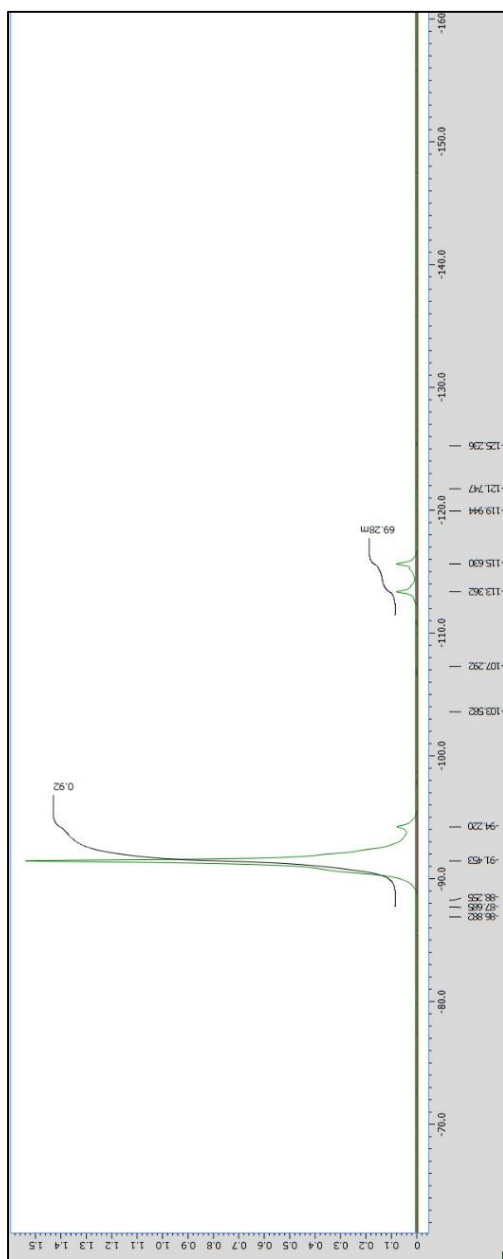


Figure E.32. ^{19}F NMR spectra for a sample of PVDF. Sample prepared in absence of CO_2 .

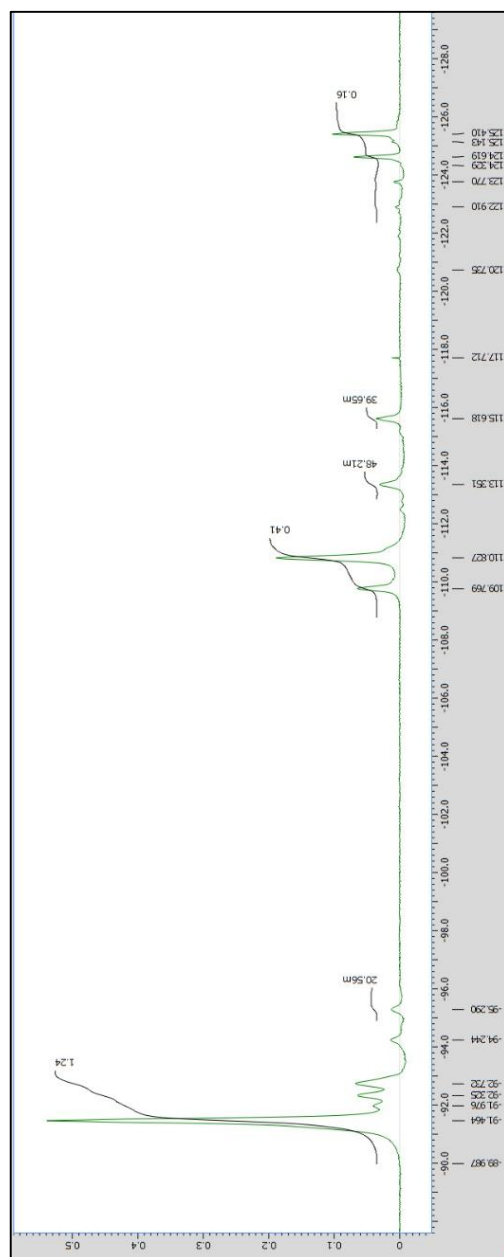


Figure E.33. ^{19}F NMR spectra for a sample of poly(VDF-*co*-TFE) containing 91 mol% VDF and 9 mol% TFE. Sample prepared in absence of CO_2 .

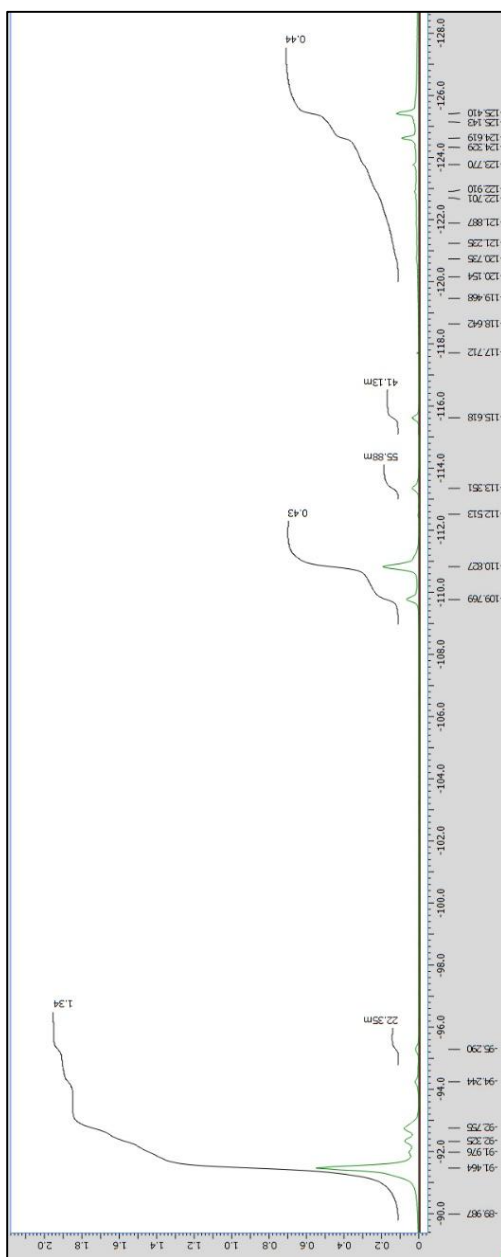


Figure E.34. ^{19}F NMR spectra for a sample of poly(VDF-co-TFE) containing 85 mol% VDF and 15 mol% TFE. Sample prepared in absence of CO_2 .

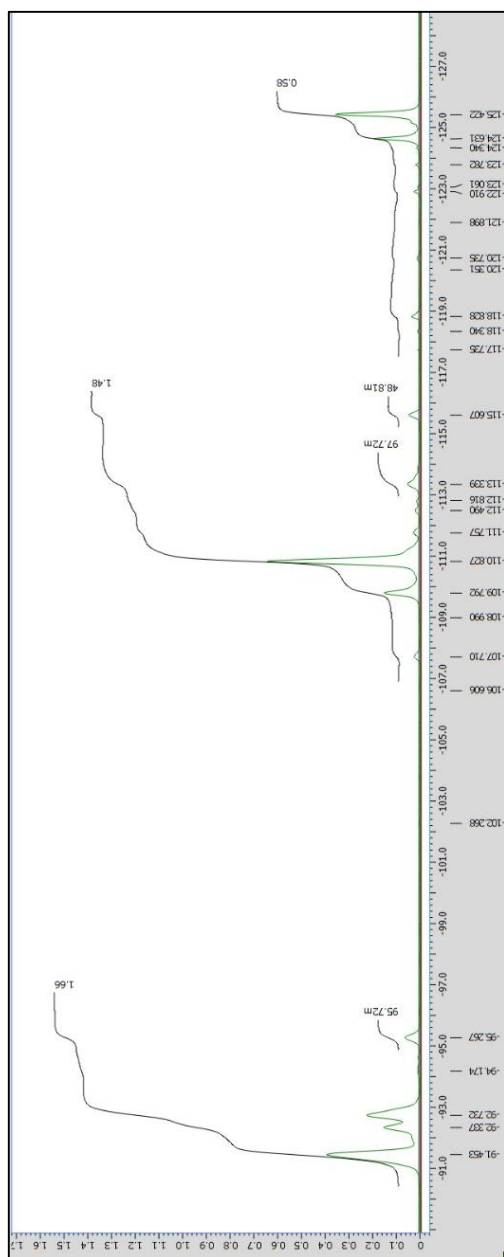


Figure E.35. ^{19}F NMR spectra for a sample of poly(VDF-*co*-TFE) containing 82 mol% VDF and 18 mol% TFE. Sample prepared in absence of CO_2 .

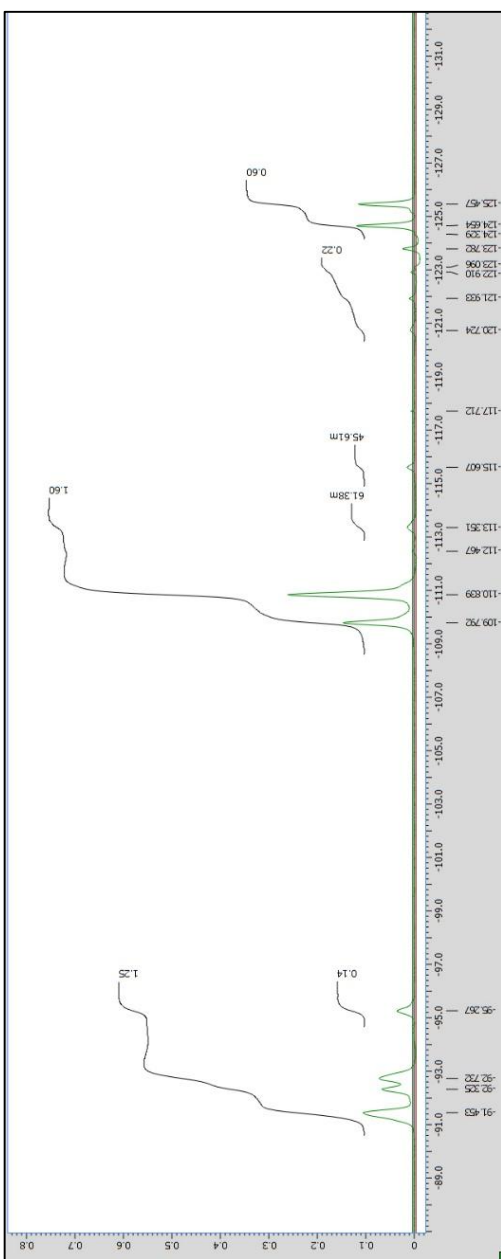


Figure E.36. ^{19}F NMR spectra for a sample of poly(VDF-*co*-TFE) containing 74 mol% VDF and 26 mol% TFE. Sample prepared in absence of CO_2 .

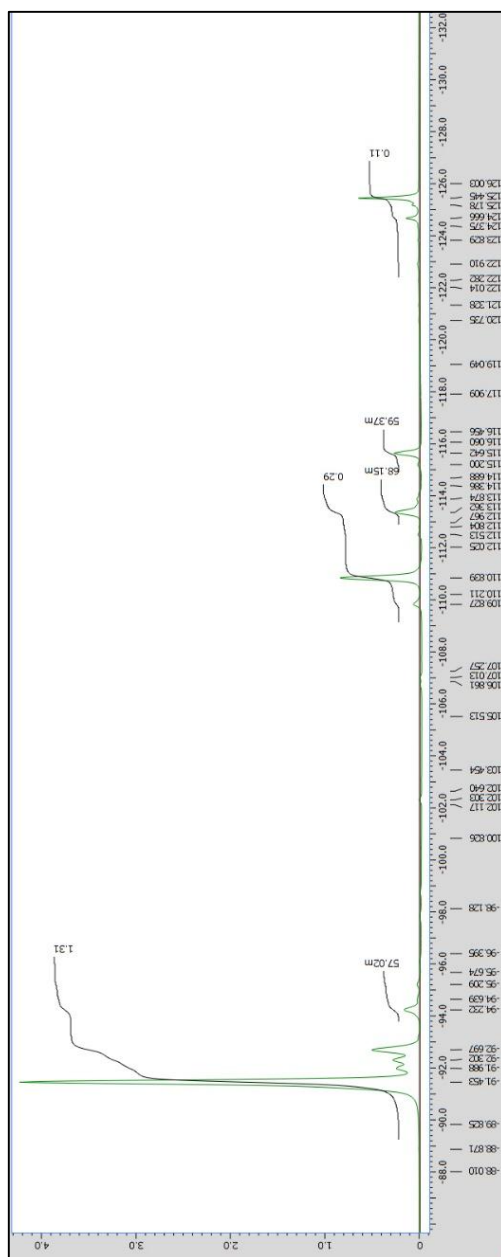


Figure E.37. ^{19}F NMR spectra for a sample of poly(VDF-*co*-TFE) containing 92 mol% VDF and 8 mol% TFE. Sample prepared in presence of CO_2 .

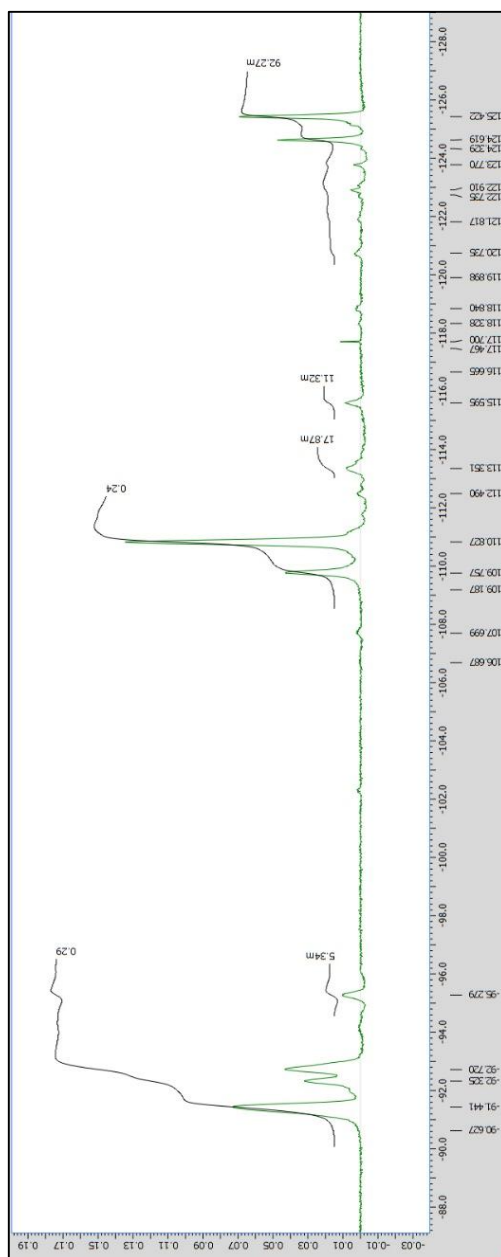


Figure E.38. ^{19}F NMR spectra for a sample of poly(VDF-*co*-TFE) containing 81 mol% VDF and 19 mol% TFE. Sample prepared in presence of CO_2 .

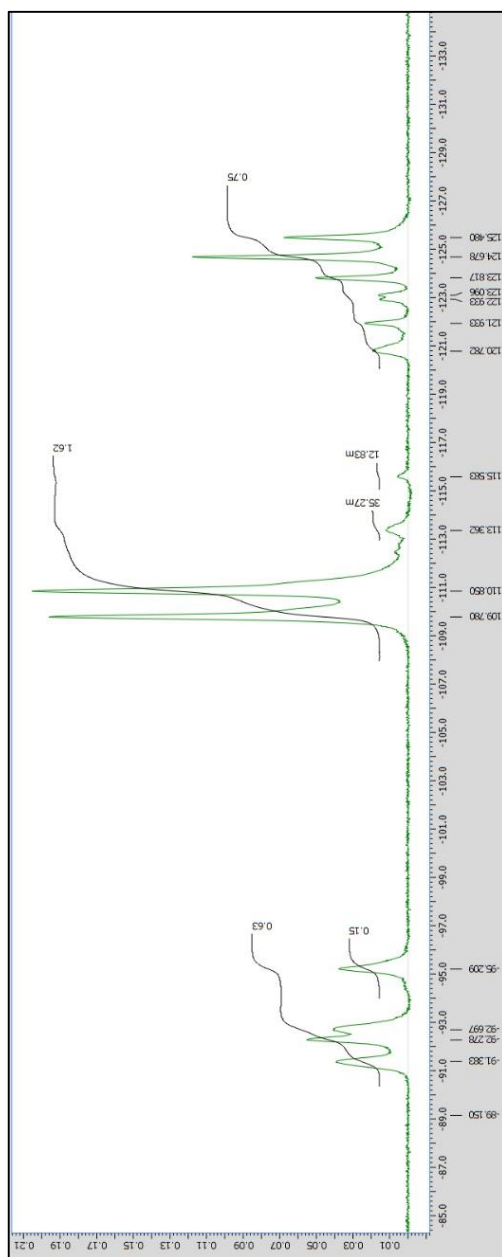


Figure E.39. ^{19}F NMR spectra for a sample of poly(VDF-*co*-TFE) containing 67 mol% VDF and 33 mol% TFE. Sample prepared in presence of CO_2 .

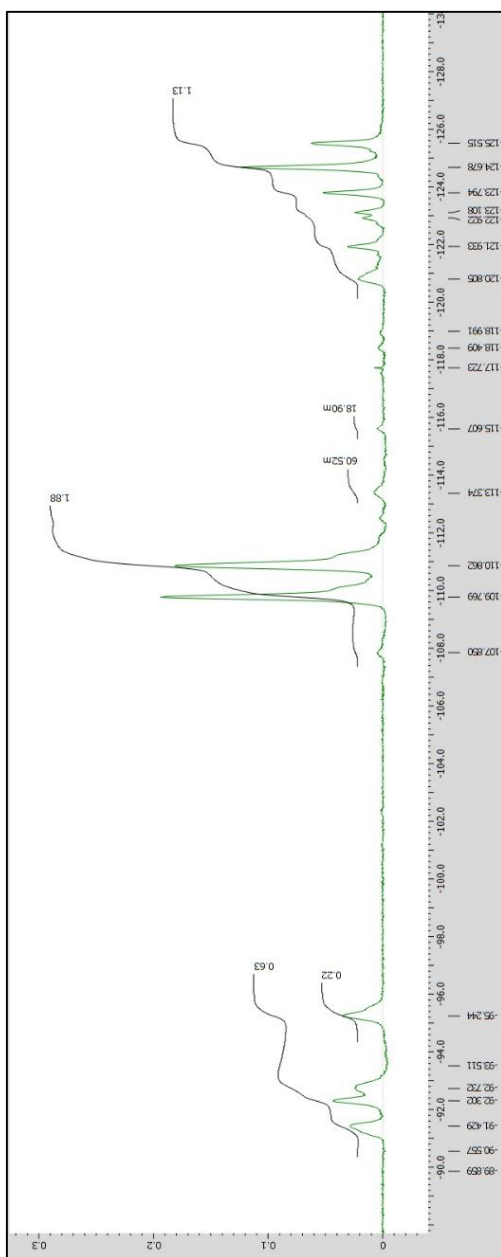


Figure E.40. ^{19}F NMR spectra for a sample of poly(VDF-*co*-TFE) containing 64 mol% VDF and 36 mol% TFE. Sample prepared in presence of CO_2 .

Appendix F

Supporting Information for Chapter 5.

F.1. ATR-FTIR results of commercial samples of poly(TFE-*co*-PSEPVE).

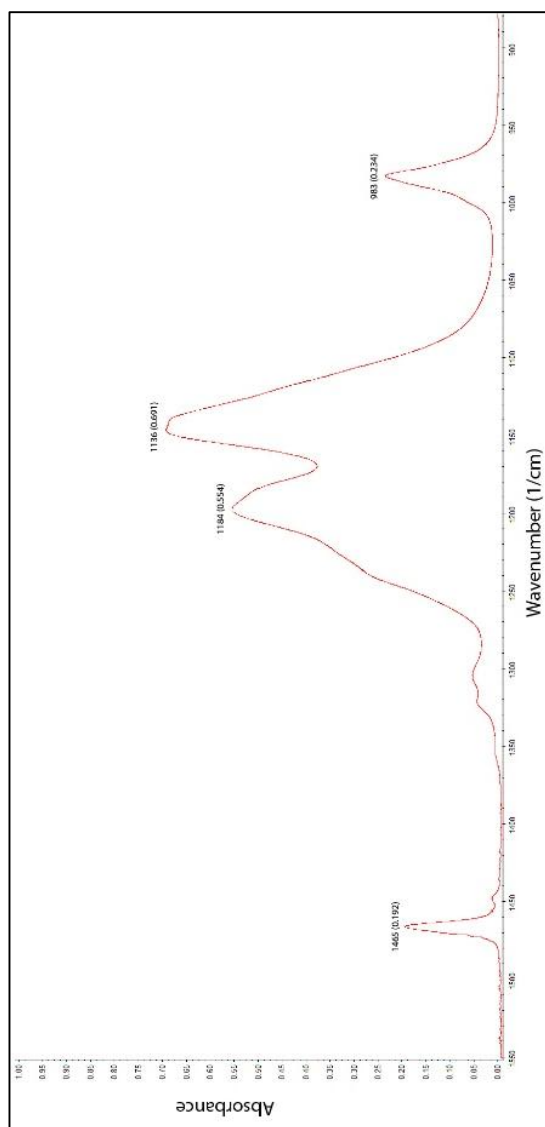


Figure F.1. Example spectra for a commercial sample of Nafion[®] 920-SR also denominated as poly(TFE-*co*-PSEPVE) in the sulfonyl fluoride form.

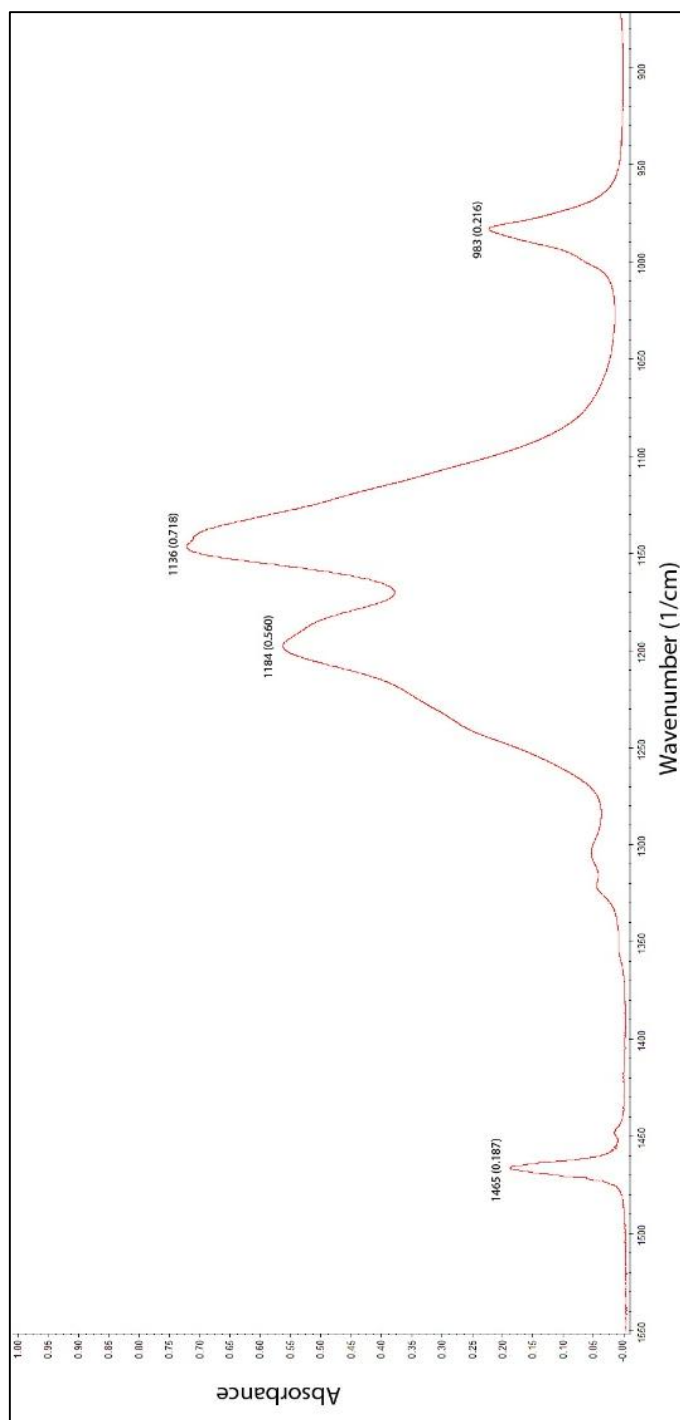


Figure F.2. Example spectra for a commercial sample of Nafion[®] 1000-SR also denominated as poly(TFE-*co*-PSEPVE) in the sulfonyl fluoride form.

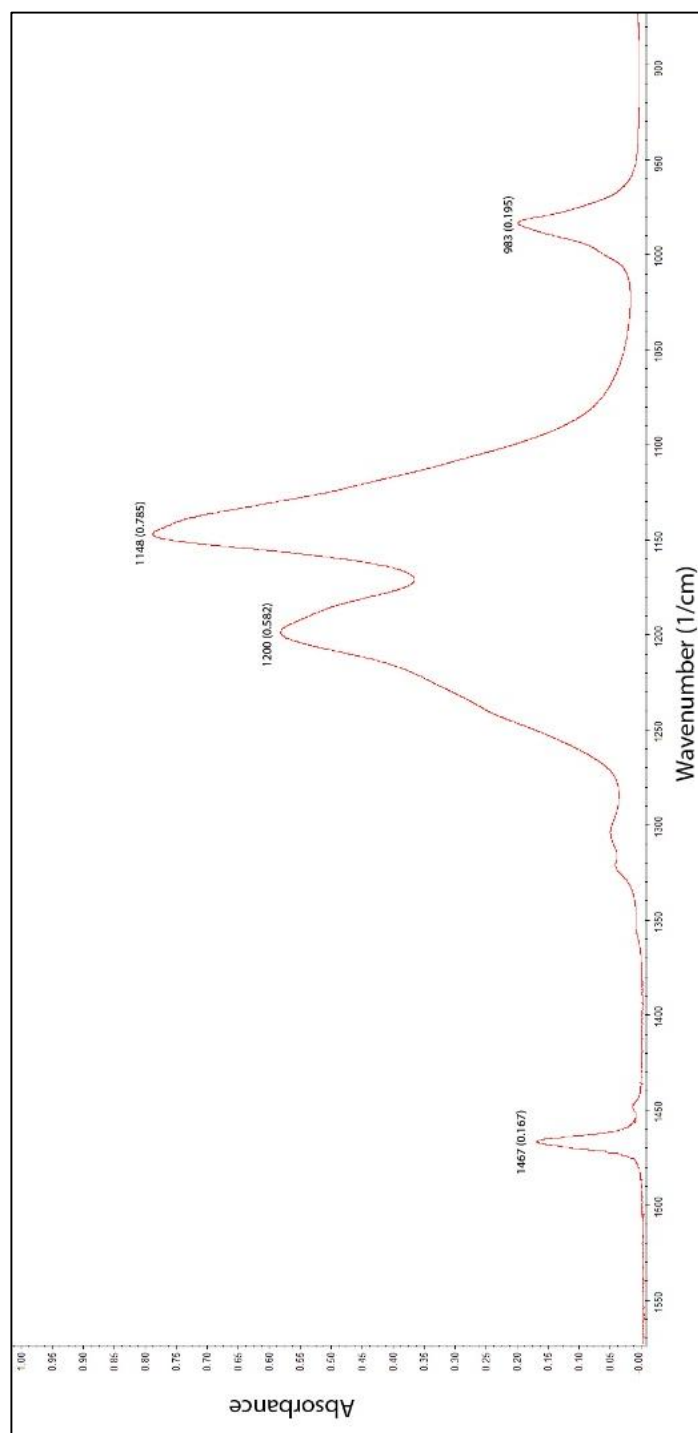


Figure F.3. Example spectra for a commercial sample of Nafion[®] 1200-SR also denominated as poly(TFE-*co*-PSEPVE) in the sulfonyl fluoride form.

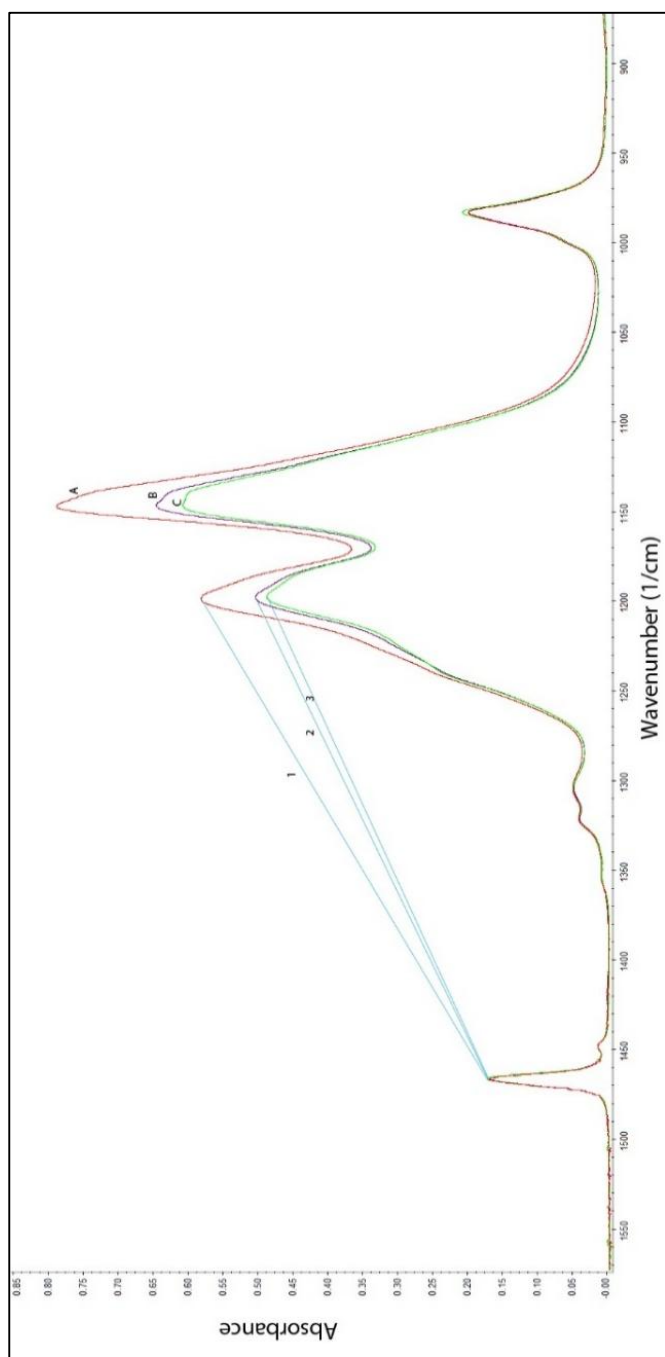


Figure F.4. Normalized infrared spectra for samples of poly(TFE-*co*-PSEPVE) featuring the ratios of absorbances used for Method I. A is the spectra for Nafion[®] 1200-SR, B is 1000-SR, and C is 920-SR.

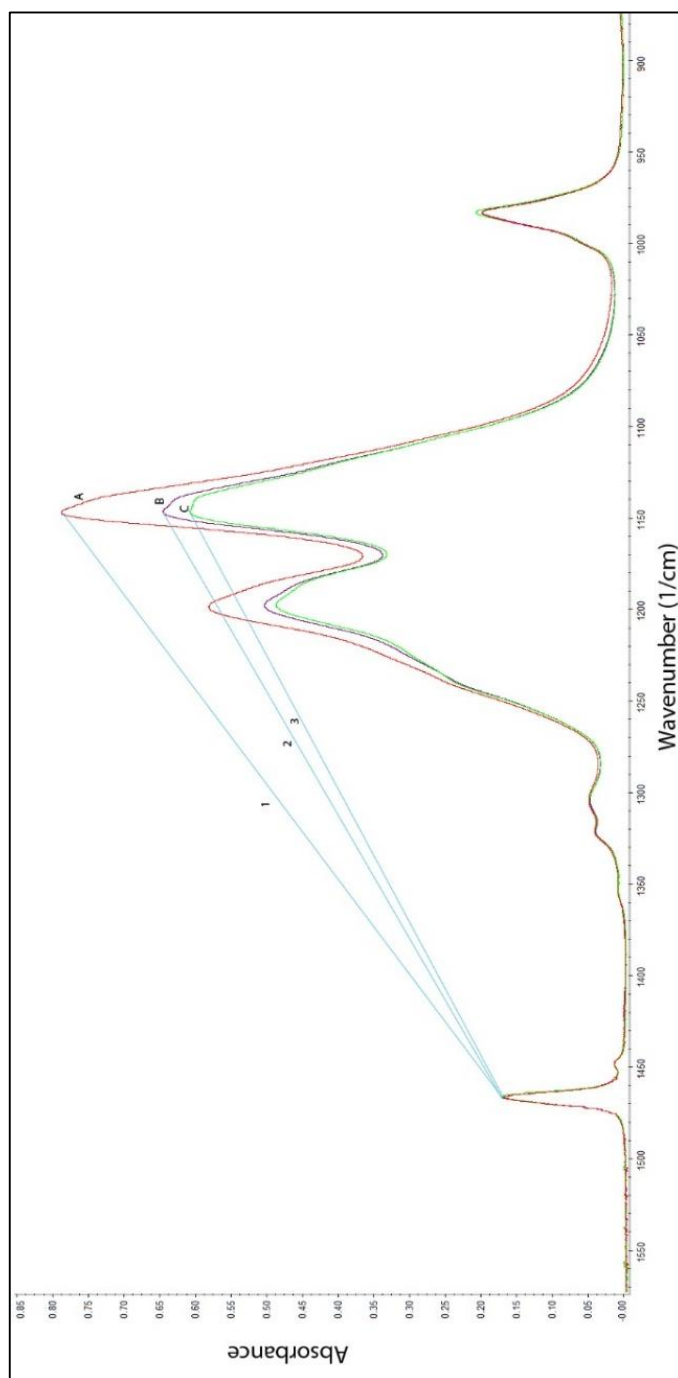


Figure F.5. Normalized infrared spectra for samples of poly(TFE-*co*-PSEPVE) featuring the ratios of absorbances used for Method II. A is the spectra for Nafion[®] 1200-SR, B is 1000-SR, and C is 920-SR.

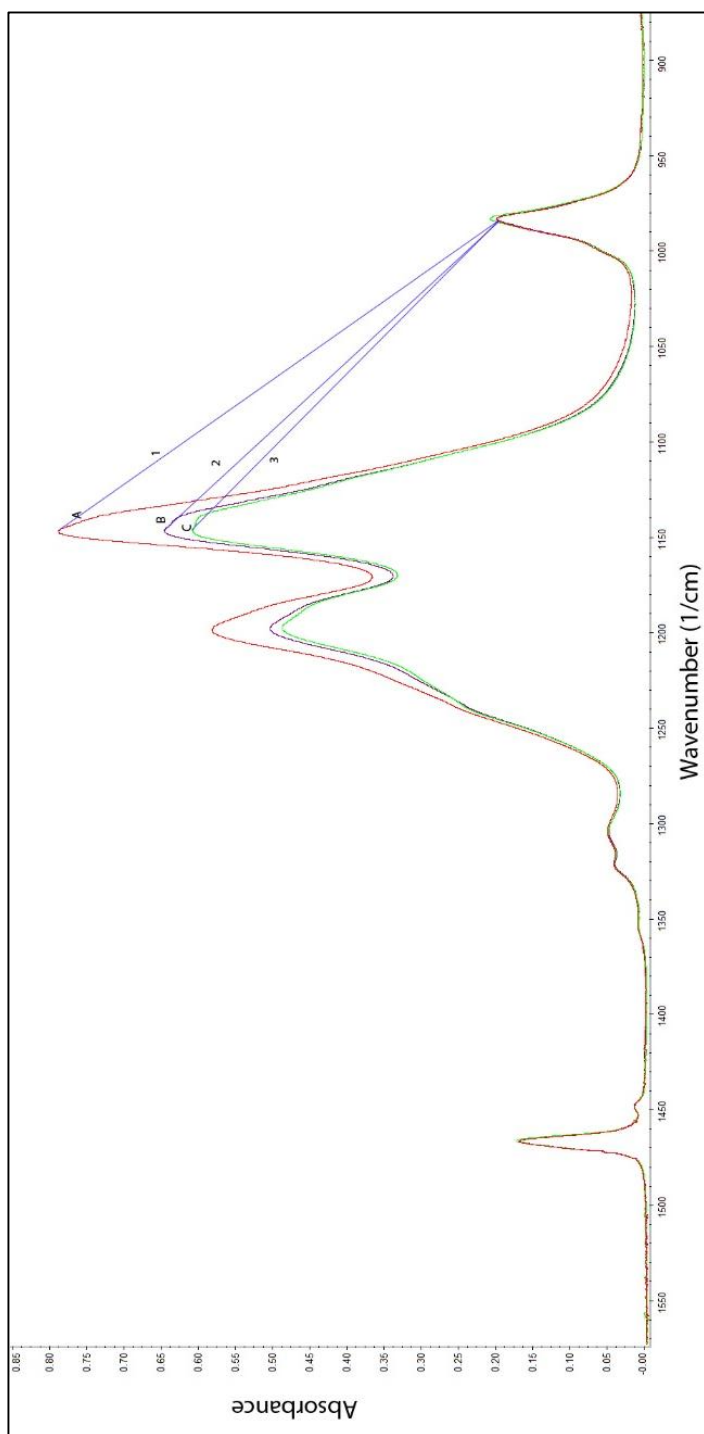


Figure F.6. Normalized infrared spectra for samples of poly(TFE-*co*-PSEPVE) featuring the ratios of absorbances used for Method III. A is the spectra for Nafion[®] 1200-SR, B is 1000-SR, and C is 920-SR.

Table F.1. Ratios of absorbances used for the experimental determination of equivalent weight linear regressions (Method I, II, and III).

Method	Point 1 (ABS)	Point 2 (ABS)	Ratio (ABS1/ABS2)	Nominal EW (g/mol)	EW from Titration (g/mol)
I	0.166	0.485	2.92	920	926
	0.166	0.500	3.01	1000	1020
	0.166	0.580	3.49	1200	1181
II	0.166	0.606	3.65	920	926
	0.166	0.645	3.89	1000	1020
	0.166	0.786	4.73	1200	1181
III	0.228	0.485	2.12	920	926
	0.228	0.500	2.19	1000	1020
	0.228	0.580	2.54	1200	1181

F.2. Equivalent Weight Results Obtained from FTIR Sample Analysis.

The following two tables (Table F.2 and Table F.3) are the calculated EW based on the Original Method for calculating Equivalent Weights from poly(TFE-*co*-PSEPVE) samples in the sulfonyl fluoride form using ATR-FTIR spectroscopy. The bands are named A, B, C, and D based on Figure F.7 where a typical ATR-FTIR spectra of a poly(TFE-*co*-PSEPVE) sample is shown.

Table F.2. Experimental determination of constants used for the equivalent weight calculation of samples of poly(TFE-*co*-PSEPVE) as detailed by the method published in the Chinese patent literature. Samples were prepared in absence of CO₂.

Sample	Band	Absorbance (abs)	h	j	R	Const	1/S	S	EW
S1	A	0.112	0.251	0.625	2.460	0.100	4.386	0.228	785
	B	0.283							
	C	0.342							
	D	0.139							
S2	A	0.122	0.275	0.757	2.686	0.091	5.036	0.199	850
	B	0.346							
	C	0.411							
	D	0.153							
S3	A	0.117	0.282	0.898	3.055	0.079	6.097	0.164	956
	B	0.394							
	C	0.504							
	D	0.165							
S4	A	0.145	0.350	1.179	3.273	0.074	6.727	0.149	1019
	B	0.508							
	C	0.671							
	D	0.205							
S5	A	0.158	0.358	1.301	3.725	0.069	8.028	0.125	1149
	B	0.556							
	C	0.745							
	D	0.200							

Where h, j, R, C are calculated values based on the patented EW equation denominated as the Original Method for calculating Equivalent Weights as explained in Chapter 5.

Table F.3. Experimental determination of constants used for the equivalent weight calculation of samples of poly(TFE-*co*-PSEPVE) as detailed by the method published in the Chinese patent literature. Samples were prepared in precense of CO₂.

Sample	Band	Absorbance (abs)	h	j	R	C	1/S	S	EW
S6	A	0.202	0.446	1.231	2.791	0.091	5.338	0.187	880
	B	0.550							
	C	0.681							
	D	0.244							
S7	A	0.122	0.282	0.866	2.994	0.081	5.922	0.169	938
	B	0.387							
	C	0.479							
	D	0.160							
S8	A	0.204	0.429	1.289	3.182	0.083	6.465	0.155	992
	B	0.573							
	C	0.716							
	D	0.225							
S9	A	0.121	0.273	0.976	3.612	0.070	7.702	0.130	1116
	B	0.427							
	C	0.549							
	D	0.152							
S10	A	0.118	0.272	1.016	3.734	0.067	8.053	0.124	1151
	B	0.441							
	C	0.575							
	D	0.154							

Where h, j, R, C are calculated values based on the patented EW equation denominated as the Original Method for calculating Equivalent Weights as explained in Chapter 5.

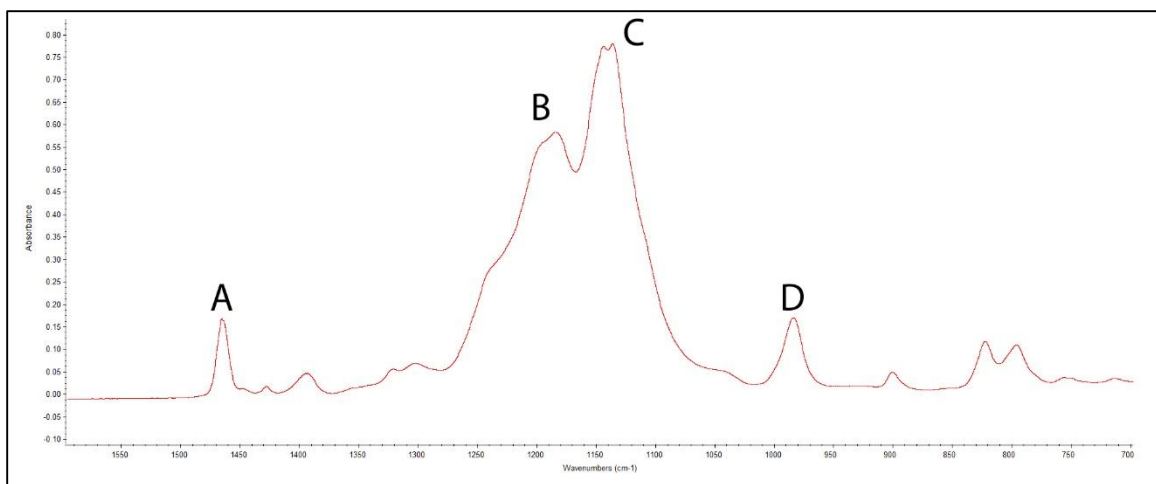


Figure F.7. Example ATR-FTIR spectra of poly(TFE-*co*-PSEPVE) of Equivalent Weight of 1116 g/mol.

Table F.4. Experimental results for acid base titration of commercial samples of poly(TFE-*co*-PSEPVE) originally obtained in the sulfonyl fluoride form from DuPont.

Sample Nominal EW (g/mol)	Experimental EW (g/mol)	Average EW (g/mol)
920	921	927 ± 25
	905	
	955	
1000	1009	1019 ± 25
	1016	
	1035	
1200	1199	1181 ± 25
	1170	
	1174	

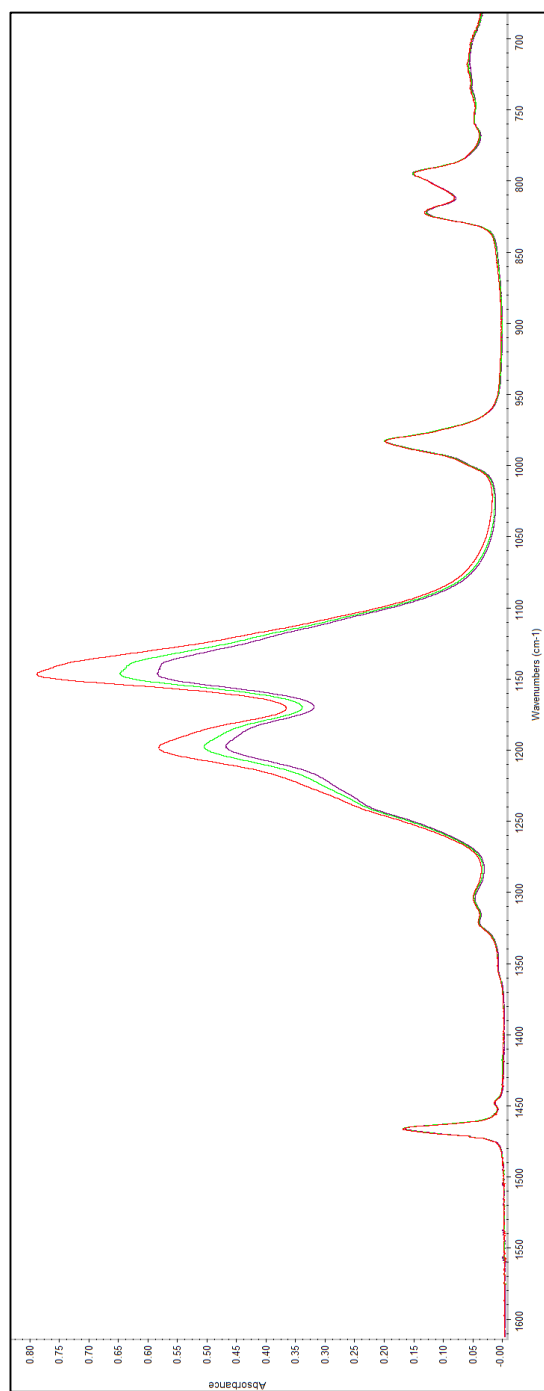


Figure F.8. Overlay of infrared spectra of poly(TFE-*co*-PSEPVE) samples used to create the calibration curves. Purple: 927 g/mol, Green: 1019 g/mol, and Red: 1181 g/mol.

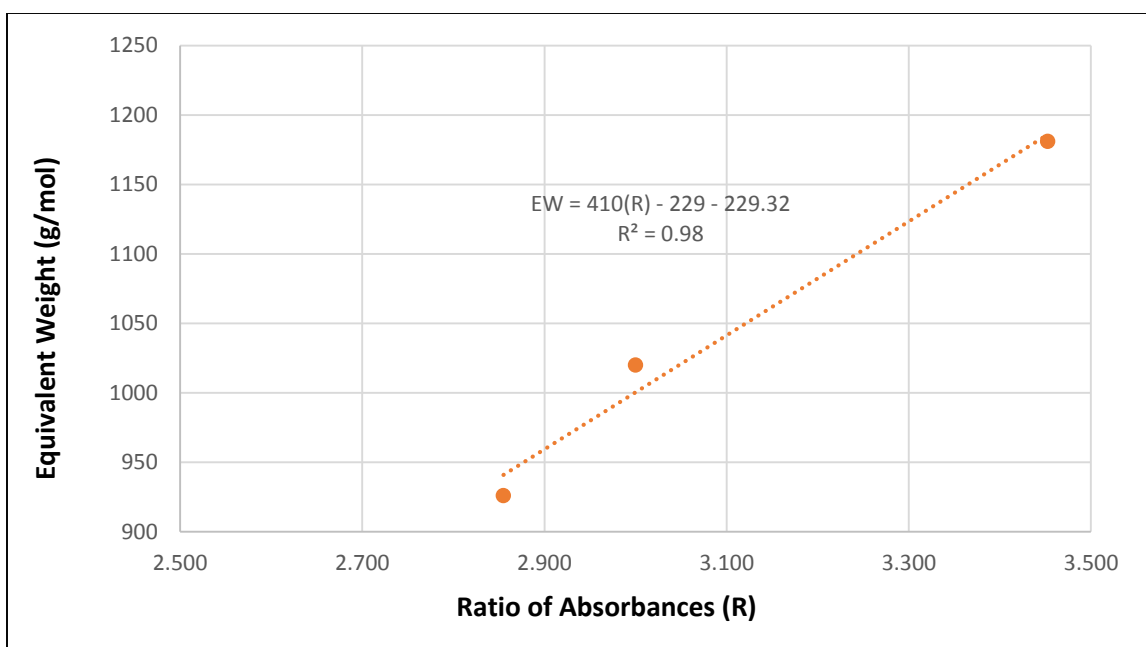


Figure F.9. Linear correlation in between absorbance ratios and Equivalent weights for samples of poly(TFE-*co*-PSEPVE). This curve is also denominated Method I.

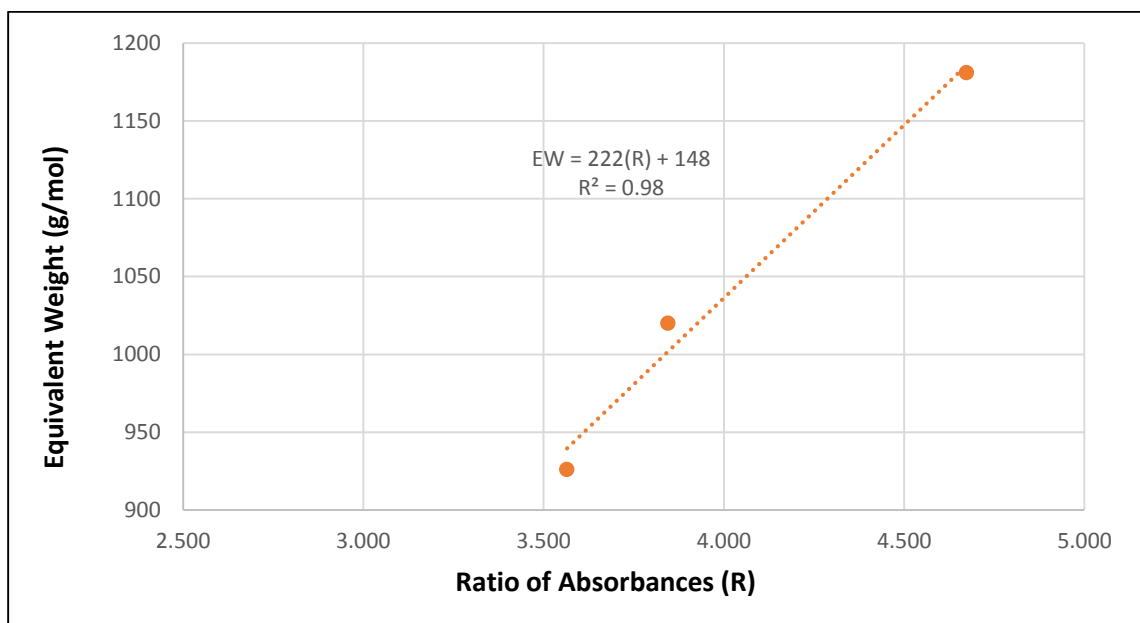


Figure F.10. Linear correlation in between absorbance ratios and Equivalent weights for samples of poly(TFE-*co*-PSEPVE). This curve is also denominated Method II.

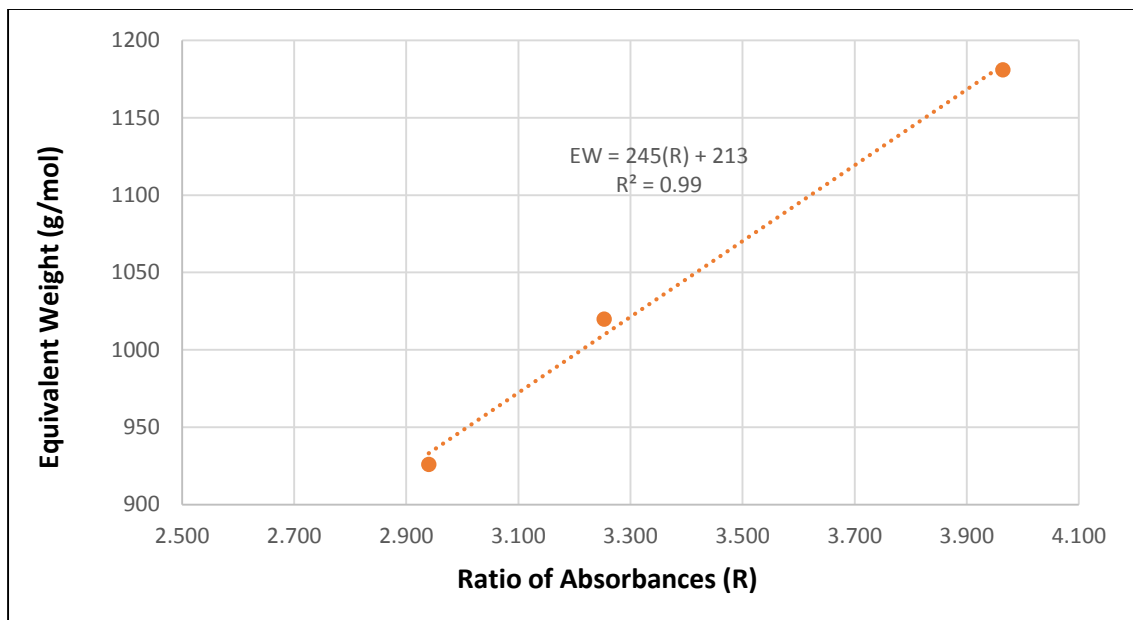


Figure F.11. Linear correlation in between absorbance ratios and Equivalent weights for samples of poly(TFE-*co*-PSEPVE). This curve is also denominated Method III.

F.3. Experimental Results from Polymerization Reactions of poly(TFE-*co*-PSEPVE).

Table F.5. Composition analysis for the feed and final monomer composition on experimental samples of poly(TFE-*co*-PSEPVE). Samples S1-S5 were prepared in absence of CO₂, while samples S6-S10 were prepared in presence of CO₂.

Sample	Polymer Composition (Molar Fraction)		Monomer Feed Composition (Molar Fraction)	
	TFE	PSEPVE	PSEPVE	TFE
S1	0.77	0.23	0.20	0.80
S2	0.80	0.20	0.26	0.74
S3	0.84	0.16	0.30	0.70
S4	0.85	0.15	0.33	0.67
S5	0.88	0.12	0.37	0.63
S6	0.81	0.19	0.26	0.74
S7	0.83	0.17	0.29	0.71
S8	0.85	0.15	0.33	0.67
S9	0.87	0.13	0.35	0.65
S10	0.88	0.12	0.40	0.60

Table F.6. Fineman and Ross, and Kelen and Tüdös parameters for the determination of reactivity ratios of the monomers in poly(TFE-*co*-PSEPVE). Samples S1-S5 were prepared in absence of CO₂, while samples S6-S10 were prepared in presence of CO₂.

Sample	X	Y	G	H	N	E	A
S1	0.25	3.39	0.18	0.02	3.52	0.37	0.03
S2	0.35	4.04	0.26	0.03	4.25	0.49	0.03
S3	0.43	5.09	0.34	0.04	5.09	0.53	0.03
S4	0.49	5.72	0.41	0.04	5.49	0.57	0.03
S5	0.59	7.02	0.50	0.05	6.24	0.61	0.03
S6	0.35	4.33	0.27	0.03	3.81	0.40	0.04
S7	0.41	4.92	0.33	0.03	4.26	0.44	0.04
S8	0.49	5.46	0.40	0.04	4.63	0.51	0.04
S9	0.54	6.70	0.46	0.04	5.35	0.50	0.04
S10	0.67	7.05	0.57	0.06	5.42	0.60	0.04

F.4. Experimental Results from Polymerization Reactions of poly(TFE-*co*-PSVE).

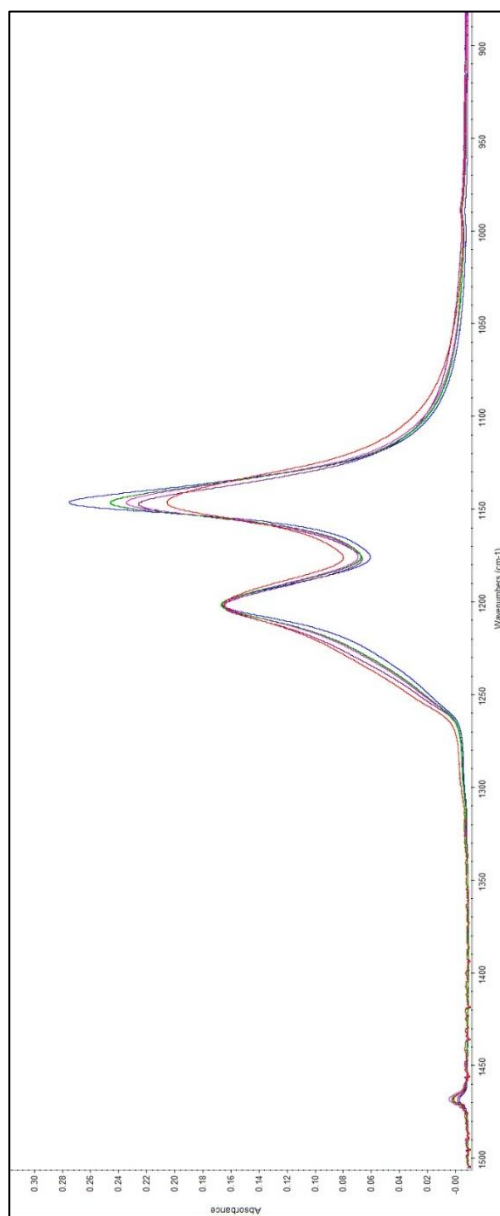


Figure F.12. Infrared spectra of experimental samples of poly(TFE-*co*-PSVE) normalized to the S-F stretch frequency for comparison. In increasing order of EW the samples are 1340, 1420, 1438, and 1509 g/mol.

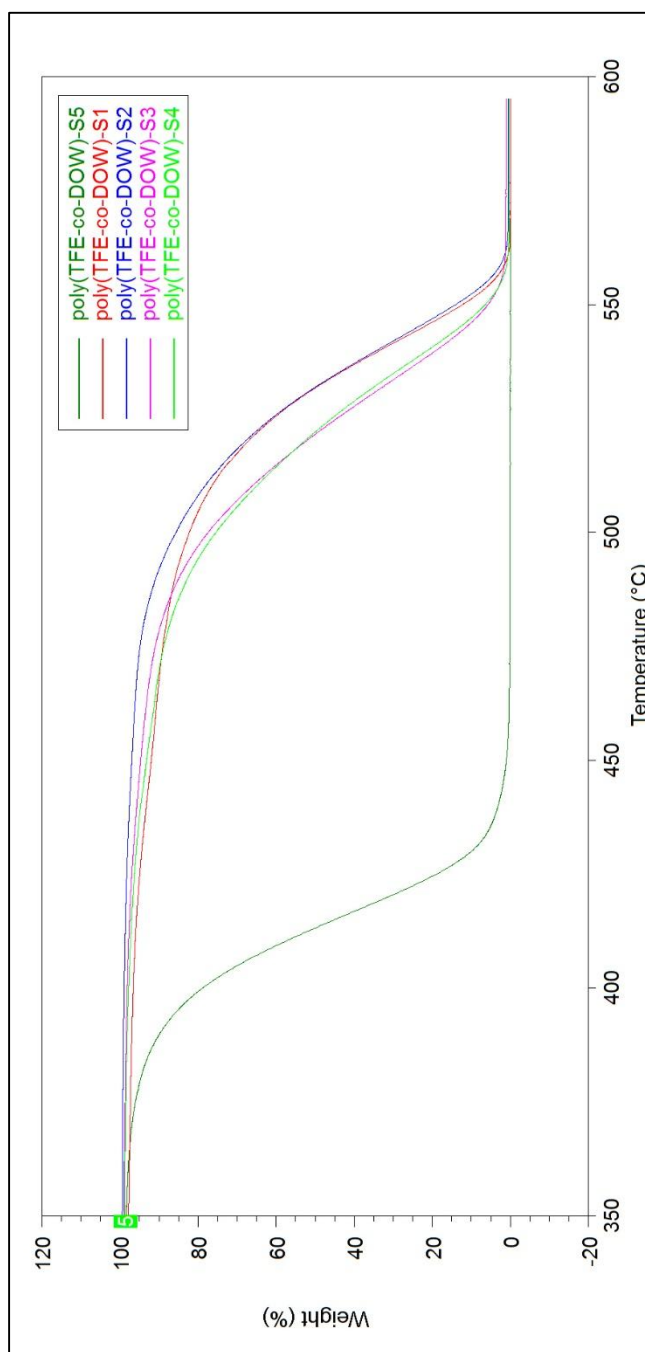


Figure F.13. TGA analysis comparison of the experimental samples of poly(TFE-*co*-PSVE) compared to a standard sample of the same polymer of EW of 700 g/mol. EW of samples is as follows: sample 1 is 1340, sample 2 is 1420, sample 3 is 1438, sample 4 is 1509, and sample 5 is 700 g/mol.

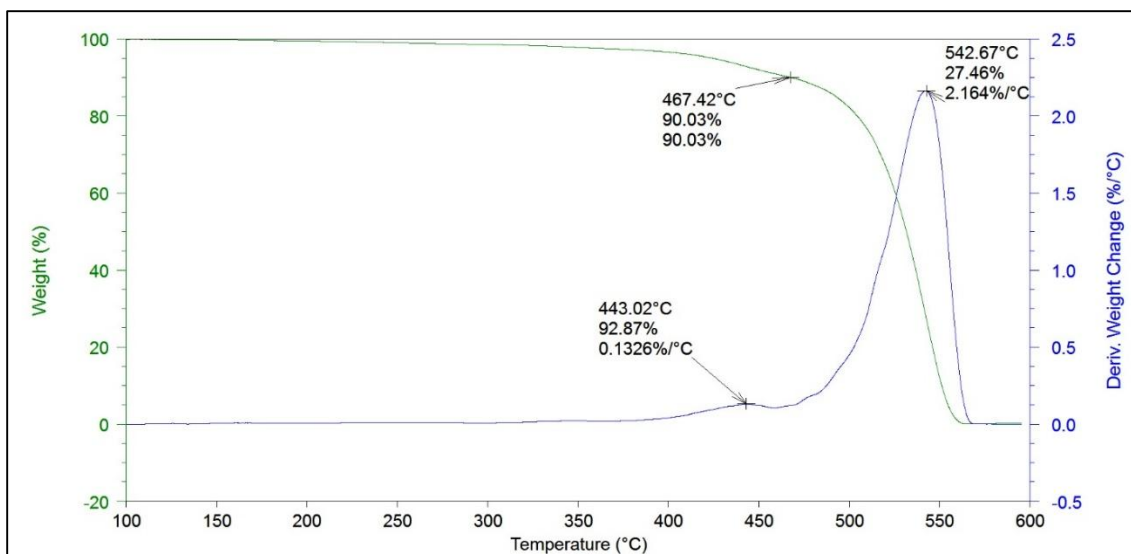


Figure F.14. TGA results for a sample of poly(TFE-co-PSVE) of EW of 1340 g/mol.

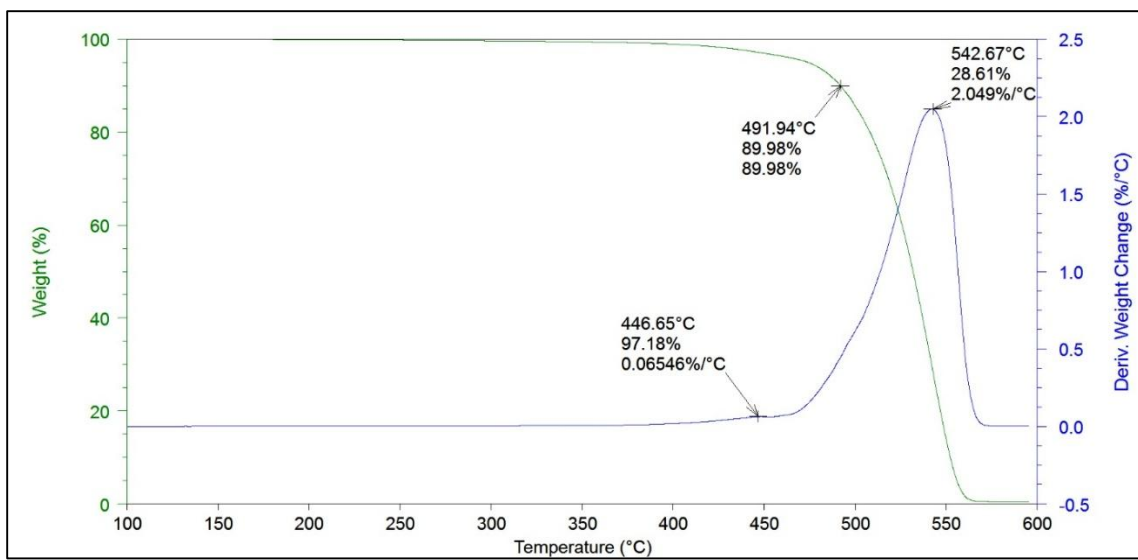


Figure F.15. TGA results for a sample of poly(TFE-co-PSVE) of EW of 1420 g/mol.

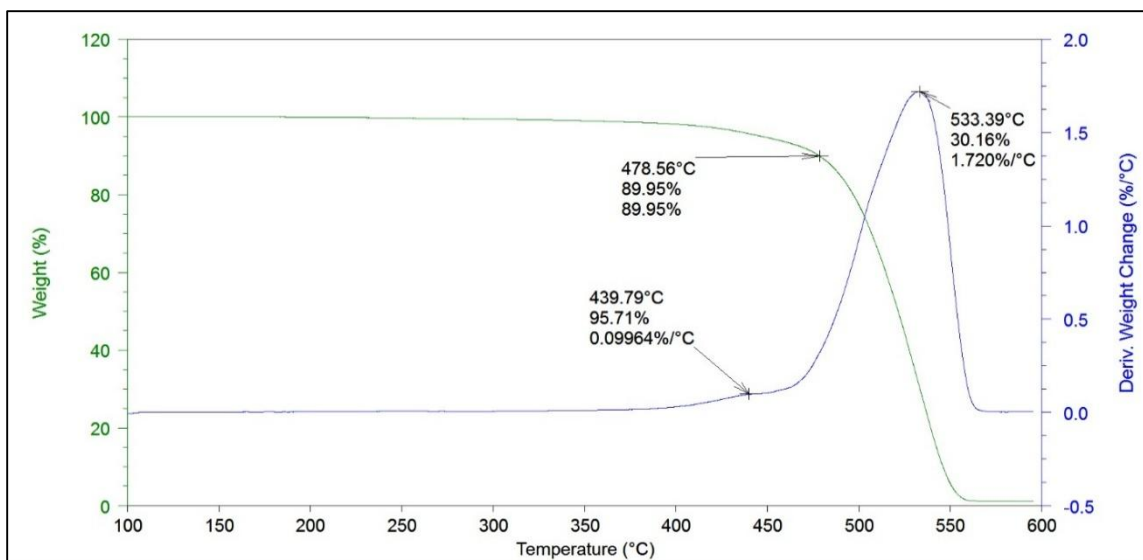


Figure F.16. TGA results for a sample of poly(TFE-co-PSVE) of EW of 1428 g/mol.

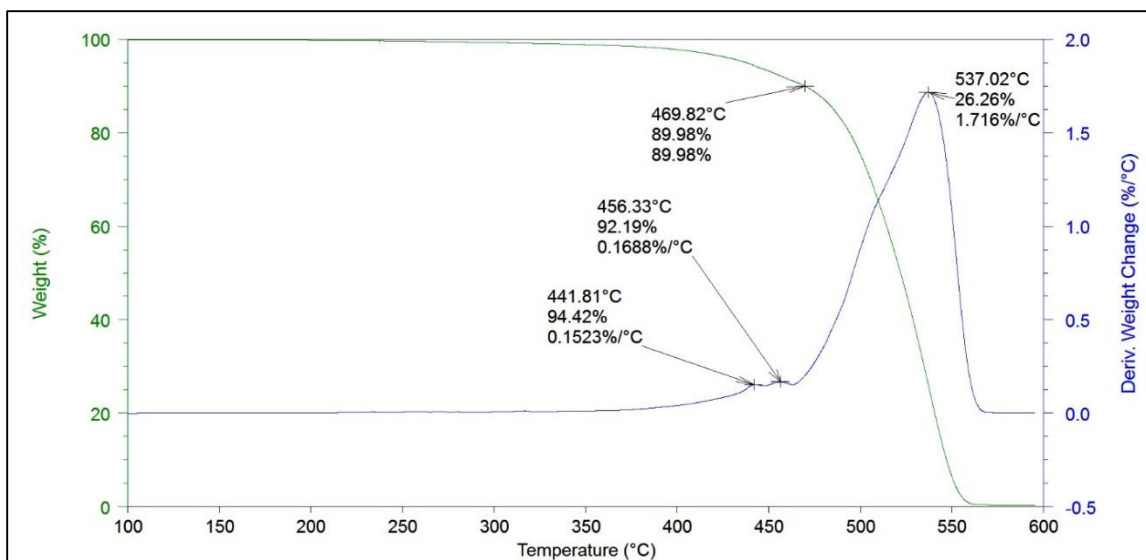


Figure F.17. TGA results for a sample of poly(TFE-co-PSVE) of EW of 1509 g/mol.

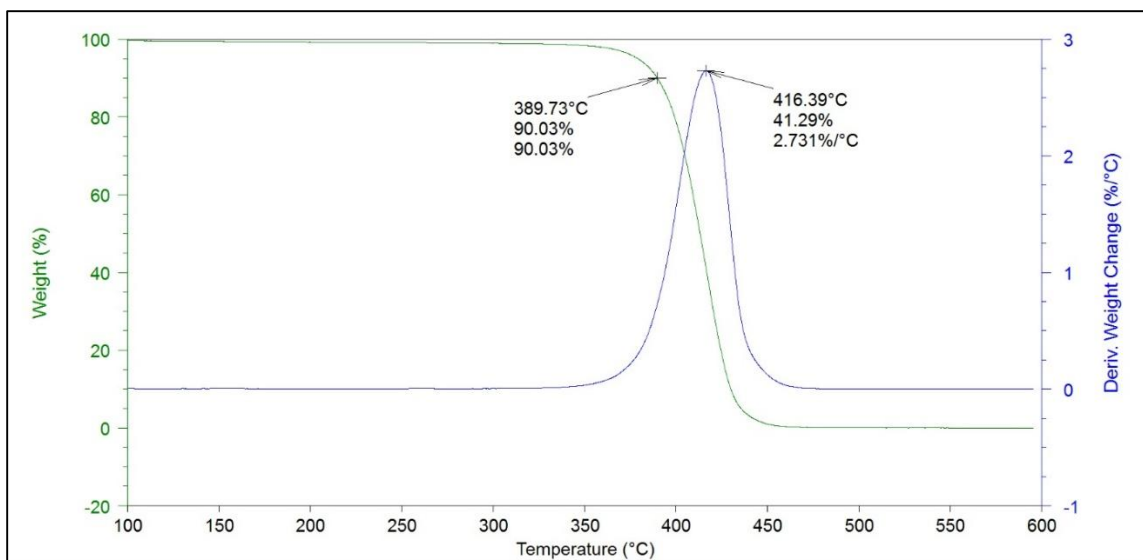


Figure F.18. TGA results for a standard sample of poly(TFE-*co*-PSVE) of EW of 700 g/mol.

F.5. Experimental Results from Polymerization Reactions of poly(TFE-*co*-DEVE).

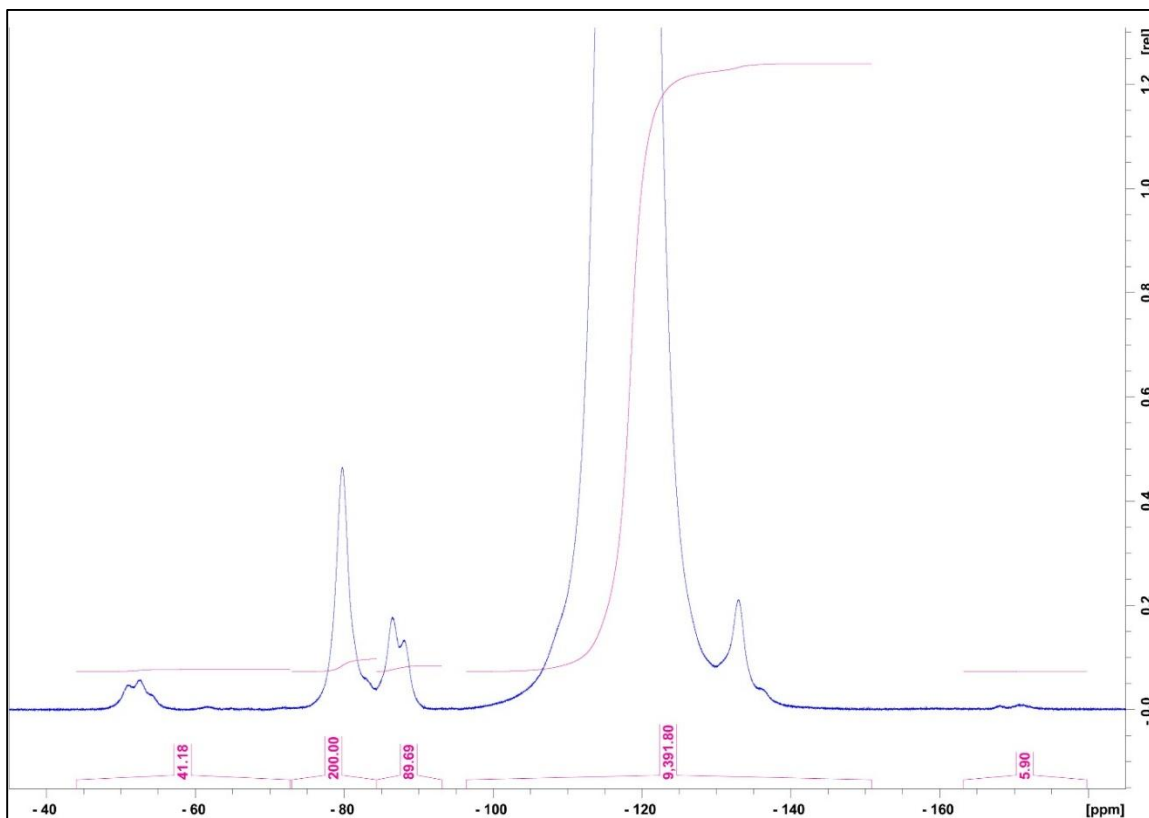


Figure F.19. Fluorine-19 melt NMR spectra of a poly(TFE-*co*-DEVE) sample of a composition of 4.3 mol% of DEVE and 95.7 mol% of TFE.

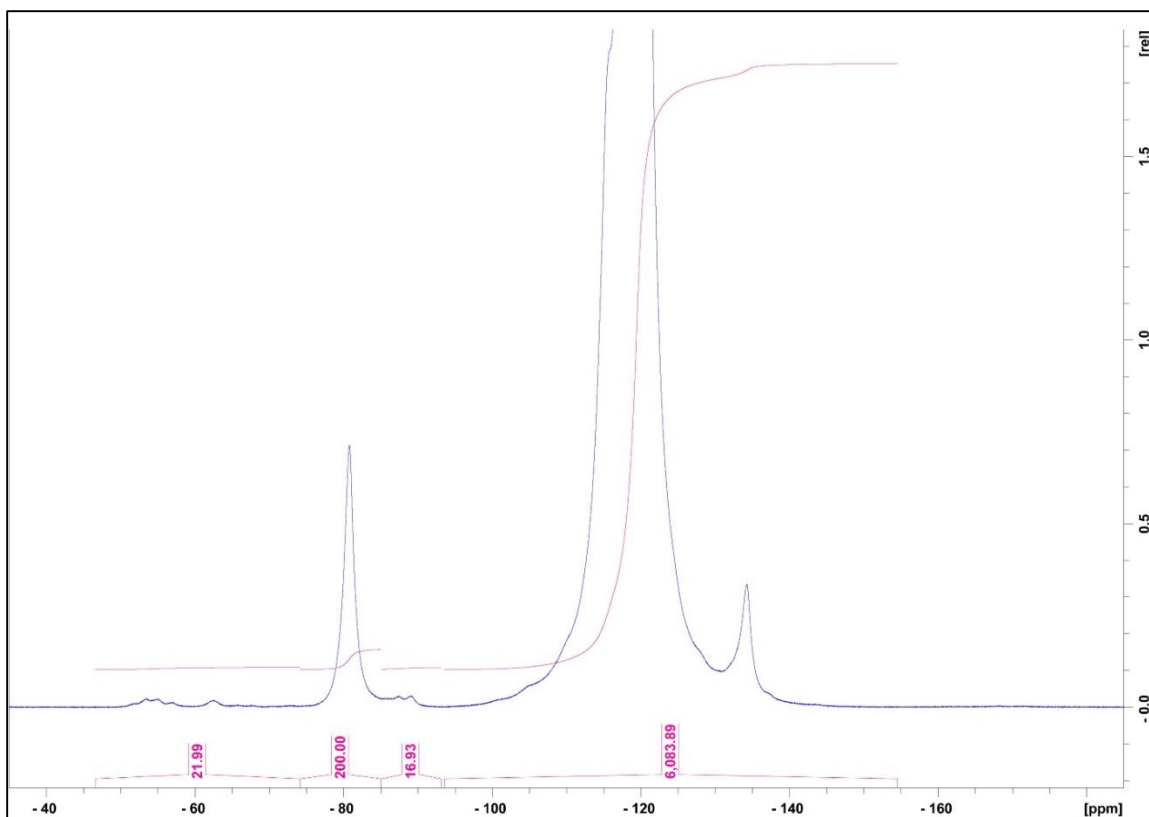


Figure F.20. Fluorine-19 melt NMR spectra of a poly(TFE-*co*-DEVE) sample of a composition of 6.7 mol% of DEVE and 93.3 mol% of TFE.

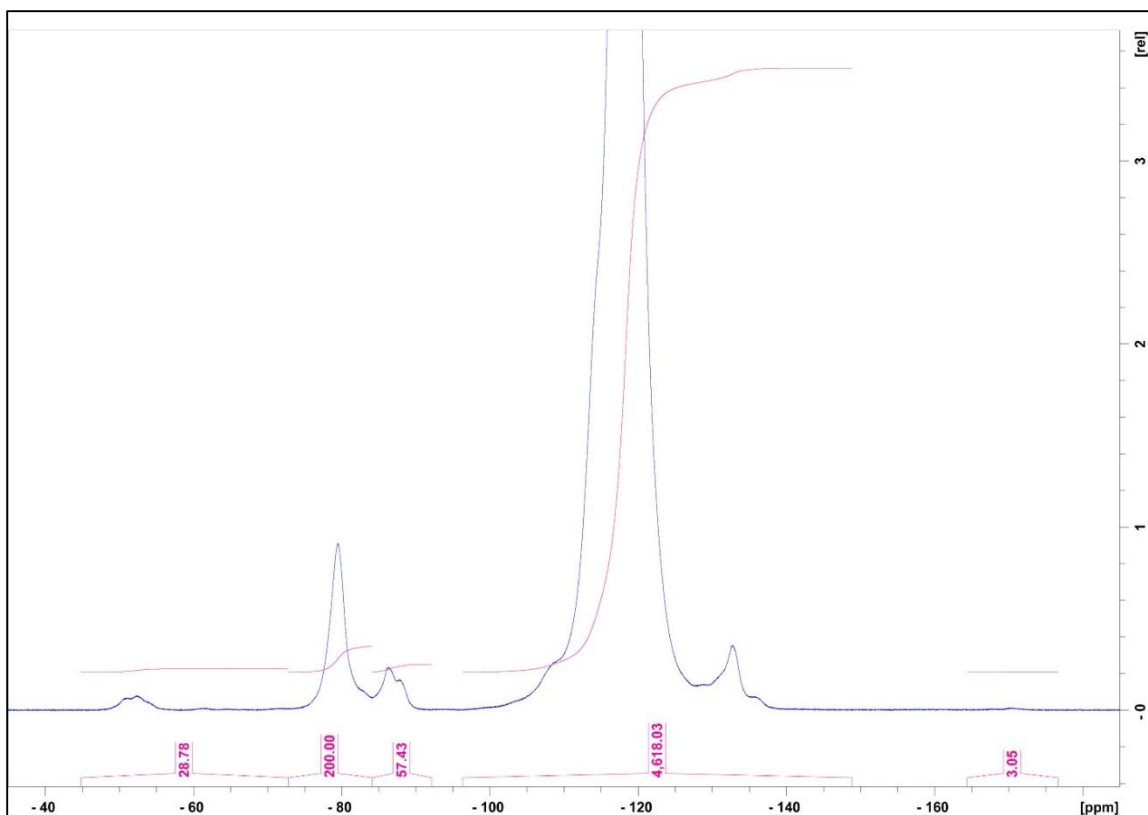


Figure F.21. Fluorine-19 melt NMR spectra of a poly(TFE-*co*-DEVE) sample of a composition of 8.9 mol% of DEVE and 91.1 mol% of TFE.

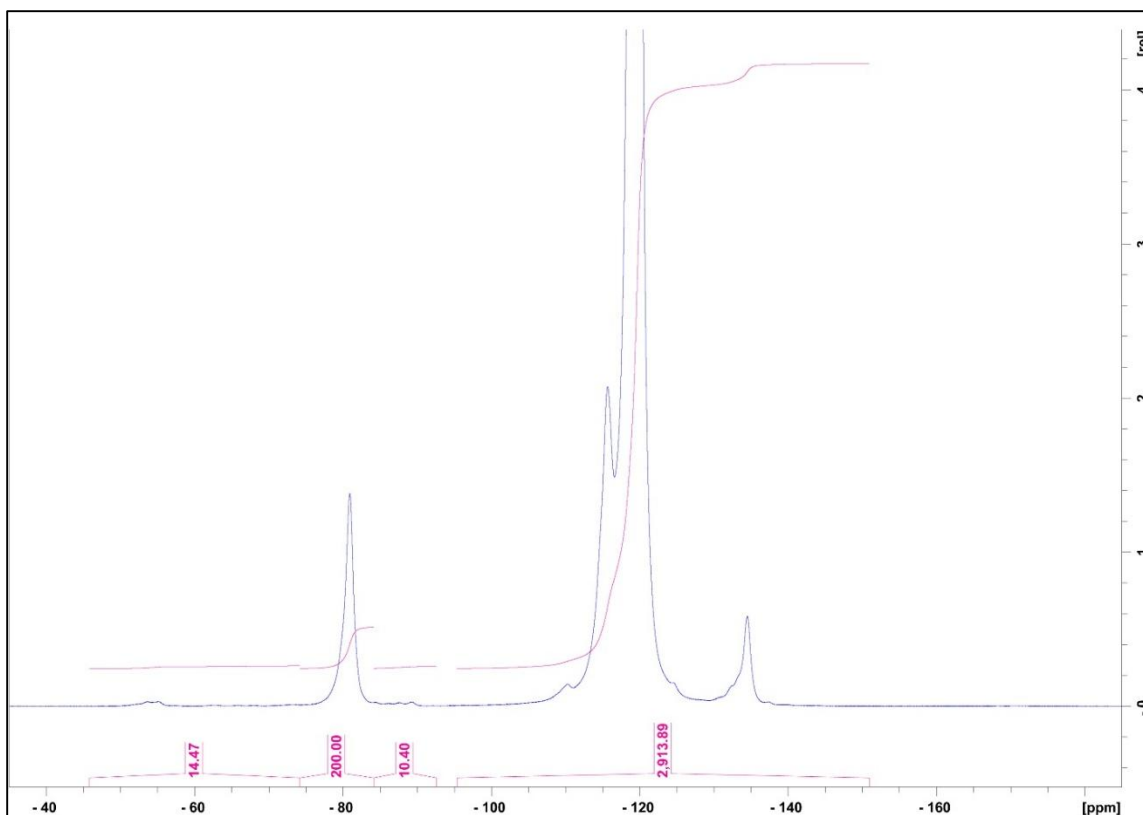


Figure F.22. Fluorine-19 melt NMR spectra of a poly(TFE-*co*-DEVE) sample of a composition of 14.2 mol% of DEVE and 85.8 mol% of TFE.

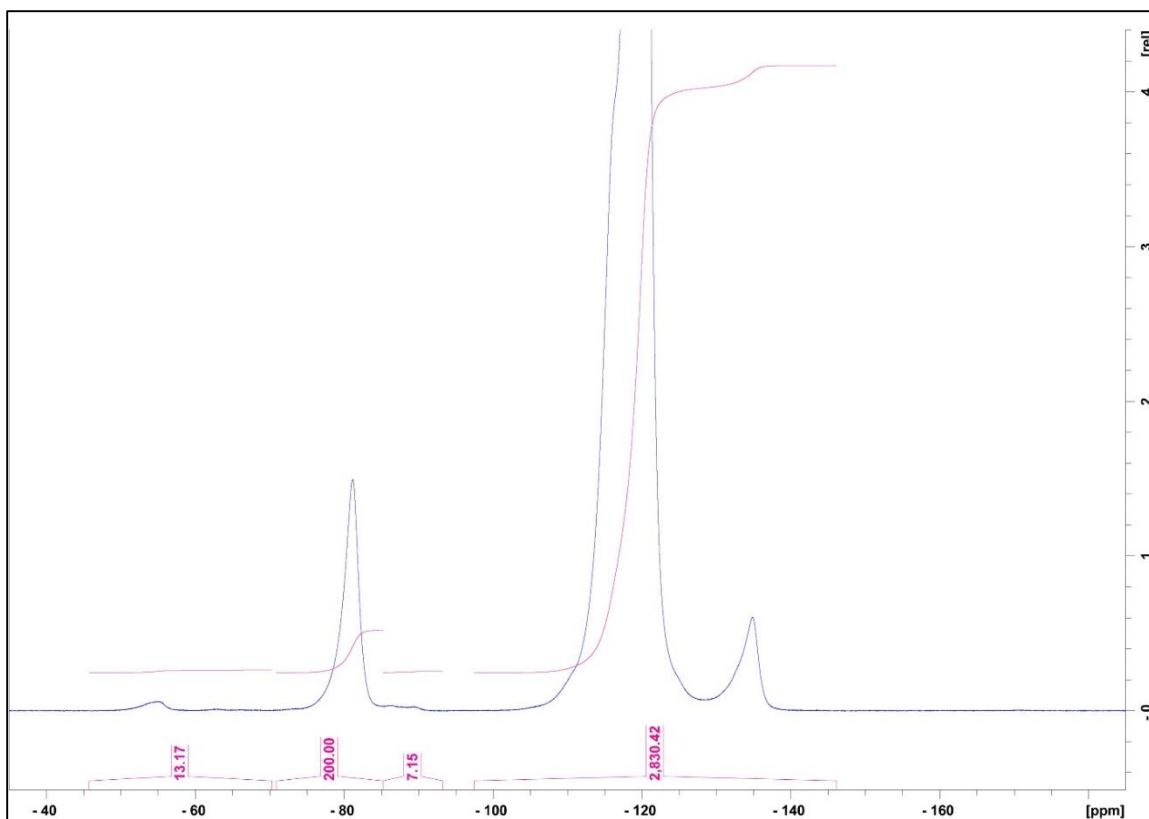


Figure F.23. Fluorine-19 melt NMR spectra of a poly(TFE-*co*-DEVE) sample of a composition of 14.7 mol% of DEVE and 85.3 mol% of TFE.

Table F.7. Calculation of initial composition molar fractions of monomer feed for the preparation of samples of poly(TFE-*co*-DEVE).

Sample	DEVE (g)	DEVE (mol)	TFE (SL)	TFE (mol)	Molar fraction of DEVE	Molar fraction of TFE
4	62	0.242	3.9	0.174	0.582	0.418
8	62	0.242	2.5	0.112	0.685	0.315
5	33	0.129	6.6	0.295	0.304	0.696
6	60	0.234	5.4	0.241	0.493	0.507
7	60	0.234	2.3	0.103	0.695	0.305

Table F.8. Final composition

Sample	Int A	Int B	DEVE (mol%)	TFE (mol%)	DEVE (molar fraction)	TFE (molar fraction)
A	200	4618	8.9	91.1	0.089	0.91
B	200	9391	4.3	95.7	0.043	0.96
C	200	6083	6.7	93.3	0.067	0.93
D	200	2913	14.2	85.8	0.142	0.86
E	200	2830	14.7	85.3	0.147	0.85

Note: Int A and Int B are the integration constants obtained for the regions A and B of the fluorine-19 NMR spectra for the samples of poly(TFE-*co*-DEVE). Int A corresponds to the range of -75 to -85 ppm and Int B range is -90 to -155 ppm. Sample A was ran at 290 °C, B at 290 °C, C at 255 °C, D at 250 °C, and E at 240 °C accordingly to the thermal data (TGA and DSC) supplied to Chemours.

The general formula of the DEVE monomer is $\text{CF}_2^{\text{a}}=\text{CF}^{\text{b}}-\text{O}-\text{CF}_2^{\text{c}}\text{CF}_2^{\text{d}}\text{C}(\text{O})\text{OCH}_3$.

Int A value covers the fluorines marked as “c” while Int B covers the fluorines marked as “a”, “b”, “d” and the 4 fluorines from the TFE monomer. The formula used to calculate the mol% of each monomer in the final composition of the copolymer are detailed below. First a constant value for the number of fluorines from DEVE and TFE should be calculated (n_{DEVE} and n_{TFE} respectively) and then a percentage ratio of both of them can be calculated.

$$n_{\text{DEVE}} = \frac{\text{Int A}}{2}$$

$$n_{\text{TFE}} = \frac{\text{Int B} - (5)(\text{Int A}/2)}{4}$$

$$\text{DEVE (mol\%)} = \frac{n_{\text{DEVE}} \times 100}{n_{\text{DEVE}} + n_{\text{TFE}}}$$

$$TFE \text{ (mol\%)} = \frac{nTFE \times 100}{nDEVE + nTFE}$$

Table F.9. Fineman and Ross parameters used to calculate the relative reactivity ratios of DEVE and TFE in the samples of poly(TFE-co-DEVE) obtained experimentally.

Sample	Initial Feed SL (molar fraction)		Copolymer Composition (molar fraction)		X	Y	G	H
	DEVE	TFE	DEVE	TFE				
A	0.58	0.42	0.09	0.91	0.72	10.24	0.65	0.05
B	0.70	0.30	0.04	0.96	0.43	24.00	0.41	0.01
C	0.49	0.51	0.07	0.93	1.03	13.93	0.95	0.08
D	0.70	0.30	0.14	0.86	0.44	6.04	0.37	0.03
E	0.68	0.32	0.15	0.85	0.46	5.80	0.38	0.04

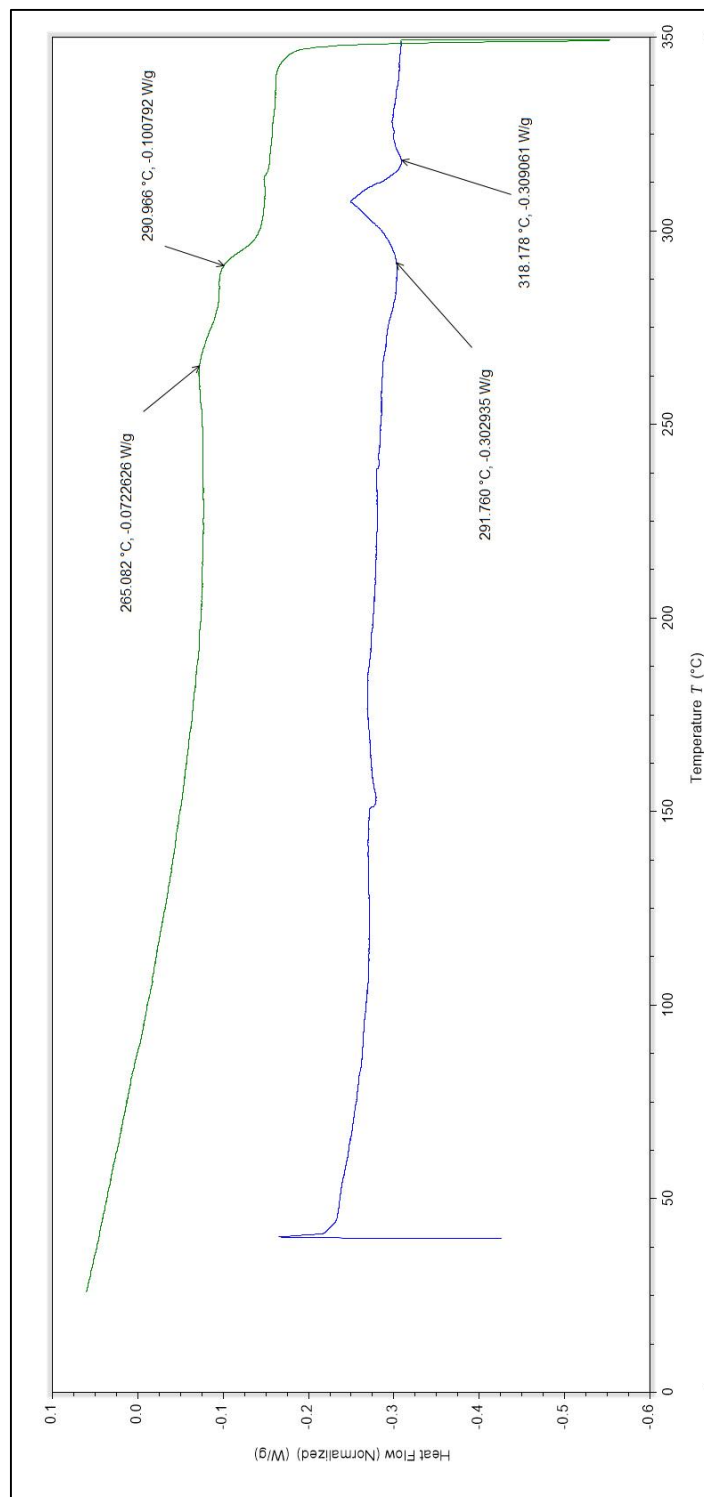


Figure F.24. DSC thermogram of a sample name "A" of poly(TFE-co-DEVE).

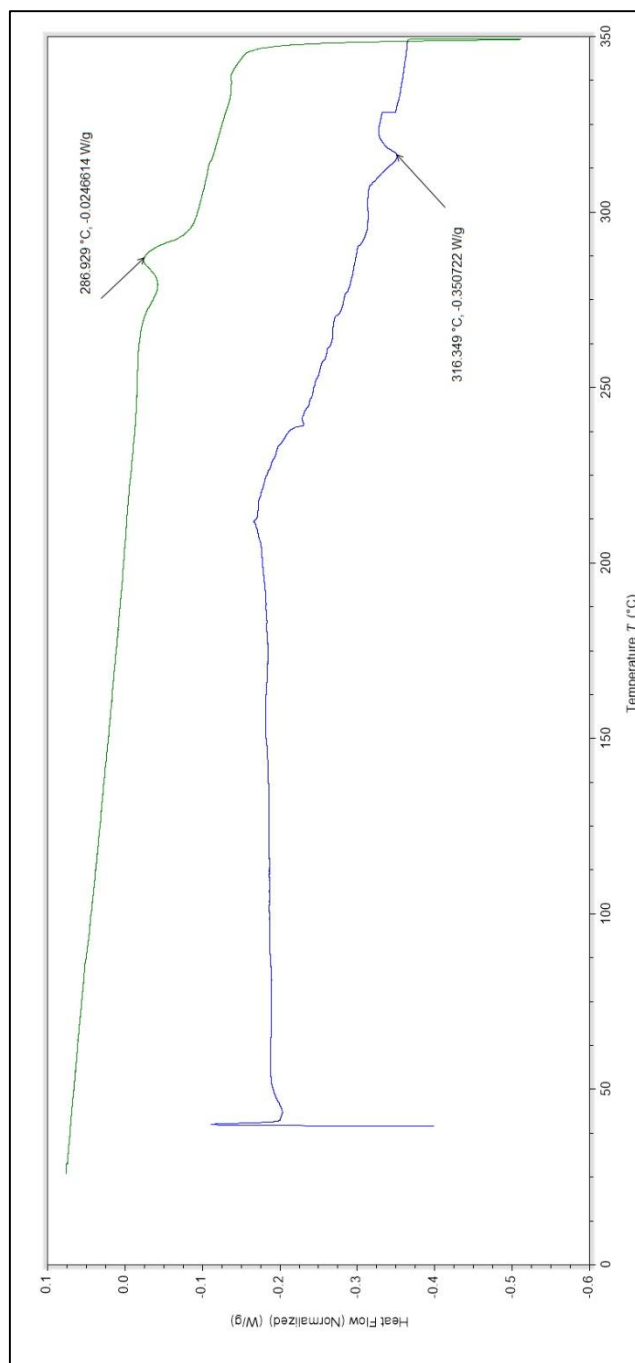


Figure F.25. DSC thermogram of a sample name “B” of poly(TFE-*co*-DEVE).

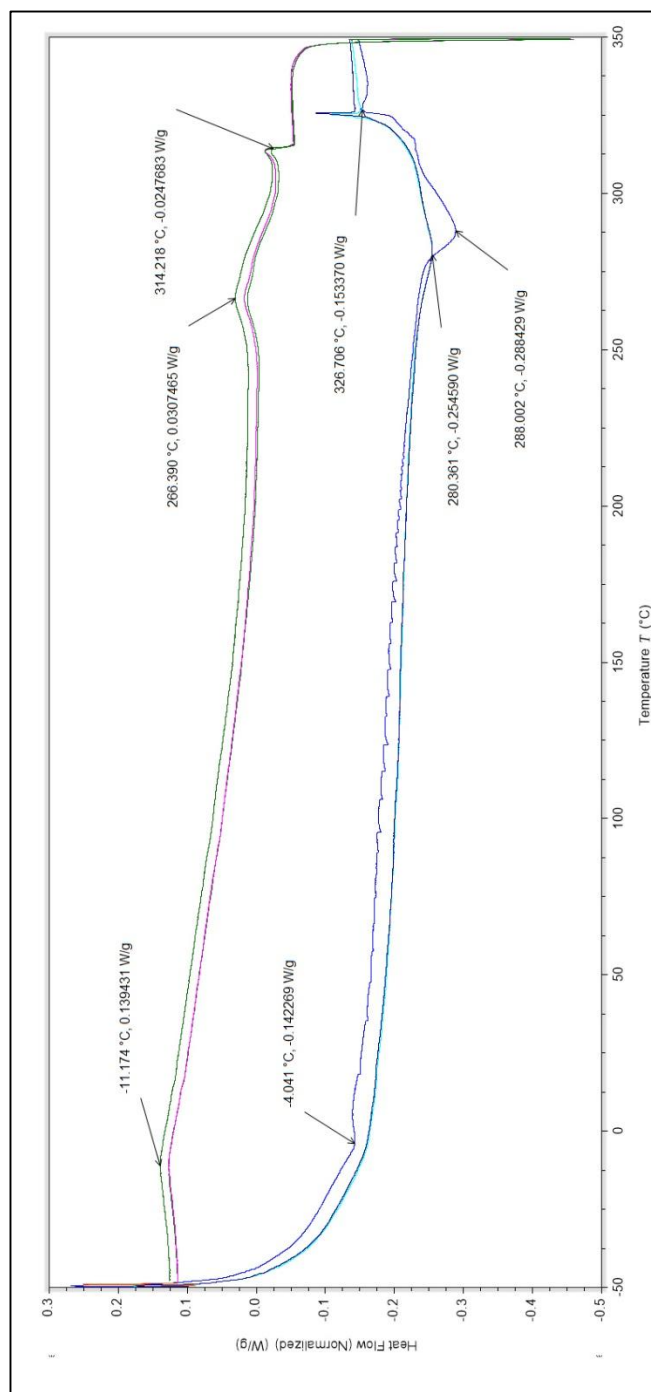


Figure F.26. DSC thermogram of a sample name “C” of poly(TFE-*co*-DEVE).

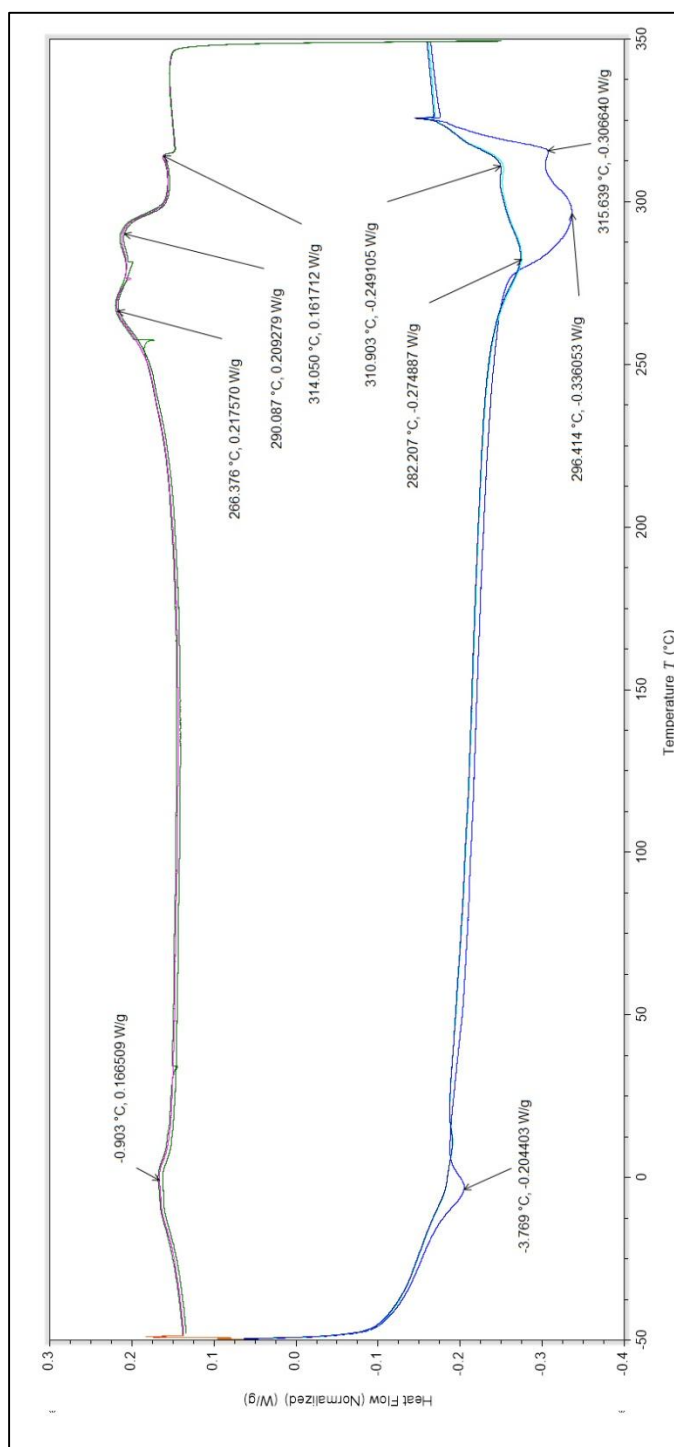


Figure F.27. DSC thermogram of a sample name “D” of poly(TFE-*co*-DEVE).

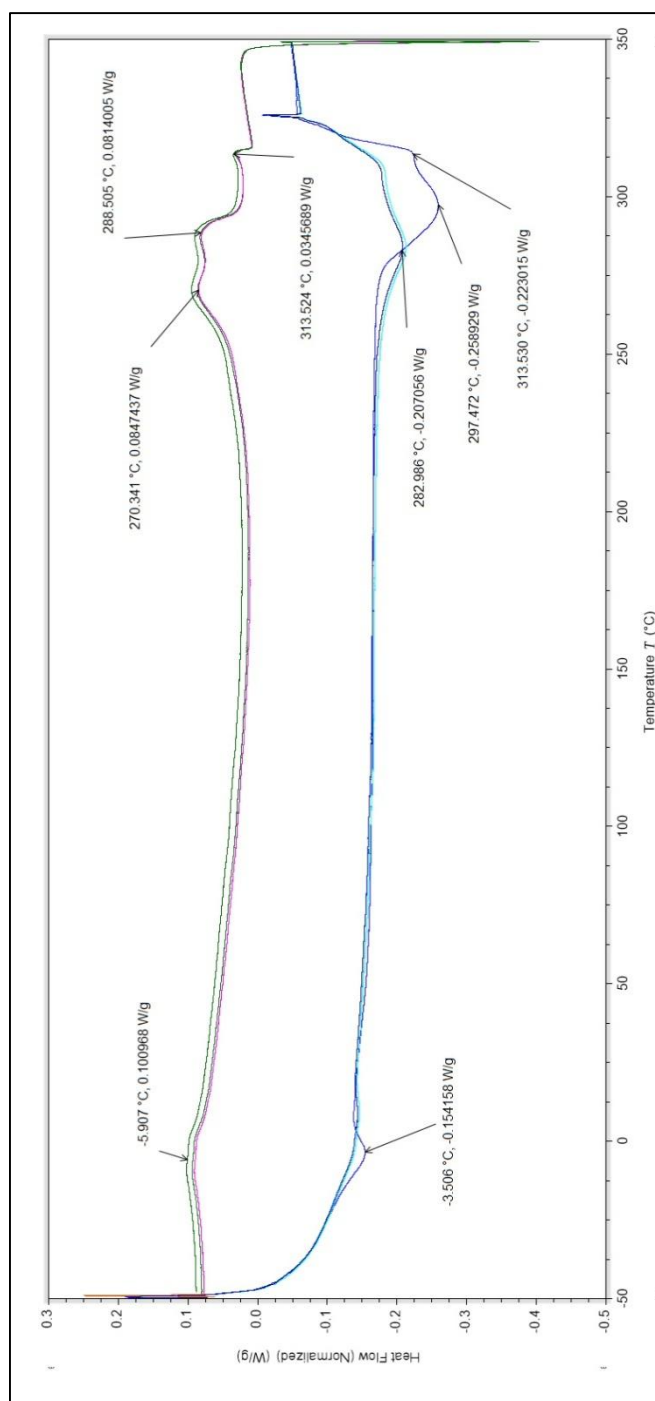


Figure F.28. DSC thermogram of a sample name “E” of poly(TFE-*co*-DEVE).

F.5. Fluorine-19 NMR Characterization of PSEPVE, PSVE, DEVE and 8-CNVE Monomers.

All the monomers were characterized via fluorine-19 NMR spectroscopy using a JEOL 300 MHz NMR spectrometer. The transients were recorded at 15 Hz and room temperature. Monomers were dissolved in deuterated acetonitrile, and CFCl_3 and TMS were used as the internal standards.

F.5.1. Fluorine-19 NMR spectrum of PSEPVE.

The formula of PSEPVE is $\text{CF}_2^{\text{aa}'}=\text{CF}^{\text{b}}-\text{O}-\text{CF}_2^{\text{c}}-\text{CF}^{\text{d}}(\text{CF}_3^{\text{e}})-\text{O}-\text{CF}_2^{\text{f}}-\text{CF}_2^{\text{g}}-\text{SO}_2\text{F}^{\text{h}}$ and its chemical name is perfluoro-2-(2-fluorosulfonylethoxy) propyl vinyl ether. Fluorine-19 NMR recorded neat: δ_{a} -118.3 (dd, $J_{\text{aa}'} = 86.9$ Hz, $J_{\text{ab}} = 66.4$ Hz, 1F), $\delta_{\text{a}'}$ -125.9 (dd, $J_{\text{a}'\text{b}} = 111.5$ Hz, $J_{\text{a}'\text{a}} = 86.1$ Hz, 1F), δ_{b} -139.9 (dd, $J_{\text{ba}'} = 111.5$ Hz, $J_{\text{ba}} = 67.2$ Hz, 1F), δ_{c} -82.5 (m, 2F), δ_{d} -147.6 (t, $J_{\text{d}} = 22.9$ Hz, 1F), δ_{e} -83.6 (m, 3F), δ_{f} -88.1 (m, 2F), δ_{g} -115.8 (s, 2F), δ_{h} 41.5 (s, 1F).

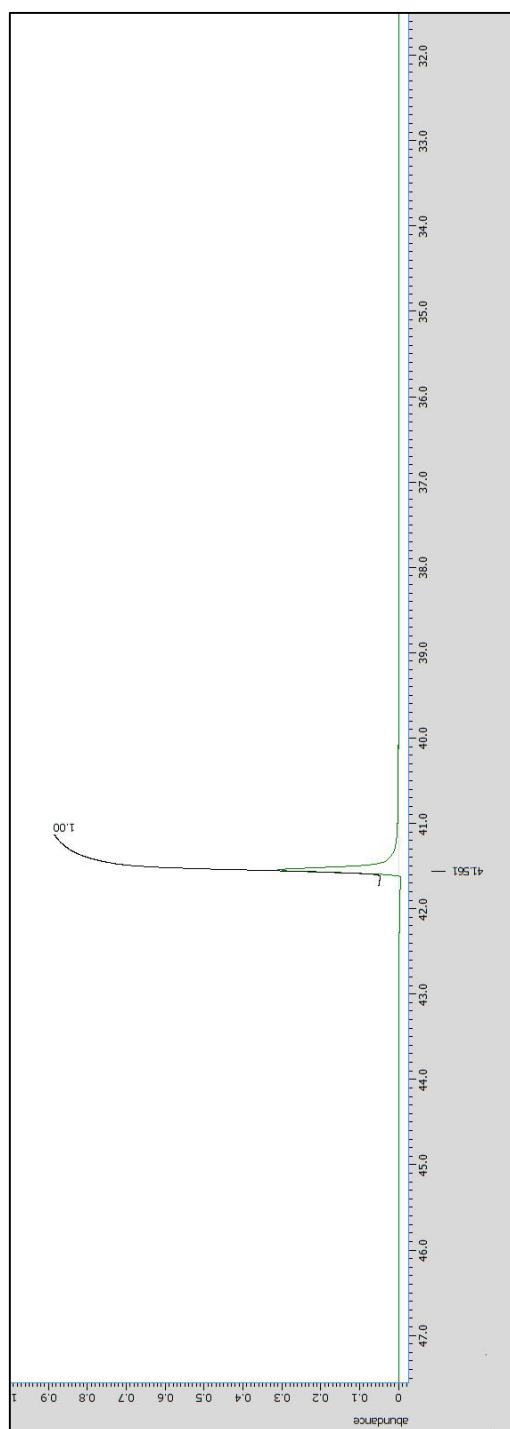


Figure F.29. Fluorine-19 NMR spectra (1 of 3 views) of PSEPVE recorded neat.

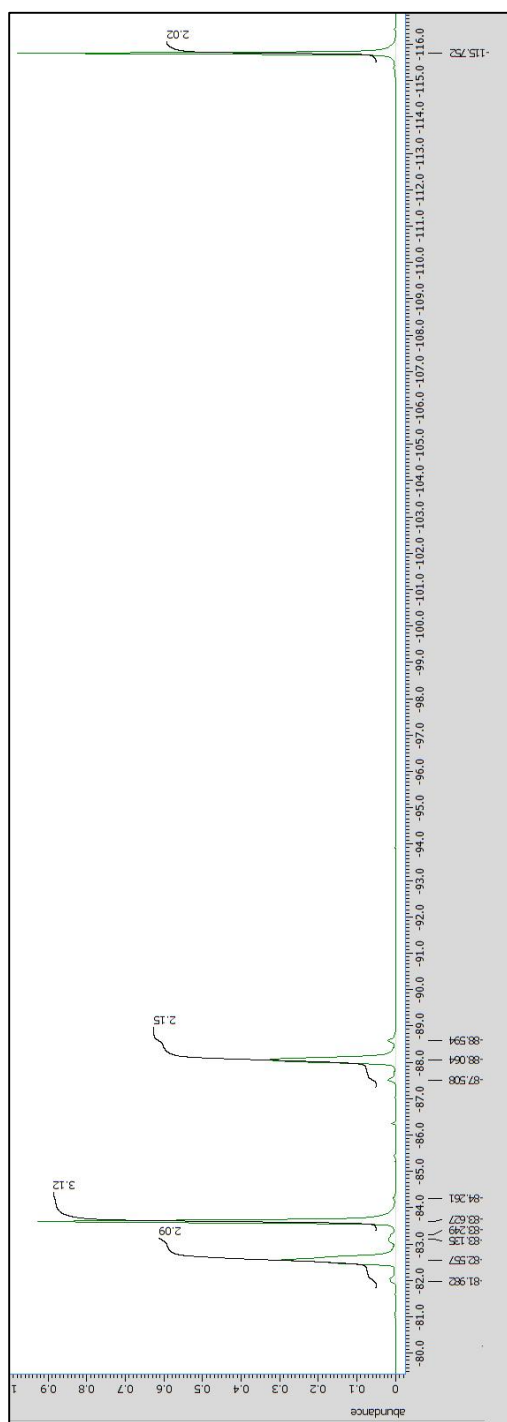
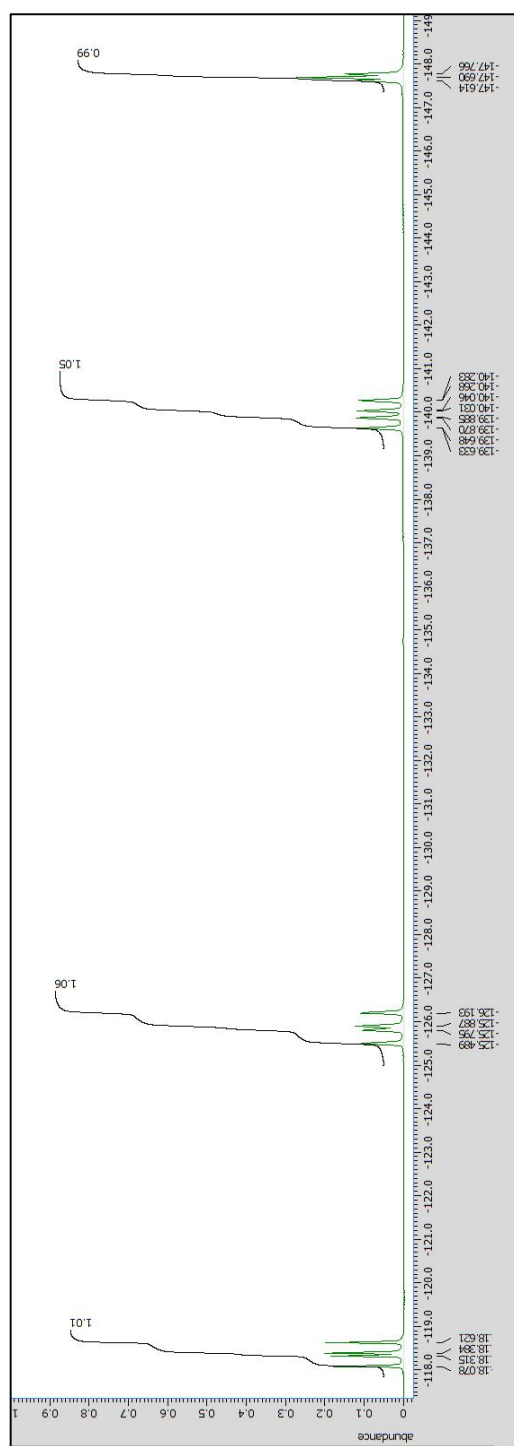


Figure F.30. Fluorine-19 NMR spectra (2 of 3 views) of PSEPVE recorded neat.



F.5.2. Fluorine-19 NMR spectrum of PSVE.

The formula of PSVE is $\text{CF}_2^{\text{aa}'}=\text{CF}^{\text{b}}-\text{O}-\text{CF}_2^{\text{c}}-\text{CF}_2^{\text{d}}-\text{SO}_2\text{F}^{\text{e}}$ and its chemical name is perfluoro(3-oxa-4-pentene)sulfonyl fluoride. Fluorine-19 NMR recorded neat: $\delta_{\text{a}} -113.4$ (dd, $J_{\text{aa}'} = 82.0$ Hz, $J_{\text{ab}} = 67.2$ Hz, 1F), $\delta_{\text{a}'} -120.0$ (dd, $J_{\text{a'b}} = 113.1$, $J_{\text{a'a}} = 85.2$, 1F), $\delta_{\text{b}} -136.4$ (ddt, $J_{\text{ba}'} = 111.5$ Hz, $J_{\text{ba}} = 67.2$ Hz, $J_{\text{bc}} = 6.54$ Hz, 1F), $\delta_{\text{c}} -83.5$ (m, 2F), $\delta_{\text{d}} -111.6$ (m, 1F), $\delta_{\text{e}} 45.3$ (s, 1F).

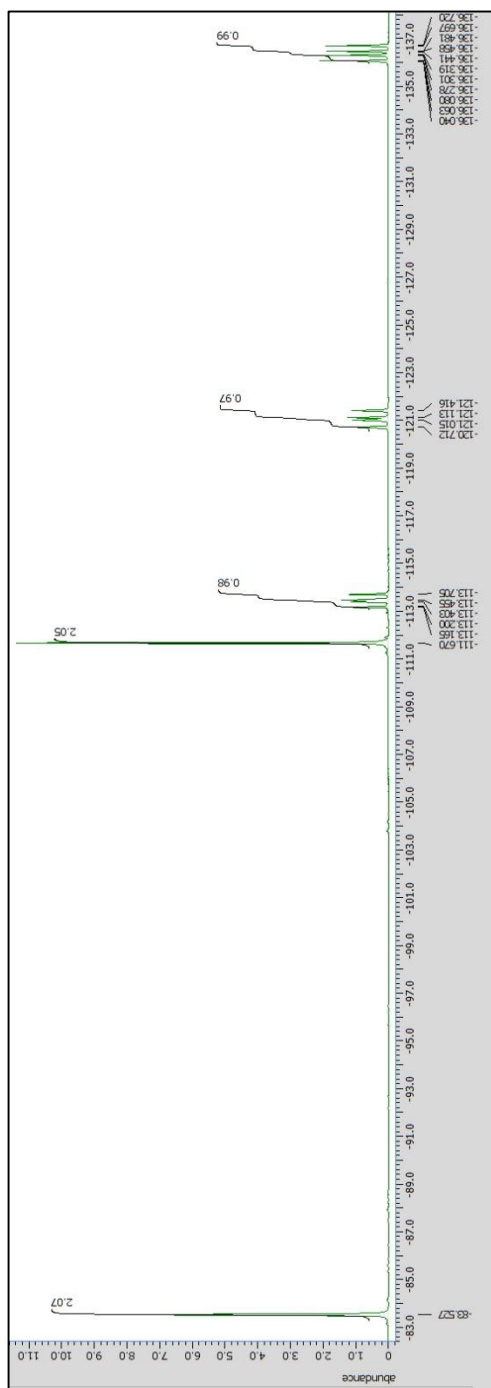


Figure F.32. Fluorine-19 NMR spectra (1 of 4 views) of PSVE recorded neat.

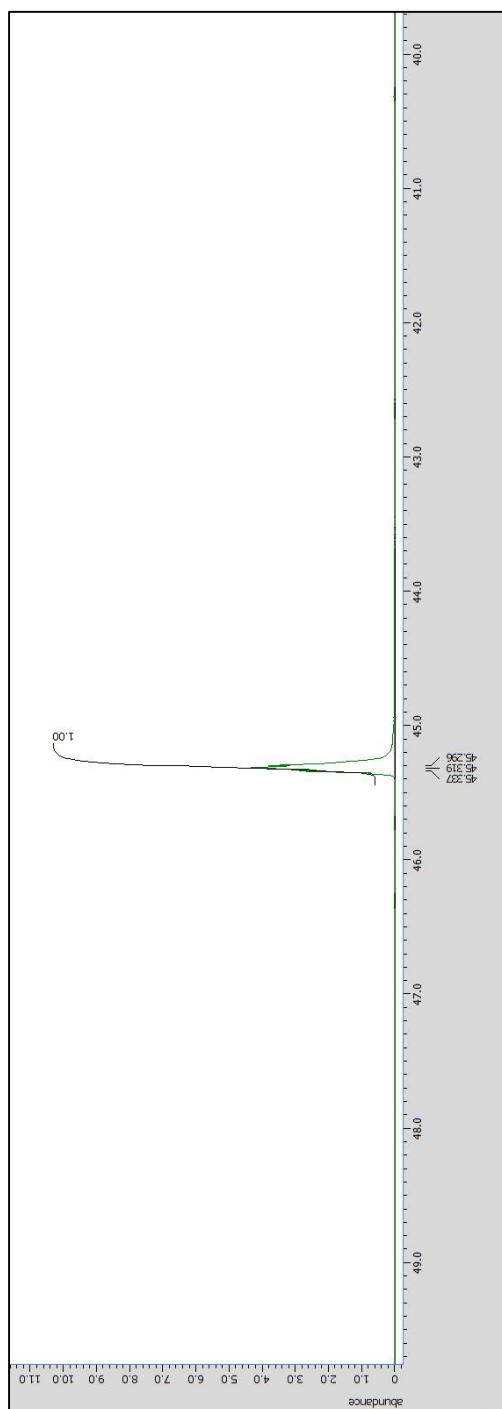
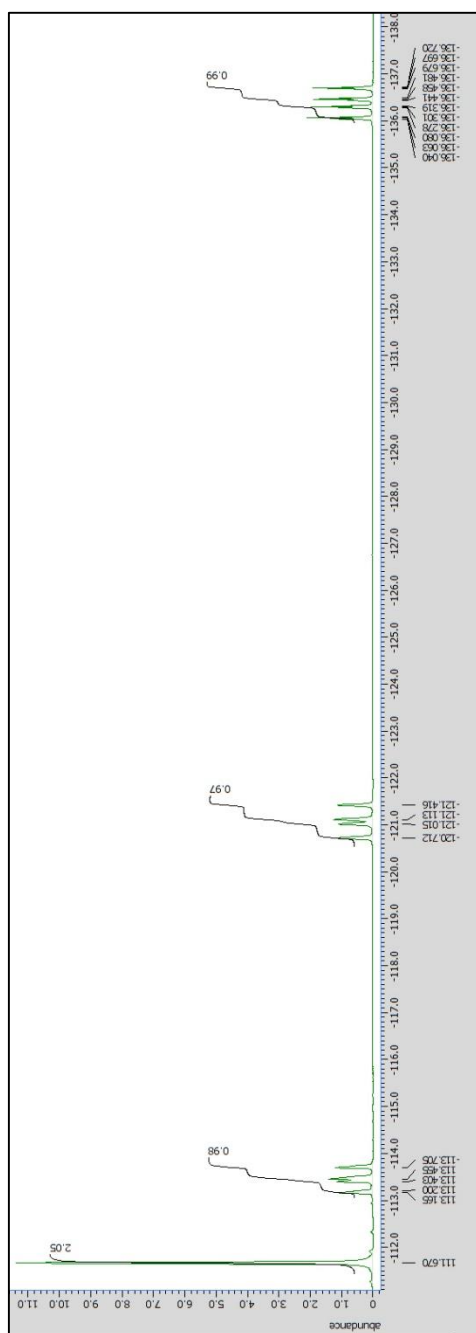


Figure F.33. Fluorine-19 NMR spectra (2 of 4 views) of PSVE recorded neat.



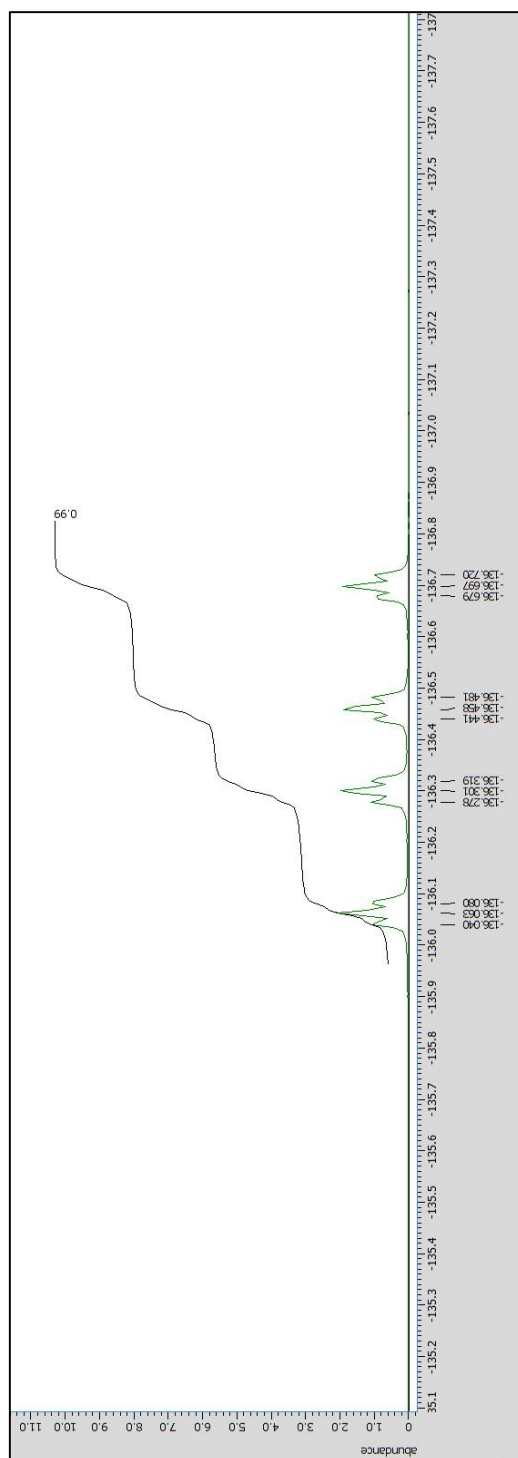


Figure F.35. Fluorine-19 NMR spectra (3 of 4 views) of PSVE recorded neat.

F.5.3. Fluorine-19 and Hydrogen-1 NMR spectrum of DEVE.

The formula of DEVE is $\text{CF}_2^{\text{aa}'}=\text{CF}^{\text{b}}-\text{O}-\text{CF}_2^{\text{c}}-\text{CF}_2^{\text{d}}-\text{C}(\text{O})\text{OCH}_3^{\text{e}}$ and its chemical name is methyl perfluoro-(3-oxa-4-hexenoate). Fluorine-19 NMR recorded in CD_3CN : δ_{a} -114.4 (dd, $J_{\text{aa}'} = 84.6$ Hz, $J_{\text{ab}} = 65.1$ Hz, 1F), $\delta_{\text{a}'}$ -122.3 (ddt, $J_{\text{a}'\text{b}} = 111.1$, $J_{\text{a}'\text{a}} = 103.2$, $J_{\text{a}'\text{c}} = 5.0$ Hz, 1F), δ_{b} -135.4 (ddt, $J_{\text{ba}'} = 111.1$ Hz, $J_{\text{ba}} = 64.2$ Hz, $J_{\text{bc}} = 6.48$ Hz, 1F), δ_{c} -87.1 (s, 2F), δ_{d} -121.2 (s, 1F), δ_{e} 3.98 (s, 3H).

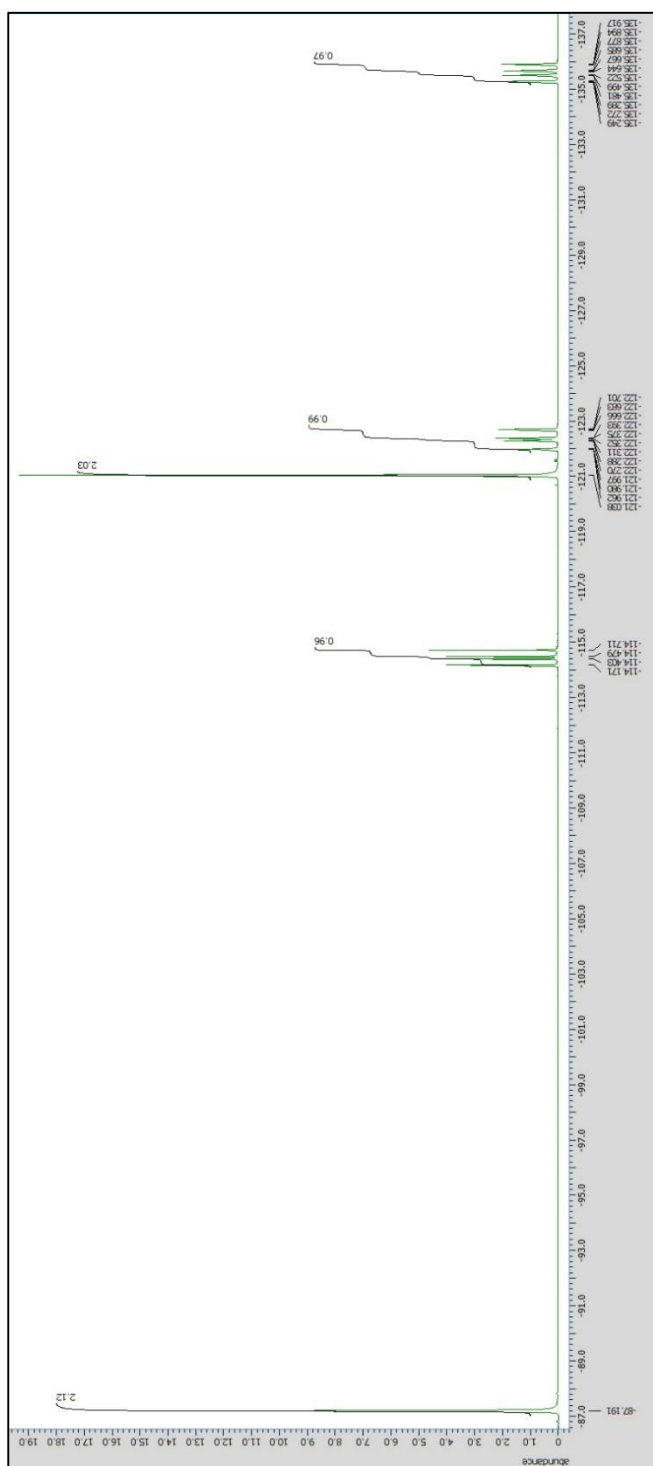
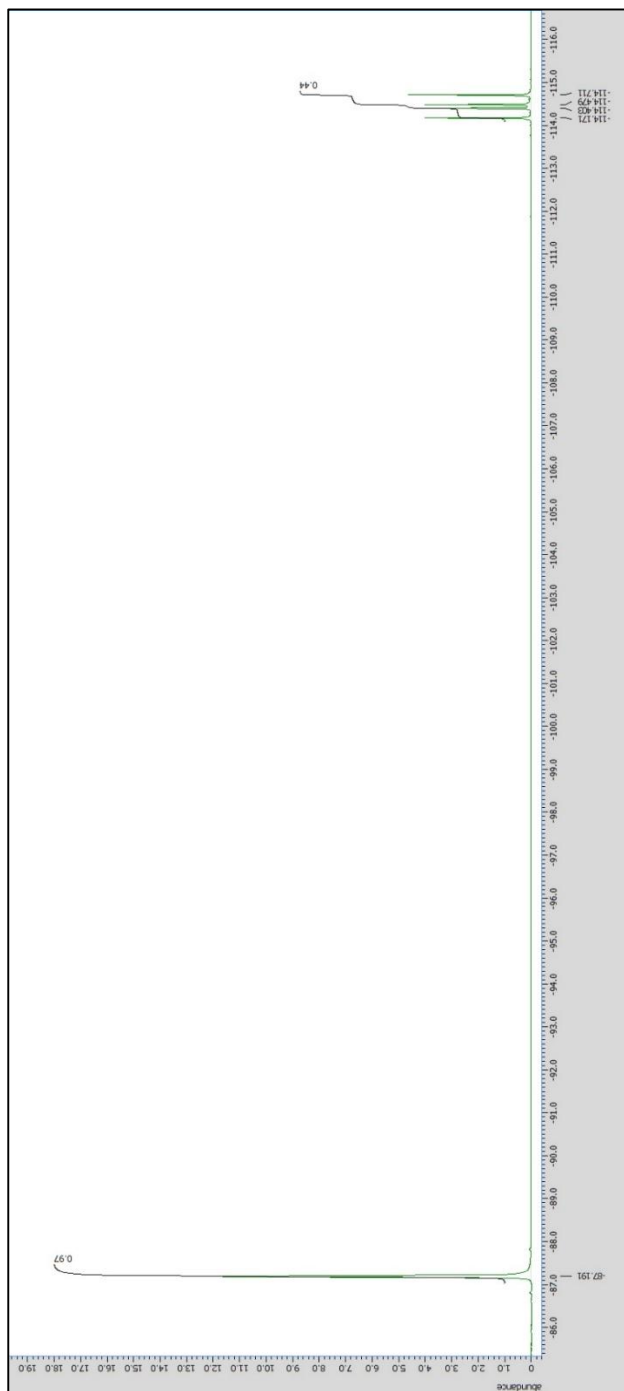


Figure F.36. Fluorine-19 NMR spectra (1 of 3 views) of DEVE recorded in CD₃CN.



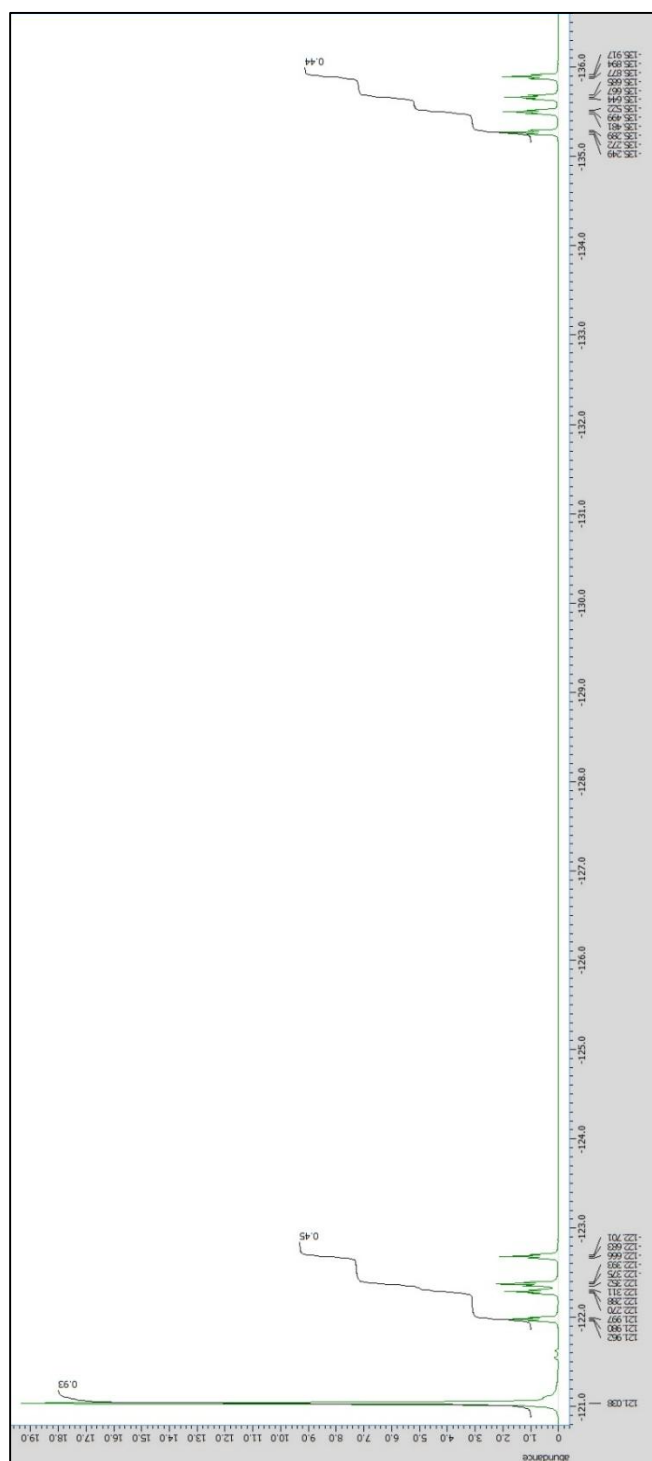


Figure F.38. Fluorine-19 NMR spectra (3 of 3 views) of DEVE recorded in CD_3CN .

F.5.4. Fluorine-19 NMR spectrum of 8-CNVE.

The formula of 8-CNVE is $\text{CF}_2^{\text{aa}'}=\text{CF}^{\text{b}}-\text{O}-\text{CF}_2^{\text{c}}-\text{CF}^{\text{d}}(\text{CF}_3^{\text{e}})-\text{O}-\text{CF}_2^{\text{f}}-\text{CF}_2^{\text{g}}-\text{CN}$ and its chemical name is perfluoro-(8-cyano-5-methyl-3,6-dioxo-1-octene). Fluorine-19 NMR recorded neat: $\delta_{\text{a}} -114.4$ (dd, $J_{\text{aa}'} = 86.9$ Hz, $J_{\text{ab}} = 66.4$ Hz, 1F), $\delta_{\text{a}'} -121.9$ (dd, $J_{\text{a}'\text{b}} = 111.5$ Hz, $J_{\text{a}'\text{a}} = 85.2$ Hz, 1F), $\delta_{\text{b}} -136.2$ (dd, $J_{\text{ba}'} = 111.5$ Hz, $J_{\text{ba}} = 62.9$ Hz, 1F), $\delta_{\text{c,f}} -84.1$ (m, 4F), $\delta_{\text{d}} -144.0$ (t, $J_{\text{d}} = 21.3$ Hz, 1F), $\delta_{\text{e}} -79.9$ (m, 3F), $\delta_{\text{g}} -108.1$ (s, 2F).

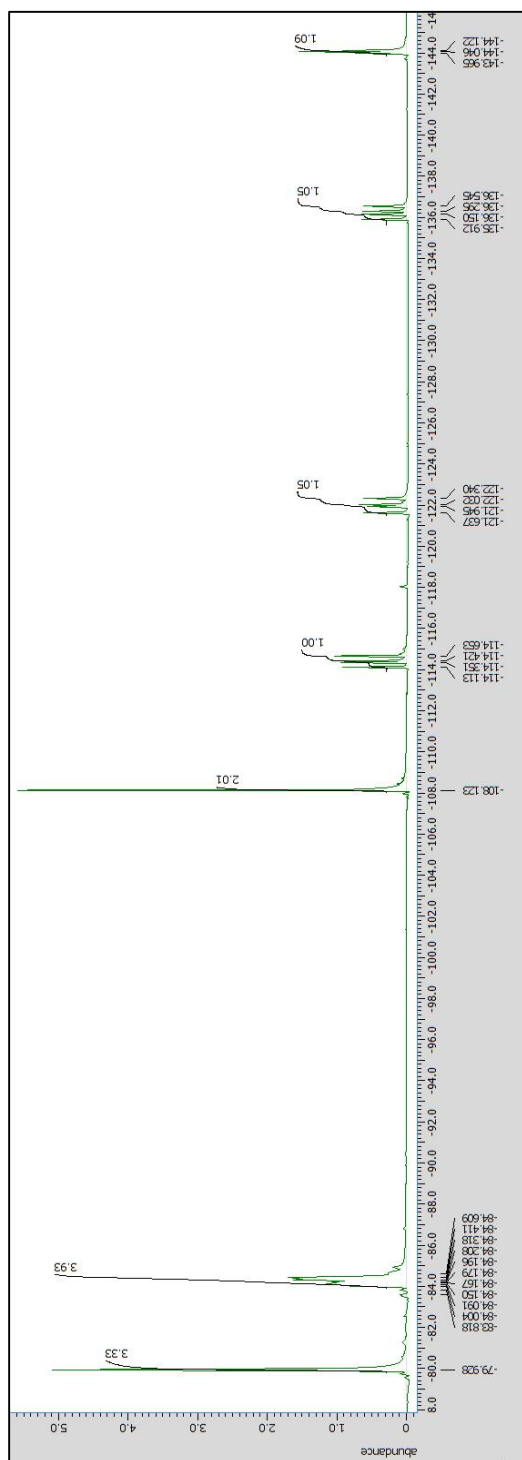


Figure F.39. Fluorine-19 NMR spectra (1 of 4 views) of 8-CNVE recorded neat.

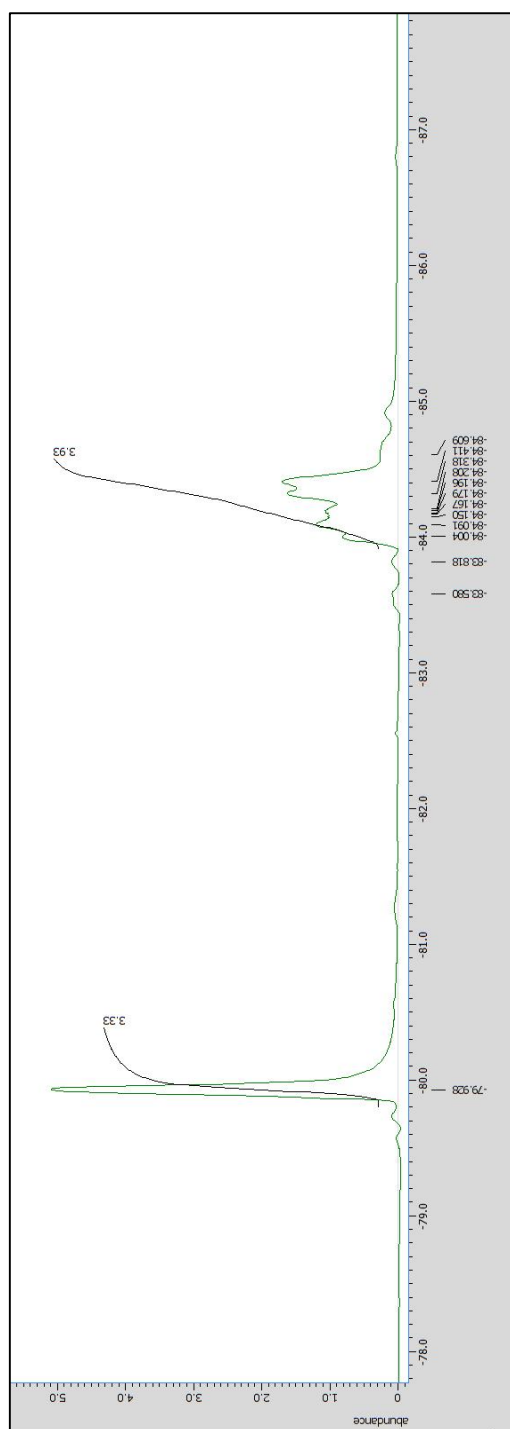


Figure F.40. Fluorine-19 NMR spectra (2 of 4 views) of 8-CNVE recorded neat.

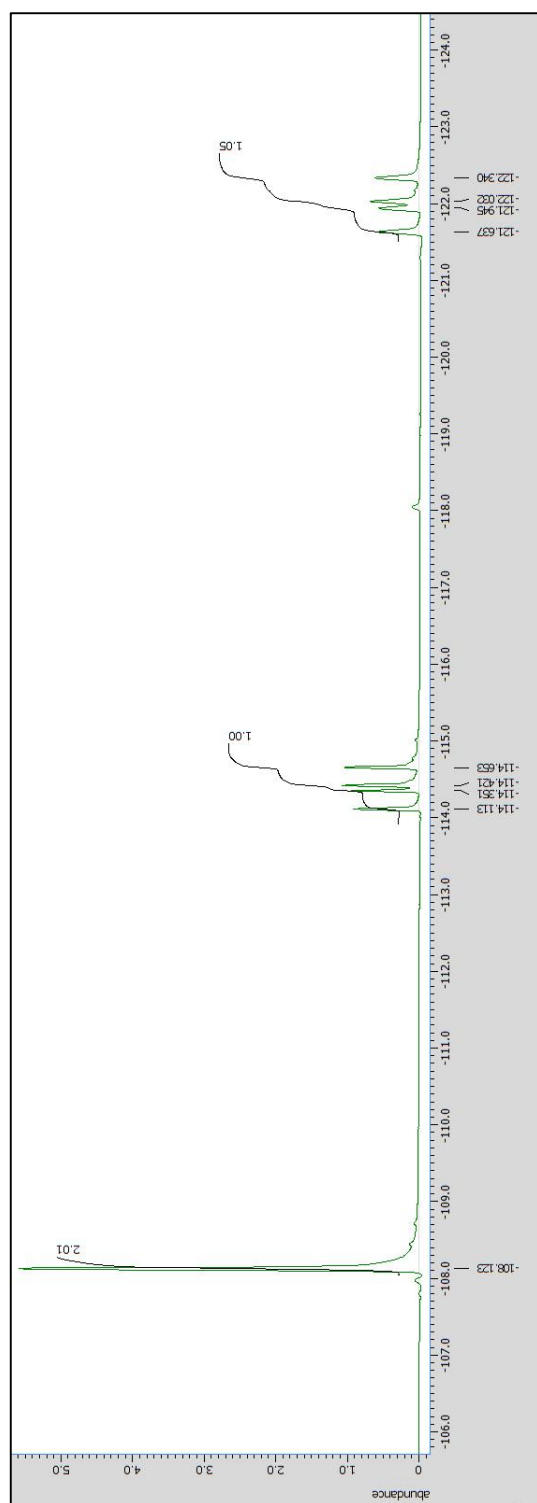


Figure F.41. Fluorine-19 NMR spectra (3 of 4 views) of 8-CNVE recorded neat.

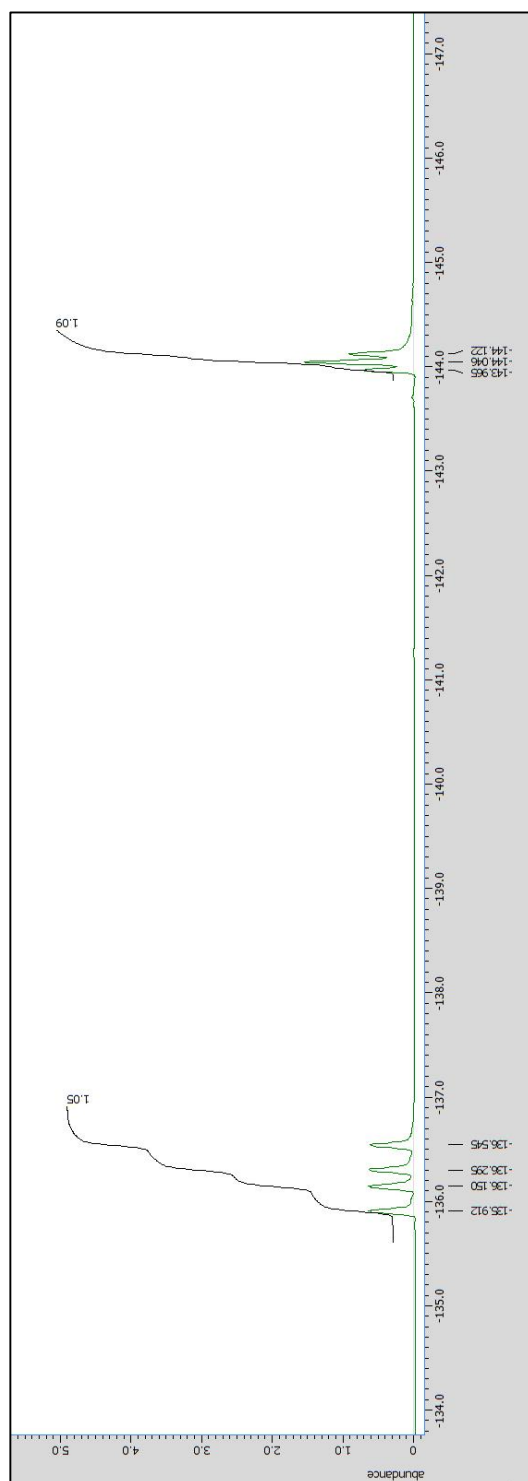


Figure F.42. Fluorine-19 NMR spectra (4 of 4 views) of 8-CNVE recorded neat.